ADAPTIVE COMPENSATION BASED ACTUATOR FAULT TOLERANT CONTROL OF NONLINEAR UNCERTAIN SYSTEMS WITH EMPHASIS ON TRANSIENT PERFORMANCE IMPROVEMENT

A
thesis submitted
for the award of the degree of

DOCTOR OF PHILOSOPHY

by

ARGHYA CHAKRAVARTY

Department of Electronics and Electrical Engineering
Indian Institute of Technology Guwahati
Guwahati - 781 039, INDIA.
NOVEMBER 2018

ADAPTIVE COMPENSATION BASED ACTUATOR FAULT TOLERANT CONTROL OF NONLINEAR UNCERTAIN SYSTEMS WITH EMPHASIS ON TRANSIENT PERFORMANCE IMPROVEMENT

ARGHYA CHAKRAVARTY

Certificate

This is to certify that the thesis entitled "**ADAPTIVE COMPENSATION BASED ACTUATOR FAULT TOLERANT CONTROL OF NONLINEAR UNCERTAIN SYSTEMS WITH EMPHASIS ON TRANSIENT PERFORMANCE IMPROVEMENT**", submitted by **Arghya Chakravarty** (11610211), affiliated to the *Department of Electronics and Electrical Engineering, Indian Institute of Technology Guwahati*, for the award of the degree of **Doctor of Philosophy**, is a record of an original research work carried out by him under my supervision and guidance. The thesis has fulfilled all requirements as per the regulations of the Institute and in my opinion has reached the standard needed for submission. The results embodied in this thesis have not been submitted to any other University or Institute for the award of any degree or diploma.

Dated:
Guwahati.

Dr. Chitralekha Mahanta
Professor
Dept. of Electronics and Electrical Engg.
Indian Institute of Technology Guwahati
Guwahati - 781039, India.

To my beloved mother Mrs. *Banani Chakravarty*, the memory of my father Mr. *Ashoke Chakravarty* and my research inspiration Professor *Francesco Bullo*

I have an angel watching over me an I call him my Father. I would always remember the things you taught me and how much you did love me. I have no words to acknowledge the sacrifices you and mother made and the dreams you both had to let go, just to give me the opportunity to achieve mine.

"To leave everything to the fate and to not actively contribute to the music of the universe is a sign of sheer ignorance. You might not change your instrument, but how well you play is entirely upto you. Whatever happens in your life, no matter how troubling things might seem, do not enter the neighbourhood of despair. Even when all doors remain closed, God will open up a new path only for you. Be thankful! for not only what you have been given but also for what you have been denied...!"

-from *The Forty Rules of Love* by **Elif Shafak**

Acknowledgement

First and foremost, I am grateful to Almighty for having guided me through the righteous path and bestowed upon me his grace to complete this PhD thesis successfully.

I take this opportunity to express my deepest gratitude and heartfelt thanks to my thesis advisor Prof. Chitralekha Mahanta for her incisive expertise, consistent guidance and her intense support. I am extremely grateful to her for giving me the opportunity to pursue a research career and introducing me to the field of robust adaptive control theory. Her unmatched supervision, support and untiring efforts (given that I was a direct entrant into Ph.D. after my B. Tech.) ever since the days I joined the Institute eventually made me a successful researcher I am today. Her sincere dedication, accessibility and keen attention to minor details in my research were of immense motivation to me. I must acknowledge her kindness, patience and extreme diligence in correcting all my manuscripts.

I would always be indebted to my doctoral committee chair Dr. Indrani Kar for her constructive criticisms of my work, her generous support in all possible ways she could and her trust on me more than what I deserve. Some of her bright thoughts were very helpful in shaping up my thoughts and were beneficial to my research. My deep appreciation and sincere thanks to her. Words would not be enough to express my sincere gratitude towards her for the guidance, constant encouragement and support she has imparted me throughout my PhD tenure in IIT Guwahati. I would really miss my daily discussions with her and most specifically, the delicious chocolate truffle cakes she gifted me every year on my birthday on New Year mornings.

I owe a debt of gratitude to other members of my doctoral committee, Dr. Srinivasan Krishnaswamy and Dr. Sisir Kumar Nayak for devoting their precious time in evaluating the progress of my research. Their critique and quality inputs counseled on timely basis have been of great help to me. I am thankful to the Ministry of Human Resource Development (MHRD), Government of India for providing me the necessary fellowship grant to pursue the Ph.D programme.

A special thanks and admiration to the person, I share a strong bond of friendship with, my dear friend Tousif Khan Nizami. Thank you for having stood beside me against all odds and being there for me in both difficult and good times during my stay. Your consistent encouragement and faith in my abilities have helped me immensely to overcome the challenges and finally led to the successful completion of this thesis. I am extremely thankful to Dr. Sanjoy Mondal (now at NTU Singapore) for his guidance and I should submit that a greater share of the knowledge and ability I have gathered so far in research, should be accredited to him. I also extend my deep sense of gratitude to my dearest friends Rohan Kumar Das (now at NUS, Singapore), Saurabh Pandey (now at Dalian University of Technology, China), Abdul Basit Andrabi, Tasaduq Hussain and Karteek for their constant motivating discussions, support and joyful company. Especially, I am greatly indebted in Saurabh and Basit for

supporting and upholding my confidence and sanguineness in all possible ways throughout the days of writing this research monograph. I deeply appreciate their efforts in keeping me happy and bearing with me all throughout my final struggling days at IIT Guwahati. During my toughest times here in Guwahati, Basit's intense support and guidance being my dearest brother, have been invaluable and certainly beyond words. Though I have been miles apart from my family, I should definitely admit that my years at IIT Guwahati had been like staying at home away from home in the company of these wonderful people. I greatly acknowledge the help from my colleague and friend Manmohan Sharma in the experimental realization of the algorithms in this thesis.

I would also like to acknowledge the love and encouragement from my dear friends Murat (Aniruddha Mazumdar), Abhijit Mazumdar and Nayanjyoti Kakoti. Just expressing gratitude to the unconditional and unparalleled support from my international friends *Babba* Ali Jraisheh, *Grandfather* Moustafa Najm, *Anne* Ghadir Nofal, *çocuk* Ahmad AlMamo, Sami AlIssa and Malek AlHasan, would not be enough and I would always be indebted in them for their kindness and deep affection for me. I would also like to take this opportunity to thank Mr. Nizam Ali Khan (Tousif's father) for bestowing his affection on me and our thought-provoking discussions which have helped me immensely all throughout my journey so far.

This journey would not have been complete without the love and affection of my dear friends Vinay Kumar Pandey (now R&D Scientist in Mercedes, Germany), Pravin Kumar Chaturvedi, Vibhuti Kumar, Khalid Wani, Syed Zainul Aabidin, Ankit Bansal, Resmi N. Chandrasekharan (Chechi), Subhasis Mandal, Nabanita Adhikary, Jyoti Prakash Medhi & his family, Jasvindar Singh, Shadab Illahi, Ajaz Ahmad Dar, Deepak Joshi and Satyabrata Dash. Also, my acknowledgment to my faculty and friend Mrs. Papiya Debnath for her confidence in my worthiness.

I am grateful to the staff of the Academic Section at IIT Guwahati, Mr. Manas Sarma in particular, and Mr. Sidananda Sonowal, for their valuable advice, encouragement and kind assistance in all times throughout my PhD tenure. I also extend my thankfulness to Mrs. Kajallata Brahma and Mrs. Trishna Choudhury for their generous help and cooperation in regards to the formalities involved in potential funding for my research visit to France in July 2017. I soulfully thank my colleagues from Control & Instrumentation Laboratory, who have made this journey, a learning and a joyful experience. Among them my appreciation to Dr. Bajarangbali, Dr. Ezhil Reena Joy, Mandar Maitra, Madhulika Das, Mridul K. Malakar, Gautam Rituraj, Kamakshi Manjari, Suman Roy, Mriganka Biswas and Karnika Biswas. Last but definitely not the least, I do not find words to describe the extent of debt I owe to my family. The unlimited sacrifices and relentless hardwork of my mother Mrs. Banani Chakravarty and my sister Ananya Chakravarty have been truly motivating and been a consistent source of encouragement to me. The contributions of my Godfather Mr. Satyabrata Jana, Mrs. Subhra Jana and Mrs. Dolly Bose (*Madame*) are much beyond words and I feel privileged to have had them in my life. Their unmatched love and patience have been undeniable, without whom my dreams would not have taken a shape.

Arghya Chakravarty
Fall 2018, IIT Guwahati

Abstract

Growing demands of reinforced reliability, survivability, safety and stringent performance requirements in complex critical systems have led to the inception of a new control paradigm, widely known as Fault Tolerant Control (FTC). Systems equipped with an FTC module are, in general, presumed to be resilient to uncertain eventualities of faults and failures. Ever since its outset, FTC has been well recognized as a promising research domain and extensive contributions have been reported so far, however, largely in the context of linear dynamical systems. Given the fact that almost all physical systems existing in nature exhibit an inherent nonlinear behavior; FTC schemes for linear systems may not be fruitful when the operating regime is desired to large and precise fault tolerant control performance also becomes a critical design attribute. In addition to actuator faults/failures, the presence of unknown parametric uncertainties, modeling imperfections and external disturbances combined with structural limitations in such systems pose numerous challenges to the problem of an effective active FTC design. Therefore, this thesis resorts to an fault estimation based FTC (FE/FTC) architecture and attempts to propose some new adaptive FTC methodologies for nonlinear uncertain dynamical systems assuming the occurrence of unanticipated actuator failures. The emphasis of the design algorithms is laid on achieving an improvement in start up and post failure transients without yielding to any decrement in input performance (quantified in terms of total variation and energy of input signal). Such ambitious objectives are attained through an amalgamation of robust control ideas with the inherent online learning capabilities of adaptive control.

Firstly, a direct adaptive actuator failure compensation is designed for nonlinear uncertain systems offering asymptotic output tracking and an improved transient and steady state performance with no additional control energy spent. Unlike conventional adaptive backstepping and sliding mode control strategies compensating actuator failures, the improvement in output transient performance is achieved without any trajectory initialization or increase in virtual control gains. Following the above, the shortcomings of direct adaptive control methods are discussed and mathematically proved. Obviating the drawbacks, a new adaptive control scheme in the context of FTC, is designed using multiple models with a two layer adaptation to alleviate the adverse effects of finite as well as infinite actuator failures. Start up and post failure transient performance improvement has been theoretically proved. The control development is supported by a rich and rigorous stability analysis unveiling the benefits of the proposed control design with the most important attributes being the modular behavior of the controller-estimator pair and global boundedness of closed loop trajectories. The proposed methodology is extended to a more challenging problem of FTC design for multi input multi output (MIMO) system with unknown subsystem coupling. Results obtained through numerical simulations and exper-

imental investigations are indeed encouraging and showcases the potential of the control algorithm in real time applications. Within the ambit of a similar indirect adaptive design philosophy, to alleviate computational complexity and anticipating reinforced robust fault tolerant performance, the multiple model adaptive estimator is replaced by a novel finite time parameter estimator. The rapidity and correctness apart from a time bound estimation allows for a promising initial and post failure transients. Besides, the fault-free tracking performance of the nominal closed-loop system during the entire time period including the transients due to abrupt actuator faults/failures is recovered in an explicitly measurable finite time. Following the above work, to render to the crucial requirement of rapid estimation and compensation of unknown failures in safety critical systems, a parametrization free finite time adaptive estimation based nonlinear adaptive controller is developed for nonlinear systems. The proposed adaptive controller is based on the design philosophy of active disturbance rejection control (ADRC) strategies and is so formulated such that controller-estimator modularity is ensured and the *separation principle* is satisfied. The controller augmented with the adaptive finite time uncertainty estimator effectively compensates infinitely occurring actuator failures, system uncertainties and time varying exogenous disturbances. This new result has proved to be instrumental in achieving output asymptotic stability when exposed to adverse situations of finite occurrences of actuator failures, unknown modelling imperfections and subsystem interconnections. The most unique aspect which is indigenous to this scheme is exact nominal performance recovery ascribed to the finite time estimation independent of knowledge of uncertainty structure as well as its bounds. Further, these control designs strategies are also able to compensate high degree of uncertainties and hence are applicable for a large class of nonlinear systems. The proposed control design offers an excellent output transient performance spending only as much control effort as required. All of the adaptive control strategies are free from any controller reconfiguration/redesign and exhibit a retrofitting feature. Such a design characteristic along with computational simplicity indeed enables them to transcend theoretical boundaries and qualify to be a promising choice for FTC applications in real time. Results obtained from extensive numerical simulation and experimental investigations support theoretical propositions presented in this thesis and substantiate their suitability for practical FTC applications.

Contents

List of Figures xi

List of Tables xvi

List of Acronyms xvii

List of Symbols xix

List of Publications xxi

1 Introduction 1

1.1 Introduction . . . 2

1.1.1 Fault Tolerant Control . . . 3

1.1.1.1 Approaches to FTC Design . . . 6

1.2 Literature Review . . . 10

1.3 Research Motivation . . . 14

1.4 Contributions of the Thesis . . . 17

1.5 Thesis Organization . . . 19

2 Adaptive Robust Fault Tolerant Controller (ARFTC) Design for Nonlinear Uncertain Systems with Actuator Failures 21

2.1 Introduction . . . 22

2.2 Adaptive Robust Fault Tolerant Controller (ARFTC) . . . 23

2.2.1 System Dynamics with Actuator Failures . . . 23

2.2.2 Problem Statement . . . 25

2.2.3 Proposed Actuator Failure Compensator Design . . . 26

2.2.4 Stability Analysis . . . 30

2.2.5 Simulation Results and Discussion . . . 39

2.3 Summary . . . 45

3 Adaptive Multiple Model Fault Tolerant Control (AMMFTC) of Nonlinear Uncertain Systems with Actuator Failures 46

3.1 Introduction . . . 47

3.2 Adaptive Multiple Model Fault Tolerant Control (AMMFTC) for Infinite Actuator Failures 51

3.2.1 Problem Statement . . . 52

3.2.2 Adaptive Fault Tolerant Control Design . . . 54

3.2.2.1 Parameter Estimation using Multiple Identifiers with Dual Layer Adaptation . . . 55
3.2.2.2 Backstepping Control Design . . . 60
3.2.3 Main Results . . . 62
3.2.3.1 Stability Analysis of the Proposed Control System . . . 62
3.2.3.2 Transient Performance Analysis for the Proposed AMMFTC . . . 77
3.2.4 Simulation Studies . . . 80
3.2.4.1 Numerical Example . . . 81
3.2.4.2 Application to an Aircraft System . . . 86
3.3 Adaptive Multiple Model Fault Tolerant Control (AMMFTC) for Uncertain Multi-Input-Multi-Output (MIMO) Nonlinear Systems . . . 90
3.3.1 Problem Formulation . . . 91
3.3.2 Adaptive Multiple Model Fault Tolerant Control (AMMFTC) Design . . . 94
3.3.2.1 Controller Synthesis . . . 95
3.3.2.2 Design of Parameter Estimator using Multiple Identification Models . . . 99
3.3.3 Main Results: Stability Analysis of the Proposed Control System . . . 103
3.3.4 Simulation Study . . . 113
3.3.5 Experimental Study on a Twin Rotor MIMO System . . . 118
3.4 Summary . . . 126

4 Finite Time Adaptation based Compensation (FTAC) of Actuator Failures in Nonlinear Uncertain Systems 127
4.1 Introduction . . . 128
4.2 Finite Time Adaptation based Compensation (FTAC) of Infinite Actuator Failures . . . 132
4.2.1 Some Preliminary Definitions . . . 132
4.2.2 Problem Formulation . . . 133
4.2.2.1 Design Assumptions . . . 134
4.2.3 Fault Tolerant Control Design with Finite Time Adaptation . . . 134
4.2.3.1 Design of Finite Time Parameter Estimator . . . 136
4.2.3.2 Controller Design . . . 146
4.2.4 Stability Analysis . . . 147
4.2.5 Simulation Studies . . . 158
4.3 Finite Time Adaptation based Compensation (FTAC) of Actuator Failures in Multi-Input-Multi-Output (MIMO) Nonlinear Uncertain Systems . . . 165
4.3.1 Problem Formulation . . . 165
4.3.2 Proposed Finite Time Adaptation based Controller (FTAC) . . . 168
4.3.2.1 Controller Synthesis . . . 168
4.3.2.2 Design of Parameter Estimator with Finite Time Convergence . . . 170
4.3.3 Stability Analysis of the Proposed Control System . . . 172
4.3.4 Simulation Study . . . 180
4.3.5 Experimental Study on a Twin Rotor MIMO System . . . 182

4.4 Summary . . . 187

5 Parametrization-free Finite Time Estimation based Adaptive Compensation of Actuator Failures in Nonlinear Uncertain Systems 189

5.1 Introduction . . . 190

5.2 Parametrization-free Finite Time Estimation based Adaptive Compensation of Actuator Failures in Nonlinear uncertain Systems . . . 192

5.2.1 Mathematical Notations and Definitions . . . 192

5.2.2 Problem Formulation . . . 193

5.2.3 Proposed Adaptive FTC Design for Infinite Actuator Failures . . . 195

5.2.3.1 Controller Design . . . 195

5.2.3.2 Failure Induced Uncertainty Estimation . . . 196

5.2.4 Stability Analysis of the Proposed Control System under Infinite Actuator Failures 197

5.2.4.1 Piecewise Boundedness of Closed-Loop Signals . . . 197

5.2.4.2 Further Results on Stability of the Closed-loop System under Infinite Actuator Failures . . . 203

5.2.5 Simulation Studies . . . 210

5.3 Summary . . . 214

6 Conclusions and Scope for Future Work 216

6.1 Conclusions . . . 217

6.2 Recommendations for Future Research . . . 220

A Appendix 222

A.1 Definition of Performance Indices . . . 223

A.2 Some Useful Definitions and Inequalities . . . 224

A.2.1 Definition of Signal Norms and $\mathcal{L}_p$ Spaces . . . 224

A.2.2 Signal Convergence Lemmas . . . 224

A.2.3 Important Inequalities . . . 224

A.2.4 Convex Sets . . . 225

A.3 Nonlinear State Estimation: Extended Kalman Filter (EKF) . . . 226

A.3.1 Design Motivation . . . 226

A.3.2 Design of Extended Kalman Filter (EKF) . . . 227

A.4 Proof of Lemma 4.1 . . . 228

References 230

List of Figures

1.1 Centrifugal governor [1] . . . 2
1.2 Illustration of the types of actuator faults and failures in dynamical systems. . . . 4
1.3 Demonstration of actuator faults and failures of control surfaces in Boeing 747 aircraft. 4
1.4 A photo of the Jet Airways Flight 9W 2374 which suffered a rare engine failure on December 27, 2016. . . . 5
1.5 Major approaches to fault tolerant control (FTC) design (adapted from [2]). . . . 6
1.6 Schematic block diagrammatic representation of active fault tolerant control (AFTC) architecture. . . . 8
1.7 An event-driven interpretation and illustration of active fault tolerant control (AFTC) architecture [3]. . . . 8
1.8 Structure and operational flow of active fault tolerant control (AFTC) scheme adopted in the thesis. . . . 9
1.9 An event-driven interpretation and illustration of active fault tolerant control (AFTC) scheme adopted in the thesis. . . . 9

2.1 Schematic representation the proposed fault tolerant control scheme . . . 31
2.2 Visualization of the calculated invariant sets with the proposed scheme, for systems with relative degree $\wp = 2$ . . . 37
2.3 Plant response and control inputs under the considered fault scenario (2.79) using the proposed control scheme. (a) Output tracking error comparison of the proposed controller (red) with ASMC (blue) [4] and ABSC (green) [5]; (b) Pitch angle θ tracking using the proposed ARFTC; (c) Pitch rate q under the proposed ARFTC; (d) Control inputs u_1 and u_2 corresponding to proposed ARFTC; (e) Control inputs u_1 and u_2 using ASMC [4]; (f) Control inputs u_1 and u_2 using ABSC procedure [5]. . . . 44

3.1 Schematic block diagram representation of a basic MMAC scheme with switching and tuning . . . 49
3.2 Bidirectional robustness interactions transformed to unidirectional interaction under the proposed FTC strategy . . . 50
3.3 Block diagrammatic representation of the proposed adaptive fault tolerant control scheme (AMMFTC). . . . 62

3.4 Illustration explaining the interdependence between $\|z\|_\infty$, controller gain parameters and actuator failure transit time T^* 77
3.5 Comparison of start-up output transient performance and parameter convergence obtained with Modular Backstepping Control (MBSC) [6], single model adaptive control and proposed multiple model adaptive control 83
3.6 System states and control input with no actuator fault under Scenario 1 (3.126) from $t = 0 \sim 50$ s. (a) Output state $\xi_2 = x_1$;(b) state ξ_1;(c) state $\xi_3 = x_2$; (d) control inputs u_1 and u_2 84
3.7 Scenario 1. Comparison of post-failure output transient performance and parameter convergence obtained with Modular Backstepping Control (MBSC) [6], single model adaptive control and proposed multiple model adaptive control 85
3.8 System states and control inputs with actuator fault under Scenario 1 (3.126) at $t = 50$ s. (a) Output state $\xi_2 = x_1$;(b) state ξ_1;(c) state $\xi_3 = x_2$; (d) control inputs u_1 and u_2 86
3.9 Comparison of post failure transient performance obtained with Modular Backstepping Control (MBSC), single model adaptive control and proposed multiple model adaptive control in case of infinite actuator failures 87
3.10 System states and control inputs with intermittent actuator fault/failures under Scenario 2 (3.127). (a) Output state $\xi_2 = x_1$;(b) state ξ_1;(c) state $\xi_3 = x_2$; (d) control inputs u_1 and u_2 88
3.11 Comparison of start up and post failure transient performance obtained with Modular Backstepping Control (MBSC), single model adaptive control and multiple model adaptive control in case of infinite actuator failures 89
3.12 (a) aircraft pitch angle tracking error;(b) actual and desired aircraft pitch angle $\theta = x_3$; (c) aircraft pitch rate x_4; (d) control inputs u_1 and u_2; 90
3.13 Schematic diagram of a coupled mass-spring-damper system 114
3.14 (a) Tracking error comparison in displacement output y_1;(b) Tracking error comparison in displacement output y_2; using the proposed adaptive FTC using multiple models and under a single model adaptive FTC strategy. 116
3.15 (a) Time evolution of $y_1(t)$ under the proposed adaptive FTC using multiple models;(b) Time evolution of $y_2(t)$ under the proposed adaptive FTC using multiple models;(c) Control inputs u_1 and u_2 under the proposed FTC scheme using multiple models; (d) Control inputs u_1 and u_2 under adaptive FTC scheme using a single model. 117
3.16 (a) The experimental setup of a twin rotor MIMO system (TRMS) emulating a 2-DOF helicopter; (b) Schematic physical description of the twin rotor MIMO system (TRMS). 118
3.17 Schematic of cross-coupled twin rotor MIMO system or a 2-DOF helicopter for control development 119
3.18 (a) pitch and yaw angle tracking error (rad) ; (b) pitch angle $\theta_v = x_1$(rad); (c) yaw angle $\theta_h = x_3$(rad); (d) control input voltages u_v and u_h (V). 124
3.19 (a) pitch and yaw angle tracking error (rad) ; (b) pitch angle $\theta_v = x_1$(rad); (c) yaw angle $\theta_h = x_3$(rad); (d) control input voltages u_v and u_h (V). 125

4.1 Block diagrammatic representation of the proposed FTAC strategy 148
4.2 (Left) Comparison of parameter estimation performance; (Right) Comparison of start up transient performance; obtained with AMMFTC, Modular Backstepping Control (MBSC) and proposed FTAC method under no failure from $t = 0s - 25s$. 160
4.3 (Left) Comparison of parameter estimation performance; (Right) Comparison of post failure transient and steady state performance; obtained with AMMFTC, Modular Backstepping Control (MBSC) and proposed FTAC method under no failure from $t = 50s - 100s$. 161
4.4 System states and control inputs with actuator fault under Case 1 (4.117) at $t = 50$ s. (a) Output state $\xi_2 = x_1$;(b) state ξ_1;(c) state $\xi_3 = x_2$; (d) control inputs u_1 and u_2 . . 162
4.5 Comparison of tracking performance under infinite actuator failures Case 2 (4.118) showing performance improvement with increasing T^*; (Left) tracking error performance for $T^* = 5s$; (Right) tracking error performance for $T^* = 15s$; between Modular Backstepping Control (MBSC) [6], Multiple Model (AMMFTC) and FTAC method in case of infinite actuator failures 163
4.6 System states and control inputs for Case 2 (4.118) with $T^* = 5$s. (a) Output state $\xi_2 = x_1$;(b) state ξ_1;(c) state $\xi_3 = x_2$; (d) control inputs u_1 and u_2 164
4.7 (a) Tracking error comparison in displacement output y_1;(b) Tracking error comparison in displacement output y_2; under the action of the proposed FTAC based FTC strategy and AMMFTC 182
4.8 (a) Time evolution of $y_1(t)$ under the proposed adaptive FTC using FTAC;(b) Time evolution of $y_2(t)$ under the proposed adaptive FTC using FTAC;(c) Control inputs u_1 and u_2 under the proposed FTC scheme using FTAC; (d) Control inputs u_1 and u_2 under AMMFTC. 183
4.9 (a) Time evolution of the pitch angle $\theta_v = x_1$ (rad) tracking the reference signal $y_{r,1}$;(b) Time evolution of the yaw angle $\theta_h = x_3$ (rad) tracking the reference signal $y_{r,2}$. 185
4.10 (a) pitch and yaw tracking error (rad); (b) control input voltages u_v and u_h for the main rotor and the tail rotor. 186

5.1 Bidirectional robustness interactions transformed to unidirectional interaction under the proposed FTC strategy 198
5.2 Illustration of the trajectory starting from $(z(0), \tilde{\kappa}(0)) \in \Omega_{(z,\tilde{\kappa})}$ and $\sigma(0) \notin \mathcal{N}_\sigma$ converges into $(z, \tilde{\kappa}, \sigma) \in \mathcal{M}_{(z,\tilde{\kappa})} \times \mathcal{N}_\sigma$. 201
5.3 Time evolution of $z(t)$ and $\tilde{\kappa}(t)$ starting in $\Omega_{(z,\tilde{\kappa})}$ traversing through the set $\mathcal{M}_{(z,\tilde{\kappa})}$ and ultimately exponentially asymptotically converging to origin. The radius k defines the decaying exponential envelope along which $z(t)$ converges to the origin with $k \to 0$ as $t \to \infty$. 210

5.4 Scenario 1: System response with the proposed fault tolerant control scheme with T^*= 10s. (a) Comparison of output pitch angle tracking error $z_1 = x_3 - y_r$ using the proposed controller and modular backstepping control (MBSC) [6], (b) Pitch angle $x_3 = \theta$ using the proposed FTC scheme, (c) Pitch rate $x_4 = q$ using the proposed FTC, (d) The estimate of the lumped uncertainty $\hat{\bar{\Delta}}_2$ incurred due to actuator faults/failures and modeling uncertainties, (e) Proposed control inputs $u_1(t)$ and $u_2(t)$, (f) Control inputs $u_1(t)$ and $u_2(t)$ using modular backstepping control based FTC proposed by Wang & Wen [6] 212

5.5 Scenario 2: System response with the proposed fault tolerant control scheme with T^*= 10s. (a) Comparison of output pitch angle tracking error $z_1 = x_3 - y_r$ using the proposed controller and modular backstepping control (MBSC) [6], (b) Pitch angle $x_3 = \theta$ using the proposed FTC scheme, (c) Pitch rate $x_4 = q$ using the proposed FTC, (d) The estimate of the lumped uncertainty $\hat{\bar{\Delta}}_2$ incurred due to actuator faults/failures and modeling uncertainties, (e) Proposed control inputs $u_1(t)$ and $u_2(t)$, (f) Control inputs $u_1(t)$ and $u_2(t)$ using modular backstepping control based FTC proposed by Wang & Wen [6] 213

5.6 Scenario 3: System response with the proposed fault tolerant control scheme. (a) Pitch angle $x_3 = \theta$ using the proposed FTC scheme, (b) Pitch rate $x_4 = q$ using the proposed FTC, (c) The estimate of the lumped uncertainty $\hat{\bar{\Delta}}_2$ incurred due to actuator faults/failures and modeling uncertainties, (d) Proposed control inputs $u_1(t)$ and $u_2(t)$ 214

A.1 Illustration of convex sets 225

A.2 Illustration of construction of convex hull in the parameter space for estimating a parameter of dimension $N = 1, 2, 3$ (from left to right). 226

List of Tables

2.1 Aircraft model parameters 40
2.2 Values of aircraft parameters in simulation 40
2.3 Post failure tracking performance with 70% loss of effectiveness of u_1 at $t = 20s$ and stuck failure of u_2 at $t = 40s$ 45

3.1 Tabular comparison of output and input performance under Scenario 1 (3.126). 83
3.2 Tabular comparison of output and input performance for Scenario 2 (3.127) describing infinite actuator failures with $T^* = 5$ s and $T^* = 15$ s 85
3.3 Tabular comparison of output and input performances under proposed AMMFTC and adaptive FTC using a single identification model 116
3.4 Physical parameters of the TRMS 121
3.5 Tabulation of input and output performances quantified using suitable performance measures 123

4.1 Tabular comparison of output and input performance under Case 1 (4.117). 161
4.2 Case 2: Performance Comparison between three adaptive control schemes, namely, finite time adaptation based control (FTAC), adaptive control using multiple models, single model adaptive control and modular backstepping control (MBSC) [6] 163
4.3 Tabular comparison of output and input performances under proposed FTC under finite time adaptation based control (FTAC), AMMFTC and adaptive FTC using a single identification model 183
4.4 Tabulation of output and input performances using the proposed FTAC methodology when applied to attitude tracking problem of TRMS. 187

List of Acronyms

ABSC	Adaptive backstepping control
ADRC	Active disturbance rejection control
ADSC	Adaptive dynamic surface control
AMMFTC	Adaptive multiple model fault tolerant control
ARFTC	Adaptive robust fault tolerant control
ARC	Adaptive robust control
ASMC	Adaptive sliding mode control
BIBS	Bounded input bounded state stable
CE	Certainty equivalence
CMMAC	Combined multiple model adaptive control
DOB	Disturbance observer
DOF	Degrees of freedom
EKF	Extended Kalman filter
FDD	Fault detection and diagnosis
FDI	Fault detection and isolation
FE	Fault/Failure estimation
FTAC	Finite time adaptation based control
FTC	Fault tolerant control
HOSMC	Higher order sliding mode control
IAE	Integral absolute error
IE	Initial excitation
ISMC	Integral sliding mode control
ITAE	Integral time absolute error
LIP	Lock in place
LMI	Linear matrix inequality
MBSC	Modular backstepping control
MIMO	Multiple input multiple output
MISO	Multiple input single output
MMAC	Multiple model adaptive control
NDOB	Nonlinear disturbance observer
PCI	Peripheral component interconnect
PE	Persistenly exciting

PLF	Piecewise Lyapunov function
PLOE	Partial loss of effectiveness
PPB	Prescribed performance bound
RMSE	Root mean square error
SMC	Sliding mode control
SOSM	Second order sliding mode
TLOE	Total loss of effectiveness
TRMS	Twin rotor MIMO system
TV	Total variation
UUB	Uniformly ultimately bounded

List of Symbols

$:=$	defined as
$\triangleq$	by definition
$\subset$	proper subset of
$\supset$	proper superset of
$\subseteq$	subset of
$\supseteq$	superset of
$\forall$	for all
$\cap$	intersection
$(\cdot)^{\dagger}$	pseudo inverse of the argument
$\in$	belongs to
$\ni$	does not belong to
$\exists$	there exists
$\square$	designating the completion of proofs
$\rightarrow$	tends to
$\Longrightarrow$	implies that
$\mathbb{R}$	the space of real numbers
$\mathbb{R}_+$	the space of positive real numbers
$\mathbb{R}^n$	the space of real valued vectors of dimension n
$\mathbb{R}^{m\times n}$	the space of real valued $m \times n$ matrices
$\mathbb{W}$	the set of whole numbers
$\mathbb{N}$	the set of natural numbers
$2\mathbb{N}$	the set of all even numbers
$\mathbb{N}/2\mathbb{N}$	the set of all odd numbers
$\mathbb{Z}_+$	the set of positive integers
$\lvert\cdot\rvert$	absolute value of a scalar argument
$(\cdot)^T$	transpose of the argument (vector or matrix)
$\lVert A\rVert_\infty$	induced $\infty-$norm of a matrix
$\lVert A\rVert_{\mathscr{F}}$	the Frobenius norm of the matrix A
$\max\{\cdot\}$	the maximum of the arguments
$\min\{\cdot\}$	the minimum of the arguments
sup	the least upper bound
$Tr\{A\}$	the trace of the matrix A

$det(A)$	the determinant of matrix A
$f : S_1 \rightarrow S_2$	a function f mapping space S_1 onto space S_2
$\mapsto$	maps to
$\|\cdot\|_p$	$\mathcal{L}_p$ norm for $p \in [1, \infty)$ of the argument vector
$\|\cdot\|_\infty$	$\mathcal{L}_\infty$ norm of the argument vector
$\bar{(\cdot)}$	upper bound of the argument
$\underline{(\cdot)}$	lower bound of the argument
$\mathcal{L}_1[a, b]$	the signal space $\mathcal{L}_1[a, b] = \{x(t) \in \mathbb{R}^n \mid \|x\|_1 < \infty \text{ for } t \in [a, b]\}$
$\mathcal{L}_2[a, b]$	the signal space $\mathcal{L}_2[a, b] = \{x(t) \in \mathbb{R}^n \mid \|x\|_2 < \infty \text{ for } t \in [a, b]\}$
$\mathcal{L}_\infty[a, b]$	the signal space $\mathcal{L}_\infty[a, b] = \{x(t) \in \mathbb{R}^n \mid \|x\|_\infty < \infty \text{ for } t \in [a, b]\}$
$\mathcal{L}_1$	the signal space $\mathcal{L}_1 = \{x(t) \in \mathbb{R}^n \mid \|x\|_1 < \infty \text{ for } t \in [0, \infty)\}$
$\mathcal{L}_2$	the signal space $\mathcal{L}_2 = \{x(t) \in \mathbb{R}^n \mid \|x\|_2 < \infty \text{ for } t \in [0, \infty)\}$
$\mathcal{L}_\infty$	the signal space $\mathcal{L}_\infty = \{x(t) \in \mathbb{R}^n \mid \|x\|_\infty < \infty \text{ for } t \in [0, \infty)\}$
$\dot{y}$, $\ddot{y}$	first and second derivative of y with respect to time
$y^{(i)}$	the i^{th} time derivative of y with respect to time
$\overline{\lambda}(\cdot)$	maximum eigen value of the matrix argument
$\underline{\lambda}(\cdot)$	minimum eigen value of the matrix argument
A/B	quotient operation between two sets A and B, i.e., $A - B$
$A \times B$	the cartesian product between two sets
$\text{diag}\{a_1, \ldots, a_n\}$	an $n \times n$ diagonal matrix with diagonal elements a_1 to a_n
$L_f(\cdot)$	the Lie derivative along the direction of vector field f
I_n or $\mathbf{I}_n$	the identity matrix of dimension $n \times n$
m, q, p	dimension of system input, output and unknown parameter vector
$\text{Proj}(\cdot)$	the projection operator
$\wp$	the relative degree of a system
$\wp_i$	the relative degree of i^{th} subsystem
$\text{sign}(x)$	the signum function such that sign(x) is 1, 0 or -1
	respectively, according as $x > 0, x = 0, x < 0$
$\delta(t - a)$	the impulse function defined at $t = a$
$U(t - a)$	the unit step function defined at $t = a$
$M_p\%$	the percentage of peak overshoot
$M_u\%$	the percentage of peak undershoot

List of Publications

International Refereed Journals

1. A. Chakravarty and C. Mahanta, "Actuator fault-tolerant control (FTC) design with post-fault transient improvement for application to aircraft control", *International Journal of Robust and Nonlinear Control, Wiley*, vol. 26(10), pp. 2049-2074, 2016.

Manuscript Under Preparation

1. A. Chakravarty, I. Kar and C. Mahanta, "A new interacting multiple model adaptive control approach to compensate infinite actuator failures in nonlinear uncertain systems: stability, convergence and performance", *IEEE Transactions on Automatic Control*, Draft prepared to be submitted.

2. A. Chakravarty and C. Mahanta, "Enhanced Parameter convergence and output performance improvement via a novel finite time adaptation based fault tolerant controller for nonlinear uncertain systems", *Automatica*, Draft prepared to be submitted.

3. A. Chakravarty, C. Mahanta and I. Kar, "Adaptive compensation of parametrization-free infinite actuator failures in nonlinear uncertain systems with finite time performance recovery", *IEEE Transactions on Automatic Control*, Draft prepared to be submitted.

4. A. Chakravarty, C. Mahanta and K. S. Amezquita, "Adaptive compensation of actuator failures in MIMO nonlinear uncertain systems with finite time fault estimation and improved transient performance applied to aircraft control", *IEEE Control Systems Letters*, To submit.

Conference Proceedings

1. A. Chakravarty, T. K. Nizami, I. Kar and C. Mahanta, "Adaptive compensation of actuator failures using multiple models", *20th IFAC World Congress,* Vol 50, No. 1, Toulouse, France, 2017, pp. 10350-10356.

2. A. Chakravarty and C. Mahanta, "Compensating actuator failures in near space vehicles using adaptive finite time disturbance observer based backstepping controller", *Proc. of 2016 European Control Conference (ECC),* Aalborg, Denmark, 2016, pp. 98-103.

3. A. Chakravarty and C. Mahanta, "Finite time actuator failure compensation of near space vehicles using an observer based backstepping method", *Proc. of LAMSYS-2016,* Satish Dhawan Space Centre, Sriharikota, ISRO, India, 2016.

4. A. Chakravarty and C. Mahanta, "Backstepping enhanced adaptive second order sliding mode controller to compensate actuator failures", *Proc. of 2014 Annual IEEE India Conference (INDICON),* Pune, India, 2014, pp. 1-6.

5. A. Chakravarty and C. Mahanta,"Actuator fault tolerant control scheme for nonlinear uncertain systems using backstepping based sliding mode", *Proc. of 2013 Annual IEEE India Conference (INDICON),* Mumbai, India, 2013, pp. 1-6.

1

Introduction

Contents

1.1 Introduction 2
1.2 Literature Review 10
1.3 Research Motivation 14
1.4 Contributions of the Thesis 17
1.5 Thesis Organization 19

1.1 Introduction

Control theory plays an integral role in deciding the behavior of all dynamical systems existing in nature. The concept of *feedback* is central to almost all control systems and has indeed been instrumental in acheiving system output regulation or desired reference trajectory tracking. With overwhelming technological developments and spectacular success of the industrial revolution, the early 19th century witnessed the first instances of feedback control systems in the form of Watt's centrifugal governor shown in Figure 1.1 [1]. The centrifugal governor was intended to control the output shaft speed of the steam engine. Until 1868, the design of control systems in such mechanical and electrical machineries, was primarily an art procured from intuition, experience and engineering ingenuity. Such approaches abstained from representing the *control problem*, its objectives and imposed constraints in terms of mathematical relationships. As a result, these ad hoc control solutions failed to provide analytical

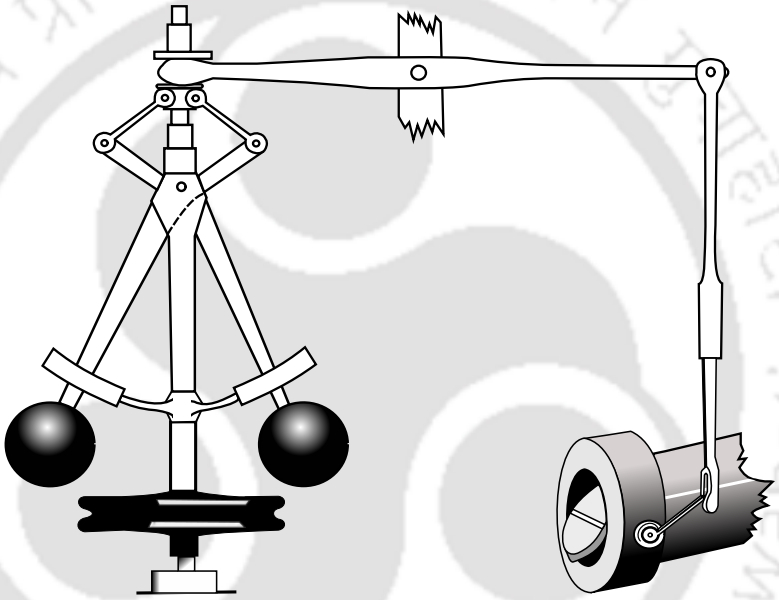

Figure 1.1: Centrifugal governor [1]

insights into system behavior in the event of parameter variations and unanticipated disturbances; and hence attaining a robust and optimized performance was certainly questionable. By then, a formal mathematical analysis had already begun with the study of governor dynamics by physicist J.C. Maxwell [1]. Eventually, the analysis led to the introductory concept of limit cycle oscillations and the fundamental notion of instability in dynamical systems under feedback. In consequence, these issues motivated several analytical developments regarding dynamic instability of linear systems in the West; the most remarkable one being the celebrated Routh-Hurwitz stability criterion. Alternatively, one of the greatest developments in the theory of stability of dynamic systems was the publication of Lyapunov's famous memoir in 1892 followed by promising methods on stability analysis. By World War II, owing to demands of high performance and stability of closed-loop feedback control systems, mathematical research on automatic control theory gained enough impetus for applications in missile guidance and control, ship steering, and aircrafts. Servomechanisms in frequency domain were de-

signed from theoretical results on dynamic stability using frequency response, bandwidth, gain and phase margins. Restricted to linear systems, these methods lacked severely in achieving performance robustness and resulted in a very limited dynamically stabilizable operating regime. In contrary, the stability results independently proposed by Lyapunov in the Soviet Union, was more general and was applicable to systems regardless of their input-output characteristics. These results were indeed a major scientific breakthrough for the Soviet Union which marked the emergence of modern control theory and the inception of new control paradigms based on state space approaches.

1.1.1 Fault Tolerant Control

Apart from stability; safety, reliability and performance are among the essential operational characteristics sought for in control of dynamical systems, especially in mission critical applications. Besides, cost effectiveness has also been an added design objective to be possibly met. Imperfections in system modeling, uncertain operating environment, large variations in parameters, malfunctioning or damage of system components further complicate the synthesis of a stable controller. On similar lines, it is extremely difficult to ensure the existence of sustainable closed-loop system solutions respecting the foregoing design attributes using conventional feedback control. Consistent attempt to address these design challenges gradually motivated the development of retrofit control technologies for complex safety critical systems to render resilience to uncertain eventualities. In this direction, the first pioneering effort was the launch of Self Repairing Flight Control System Program [7] by the US Air Force in 1984. Eventually followed up by the National Aeronautics and Space Administration (NASA), this initiative led to the inception of a new research avenue in the field of control theory applications known as fault tolerant control (FTC) [8]. Hence, FTC systems are defined as *control systems that are equipped with the ability to accommodate system, component faults or failures automatically and are capable of maintaining overall system stability and acceptable performance in the event of such fault or failure* [8–10].

Fault can be defined as an undesired change in a system parameter that degrades performance. Whereas, *failure* is an eventuality that results in catastrophic or complete breakdown of a component or function which can be compared to a fault which is a tolerable malfunction. Having defined the terminologies, a broad classification comprises of actuator, sensor and system faults/failures. Changes in operating points, large uncertain abrupt variation in system parameters, payload variations, etc. are termed as system faults. On the other hand, sensor faults manifest themselves in incorrect measurements with noise, measurement bias, freezing and drift. Actuator faults/failures and their types are illustrated in Figure 1.2. The variable t_f denotes the failure instant and $u_{\max}, u_{\min}$ are the maximum/minimum limits of actuation magnitude. Different types of actuator failures are demonstrated using an aircraft example. Figure 1.3 shows a commercial aircraft exhibiting faults and failures in ailerons (f_{al}), elevators (f_e) and rudder (f_r). Faults in such control surfaces occur in the form of partial loss of effectiveness (PLOE) as shown in Figure 1.2(d), wherein the actuator operates with reduced efficiency after time t_f. Total actuator failures manifests in three forms, namely, *float*, *lock-in-place* (LIP) and *hard-over* failures (Figure 1.2(a)-(c)). Float failure is a condition when the control surface moves freely and has no moment contribution to the aircraft. While LIP failure results in the condition

where the actuator is stuck or jammed at a certain value. The most catastrophic form of actuator failure is the hard-over failure where the actuator actuates at its maximum rate limit until its position reaches the blowdown limit.

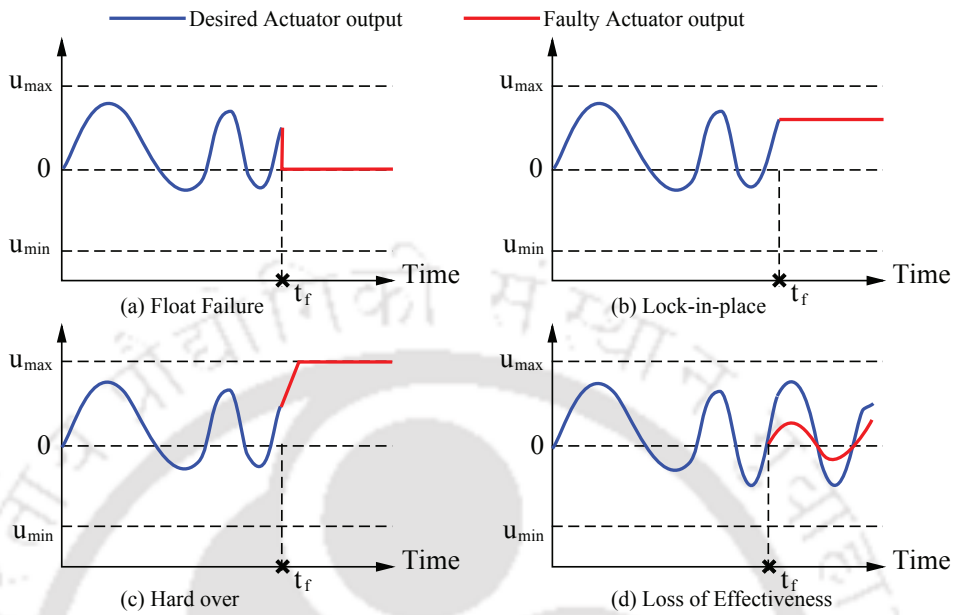

Figure 1.2: Illustration of the types of actuator faults and failures in dynamical systems.

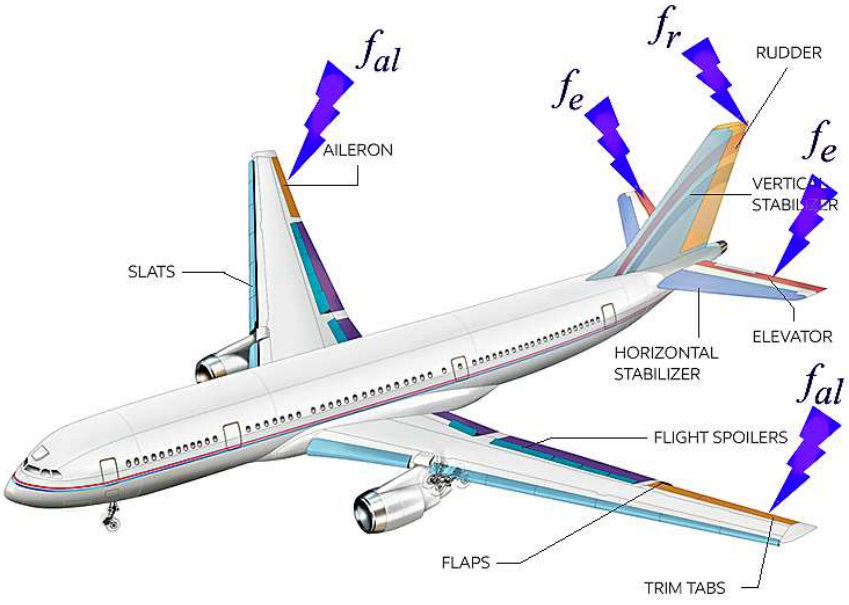

Figure 1.3: Demonstration of actuator faults and failures of control surfaces in Boeing 747 aircraft.

This thesis broadly concerns the design, development and analysis of fault tolerant controllers to compensate actuator faults and failures in addition to system uncertainties and external disturbances. The generalized problem of FTC has not been attempted and hence sensor failures are beyond the

Figure 1.4: A photo of the Jet Airways Flight 9W 2374 which suffered a rare engine failure on December 27, 2016.

scope of this work. In what follows, some practical motivation for actuator FTC research in aerospace systems ranging from commercial aircrafts to unmanned aerial vehicles (UAV) are provided. The basic premise of FTC systems is the availability of redundancy which can be used judiciously in emergency conditions to maintain system stability and an allowable performance degradation. There have been several instances of malfunctioning and shut down of actuators in aircrafts when the pilots were still able to safely land the aircraft utilizing their expertise and redundant system components. For example, on 9 October 2002, the Boeing 747-400 Airline Flight 85 suffered a lower rudder hard-over failure at an altitude of 35,000 ft (404 people on board including 4 crew members and 14 flight attendants) [11]. On account of such a failure, the rudder deflected left to the maximum position limit causing excessive roll. The crew members managed to land the aircraft safely in Anchorage, Alaska by manipulating the upper rudder and the ailerons together with differential engine thrust. More recently, on 27 December 2016, the Jet Airways Flight 9W 2374 (154 passengers, 7 crew members) departing from Goa (Figure 1.4), India underwent a rare engine failure during take-off where the right reverser got engaged and the right engine started producing a thrust in reverse direction while that on the left was producing a forward thrust [12, 13]. The aircraft veered off the runway with excessive spinning. This was indeed dangerous given the fact that the extremely high force which catapults the aircraft into the air was now engaged in spinning it. However, the promptness and expertise of the pilot within the reaction time of such a scenario avoided a catastrophic accident with no human casualties. It is certainly clear from these incidents that the presence of redundancy and the use of pilot skills were central to achieving aircraft stability in such seriously adverse operating conditions. The solutions given by the pilots in these emergency scenarios should be automatically and autonomously found by the onboard autopilot embedded with an FTC unit. Thus, the research on FTC design for commercial/military aircraft systems is highly motivated and undubiously promising. Recent years have seen a tremendous use of unmanned aerial vehicles (UAV) in a multitude of applications including surveillance and reconnaissance, searching and inspection, high resolution imaging, goods delivery and

in-flight refueling and various military missions. Therefore, their relentless deployment in fire-fighting and surveillance operations largely under rough environmental conditions including natural disasters, make them highly vulnerable to on-flight actuator failures. Of late, in this regard, the Washington Post has reported more than 400 crashes of military UAVs in the United States since 2001 [14, 15]. Besides mission failures, these crashes have led to huge loss of property including but not limited to, destruction of houses, farms, forest fires, airport and naval base infrastructures, etc, which is also unfortunate. Indeed, with years of rapid technological advancements in the 21st century, new inventions of mechanical/aerospace systems and their multifaceted applications have come up with several design and operational issues including reliability and safety. Thus, from a control design perspective, these burgeoning issues and their subsequent challenges leave a exciting aura for further research on actuator FTC synthesis for dynamical systems.

1.1.1.1 Approaches to FTC Design

Approaches to FTC design are broadly classified into two categories, namely, an active and a passive approach. Figure 1.5 depicts the classification of FTC along with the segregation between various important control methodologies as active and passive methods.

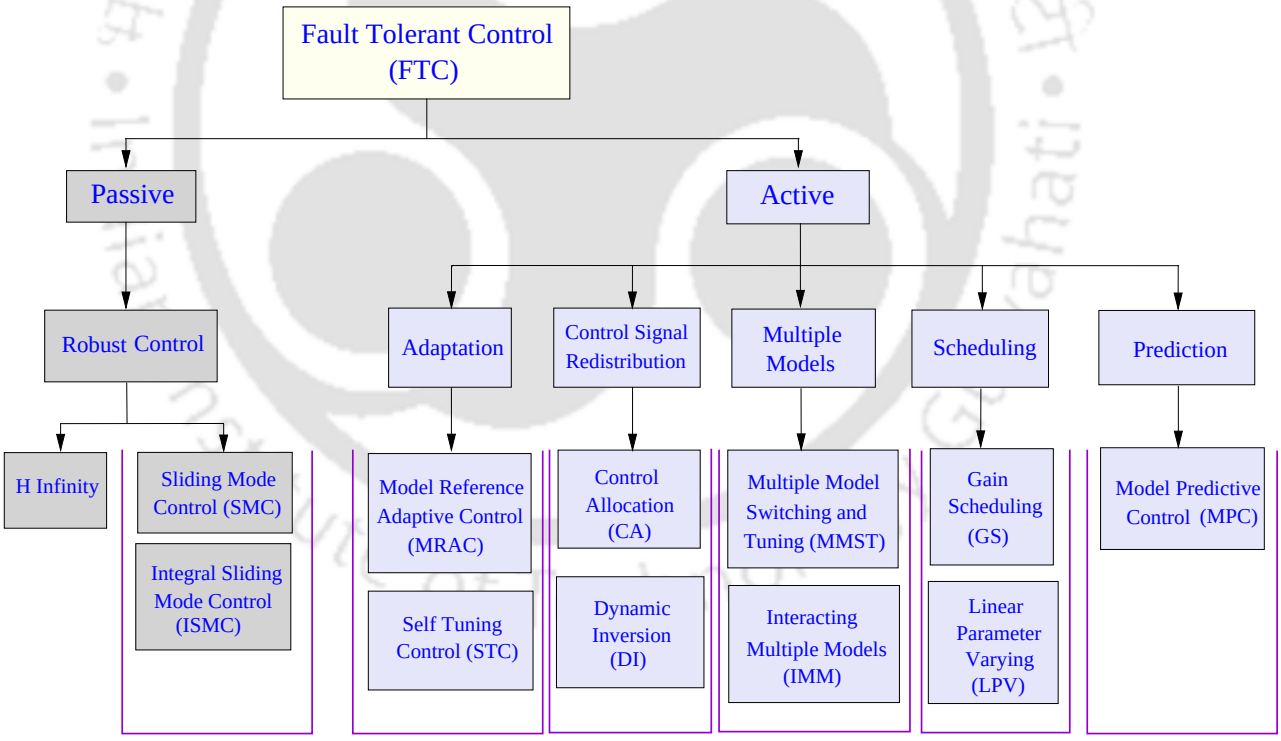

Figure 1.5: Major approaches to fault tolerant control (FTC) design (adapted from [2]).

Active fault tolerant controllers are online self repairing strategies which rely on three fundamental units, namely, an fault detection and isolation (FDI) unit, a reconfigurable controller and a control reconfiguration mechanism to achieve fault tolerance and nominal performance recovery. A schematic

block diagram representing the basic design structure of active FTC is shown in Figure 1.6. These three units have to work in a cooperative manner to guarantee system stability and optimal excellent output performance in the event of a failure. The illustration in Figure 1.7 shows the operational procedure of an active FTC scheme from an event-driven perspective sarting from the occurence of a fault/failure until it is recovered. The operation modes of the system are denoted by H (healthy/faultfree), F (faulty), D (fault diagnosed) and R (reconfigured). The terms E_f, E_d, E_{rc} and E_r denote the events resulting in the transition from one operational mode to the other. The explanation of an active FTC scheme based on FDI is as follows: The controller starts to operate in H (faultfree) operation mode. Due to occurrence of a fault/failure event E_f, the control system transits from H mode to F(faulty) mode. Thereafter, from the diagnosis event E_d and mode D, the reconfiguration event E_{rc} enables the system to attain a desirable reconfiguration mode (R) where it should be at least stable and should satisfy the design objectives as much as possible. Following the synthesis of the reconfigurable controller, a suitable reconfiguration strategy is designed to make the system transit to its (H) healthy mode through the recovery event E_r. The timing diagram in Figure 1.7(right) shows the temporal relation between the events incurred within this active FTC architecture. Although appearing to be apparently advantageous, it exhibits the following shortcomings: (a) The success of fault tolerance solely depends on the correctness of the FDI unit. However, guaranteeing robustness FDI results to modeling uncertainties is difficult and hence false alarms are often incurred. This eventually leads to incorrect reconfiguration thereby degrading performance and at times may destabilize the system; (b) In safety critical systems, where time is a crucial parameter, there is a time interval within which the active FTC system should detect the fault and subsequently resort to reconfiguration and FTC action. This time is known as the *critical reaction time*. Therefore, as shown in the timing diagram in Figure 1.7(right) if the time delay incurred in fault diagnosis E_d until reconfiguration E_{rc} is greater than the critical reaction time, the fault/failure is not recoverable and the system experiences instability which is undesirable; (c) Further, the switching action (reconfiguration) between optimal control solutions aligned to each type of faults/failures based on a reconfiguration criterion results in harmful switching transients. These transients contribute to sabotage the fault tolerant performance of the active FTC system. Further, closed loop instability can occur in case the system considered does not have a positive dwell time; (d) The reconfiguration procedure involves a complex decision making process which is computationally intense. The reconfiguration time adds to the computation time of the reconfiguration solution which increases with the growing dimension of the system. All these factors inhibit a successful implementation of an integrated FDI based FTC system.

Owing to practical implementation challenges of an integrated FDI based FTC design, an integrated fault estimation(FE) based FTC emerges to be a promising alternative. The basic architecture of an FE based FTC system is illustrated in the block diagram presented in Figure 1.8. Similar to the explanation of an FDI based FTC, to elucidate the working of an FE/FTC strategy, an event driven architecture of the same is depicted as a finite state automaton in Figure 1.9. Such a FTC design topology comprises of three operation modes and three events to allow transition between each of the modes. The operation modes are denoted by H (healthy/faultfree), F (faulty) and E(fault estimated) while the events are represented as E_f, E_e and E_r defining the occurrence of fault, fault estimation and failure recovery,

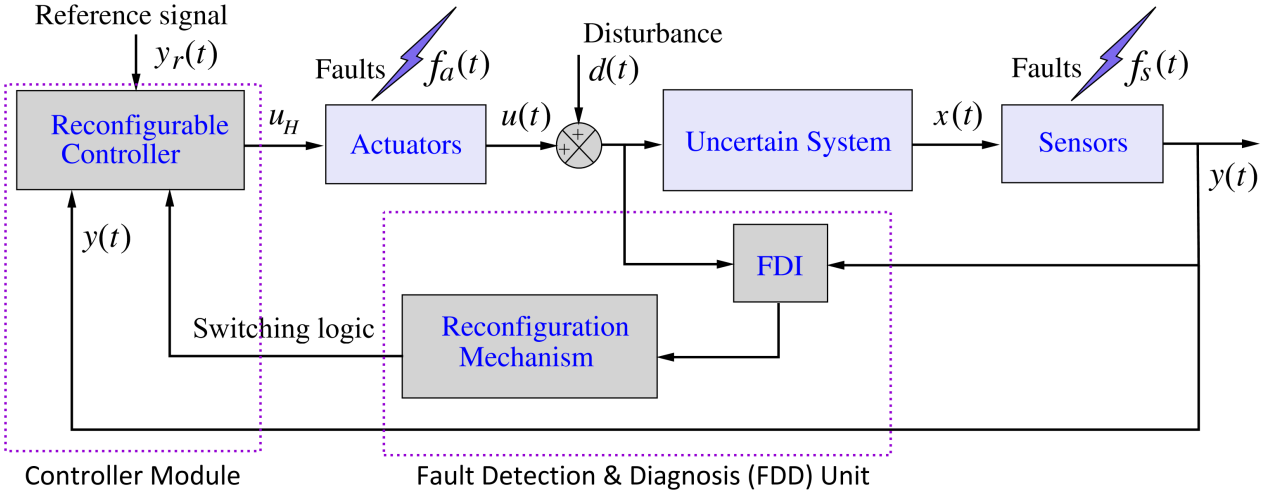

Figure 1.6: Schematic block diagrammatic representation of active fault tolerant control (AFTC) architecture.

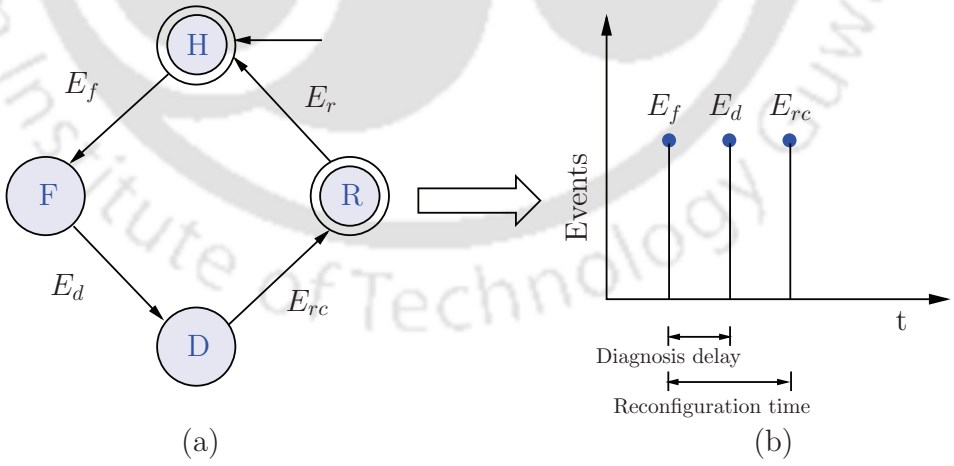

Figure 1.7: An event-driven interpretation and illustration of active fault tolerant control (AFTC) architecture [3].

respectively. This design framework does not rely on any switching or reconfiguration strategy and controller reconfiguration. It consists of a single controller wherein the fault estimation from the FE module can be retrofitted to achieve fault tolerance and improved output performance. Hence, the design is indeed computationally appealing with increased design freedom and has great potential for practical use in FTC applications. Besides, closed loop stability analysis of the integrated FE/FTC scheme is comparatively tractable. Apart from the aforementioned advantages, system performance recovery cannot be guaranteed if the critical reaction time is lesser than the time required for fault estimation. Several active FTC methodologies have been proposed in literature using model reference adaptive control [16, 17], self tuning [18], control allocation [19–21], multiple models [22–24], gain scheduling [25], linear-parameter varying approaches [26], model predictive control [27, 28], adaptive sliding mode control [4, 29, 30], adaptive backstepping control [5, 31, 32].

[33] On the other hand, passive FTC schemes are off-line strategies based on robust control ideas

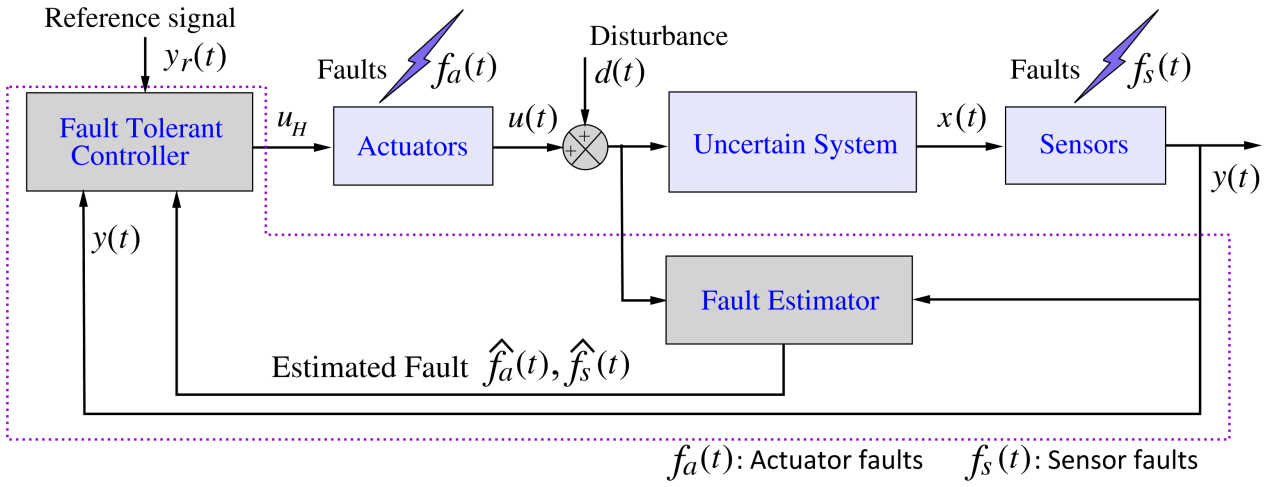

Figure 1.8: Structure and operational flow of active fault tolerant control (AFTC) scheme adopted in the thesis.

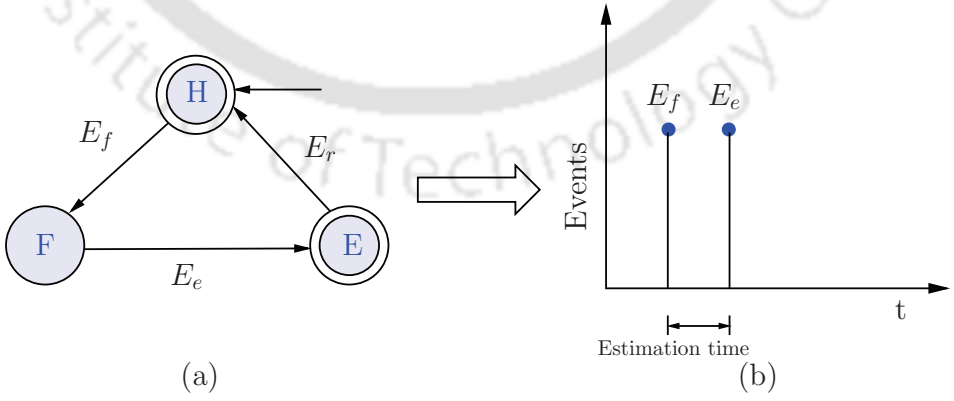

Figure 1.9: An event-driven interpretation and illustration of active fault tolerant control (AFTC) scheme adopted in the thesis.

and do not require any online scheme of fault detection and diagnosis. A single fixed controller is

designed by considering a predetermined set of faults and failures that can probably occur, during the design stage. The fundamental objective of passive FTC methods is to maintain stability of the system in the event of multiple failures without striving for optimal performance corresponding to any specific fault. Therefore, any passive FTC design is conservative in terms of performance and hence not suitable for performance critical systems. Passive FTC basically makes a trade-off between system performance and stability. Further, since most passive FTC designs are formulated as optimization problems, it is very likely to encounter ill posed problems wherein, the existence of solutions is not guaranteed. Hence, performance robustness of passive schemes are limited to a restrictive repertoire of anticipated actuator failures. Various passive FTC methodologies have been proposed in literature, for instance, $\mathcal{H}_\infty$ control [34–39], sliding mode control (SMC) [40–42] and integral sliding mode control (ISMC) [43, 44].

This thesis adopts an active FTC approach to guarantee robustness to large class of faults and failures, maintain optimal performance and therefore attempts to increase its reliability and applicability. In what follows, the active FTC methodologies pertaining to nonlinear uncertain systems are reviewed.

1.2 Literature Review

The basic premise of an actuator fault tolerant control (FTC) system is to achieve fault tolerance and maintain a stable post fault/failure output tracking by redesigning/reconfiguring the control input. Besides, in safety and mission critical systems, owing to a large variation in operating points, the FTC design should ensure increased stability margins and an expanded dynamically stable operating regime. In addition, robust output performance in presence of system uncertainties and external disturbances is another design objective in FTC. For example, in aircrafts, UAVs, spacecrafts, the wide variations in aerodynamic coefficients, Mach, altitude, dynamic pressure, angle of attack (AoA) and payload are inevitable. Payload variations may occur due to fuel consumption, release of missiles and carriage. Apart from actuator failures, these factors, if not compensated, also contribute to decreased flight envelope with degraded flying quality and may be a factor for potential instability as well. Thus, design of an actuator failure resilient control system which automatically adapts to the change in operating conditions and guarantees closed loop stability over its entire operating envelope, is indeed a *Herculean* task. Moreover, considering the system to be nonlinear, further adds a dimension to the difficulty of the foregoing FTC design. Aligned with the aforementioned control design problem, different FTC strategies based on passive and active philosophies have been proposed for both linear and nonlinear systems. However, none of the methodologies has been able enough to address the design objectives in a unified manner. Passive FTC methodologies and their shortcomings have been reviewed in the previous section. To be specific with the development of the thesis objectives within the ambit of active FTC; in the following, a brief survey of relevant literature on various active FTC methods for nonlinear dynamical systems is provided.

In the context of nonlinear systems, a number of active FTC schemes have been proposed, such as, control allocation [45–47], neural networks/fuzzy logic based control [48–52], multiple model adaptive

control [24, 53–56], reconfigurable control with learning [57], model predictive control [27, 28, 58], and SMC/ISMC with control signal redistribution [59–61]. These control strategies solely rely on an FDI based control design architecture (Figure 1.6) and hence are more likely to suffer from its inherent drawbacks. Besides, assumption of existence of system dwell time, switching mechanism, increasing computational burden and excessive input usage proportional to output performance; are some of the features exhibited by the above-mentioned active FTC design. In view of these foregoing issues, practical implementation of such schemes is difficult and hence, their applicability is largely restricted to a specific class of nonlinear systems only.

On the other hand, adaptive control methodologies are found to be intuitively appealing in the design of efficient active fault tolerant controllers for nonlinear systems. Among all active FTC schemes, adaptive controllers offer two major conceptual advantages. Firstly, only a single adaptive controller is needed to compensate actuator failures. Secondly and more importantly, these controllers do not require an explicit fault detection and diagnosis (FDD) module eluding the implementation issues of FDD and subsequent reconfiguration in real time. This motivated the design of active fault tolerant controllers for nonlinear systems subjected to complete actuator failures. With an aim to achieve total failure tolerance in uncertain nonlinear systems, direct adaptive control strategies have been proposed for multiple input single output and multiple input multiple output nonlinear uncertain systems using adaptive feedback linearization [62–65], adaptive backstepping control (ABSC) [5, 32, 54] and adaptive dynamic surface control (ADSC) methodologies [66, 67]. Although, adaptive feedback linearization [68] procedures of actuator FTC design reported in [62–65] are methodically attractive and ensure a faithful compensation of actuator failures, the design requires an accurate and complete knowledge of system dynamics. In real time, the presence of parametric uncertainties in system dynamics is obvious and their adverse effects on system performance is inevitable. However, apart from actuator failures, incorporating compensation of uncertain system parameters into feedback linearization design leads to a large dimension of parameter estimates. As a result, overparameterization prevails, culminating in high computational burden and the closed loop solutions may experience numerical instability. Whereas, ABSC [69] and ADSC [70] methodologies [5, 32, 54, 66, 67] address the issues of compensating coexisting system uncertainties along with actuator failures and ensure stable fault tolerant output tracking. However, an FTC based on ADSC does not offer asymptotic stability and its transient and steady state performances are dependent on the chosen time constants of intermediate low pass filters encountered in the course of design. Further, a robust adaptive output feedback controller designed using backstepping procedure was developed in [71, 72] to stabilize a nonlinear system affected by uncertain linearly parameterized actuator failures. Eventually, the results of [71, 72] were extended in [73] to compensate parameterizable as well as non-parameterizable actuator failures. The aforementioned methodologies are reported to yield promising results in the event of uncertain actuator failures in presence of state dependent matched and unmatched uncertainties only. Actuator failures in nonlinear systems with model uncertainties, have also been compensated using adaptive sliding mode control (ASMC) [4,30,74]. With the ASMC in action, the closed-loop system exhibits fast response and makes the system output invariant to actuator faults/failures. The design of ASMC is primarily based on the bound estimation of lumped uncertainty encompassing state dependent system uncertainties, external disturbances and

actuator failures. Moreover, the lumped uncertainty should necessarily satisfy the matched condition. Further, unlike [5, 32, 54, 62–67], the most severe drawback of ASMC is its discontinuity across sliding surfaces which leads to chattering and subsequent excitation of neglected high-frequency dynamics. To make ASMC strategies practically feasible for FTC, efforts to alleviate chattering using sigmoid function based smoothing and boundary layer approximation have been proposed. However, the tracking precision is severely compromised with control smoothing. Although transient performance is still acceptable, asymptotic stability is lost. In summary, translation of ASMC techniques from theory to practice suffers from a trade-off between output performance and control bandwidth. Inspired by prescribed performance bound (PPB) based adaptive controllers, using a variable transformation, ABSC is designed to compensate actuator failures [31]. Such a method ensures that the output trajectory never escapes the pre-defined exponential envelope and hence, offers a guaranteed transient and steady state performance. Recently, a bound estimation based backstepping control approach using tuning functions [75] is proposed for nonlinear systems with uncertainties, to compensate finite as well as possibly infinite (intermittent) actuator failures. However, the proposed adaptive control solution and its ultimate transient bounds explicitly depend on time. Besides, another direct adaptive backstepping controller is proposed using a fusion of tuning function approach, nonlinear damping and a projection based parameter adaptation [76]. The review of direct adaptive FTC approaches herein shows their design flexibility and potential to be retrofitted into an existing control loop in complex critical systems to ensure fault tolerance.

Indirect adaptive FTC strategies have also been proposed for nonlinear systems assuming the presence of decoupling between the estimator-controller pair. Herein, the unknown parameters are estimated first and then the control signal comprising of functions of these unknown parameters is calculated using these estimates. These controllers are characterized by a poor oscillatory transient behaviour during their learning phase. Their output performance is directly correlated to the accuracy and fastness of parameter estimation. Moreover, overparameterization is absent. Very few works have been reported in adaptive FTC literature so far on deriving an indirect adaptive compensator for linearly parametrized nonlinear systems affected by actuator failures. It is our belief that such a cold attitude towards adopting an indirect adaptive approach for FTC design is ascribed to its poor output transient performance. Within a certainty equivalence (CE) based indirect adaptive control structure, introduction of large parameteric uncertainties due to actuator failures may result in high output overshoots which may trespass the safety limits of the system. Further, to ensure modularity between controller and the estimator, the nonlinear system should be necessarily globally Lipschitz. Further, the closed loop stability analysis and proof of asymptotic stability is not straightforward. Although substantial number of these controllers contribute to FTC literature on linear systems, solving the failure compensation design problem using similar strategies for nonlinear systems has rarely been considered by researchers. Lately, the problem of actuator failure compensation in nonlinear MIMO systems with linearly parameterizable uncertainties, is attempted using a multiple model adaptive control with switching and tuning [24]. Assuming modularity of controller-identifier pair, the proposed backstepping controller follows an indirect adaptive control design philosophy and the transient performance is improved by the use of multiple identification models in conjunction with PPB control. The

first seminal work on adaptive compensation of infinite actuator failures in nonlinear uncertain systems is based on a modular adaptive backstepping control [6]. Except for switching multiple model based adaptive control (MMAC) approaches to FTC, active FTC methods based on indirect adaptive control are based on an fault estimator (FE) based FTC architecture driven by three events and a single controller, without any reconfiguration/switching strategy between a bank of controllers/estimators (see Figures 1.8-1.9). With reference to FE/FTC design topology, some of the major active FTC techniques for parametrization free system uncertainties and actuator failures are discussed below. Based on the fault estimate from a nonlinear unknown input observer, an adaptive sliding mode fault tolerant controller is designed [77] for Lipschitz nonlinear systems. The observer and the control gains are obtained from solutions of an $\mathcal{H}_\infty$ optimization problem to minimize the bidirectional robustness interactions between the controller and the observer. In [78], differential geometric tools are utilized to design an FE integrated FTC scheme. A neural network observer based backstepping controller is proposed in [79] to estimate the failure pattern and magnitude for multivariable nonlinear systems.

Active disturbance rejection controllers (ADRC) using nonlinear disturbance observers (NDOB) have recently earned great popularity due to excellent estimation and output transient performance. They are indeed applicable to a large class of nonlinear systems owing to their capability to handle a large class of nonlinear and linear uncertainties and disturbances. Herein, the design procedure first assumes that the system is bounded under the action of a nominal control law. Thereafter, a disturbance observer is designed which estimates the temporal profile of the lumped uncertainty comprising of state dependent system uncertainties, external disturbances and parameterization free actuator failure induced perturbations. Some of the recent works on ADRC based active actuator failure compensators can be found in [80–83] and the references therein. These disturbance observers (DOB) utilize the information from the disturbance prediction error and/or the state prediction error to estimate the distubance. Subsequently, the estimated disturbance is fed back to the nominal controller for subsequent cancellations. ADRC startegies can be categorically placed under an indirect adaptive FTC design scheme for nonlinear systems affected by uncertainties and actuator failures which are not necessarily parameterized. Further, adaptive neural FTC based on disturbance observers with composite adaptation have also been proposed recently in [84–88]. These estimator based control algorithms follow an integrated design approach where the disturbance observer utilizes the disturbance prediction error for its estimation. Neural networks with online learning are used to estimate unknown state dependent nonlinearities and disturbance estimation error for subsequent compensation. The online learning herein is based on the information from either the tracking error, the state prediction error or both. Although through proper tuning of controller gains, output transient performance is preserved at large; asymptotic stability of the output is lost. Globally uniformly ultimately bounded closed loop trajectories are not guaranteed. Finally, it is observed that ADRC startegies at large are also easy to be integrated to any nominal existing control loop without changing the control structure. Hence, with the retrofit property, DOB based adaptive control qualifies to be a potential choice for FTC applications in real time.

1.3 Research Motivation

It is evident from the literature review in the preceding section that the area of active FTC design, has been extensively researched upon. Fruitful results within the active framework have been reported as regards control of nonlinear uncertain systems to compensate unknown actuator faults and failures. However, there are still a number of challenging problems which are yet to be addressed. Some of the open theoretical issues drawing our attention are discussed below.

- Control design using a direct adaptive backstepping technique is known to offer a promising output transient performance through trajectory initialization and initial increase of the virtual control gains. The same ideology translates analogously to transient performance improvement in adaptive sliding mode control (ASMC) through increment in the sliding surface coefficients. However, actuator faults and failures are unknown in time, and hence, trajectory initialization is not so feasible. Further, it has been mathematically proved in [69] that an increase in the virtual control gains may improve the start-up transients while such a measure will increase the value of the tracking error at the instant of actuator fault/failure. In consequence, the post-fault transient performance is degraded and the output experiences cumulatively high overshoots with each instance of failures, which is undesirable. Addressing this design issue, an adaptive backstepping control based failure compensation is proposed in [31] guaranteeing prescribed output transient performance in the event of complete actuator failures and PLOE faults. However, since the design philosophy relies on the ideology of high gain adaptive controllers using performance funnels, the control energy, in this case, varies inversely with the prescribed error bounds. Although being theoretically promising, owing to design and physical constraints in practical systems, rewarding application of such controllers to crucial FTC problems is doubtful and may not be promising. Therefore, it would be interesting to develop new backstepping based adaptive control strategies wherein the output transients in failure cases can be improved independent of the choice of virtual control gains and trajectory initialization without any significant increase in the control effort.

- From the perspective of active approaches, most of the active FTC schemes rely on fault detection and isolation (FDI) unit for controller reconfiguration in the event of uncertain eventualities of actuator faults and failures. However, the performance and correctness of such residual based FDI schemes are largely affected by system modeling errors, parametric uncertainties and external disturbances, which may often lead to false alarms. Thus, FDI strategies strictly require an optimal determination of residual signals and a selection of detection thresholds so as to successfully differentiate between an actuator failure and an uncertainty. Thereafter, a reconfiguration strategy based on the information from FDI unit is to be formulated to conform the system with the failure induced changes and maintain stability. Nevertheless, an integrated FDI based FTC design is very difficult to realize and implement [89, 90], owing to a discrete event structure of reconfiguration, time delay in FDI and optimality factors regarding modeling imperfections and external disturbances during the detection phase. In summary, the integrated FDI/FTC design problem essentially reduces to a hard optimization problem and finding a solution satisfying the

design constraints is indeed difficult, if not impossible [9, 10]. Although being apparently advantageous, the aforementioned design issues along with implementation complexity inhibits its translation to practice, especially in systems, where safety is an overriding concern. Moreover, the design is far more difficult for general nonlinear dynamical systems. Most of the research on FTC conducted till date, is on model based FDI without an FTC function or on fault tolerant control (FTC) design without the requirement of FDI module for computational simplicity.

As an alternative, an integrated fault estimator (FE) based active FTC architecture can be resorted to. Such a design can be realized in either ways by adopting a direct or an indirect adaptive control philosophy. However, FE/FTC design based on the philosophy of direct adaptive control is believed to exhibit high and aggressive control effort since its learning is directly dependent on the output [91]. To economize the control requirement, FE/FTC synthesis on the basis of indirect adaptive control methodology seems to be a suitable choice. Nevertheless, to the best of our knowledge, an FE/FTC design for nonlinear systems guaranteeing global/semiglobal output stability is not trivial. The bidirectional robustness interaction between the controller and the estimator in nonlinear systems results in the breakdown of the *separation principle*. With the loss of design modularity, the stability margins of the closed loop system are substantially decreased and the trajectories will experience a finite escape time. The active FTC algorithms proposed so far in this context largely assume systems with Lipschitz nonlinearities. Moreover, integrated FE/FTC design has been proposed for general nonlinear dynamics using neural networks and NDOB based control approaches [80–88] only guarantee semi global uniformly ultimately bounded (UUB) closed loop trajectories. The assumptions are neither rigorously analyzed nor are well justified from a theoretical design perspective. Estimation accuracy is unguaranteed. Herein, disturbance observers are used to estimate time dependent unknown signals and neural networks/fuzzy observers with a composite weight learning law are used to estimate unknown system nonlinearities and failure induced uncertainties. Owing to the usage of both disturbance observers and neural network/fuzzy estimators, these control methodologies are computationally intensive and also exhibit high control usage. Bidirectional uncertainty interactions now exist between the neural network estimator, disturbance observer and the controller which adversely effect estimation performance thereby affecting the output. However, such robustness interaction issues have not at all been investigated in the above works and other pertinent literature. On the same lines, rigorous mathematical analysis proving the modularity of the triple along with insights on estimation correctness of the coexisting neural network estimator and the disturbance observer, is challenging and remains open. On the other front, development of globally stable FE/FTC for nonlinear systems using only disturbance observers which can successfully compensate state dependent nonlinearities, actuator faults/failures(not necessarily parameterized) and external disturbances, will be an interesting and impactful contribution. In this direction, when an ADRC strategy using an NDOB [92, 93], is adopted into the FE/FTC framework, a bidirectional robustness interaction between the control system and the estimator creeps in. To remove these interactions, the existing ADRC methods based on NDOB, presume that the time derivative of the unknown lumped disturbance is zero which is restrictive. Therefore, apart from

FE/FTC, with the perspective of proposing a general methodology for control of nonlinear systems guarantees of global output asymptotic stability and relaxation of the foregoing assumption will definitely attract applicability to a wide range of systems.

As an addition to the preceding problem, the following issue is certainly generic to any integrated FE based FTC intended for nonlinear uncertain systems. Within such an active FTC architecture, the time available for fault estimation and subsequent recovery plays a crucial role in deciding the existence of stable adaptive solutions. Considering practical situations such as in mission critical systems, where the time window in which the faulty system is stabilizable is very short [8,94]. As a matter of fact, if the actuator fault/failure is not accommodated within a specific finite time, the inputs and outputs will encroach their safety limits and eventually lead to mission failures, which is undesirable. Therefore, finite time system performance recovery from the effects of actuator failure is necessary for complex safety systems, where time is a crucial parameter. To the best of our knowledge, the simultaneous treatment of all these factors within an FE/FTC scheme for nonlinear systems has not yet been explicitly considered.

- Most of the existing results on adaptive compensation of actuator failures assume the occurrence of a finite number of faults and failures, meaning that a single actuator fails only once and does not recover thereafter. In other words, this implies that there exists a finite time after which the failure topology never changes and the system is not subjected to any further faults/failures. These existing results are derived from the closed-loop stability analysis using Lyapunov functions involving unknown fault/failure parameter estimation errors. Hence, the Lyapunov functions will experience jumps at the time instances when failures occur. Moreover, boundedness of the Lyapunov function or rather that of the output tracking error, at all instances of failures can only be guaranteed if and only if the jumps are limited to be finite. This validates the presumption on the applicability of direct adaptive control strategies to the problem of FTC which states the existence of an upper bound on the total number of actuator failures and restricts any change in the failure pattern after a finite span of time. However, in practice, the actuator failure topology may change intermittently without violating the relative degree condition. More generally, this implies that an actuator can infinitely switch between its faulty and healthy states provided that there is a finite time lapse between its two states of operation. In contrast to finite number of actuator failures, an adaptive compensation of possibly infinite number of unknown actuator failures using direct adaptive control methodologies [5,32,54,66,67,95] fail to ensure boundedness of the overall closed loop system dynamics. Very few results on adaptive compensation of infinite actuator failures in nonlinear systems have been reported in literature [6], [75]. The method proposed in [6] assures convergence of the tracking error in the mean square sense. However, no explicit calculation of $\mathcal{L}_2$ or $\mathcal{L}_\infty$ on the tracking errors is derived which could hint on the tuning of parameters to achieve better performance. Different from [6], the bound estimation based approach in [75] suffers from a very high control requirement. No rigorous analysis is reported and the upper bound on the tracking error is not time invariant. Further, no insights on transient and input performance improvements are provided and the work only focuses on achieving boundedness of closed loop trajectories. Improvement of output transient performance

and its consequent quantification have always been an exciting problem in adaptive control of nonlinear systems irrespective of the parametrization of uncertainties. Efforts are needed towards proposal of new indirect adaptive control strategies for FTC applications in nonlinear systems which yield an improvement in output transient and steady state performance without substantially increasing the input usage. Besides, the problems of finite time estimation based adaptive compensation of infinite actuator failures in nonlinear systems characterizing linearly parametrizable/unparametrizable uncertainties and actuator failures, are not yet addressed in FTC literature and still remain open.

Compared to direct adaptive FTC strategies, one of the major advantages of the estimator/identifier based fault compensation design is that it uses only as much control effort as needed [96]. Hence, following development of a direct ARFTC to improve the transient performance without increasing the control usage, we adopt an indirect adaptive framework for FTC is adopted all throughout to have a judicious usage of control. Thereafter, one can come up with various ideas to improve the output transient performance without significantly effecting the control input requirement. An example of such an advancement are the ABSC strategies proposed in this thesis, as they restrain from increasing the virtual control gains to render improved transients and resort to the thought for alternatives which contribute to the input performance as well.

Motivated by the above-mentioned open research issues, the contributions of this thesis are enumerated and briefly discussed in the following section.

1.4 Contributions of the Thesis

The contributions made under each chapter in the thesis are highlighted below.

(i) **Adaptive robust fault tolerant controller(ARFTC) design for nonlinear uncertain systems with actuator failures**

An FTC algorithm is proposed using a direct adaptive backstepping methodology augmented with second order sliding modes for nonlinear uncertain systems. The motivation behind were the drawbacks of ABSC and ASMC which are listed as: (1) Transient performance can be improved using trajectory initialization. However, faults occur abruptly and are uncertain in time, pattern and magnitude and hence trajectory initialization is not feasible in such problems. (2) Alternatively, the virtual control gains/sliding surface parameters can be increased to achieve a good start up transient performance at the cost of high control usage. Nevertheless, this will result in a cumulative increment in the $\mathcal{L}_2$ and $\mathcal{L}_\infty$ output transient performance bounds with subsequent occurrences of actuator faults/failures leading to degraded post fault transients with high overshoots, which is undesirable. The proposed control algorithm circumvents the aforementioned issues (1) and (2) while instilling robustness to modeling imperfections, exogeneous disturbances and failure induced parametric and nonparametric uncertainties. Two modified adaptive laws are formulated, to approximate the bounds of uncertainties due to modeling and to estimate the fault-induced parametric uncertainties. The proposed scheme ensures robustness

towards linearly parameterized mismatched uncertainties, in addition to parametric and nonparametric matched perturbations. Improved post fault transient performance is achieved without increasing the virtual control gains and the proposed method characterizes no significant increase in the control energy spent.

(ii) **Adaptive multiple model fault tolerant control (AMMFTC) of nonlinear uncertain systems with actuator failures**

A novel actuator failure compensation scheme is proposed for affine nonlinear uncertain systems subject to actuator faults/failures unknown in time, magnitude and pattern. The proposed control methodology utilizes a modular backstepping control augmented with multiple estimation models to estimate failure induced parametric uncertainties and unknown system parameters. The output transient performance at start up and post-failure instances, is improved on account of the two layer adaptation which enhances the convergence speed and accuracy of parameter estimates. Further, the same methodology is extended to the design of adaptive control design to compensate possibly infinite actuator failures. The proposed fault tolerant control (FTC) method yields a faithful accommodation of uncertain finite as well as infinite actuator failures while ensuring satisfactory output transient and steady state performances. Further, compared to existing multiple model based adaptive FTC design for nonlinear systems, the proposed methodology circumvents the issues of stability due to switching between different models and utilizes a minimum number of estimation models for parameter estimation without sacrificing the output performance and thereby reduces the computational burden. Using the concepts from stability analysis in random nonlinear impulsive systems, the $\mathcal{L}_\infty$ and $\mathcal{L}_2$ bounds on tracking error $\forall t \in [0, \infty)$ are derived in the case of infinite actuator failures. The improvement of output transient performance in the proposed control scheme, is theoretically proved. Further, the proposed methodology is extended for a challenging adaptive FTC design intended for MIMO nonlinear systems with actuator failures, system uncertainties and strong coupling. Experimental investigations on the attitude control of a 2DOF helicopter system (twin rotor MIMO system) justify the efficacy and practical suitability of the proposed control algorithm.

(iii) **Finite time adaptation based compensation (FTAC) of actuator failures in nonlinear uncertain systems**

A new finite time parameter estimator is proposed to further improve the output transient and steady state performance in adaptive control. The parameter estimation algorithm achieves a fast and exact estimation of unknown system and actuator failure induced parameters. While the parameter estimates are robust to external disturbances and their convergence do not require the PE condition, such an estimation methodology is also applicable for unstable systems. The finite time parameter estimator based backstepping controller is proposed for adaptive compensation of infinite actuator failures in nonlinear uncertain systems. Rigorous stability analysis is provided which proves the global stability of closed loop trajectories and boundedness of the tracking error in the absolute sense $\forall t \in [0, \infty)$. An FTC scheme using the proposed FTAC methodology is also designed for a strongly coupled MIMO nonlinear system affected by finite actuator failures. Finite time perfromance recovery in the event of actuator failure adds to the improvement of output

transients and asymptotic convergence of the output to the origin is guaranteed. The proposed FTAC method achieves global stability results. Experimental investigations are conducted on the twin rotor MIMO system (TRMS) to control its attitude using the proposed controller. The results obtained justify the superiority of the adaptive control technique and substantiate its potential of translation to practical engineering applications.

(iv) **Parametrization-free finite time estimation based adaptive compensation of actuator failures in nonlinear uncertain systems**
A new adaptive control scheme is proposed for nonlinear systems affected by infinite failures with inherent modeling uncertainties and matched/mismatched perturbations. The actuator failures need not be linearly parametrized and can be function of system states as well. The proposed controller appropriately utilizes direct adaptive backstepping approach till the $(n-1)$ coordinate to guarantee an appreciable transient performance and inducts an adaptive finite time estimator based control to counteract the lumped uncertainty at the last coordinate (comprising of system uncertainties and perturbations induced due to finite/infinite actuator failures). The attributes of the proposed control methodology are boundedness of all closed loop trajectories; finite time output transient and steady state performance recovery in the event of failures; asymptotic exact output tracking; finite time exact estimation of system and failure induced uncertainties; and potential to compensate infinite actuator failures. A rigorous stability analysis of the closed loop system using the proposed adaptive estimator integrated backstepping controller is conducted to prove stability of the overall controlled system for all time $t \in [0, \infty)$.

The implicit details of the contributions mentioned above are provided clearly in each of the chapters.

1.5 Thesis Organization

The thesis contains 6 chapters which are organized as follows.

- **Chapter 2:** In this chapter, a new direct adaptive robust controller is designed using a backstepping technique augmented with an adaptive second order sliding mode control strategy to compensate actuator failures in nonlinear systems with norm bounded modeling uncertainties. Output transient performance improvement is achieved through finite time convergence of the error variable obtained at the last coordinate of backstepping. Different from other ARC strategies, it separately estimates the fault parameters and the upper bound on modeling uncertainties. Compared to ASMC, the most celebrated ARC method, input usage is decreased by the use of a second order sliding mode controller; without compromising the robustness and asymptotic stability of output tracking both in nominal and post failure scenarios.

- **Chapter 3:** A multiple model based backstepping controller with two layer adaptation is proposed in the context of FTC of nonlinear uncertain systems. The problem of adaptive compensation of infinite actuator failures is discussed followed by proofs which show the inability of direct adaptive control strategies and the method proposed in Chapter 2, to ensure stable solutions in

such scenarios.Thereafter, AMMFTC strategy is proposed to compensate intermittently occurring actuator failures apart from system uncertainties followed by transient performance analysis. The quantification of transient performance is provided to show the performance superiority over single model adaptive control. Following the results, the proposed AMMFTC is applied to nonlinear coupled MIMO systems to compensate finite actuator failures and ensure enhancement of transient and steady state output performance.

- **Chapter 4:** A new finite time adaptation based controller (FTAC) is designed to ensure finite time output nominal performance recovery and promising transient behavior both at start-up and post failure instances. The proposed FTAC is then extended for applications to compensate infinite actuator failures followed by a rigorous stability proof to arrive at the boundedness of tracking error in the absolute sense. The theoretical results are justified through simulation results. Thereafter, the proposed adaptive controller with finite time adaptation is adopted in the design of FTC for a MIMO coupled nonlinear system. An involved analysis followed by simulation and experimental results demonstrate the proficiency of the control algorithm.

- **Chapter 5:** This chapter proposes a novel finite time converging adaptive disturbance observer based backstepping controller for nonlinear uncertain systems. The system uncertainties and those induced due to actuator failures do not require any kind of parametrization for DOB based estimation and backstepping control. Rigorous stability analysis proves the closed loop signal boundedness and global asymptotic stability of the tracking error in the event of infinite and finite actuator failures for all time. Fast and exact disturbance estimation at steady state are indeed very important to the improvement of output transient and steady state performance. The bidirectional interactions between control-DOB estimator pair is reduced to a unidirectional interaction from the observer to the controller and hence the separation principle is satisfied which offers more design freedom into FE design.

- **Chapter 6:** In this section, the conclusions from all the proposed adaptive FTC methodologies are discussed. These inferences are followed by several useful recommendations for future research in adaptive FTC and applications.

2

Adaptive Robust Fault Tolerant Controller (ARFTC) Design for Nonlinear Uncertain Systems with Actuator Failures

Contents

2.1 Introduction 22
2.2 Adaptive Robust Fault Tolerant Controller (ARFTC) 23
2.3 Summary 45

2.1 Introduction

The objective of this chapter is to propose a fault tolerant controller ensuring enhanced post fault transient performance in conjunction with the issue of reaching a trade-off between improved transients and control effort respectively. Robustness towards modeling uncertainties is another design requirement of the proposed controller. The essence of exploring the complimentary relation between two different control methodologies is the main driving force behind the synthesis of the proposed control algorithm. The main contribution lies in the proposed design of an adaptive second order sliding mode controller embedded in a backstepping framework for FTC design of uncertain nonlinear systems. The designed FTC scheme has been specifically aimed for potential applications in aircraft control. Further, a systematic and rigorous closed loop stability analysis of the proposed control scheme has been conducted which suggests an improvement in post fault transient performance using the proposed design methodology. The benefits of both backstepping [69] and sliding mode [97] controllers are encashed in the proposed approach. Moreover, to the best of the authors' knowledge, there are no results available pertaining to the defined objective of this work in accommodating actuator faults and failures in addition to system uncertainties. The proposed methodology offers numerous advantages.

The proposed control strategy is applicable to both linear and nonlinear systems affected by matched or mismatched uncertainties which may not be necessarily linearly parameterized. In addition, failure induced mismatched perturbations and exogenous disturbances are also tackled faithfully by the proposed controller. Unlike the backstepping based methodologies proposed in [5, 32, 54, 65, 98, 99], the proposed control strategy neither requires trajectory initialization nor resorts to an increment in the virtual control gains for the improvement in post fault tracking error performance. The contribution of this study relative to SMC based fault tolerant controllers [19, 20, 44, 61] is that the proposed design totally eradicates intruding matched and mismatched uncertainties (rather than minimizing) due to actuator failures without any control reallocation scheme requiring an explicit detection and isolation of such uncertain eventualities. In addition, robustness towards modeling uncertainties is also guaranteed. The proposed scheme attains the desired control objective for uncertain nonlinear systems yielding improved post fault transients with a considerably lower control energy requirement compared to the schemes based on control allocation and adaptive sliding mode control [4, 29, 30]. Moreover, the proposed control input is smooth with no chattering and therefore expected to satisfy physical constraints more effectively in comparison to the existing SMC based FTC strategies for aircraft systems, making it suitable for practical applications. It is to be noted that while using an ASMC based FTC strategy, an increase in the values of the sliding surface coefficient may improve the initial transient response of the system. However, in consequence, the post fault output transient performance degrades resulting in high overshoots which is strictly undesirable in safety critical systems. Further, no detailed investigations regarding ASMC based control of nonlinear systems in the face of actuator failures have been reported in literature. Moreover, no rigorous analysis of the transient performance is available in literature to give an insight as to how the post fault transients can be improved. In contrast to multiple model based adaptive approaches to FTC [22, 23, 100, 101], the proposed control methodology does not require any knowledge about the bounds of the failure nor does it depend on any switching logic for controller reconfiguration in the event of unanticipated actuator failures. The

proposed control scheme utilizes two adaptive laws to distinguish between actuator faults/failures and uncertainties/disturbances. In practice, sliding motion is never ideal and hence the adaptive estimates here can be unbounded. Hence, in the proposed controller, the adaptive laws are formulated suitably to ensure boundedness of adaptation and thereby prevent overestimation. Compared to traditional backstepping based methods and dynamic surface control (DSC) based techniques [66], the proposed control scheme reduces the computational complexity without compromising on the asymptotic stability of the output error dynamics. Moreover, in the proposed control technique, the discontinuous sign function is made to act on the time derivative of the control input resulting in a continuous control signal and hence chattering is totally eliminated.
The proposed scheme is applied to pitch control problem of a nonlinear longitudinal model of a large transport aircraft (Boeing 747-100/200), potentially affected by parametric uncertainties, sudden actuator faults, float and lock-in-place failures. Simulation studies confirm that the proposed controller yields satisfactory tracking performance and fast nominal performance recovery under fault and failures, thereby outperforming the basic approaches based on backstepping and sliding mode ideologies individually.

The chapter is organized as follows. Firstly the dynamics of the considered nonlinear systems with actuator failures are described in Section 2.2.1. Thereafter, the objective of the proposed actuator FTC with the inherent assumptions is formulated in Section 2.2.2. The proposed design procedure and stability analysis of the proposed controller are explained in Sections 2.2.3-2.2.4. In Section 2.2.5, simulation studies are performed by applying the proposed controller to longitudinal control of a Boeing 747-100/200 aircraft. Finally, the solution proposed for the FTC problem and its design attributes are summarized in Section 2.2.6.

2.2 Adaptive Robust Fault Tolerant Controller (ARFTC)

2.2.1 System Dynamics with Actuator Failures

Let us consider a class of multi-input (m) single output affine nonlinear system as follows,

$$\sum_p : \begin{cases} \dot{x} = f(x) + \sum_{j=1}^{m} b_j g_j(x) u_j \\ y = h(x) \end{cases} \tag{2.1}$$

where $x := [x_1, \cdots, x_n]^T \in \mathcal{D} \subseteq \mathbb{R}^n$ is the state vector representing the states of the system, $y \in \mathbb{R}$ is the output and $u_j \in \mathbb{R}$ for $j = 1, 2, \cdots, m$ denotes the j^{th} input to the system which may be faulty during operation due to malfunctioning of the actuators. The functions $f(x),\ g_j(x) : \mathcal{D} \longrightarrow \mathbb{R}^n$ for $j = 1, 2, \cdots, m$ are assumed to be smooth nonlinear functions, that is $f(x),\ g_j(x) \in \mathfrak{C}^{\infty}(\mathbb{R}^n)$. The output function $h(x) \in \mathbb{R}$ is assumed to be a known smooth nonlinear function and b_j for $j = 1, 2, \cdots, m$ denotes the unknown control coefficients of the plant given by $\sum_p$ in (2.1).
Assuming that the actuators can encounter uncertain catastrophic events identified as partial loss of effectiveness (PLOE) and total failures, the actuator input-output relationship can be mathematically

modeled as,

$$u_j = \begin{cases} K_j u_{Hj} + \bar{u}_{Fj}, & \forall\ t \geq t_j \\ u_{Hj}, & \forall\ t < t_j \end{cases} \quad j = 1, 2, \cdots, m \tag{2.2}$$

where, $K_j \in [0,\ 1)$ defines the factor signifying the degree of PLOE incurred by the j^{th} actuator. The actuator model considered here characterizes stuck failures and the magnitude at which the j^{th} actuator is stuck is denoted by $\bar{u}_{Fj}$. Furthermore, the term u_{Hj} represents the controller output fed as input to the j^{th} actuator. The actuator faults and failures are ascertained to be unknown and uncertain in time, pattern and magnitude and hence the sudden failure of an actuator at an unknown time instant t_j unfolds the following three failure cases, (a) $K_j \neq 0$ and $\bar{u}_{Fj} = 0$, (b) $K_j = 0$ and $\bar{u}_{Fj} \neq 0$, (c) $K_j = 0$ and $\bar{u}_{Fj} = 0$. In contemplating the problem statement concerning actuator failure scenarios in class of systems described by (2.1), the following assumptions are necessary,

Assumption 2.1. *The system $\sum_p$ in (2.1) has well defined relative degree $\wp$, $1 \leq \wp \leq n$ with respect to the output function $y = h(x)$ [102], corresponding to each actuation functions $g_j : \mathcal{D} \longrightarrow \mathbb{R}^n$, such that,*

$$\begin{aligned} L_{g_j} L_f^r h(x) &= 0 \quad \forall r = \{0, 1, \cdots, \wp - 2\} \\ L_{g_j} L_f^{\wp-1} h(x) &\neq 0 \quad \forall j = \{1, 2, \cdots, m\} \end{aligned} \tag{2.3}$$

where, $L_f h(x) = (\partial h(x)/\partial x)^T f(x)$ denotes the Lie derivative of $h(x)$ along the flow of the vector field $f(x)$. This ensures that the output $y = h(x)$ is associated with at least one control input u_j. In order to meet the controller design requirements, the system $\sum_p$ is considered as transformable into a strict feedback form with relative degree $1 \leq \wp \leq n$.

Assumption 2.2. *The system under consideration is assumed to achieve the desired control objective in the event of at most $(m-1)$ actuator total failures. This assumption assures controllability of the system $\sum_p$ in (2.1) under such eventualities and thereafter guarantees the existence of stable solutions for (2.1), considering a suitably designed failure compensation scheme [32].*

Therefore, in accordance with the *Assumption* 2.2, there exists a diffeomorphism $[\xi, \eta]^T = \mathscr{T}(x) = [\mathscr{T}_c(x), \mathscr{T}_z(x)]^T$, $\xi \in \mathbb{R}^\wp$ and $\eta \in \mathbb{R}^\ell$, $\wp + \ell = n$, defined as,

$$\xi = \mathscr{T}_c(x) = \begin{bmatrix} h(x) \\ L_f h(x) \\ \vdots \\ L_f^{\wp-1} h(x) \end{bmatrix} = \begin{bmatrix} \xi_1 \\ \xi_2 \\ \vdots \\ \xi_\wp \end{bmatrix}, \quad \text{and} \quad \eta = \mathscr{T}_z(x) = \begin{bmatrix} \mathscr{T}_{\wp+1}(x) \\ \mathscr{T}_{\wp+2}(x) \\ \vdots \\ \mathscr{T}_n(x) \end{bmatrix} = \begin{bmatrix} \eta_1 \\ \eta_2 \\ \vdots \\ \eta_{n-\wp} \end{bmatrix}$$

to decompose the system (2.1), dividing the actuator failure model in (2.2), into a controllable part $\sum_c$ and its uncontrollable counterpart $\sum_z$ as follows,

$$\sum\nolimits_c : \begin{cases} \dot{\xi}_1 = \xi_2 \\ \dot{\xi}_i = \xi_{i+1}, \qquad i = 2, 3, \cdots, \wp - 1 \\ \dot{\xi}_\wp = a(\xi, \eta) + \sum\limits_{j=1}^{m} b_j \beta_j(\xi, \eta)(K_j u_{Hj} + \bar{u}_{Fj}) \\ y = \xi_1 \end{cases} \tag{2.4}$$

$$\sum\nolimits_z : \qquad \dot{\eta} = \varrho(\xi, \eta) \tag{2.5}$$

In (2.5), $\sum_z$ describes the internal dynamics of the overall system $\sum_p$ driven by ξ as its input. Suppose, in (2.5), it is assumed that $\xi = 0$, which implies $\sum_z$ is affected by a zero input and suffices to describe the zero dynamics of the system (2.1). The reference trajectory to be tracked by the system is the output of the reference state variable model with relative degree $\wp$ as given below in (2.6).

$$\sum\nolimits_d : \begin{cases} \dot{\xi}_d = A_d \xi_d + B_d y_d \\ y_r = C_d \xi_d \end{cases} \tag{2.6}$$

where, $A_d = \begin{bmatrix} 0 & 1 & 0 & \cdots & 0 & 0 \\ 0 & 0 & 1 & \cdots & 0 & 0 \\ \vdots & \ddots & \cdots & \cdots & \ddots & \vdots \\ 0 & 0 & \cdots & 0 & 0 & 1 \\ -a_1 & -a_2 & \cdots & -a_{\wp-2} & -a_{\wp-1} & -a_\wp \end{bmatrix} \in \mathbb{R}^{\wp \times \wp}, \quad B_d = \begin{bmatrix} 0 \\ 0 \\ \vdots \\ 0 \\ 1 \end{bmatrix} \in \mathbb{R}^{\wp \times 1}$

$C_d = [1 \;\; 0 \cdots \;\; \cdots \;\; 0 \;\; 0] \in \mathbb{R}^{1 \times \wp}$

The constants $a_1,\ a_2, \ldots, a_\wp$ are coefficients of the Hurwitz polynomial $P(s) = |sI - A_d| \in \mathbb{R}[s]$ and the rest can be concluded by stating the following assumption.

Assumption 2.3. *The reference signal y_r and its successive time derivatives upto the $\wp^{th}$ order are known, bounded, piecewise continuous and hence belong to a compact set.*

Assumption 2.4. *The zero dynamics of the system given by $\sum_z$ is input-to-state stable (ISS) with $\xi = 0$ as its input. The control coefficients b_j in (2.4) are unknown in magnitude and moreover, the terms $\beta_j(\xi, \eta) \neq 0$ for $j = 1,\ 2, \cdots, m$.*

Now, let us define a set $\mathscr{B} = \{j_1,\ j_2, \cdots, j_m\}$ and two subsets of the set $\mathscr{B}$ as $\mathscr{B}_{tot_F} = \{j_1,\ j_2, \cdots, j_k\}$, for $k = 1,\ 2, \cdots, (m-1)$ and $\mathscr{B}_{par_H} = \mathscr{B} \backslash \mathscr{B}_{tot_F}$. The subset $\mathscr{B}_{par_H}$ contains the indices corresponding to the partially effective or total healthy actuators. On the contrary, the other subset $\mathscr{B}_{tot_F}$ consists of elements characterizing the totally failed actuators. Finally, the controllable part (2.4) of system (2.1) can be re-casted as,

$$\begin{cases} \dot{\xi}_i = \xi_{i+1}, \qquad i = 1, 2, \cdots, \wp - 1 \\ \dot{\xi}_\wp = a_0(\xi, \eta) + \Delta a(\xi, \eta) + \sum\limits_{j_k \in \mathscr{B}_{tot_F}}^{m} b_j \beta_j(\xi, \eta) \bar{u}_{Fj} + \sum\limits_{j \in \mathscr{B}_{par_H}}^{m} b_j \beta_j(\xi, \eta) K_j u_{Hj} \end{cases} \tag{2.7}$$

where, $a_0(\xi, \eta)$ denotes the nominal part of $a(\xi, \eta)$ whereas $\Delta a(\xi, \eta)$ characterizes the modeling imperfections or imprecisions in the latter.

2.2.2 Problem Statement

By virtue of the above mentioned assumptions, the problem concerns a control design for the nonlinear system (2.1), in the event of unanticipated actuator faults and failures, in addition to mod-

eling uncertainties, guaranteeing global asymptotic stability of the closed loop tracking error dynamics. Furthermore, the improvement of transient and steady state performance of the tracking error $e(t) = y(t) - y_r(t)$, at the onset of faults and failures in terms of maximum overshoot, convergence time and steady state error has to be ascertained. The failure compensation design assumes no apriori knowledge of the active actuators in action on the system (2.1) under the total loss of atmost $(m-1)$ of them.

Assumption 2.5. *The uncertainties in system dynamics given by $\Delta a(\xi, \eta)$ and that incurred due to fault and failures in the actuators, along with their time derivatives are assumed to be bounded with unknown upper bounds i.e. $|\Delta a(\xi, \eta)| \leq a^*$, which holds similar for the faults and failures also and will be defined later.*

2.2.3 Proposed Actuator Failure Compensator Design

The control objective is attained by designing a controller based on the systematic backstepping procedure [69] in conjunction with an adaptive second order sliding mode control (SOSMC) strategy [97], embedded in an integral sliding mode concept (ISMC) [103]. This yields a transformed system, described by $(\wp-1)$ differential equations augmented with an extended uncertain second order nonlinear dynamics. This extended system is firstly stabilized in finite time with the adaptive SOSMC in action and subsequently being acted upon by the backstepping controller, the remaining $(\wp-1)^{th}$ order tracking error dynamics pursue an asymptotically stable behavior in the global sense. The benefits provided by the proposed methodology will be evident in the sequel.

The control signal u_{Hj} is designed following the procedure proposed in [104] with modifications, since the authors have considered only the case of partial loss of actuators. Moreover, no insight has been provided, pertaining to the tuning of controller parameters for transient performance enhancement and their subsequent effects on the overall stability of the system. The crucial issue of transient improvements have been rigourously dealt with, in this section, in addition to the problem of controller design. The generation of u_{Hj} initiates, firstly by defining $\wp$ error variables as,

$$z_1 = \xi_1 - y_r \tag{2.8}$$

$$z_i = \xi_i - \alpha_{i-1} - y_r^{(i-1)} \qquad i = 2, \cdots, \wp \tag{2.9}$$

Now, these tracking error variables $z_1, z_2, \cdots, z_\wp$ are stabilized by α_i serving as the smooth virtual control inputs determined at the i^{th} step as,

$$\alpha_i = -z_{i-1} - c_i z_i + \sum_{k=1}^{i-1} \frac{\partial \alpha_{i-1}}{\partial \xi_k} \xi_{k+1} + \sum_{k=0}^{i-1} \frac{\partial \alpha_{i-1}}{\partial y_r^{(k)}} y_r^{(k+1)} \tag{2.10}$$

where, the subscript $i = 2, \cdots, \wp - 1$. Finally, retaining the $(\wp-1)$ steps of backstepping, the $\wp^{th}$ step of the proposed scheme is different from the conventional backstepping procedure and is elaborated

below. For $i = \wp$, the $\wp^{th}$ error variable dynamics is given by,

$$\dot{z}_\wp = \dot{\xi}_\wp - \dot{\alpha}_{\wp-1} - y_r^{(\wp)} = a_0(\xi,\eta) + \Delta a(\xi,\eta) + \sum_{j_k \in \mathscr{B}_{tot_F}}^{m} b_j \beta_j(\xi,\eta)\bar{u}_{Fj} + \sum_{j \in \mathscr{B}_{par_H}}^{m} b_j \beta_j(\xi,\eta) K_j u_{Hj} - \left(\sum_{k=1}^{\wp-1} \frac{\partial \alpha_{\wp-1}}{\partial \xi_k} \xi_{k+1} + \sum_{k=0}^{\wp-1} \frac{\partial \alpha_{\wp-1}}{\partial y_r^{(k)}} y_r^{(k+1)} \right) - y_r^{(\wp)} \tag{2.11}$$

The uncertainties introduced into the system at the onset of faults and failures of j actuators in (2.11), for the sake of simplicity, can be expressed as,

$$\Delta_1 = \sum_{j_k \in \mathscr{B}_{tot_F}}^{m} b_j \beta_j(\xi,\eta)\bar{u}_{Fj}, \qquad \Delta_2 = \sum_{j \in \mathscr{B}_{par_H}}^{m} b_j K_j$$

Furthermore,

$$\ddot{z}_\wp = \dot{a}_0(\xi,\eta) - \left(\sum_{k=1}^{\wp-1} \frac{\partial}{\partial \xi_k} \left(\sum_{k=1}^{\wp-1} \frac{\partial \alpha_{\wp-1}}{\partial \xi_k} \xi_{k+1} \right) \xi_{k+1} + \sum_{k=0}^{\wp-1} \frac{\partial}{\partial y_r^{(k)}} \left(\sum_{k=0}^{\wp-1} \frac{\partial \alpha_{\wp-1}}{\partial y_r^{(k)}} y_r^{(k+1)} \right) y_r^{(k+1)} \right) - y_r^{(\wp)} + \frac{d}{dt}(\Delta a(\xi,\eta)) + \frac{d}{dt}(\Delta_1) + \Delta_2 \underbrace{\frac{d}{dt}(\beta_j(\xi,\eta)u_{Hj})}_{v} \tag{2.12}$$

$$\ddot{z}_\wp = \dot{a}_0(\xi,\eta) - \left(\sum_{k=1}^{\wp-1} \frac{\partial}{\partial \xi_k} \left(\sum_{k=1}^{\wp-1} \frac{\partial \alpha_{\wp-1}}{\partial \xi_k} \xi_{k+1} \right) \xi_{k+1} + \sum_{k=0}^{\wp-1} \frac{\partial}{\partial y_r^{(k)}} \left(\sum_{k=0}^{\wp-1} \frac{\partial \alpha_{\wp-1}}{\partial y_r^{(k)}} y_r^{(k+1)} \right) y_r^{(k+1)} \right) - y_r^{(\wp)} + \frac{d}{dt}(\Delta a(\xi,\eta)) + \frac{d}{dt}(\Delta_1) + \underbrace{\Delta_2}_{\zeta(\cdot)} v \tag{2.13}$$

where, all the terms in (2.13) except the last term, are collectively represented by the function $\varphi(\cdot)$. Thereafter, in order to accommodate the second order sliding mode strategy within the backstepping procedure, the second time derivative of $z_\wp$ in (2.13) is used to yield an uncertain extended second order system in $s = z_\wp$ and $\dot{s} = \dot{z}_\wp$ as,

$$\ddot{s} = \varphi(\cdot) + \zeta(\cdot)v \tag{2.14}$$

where, the sliding variable and its first time derivative are designated by the terms $s(\xi,t)$ and $\dot{s}(\xi,t)$ respectively. Here the control objective is to ensure $s(\xi,t) = 0$ and $\dot{s}(\xi,t) = 0$ in finite time to guarantee the existence of a second order sliding mode. Hence, before proceeding any further, the definition of SOSMC followed by some remarks are given below.

Definition 2.1. *Let us consider the second order nonlinear dynamics in (2.14) closed by a discontinuous feedback v. Assuming that s and $\dot{s}$ are continuous functions and the set $\mathcal{S}^2 = \{\xi \mid s(\xi,t) = \dot{s}(\xi,t) = 0\}$, called a second order sliding set, is nonempty and is locally an integral set in the Filippov sense, the motion on $\mathcal{S}^2$ is called second order sliding mode with respect to the sliding variable $s(\xi,t)$ [97].*

Remark 2.1. *The solutions of (2.14) are understood in the Filippov sense [105] and the control law v is Lebesgue measurable.*

Remark 2.2. *The uncertain functions $\varphi(\cdot)$ and $\zeta(\cdot)$ in (2.14) are known to be bounded with unknown upper bounds.*

Therefore, the second order sliding mode control of (2.14) with respect to sliding variable s reduces to the finite time stabilization of the perturbed double integrator dynamics given by,

$$\begin{aligned} \dot{s}_1 &= s_2 \\ \dot{s}_2 &= \varphi(\cdot) + \zeta(\cdot)v = \underbrace{\varphi(\cdot) + (\zeta(\cdot) - 1)v}_{\psi(\cdot)} + v \end{aligned} \tag{2.15}$$

with $[s_1 \;\; s_2]^T = [s \;\; \dot{s}]^T$. The following lemma gives an affirmation as to how the dependent variables involved in a double integrator dynamics driven by an external input v, can be steered to the origin in finite time.

Lemma 2.1. *Let us consider an n-integrator system described as:*

$$\begin{aligned} \dot{\xi}_i &= \xi_{i+1} \\ \dot{\xi}_n &= v_{nom} \qquad i = 1, \cdots, n-1 \end{aligned} \tag{2.16}$$

Let $\beta_1, \beta_2, ..., \beta_n > 0$ be such that the polynomial $\phi(\lambda) = \lambda^n + \sum_{k=1}^{n} \beta_k \lambda^{k-1}$ is Hurwitz. For the system (2.16), $\exists\ \varrho \in (0,1)$ such that for every $\vartheta_k \in (1-\varrho, 1)$, $k = 1, ..., n$, the origin is a globally stable equilibrium in finite time under the feedback, $v_{nom}(x) = -\sum_{k=1}^{n} \beta_k sign(\xi_k)|\xi_k|^{\vartheta_k}$, where $\vartheta_1, ...\vartheta_n$ satisfy $\vartheta_{k-1} = \frac{\vartheta_k \vartheta_{k+1}}{2\vartheta_{k+1} - \vartheta_k}$, $k = 2, ..., n$ and $\vartheta_{n+1} = 1$.

Proof.
Please refer to the work in [106]. □

Attaining finite time stability of (2.15) requires the design of an auxiliary integral sliding manifold σ with an embedded nominal control law v_{nom} and thereafter a discontinuous control law to ensure finite time stability and invariance of (2.15) to perturbations [107] collectively represented by $\psi(\cdot)$. Let the integral sliding manifold be defined as,

$$\sigma := s_2(t) - s_2(t_0) - \int_{t_0}^{t} v_{nom} dt' \tag{2.17}$$

Now under the action of a discontinuous control law, sliding mode is established on the sliding surface defined by the set $\mathcal{S}_{\int} = \{\ [s_1,\ s_2]^T \in \mathbb{R}^2 \mid \sigma = 0\}$ for $t \geq 0$ and hence the reaching phase is totally eliminated. Therefore, an invariance towards matched uncertainties is achieved from the very beginning and robustness is guaranteed over the entire state space. Finally, the synthesis of the overall control law v is based on Gao's reaching law approach [108] and subsequent analysis of the motion equations

on the sliding surface $\sigma = 0$ using the equivalent control method proposed in [103]. Hereinafter, the constant plus proportional reaching law is considered as, $\dot{\sigma} = -\varepsilon\sigma - \tau sign(\sigma)$. Where ε, τ are design constants which characterize the rate at which σ converges to zero.

Now, since the only knowledge available about the uncertainties is their property of boundedness and that too is unknown, the reaching law will be incompetent in establishing a sliding mode along $\sigma = 0$ in the event of unknown actuator failures. Therefore, it is quite relevant to append an adaptive counterpart to the control law v, in order to ensure that the constraint $\sigma = 0 \ \forall \ t \geq 0$ is fulfilled. Moreover, the partitioning of modeling uncertainties from the impact of faults and failures will be clearly visible in the course of design. Consequently, from (2.13) and (2.17), the first time derivative of σ can be derived as,

$$\begin{aligned}\dot{\sigma} = \dot{a}_0(\xi,\eta) - \left(\sum_{k=1}^{\wp-1}\frac{\partial}{\partial\xi_k}\left(\sum_{k=1}^{\wp-1}\frac{\partial\alpha_{\wp-1}}{\partial\xi_k}\xi_{k+1}\right)\xi_{k+1} + \sum_{k=0}^{\wp-1}\frac{\partial}{\partial y_r^{(k)}}\left(\sum_{k=0}^{\wp-1}\frac{\partial\alpha_{\wp-1}}{\partial y_r^{(k)}}y_r^{(k+1)}\right)y_r^{(k+1)}\right) \\ - y_r^{(\wp)} + \frac{d}{dt}(\Delta a(\xi,\eta)) + \sum_{j\in\mathscr{B}_{tot_F}}^{m} b_j\bar{u}_{Fj}\beta_j(\xi,\eta) + \sum_{j\in\mathscr{B}_{par_H}}^{m} b_jK_jv - v_{nom} \\ = \left(\sum_{j\in\mathscr{B}_{par_H}}^{m}|b_j|K_j\right)\theta^{*^T}\Phi(\xi) + \sum_{j\in\mathscr{B}_{par_H}}^{m} b_jK_jv + \frac{d}{dt}(\Delta a(\xi,\eta)) \end{aligned} \tag{2.18}$$

where, $\theta^* := [\theta_1^* \quad \theta_2^*]^T$ and $\theta_2^* := [\theta_{2,1}^* \quad \theta_{2,2}^* \cdots \ \theta_{2,m-1}^*]^T$. These unknown parameters are now defined below as,

$$\theta_1^* := \frac{1}{\sum\limits_{j\in\mathscr{B}_{par_H}}^{m}|b_j|K_j}, \qquad \theta_{2,j}^* := \frac{\{b_j\bar{u}_{Fj}\}_{j\in\mathscr{B}_{tot_F}}}{\sum\limits_{j\in\mathscr{B}_{par_H}}^{m}|b_j|K_j}$$

Furthermore, the regressor matrix $\Phi(\xi) := [\Phi_1(\xi) \ \Phi_2(\xi)]^T$ is known and whose components are defined as follows.

$$\begin{aligned}\Phi_1(\xi) &= \dot{a}_0(\xi,\eta) - \left(\sum_{k=1}^{\wp-1}\frac{\partial}{\partial\xi_k}\left(\sum_{k=1}^{\wp-1}\frac{\partial\alpha_{\wp-1}}{\partial\xi_k}\xi_{k+1}\right)\xi_{k+1} + \sum_{k=0}^{\wp-1}\frac{\partial}{\partial y_r^{(k)}}\left(\sum_{k=0}^{\wp-1}\frac{\partial\alpha_{\wp-1}}{\partial y_r^{(k)}}y_r^{(k+1)}\right)y_r^{(k+1)}\right) - y_r^{(\wp)} \\ &\quad - v_{nom} \\ \Phi_2(\xi) &= [\beta_1(\xi,\eta) \quad \beta_2(\xi,\eta) \ \ldots \ \beta_{m-1}(\xi,\eta)]^T\end{aligned}$$

Further, (2.18) clearly reveals the separation between modeling uncertainties and the fault induced perturbations. Accordingly, this demands two adaptive laws to counteract the effect of uncertainties due to faults and that of modeling in a decoupled fashion. Thereafter, analyzing the dynamics along the sliding surface $\sigma = 0$, the total control law v satisfying the μ-reachability condition is derived as,

$$v = (-\hat{\theta}^T\Phi(\xi) - \varepsilon\sigma - \tau sgn(\sigma) - \hat{\Gamma}sgn(\sigma))sgn(b_j) \tag{2.19}$$

The first and the third part on the right hand side of (2.19) characterize the adaptive part of v. In

consequence, the actual control law for the system (2.1) is straightaway found to be,

$$u_j = u_{Hj} = sgn(b_j)\frac{1}{\beta_j(\xi,\eta)}\int_{t_0}^{t}(-\hat{\theta}^T\Phi(x) - \varepsilon\sigma - \tau sgn(\sigma) - \hat{\Gamma}sgn(\sigma))dt' \tag{2.20}$$

for $j = 1, 2, ..., m$. Moreover, $\hat{\theta}$ and $\hat{\Gamma}$ are the estimates of θ^* and Γ^* respectively. Γ^* signifies the upper bound of system uncertainties, that is $\left|\frac{d\Delta a}{dt}\right| \leq \Gamma^*$ and θ^* denotes the failure induced adversities on the plant. Moreover, the adaptive parameter update laws are given as,

$$\dot{\hat{\theta}} = -P\epsilon_2\hat{\theta} + P\Phi\sigma \tag{2.21}$$

$$\dot{\hat{\Gamma}} = -\gamma\epsilon_1\hat{\Gamma} + \gamma|\sigma| \tag{2.22}$$

The matrix P is user defined and is a solution of the Lyapunov equation, $A^TP + PA = -Q$. Here, A is a Hurwitz stable matrix chosen by the designer and the matrix Q is positive definite. The finite time stabilizing nominal control law v_{nom} is formulated from Lemma 2.1 as,

$$v_{nom} = -\beta_1 sign(s_1) \mid s_1 \mid^{\vartheta_1} -\beta_2 sign(\dot{s}_1) \mid \dot{s}_1 \mid^{\vartheta_2} \tag{2.23}$$

The terms $\gamma,\ \epsilon_1,\ \epsilon_2,\ \beta_1,\ \beta_2\ >\ 0$ and $c_i\ >\ 0$ for $i\ =\ 1,\ 2, \cdots,\ \wp - 1$ are positive constants and depend on the designer's choice. The block diagrammatic representation of the proposed control scheme is shown in Figure 2.1.

2.2.4 Stability Analysis

The closed loop stability of the overall system in the event of finite number of actuator failures is investigated.

Theorem 2.1. *Considering the system (2.1) potentially affected by possible actuator faults and failures (2.2) in addition to modeling uncertainties, assuming the zero dynamics to be input to state stable (ISS) [109], the controller given by (2.20) with the update laws (2.21)-(2.22), under the assumptions (2.1)-(2.5), guarantees asymptotic output tracking, meaning* $\lim_{t\to\infty}(y(t) - y_r(t)) = 0$ *and closed loop trajectories are bounded and finally evolve in the vicinity of the origin defined by* $\mathscr{S}^*$ *as,*

$$\mathscr{S}^* := \left\{ Z \in \mathbb{R}^{\wp+1} \mid \|Z\|_2 \leq \left(\left(\frac{1}{\mathscr{C}_{min}\nu} + 1 \right) \left(\frac{2\lambda\beta_2}{\beta_1(2-\vartheta)} \right)^{2-\vartheta} + \left(\frac{|\dot{\sigma}_{\max}|}{\beta_2} \right)^{\frac{2}{\vartheta}} \right)^{1/2} \right\}$$

where, Z is the $(\wp+1)^{th}$ order tracking error vector and $\mathscr{C}_{min}, \nu, \lambda, \beta_1, \beta_2, \vartheta$ are user defined parameters.

Proof.

The aim is to prove the asymptotic stability of the error variables $z_1, z_2, z_3, \cdots, z_\wp$ defined in (2.8). The proof will be established in a systematic way adopting a stepwise procedure as follows,

Regarding the stabilization of z_1, the first Lyapunov function is taken as, $V_1 = \frac{1}{2}z_1^2$. The time derivative

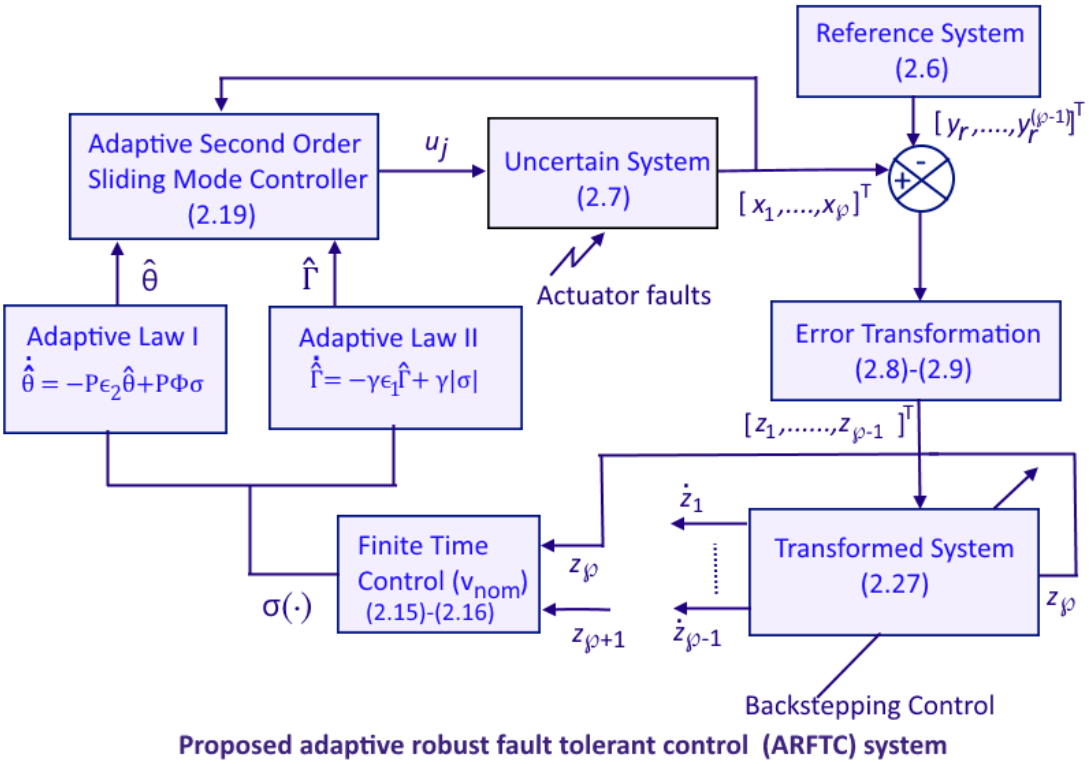

Figure 2.1: Schematic representation the proposed fault tolerant control scheme

of V_1 is given by,

$$\dot{V}_1 = z_1\dot{z}_1 = z_1(\xi_2 - \dot{y}_r) = z_1(z_2 + \alpha_1 + \dot{y}_r - \dot{y}_r)$$

Using (2.10) yields,

$$\dot{V}_1 = z_1 z_2 + z_1(-c_1 z_1) = -c_1 z_1^2 + z_1 z_2 = -\kappa_1 V_1 + z_1 z_2 \tag{2.24}$$

where, $\kappa_1 = 2c_1,\ c_1 > 0$. Clearly, if $z_2 = 0$, then $\dot{V}_1 = -\kappa_1 V_1$ and hence z_1 is guaranteed to converge to zero asymptotically.

Now, for $i = 2, \cdots, \wp-1$, concerning the stability of each error variable $z_2, ..., z_i, ...z_{\wp-1}$, the Lyapunov function is defined as, $V_i = \frac{1}{2}z_i^2$. Taking the time derivative of V_i and using equality (2.10) results in,

$$\dot{V}_i = z_i\dot{z}_i = z_i\left(z_{i+1} + \alpha_i + y_d^{(i)} - \sum_{k=1}^{i-1}\frac{\partial\alpha_{i-1}}{\partial\xi_k}\xi_{k+1} - \sum_{k=0}^{i-1}\frac{\partial\alpha_{i-1}}{\partial y_r^{(k)}}y_r^{(k+1)} - y_r^{(i)}\right)$$

$$= z_i(z_{i+1} - c_i z_i - z_{i-1}) = z_i z_{i+1} - c_i z_i^2 - z_{i-1}z_i \tag{2.25}$$

$$\dot{V}_i = -\kappa_i V_i + z_i z_{i+1} - z_{i-1}z_i, \quad \text{for} \quad \kappa_i = 2c_i,\ c_i > 0 \tag{2.26}$$

Now,

$$\begin{bmatrix} \dot{z}_1 \\ \dot{z}_2 \\ \dot{z}_3 \\ \vdots \\ \dot{z}_{\wp-1} \end{bmatrix} = \underbrace{\begin{bmatrix} -c_1 & 0 & 0 & \cdots & 0 \\ 0 & -c_2 & 1 & \cdots & 0 \\ 0 & -1 & -c_3 & \cdots & 0 \\ \vdots & \vdots & \vdots & \ddots & \vdots \\ 0 & 0 & \cdots & -1 & -c_{\wp-1} \end{bmatrix}}_{\mathcal{A}_z} \begin{bmatrix} z_1 \\ z_2 \\ z_3 \\ \vdots \\ z_{\wp-1} \end{bmatrix} + \underbrace{\begin{bmatrix} 0 \\ 0 \\ 0 \\ \vdots \\ 1 \end{bmatrix}}_{\mathcal{B}_z} z_\wp \tag{2.27}$$

Here (2.27) describes the $(\wp-1)^{th}$ order tracking error dynamics controlled by the $\wp^{th}$ error variable. It is obvious that, $z_\wp = 0$ guarantees an asymptotically stable behavior for the solutions of the dynamics in (2.27) since the matrix $\mathcal{A}_z$ is Hurwitz. Alternatively, stability can also be proved through the choice of a total Lyapunov function given by $V = \sum_{i=1}^{\wp-1} V_i$ and subsequently proving its first time derivative to be negative as,

$$\dot{V} = \sum_{i=1}^{\wp-1} \dot{V}_i = \sum_{i=1}^{\wp-1} c_i z_i^2 + z_{\wp-1} z_\wp = -\sum_{i=1}^{\wp-1} \kappa_i V_i + z_{\wp-1} z_\wp = -\min\{\kappa_i\}_{i=1}^{\wp-1} \sum_{i=1}^{\wp-1} V_i + z_{\wp-1} z_\wp \tag{2.28}$$

Considering $z_\wp = 0$, the negative definiteness of (2.28) is proved. Hence, it can be stated that finite time stability of $z_\wp$ ensures asymptotic stability of the $(\wp-1)^{th}$ order error dynamics. Now, the finite time stability of $z_\wp$ and other extended state variables explored in the accomplishment of the proposed design are proved. This objective was achieved through the design of an integral sliding manifold (2.17), which when proved to be attractive and converge to zero in finite time, ensured the convergence of the state $z_\wp$ or conversely the pair $\{s_1, \dot{s}_1\}$, to the origin in finite time. To study the stability properties of the auxiliary sliding surface $\sigma = 0$ and parameter convergence, a Lyapunov function candidate is chosen as,

$$V_\sigma = \frac{1}{2}\sigma^2 + \frac{1}{\gamma} \sum_{j \in \mathscr{B}_{par_H}}^{m} \frac{|b_j| K_j}{2} \tilde{\Gamma}^2 + \sum_{j \in \mathscr{B}_{par_H}}^{m} \frac{|b_j| K_j}{2} \tilde{\theta}^T P^{-1} \tilde{\theta} \tag{2.29}$$

where, $\tilde{\Gamma} := \hat{\Gamma} - \Gamma^*$ and $\tilde{\theta} := \hat{\theta} - \theta^*$. Additionally let us define $\Gamma^* := \theta_1^* \omega^* \geq \theta_1^* |\frac{d}{dt}(\Delta a(\xi, \eta))|$. Now $\dot{V}_\sigma$ is obtained as,

$$\dot{V}_\sigma = \sigma\dot{\sigma} + \sum_{j \in \mathscr{B}_{par_H}}^{m} \frac{|b_j| K_j}{\gamma} \tilde{\Gamma}\dot{\hat{\Gamma}} + \sum_{j \in \mathscr{B}_{par_H}}^{m} |b_j| K_j \tilde{\theta} P^{-1} \dot{\tilde{\theta}} = \sigma\dot{\sigma} + \frac{1}{\theta_1^* \gamma} \tilde{\Gamma}\dot{\hat{\Gamma}} + \frac{1}{\theta_1^*} \tilde{\theta} P^{-1} \dot{\tilde{\theta}} \tag{2.30}$$

$$= \sigma \left(\frac{\theta^{*T} \Phi}{\theta_1^*} + \sum_{j \in \mathscr{B}_{par_H}}^{m} b_j K_j v + \frac{\theta_1^*}{\theta_1^*} \frac{d}{dt}(\Delta a(\xi, \eta)) \right) + \frac{1}{\theta_1^* \gamma} \tilde{\Gamma}\dot{\hat{\Gamma}} + \frac{1}{\theta_1^*} \tilde{\theta} P^{-1} \dot{\tilde{\theta}} \tag{2.31}$$

Substituting the control law v from (2.19) yields,

$$\dot{V}_\sigma = \sigma\left(\frac{\theta^{*T}\Phi}{\theta_1^*} + \sum_{j\in\mathscr{B}_{par_H}}^{m} b_j K_j\left((-\hat{\theta}^T\Phi(\xi) - \varepsilon\sigma - \tau sgn(\sigma) - \hat{\Gamma}sgn(\sigma))sgn(b_j)\right) + \frac{\theta_1^*}{\theta_1^*}\frac{d}{dt}(\Delta a(\xi,\eta))\right) + \frac{1}{\theta_1^*\gamma}\tilde{\Gamma}\dot{\hat{\Gamma}} + \frac{1}{\theta_1^*}\tilde{\theta}P^{-1}\dot{\hat{\theta}} \tag{2.32}$$

$$= \sigma\left(\frac{\theta^{*T}\Phi}{\theta_1^*} + \frac{1}{\theta_1^*}\left(-\hat{\theta}^T\Phi(\xi) - \varepsilon\sigma - \tau sgn(\sigma) - \hat{\Gamma}sgn(\sigma)\right) + \frac{\theta_1^*}{\theta_1^*}\frac{d}{dt}(\Delta a(\xi,\eta)\right) + \frac{1}{\theta_1^*\gamma}\tilde{\Gamma}\dot{\hat{\Gamma}} + \frac{1}{\theta_1^*}\tilde{\theta}P^{-1}\dot{\hat{\theta}}$$

Utilizing the adaptive laws from (2.21) and (2.22),

$$\begin{aligned}
\dot{V}_\sigma &= -\sigma\frac{1}{\theta_1^*}(\hat{\theta}^T - \theta^{*T})\Phi - \sigma\frac{1}{\theta_1^*}\hat{\Gamma}sgn(\sigma) - \frac{1}{\theta_1^*}\varepsilon\sigma^2 - \sigma\frac{1}{\theta_1^*}\tau sgn(\sigma) + \frac{1}{\theta_1^*}\Gamma^*\sigma + \frac{1}{\theta_1^*}\tilde{\Gamma}|\sigma| - \frac{1}{\theta_1^*}\epsilon_1\tilde{\Gamma}\hat{\Gamma} \\
&\quad + \frac{1}{\theta_1^*}\tilde{\theta}^T P^{-1}P\Phi\sigma - \frac{1}{\theta_1^*}\tilde{\theta}^T P^{-1}P\epsilon_2\hat{\theta} \\
&\le -\frac{1}{\theta_1^*}\varepsilon\sigma^2 - \frac{1}{\theta_1^*}\tau\sigma sgn(\sigma) - \frac{1}{\theta_1^*}\epsilon_1\hat{\Gamma}^2 + \frac{1}{\theta_1^*}\epsilon_1\Gamma^*\hat{\Gamma} - \frac{1}{\theta_1^*}\epsilon_2\hat{\theta}^T\hat{\theta} + \frac{1}{\theta_1^*}\epsilon_2\theta^{*T}\hat{\theta} \\
&\le -\frac{1}{\theta_1^*}\varepsilon\sigma^2 - \frac{1}{\theta_1^*}\tau\sigma - \frac{1}{\theta_1^*}\epsilon_1\left(\hat{\Gamma} - \frac{1}{2}\Gamma^*\right)^2 - \frac{1}{\theta_1^*}\epsilon_2(\left(\hat{\theta}_1 - \frac{1}{2}\theta_1^*\right)^2 + \left(\hat{\theta}_{2,1} - \frac{1}{2}\theta_{2,1}^*\right)^2 + \left(\hat{\theta}_{2,2} - \frac{1}{2}\theta_{2,2}^*\right)^2 \\
&\quad + \cdots + \left(\hat{\theta}_{2,(m-p)} - \frac{1}{2}\theta_{2,(m-p)}^*\right)^2) + \frac{1}{4}\frac{1}{\theta_1^*}\epsilon_1\Gamma^{*2} + \frac{1}{4}\frac{1}{\theta_1^*}\epsilon_2\left(\theta_1^{*2} + {\theta_{2,1}^*}^2 + {\theta_{2,2}^*}^2 + \cdots + {\theta_{2,(m-p)}^*}^2\right) \\
&\le -\frac{1}{\theta_1^*}\varepsilon\sigma^2 - \frac{1}{\theta_1^*}\tau|\sigma| - \frac{1}{\theta_1^*}\epsilon_1\left(\hat{\Gamma} - \frac{1}{2}\Gamma^*\right)^2 - \frac{1}{\theta_1^*}\epsilon_2\|\hat{\theta} - \frac{1}{2}\theta^*\|^2 + \frac{1}{4}\frac{1}{\theta_1^*}\epsilon_1\Gamma^{*2} + \frac{1}{4}\frac{1}{\theta_1^*}\epsilon_2\|\theta^*\|^2 \\
&\le -\frac{1}{\theta_1^*}\varepsilon\sigma^2 - \frac{1}{\theta_1^*}\tau|\sigma| + \frac{1}{4}\frac{1}{\theta_1^*}(\epsilon_1\Gamma^{*2} + \epsilon_2\|\theta^*\|^2) \\
&\le -\frac{1}{\theta_1^*}\varepsilon\sigma^2 - \frac{1}{\theta_1^*}\tau|\sigma| + \frac{1}{4}\left(\epsilon_1\frac{\Gamma^{*2}}{\theta_1^*} + \epsilon_2\left(\theta_1^* + \frac{{\theta_{2,1}^*}^2}{\theta_1^*} + \frac{{\theta_{2,2}^*}^2}{\theta_1^*} + \frac{{\theta_{2,3}^*}^2}{\theta_1^*} + \cdots + \frac{{\theta_{m-p}^*}^2}{\theta_1^*}\right)\right) \\
&\le -\frac{1}{\theta_1^*}\varepsilon\sigma^2 - \frac{1}{\theta_1^*}\tau|\sigma| + \frac{1}{4\theta_1^*}\underbrace{\left(\epsilon_1\Gamma^{*2} + \epsilon_2(\theta_1^{*2} + {\theta_{2,1}^*}^2 + {\theta_{2,2}^*}^2 + {\theta_{2,3}^*}^2 + \cdots + {\theta_{m-p}^*}^2)\right)}_{\bar{\theta}^*}
\end{aligned} \tag{2.33}$$

Now, negative definiteness of $\dot{V}_\sigma$ in (2.33) can only be attained on satisfying the conditions,

$$\|\sigma\| > \sqrt{\frac{\bar{\theta}^*}{4\varepsilon}} \quad \text{and} \quad |\sigma| > \frac{\bar{\theta}^*}{4\tau} \tag{2.34}$$

Hence, it can be inferred that the trajectories of the closed loop system are upper bounded in the region defined as a compact subset and a positively invariant set in $\mathbb{R}$ given as,

$$\mathscr{V} := \left\{\sigma : \mathbb{R}^2 \times \mathbb{R}_+ \longrightarrow \mathbb{R}, z_1, z_2, \ldots, z_{\wp+1} \in \mathbb{R} \;\middle|\; int(\dot{V}_\sigma = 0),\ \left(\|\sigma\|^2 \le \frac{\bar{\theta}^*}{4\varepsilon}\right) \cap \left(|\sigma| \le \frac{\bar{\theta}^*}{4\tau}\right)\right\} \tag{2.35}$$

Application of the control therefore first drives the pair $\{s_1,\ \dot{s}_1\}$ into this small set around the origin defined in (2.35) and then it attains a finite time stable behavior to the origin. The analysis of the

closed loop signals is commenced after the sliding mode is procured. As per *Lemma* 2.1, when real sliding mode is attained, i.e. $|\sigma| < |\sigma_{\max}|$, finite time convergence of s_1 and $\dot{s}_1$ is guaranteed. The term $\sigma_{\max}$ designates a small boundary region around the sliding surface $\sigma = 0$ defined as $\mathscr{V}$ in (2.35). This fact is also evident from (2.15) and (2.17) leading to the dynamics,

$$\begin{aligned} \dot{s}_1 &= s_2 \\ \dot{s}_2 &= -\beta_1 sgn(s_1)|s_1|^{\frac{2}{2-\vartheta}} - \beta_2 sgn(s_2)|s_2|^{\vartheta} + |\dot{\sigma}_{\max}| \end{aligned} \tag{2.36}$$

Assuming, $\|\Phi\|$ to be upper bounded, the term, $|\dot{\sigma}_{\max}|$, is the maximum value belonging to the residing set of $\dot{\sigma}$, given as,

$$\dot{\sigma} \in \left(|\dot{\sigma}| \leq \frac{1}{\theta_1^*} \left| \sqrt{\frac{\theta^* - \epsilon_1 \Gamma^{*2}}{\epsilon_2}} \|\Phi\| + \Gamma^* - \varepsilon|\sigma_{\max}| - \tau \right| \right)$$

Guaranteeing finite time stability of the dynamics in (2.36) requires that the associated vector field has a negative degree of homogeneity in addition to the system dynamics being asymptotically stable. This notion of finite time stability for n integrator dynamics has been given by Bhat and Bernstein in their work [106]. The vector field on $\mathbb{R}^2$ in (2.36) is given by,

$$\mathscr{F} := \mathscr{F}_1(s_1, s_2)\frac{\partial}{\partial s_1} + \mathscr{F}_2(s_1, s_2)\frac{\partial}{\partial s_2} \tag{2.37}$$

where, $\mathscr{F}_1(s_1, s_2) = s_2$ and $\mathscr{F}_2(s_1, s_2) = -\beta_1 sgn(s_1)|s_1|^{\frac{2}{2-\vartheta}} - \beta_2 sgn(s_2)|s_2|^{\vartheta}$. Now let us consider a variable $r > 0$ and evaluate the degree of homogeneity of the vector field $\mathscr{F}$. It is observed that,

$$\mathscr{F}_1(r^{2-\vartheta}s_1, rs_2) = r^{(2-\vartheta)+(\vartheta-1)}\mathscr{F}_1(s_1, s_2) \tag{2.38}$$

$$\mathscr{F}_2(r^{2-\vartheta}s_1, rs_2) = r^{1+(\vartheta-1)}\mathscr{F}_2(s_1, s_2) \tag{2.39}$$

Therefore, the degree of homogeneity of $\mathscr{F}$ is equal to $(\vartheta - 1)$ being negative, since $\vartheta < 0$ follows from Lemma 2.1. The negative degree of homogeneity has now been proved. Now, it is to be shown that the dynamics (2.36) is asymptotically stable.

There exists a Lyapunov function $V_{s_1 s_2} : \mathbb{R}^2 \longrightarrow \mathbb{R}$ which is $\mathfrak{C}^1$ on $\mathbb{R}^2/\{0\}$ such that $\dot{V}_{s_1 s_2}$ is continuous and negative definite. Let the Lyapunov function $V_{s_1 s_2}$ be defined as,

$$V_{s_1 s_2} := \frac{\beta_1}{\beta_2}\frac{2-\vartheta}{2}|s_1|^{\frac{2}{2-\vartheta}} + \frac{1}{2\beta_2}{s_2}^2 \tag{2.40}$$

Subsequently,

$$\begin{aligned}\dot{V}_{s_1s_2} &= \frac{\beta_1}{\beta_2}\left(\frac{2-\vartheta}{2}\right)\left(\frac{2}{2-\vartheta}\right)|s_1|^{\frac{2}{2-\vartheta}}sgn(s_1)\dot{s}_1 + \frac{1}{\beta_2}s_2\dot{s}_2 \qquad (2.41)\\ &= \frac{\beta_1}{\beta_2}s_2|s_1|^{\frac{\vartheta}{2-\vartheta}}sgn(s_1) + \frac{1}{\beta_2}s_2\left(-\beta_1 sgn(s_1)|s_1|^{\frac{2}{2-\vartheta}} - \beta_2 sgn(s_2)|s_2|^{\vartheta} + |\dot{\sigma}_{\max}|\right)\\ &= -|s_2|^{\vartheta}sgn(s_2)s_2 + \frac{1}{\beta_2}|\dot{\sigma}_{\max}|s_2\\ \dot{V}_{s_1s_2} &\leq -|s_2|^{\vartheta+1} + \frac{1}{\beta_2}|\dot{\sigma}_{\max}||s_2| \qquad (2.42)\end{aligned}$$

For $\dot{V}_{s_1s_2} < 0$, the following condition, $|s_2|^{\vartheta} > |\dot{\sigma}_{\max}|/\beta_2$, must be satisfied. Now, let the minimum value that $V_{s_1s_2}$ can achieve be given by $\mathscr{C}_{min}$. This implies that,

$$|s_1|^{\frac{2}{2-\vartheta}} = \frac{1}{\beta_1(2-\vartheta)}\left(2\beta_2\mathscr{C}_{min} - \left(\frac{|\dot{\sigma}_{\max}|}{\beta_2}\right)^{\frac{2}{\vartheta}}\right) \qquad (2.43)$$

For $|s_1|^{\frac{1}{2-\vartheta}}$ to exist in the real space $\mathbb{R}$, calls for, $\mathscr{C}_{min} > \frac{1}{2\beta_2}\left(\frac{|\dot{\sigma}_{\max}|}{\beta_2}\right)^{\frac{2}{\vartheta}}$. Now if $\mathscr{C}_{min} = \frac{1}{2\beta_2}\left(\frac{|\dot{\sigma}_{\max}|}{\beta_2}\right)^{\frac{2}{\vartheta}}$ is achieved, $|s_1| = 0$ in finite time which in turn guarantees the asymptotic stability of the $(\wp-1)^{th}$ order tracking error dynamics. The invariant set is hence defined as,

$$\mathscr{S}_1 := \left\{(s_1, s_2) \in \mathbb{R}^2 \mid int(\dot{V}_{s_1s_2} = 0),\ |s_1| = 0,\ |s_2| \leq \left(\frac{|\dot{\sigma}_{\max}|}{\beta_2}\right)^{\frac{1}{\vartheta}}\right\} \qquad (2.44)$$

From (2.28) and (2.44), utilizing Barbalat's Lemma [110] and Lasalle's theorem [69] yields,

$$\dot{V} = -\sum_{i=1}^{\wp-1}\kappa_i V_i = -min\{\kappa_i\}_{i=1}^{\wp-1}\sum_{i=1}^{\wp-1}V_i \leq 0 \qquad (2.45)$$

Therefore, from (2.44), the signal vector $[z_1\ z_2 \dots z_{\wp-1}]^T \in \mathcal{L}_2 \cap \mathcal{L}_\infty$ and thereafter $[\dot{z}_1\ \dot{z}_2 \dots \dot{z}_{\wp-1}]^T \in \mathcal{L}_\infty$. Utilizing the signal convergence lemma, the closed loop stability is established and asymptotic output tracking is guaranteed, which means, $\lim_{t\to\infty} z_1 = \lim_{t\to\infty}(\xi_1 - y_r) = 0$.
Now, if $\mathscr{C}_{min}$ is not achieved as $t \to t_f$, a finite time, its consequence on the stability of the closed loop system is investigated below.
In order to circumvent the problem mentioned above, let us define a variable $\lambda > 0$, denoting the difference between the steady state and the instantaneous value of $\mathscr{C}_{min}$. This yields the modified invariant set $\mathscr{S}_1'$ defined as,

$$\mathscr{S}_1' := \left\{(s_1, s_2) \in \mathbb{R}^2 \mid int(\dot{V}_{s_1s_2} = 0),\ |s_1| \leq \left(\frac{2\lambda\beta_2}{\beta_1(2-\vartheta)}\right)^{\frac{2-\vartheta}{2}},\ |s_2| \leq \left(\frac{|\dot{\sigma}_{\max}|}{\beta_2}\right)^{\frac{1}{\vartheta}}\right\} \qquad (2.46)$$

From (2.46), it is obvious that the notion of asymptotic stability of the $(\wp-1)^{th}$ order error dynamics to the origin will be violated. However, stability is guaranteed in the vicinity of the origin as shown below.

Referring to (2.28), gives,

$$\dot{V} = -\sum_{i=1}^{\wp-1} \kappa_i V_i + z_{\wp-1} z_{\wp} \leq -\sum_{i=1}^{\wp-1} \kappa_i V_i + |z_{\wp-1}||z_{\wp}| \tag{2.47}$$

Application of Peter-Paul inequality (Appendix A.2.3) to (2.47), for every $0 < \nu < 2c_{\wp-1}$, yields,

$$\dot{V} \leq -\sum_{i=1}^{\wp-1} c_i z_i^2 + \frac{\nu |z_{\wp-1}|^2}{2} + \frac{|z_{\wp}|^2}{2\nu} \leq -\underbrace{2\left[c_1 \; c_2 \ldots\ldots \left(c_{\wp-1} - \frac{\nu}{2}\right)\right]}_{C} \begin{bmatrix} 0.5z_1^2 \\ 0.5z_2^2 \\ \vdots \\ 0.5z_{\wp-1}^2 \end{bmatrix} + \frac{|z_{\wp}|^2}{2\nu}$$

$$\leq -\min\{C = C_i\}_{i=1}^{\wp-1} \sum_{i=1}^{\wp-1} V_i + \frac{|z_{\wp}|^2}{2\nu} \tag{2.48}$$

From the invariant set $\mathscr{S}_1'$, it is known that $|z_{\wp}| = |s_1| \leq \left(\frac{2\lambda\beta_2}{\beta_1(2-\vartheta)}\right)^{\frac{2-\vartheta}{2}}$, therefore (2.48) reduces to,

$$\dot{V} \leq -\min\{C = C_i\}_{i=1}^{\wp-1} \sum_{i=1}^{\wp-1} V_i + \frac{1}{2\nu}\left(\frac{2\lambda\beta_2}{\beta_1(2-\vartheta)}\right)^{2-\vartheta} \tag{2.49}$$

$$\implies V \leq V(t_0) exp(-C_{\min} t) + \frac{1}{2C_{\min}\nu}\left(\frac{2\lambda\beta_2}{\beta_1(2-\vartheta)}\right)^{2-\vartheta} \tag{2.50}$$

Considering the steady state, the following evolves from inequality (2.50),

$$\left|(z_1^2 + z_2^2 + \ldots + z_{\wp-1}^2)^{1/2}\right| \leq \frac{1}{\sqrt{C_{\min}\nu}}\left(\frac{2\lambda\beta_2}{\beta_1(2-\vartheta)}\right)^{\frac{2-\vartheta}{2}} \tag{2.51}$$

In consequence, another positively invariant set $\mathscr{S}_2$ using (2.51) is defined as,

$$\mathscr{S}_2 := \left\{(z_1, z_2, \ldots, z_{\wp-1}) \in \mathbb{R}^{\wp-1} \;\middle|\; \left|(z_1^2 + z_2^2 + \ldots + z_{\wp-1}^2)^{1/2}\right| \leq \frac{1}{\sqrt{C_{min}\nu}}\left(\frac{2\lambda\beta_2}{\beta_1(2-\vartheta)}\right)^{\frac{2-\vartheta}{2}}\right\} \tag{2.52}$$

It is quite relevant that the visualization of set $\mathscr{S}_2$ is possible if and only if $\wp \leq 4$. Thereupon considering $\wp = 4$ yields a set $\mathscr{S}_2$, which is a ball of radius $\frac{1}{\sqrt{C_{\min}\nu}}\left(\frac{2\lambda\beta_2}{\beta_1(2-\vartheta)}\right)^{\frac{2-\vartheta}{2}}$ centered around the origin. Eventually, it is now possible to define the final compact and positively invariant set $\mathscr{S}^*$ with the help of (2.46) and (2.52). Defining $Z := [z_1 \; z_2 \; z_3 \ldots z_{\wp-1} \; z_{\wp} \; z_{\wp+1}]^T$, results in,

$$\mathscr{S}^* := \left\{Z \in \mathbb{R}^{\wp+1} \;\middle|\; \|Z\|_2 \leq \sqrt{\left(\frac{1}{\mathscr{C}_{\min}\nu} + 1\right)\left(\frac{2\lambda\beta_2}{\beta_1(2-\vartheta)}\right)^{2-\vartheta} + \left(\frac{|\dot{\sigma}_{\max}|}{\beta_2}\right)^{\frac{2}{\vartheta}}}\right\} \supseteq \mathscr{S}_1' \times \mathscr{S}_2 \tag{2.53}$$

Ultimately the set $\mathscr{S}^*$ is the largest possible positively invariant set, where the closed loop trajectories of the system (2.4) evolve finally and live there for all future time under the action of the proposed controller. It is also clear from (2.35) and (2.53) and can also be concluded that $\mathscr{S}^* \subset \mathscr{V}$. Considering,

relative degree $\wp$=2, the invariant sets $\mathscr{S}_1', \mathscr{S}_2, \mathscr{S}_1' \times \mathscr{S}_2$ and $\mathscr{S}^*$ are shown in Figure 2.2. The points O, A and A′ denote the origin $(0, 0, 0)$ and the maximum positive and negative bounds on the output tracking error z_1. The sets can be made smaller by proper adjustment of the controller parameters yielding a high precision in tracking accuracy.

The proof is not yet complete. Now, it has to be proved that the results derived above hold

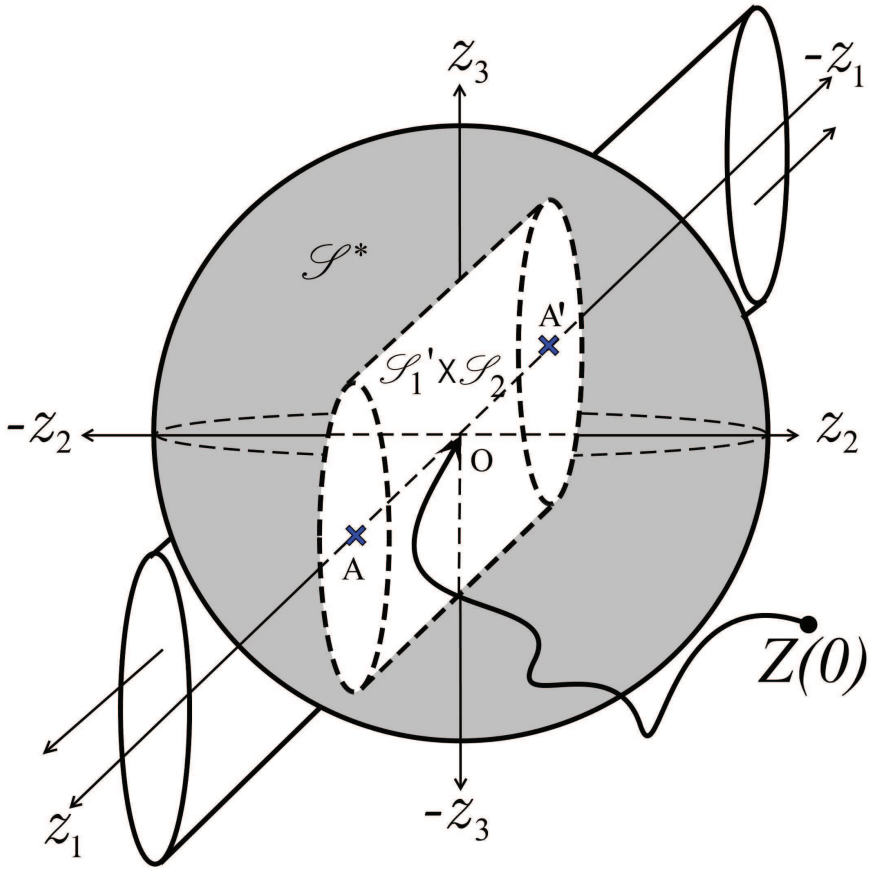

Figure 2.2: Visualization of the calculated invariant sets with the proposed scheme, for systems with relative degree $\wp = 2$

true even in the presence of unknown actuator failure scenarios occurring at unknown time instances $T_1, T_2, \cdots, T_h$ and $T_0 < T_1 < T_2 < \cdots < T_h$ subject to a finite $h \leq (m-1)$ and $h \in \mathbb{Z}_+$. In other words, closed-loop signal boundedness and asymptotic stability of the $(\wp-1)^{th}$ order tracking error dynamics have to be proved at each uncertain time instant when failures are encountered.
Let us define the Lyapunov function $V_h(t) : \mathcal{T}_h \to \mathbb{R}_+$ for each sub-domain $\mathcal{T}_h := [T_h, T_{h+1})$ from the total time interval $[T_0, T_{m-1+1}]$ in which all possible failures, which can be compensated, occur.

$$V_h = \frac{1}{2}\sum_{i=1}^{\wp-1} z_i^2 + \frac{1}{2}\sigma^2 + \frac{1}{\gamma}\sum_{j\in\mathscr{B}_{par_H}}^{m} \frac{|b_j|K_j}{2}\tilde{\Gamma}^2 + \sum_{j\in\mathscr{B}_{par_H}}^{m} \frac{|b_j|K_j}{2}\tilde{\theta}^T P^{-1}\tilde{\theta} \quad \text{for} \quad h = 0, 1, \ldots, (m-1) \tag{2.54}$$

From (2.45) and (2.33), it is evident that $\dot{V}_h < 0$. This in turn proves that the positive definite function V_h is a monotonically decreasing function in $\mathcal{T}_h$. Now, the piecewise continuity of V_h at various subdomains $[T_h, T_{h+1})$ has to be established using the continuity criterion for monotone functions. Since

$$V_h(T_{h+1}^-) = \lim_{\delta t \to 0^-} V_h(T_{H+1} + \delta t) \tag{2.55}$$

$$V_h(T_h^+) = \lim_{\delta t \to 0^+} V_h(T_h + \delta t) = V_h(T_h^+) = V_h(T_h^+) = V_h(T_h) \tag{2.56}$$

the function $V_h(\mathcal{T}_h)$ suffices to be an interval and thereafter by virtue of the Intermediate Value Theorem, the piecewise continuity of $V_h(t)$ is proved. Furthermore, the monotonic decreasing nature of V_h during the time interval $\mathcal{T}_h$, $h = 0, 1, \ldots, (m-1)$, points out the fact that $T_h < T_{h+1}$ implying $V_h(T_h^+) = V_h(T_h) \geq V_h(T_{h+1}^-)$. The interval in which no fault occurs is $\mathcal{T}_0$ during which $V_0(T_0^+) = V_0(T_0) \geq V_0(T_1^-)$ and since $V_0(T_0)$ is finite, it is inferred that $(z_1, z_2, \ldots, z_{\wp-1}) \in \mathcal{L}_2 \cap \mathcal{L}_\infty$ and $(\dot{z}_1, \dot{z}_2, \ldots, \dot{z}_{\wp-1}) \in \mathcal{L}_\infty$. Now, considering the first time interval $\mathcal{T}_1$ in which the first failure is encountered and recovered, $V_1(T_1^+) = V_0(T_1^-) + \delta V_1$. The term δV_1 is finite and arises from the torments in the adaptive parameters at the occurrence of failures, subsequently affecting the related terms in V_1 from (2.54). Hence $V_1(T_1^+)$ is bounded in $\mathcal{T}_1$ if and only if $V_0(T_1^-)$ defined on $\mathcal{T}_0$ is bounded. In similar words, it can be argued that boundedness of $V_h(T_{h+1}^-)$ over the set $\mathcal{T}_r$ ensures the boundedness of $V_{h+1}(T_{h+1}^+)$ in $\mathcal{T}_{r+1}$. Subsequently, the boundedness of all the closed loop signals at each interval between the onset and recovery of the failure, is guaranteed. Finally, this completes the proof. □

Remark 2.3. *The positive gain parameters ε and τ in the control law (2.20) must be chosen large enough in order to ensure a bounded motion around the sliding surface such that $\dot{V}_\sigma < 0$ is satisfied outside and on the set $\mathscr{V}$ containing the equilibrium point. In addition, the adaptive rates ϵ_1 and ϵ_2 define the span of $\mathscr{V}$ and should be chosen small enough to guarantee ideal sliding mode dynamics along the sliding surface $\sigma = 0$. However, contraction of the set $\mathscr{V}$ by small enough choice of ϵ_1 and ϵ_2 results in slow convergence of the adaptive parameters thereby adversely affecting the transient performance. Hence, a trade-off must be made between the adaptive rate parameters and achievement of ideal sliding motion.*

Remark 2.4. *The transient performance of the output $y = \xi_1$ in the proposed scheme solely depends on that of the auxiliary sliding manifold σ. Improvements in the $\mathcal{L}_1$ sense can be achieved by increasing the values of parameters τ, ε, γ, P and decreasing the magnitude of ϵ_1, ϵ_2 judiciously without any significant effect on the convergence of adaptive parameters, guaranteeing close to ideal sliding motion. Furthermore, the gains β_1 and β_2 must be chosen in a way, such that, $\beta_2/\beta_1 > 1$ and β_2 being sufficiently large in order to ensure a low value of s_2 without any noticeable increase in the control energy. This in turn yields low overshoots in $z_\wp$ and hence its impact on the output error $z_1 = \xi_1 - y_r$ is quite insignificant. Therefore, in contrast to backstepping, the transient performance of the output can be improved without increasing the virtual control gains $c_1, c_2, \ldots, c_\wp$ and trajectory initialization even when unanticipated actuator failures are encountered. Furthermore, transient performance of the output in sliding mode depends on the sliding surface coefficients, which are equivalent to the virtual control gains $c_1, c_2, \ldots, c_\wp$. Increasing the values of these coefficients can initially result in a good transient response but will result in high overshoots at the time instances of uncertain faults and failures*

($\mathcal{L}_2$ bound of the output error increases), which is undesirable. Hence, the superiority of the proposed scheme in offering better transient response is well clarified from the stability analysis leading to the inferences as discussed above.

2.2.5 Simulation Results and Discussion

In order to investigate the performance of the proposed controller, simulation study is carried out on the nonlinear longitudinal model of a Boeing 747-100/200 aircraft subjected to uncertain actuator faults and failures in addition to uncertainties inherent in their modeling. The detailed modeling of the longitudinal motion of the aircraft is not reproduced here and instead can be referred to in [4,111]. An approximately fitted nonlinear longitudinal model of Boeing 747-100/200 aircraft is used for the purpose of controller design by fitting the aerodynamic coefficients as polynomial functions of angle of attack and velocity for level flight [111]. The Boeing 747-100/200 aircraft longitudinal nonlinear dynamics are considered as described in [4, 111, 112] and are given below,

$$\dot{\alpha} = q + \frac{-F_x \sin\alpha + F_z \cos\alpha}{mV_T}, \qquad \dot{\theta} = q \tag{2.57}$$

$$\dot{V}_T = \frac{F_x \cos\alpha + F_z \sin\alpha}{m}, \qquad \dot{q} = \frac{M_y}{I_y} \tag{2.58}$$

where, the forces F_x, F_z and the moment M_y along the x, z and y body axes are given by,

$$F_x = \bar{q}SC_x + \sum_{i=1}^{4} P_{n_i} - mg\sin\theta, \;\; F_z = \bar{q}SC_z - 0.0436\sum_{i=1}^{4} P_{n_i} + mg\cos\theta \tag{2.59}$$

$$M_y = \bar{q}S\bar{c}C_M + \sum_{i=1}^{4} z_{\text{eng}_i} P_{n_i} \tag{2.60}$$

where, $C_x = -C_D\cos\alpha + C_L\sin\alpha$, $C_z = -C_D\sin\alpha - C_L\cos\alpha$, $\bar{q} = \frac{1}{2}\rho V_T^2$. Further, C_L, C_M and C_D are functions defined as,

$$C_L = C_{L_b} + \frac{\bar{c}}{2V_T}\frac{dC_L}{dq}q + \frac{dC_M}{d\delta_{e_1}}\delta_{e_1} + \frac{dC_M}{d\delta_{e_2}}\delta_{e_2} \tag{2.61}$$

$$C_M = C_{M_b} + \frac{\bar{c}q}{2V_T}\frac{dC_M}{dq} + \frac{dC_M}{d\phi_s}\phi_s + \frac{dC_M}{d\delta_{e_1}}\delta_{e_1} + \frac{dC_M}{d\delta_{e_2}}\delta_{e_2} \tag{2.62}$$

$$C_D = C_{D_m} = C_{D_{m3}}\alpha^2 + C_{D_{m2}}\alpha + C_{D_{m1}}V_T + C_{D_{m0}} \tag{2.63}$$

In (2.61)-(2.63), the coefficient functions are given by $C_{L_b} := C_{L_{b2}}\alpha + C_{L_{b1}}V_T + C_{L_{b0}}$, $C_{M_b} := C_{M_{b3}}\alpha^2 + C_{M_{b2}}\alpha + C_{M_{b1}}V_T + C_{M_{b0}}$, $D_{\delta_{e_1}}(C_L) = D_{\delta_{e_2}}(C_L) := C_{L_2}V_T^2 + C_{L_1}V_T + C_{L_0}$ and $D_{\delta_{e_1}}(C_M) = D_{\delta_{e_2}}(C_M) := C_{M_2}V_T^2 + C_{M_1}V_T + C_{M_0}$. These coefficients are further approximated as polynomial functions of velocity and angle of attack as follows,

$$\begin{aligned} C_{L_b} &= C_{L_{b2}}\alpha + C_{L_{b1}}V_T + C_{L_{b0}} \\ C_{M_b} &= C_{M_{b3}}\alpha^2 + C_{M_{b2}}\alpha + C_{M_{b1}}V_T + C_{M_{b0}} \end{aligned}$$

Table 2.1: Aircraft model parameters

Terminologies for the aircraft model	
α	The angle of attack (AoA)
V_T	The velocity or true air speed
θ	The pitch angle
q	The pitch rate
$\delta_{e_1},\ \delta_{e_2}$	The elevator deflections of a two-piece augmented elevator
m	The mass of the aircraft
I_y	The moment of inertia along the body y
ρ	The air density
S	The wing area
$\bar{c}$	The mean chord
P_{n_i}	Thrust produced by the i^{th} engine
ϕ_s	The horizontal stabilizer deflection angle
$\bar{q}$	The velocity head

Table 2.2: Values of aircraft parameters in simulation

Aircraft parameters in simulation		
$m = 3{\times}10^5$kg	$C_{D_{\text{m}2}} = 0.0348$	$C_{L_{\text{b}0}} = 0.00615$
$I_y = 4.5278{\times}10^7$kg	$C_{D_{\text{m}1}} = 4.45{\times}10^{-5}$	$C_{M_{\text{b}3}} = 2.39$
$\bar{c} = 8.324$m	$C_{D_{\text{m}0}} = 0.00992$	$C_{M_{\text{b}2}} = -1.46$
$S = 511\text{m}^2$	$C_{L_2} = -8.25{\times}10^{-6}$	$C_{M_{\text{b}1}} = -0.00032$
$\rho = 0.59\text{kg/m}^3$	$C_{L_1} = 2.44{\times}10^{-3}$	$C_{M_{\text{b}0}} = 0.12$
$z_{\text{eng}_1} = z_{\text{eng}_4} = 0.94$m	$C_{L_0} = 0.1839$	$C_{M_2} = 2.492{\times}10^{-5}$
$z_{\text{eng}_2} = z_{\text{eng}_3} = 2.53$m	$C_{L_{\text{b}2}} = 5.15$	$C_{M_1} = -6.64{\times}10^{-3}$
$C_{D_{\text{m}3}} = 3.27$	$C_{L_{\text{b}1}} = 0.00121$	$C_{M_0} = -1$
$P = 41631$ N	$\phi_s = 0.0128$	$\frac{dC_M}{d\phi_s} = -2.8374$

$$\frac{dC_L}{d\delta_{e_1}} = \frac{dC_L}{d\delta_{e_2}} = C_{L_2}V_T^2 + C_{L_1}V_T + C_{L_0}$$
$$\frac{dC_M}{d\delta_{e_1}} = \frac{dC_M}{d\delta_{e_2}} = C_{M_2}V_T^2 + C_{M_1}V_T + C_{M_0} \tag{2.64}$$

The terminologies used for the model in (2.57)-(2.58) are illustrated in Table 2.1. The aircraft parameters used in the simulation are set based on the data sheet in [111] and are reproduced in Table 2.2. The state variables are chosen as $[x_1,\ x_2,\ x_3,\ x_4] = [\alpha,\ V_T,\ \theta,\ q]$, respectively. Longitudinal control is performed through four elevator segments and by thrust from the four engines. Pitch angle control is achieved mainly through the four piece elevator segments. Under normal operation, the inboard and outboard elevators move together and hence a two piece elevator can be formed with an outer and an inner elevator segment. This is done for mere simplicity in modeling and control design for the aircraft. The elevator deflection angles of such a two piece augmented elevator is designated as δ_{e1} and δ_{e2} and chosen as the two actuators u_1 and u_2. Moreover, the term P_n $(Newton)$ collectively defines the thrust generated by the four engines of the aircraft, that is, $P_{n_1} = P_{n_2} = P_{n_3} = P_{n_4} = P_n$. Furthermore, ϕ_s represents the horizontal stabilizer deflection angle. The trim point is given as $\alpha_{trim} = 0.0162\ rad$, $q_{trim} = 0\ rad/s$, $V_{T_{trim}} = 230\ m/s$, $\theta_{trim} = 0.0162\ rad$, $\delta_{e_{trim}} = 0$, $\phi_{s_{trim}} = 0.0128\ rad$, $P_{ntrim} = 41631\ N$. The magnitude of the unknown control coefficients are given as $b_1 = b_2 = 2.77 \times 10^{-5}$.

The control objective is to design an actuator fault tolerant control strategy to control the elevator deflection angles u_1 and u_2 such that the pitch angle θ given by x_3 tracks a reference signal y_r generated from a reference system $\sum_d$ even if the actuators driving the elevators lose their effectiveness partially or experience an uncertain stuck failure. As explained in Section 2, there exists a diffeomorphism, which transforms the system $\sum_p$ to $\sum_c$ in strict feedback form and $\sum_z$ denoting the internal dynamics of the system. The diffeomorphism for the aircraft model (2.57)-(2.58) is given by $\mathscr{T}(x) = [\eta_1 \;\; \eta_2 \;\; \xi_3 \;\; \xi_4]^T = [\mathscr{T}_1(x) \;\; \mathscr{T}_2(x) \;\; x_3 \;\; x_4]^T$ yielding $\sum_c$ as,

$$\begin{aligned}\dot{\xi}_3 &= \xi_4 \\ \dot{\xi}_4 &= a(\xi,\eta) + \sum_{j=1}^{m} b_j\beta_j(\xi,\eta)(K_j u_{Hj} + \bar{u}_{Fj})\end{aligned} \tag{2.65}$$

Accordingly, the transformations $\mathscr{T}_1(x)$ and $\mathscr{T}_2(x)$ are found as solutions to the partial differential equations given below.

$$\frac{\partial \mathscr{T}_1}{\partial x_1}g_1(x) + \frac{\partial \mathscr{T}_1}{\partial x_2}g_2(x) + \frac{\partial \mathscr{T}_1}{\partial x_3}g_3(x) + \frac{\partial \mathscr{T}_1}{\partial x_4}g_4(x) = 0 \tag{2.66}$$

$$\frac{\partial \mathscr{T}_2}{\partial x_1}g_1(x) + \frac{\partial \mathscr{T}_2}{\partial x_2}g_2(x) + \frac{\partial \mathscr{T}_2}{\partial x_3}g_3(x) + \frac{\partial \mathscr{T}_2}{\partial x_4}g_4(x) = 0 \tag{2.67}$$

where, g_1, g_2, g_3, g_4 are nonlinear smooth actuation functions in x_2 described as,

$$\begin{bmatrix} g_1(x) \\ g_2(x) \\ g_3(x) \\ g_4(x) \end{bmatrix} = \begin{bmatrix} -0.000502483x_2(0.00321 + 0.0000426x_2 - 1.44\times10^{-7}x_2^2) \\ 0 \\ 0 \\ 0.0000277133x_2^2(-0.0176 - 0.000116x_2 + 4.35\times10^{-7}x_2^2) \end{bmatrix}$$

Thereafter solving the partial differential equations (PDEs) in (2.66) and (2.67) yields,

$$\eta_1 = \mathscr{T}_1(x) = x_1x_2 - 6.6586261x_4 \tag{2.68}$$

$$\eta_2 = \mathscr{T}_2(x) = x_2 \tag{2.69}$$

Hence, the unforced zero dynamics can be expressed as $\dot{\eta} = \varrho(\eta_1, \eta_2, 0, 0)$ with $\xi_3 = \xi_4 = 0$ as the input. It is now shown that the zero dynamics is locally input to state stable (ISS) [109]. The equilibrium point of $\dot{\eta} = \varrho(\eta_1, \eta_2, 0, 0)$ is found to be $\eta_e = [0 \;\; 3806.14]^T$. The stability of the unforced zero dynamics at equilibrium is investigated by checking the eigen values of $\partial\varrho(\eta, 0)/\partial\eta$ at η_e. The eigen values are found to be -9.17485 and -1.00182, and since $\Re(\lambda(\partial\varrho(\eta,0)/\partial\eta|_{\eta_e})) < 0$, it is proved that the unforced zero dynamics are locally asymptotically stable.

The controller is designed following the strategy discussed in Section 2.2.3 and the control law given by (2.20), with relative degree $\wp = 2$. The initial state conditions are assumed to be $[\,0.794 \;\; 230 \;\; 0.0162 \;\; 0\,]^T$. The rate parameters in the adaptive law are chosen as $\gamma = 0.5, \epsilon_1 = 0.5, \epsilon_2 = 0.6$ and $P = 0.5I_2$ and that in the virtual control law α_1 is considered to be $c_1 = 30$. The parameters in the nominal control law w_{nom} are selected as β_1 =40.5, β_2 =30.5, $\vartheta_1 = \frac{3}{5}$ and $\vartheta_2 = \frac{3}{4}$. The reference signal y_r to be tracked

is generated from the reference system as in [4], given by $G_d(s) = \frac{1}{s^2 + 3s + 4}$ with y_d as the reference input, meaning that $y_r = L^{-1}[G_d(s)] * y_d$. The notations $L^{-1}[\cdot]$ and $*$ denote the inverse Laplace transform and the convolution operator respectively. The signal y_d is given as,

$$y_d(t) = \begin{cases} 0 & 0s \leq t < 5s \\ 0.1 & 5s \leq t < 10s \\ 0 & 10s \leq t < 15s \\ -0.1 & 15s \leq t < 20s \\ 0 & 20s \leq t < 25s \end{cases} \tag{2.70}$$

This pattern of $y_d(t)$ in (2.70) is repeated for the next 25 s. The initial value of the adaptive parameters $\hat{\xi}$ and $\hat{\Gamma}$ are set as $\hat{\xi}(0) = [1 \quad 0]^T$ and $\hat{\Gamma}(0) = 0$. The functions β_1 and β_2 are given by, $\beta_1 = \beta_2 = x_2^2(-0.0088 - 0.000058x_2 + 2.175 \times 10^{-7}x_2^2)$.

Remark 2.5. *The performance of the proposed methodology is compared with similar existing schemes. For this purpose, an adaptive failure compensation method based on backstepping (BS) proposed in [32] is considered. Also, an adaptive sliding mode control (ASMC) based failure control scheme has also been designed based on a partial actuator loss compensation method proposed in [4], for the sake of further comparison.*

For the longitudinal aircraft model of Boeing 747-100/200, the basic controller proposed in [5] based on adaptive backstepping control (ABSC) is obtained considering similar notations as follows,

$$u_{j_{BS}} = -sgn(b_j)\frac{1}{b_j}\left[\hat{\theta}_1\left(z_1 + c_2 z_2 + a_0(\xi,\eta) + \hat{\Gamma}a_0(\xi,\eta) - \left(\frac{\partial \alpha_1}{\partial \xi_3}\xi_4 + \frac{\partial \alpha_1}{\partial \dot{y}_r}\ddot{y}_r\right) - \ddot{y}_r\right) + \beta_j\hat{\theta}_{2,j}\right] \tag{2.71}$$

$$\dot{\hat{\theta}}_1 = \gamma_1\left[\left(z_1 + c_1 z_1 + a_0(\xi,\eta) + \hat{\Gamma}a_0(\xi,\eta) - \left(\frac{\partial \alpha_1}{\partial \xi_3}\xi_4 + \frac{\partial \alpha_1}{\partial \dot{y}_r}\ddot{y}_r\right) - \ddot{y}_r\right)\right]z_2 \tag{2.72}$$

$$\dot{\hat{\theta}}_{2,j} = \gamma_{2,j}\beta_j z_2, \qquad j = 1, 2 \tag{2.73}$$

$$\dot{\hat{\Gamma}} = 0.0005a_0(\xi,\eta)z_2 \tag{2.74}$$

where, z_1, z_2 denote the error variables and α_1 defines the virtual control as, $z_1 = \xi_3 - y_r$, $z_2 = \xi_4 - \alpha_1 - \dot{y}_r$, $\alpha_1 = -c_1 z_1$ The design parameters are chosen as $c_1 = 25, c_2 = 25, \gamma_1 = 1$ and $\gamma_{2,1} = 0.1$. Here $j = 1$ is only considered since case of total loss of only one actuator is possible for this particular illustration of aircraft control. Similarly, the adaptive sliding mode control (ASMC) methodology proposed in [4] assuming known control coefficients and modified to deal with partial loss as well as total actuator failure, is given as,

$$u_{j_{ASMC}} = \frac{1}{b_j \beta_j}(c(\dot{y}_r - \xi_4) - a_0(\xi, \eta) + \ddot{y}_r + \hat{\rho} sgn(\sigma) + \hat{\gamma}|\psi_0| sgn(\sigma)) \tag{2.75}$$

$$\psi_0 = c(\dot{y}_r - \xi_4) - a_0(\xi, \eta) + \ddot{y}_r \tag{2.76}$$

$$\sigma = (\dot{y}_r - \xi_4) + c(y_r - \xi_3) \tag{2.77}$$

$$\dot{\hat{\rho}} = a_\rho |\sigma|, \quad \dot{\hat{\gamma}} = a_\gamma |\psi_0||\sigma| \tag{2.78}$$

where, $c = 3, a_\rho = 0.3$ and $a_\gamma = 5$ are chosen values of the user defined parameters.
Simulation studies have been carried out considering a severe actuator failure scenario with modeling uncertainties. Transient performance is assessed on the basis of the integral time absolute error (ITAE) and settling time (t_s) which are desired to be of low magnitude. A small value of ITAE ensures minimum overshoots and oscillations in the output under the action of the controller. The output tracking performance is evaluated in terms of the integral absolute error (IAE), which is widely used as a performance criterion in the design of efficient controllers. To evaluate the manipulated input usage, the total variation (TV) [113] is calculated as, $\sum_{i=1}^{n} |u_i - u_{i+1}|$, which should have a small value. Energy of the control input is measured by using the 2-norm method.
The failure scenario is as follows: 20% uncertainties in system dynamics and the actuator failure pattern is given as,

$$u_1(t) = \begin{cases} 0.3u_{H1}(t), & t \in [20,\ \infty) \\ u_{H1}(t), & t \in [0,\ 20) \end{cases}, \qquad u_2(t) = \begin{cases} 2, & t \in [40,\ \infty) \\ u_{H2}(t), & t \in [0,\ 40) \end{cases} \tag{2.79}$$

The tracking performance of the proposed controller is compared with those of ASMC [4] and ABSC [5] schemes in Figures 2.3(a)-(f). The tracking error obtained by using the proposed method and the control methodologies proposed in [4] and [5] are plotted in Figure 2.3(a). It is observed from Figure 2.3(a) that in comparison to [4] and [5], the system output $y = \xi_3$ (pitch angle θ) with the proposed scheme is capable of tracking the desired trajectory y_r with marginal error and negligible overshoots in addition to a substantially low settling time. In contrast, the ASMC based scheme (2.75) exhibits a degraded transient performance with the output error swinging between -0.0125 and 0.7×10^{-4} and never reaches an acceptable steady state value. Further, the tracking error obtained using the adaptive backstepping controller (ABSC) (2.71) never achieves a steady state and oscillates in the interval (-0.001 , 0.002). The output tracking of the pitch angle θ using the proposed control strategy is shown in Figure 2.3(b) and the equivalent pitch rate q is shown in Figure 2.3(c). Figures 2.3(d)-(f) show the control signals utilizing the proposed method, ASMC and adaptive backstepping control (ABSC) respectively. The output tracking performance of each controller is measured in terms of ITAE and IAE. Comparison of tracking performances using the proposed scheme, ASMC [4] and backstepping [5] can be found in Table 2.3. In Table 2.3, it is observed that the proposed control strategy yields an ITAE of 0.00947 in contrast to comparatively higher ITAE values of 0.481 and 0.523 using ASMC [4] and ABSC [5] methods. Further, Table 2.3 shows that the proposed scheme yields an IAE of 0.00989 indicating small sustained oscillations in the output compared to significantly high IAE values of 0.044 and 0.025 in [4] and [5]. The total variation (TV) values for the inputs u_1 and u_2 in the proposed control scheme are measured to be 277.01 and 258.22 in comparison to quite high values in [4].

The time window between the onset of the fault or failure and its subsequent estimation is very

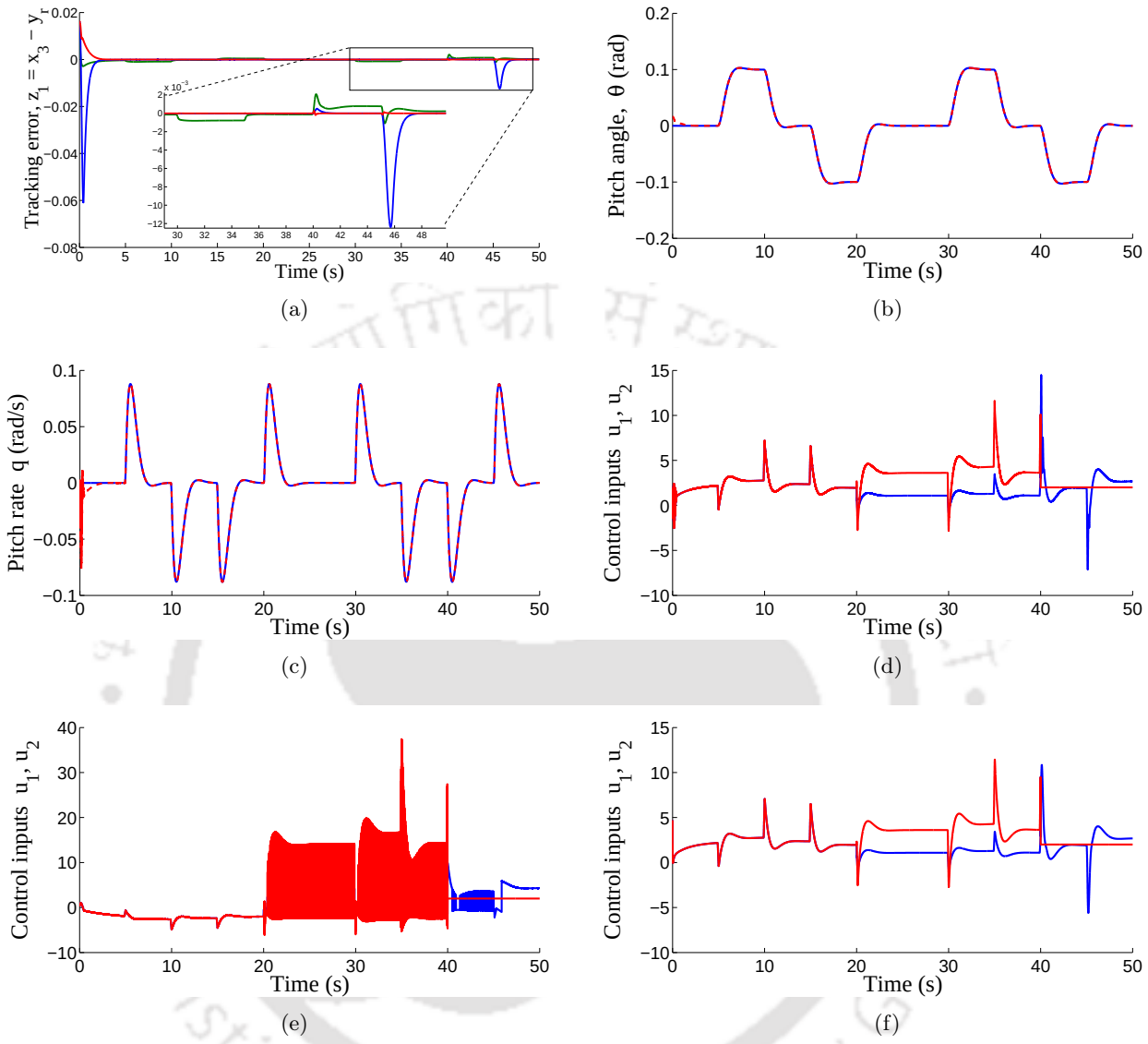

Figure 2.3: Plant response and control inputs under the considered fault scenario (2.79) using the proposed control scheme. (a) Output tracking error comparison of the proposed controller (red) with ASMC (blue) [4] and ABSC (green) [5]; (b) Pitch angle θ tracking using the proposed ARFTC; (c) Pitch rate q under the proposed ARFTC; (d) Control inputs u_1 and u_2 corresponding to proposed ARFTC; (e) Control inputs u_1 and u_2 using ASMC [4]; (f) Control inputs u_1 and u_2 using ABSC procedure [5].

crucial from the point of FTC design and must be as small as possible. This time window can be made analogous to the settling time measure, signifying the time required by the overall control system to recover its performance after the failure occurs. The settling time t_s has been measured at $t = 40$ s, when u_1 experiences a partial loss of effectiveness and u_2 undergoes a total loss. It is clear from the Figure 2.3 and Table 2.3 that using the proposed FTC scheme, the post fault overshoots and settling time could be substantially reduced. Moreover, the proposed FTC scheme spends lesser control effort than that in [4] with the faithful realization of its objective. The control energy spent by the proposed

controller is found to be almost at par with that of the basic controller (2.71) based on adaptive backstepping control (ABSC) [5]. However, the proposed design outperforms ABSC [5] and exhibits a superior post failure tracking performance. Besides, the scheme performs well in the presence of unknown control coefficients b_j compared to ASMC [4] and ABSC [5]. Further, the control input using ASMC in [4] is not smooth and experiences chattering which is undesired. However, the control signals using the proposed ARFTC strategy is continuous and smooth.

Table 2.3: Post failure tracking performance with 70% loss of effectiveness of u_1 at $t = 20s$ and stuck failure of u_2 at $t = 40s$

Performance Criteria		**ARFTC**	**ASMC** [4]	**ABSC** [5]
ITAE		0.00947	0.48141	0.52341
IAE		0.00989	0.04483	0.02505
Settling time t_s		0.73 s	-	-
Control energy	u_1	472.99	525.38	474.14
	u_2	685.23	695.53	684.01
Total variation(TV)	u_1	277.01	1.31×10^3	103.61
	u_2	258.22	3.24×10^4	94.79

2.3 Summary

An actuator failure compensation strategy is designed for affine nonlinear uncertain systems affected by faults in the form of partial and total loss of effectiveness of actuators. The proposed strategy is based on backstepping and second order sliding mode control methodologies. Applicability of the proposed controller to longitudinal control of Boeing 747-100/200 aircraft has been investigated. Simulation studies are performed to realize the different degrees of actuator failure and severity of uncertainty affecting the aircraft system. Enhancement of transient performance is shown through a rigorous stability analysis of the proposed scheme. Simulation results also confirm that the proposed controller yields enhanced transient and input performance with no chattering in the control input in comparison to a dedicated backstepping or sliding mode controller. Hence the proposed scheme promises to be a suitable control scheme for aircraft control as well as FTC applications.

3

Adaptive Multiple Model Fault Tolerant Control (AMMFTC) of Nonlinear Uncertain Systems with Actuator Failures

Contents

3.1 Introduction 47

3.2 Adaptive Multiple Model Fault Tolerant Control (AMMFTC) for Infinite Actuator Failures 51

3.3 Adaptive Multiple Model Fault Tolerant Control (AMMFTC) for Uncertain Multi-Input-Multi-Output (MIMO) Nonlinear Systems 90

3.4 Summary 126

3.1 Introduction

In Chapter 2, an adaptive robust fault tolerant controller (ARFTC) was developed by integrating adaptive and robust control ideas, to compensate actuator failures along with system uncertainties. The controller resorted to the online estimation of fault/failure induced unknown parameters (instead of their bounds) and unknown system uncertainty bounds for ensuring closed loop signal boundedness and output asymptotic stability in the event of actuator faults/failures. Although assuring improvement of transient performance, most of the existing results on direct adaptive control for actuator failure compensation including those mentioned above, strongly rely on the following design assumptions, (1) the number of actuator faults/failures is finite; (2) the transit time between the occurrence of two successive actuator failures is sufficiently large, and; (3) the time derivative of the fault/failure induced parametric uncertainties is zero. The first presumption ensures that any actuator will undergo a total or a partial failure once and it never recovers thereafter. Hence, there exists a finite time after which no actuator fault/failure occurs. In other words, a system with m inputs and q outputs can be subjected to a maximum of $(m-q)$ actuator failures, provided all such actuator failure patterns satisfy the conditions for existence of control characteristic indices corresponding to q outputs. This implies that even if the actuator failure parameters experience jumps at the failure instances, the collective magnitude of $(m-q)$ jumps are still bounded. Hence, closed loop stability and asymptotic convergence of output tracking error to the origin in the event of finite actuator failures follow [95]. The second assumption implicitly states that the unknown parameters should be slowly time varying while the third supposition directs towards failure induced parametric uncertainties to be constants for all $t \in [0, \infty)$. However, as will be discussed in the sequel, that actuator fault/failure induced parameters are unknown, time varying and piecewise constant functions of time. Further, as a consequence of intermittent actuator faults and failures, the infinite sequence of total magnitude of failure induced parameter jumps turns out to be monotonically increasing. This leads to a perpetual increase of the Lyapunov function and jeopardizes the existence of stable $\mathcal{L}_2$ and $\mathcal{L}_\infty$ bounds for the tracking error. Thus, in simple words, closed loop stability of the system is lost. On an additional note, intermittent failure induced parametric uncertainties are not necessarily slowly varying and hence their estimation over a continuum is challenging. Hence, direct adaptive strategies proposed in literature and that developed in the previous chapter are unable to compensate infinite actuator failures. Hence, finding an adaptive control solution to the problem of compensating infinitely occurring actuator failures in nonlinear uncertain systems, independent of the foregoing design presumptions and shortcomings is indeed not trivial.

Owing to its applicability to a larger class of systems, design modularity and comparatively lower control usage, indirect adaptive control based failure compensation design can be proclaimed as a potential active FTC alternative to solve the foregoing control problem. Herein, an integrated fault estimation (FE) based control, as depicted in Figure 1.8, is resorted to, which seeks to overcome some of the aforementioned difficulties, while retaining the fundamental ideas and advantages of active FTC for nonlinear systems. Such an active FTC architecture consists of a fault/failure parameter estimation module appended to a single controller. Nevertheless, the design and realization of the abovestated active FTC paradigm is also not straightforward, and certainly puts forth several theoretical and prac-

tical challenges. Regardless of the actuator failure eventualities being intermittent or finite, catering to joint multiple objectives of robust closed loop stability and robust fault estimation in presence of modeling uncertainties (Figure 1.6) is undeniably difficult, especially for nonlinear systems. Resorting to the above FTC design philosophy, in order to ensure a globally stable closed loop system, it is necessary that the controller assumes the regressor functions associated with the unknown parameters to be globally Lipschitz. Such an assumption, in turn, ensures modularity between the certainty equivalence (CE) based adaptive controller and stable parameter estimator. However, the presence of non-Lipschitz functions in the regressor matrix results in *bi-directional robustness interaction* between the certainty equivalence (CE) controller and estimator (Figure 3.2 (left)), breaking down the *Separation Principle*. As a consequence, the region of attraction or the operating region and performance robustness is decreased significantly which is undesirable. The occurrence of infinite actuator failures will further degrade the performance eventually leading to instability.

As a matter of fact, even if the identifier and controller are decoupled, indirect adaptive control strategies characterize poor transient performance at the learning phase which is detrimental for FTC applications. Similar to direct adaptive control, the output transients herein can be improved by increasing the control gains and adaptive rate which eventually lead to an increased control usage and a proportional decrease in robust stability margins [114]. Of late, as an alternative procedure, multiple model adaptive control (MMAC) using switching and tuning [115,116] has become popular in achieving substantial improvement in output transient performance in linear and Lipschitz nonlinear uncertain systems [117–120]. The basic functional block diagram of MMAC is presented in Figure 3.1 which summarizes its operation. However, to achieve an enhanced transient performance, these MMAC schemes require large number of models which grows exponentially with the dimension of the unknown parameter vector. Hence, computational burden is heavily increased. In addition, at least one identification model should be near to the unknown parameter to ensure stability in the face of switching transients and an improved performance. It is worth mentioning that all existing MMAC strategies for nonlinear uncertain systems including those cited above, are applicable only when the system nonlinearities or the associated regressor matrix for unknown parameters are globally Lipschitz. Further, in some works, the system is pre-assumed to be bounded input bounded state (BIBS) stable to facilitate a decoupling design of the CE control and identifier. The nonlinear system should also exhibit a positive dwell time. In such a case, if the system dynamics characterize exploding nonlinearities (no linear growth), the aforesaid assumptions for the existent multiple model adaptive control design algorithms, do not hold. In consequence, as discussed earlier, bidirectional uncertainty interactions creep in; thereby ruling out the guarantees of global/semi-global boundedness and asymptotic stability of controlled system dynamics. Besides, stability and performance robustness margins are also largely compromised. In conjunction with the above limitations, the theoretical quantification of the transient performance using MMAC in terms of $\mathcal{L}_\infty$ and $\mathcal{L}_2$ bounds in no failure and finite failure cases is yet to be reported and remains as an open problem.

In this chapter, an effective indirect adaptive FTC using multiple identifiers/models is proposed which addresses the design issues and problems identified in the foregoing discussion. The proposed approach, named as adaptive multiple model fault tolerant control (AMMFTC), is summarized as

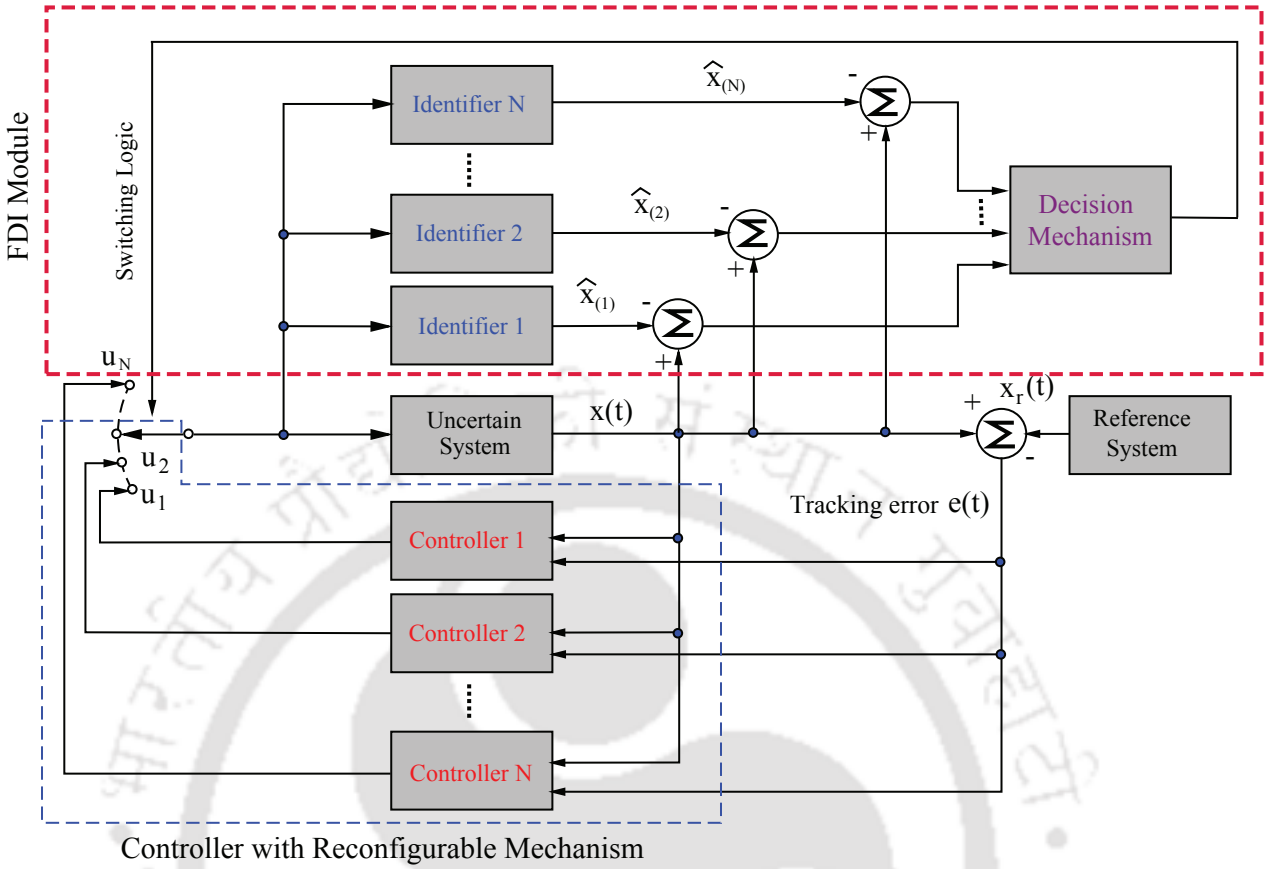

Figure 3.1: Schematic block diagram representation of a basic MMAC scheme with switching and tuning

follows. The controller is designed using a backstepping approach with suitable damping functions [69], to strengthen the CE controller by enhancing its stability margins with respect to the parameter estimation error and its derivative. The unknown parameters due to actuator faults/failures and system uncertainties are adaptively estimated using multiple identifiers with two layers of adaptation. The first layer of adaptation in the AMMFTC scheme developed herein involves a gradient based parameter update law corresponding to each of the multiple identifiers. Thereafter, exploiting the property of convex sets, the second layer of adaptation essentially produces an adaptive weighted convex combination of parameter estimates obtained from each of the identification models at the first adaptation layer. The improvement of transient and steady state performance is strongly accredited to such an efficient mixing strategy. Thus, unlike in switching based MMAC schemes, the information from each of the identifiers is aptly utilized. Following the same, the number of identification models in the proposed MMAC architecture is reduced to$(N+1)$, provided the dimension of unknown parameter vector is N. Therefore, the computational burden of the proposed MMAC scheme is drastically reduced compared to MMAC with switching. It is proved that the states of the closed loop system are bounded whenever, the parameter estimation error is bounded and its derivative is square integrable. These desirable convergence properties of the estimation signals are achieved using multiple identification

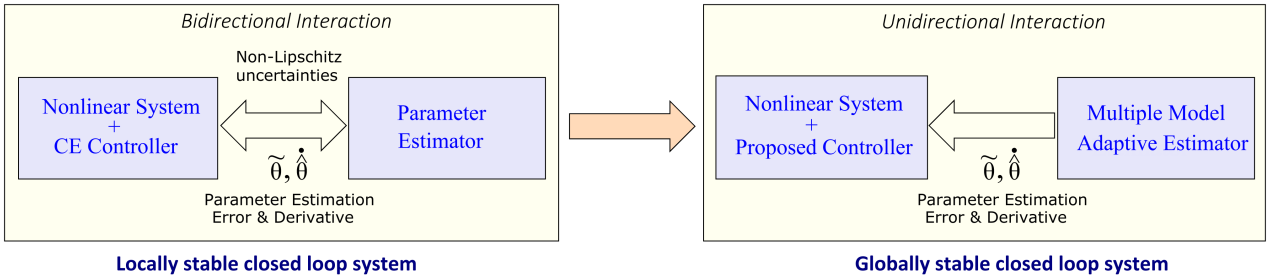

Figure 3.2: Bidirectional robustness interactions transformed to unidirectional interaction under the proposed FTC strategy

models with two layers of adaptation independent of the boundedness of the regressor matrix. It is therefore concluded that the proposed FE/FTC strategy transforms the bidirectional interaction to a unidirectional one as shown in Figure 3.2 (right). Hence, the design modularity is restored and the BIBS design presumption on the system dynamics is eliminated. Furthermore, finite and infinite actuator failures apart from unknown parametric uncertainties are also observed to be compensated using a single controller without switching between identifiers or controllers. Thus, a piecewise continuous and smooth control signal is obtained and the assumption of existence of positive dwell time is relaxed.

Hence, relative to existing results in literature with relevance to the problem of compensating finite and infinite actuator failures, the major contributions of this chapter are enumerated below.

- To the best of the authors' knowledge, this is the first time that an MMAC strategy is proposed to compensate possibly infinite actuator failures. The proposed control scheme ensures boundedness of closed loop signals. The incorporation of a two layer adaptation without switching into the control design results in substantial improvement in transient and steady state performance, under no failure, finite and infinite actuator failure scenarios with almost no additional control usage. The proposed MMAC strategy from its design perspective overcomes all the limitations of earlier multiple model adaptive controllers and hence can be applied to a wider class of nonlinear uncertain systems. Thus, the work presented in this chapter contributes to bridge the potential research gaps in MMAC as well as active FTC literature for nonlinear dynamical systems.

- A rigorous integrated stability analysis of the closed loop system under infinite actuator failures for all $t \in [0, \infty)$ is conducted using a piecewise defined Lyapunov function. A piece of time herein defines the time interval within which the actuator failure pattern does not change. Since occurrence of infinite actuator failures is not deterministic, the closed loop system is first represented as a random nonlinear impulsive system in terms of the piecewise Lyapunov function (PLF). Thereafter, a subsequent recursive formulation of the closed-loop system dynamics in terms of the PLF is arrived at. Global boundedness of closed loop trajectories over all time $t \in [0, \infty)$, is concluded thereafter. Unlike [6, 75], explicit expressions for $\mathcal{L}_\infty$ and $\mathcal{L}_2$ bounds on the output tracking error are derived for $t \in [0, \infty)$ considering both first and second layer of adaptation.

- The interrelation of the output transient performance bounds with the minimum transit time

between two consecutive changes in failure patterns and controller gains is mathematically deduced.

- In case of finite actuator failures or no failure conditions, global asymptotic (exponential) stability of output tracking error is established. Further, the transient performance improvement using the proposed MMAC strategy over single model adaptive control is theoretically proved.
- Decoupling between the controller and the identifier in the proposed MMAC based FE/FTC scheme provides greater design freedom in determining the type of parameter estimator.
- The proposed MMAC scheme with two layer adaptation is further applied to FTC design problem for uncertain nonlinear coupled MIMO systems affected by finite actuator failures. Similar stability properties and convergence characteristics are obtained. Further, transient and steady state performance improvements are observed at the output without any significant increment in the control usage. Results obtained through extensive simulation studies support theoretical propositions. Further, experimental validation on a twin rotor MIMO system demonstrates the practical feasibility and applicability of the proposed MMAC technique.

In view of the above design attributes and advantages, the proposed AMMFTC algorithm proves to be an appealing choice for applications demanding reinforced robust stability and high performance. The chapter is organized as follows: Section 3.2 discusses the proposed adaptive FTC design for multi input single output (MISO) nonlinear systems affected by infinite actuator failures. The design methodology spans through subsections 3.2.1-3.2.2 followed by closed-loop stability analysis in subsection 3.2.3.1 and transient performance analysis in subsection 3.2.3.2. An extensive simulation study is provided in subsection 3.2.4. Next, the proposed MMAC approach is extended for application to the problem of FTC design in MIMO nonlinear systems in Section 3.3. The problem formulation, control design methodology, stability analysis and simulation study are provided in subsections 3.3.1-3.3.4. Experimental study on a twin rotor MIMO system using the proposed AMMFTC is provided under subsection 3.3.5. followed by summary in Section 3.4.

3.2 Adaptive Multiple Model Fault Tolerant Control (AMMFTC) for Infinite Actuator Failures

In this section, an adaptive control strategy will be developed for nonlinear systems with parametric uncertainties and affected by possibly infinite actuator failures.

3.2.1 Problem Statement

The same class of multi-input-single-output (MISO) nonlinear uncertain systems is considered as in [6] and is rewritten below for completeness,

$$\begin{aligned}
\dot{x}_i &= x_{i+1} + f_i(\bar{x}_i)^T\kappa^*, \quad i = \overline{1, \wp - 1} \\
\dot{x}_\wp &= f_0(x,\eta) + f_\wp(x,\eta)^T\kappa^* + \sum_{j=1}^{m} b_j\beta_j(x,\eta)u_j \\
\dot{\eta} &= \Lambda_0(x,\eta) + \sum_{i=1}^{p}\kappa_i^*\Lambda_i(x,\eta) \\
y &= x_1
\end{aligned} \tag{3.1}$$

where,the state vector is defined as $x := [x_1, x_2, \ldots, x_\wp]^T \in \mathbb{R}^\wp$ and $\bar{x}_i := [x_1, x_2, \ldots, x_i]^T \in \mathbb{R}^i$. The term $\wp$ is the relative degree of the system concerned with x_1 as the output. The nonlinearities $f_i(x,\eta) : \mathbb{R}^\wp \times \mathbb{R}^{n-\wp} \to \mathbb{R}^p$ for $i = \overline{0, \wp}$ are assumed to be vectors of known smooth functions. The actuation functions $\beta_j(x,\eta) : \mathbb{R}^\wp \times \mathbb{R}^{n-\wp} \to \mathbb{R} \in \mathfrak{C}^\infty$ for $j = \overline{1, m}$ are known and may be linear or nonlinear in its arguments. The function $y(t) \in \mathbb{R}$ defines the system output and $u_j : [0, \infty) \to \mathbb{R}$ represents the j^{th} control input or rather the output from the j^{th} actuator fed to the plant. Further, $\kappa^* := [\kappa_1^*, \kappa_2^*, \ldots, \kappa_p^*]^T \in \mathbb{R}^p$ and $\{b_j\}_{j=1}^m$ defines the vector of unknown parameters of the plant and unknown actuation coefficients, respectively.

Now, in general, the output of the j^{th} actuator given by u_j is equal to its input u_{Hj}. However, the actuators in the system may experience malfunctioning in the form of partial loss of effectiveness (PLOE), lock-in-place (LIP) and float failures. Further, the actuator failures can occur intermittently and hence, the cardinality of such events are not limited to $(m-1)$. Nevertheless, one actuator should always remain healthy at any failure instant to satisfy the controllability criterion. Therefore, a unified model reflecting the input-output (i/o) characteristics of the j^{th} actuator encompassing the aforementioned types of faults/failures for, $t \in [t_{j,h}^o,\ t_{j,h}^e)$, $h \in \mathbb{Z}_+$ is given below [6].

$$u_j(t) = \begin{cases} K_{j,h}u_{Hj} + \bar{u}_{Fj,h}, & t \in [t_{j,h}^o, t_{j,h}^e) \\ u_{Hj}, & t \in [t_{j,h}^e, t_{j,h+1}^o) \end{cases} \tag{3.2}$$

Herein, $h = 1, 2, \ldots, \infty$ and $K_{j,h} \in [0, 1]$ define the cardinality of occurrence of actuator failures and the state of health of the j^{th} actuator at the h^{th} instant of the failure. The term u_{Hj} is the designed control input to be fed to the j^{th} actuator and u_j defines the j^{th} input of the system. The time variables $t_{j,h}^o$ and $t_{j,h}^e$ denote the time instances at which the h^{th} failure of the j^{th} actuator commences and ends, respectively. Further, the j^{th} actuator remains healthy for the time interval $[t_{j,h}^e, t_{j,h+1}^o)$ until the onset of the $(h+1)^{th}$ failure at $t = t_{j,h+1}^o$. In addition, during the time $[t_{j,h}^o,\ t_{j,h}^e)$, the degree of severity of the j^{th} actuator failure described by K_j and the value at which the actuator is stuck under LIP failure are unknown.

The actuator failure model in (3.2) encompasses i/o characteristics of healthy actuators as well as typical PLOE, LIP and float actuator failures.

- $K_{j,h} = 1$ and $\bar{u}_{Fj,h} = 0$ for $j = \overline{1,m}$, means that the actuators are free from faults and failures.
- $K_{j,h} \in (0,1)$ and $\bar{u}_{Fj,h} = 0$ for $j = \overline{1,m}$ in (3.2) indicates that the actuator suffers from partial loss of effectiveness (PLOE).
- $K_{j,h} = 0$ and $\bar{u}_{Fj,h} \neq 0$ for $j = \overline{1,q}$ with $q \leq m-1$ in the fault model (3.2) reveals that the actuator undergoes a total loss and such a failure typically leaves the actuator jammed at an unknown value denoted by $\bar{u}_{Fj,h}$. Further, $K_j = 0$ and $\bar{u}_{Fj,h} = 0$ for $j = \overline{1,q}$ with $q \leq m-1$ describes actuator float failures.

Prior to the problem statement, the following assumptions are necessary.

Assumption 3.1. *The nonlinear dynamical system in* (3.1) *is so designed that the desired output performance can only be achieved in the event of at most $q \leq m-1$ actuator failures unknown in time, pattern and magnitude.*

Assumption 3.2. *The actuators are assumed to undergo a transition from their normal mode of operation to various failure modes and vice-versa, infinitely many times. Therefore, there exists a non-zero finite transit time $T^* := t^o_{j,h+1} - t^e_{j,h} > 0$ between the occurrence of two consecutive actuator failure patterns. (This assumption is justified later to be instrumental to achieve global boundedness of all closed loop signals)*

Assumption 3.3. *The actuation functions in* (3.1)*, given by $\beta_j(x,\eta)$ are assumed to be non-zero and the sign of the actuation coefficients, that is, sign(b_j) for $j = \overline{1,m}$ are known.*

Assumption 3.4. *The reference trajectory and its successive time derivative signals $(y_r,\ \dot{y}_r,\ \ddot{y}_r, \ldots, y_r^{(\wp)})$ are known, piecewise continuous, bounded and hence belong to a compact set.*

Assumption 3.5. *The upper/lower bounds on actuation coefficients $0 < \underline{b}_j \leq |b_j| \leq \overline{b}_j$, $|\bar{u}_{Fj,h}| < \bar{u}$ and $0 < \underline{K}_j \leq K_j \leq 1$ are known which means that $\underline{b}_j$, $\overline{b}_j$, $u_{\max}$ and $\underline{K}_j$ for $j = \overline{1,m}$ are known finite positive constants. The unknown parameter vector κ^* belongs to a known convex compact set, i.e., $\kappa^* \in \mathcal{S}_{\kappa^*} \subset \mathbb{R}^p$. Here, $\mathcal{S}_{\kappa^*}$ denotes the parameter space in $\mathbb{R}^p$ and $\forall \kappa_1, \kappa_2 \in \mathcal{S}_{\kappa^*}$, the relation $\|\kappa_1 - \kappa_2\| \leq \kappa_{\max}$ holds.*

Assumption 3.6. *The subsystem dynamics given by $\dot{\eta} = \Lambda_0(x,\eta) + \sum_{i=1}^{p} \kappa_i^* \Lambda_i(x,\eta)$ is input-to-state-stable (ISS) with x as its input. This implies that system dynamics is assumed to exhibit a minimum phase behavior.*

Having stated the assumptions, the control objectives of this work are as follows:

- To compensate the adverse effects of infinite actuator failures unknown in time, pattern and magnitude and ensure boundedness of all closed loop signals $\forall t \in [0,\infty)$ in presence of unknown parametric uncertainties.
- To enhance the output transient performance at start-up and in the event of unknown actuator failures considered in (3.2). The aim is to quantify the output transient performance using $\mathcal{L}_2$

and $\mathcal{L}_\infty$ bounds and thereafter prove the improvement in transient performance theoretically. It is worth mentioning that usually, an improved output performance is achieved at the cost of high input usage. However, such a practice may result in a degraded input performance. Thus, the control design algorithm is to be aimed at guaranteeing a promising output transient performance without any significant increment of the control energy spent. The intended objective behind is to *surpass the conventional trade-off between output and input performance* at both instances of start-up and post actuator failures.

- To ensure that the output tracking error $y - y_r$ converges to a arbitrarily small set in the vicinity of the origin. Further, explicit expressions to calculate the ultimate bounds on the tracking error are to be derived.
- To achieve asymptotic stability of the tracking error dynamics in the event of finite actuator failures, i.e., $\lim_{t\to\infty}(y(t) - y_r(t)) = 0$.

3.2.2 Adaptive Fault Tolerant Control Design

Firstly, for simplicity of representation, let us define the index set of actuators as $\mathscr{B} := \{j_1, j_2, \ldots, j_m\}$. Thereafter, another two subsets of $\mathscr{B}$ as $\mathscr{B}_{tot_F} := \{j_1, j_2, \ldots, j_{q_h}\}$ and $\mathscr{B}_{tot_H} := \mathscr{B}/\mathscr{B}_{tot_F}$ are defined. Denoting T_h for $h \in \mathbb{Z}_+$ to be the time instant when the failure pattern changes, it has been discussed in the previous section that the fault pattern remains fixed until the time instant T_{h+1}. Further, in accordance with Assumption 3.4, stable solutions to the adaptive fault tolerant control problem can be ensured only if there are at most $q_h (0 \leq q_h \leq m-1)$ actuator failures during the time interval $(T_h,\ T_{h+1})$. Therefore, the set $\mathscr{B}_{tot_F}$ contains indices corresponding to totally failed actuators. However, the remaining healthy and partially failed actuator indices belong to the set $\mathscr{B}_{tot_H}$. Incorporating the actuator failure model (3.2) into the system dynamics and substituting the j^{th} control input as $u_{Hj} = \text{sign}(b_j)v/\beta_j$ unfolds two different dynamical equations at the $\wp^{th}$ step corresponding to faulty and fault free conditions as shown below.

- No fault condition

$$\dot{x}_\wp = f_0(x,\eta) + f_\wp(x,\eta)^T\kappa^* + \sum_{j=1}^{m}|b_j|v \tag{3.3}$$

- Faulty condition

$$\dot{x}_\wp = f_0(x,\eta) + f_\wp(x,\eta)^T\kappa^* + \sum_{j\in\mathscr{B}_{tot_H}} K_{j,h}|b_j|v + \sum_{\mathscr{B}_{tot_F}} b_j\bar{u}_{Fj,h}\beta_j \tag{3.4}$$

Therefore, a unified mathematical model with an actuator failure parametrization encompassing faulty and fault-free system dynamics in (3.4) and (3.3) can be framed as,

$$\begin{aligned}\dot{x}_i &= x_{i+1} + f_i(\bar{x}_i)^T\kappa^*, \qquad i = \overline{1, \wp-1}\\ \dot{x}_\wp &= f_0(x,\eta) + f_\wp(x,\eta)^T\kappa^* + b^*v + \beta^T\bar{u}^*\end{aligned} \tag{3.5}$$

where,

$$b^* := \begin{cases} \sum_{j=1}^{m} |b_j|, & \text{for } K_{j,h} = 1 \text{ and } \bar{u}_{Fj,h} = 0 \forall\ j\ \in \mathscr{B} \\ \sum_{j \in \mathscr{B}_{tot_H}} K_{j,h}|b_j|, & \text{for } K_{j,h} \in [0,1) \text{ and } \bar{u}_{Fj,h} \neq 0\ \forall\ j\ \in \mathscr{B}_{tot_F} \end{cases} \tag{3.6}$$

$$\bar{u}^* := [0, \ldots, 0]^T \in \mathbb{R}^m, \text{ for } K_{j,h} = 1 \text{ and } \bar{u}_{Fj,h} = 0\ \forall\ j\ \in \mathscr{B} \tag{3.7}$$

$$\bar{u}^* := [\{b_{j_k}\bar{u}_{Fj_k,h}\}_{k=1}^{q_h}, 0, \ldots, 0]^T \in \mathbb{R}^m \text{ for } K_{j,h} \in [0,1) \text{ and } \bar{u}_{Fj,h} \neq 0\ \forall\ j\ \in \mathscr{B}_{tot_F} \tag{3.8}$$

Further, $\beta := [\{\beta_j(x,\eta)\}_{j=1}^m]^T \in \mathbb{R}^m$ is the vector of actuation functions. The unknown system parameters and those induced due to actuator failures are redefined using a lumped parameter vector $\theta^* := [\theta_1^*,\ \theta_2^*,\ \theta_3^*]^T = [b^*,\ \kappa^*,\ \bar{u}^*]^T \in \mathbb{R}^{m+p+1}$. The actuator failure induced unknown parameters θ_1^* and θ_3^* are time varying and hence are characterized by piecewise constant time dependent signals instead of being constants for all $t > 0$. These parameters experience jumps at the occurrence of abrupt actuator faults and failures. Therefore, from assumption 3.5, it is further assumed that $\theta_1^* \geq \ell := \min_{1 \leq j \leq m}\{\underline{K_j}\underline{b_j}\} > 0$. Besides, at the time instant t in the event of occurrence of an actuator failure, the failure induced parameter jumps satisfy $|\theta_1^*(t^+) - \theta_1^*(t^-)| \leq \sum_{j=1}^{m} \overline{b}_j - \ell$ and $|\theta_{3j}^*(t^+) - \theta_{3j}^*(t^-)| \leq 2\overline{b}_j\overline{u}$. Since, one actuator should always be alive to satisfy the controllability condition, the inequality $b^* > \ell$ holds. Given that the parametrization of the fault affected system is complete (referred to (3.5)), it is now possible to proceed with the design of the proposed multiple model estimator based indirect adaptive backstepping controller to compensate possibly infinite actuator failures.

3.2.2.1 Parameter Estimation using Multiple Identifiers with Dual Layer Adaptation

In this section, firstly the design of the online parameter estimator using multiple identification models with first layer of adaptation is explained. Thereafter, a piecewise stability analysis is conducted to infer the boundedness and convergence properties of parameter estimation error and observer error dynamics corresponding to each of the multiple (N) adaptive identification models.

To initiate the design of observers, the fault/failure parameterized dynamics in (3.5) are rewritten in parametric x-model as,

$$\dot{x} = f(x) + \Phi^T(x,v)\theta^* \tag{3.9}$$

Wherein the function vector $f(x)$ and the regressor matrix $\Phi(x,v)$ are defined as,

$$f(x) = [x_2,\ x_3, \ldots,\ x_\wp,\ f_0(x,\eta)]^T \in \mathbb{R}^\wp\ \&\ \Phi^T(x,\eta) = \begin{bmatrix} 0 & f_1(x_1)^T & 0_{1\times m} \\ 0 & f_2(\bar{x}_2)^T & 0_{1\times m} \\ \vdots & \vdots & \vdots \\ v & f_p(x,\eta)^T & \beta^T \end{bmatrix} \in \mathbb{R}^{\wp \times p+m+1}. \tag{3.10}$$

From assumption 3.9, it is known that the unknown parameter vector resided within a closed compact

set $\mathcal{S}_{\theta^*}$ defined as

$$\mathcal{S}_{\theta^*} := [\underline{\theta_1^*}, \overline{\theta_1^*}] \times [\underline{\theta_{21}^*}, \overline{\theta_{21}^*}] \times \ldots \times [\underline{\theta_{2p}^*}, \overline{\theta_{2p}^*}] \times [\underline{\theta_{31}^*}, \overline{\theta_{31}^*}] \times \ldots \times [\underline{\theta_{3m}^*}, \overline{\theta_{3m}^*}]$$

Where, $\underline{\theta_i^*}$ and $\overline{\theta_i^*}$ denote the lower and upper bounds on the unknown parameters θ_i^* for $i = 1, \ldots, (p+m+1)$.

A. First Layer Adaptation

The N adaptive identifiers/estimators are described by differential equations with non-zero initial values of the unknown parameter vector as follows,

$$\dot{\hat{x}}_{(\mu)} = A_\mu(x,t)(\hat{x}_{(\mu)} - x) + f(x) + \Phi^T(x,v)\hat{\theta}_{(\mu)} \tag{3.11}$$

$$\hat{\theta}_{(\mu)}(t) = \hat{\theta}_{(\mu)}(t_0) + \Gamma_\mu \int_{t_0}^{t} \text{Proj}[\Phi(x,v)P_\mu(x - \hat{x}_{(\mu)})]d\tau \tag{3.12}$$

The subscript $\mu = 1, \ldots, N$ denotes each of the adaptive identification models, $\hat{x}_{(\mu)}$ and $\hat{\theta}_{(\mu)}$ are the estimates of the state vector and the unknown parameter vector θ^*, respectively from the μ^{th} identification model. The operator Proj$\{\cdot\}$ is a smooth projection operator to ensure that the parameter estimate $\hat{\theta}_{(\mu)}$ resides in $\mathcal{S}_{\theta^*}$. The matrix $A_\mu(x,t) := A_{\mu 0} - \gamma\Phi(x,v)^T\Phi(x,v)P_\mu$ is so chosen to ensure boundedness of μ^{th} estimator error dynamics irrespective of the boundedness of the regressor matrix $\Phi(x,v)$ for $\mu \in \{1, 2, \ldots, N\}$. The adaptation rate for each of the N models is given by a user designed positive definite matrix $\Gamma_\mu \in \mathbb{R}^{p+m+1 \times p+m+1}$. Further, $A_{\mu 0}$ is a stable matrix satisfying the Lyapunov equation, that, is,

$$A_{\mu 0}^T P_\mu + P_\mu A_{\mu 0} = -Q_\mu, \;\; P_\mu, \; Q_\mu \; \in \; \mathbb{R}^{\wp \times \wp} \text{ and } \mu = \{1, \ldots, N\} \tag{3.13}$$

In addition P_μ and Q_μ are positive definite symmetric matrices chosen by the designer and may have the same values for all the N identification models.

Let us now define the identification error and the parameter estimation error corresponding to the μ^{th} identification model as $\tilde{x}_{(\mu)} := x - \hat{x}_{(\mu)}$ and $\tilde{\theta} := \theta^* - \hat{\theta}_{(\mu)}$, respectively for $\mu \in \{1, 2, \ldots, N\}$. Referring to equations (3.11)-(3.12), the identification error dynamics for each of the N adaptive estimators are derived as,

$$\dot{\tilde{x}}_{(\mu)} = (A_{\mu 0} - \gamma\Phi(x,v)^T\Phi(x,v)P_\mu)\tilde{x}_{(\mu)} + \Phi^T(x,v)\tilde{\theta}_{(\mu)} \tag{3.14}$$

where, $\hat{\theta}_{(\mu)}(t_0) \in \Omega(t_0) \subseteq \mathcal{S}_{\theta^*}$ for $\mu = 1, \; 2, \ldots, \; N$. The stability and convergence properties of all the N adaptive estimators are summarized in Theorem 3.1. Since the FTC design aims at compensating infinite actuator failures, following a piecewise stability analysis at this point would be helpful in analyzing the stability of the overall closed loop system dynamics for $t \in [0, \infty)$. It is assumed that the actuator fault/failure pattern does not change within the time interval $[T_h, \; T_{h+1})$ for $h \in \mathbb{Z}_+$.

Remark 3.1. *The rationale behind the use of N adaptive identification models is to improve the output transient performance. Now, considering the parameter space S_{θ^*} defined earlier, the number of identification models required is given by $N = 2^{p+m+1}$. Therefore, the nonzero initial values of the*

unknown parameter estimates $\hat{\theta}_{(\mu)}$ with respect to each of the N adaptive identifiers should be so chosen such that $\mathcal{S}_{\theta^*} \supseteq \Omega(t_0)$. $\Omega(t_0)$ is a convex set formed by the initial parameter estimates $\{\hat{\theta}_{(\mu)}(t_0)\}_{\mu=1}^{N}$ and the actual unknown parameter vector θ^* resides in the set $\Omega(t_0)$. Nevertheless, it is evident that as the number of unknown parameters increase, the number of identification models N also escalates. Although increment in the number of models results in a fair transient performance, it is achieved at the cost of a high computational complexity. Increase in computational burden manifests itself in the form of input delays, state delays and communication delays in real time systems resulting in degraded system behavior and is therefore not desirable in safety critical applications.

Theorem 3.1. *(First layer of adaptation) Let us consider that the solutions of the adaptive identifiers given by* (3.11)-(3.12) *and the identification error dynamics in* (3.14) *for $\mu = \{1, \ldots, N\}$, are defined on the interval $[T_h,\ T_{h+1})$. Then the following properties hold under the framework of first layer adaptation for each of the N adaptive identification models for $\Gamma_\mu,\ P_\mu,\ Q_\mu > 0$.*

(i) $\tilde{\theta}_{(\mu)}(t) \in \mathcal{L}_\infty[T_h,\ T_{h+1})$

(ii) $\tilde{x}_{(\mu)}(t) \in \mathcal{L}_2[T_h,\ T_{h+1}) \cap \mathcal{L}_\infty[T_h,\ T_{h+1}),\ \dot{\tilde{x}}_{(\mu)}(t) \in \mathcal{L}_\infty[T_h,\ T_{h+1})$

(iii) $\dot{\hat{\theta}}_{(\mu)}(t) \in \mathcal{L}_2[T_h,\ T_{h+1})$

Proof.

Let us take a Lyapunov function $V_{(\mu),h}(\tilde{x}_{(\mu)}, \tilde{\theta}_{(\mu)}, t) : \mathbb{R}^{\wp} \times \mathbb{R}^{p+m+1} \times [T_h,\ T_{h+1})$ as,

$$V_{(\mu),h} = \frac{1}{2}\tilde{x}_{(\mu)}^T P_\mu \tilde{x}_{(\mu)} + \frac{1}{2}\tilde{\theta}_{(\mu)}^T \Gamma_\mu^{-1} \tilde{\theta}_{(\mu)} \tag{3.15}$$

Given the identification error dynamics (3.14) and owing to the fact that the failure pattern remains fixed for $[T_h,\ T_{h+1})$ results in, $\dot{\tilde{\theta}} = -\dot{\hat{\theta}}$ for $[T_h,\ T_{h+1})$. The first time derivative of $V_{(\mu)}$ yields the following,

$$\dot{V}_{(\mu),h} = -\tilde{x}_{(\mu)}^T Q_\mu \tilde{x}_{(\mu)} - \gamma \tilde{x}_{(\mu)}^T P_\mu \Phi^T \Phi P_\mu \tilde{x}_{(\mu)} + \tilde{\theta}_{(\mu)}^T \Phi P_\mu \tilde{x}_{(\mu)} - \tilde{\theta}_{(\mu)}^T \Gamma_\mu^{-1} \dot{\hat{\theta}}_{(\mu)} \tag{3.16}$$

where the matrix $Q_\mu := -(A_{\mu 0}^T P_\mu + P_\mu A_{\mu 0})/2 > 0$ and as defined earlier, P_μ is a positive definite symmetric matrix. Substituting the parameter update law (3.12) in (3.16) and using the properties of projection operator from [69] as $-\tilde{\theta}_{(\mu)}^T \Gamma_\mu^{-1} \text{Proj}(\Gamma_\mu \Phi P_\mu \tilde{x}_{(\mu)}) \leq -\tilde{\theta}_{(\mu)}^T \Gamma_\mu^{-1} \Gamma_\mu \Phi P_\mu \tilde{x}_{(\mu)}$, we arrive at the following,

$$\dot{V}_{(\mu),h} \leq -\underline{\lambda}(Q_\mu)\|\tilde{x}_{(\mu)}\|^2 - \gamma\|\Phi P_\mu \tilde{x}_{(\mu)}\|^2 < 0 \tag{3.17}$$

Thereafter, integrating the above inequality (3.17) for the time interval $t \in [T_h,\ T_{h+1})$, rearranging and using the notation $x^T P x = \|x\|_P^2$ yields,

$$\|\tilde{x}_{(\mu)}\|_{\mathcal{L}_2[T_h, T_{h+1})} = \frac{1}{\sqrt{2\underline{\lambda}(Q_\mu)}}(\|\tilde{x}_{(\mu)}(T_h)\|_{P_\mu}^2 + \|\tilde{\theta}_{(\mu)}(T_h)\|_{\Gamma_\mu^{-1}}^2)^{\frac{1}{2}} \tag{3.18}$$

Since a projection operator is used for parameter estimation, it is very straightforward to conclude that $\tilde{\theta}_{(\mu)} \in \mathcal{L}_\infty[T_h,\ T_{h+1})$. Further, from (3.18) and the inequality $\tilde{x}_{(\mu)}^T P_\mu \tilde{x}_{(\mu)} \leq 2V_{(\mu)}(t) \leq 2V_{(\mu)}(T_h)$, the signal properties $\tilde{x}_{(\mu)}(t) \in \mathcal{L}_2 \cap \mathcal{L}_\infty$ are inferred. From the above arguments, $\dot{\tilde{x}}_{(\mu)}(t) \in \mathcal{L}_\infty$ follows. Thereafter using (3.17), the $\mathcal{L}_2$-integrability is proved and its $\mathcal{L}_2$ bound is given as,

$$\|\dot{\tilde{\theta}}_{(\mu)}\|_{\mathcal{L}_2[T_h,T_{h+1})} = \sqrt{\frac{\overline{\lambda}(\Gamma_\mu^2)}{2\gamma}}(\|\tilde{x}_{(\mu)}(T_h)\|_{P_\mu}^2 + \|\tilde{\theta}_{(\mu)}(T_h)\|_{\Gamma_\mu^{-1}}^2)^{\frac{1}{2}} \tag{3.19}$$

The proof is complete. □

Now, to develop the proposed parameter estimation procedure based on multiple models, the following lemma would be helpful.

Lemma 3.1. *Let us consider the N adaptive estimators defined by* (3.11) *and the adaptive laws given in* (3.12) *with initial conditions $\hat{\theta}_{(\mu)}(t_0) \in \Omega(t_0)$. If the unknown parameter vector θ^* is contained in the convex hull $\Omega(t_0)$ of the set $\{\hat{\theta}_{(\mu)}(t_0)\}_{\mu=1}^N$, then it also resides within the convex hull $\Omega(t)$ of the set $\{\hat{\theta}_{(\mu)}(t)\}_{\mu=1}^N \forall t \geq t_0$.*

Proof. The proof is simple and follows from the linear algebra of convex sets. □

B. Second Layer of Adaptation

Speed and accuracy of unknown parameter estimation $\hat{\theta}$, are two essential attributes which primarily decide the output performance of an indirect adaptive control system. Essentially, since the proposed design assumes the knowledge of unknown parameter bounds, such bounds may be located far away from the actual parameter vector θ^*. Hence, the lumped parameter space $\mathcal{S}_{\theta^*}$ can be arbitrarily large and therefore the estimation from each of the N observers with first layer of adaptation will experience a slow parameter estimation with high overshoots exhibiting oscillatory behavior. This will eventually translate in a degradation of the output transient performance, which is undesirable in safety critical applications. Consequently, exploiting the convex set properties of the parameter space $\mathcal{S}_{\theta^*}$ in Lemma 3.1, a second layer of adaptation is resorted to in order to achieve a fast and accurate estimation of unknown parameters. From the theory of convex sets and convex hull, it is clear that the initial parameter estimation set $\Omega(t_0) \subset \mathcal{S}_{\theta^*}$ can still enclose the actual parameter vector θ^* if the number of adaptive identification models is chosen to be $N = p + m + 1 + 1$. Following this procedure can significantly decrease the number of estimation models thereby reducing computational burden. In the second adaptation layer, a weighted convex combination of the parameter estimates $\hat{\theta}_{(\mu)}$ for $\mu = \{1, \ldots, N\}$ with adaptive learning is resorted to. The rationale behind such a combination is that the estimate of the parameter vector after such a weighted combination gains closer proximity to the actual parameter vector θ^* in the convex set $\mathcal{S}_{\theta^*}$ compared to $\hat{\theta}_{(\mu)}$ from each of the $(p + m + 2)$ identification models (indexed by $\mu = \{1, \ldots, p + m + 2\}$) with every iteration and results in fast estimation.

The procedure is mathematically described as follows. Let the weighted convex combination of the parameter estimates obtained from first adaptation layer be denoted as $\hat{\theta}_s$. As per definition the final

parameter estimate is mathematically represented as,

$$\hat{\theta}_s := \sum_{\mu=1}^{(p+m+2)} w_\mu^* \hat{\theta}_{(\mu)}, \quad w_\mu^* \in [0,1] \text{ and } \sum_{\mu=1}^{(p+m+2)} w_\mu^* = 1$$

where, w_μ^* for $\mu = \{1, \ldots, p+m+2\}$ are the weights assigned to the parameters estimated for the N identification models. However, these weights would be generally unknown and time varying depending on the uncertainties affecting the system. Therefore, a Lyapunov based adaptive weight learning law is formulated which eliminates the requirement of the knowledge of weight parameters w_μ^*. In what follows next, the formulation of the weight update law is presented and its stability properties are derived.

In order to formulate the update laws for adaptive weight learning, constructing a suitable estimation model is necessary and is formed as follows. A similar approach as presented in [121], is adopted for learning the weights w_μ online. Assuming $\theta^* = \sum_{\mu=1}^{p+m+2} w_\mu^* \hat{\theta}_{(\mu)}$, and subtracting θ^* from both sides yields, $\sum_{\mu=1}^{p+m+2} w_\mu^* (\hat{\theta}_{(\mu)} - \theta^*) = 0$. Taking the time derivative of the resulting equality leads to,

$$\sum_{\mu=1}^{p+m+2} w_\mu^* (\dot{\hat{\theta}}_{(\mu)} - \dot{\theta}^*) = 0 \tag{3.20}$$

Rearranging the above equation (3.20) gives,

$$\sum_{\mu=1}^{p+m+1} w_\mu^* (\dot{\hat{\theta}}_{(\mu)} - \dot{\hat{\theta}}_{(p+m+2)}) = -\dot{\hat{\theta}}_{(p+m+2)} \Longrightarrow \sum_{\mu=1}^{p+m+1} w_\mu^* (\tilde{x}_{(\mu)} - \tilde{x}_{(p+m+2)}) = -\tilde{x}_{(p+m+2)} \tag{3.21}$$

Defining $w^* := [\{w_\mu^*\}_{\mu=1}^{p+m+1} \; w_{p+m+2}^*]^T$, $\bar{w}^* := [\{w_\mu^*\}_{\mu=1}^{p+m+1}]^T$, $\triangle\tilde{X}(t) := [\text{diag}\{\tilde{x}_{(\mu)} - \tilde{x}_{(p+m+2)}\}_{\mu=1}^{p+m+1}] \in \mathbb{R}^{\wp \times (p+m+1)}$ and $r(t) := -\tilde{x}_{(p+m+2)} \in \mathbb{R}^{\wp}$, equation (3.21) can be rewritten in a vector form as, $\triangle\tilde{X}(t)\bar{w}^* = r(t)$. Therefore, since the elements of the vector $\triangle\tilde{X}(t)$ and $r(t)$ are known with the weight vector w^* being unknown, the weight estimation model can be framed as,

$$\triangle\tilde{X}(t)\hat{\bar{w}} = \hat{r}(t) \tag{3.22}$$

Further, using the weight estimation model (3.22), the weight update law is chosen as

$$\dot{\hat{\bar{w}}}(t) = -\triangle\tilde{X}(t)^T \triangle\tilde{X}(t)\hat{\bar{w}}(t) + \triangle\tilde{X}(t)^T r(t); \quad \hat{w}_{p+m+2} = 1 - \sum_{\mu=1}^{p+m+1} \hat{w}_\mu \tag{3.23}$$

Finally, the unknown parameter vector θ^* is estimated as $\hat{\theta}_s := \sum_{\mu=1}^{p+m+2} \hat{w}_\mu \hat{\theta}_{(\mu)}$.

Theorem 3.2. *Let us consider the second layer of adaptive parameter estimate* $\hat{\theta}_s := \sum_{\mu=1}^{p+m+2} \hat{w}_\mu \hat{\theta}_{(\mu)}$

and the weight learning law given by (3.23) *defined within the time interval* $[T_h,\ T_{h+1})$. *The following properties hold: (i)* $\hat{w} \in \mathcal{L}_\infty[T_h,\ T_{h+1})$; *(ii)* $\dot{\hat{w}} \in \mathcal{L}_\infty[T_h,\ T_{h+1})$.

Proof.

To prove the properties of the adaptive weight estimates $\hat{w}_\mu$ for $\mu = \{1, \ldots, p+m+2\}$, a Lyapunov function defined over the time interval $[T_h,\ T_{h+1})$ is called upon as $V_{w,h} : \mathbb{R}^{p+m+1} \times [T_h,\ T_{h+1}) \to \mathbb{R}_+$ given by,

$$V_{w,h} = \frac{1}{2}\tilde{\bar{w}}^T(t)\tilde{\bar{w}}(t) \tag{3.24}$$

where, $\tilde{\bar{w}}(t) := \bar{w}^*(t) - \hat{\bar{w}}(t)$. Taking the time derivative of $V_{w,h}$ and the subsequent substitution of the weight adaptation law (3.23) yields,

$$\begin{aligned}\dot{V}_{w,h} &= -(\bar{w}^* - \hat{\bar{w}})^T(-\triangle\tilde{X}(t)^T\triangle\tilde{X}(t)\hat{\bar{w}}(t) + \triangle\tilde{X}(t)^T\triangle\tilde{X}(t)\bar{w}^*(t)) \\ &= -(\bar{w}^* - \hat{\bar{w}})^T\triangle\tilde{X}(t)^T\triangle\tilde{X}(t)(\bar{w}^* - \hat{\bar{w}}) = -\tilde{\bar{w}}(t)^T M(t)\tilde{\bar{w}}(t) < 0\end{aligned} \tag{3.25}$$

Here, $M(t) := \triangle\tilde{X}(t)^T\triangle\tilde{X}(t) > 0$ and since $\dot{V}_{w,h}$ is negative definite, integrating both sides of the equality (3.25) in the interval $[T_h,\ T_{h+1})$ and using Hölder's inequality results in,

$$-\int_{T_h}^{T_{h+1}} \dot{V}_{w,h}(t)dt \leq \|M\|_\infty \int_{T_h}^{T_{h+1}} \tilde{\bar{w}}^T(t)\tilde{\bar{w}}(t)dt < \infty \tag{3.26}$$

Therefore, the negative definiteness of $\dot{V}_{w,h}$ and the above inequality (3.26) proves that $\hat{\bar{w}}, \hat{w} \in \mathcal{L}_\infty[T_h,\ T_{h+1})$ and $\dot{\hat{\bar{w}}} \in \mathcal{L}_\infty[T_h,\ T_{h+1})$. Further, $\hat{w}_{p+m+2}$ is also bounded. The proof is complete. □

3.2.2.2 Backstepping Control Design

The design procedure is initiated by defining the error variables as,

$$z_1 = x_1 - y_r, \tag{3.27}$$

$$z_i = x_i - \alpha_{i-1} - y_r^{(i-1)} \tag{3.28}$$

where $i = \overline{2, \wp}$. Now utilizing the plant dynamics in (3.1), and taking the first time derivative of the error variables yields,

$$\dot{z}_i = z_{i+1} + \alpha_i + f_i(\bar{x}_i)\theta_2^* - \dot{\alpha}_{i-1} \tag{3.29}$$

$$\dot{z}_\wp = f_0(x,\eta) + f_\wp(x,\eta)^T\theta_2^* + \theta_1^* v + \beta^T\theta_3^* - \dot{\alpha}_{\wp-1} \tag{3.30}$$

Here $i = \overline{1, \wp - 1}$. The variables α_i are the virtual control inputs stabilizing each of the tracking error subsystem dynamics in z_i (3.29)-(3.30). These stabilizing functions α_i are given by (3.31).

$$\alpha_i = -z_{i-1} - c_i z_i - \bar{c}_i \|\psi_i\|^2 z_i - g_i \left\| \frac{\partial \alpha_{i-1}}{\partial \hat{\theta}_2} \right\|^2 z_i - \psi_i^T \hat{\theta}_2 + \sum_{k=1}^{i-1} \left(\frac{\partial \alpha_{i-1}}{\partial x_k} x_{k+1} + \frac{\partial \alpha_{i-1}}{\partial y_r^{(k-1)}} y_r^{(k)} \right) \tag{3.31}$$

with $i = \overline{1, \wp - 1}$ and $\psi_i := f_i(\bar{x}_i) - \sum_{k=1}^{i-1} \frac{\partial \alpha_{i-1}}{\partial x_k} f_k(\bar{x}_k)$. Due to actuator failure induced uncertainties, the $\wp^{th}$ design step is quite different from the procedure followed in the previous steps. In Step $\wp$, the controller design is initiated by defining the $z_\wp$-dynamics in an expanded form with the actual control law $v = v_1 + v_2$, as follows.

$$\begin{aligned} \dot{z}_\wp = {} & f_0(x, \eta) + f_\wp(x, \eta)^T \hat{\theta}_2 + \beta^T \hat{\theta}_3 + \hat{\theta}_1 v_1 + \tilde{\theta}_1 v_1 + \theta_1^* v_2 - y_r^{(\wp)} - \sum_{k=1}^{\wp-1} \left(\frac{\partial \alpha_{\wp-1}}{\partial x_k} x_{k+1} - \frac{\partial \alpha_{\wp-1}}{\partial y_r^{(k-1)}} y_r^{(k)} \right) \\ & + \left(\beta^T \tilde{\theta}_3 + \psi_\wp^T \tilde{\theta}_2 - \frac{\partial \alpha_{\wp-1}}{\partial \hat{\theta}_2} \dot{\hat{\theta}}_2 \right) \end{aligned} \tag{3.32}$$

The first part of the control input $v(t)$ is chosen as follows,

$$v_1 = \frac{1}{\hat{\theta}_1} (-f_0(x, \eta) - f_\wp(x, \eta)^T \hat{\theta}_2 - \beta^T \hat{\theta}_3 - z_{\wp-1} + \sum_{k=1}^{\wp-1} \left(\frac{\partial \alpha_{\wp-1}}{\partial x_k} x_{k+1} - \frac{\partial \alpha_{\wp-1}}{\partial y_r^{(k-1)}} y_r^{(k)} \right) + y_r^{(\wp)}), \tag{3.33}$$

Such a choice of $v_1(t)$ yields the resulting $z_\wp$-dynamics as given below,

$$\dot{z}_\wp = -z_{\wp-1} + \theta_1^* v_2 + \tilde{\theta}_1 v_1 + \beta^T \tilde{\theta}_3 + \psi^T \tilde{\theta}_2 - \frac{\partial \alpha_{\wp-1}}{\partial \hat{\theta}_2} \dot{\hat{\theta}}_2 \tag{3.34}$$

Now being left with the design of v_2 to arrive at the final control law v, the signal v_2 is chosen as follows,

$$v_2 = \ell^{-1} \big(- c_\wp z_\wp - \bar{c}_\wp \big(|v_1|^2 + \|\beta\|^2 + \|\psi_\wp\|^2 \big) z_\wp - g_\wp \left\| \frac{\partial \alpha_{\wp-1}}{\partial \hat{\theta}_2} \right\|^2 z_\wp \big) \tag{3.35}$$

Thereafter, substituting the expression for v_2 in (3.34) and using the sum of squares inequality leads to,

$$z_\wp \dot{z}_\wp \leq \frac{\theta_1^*}{\ell} c_\wp z_\wp^2 + \frac{1}{4\bar{c}_\wp} \big(\|\tilde{\theta}_1\|^2 + \|\tilde{\theta}_2\|^2 + \|\tilde{\theta}_3\|^2 \big) + \frac{\|\dot{\hat{\theta}}_2\|^2}{4 g_\wp} - z_\wp z_{\wp-1} \tag{3.36}$$

The inequality in (3.36) would be useful while deriving the stability results of the proposed control. Finally, we arrive at the actual control law $v(t)$ as,

$$v(t) = v_1(t) + v_2(t) \tag{3.37}$$

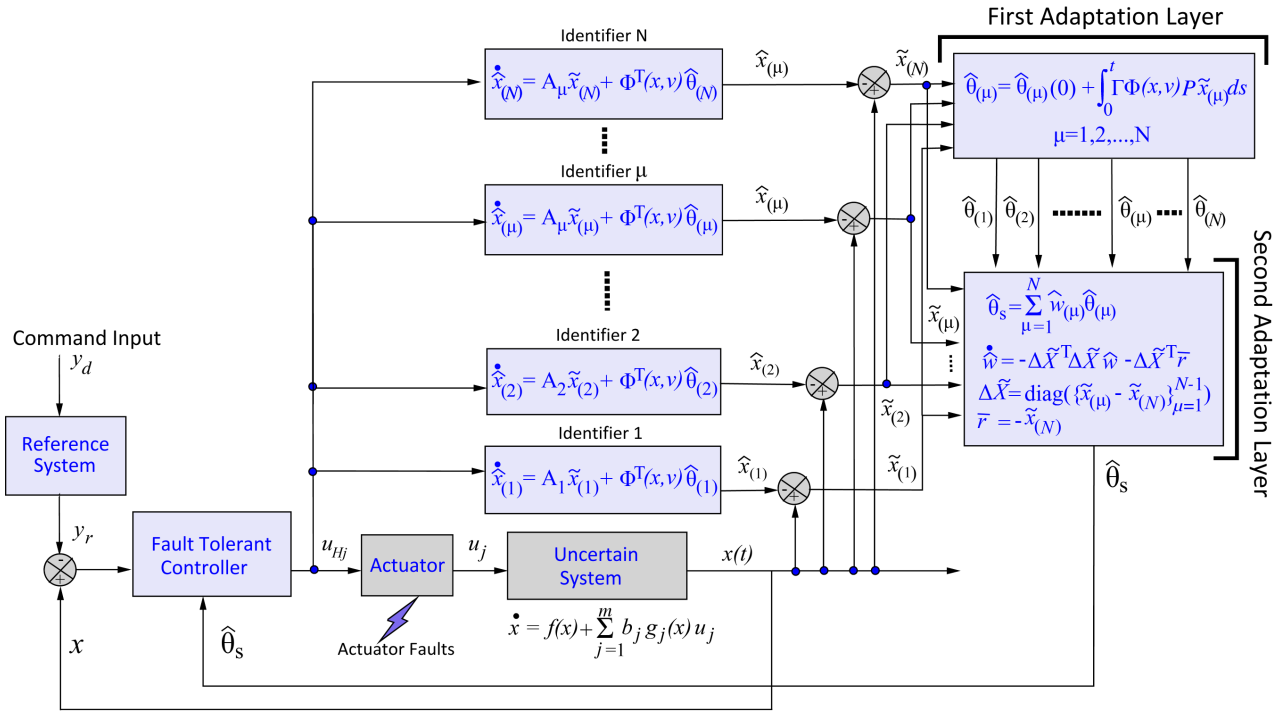

Figure 3.3: Block diagrammatic representation of the proposed adaptive fault tolerant control scheme (AMMFTC).

where the signals $v_1(t)$ and $v_2(t)$ have been defined in the preceding text in equations (3.33) and (3.35). The equations (3.29)-(3.30), (3.31) and (3.33)-(3.35) are the fundamental equations which would be required in implementation of the proposed control law. The control design parameters c_i, $\bar{c}_i$, $g_{\wp}$ are positive scalars.

Figure 3.3 shows a schematic block diagram summarizing the proposed control design procedure.

3.2.3 Main Results

3.2.3.1 Stability Analysis of the Proposed Control System

Herein, prior to the closed loop stability analysis of the proposed adaptive control system, the following preliminary calculations and statements are necessary in the subsequent analysis. As mentioned earlier, the compact set wherein the parameter θ^* resides is denoted by $\mathcal{S}_{\theta^*}$ defined as,

$$\mathcal{S}_{\theta^*} := \{\theta^* \in \mathbb{R}^{p+m+1} |\ \ell \leq \theta_1^* \leq \sum_{j=1}^{m} \bar{b}_j,\ \theta_2 \in \mathcal{S}_{\kappa^*} \subseteq \mathbb{R}^p,\ |\theta_{3j}^*| \leq \bar{b}_j \bar{u}_j,\ j = \overline{1,m}\} \tag{3.38}$$

Lemma 3.2. *The projection operator utilized in the parameter estimation law* (3.12) *has the following properties [69]: (i) The mapping Proj:*$\mathbb{R}^{p+m+1} \times \mathcal{S}_{\theta^*} \rightarrow \mathbb{R}^{p+m+1}$ *is locally Lipschitz in its arguments; (ii)* $Proj\{\tau\}^T \Gamma_\mu^{-1} Proj\{\tau\} \leq \tau^T \Gamma_\mu^{-1} \tau\ \forall\ \hat{\theta}_{(\mu)} \in \mathcal{S}_{\theta^*}$*; (iii) The solution* $\hat{\theta}_{(\mu)}$ *remains in* $\mathcal{S}_{\theta^*}\ \ \forall\ \hat{\theta}_{(\mu)}(t_0) \in \mathcal{S}_{\theta^*}$*; (iv)* $-\tilde{\theta}_{(\mu)}^T \Gamma_\mu^{-1} Proj\{\tau\} \leq -\tilde{\theta}_{(\mu)}^T \Gamma_\mu^{-1} \tau,\ \ \forall\ \hat{\theta}_{(\mu)},\ \theta^* \in \mathcal{S}_{\theta^*}$.

Proof. The proof can be referred to [69] (Refer Lemma E.1 on page 512).

Hence from property (iii) of the projection operator stated in Lemma 3.2, it can be easily concluded that the parameter estimation error $\tilde{\theta}_{(\mu)}$ is bounded as,

$$\|\tilde{\theta}_{(\mu)}\| \leq \sqrt{(\sum_{j=1}^{m} \overline{b}_j - \ell)^2 + \kappa_{\max}^2 + 4\sum_{j=1}^{m} \overline{b}_j^2 \bar{u}_j^2} := \overline{\theta},\ \mu = \overline{1,\ p+m+1} \tag{3.39}$$

The stability results would be derived in a generalized form such that conclusions on the convergence of all the closed loop signals can be drawn for cases of no actuator failure, finite number of actuator failures and infinite actuator failures. Therefore, let us construct an overall Lyapunov function $V(z, \tilde{x}_{(\mu)}, \tilde{\theta}_{(\mu)}, t) : \mathbb{R}^{\wp} \times \mathbb{R}^{\wp} \times \mathbb{R}^{p+m+1} \times [t_0, \infty) \to \mathbb{R}_+$ for $\mu = \overline{1, p+m+2}$ as,

$$V(z, \tilde{x}_{(\mu)}, \tilde{\theta}_{(\mu)}, t) = \frac{\epsilon}{2}\|z\|^2 + \frac{1}{2}\tilde{x}_{(\mu)}^T P_\mu \tilde{x}_{(\mu)} + \frac{1}{2}\tilde{\theta}_{(\mu)}^T \Gamma_\mu^{-1} \tilde{\theta}_{(\mu)} \tag{3.40}$$

The function $V(t)$ is piecewise continuous and differentiable in $t \in [T_h,\ T_{h+1})$ and let us define $V(t) = V_h(t)\ \forall t \in [T_h,\ T_{h+1}),\ h \in \mathbb{W}$. The time T_h for $h = 0$ denotes the initial time t_0. Owing to the fact that $V(t)$ experiences sudden jumps at each instants of actuator failure T_h $(h = 1, \ldots, \infty)$, it is discontinuous over $t \in [0, \infty)$ and is not differentiable at its points of discontinuity. Although the function $V(t)$ satisfies to be a Lyapunov function for $t \in [T_h,\ T_{h+1})$, the same does not hold true for $t \in [0, \infty)$. Assuming that the actuator failure pattern does not change for $t \in [T_h,\ T_{h+1})$, the stability/boundedness properties of the triple $(z(t), \tilde{x}_\mu, \tilde{\theta}_{(\mu)})$ for $t \in [T_h,\ T_{h+1})$ can be easily derived considering $V_h(t)$ as the Lyapunov function candidate. However, proving the closed loop signal boundedness of the triple $(z(t), \tilde{x}_\mu, \tilde{\theta}_{(\mu)})$ over the entire time range $t \in [0, \infty)$ under the occurrence of infinitely changing actuator failure patterns, is not straightforward. Further, it is also not trivial to deduce an explicit expression for the $\mathcal{L}_\infty[0, \infty)$ and $\mathcal{L}_2[0, \infty)$ bounds of the output tracking error in this case. In the following, the closed loop stability of the system (3.1) under the action of the control law v in (3.37) is investigated for $t \in [T_h,\ T_{h+1})$ and the results are summarized in Theorem 3.3. Thereafter, the main results on boundedness of closed loop signals and transient performance improvement in the case of intermittent actuator failures are derived for all $t \in [0, \infty)$.

By substituting the stabilizing functions α_i in (3.31), the control input $v(t)$ given by (3.37) and the parameter estimation law $\dot{\tilde{\theta}}_{(\mu)}(t)$ in (3.12) into the fault parameterized system dynamics (3.5), the output tracking error dynamics takes the following form,

$$\dot{z} = \underbrace{\begin{bmatrix} -(c_1+s_1) & 1 & \ldots & 0 \\ -1 & -(c_2+s_2) & \ldots & 0 \\ \vdots & \ldots & \ldots & 1 \\ 0 & \ldots & -1 & -(c_\wp+s_\wp)\frac{b^*}{\ell} \end{bmatrix}}_{\mathcal{A}} z + \underbrace{\begin{bmatrix} 0 & \psi_1^T & 0 \\ 0 & \psi_2^T & 0 \\ \vdots & \vdots & \vdots \\ v_1 & \psi_\wp^T & \beta^T \end{bmatrix}}_{B_{\theta^*}} \tilde{\theta}_{(\mu)} + \underbrace{\begin{bmatrix} 0 \\ -\frac{\partial \alpha_1}{\partial \hat{\kappa}_{(\mu)}} \\ \vdots \\ -\frac{\partial \alpha_{\wp-1}}{\partial \hat{\kappa}_{(\mu)}} \end{bmatrix}}_{B_{\dot{\hat{\kappa}}}} \dot{\hat{\kappa}}_{(\mu)} \tag{3.41}$$

where $z := [\{z_i\}_{i=1}^{\wp}]^T$ is the tracking error vector and the matrices in (3.41) are denoted by $\mathcal{A}(x,t) \in \mathbb{R}^{\wp \times \wp}$, $B_{\theta^*} \in \mathbb{R}^{\wp \times (p+m+1)}$ and $B_{\dot{\hat{\kappa}}} \in \mathbb{R}^{\wp}$. For simplicity of representation, the short hand notation s_i

in the matrix $\mathcal{A}$, is used for the following expressions given below.

$$s_1 = \bar{c}_1\|\psi_1\|^2,\ s_i = \bar{c}_2\|\psi_i\|^2 + g_i\left\|\frac{\partial\alpha_{i-1}}{\partial\hat{\kappa}}\right\|^2 \tag{3.42}$$

$$s_\wp = \bar{c}_\wp(\|\psi_\wp\|^2 + |v_1|^2 + \|\beta\|^2) + g_\wp\left\|\frac{\partial\alpha_{\wp-1}}{\partial\hat{\kappa}}\right\|^2 \tag{3.43}$$

As defined earlier, the parameters $c_i,\ \bar{c}_i$ and g_j for $i = \overline{1,\wp}$ and $j = \overline{2,\wp}$ are positive design constants chosen by the designer. Now, we are well equipped to state the following theorem.

Theorem 3.3. *(Piecewise stability properties under first layer of adaptation) Let us consider the output tracking error dynamics in* (3.41) *whose solutions are defined for* $t \in [T_h,\ T_{h+1})$ *for* $h \in \mathbb{W}$. *Under Assumptions 3.1-3.6, and the adaptive law* $\dot{\hat{\theta}}_{(\mu)}(t)$ *in* (3.12), *the solutions satisfy the following properties: (i)* $z(t) \in \mathcal{L}_\infty[T_h,\ T_{h+1}),\ x(t),\ \dot{z}(t) \in \mathcal{L}_\infty[T_h,\ T_{h+1})$; *(ii)* $z(t) \in \mathcal{L}_2[T_h,\ T_{h+1})$. *Further, if* $T_{h+1} \to \infty$ *and the actuator failure pattern remains fixed within* $[T_h,\ \infty]$, *asymptotic output tracking is guaranteed, that is,* $\lim_{t\to\infty} z(t) = 0$.

Proof of (i). The proof will be completed in two steps. In the first step, the boundedness of all the closed loop signals shall be proved for the interval $[T_h,\ T_{h+1})$. Secondly, to prove asymptotic stability of the tracking error $z(t)$, it would be shown to belong to class of $\mathcal{L}_2[T_h,\ T_{h+1})$ integrable signals. A Lyapunov function $V(t)$ for $t \in [T_h,\ T_{h+1})$ defined as $V_h(t)$ in (3.40) is therefore called upon. The analysis is done as follows. Using (3.29),(3.30), (3.36) and invoking the sum of squares inequality with $\theta^* := [\theta_1^*\ \theta_2^*\ \theta_3^*]^T =: [b^*\ \kappa^*\ \bar{u}]^T$ yields,

$$\begin{aligned}
\frac{d}{dt}\left(\frac{\epsilon}{2}\|z\|^2\right) &\le -\underline{\lambda}(\mathcal{Q})\epsilon\|z\|^2 + \frac{\epsilon}{4}\left[\frac{\|\tilde{\theta}_{1(\mu)}\|^2}{c_\wp} + \frac{\|\tilde{\theta}_{2(\mu)}\|^2}{\bar{c}} + \frac{\|\tilde{\theta}_{3(\mu)}\|^2}{\bar{c}_\wp} + \frac{\|\dot{\hat{\kappa}}\|^2}{\bar{g}}\right] \\
&\le -\underline{\lambda}(\mathcal{Q})\epsilon\|z\|^2 + \frac{\epsilon}{4}\left[\frac{\|\tilde{b}\|^2}{c_\wp} + \frac{\|\tilde{\kappa}\|^2}{\bar{c}} + \frac{\|\tilde{\bar{u}}\|^2}{\bar{c}_\wp} + \frac{\|\dot{\hat{\kappa}}\|^2}{\bar{g}}\right] \\
&\le -\underline{\lambda}(\mathcal{Q})\epsilon\|z\|^2 + \frac{\epsilon}{4}\left[\frac{\|\tilde{\theta}_{(\mu)}\|^2}{\bar{\bar{c}}} + \frac{\|\dot{\hat{\theta}}_{(\mu)}\|^2}{\bar{g}}\right]
\end{aligned} \tag{3.44}$$

where $\mathcal{Q} := \text{diag}\{c_1, \ldots, c_{\wp-1}, \frac{\theta_1^*}{\ell}c_\wp\} > 0$, $\bar{c} := \sum_{i=1}^{\wp}\frac{1}{4\bar{c}_i}$, $\bar{\bar{c}} := \min\{\bar{c}, \bar{c}_\wp, c_\wp\}$ and $\bar{g} := \sum_{i=2}^{\wp}\frac{1}{4\bar{g}_i}$. From Theorem 3.1, it is already proved that the projection operation within the set $\mathcal{S}_{\theta^*}$ ensures $\tilde{\theta}_{i(\mu)} \in \mathcal{L}_\infty[T_h,\ T_{h+1}),\ i = \overline{1,3}$ and $\dot{\hat{\theta}}_{(\mu)} \in \mathcal{L}_2[T_h,\ T_{h+1})$ implying $\|\dot{\hat{\kappa}}\| \in \mathcal{L}_2[T_h,\ T_{h+1})$. Therefore, the differential inequality (3.44) is solved in the interval $[T_h,\ T_{h+1})$ for $h \in \mathbb{W}$ as,

$$\|z\|_{[T_h,\ T_{h+1})} \le \|z(T_h)\|e^{-\underline{\lambda}(\mathcal{Q})t} + \frac{1}{2\sqrt{\underline{\lambda}(\mathcal{Q})}}\left[\frac{\|\tilde{\theta}_{(\mu)}\|_\infty^2}{\bar{\bar{c}}} + \frac{\|\dot{\hat{\theta}}_{(\mu)}\|_2^2}{\bar{g}}\right]^{\frac{1}{2}} \tag{3.45}$$

From (3.45), the property of $z(t) \in \mathcal{L}_\infty[T_h,\ T_{h+1})$ is proved and since the reference trajectory and its successive time derivatives are assumed to belong to a compact set so the plant state vector $x(t) \in \mathcal{L}_\infty[T_h,\ T_{h+1})$ and $\dot{z} \in \mathcal{L}_\infty[T_h,\ T_{h+1})$. Hence, the closed loop signal boundedness for $t \in [T_h,\ T_{h+1})$ ($h \in \mathbb{W}$) using the proposed controller is proved. □

Proof of (ii).

Now it has to be shown that $z(t) \in \mathcal{L}_2[T_h,\ T_{h+1})$. Therefore, proceeding with the proof, let us first represent the closed loop system in (3.41) using the definition $\theta_1^* = \tilde{\theta}_1 + \hat{\theta}_1$ as

$$\dot{z} = \underbrace{\begin{bmatrix} -(c_1+s_1) & 1 & \dots & 0 \\ -1 & -(c_2+s_2) & \dots & 0 \\ \vdots & \dots & \dots & 1 \\ 0 & \dots & -1 & -(c_\wp+s_\wp)\frac{\hat{b}}{\ell} \end{bmatrix}}_{\bar{\mathcal{A}}} z + \underbrace{\begin{bmatrix} 0 & \psi_1^T & 0 \\ 0 & \psi_2^T & 0 \\ \vdots & \vdots & \vdots \\ v & \psi_\wp^T & \beta^T \end{bmatrix}}_{\bar{B}_{\theta^*}} \tilde{\theta}_{(\mu)} + \underbrace{\begin{bmatrix} 0 \\ -\frac{\partial \alpha_1}{\partial \hat{\kappa}_{(\mu)}} \\ \vdots \\ -\frac{\partial \alpha_{\wp-1}}{\partial \hat{\kappa}_{(\mu)}} \end{bmatrix}}_{B_{\dot{\hat{\kappa}}}} \dot{\hat{\kappa}}_{(\mu)}$$

Thereafter, the matrix $\bar{B}_{\theta^*}$ is factorized such that $\bar{B}_{\theta^*} := \mathcal{M}(z, \hat{\theta}, t)\Phi^T(x, v)$. Where,

$$\mathcal{M}(z, \hat{\theta}_{(\mu)}, t) := \begin{bmatrix} 1 & 0 & \dots & 0 & 0 \\ -\frac{\partial \alpha_1}{\partial x_1} & 1 & \dots & 0 & 0 \\ \vdots & \ddots & \ddots & \ddots & \vdots \\ -\frac{\partial \alpha_{\varrho-1}}{\partial x_1} & -\frac{\partial \alpha_{\varrho-1}}{\partial x_2} & \dots & -\frac{\partial \alpha_{\varrho-1}}{\partial x_{\varrho-1}} & 1 \end{bmatrix} \tag{3.46}$$

Hereafter, we define an auxiliary variable $\vartheta := z - \mathcal{M}\tilde{x}_{(\mu)}$. With this choice of ϑ, we arrive at a dynamics in ϑ driven by only $\mathcal{L}_2$-integrable inputs $\tilde{x}_{(\mu)}$ and $\dot{\hat{\kappa}}_{(\mu)}$ described by the following differential equation defined for $t \in [T_h,\ T_{h+1})$.

$$\dot{\vartheta} = \bar{\mathcal{A}}\vartheta + \underbrace{[-\dot{\mathcal{M}} + \bar{\mathcal{A}}\mathcal{M} - \mathcal{M}A_\mu]}_{\hat{\mathcal{M}}(z, \hat{\theta}_{(\mu)}, t)} \tilde{x}_{(\mu)} + B_{\dot{\hat{\kappa}}}\dot{\hat{\kappa}}_{(\mu)} \tag{3.47}$$

Now, finally if ϑ is shown to be $\mathcal{L}_2$-integrable in the interval $[T_h,\ T_{h+1})$, the tracking error $z(t) \in \mathcal{L}_2[T_h,\ T_{h+1})$ is proved. Proceeding with this objective, we compute,

$$\begin{aligned} \frac{d}{dt}\Big(\frac{1}{2}\|\vartheta\|^2\Big) &\leq \vartheta^T\bar{\mathcal{A}}\vartheta + \vartheta^T\hat{\mathcal{M}}(z, \hat{\theta}_{(\mu)}, t)\tilde{x}_{(\mu)} + \vartheta^T B_{\dot{\hat{\kappa}}}\dot{\hat{\kappa}}_{(\mu)} \\ &\leq -\underline{\lambda}(\mathcal{Q})\|\vartheta\|^2 - \sum_{i=1}^{\wp} g_i \Big\| \frac{\partial \alpha_{i-1}}{\partial \hat{\kappa}_{(\mu)}} \Big\|^2 \vartheta_i^2 + \sum_{i=1}^{\wp} \frac{\partial \alpha_{i-1}}{\partial \hat{\kappa}_{(\mu)}} \dot{\hat{\kappa}}_{(\mu)} \vartheta_i + \vartheta^T\hat{\mathcal{M}}\tilde{x}_{(\mu)} \\ \frac{d}{dt}\Big(\frac{1}{2}\|\vartheta\|^2\Big) &\leq -\underline{\lambda}(\mathcal{Q})\|\vartheta\|^2 + \frac{\|\dot{\hat{\kappa}}_{(\mu)}\|^2}{4\bar{g}} + \vartheta^T\hat{\mathcal{M}}\tilde{x}_{(\mu)} \end{aligned} \tag{3.48}$$

Using Peter-Paul inequality (Appendix A.2.3) with the factor $\underline{\lambda}(\mathcal{Q})$ for the third term in (3.48) leads to,

$$\vartheta^T\hat{\mathcal{M}}\tilde{x}_{(\mu)} \leq \underline{\lambda}(\mathcal{Q})\frac{\|\vartheta\|^2}{2} + \frac{1}{2\underline{\lambda}(\mathcal{Q})}\|\hat{\mathcal{M}}\|_{\mathscr{F}}^2\|\tilde{x}_{(\mu)}\|^2 \tag{3.49}$$

Using (3.48) in (3.49) results in the following differential inequality given as,

$$\frac{d}{dt}\Big(\frac{1}{2}\|\vartheta\|^2\Big) \leq -\underline{\lambda}(\mathcal{Q})\|\vartheta\|^2 + \frac{\|\dot{\hat{\kappa}}_{(\mu)}\|^2}{4\bar{g}} + \frac{\|\hat{\mathcal{M}}\|_{\mathscr{F}}^2\|\tilde{x}_{(\mu)}\|^2}{2\underline{\lambda}(\mathcal{Q})} \tag{3.50}$$

The boundedness of $\hat{\mathcal{M}}(\cdot)$ is ensured if $\mathcal{M},\ \dot{\mathcal{M}},\ \bar{\mathcal{A}}$ and $A_{(\mu)}$ are bounded. The bounded variation of $\mathcal{M}$ is inferred from the choice of the virtual control laws $\alpha_i,\ i = \overline{1, \varrho-1}$ and control law v. Since $\dot{x} \in \mathcal{L}_\infty$ as shown in the earlier section of the proof, the regressor $\Phi(x, v)$ and the matrix A_μ is bounded. The matrix $\dot{\mathcal{M}}$ is also found to be bounded in t taking into account the following signal properties, $\dot{z} \in \mathcal{L}_\infty[T_h,\ T_{h+1})$, $\dot{\hat{\theta}} \in \mathcal{L}_2[T_h,\ T_{h+1})$ and the partial derivatives $\frac{\partial \mathcal{M}}{\partial z}$, $\frac{\partial \mathcal{M}}{\partial \hat{\theta}}$ being time bounded continuous functions. Therefore, the matrix $\hat{\mathcal{M}}(z, \hat{\theta}_{(\mu)}, t)$ is bounded. Finally, the inequality in (3.50) is rearranged and then integrated for the time interval $[T_h,\ T_{h+1})$ leading to,

$$\int_{T_h}^{T_{h+1}} \|\vartheta\|^2 dt \leq \frac{\|\vartheta(T_h)\|^2}{2\underline{\lambda}(\mathcal{Q})} + \frac{1}{4\bar{g}\underline{\lambda}(\mathcal{Q})}\int_{T_h}^{T_{h+1}} \|\dot{\tilde{\kappa}}_{(\mu)}\|^2 dt + \frac{1}{2\underline{\lambda}(\mathcal{Q})^2}\|\hat{\mathcal{M}}\|_{\mathscr{F}}^2 \int_{T_h}^{T_{h+1}} \|\tilde{x}_{(\mu)}\|^2 dt < \infty \quad (3.51)$$

With a reasonable consideration that $\vartheta(T_h)$ is finite and $\dot{\tilde{\kappa}}_{(\mu)},\ \tilde{x}_{(\mu)} \in \mathcal{L}_2[T_h,\ T_{h+1})$, the signal property of $\vartheta(t) \in \mathcal{L}_2[T_h,\ T_{h+1})$ is easily concluded from (3.51). Further, $z(t) \in \mathcal{L}_2[T_h,\ T_{h+1})$ follows from the $\mathcal{L}_2$-integrability property of $\vartheta(t)$. Finally, if $T_{h+1} \to \infty$, invoking Barbalat's Lemma [69], $z(t) \in \mathcal{L}_2[T_h,\ \infty) \cap \mathcal{L}_\infty[T_h,\ \infty)$ with $\dot{z}(t) \in \mathcal{L}_\infty[T_h,\ \infty)$ infers asymptotic stability of the tracking error vector $z(t)$. The proof is complete. □

As mentioned earlier prior to Theorem 3.3, that the total Lyapunov function $V(t)$ is discontinuous due to sudden jumps at the actuator failure instances T_h for $h \in \mathbb{Z}_+$. The initial time instant when no fault occurs is indexed by $h = 0$ and given by T_0. The magnitude of the jumps in $V(t)$ at the failure instants T_h, can be calculated as,

$$V(T_h^+) - V(T_h^-) \leq \frac{1}{2}\tilde{\theta}_{(\mu)}^T(T_h^+)\Gamma_\mu^{-1}\tilde{\theta}_{(\mu)}(T_h^+) - \frac{1}{2}\tilde{\theta}_{(\mu)}^T(T_h^-)\Gamma_\mu^{-1}\tilde{\theta}_{(\mu)}(T_h^-) \leq \frac{1}{2}\overline{\lambda}(\Gamma_\mu^{-1})\overline{\theta}^2 = \overline{\Delta} \quad (3.52)$$

Further, let us consider the entire time range, i.e, $t \in [T_0,\ T)$, where T_0 and T denote the initial and final time instants. Within this time interval, assume that the actuator failure pattern changes $\aleph$ times. Therefore, using (3.52), the following inequality can be established.

$$\begin{aligned} V(T^-) \leq V(T_\aleph^+) \leq V(T_\aleph^-) + \overline{\Delta} \leq V(T_{\aleph-1}^-) + 2\overline{\Delta} \leq \ldots \\ \leq \ldots \leq V(T_1) + (\aleph-1)\overline{\Delta} \leq V(T_0) + \aleph\overline{\Delta} \end{aligned} \quad (3.53)$$

where $\aleph$ denotes the total number of times the actuator failure pattern changes. From inequality (3.53), it can be inferred that if the actuator failure patterns vary with finite cardinality (finite number of times) for all $t \in [T_0,\ T)$, the overall Lyapunov function $V(T^-)$ is bounded rendering global boundedness of the closed loop signals. However, infinitely occurring actuator failures would mean that $\aleph \to \infty$ with $T \to \infty$. Subsequent unboundedness of $V(t)$ can be concluded from (3.53) for $[T_0,\ \infty)$ with infinite actuator failures. Therefore, it is not straightforward to prove the stability of the closed loop adaptive system affected by infinitely occurring actuator failures. In what follows, we provide a stability analysis ensuring closed loop signal boundedness globally for all time $t \in [T_0,\ \infty)$ and $\aleph \to \infty$. The theoretical results obtained are stated in Theorem 3.4.

Theorem 3.4. *(first layer of adaptation) Let us consider the closed loop adaptive system consisting of the nonlinear system* (3.1)*, the adaptive parameter estimation law* (3.12) *and the control law in* (3.37)*.*

By virtue of the assumptions 3.1-3.6 and choosing the initial time $T_0 = 0$, the following results hold.

(i) All the closed loop signals are globally bounded assuming that the transit time T^* between actuator failure pattern changes is finite. The tracking error $z(t)$ finally resides within a bound is given by,

$$\lim_{t\to\infty} \|z(t)\| \leq \sqrt{\overline{\theta}^2 \left(\frac{\epsilon + 2\overline{\lambda}(\Gamma_\mu^{-1})\bar{\bar{c}}}{\bar{\rho}\bar{\bar{c}}}\right)\left(\frac{2 - e^{-\bar{\rho}T^*}}{1 - e^{-\bar{\rho}T^*}}\right) + \frac{2\overline{\Delta}}{1 - e^{-\bar{\rho}T^*}}} \tag{3.54}$$

(ii) The output tracking error $z_1 = x_1 - y_r$ is energy integrable for $t \in [0,\ \infty)$ for a finite $\aleph$ and the $\mathcal{L}_2[0,\ \infty)$ bound is given by,

$$\|z\|_2 \leq \sqrt{\frac{2\|z(0)\|^2 + \overline{\mathcal{M}}^*\|\tilde{x}_{(\mu)}(0)\|^2_{P_\mu} + (\overline{\mathcal{M}}^* - \mathcal{M}^*)(\|\tilde{\theta}_{(\mu)}(0)\|^2_{\Gamma_\mu^{-1}} + 2\aleph(0,\ \infty)\overline{\Delta})}{2\underline{\lambda}(\mathcal{Q})}} \tag{3.55}$$

(iii) Asymptotic convergence of the output tracking error $z(t)$ to the origin is ensured for a finite $\aleph$, i.e., $\lim_{t\to\infty} x_1 - y_r = 0$.

Herein $\mathcal{M}^*$ and $\overline{\mathcal{M}}^*$ are user defined parameters. The parameters $\bar{\bar{c}},\ \gamma,\ \bar{\rho} := \min\{2\rho,\ \underline{\lambda}(\Gamma_\mu^{-1})\},\ \rho = \min\{\underline{\lambda}(\mathcal{Q}),\ \underline{\lambda}(Q_\mu)\},\ \epsilon := \gamma\underline{\lambda}(\Gamma_\mu^{-2})\bar{g}$ and $\Gamma_\mu > 0$ are design constant scalars and matrices. Further, $\overline{\Delta}$ is the maximum magnitude of the jump due to occurrence of actuator failure given in (3.52) and $\aleph(0,\ T)$ denotes the total number of transitions the actuator failure pattern within the time interval $[0,\ T)$. The notations $\underline{\lambda}(\cdot)$ and $\overline{\lambda}(\cdot)$ denote the minimum and maximum eigen values of the argument.

Proof of Theorem 3.4 (i)

To prove stability, the Lyapunov function candidate $V(t)$ for $t \in [T_h,\ T_{h+1})$ defined as $V_h(t)$ in (3.40) is called upon. The analysis is done as follows. From the inequality (3.17) in the proof of Theorem 3.1 with the choice of $P_\mu = I_\wp$, the following inequality is deduced.

$$\begin{aligned}\frac{d}{dt}\Big(\frac{1}{2}\|\tilde{x}_{(\mu)}\|^2 + \frac{1}{2}\tilde{\theta}^T_{(\mu)}\Gamma_\mu^{-1}\tilde{\theta}_{(\mu)}\Big) &\leq -\tilde{x}^T_{(\mu)}Q_\mu\tilde{x}_{(\mu)} - \gamma\|\Phi P_\mu\tilde{x}_{(\mu)}\|^2 \\ &\leq -\underline{\lambda}(Q_\mu)\|\tilde{x}_{(\mu)}\|^2 - \frac{\gamma}{2}\underline{\lambda}(\Gamma_\mu^{-2})\|\dot{\hat{\theta}}_{(\mu)}\|^2\end{aligned} \tag{3.56}$$

Further, from (3.44), it has been found that the following inequality holds,

$$\frac{d}{dt}\Big(\frac{\epsilon}{2}\|z\|^2\Big) \leq -\underline{\lambda}(\mathcal{Q})\epsilon\|z\|^2 + \frac{\epsilon}{4}\left[\frac{\|\tilde{\theta}_{(\mu)}\|^2}{\bar{\bar{c}}} + \frac{\|\dot{\hat{\theta}}_{(\mu)}\|^2}{\bar{g}}\right] \tag{3.57}$$

Now as per the definition of $V_h(t)$ in (3.40), and using the above inequalities (3.57) and (3.44), the first time derivative of $V_h(t)$ for $t \in [T_h,\ T_{h+1})$ is calculated as,

$$\begin{aligned}\dot{V}_h(t) &= \frac{d}{dt}\Big[\frac{\epsilon}{2}\|z\|^2 + \frac{1}{2}\|\tilde{x}_{(\mu)}\|^2 + \frac{1}{2}\tilde{\theta}^T_{(\mu)}\Gamma_\mu^{-1}\tilde{\theta}_{(\mu)}\Big] \\ &\leq -\underline{\lambda}(\mathcal{Q})\epsilon\|z\|^2 - \underline{\lambda}(Q_\mu)\|\tilde{x}_{(\mu)}\|^2 - \Big(\frac{\gamma}{2}\underline{\lambda}(\Gamma_\mu^{-2}) - \frac{\epsilon}{4\bar{g}}\Big)\|\dot{\hat{\theta}}_{(\mu)}\|^2 + \frac{\epsilon}{4\bar{\bar{c}}}\|\tilde{\theta}_{(\mu)}\|^2\end{aligned} \tag{3.58}$$

Defining $\rho := \min\{\underline{\lambda}(\mathcal{Q}),\ \underline{\lambda}(Q_\mu)\}$ and choosing $\epsilon = \gamma\underline{\lambda}(\Gamma_\mu^{-2})\bar{g}$ and substituting these relations in (3.58) yields the following with solutions being defined $\forall t \in [T_h,\ T_{h+1}),\ h \in \mathbb{W}$,

$$\begin{aligned}\dot{V}_h(t) &\leq -\rho(\epsilon\|z\|^2 + \|\tilde{x}_{(\mu)}\|^2) - \frac{1}{2}\tilde{\theta}_{(\mu)}^T\Gamma_\mu^{-1}\tilde{\theta}_{(\mu)} + \left[\frac{\epsilon + 2\overline{\lambda}(\Gamma_\mu^{-1})\bar{\bar{c}}}{2\bar{\bar{c}}}\right]\overline{\theta}^2 \\ &\leq -\underbrace{\min\{2\rho,\ \underline{\lambda}(\Gamma_\mu^{-1})\}}_{\bar{\rho}} V_h(t) + \left[\frac{\epsilon + 2\overline{\lambda}(\Gamma_\mu^{-1})\bar{\bar{c}}}{2\bar{\bar{c}}}\right]\overline{\theta}^2 \leq -\bar{\rho}V_h(t) + \left[\frac{\epsilon + 2\overline{\lambda}(\Gamma_\mu^{-1})\bar{\bar{c}}}{2\bar{\bar{c}}}\right]\overline{\theta}^2 \end{aligned} \tag{3.59}$$

Now, stability of the overall control system affected by infinitely occurring actuator failures over the time interval $[0,\ \infty)$ cannot be inferred from the boundedness of $V_h(t)$ or rather $V(t)$ over the interval $[T_h,\ T_{h+1})$. Therefore at this point, let us call upon the total Lyapunov function $V(t)$ defined over $t \in [0,\ \infty)$. Due to the random variation in the actuator failure pattern at each unknown time instant $T_h (h \in \mathbb{N})$, the Lyapunov function $V(t)$ would undergo random jumps at the corresponding time instances between intervals($[T_h,\ T_{h+1})$) of continuous stable evolution in accordance with (3.59). These instantaneous changes of $V(t)$ can be approximately expressed as impulses. The overall system under infinitely varying actuator failure patterns can now be represented as a type of hybrid system comprising of continuous dynamics, discrete dynamics and the impulsive sequence $\{T_h\}\ \forall h \in \mathbb{W}$ satisfying $0 \leq T_0 < T_1 < T_2 < \ldots < T_h < \ldots < T_{\aleph} < T$ and $T \to \infty$ as given below.

$$\dot{V}(z, \tilde{x}_{(\mu)}, \tilde{\theta}_{(\mu)}, t) \leq -\bar{\rho}V(z, \tilde{x}_{(\mu)}, \tilde{\theta}_{(\mu)}, t) + \left[\frac{\epsilon + 2\overline{\lambda}(\Gamma_\mu^{-1})\bar{\bar{c}}}{2\bar{\bar{c}}}\right]\overline{\theta}^2, \qquad t \in [T_h,\ T_{h+1}) \tag{3.60}$$

$$V(z, \tilde{x}_{(\mu)}, \tilde{\theta}_{(\mu)}, T_{h+1}) \leq V(z, \tilde{x}_{(\mu)}, \tilde{\theta}_{(\mu)}, T_{h+1}^-) + \overline{\Delta}, \quad \forall h \in \mathbb{W} \tag{3.61}$$

Where, $\overline{\Delta}$ defined in (3.52) denotes the magnitude of jumps in the Lyapunov function $V(t)$ at the failure instances T_h; $V(T_{h+1}^-) := \lim_{t \to T_{h+1}^-} V(t)$ and $\overline{\theta}$ denotes the upper bound on the parameter estimation error defined earlier. Invoking the property of continuous dependence of solutions on initial conditions and parameters stated in (Theorem 3.4, [109]), the solution of the differential inequality (3.61) for any time interval $[T_h,\ T_{h+1})$ is given by,

$$V(t) \leq V(T_h)e^{-\bar{\rho}(t-T_h)} + \int_{T_h}^{t} e^{-\bar{\rho}(t-s)}\left[\frac{\epsilon + 2\overline{\lambda}(\Gamma_\mu^{-1})\bar{\bar{c}}}{2\bar{\bar{c}}}\right]\overline{\theta}^2 ds \tag{3.62}$$

Let us assume that actuator failure pattern changes occur between the considered time range $[0,\ T) \supset [T_h,\ T_{h+1})$ with a finite cardinality $\aleph(T_0,\ T) = (T - T_0)/T^*$ and $T_{\aleph} < T < \infty$. Now using (3.53) and iterating the inequality (3.62), the following is obtained for $t \in [T_0,\ T)$.

$$\begin{aligned}V(T^-) \leq V(T_0)e^{-\bar{\rho}(T-T_0)} &+ \left[\frac{\epsilon + 2\overline{\lambda}(\Gamma_\mu^{-1})\bar{\bar{c}}}{2\bar{\bar{c}}}\right]\overline{\theta}^2\left(\int_{T_0}^{T_1} e^{-\bar{\rho}(T-s)}ds + \int_{T_1}^{T_2} e^{-\bar{\rho}(T-s)}ds + \ldots + \int_{T_{\aleph(T_0,T)}}^{T} e^{-\bar{\rho}(T-s)}ds\right) \\ &+ \overline{\Delta}\left[e^{-\bar{\rho}(T-T_1)} + e^{-\bar{\rho}(T-T_2)} + \ldots + e^{-\bar{\rho}(T-T_{\aleph(T_0,T)-1})} + e^{-\bar{\rho}(T-T_{\aleph(T_0,T)})}\right]\end{aligned} \tag{3.63}$$

At this point, let us consider the initial time $T_0 = 0$ and thereafter using the notation for the index of the actuator failure pattern change h as defined earlier, the above inequality (3.63) is represented in a more compact form as follows,

$$V(T^-) \leq V(0)e^{-\bar{\rho}T} + \left[\frac{\epsilon + 2\overline{\lambda}(\Gamma_\mu^{-1})\bar{\bar{c}}}{2\bar{\bar{c}}}\right]\frac{\overline{\theta}^2}{\overline{\rho}}\left(\sum_{h=0}^{\aleph(0,T)-1} e^{-\bar{\rho}(T-T_{h+1})} - \sum_{h=0}^{\aleph(0,T)-1} e^{-\bar{\rho}(T-T_h)} - e^{-\bar{\rho}(T-T_{\aleph(0,T)})} + 1\right) + \overline{\Delta}\left[\sum_{h=1}^{\aleph(0,T)-1} e^{-\bar{\rho}(T-T_h)} + e^{-\bar{\rho}(T-T_{\aleph(0,T)})}\right] \tag{3.64}$$

It is known that two consecutive instances of occurrence of actuator failure are related by the transit time $T^* := T_{h+1} - T_h$. Further, considering the final time T with $[T_h,\ T_{h+1}) \subset [0,\ T]\ \forall h \in \mathbb{W}$, the cardinality $\aleph(0,T)$ of the index set representing the number of changes in the actuator failure pattern for $t \in [0,T)$ satisfies the inequality,

$$\aleph(T_0,\ T) = \aleph(0,\ T) - h \leq \frac{T - T_h}{T^*},\quad h \in \{0,1,2,\ldots,\aleph(0,T)\} \subset \mathbb{W} \tag{3.65}$$

The inequality above implies $(T - T_{h+1}) \geq (\aleph(0,T) - h - 1)T^*$ and $(T - T_h) \geq (\aleph(0,T) - h)T^*$ which when substituted in (3.64) yields,

$$V(T^-) \leq V(0)e^{-\bar{\rho}T} + \frac{\overline{\theta}^2}{\overline{\rho}}\left[\frac{\epsilon + 2\overline{\lambda}(\Gamma_\mu^{-1})\bar{\bar{c}}}{2\bar{\bar{c}}}\right]\left[\sum_{h=0}^{\aleph(0,T)-1} e^{-\bar{\rho}(\aleph(0,T)-h-1)T^*} + 1\right] + \overline{\Delta}\left[\sum_{h=1}^{\aleph(0,T)-1} e^{-\bar{\rho}(\aleph(0,T)-h)T^*} + 1\right] \tag{3.66}$$

$$\leq V(0)e^{-\bar{\rho}T} + \frac{\overline{\theta}^2}{\overline{\rho}}\left[\frac{\epsilon + 2\overline{\lambda}(\Gamma_\mu^{-1})\bar{\bar{c}}}{2\bar{\bar{c}}}\right]\left(\frac{1}{1 - e^{-\bar{\rho}T^*}} + 1\right) + \overline{\Delta}\left(\frac{e^{-\bar{\rho}T^*}}{1 - e^{-\bar{\rho}T^*}} + 1\right) \tag{3.67}$$

$$\leq V(0)e^{-\bar{\rho}T} + \frac{\overline{\theta}^2}{\overline{\rho}}\left[\frac{\epsilon + 2\overline{\lambda}(\Gamma_\mu^{-1})\bar{\bar{c}}}{2\bar{\bar{c}}}\right]\left(\frac{2 - e^{-\bar{\rho}T^*}}{1 - e^{-\bar{\rho}T^*}}\right) + \frac{\overline{\Delta}}{1 - e^{-\bar{\rho}T^*}} \tag{3.68}$$

Since, $\|z\|^2 \leq 2V(t)$, therefore using (3.68), the ultimate bound on the tracking error $z(t)$ under infinite actuator failures is derived as,

$$\lim_{T\to\infty} \|z\| \leq \sqrt{\overline{\theta}^2\left(\frac{\epsilon + 2\overline{\lambda}(\Gamma_\mu^{-1})\bar{\bar{c}}}{\bar{\rho}\bar{\bar{c}}}\right)\left(\frac{2 - e^{-\bar{\rho}T^*}}{1 - e^{-\bar{\rho}T^*}}\right) + \frac{2\overline{\Delta}}{1 - e^{-\bar{\rho}T^*}}} \tag{3.69}$$

With $T^* > 0$, the following stability properties are obtained from (3.68) $\forall\ t \in [0,\ \infty)$, viz. the closed loop signals $(z(t),\ \tilde{x}_{(\mu)}(t),\ \tilde{\theta}_{(\mu)}) \in \mathcal{L}_\infty[0,\ \infty)$. □

Proof of Theorem 3.4 (ii).

Although not straight forward, it is not very difficult either, to show the $\mathcal{L}_2$-integrability of $z(t)$ for

$t \in [0,\ \infty)$. From the proof of Theorem 3.1 (ii), it is known that for $t \in [T_h,\ T_{h+1})$,

$$V_{(\mu)}(T_{h+1}^-) \leq V_{(\mu)}(T_h^+) - \underline{\lambda}(Q_\mu)\int_{T_h}^{T_{h+1}} \|\tilde{x}_{(\mu)}\|^2 dt \leq V_{(\mu)}(T_h^-) - \underline{\lambda}(Q_\mu)\int_{T_h}^{T_{h+1}} \|\tilde{x}_{(\mu)}\|^2 dt + \overline{\Delta} \tag{3.70}$$

Utilizing inequality (3.70), the following holds for the final time T,

$$\begin{aligned} V_{(\mu)}(T^-) &\leq V_{(\mu)}(T_\aleph^+) - \underline{\lambda}(Q_\mu)\int_{T_\aleph}^{T} \|\tilde{x}_{(\mu)}\|^2 dt \leq V_{(\mu)}(T_\aleph^-) + \overline{\Delta} - \underline{\lambda}(Q_\mu)\int_{T_\aleph}^{T} \|\tilde{x}_{(\mu)}\|^2 dt \leq \dots \\ &\leq \dots \leq V_{(\mu)}(0) + \aleph(0,T)\overline{\Delta} - \underline{\lambda}(Q_\mu)\int_0^T \|\tilde{x}_{(\mu)}\|^2 dt \end{aligned} \tag{3.71}$$

From (3.71), the $\mathcal{L}_2$ bound on the identification error $\tilde{x}_{(\mu)}$ is calculated as follows with $T \to \infty$,

$$\int_0^\infty \|\tilde{x}_{(\mu)}\|^2 dt \leq \frac{V_{(\mu)}(0) + \aleph(0,\infty)\overline{\Delta}}{\underline{\lambda}(Q_\mu)} < \infty \tag{3.72}$$

Further, using the same procedure as in the proof of Theorem 3.1 (ii), the signal $\dot{\hat{\theta}}_{(\mu)}$ is proved to be energy integrable. For clarity, the procedure is reproduced here. From (3.17),

$$\begin{aligned} V_{(\mu)}(T^-) &\leq V_{(\mu)}(T_\aleph^+) - \gamma\int_{T_\aleph}^{T} \|\Phi P_\mu \tilde{x}_{(\mu)}\|^2 dt \leq V_{(\mu)}(T_\aleph^+) - \frac{\gamma}{\overline{\lambda}(\Gamma_\mu^{-2})}\int_{T_\aleph}^{T} \|\dot{\hat{\theta}}_{(\mu)}\|^2 dt \leq \\ &\leq V_{(\mu)}(T_\aleph^-) + \overline{\Delta} - \frac{\gamma}{\overline{\lambda}(\Gamma_\mu^{-2})}\int_{T_\aleph}^{T} \|\dot{\hat{\theta}}_{(\mu)}\|^2 dt \leq V_{(\mu)}(0) + \aleph(0,T)\overline{\Delta} - \frac{\gamma}{\overline{\lambda}(\Gamma_\mu^{-2})}\int_0^T \|\dot{\hat{\theta}}_{(\mu)}\|^2 dt \end{aligned} \tag{3.73}$$

Hence, the inequality (3.73) proves $\dot{\hat{\theta}}_{(\mu)} \in \mathcal{L}_2[0,\ \infty)$ and rearranging (3.73) yields,

$$\int_0^\infty \|\dot{\hat{\theta}}_{(\mu)}\|^2 dt \leq \frac{\overline{\lambda}(\Gamma_\mu^{-2})(V_{(\mu)}(0) + \aleph(0,\infty)\overline{\Delta})}{\gamma} \tag{3.74}$$

Using the auxiliary variable $\vartheta := z - \mathcal{M}\tilde{x}$ defined earlier in the proof of Theorem 3.3, the following inequality is inferred from (3.51), (3.74) and (3.72) that,

$$\int_0^\infty \|\vartheta\|^2 dt \leq \frac{\|\vartheta(0)\|^2}{2\underline{\lambda}(\mathcal{Q})} + \frac{1}{4\bar{g}\underline{\lambda}(\mathcal{Q})}\int_0^\infty \|\dot{\hat{\theta}}_{(\mu)}\|^2 dt + \frac{1}{2\underline{\lambda}(\mathcal{Q})^2}\|\hat{\mathcal{M}}\|_\infty^2 \int_0^\infty \|\tilde{x}_{(\mu)}\|^2 dt < \infty \tag{3.75}$$

Since, under possibly infinite actuator failures, the global boundedness of all the closed loop signals are proved in the earlier section of the proof, using similar arguments, $\hat{\mathcal{M}}(\cdot)$ is inferred bounded for $t \in [0,\ \infty)$. Hence, $\vartheta \in \mathcal{L}_2[0,\ \infty)$ and by the definition of ϑ, the tracking error vector $z(t) \in \mathcal{L}_2[0,\ \infty)$ is concluded. Finally using the inequality $(a+b)^2 \leq 2(a^2+b^2)$, the $\mathcal{L}_2[0,\ \infty)$ bound of $z(t)$ is calculated as,

$$\int_0^\infty \|z\|^2 dt \leq \frac{\|\vartheta(0)\|^2}{\underline{\lambda}(\mathcal{Q})} + \frac{1}{2\bar{g}\underline{\lambda}(\mathcal{Q})}\int_0^\infty \|\dot{\hat{\theta}}_{(\mu)}\|^2 dt + \frac{\overline{\mathcal{M}}}{\underline{\lambda}(\mathcal{Q})}\int_0^\infty \|\tilde{x}_{(\mu)}\|^2 dt \tag{3.76}$$

Where $\overline{\mathcal{M}} := (\|\hat{\mathcal{M}}\|_\infty^2 + 2\underline{\lambda}(\mathcal{Q})^2\|\mathcal{M}\|_\infty^2)/\underline{\lambda}(\mathcal{Q})$. The above expression can be further simplified as,

$$\|z\|_2 \leq \frac{1}{\sqrt{\underline{\lambda}(\mathcal{Q})}}\left[\|\vartheta(0)\|^2 + \left(\frac{\overline{\lambda}(\Gamma_\mu^{-2})}{2\bar{g}\gamma} + \frac{\overline{\mathcal{M}}}{\underline{\lambda}(Q_\mu)}\right)(V_{(\mu)}(0) + \aleph(0,\ \infty)\overline{\Delta})\right]^{\frac{1}{2}} \tag{3.77}$$

$$\leq \frac{1}{\sqrt{2\underline{\lambda}(\mathcal{Q})}}\left[2\|z(0)\|^2 + \left(\frac{\overline{\lambda}(\Gamma_\mu^{-2})}{2\bar{g}\gamma} + \frac{\overline{\mathcal{M}}}{\underline{\lambda}(Q_\mu)} + \mathcal{M}^*\right)\|\tilde{x}_{(\mu)}(0)\|_{P_\mu}^2 + \left(\frac{\overline{\lambda}(\Gamma_\mu^{-2})}{2\bar{g}\gamma} + \frac{\overline{\mathcal{M}}}{\underline{\lambda}(Q_\mu)}\right)(\|\tilde{\theta}_{(\mu)}(0)\|_{\Gamma_\mu^{-1}}^2 + 2\aleph(0,\ \infty)\overline{\Delta})\right]^{\frac{1}{2}} \tag{3.78}$$

Finally, considering the notations $\overline{\mathcal{M}}^* := 0.5\overline{\lambda}(\Gamma_\mu^{-2})\bar{g}^{-1}\gamma^{-1} + \underline{\lambda}^{-1}(Q_\mu)\overline{\mathcal{M}} + \mathcal{M}^*$ and $\mathcal{M}^* := \|\mathcal{M}\|_\infty^2$, yields the expression for $\|z\|_2$ for $t \in [0,\ \infty)$ in Theorem 3.4 (ii). □

Proof of Theorem 3.4 (iii).

Now when the number of changes in the actuator failure pattern is finite then the variable $\aleph$ is bounded by a finite natural number. Further, it has been shown in the proof of Theorem 3.4 (i) that the triple $(z,\ \tilde{x}_{(\mu)},\ \tilde{\theta}_{(\mu)}) \in \mathcal{L}_\infty[0,\ \infty)$ and $\dot{z} \in \mathcal{L}_\infty[0,\ \infty)$. Therefore, for a finite $\aleph$, inequality (3.78) leads to $z(t) \in \mathcal{L}_2[0,\ \infty)$. Therefore, invoking signal convergence Lemma, asymptotic stability of $z(t)$ to the origin is guaranteed as $t \to \infty$. The proofs are complete. □

Now, we state Theorem 3.5 which states that the closed loop system under the action of the proposed controller with dual layer adaptation hold similar signal convergence properties as those obtained from the first layer adaptation based controller. Different from first layer adaptation based controller, the proposed FTC with the second layer of adaptation substantially improves the output transient performance. This is a theoretical claim which would be proved after the stability proof of the closed loop system under the action of the proposed control law.

The following lemma would be helpful in deducing stability proofs to follow later in this section.

Lemma 3.3. *For a time varying system $\dot{\xi} = A(x(t),t)\xi$, the state transition matrix satisfies the condition, $\|\exp(A(x,t)(t-t_0))\| \leq \breve{k}\exp(-c_0(t-t_0))$, with $\breve{k}$ and c_0 being some positive constants [109].*

To analyze the convergence properties under second layer of adaptation, an additional adaptive identification model is defined as,

$$\dot{\hat{x}}_s = A(x,t)(\hat{x}_s - x) + \Phi^T(x,v)\hat{\theta}_s \tag{3.79}$$

The number of adaptive identification models is given by $N = p + m + 2$. The initial condition for the parameter estimate at the second layer of adaptation is given by $\hat{\theta}_s(t_0) = \sum_{\mu=1}^{p+m+2} \hat{w}_\mu(t_0)\hat{\theta}_{(\mu)}(t_0)$. The

adaptive law governing the parameter estimate $\hat{\theta}_s$ at this point is calculated to be,

$$\dot{\hat{\theta}}_s(t) = \sum_{\mu=1}^{p+m+2} \hat{w}_\mu \dot{\hat{\theta}}_{(\mu)} + \sum_{\mu=1}^{p+m+2} \dot{\hat{w}}_\mu \hat{\theta}_{(\mu)} = \sum_{\mu=1}^{p+m+2} \hat{w}_\mu \Gamma_\mu \Phi P_\mu \tilde{x}_{(\mu)} + \sum_{\mu=1}^{p+m+2} \dot{\hat{w}}_\mu \hat{\theta}_{(\mu)}$$

$$= \Gamma_\mu \Phi P_\mu \int_{t_0}^{t} \exp(A(x,\tau)(t-t_0-\tau)) \Phi^T \sum_{\mu=1}^{p+m+2} \hat{w}_\mu \tilde{\theta}_{(\mu)}(\tau) d\tau + \sum_{\mu=1}^{p+m+2} \dot{\hat{w}}_\mu \hat{\theta}_{(\mu)} \tag{3.80}$$

$$\leq \Gamma_\mu \Phi P_\mu \int_{t_0}^{t} \breve{k} \exp(-c_0(t-t_0-\tau)) \Phi^T \sum_{\mu=1}^{p+m+2} \hat{w}_\mu \tilde{\theta}_{(\mu)} d\tau + \sum_{\mu=1}^{p+m+2} \dot{\hat{w}}_\mu \hat{\theta}_{(\mu)} \tag{3.81}$$

Now using the equality $\tilde{\theta}_s = \theta^* - \sum_{\mu=1}^{p+m+2} \hat{w}_\mu \hat{\theta}_{(\mu)} = \theta^* - \sum_{\mu=1}^{p+m+2} \hat{w}_\mu (\theta^* - \tilde{\theta}_{(\mu)}) = \sum_{\mu=1}^{p+m+2} \hat{w}_\mu \tilde{\theta}_{(\mu)}$ in (3.80) yields,

$$\dot{\hat{\theta}}_s = \Phi(x,v) P_\mu \tilde{x}_s + \sum_{\mu=1}^{p+m+2} \dot{\hat{w}}_\mu \hat{\theta}_{(\mu)} \tag{3.82}$$

In (3.82), it is observed that if the weights $\hat{w}_\mu$ were known then $\dot{\hat{w}}_\mu = 0$. Hence, the adaptive law governing the evolution of $\hat{\theta}_s$ would be similar to those designed for the individual adaptive identification models in (3.12). This explains that the identification model (3.79) obtained through a convex combination of all the $(p+m+2)$ adaptive identification models would have the same estimation error convergence properties as stated in Theorem 3.1. Hence, the choice of the adaptive identification model in (3.79) under the second adaptation is justified. The stability results in regards to second layer adaptation are stated in Theorem 3.5.

Theorem 3.5. *(Stability properties under the proposed dual layer adapted estimation) Let us consider the closed loop adaptive system consisting of the nonlinear system* (3.1)*, the adaptive parameter estimation* $\hat{\theta}_s$ *under the second layer of adaptation given by* $\hat{\theta}_s := \sum_{\mu=1}^{p+m+2} \hat{w}_\mu \hat{\theta}_{(\mu)}$*, the weight learning law* $\dot{\hat{w}}$ *in* (3.23)*and the control law* (3.37)*. Considering assumptions 3.1-3.6 hold and choosing the initial time* $T_0 = 0$*, the following results are stated.*

(i) Considering the nonlinear system is subjected to infinite actuator failures and the transit time T^* *between actuator failure pattern changes is finite, closed loop signal boundedness is ensured for all* $t \in [0,\ \infty)$*.*

$$\lim_{t\to\infty} \|z(t)\| \leq \sqrt{2\mathscr{L}\overline{\theta}^2 \left(\frac{2 - e^{-\bar{\rho}T^*}}{1 - e^{-\bar{\rho}T^*}}\right) + \frac{2\overline{\Delta}}{1 - e^{-\bar{\rho}T^*}}} \tag{3.83}$$

(ii) The output tracking error $z_1 = x_1 - y_r$ *is energy integrable for* $t \in [0,\ \infty)$ *for a finite* $\aleph$ *(finite transitions of actuator failure patterns)*

(iii) Asymptotic stability of $z(t) = 0$ *for a finite* $\aleph$*, which means that* $\lim_{t\to\infty} x_1 - y_r = 0$*. Where,*

$\mathscr{L} := \Big(\frac{\gamma\underline{\lambda}(\Gamma^{-2})\epsilon + 2\bar{\bar{c}}}{4\bar{\bar{c}}\gamma\underline{\lambda}(\Gamma^{-2})} + \frac{\overline{\lambda}(\Gamma^{-1})}{2}\Big)\overline{\theta}^2$ *and* $\overline{\Delta}$ *is the maximum magnitude of the sudden jump in the failure induced parameters due to change in actuator failure pattern.* T^* *the finite positive transit time between two simultaneous changes in actuator failure patterns. Further,* γ, $\bar{\bar{c}}$, $\bar{g}$ *and* Γ *are positive design parameters while* $\overline{\theta}$ *denotes the bound on the parameter estimation error defined in* (3.39).

Proof of Theorem 3.5 (i).

In order to proceed with the proof, firstly, equations (3.79) and (3.80) are called upon to form the estimation error dynamics at the second layer as,

$$\dot{\tilde{x}}_s = (A_0 - \gamma\Phi(x,v)^T\Phi(x,v)P)\tilde{x}_s + \Phi(x,v)^T\tilde{\theta}_s \tag{3.84}$$

$$\dot{\hat{\theta}}_s = \Gamma\Phi(x,v)P\tilde{x}_s + \sum_{\mu=1}^{p+m+2}\dot{\hat{w}}_\mu\hat{\theta}_{(\mu)} \tag{3.85}$$

For ease of analysis, we consider $\Gamma_\mu = \Gamma$ and $P_\mu = P$ for all $\mu = \{1, 2, \ldots, p+m+2\}$. The closed loop tracking error dynamics at the second layer of adaptation can be rewritten from (3.41) as,

$$\dot{z} = \underbrace{\begin{bmatrix} -(c_1+s_1) & 1 & \ldots & 0 \\ -1 & -(c_2+s_2) & \ldots & 0 \\ \vdots & \ldots & \ldots & 1 \\ 0 & \ldots & -1 & -(c_\wp+s_\wp)\frac{b^*}{\ell} \end{bmatrix}}_{\mathcal{A}} z + \underbrace{\begin{bmatrix} 0 & \psi_1^T & 0 \\ 0 & \psi_2^T & 0 \\ \vdots & \vdots & \vdots \\ v_1 & \psi_\wp^T & \beta^T \end{bmatrix}}_{B_{\theta^*}}\tilde{\theta}_s + \underbrace{\begin{bmatrix} 0 \\ -\frac{\partial\alpha_1}{\partial\hat{\kappa}_{(\mu)}} \\ \vdots \\ -\frac{\partial\alpha_{\wp-1}}{\partial\hat{\kappa}_{(\mu)}} \end{bmatrix}}_{B_{\dot{\hat{\kappa}}}}\dot{\hat{\kappa}}_s \tag{3.86}$$

The subscript s is used here with signals undergoing the second layer of adaptation. Further, the equation (3.85) is simplified as follows,

$$\begin{aligned}\dot{\hat{\theta}}_s &= \Gamma\Phi(x,v)P\tilde{x}_s + \sum_{\mu=1}^{p+m+2}\dot{\hat{w}}_\mu\hat{\theta}_{(\mu)} \\ &= \Gamma\Phi(x,v)P\tilde{x}_s + \dot{\hat{w}}_1\hat{\theta}_{(1)} + \ldots + \dot{\hat{w}}_{p+m+1}\hat{\theta}_{(p+m+1)} - (\dot{\hat{w}}_1 + \ldots + \dot{\hat{w}}_{p+m+1})\hat{\theta}_{(p+m+2)} \\ &= \Gamma\Phi(x,v)P\tilde{x}_s - \sum_{\mu=1}^{p+m+1}\dot{\hat{w}}_\mu(\hat{\theta}_{(p+m+2)} - \hat{\theta}_{(\mu)}) = \Gamma\Phi(x,v)P\tilde{x}_s - \dot{\hat{\tilde{w}}}^T\tilde{\Theta}\end{aligned} \tag{3.87}$$

where, $\Gamma = \Gamma_\mu$, $P_\mu = P$ and $A_{\mu_0} = A_0$ are so considered for simplicity of calculations. Further, the vector $\tilde{\Theta} := [\{\hat{\theta}_{(p+m+2)} - \hat{\theta}_{(\mu)}\}_{\mu=1}^{p+m+1}]^T$. With $P = I_\wp$ as considered earlier in the proof of Theorem 3.4, $\dot{\tilde{\theta}}_s = -\dot{\hat{\theta}}_s$, equations (3.84), (3.87) and subsequently applying Peter-Paul inequality with the factor $\gamma\underline{\lambda}(\Gamma^{-2})$ yields,

$$\frac{d}{dt}\Big(\frac{1}{2}\|\tilde{x}_s\|^2 + \frac{1}{2}\tilde{\theta}_s^T\Gamma^{-1}\tilde{\theta}_s\Big) \leq -\tilde{x}_s^TQ\tilde{x}_s - \gamma\|\Phi\tilde{x}_s\|^2 + \frac{\|\tilde{\theta}_s\|^2}{2\gamma\underline{\lambda}(\Gamma^{-2})} + \frac{\gamma\underline{\lambda}(\Gamma^{-2})}{2}\|\dot{\hat{\tilde{w}}}^T\tilde{\Theta}\|^2 \tag{3.88}$$

Now invoking the inequality, $\|\Phi(x,v)\tilde{x}_s\|^2 \geq \underline{\lambda}(\Gamma^{-2})(\|\dot{\hat{\theta}}_s\|^2 + \|\dot{\tilde{w}}^T\tilde{\Theta}\|^2)$ and applying the same to (3.88) gives,

$$\frac{d}{dt}\Big(\frac{1}{2}\|\tilde{x}_s\|^2 + \frac{1}{2}\tilde{\theta}_s^T\Gamma^{-1}\tilde{\theta}_s\Big) \leq -\tilde{x}_s^T Q\tilde{x}_s + \frac{\|\tilde{\theta}_s\|^2}{2\gamma\underline{\lambda}(\Gamma^{-2})} - \frac{\gamma\underline{\lambda}(\Gamma^{-2})}{2}\|\dot{\hat{\theta}}_s\|^2 \tag{3.89}$$

From (3.44), it is already proved that the tracking error $z(t)$ satisfies ISS property. Therefore,

$$\frac{d}{dt}\Big(\frac{\epsilon}{2}\|z\|^2\Big) \leq -\underline{\lambda}(\mathcal{Q})\epsilon\|z\|^2 + \frac{\epsilon}{4}\left[\frac{\|\tilde{\theta}_s\|^2}{\bar{\bar{c}}} + \frac{\|\dot{\hat{\theta}}_s\|^2}{\bar{g}}\right] \tag{3.90}$$

With respect to the second layer of adaptation, a total Lyapunov function $V : \mathbb{R}^{\wp} \times \mathbb{R}^{\wp} \times \mathbb{R}^{p+m+1} \times [t_0, \infty) \to \mathbb{R}_+$ is considered with $V(t) = V_h(t)$ for $t \in [T_h,\ T_{h+1})$ similar to (3.40) as shown below.

$$V(t) = \frac{\epsilon}{2}\|z\|^2 + \frac{1}{2}\tilde{x}_s^T P\tilde{x}_s + \frac{1}{2}\tilde{\theta}_s^T\Gamma^{-1}\tilde{\theta}_s \tag{3.91}$$

The function $V_h(t)$ is continuous and differentiable. Adding (3.89) and (3.90) yields the derivative of $V_h(t)\ \forall t \in [T_h,\ T_{h+1})$ as,

$$\begin{aligned}\dot{V}_h(t) &\leq -\underline{\lambda}(\mathcal{Q})\epsilon\|z\|^2 - \underline{\lambda}(Q)\|\tilde{x}_s\|^2 - \Big(\frac{\gamma}{2}\underline{\lambda}(\Gamma^{-2}) - \frac{\epsilon}{4\bar{g}}\Big)\|\dot{\hat{\theta}}_s\|^2 + \Big(\frac{\gamma\underline{\lambda}(\Gamma^{-2})\epsilon + 2\bar{\bar{c}}}{4\bar{\bar{c}}\gamma\underline{\lambda}(\Gamma^{-2})}\Big)\|\tilde{\theta}_s\|^2 \\ &\leq -\rho(\epsilon\|z\|^2 + \|\tilde{x}_s\|^2) + \Big(\frac{\gamma\underline{\lambda}(\Gamma^{-2})\epsilon + 2\bar{\bar{c}}}{4\bar{\bar{c}}\gamma\underline{\lambda}(\Gamma^{-2})}\Big)\|\tilde{\theta}_s\|^2 \end{aligned} \tag{3.92}$$

The inequality (3.92) results from the choice of $\epsilon = \gamma\underline{\lambda}(\Gamma^{-2})\bar{g}$. Further, this resulting inequality can be rearranged as,

$$\dot{V}_h(t) \leq -\rho(\epsilon\|z\|^2 + \|\tilde{x}_s\|^2) - \frac{1}{2}\tilde{\theta}_s^T\Gamma^{-1}\tilde{\theta}_s + \Big(\frac{\gamma\underline{\lambda}(\Gamma^{-2})\epsilon + 2\bar{\bar{c}}}{4\bar{\bar{c}}\gamma\underline{\lambda}(\Gamma^{-2})} + \frac{\overline{\lambda}(\Gamma^{-1})}{2}\Big)\overline{\theta}^2 \tag{3.93}$$

$$\leq -\bar{\rho}V_h(t) + \Big(\frac{\gamma\underline{\lambda}(\Gamma^{-2})\epsilon + 2\bar{\bar{c}}}{4\bar{\bar{c}}\gamma\underline{\lambda}(\Gamma^{-2})} + \frac{\overline{\lambda}(\Gamma^{-1})}{2}\Big)\overline{\theta}^2 \tag{3.94}$$

Where $\bar{\rho} := \min\{2\underline{\lambda}(\mathcal{Q}),\ 2\underline{\lambda}(Q),\ \underline{\lambda}(\Gamma^{-1})\}$. For simplicity of representation let us denote the second term in inequality (3.94) as $\mathscr{L} := \Big(\frac{\gamma\underline{\lambda}(\Gamma^{-2})\epsilon + 2\bar{\bar{c}}}{4\bar{\bar{c}}\gamma\underline{\lambda}(\Gamma^{-2})} + \frac{\overline{\lambda}(\Gamma^{-1})}{2}\Big)\overline{\theta}^2$ so that (3.94) can be written as, $\dot{V}_h(t) \leq -\bar{\rho}V_h(t) + \mathscr{L}\overline{\theta}^2$. Since $\mathscr{L}$ is a function of constant design parameters and $\overline{\theta}$ is finite so $z(t) \in \mathcal{L}_\infty[T_h,\ T_{h+1})$. All other closed loop signals are proved to be piecewise bounded that is for $t \in [T_h,\ T_{h+1})$ $(h \in \mathbb{W})$.

To show the stability of the closed loop signals for all time $t \in [0,\ \infty)$ under infinite actuator failures, similar recursive analysis as in the proof of Theorem 3.4 (i) is done to infer the following. The total Lyapunov function $V(t)$ is used and following inequality relating the final value $V(T)$ and $V(0)$ is derived. Herein T denotes the final time and $T \to \infty$. The analysis is not repeated here for the sake

of brevity.

$$V(T^-) \leq V(0)e^{-\bar{\rho}T} + \mathscr{L}\overline{\theta}^2\left(\frac{2-e^{-\bar{\rho}T^*}}{1-e^{-\bar{\rho}T^*}}\right) + \frac{\overline{\Delta}}{1-e^{-\bar{\rho}T^*}} \tag{3.95}$$

$$\tag{3.96}$$

The notations in the above expression (3.95) have their usual meanings as discussed in the proof of Theorem 3.4. Therefore, the $\mathcal{L}_\infty[0,\infty)$ bound on the tracking error is derived to be,

$$\lim_{T\to\infty}\|z(t)\| \leq \sqrt{2\mathscr{L}\overline{\theta}^2\left(\frac{2-e^{-\bar{\rho}T^*}}{1-e^{-\bar{\rho}T^*}}\right) + \frac{2\overline{\Delta}}{1-e^{-\bar{\rho}T^*}}} \tag{3.97}$$

Proof of Theorem 3.5 (ii)

To prove that $z(t) \in \mathcal{L}_2[0,\ \infty)$

Since $\tilde{x}_s = \sum_{\mu=1}^{p+m+2} \hat{w_\mu}\tilde{x}_{(\mu)}$ and $\tilde{x}_{(\mu)} \in \mathcal{L}_2[0,\ \infty)$ $(\mu = \overline{1,\ p+m+2})$ is ensured from Theorem 3.4 (ii) for a finite $\aleph$, it can be concluded that $\tilde{x}_s \in \mathcal{L}_2[0,\ \infty)$. Herein, the property of convex hull will be exploited which yields $\sum_{\mu=1}^{p+m+2} \hat{w}_\mu\tilde{x}_{(\mu)} \leq \tilde{x}_{(\mu)}$ since $\hat{w}_\mu \in [0,\ 1]$ by design. Therefore, the following inequality holds.

$$\int_0^\infty \|\tilde{x}_s\|^2 dt \leq \int_0^\infty \left\| \sum_{\mu=1}^{p+m+2} \hat{w}_\mu\tilde{x}_{(\mu)} \right\|^2 dt \leq \int_0^\infty \|\tilde{x}_{(\mu)}\|^2 dt < \infty \tag{3.98}$$

Thus from (3.98) $\tilde{x}_s \in \mathcal{L}_2[0,\infty)$ follows. Thereafter, since $x(t) \in \mathcal{L}_\infty[0.\ \infty)$ from Theorem 3.3, the regressor matrix $\Phi \in \mathcal{L}_\infty[0,\ \infty)$. Further, let us define $\bar{\tilde{\Theta}} := [\{\hat{\theta}_{(\mu)} - \hat{\theta}_{(p+m+2)}\}_{\mu=1}^{p+m+1}]^T$ and then derive the expression $\dot{\tilde{\hat{w}}} = \triangle\tilde{X}^T\triangle\tilde{X}\tilde{\tilde{w}} = M(t)\tilde{\tilde{w}}$ from (3.23) with $\triangle\tilde{X} := [\{\tilde{x}_{(\mu)} - \tilde{x}_{(p+m+2)}\}_{\mu=1}^{p+m+1}]^T$. It is well known that $\mathcal{L}_2$ spaces are closed under addition, so $\triangle\tilde{X} \in \mathcal{L}_2[0,\ \infty]$. The parameter adaptation law at the second layer is given by,

$$\dot{\hat{\theta}}_s = \Gamma\Phi P\tilde{x}_s + \dot{\tilde{\hat{w}}}^T\bar{\tilde{\Theta}} \tag{3.99}$$

Squaring both sides of (3.99), using the inequality $(a+b)^2 \leq 2(a^2+b^2)$ and subsequent application of the integral inequality yields,

$$\int_0^\infty \|\dot{\hat{\theta}}_s\|^2 dt \leq 2\overline{\lambda}(\Gamma^2)\overline{\lambda}(P^2)\|\Phi\|_\infty^2 \int_0^\infty \|\tilde{x}_s\|^2 dt + 2\|\bar{\tilde{\Theta}}\|_\infty^2 \int_0^\infty \|\dot{\tilde{\hat{w}}}\|^2 dt \tag{3.100}$$

$$\leq 2\overline{\lambda}(\Gamma^2)\overline{\lambda}(P^2)\|\Phi\|_\infty^2 \int_0^\infty \|\tilde{x}_s\|^2 dt + 2\|\bar{\tilde{\Theta}}\|_\infty^2\|M\|_\infty\|\tilde{\tilde{w}}\|_\infty^2 \int_0^\infty \|\triangle\tilde{X}^T\triangle\tilde{X}\|dt \tag{3.101}$$

Now the boundedness of the integral in the second term of inequality (3.101) is inferred by applying

Holder's inequality and thereafter invoking the $\mathcal{L}_2$ integrability property of $\triangle\tilde{X}(t)$ as follows,

$$\int_0^\infty \|\triangle\tilde{X}^T\triangle\tilde{X}\|dt \leq \int_0^\infty \|\triangle\tilde{X}\|\|\triangle\tilde{X}\|dt \leq \sqrt{\int_0^\infty \|\triangle\tilde{X}(t)\|^2dt}\sqrt{\int_0^\infty \|\triangle\tilde{X}(t)\|^2dt} < \infty \tag{3.102}$$

Hence, from (3.101) and (3.102), it is proved that $\dot{\hat{\theta}}_s(t) \in \mathcal{L}_2[0,\ \infty)$. At this point, let us define an auxiliary variable $\vartheta := z - \mathcal{M}\tilde{x}_s$ which is similar to the one defined in Theorem 3.3 to prove $z(t) \in \mathcal{L}_2[T_h,\ T_{h+1})$. Using the closed loop output tracking error dynamics (3.86) and (3.84), the dynamics of the transformed variable ϑ is described by,

$$\dot{\vartheta} = \bar{A}\vartheta + \hat{\mathcal{M}}\tilde{x}_s + B_{\hat{\kappa}}\dot{\tilde{\kappa}}_s \tag{3.103}$$

Where $\hat{\mathcal{M}} := -\dot{\mathcal{M}} + \bar{\mathcal{A}}\mathcal{M} - \mathcal{M}\bar{A}$ and $\bar{A} = A_0 - \gamma\Phi^T\Phi P$. The matrix $\mathcal{M}$ has been defined earlier in (3.46). Now the system dynamics in (3.103) is driven only by $\mathcal{L}_2$ inputs. The analysis until the derivation of finite $\mathcal{L}_2$ bound for the signal $\vartheta(t)$ is same and hence not repeated for brevity. Instead, the derived inequality (3.51) is utilized to infer the following,

$$\int_0^\infty \|\vartheta\|^2dt \leq \frac{\|\vartheta(0)\|^2}{2\underline{\lambda}(\mathcal{Q})} + \frac{1}{4\bar{g}\underline{\lambda}(\mathcal{Q})}\int_0^\infty \|\dot{\hat{\theta}}_s\|^2dt + \frac{1}{2\underline{\lambda}(\mathcal{Q})^2}\|\hat{\mathcal{M}}\|_F^2\int_0^\infty \|\tilde{x}_s\|^2dt < \infty \tag{3.104}$$

Hence, using inequalities (3.98), (3.101) and (3.102), it can be concluded from (3.104), that $\vartheta(t) \in \mathcal{L}_2[0,\infty)$ implying $z(t) \in \mathcal{L}_2[0,\ \infty)$.

Proof of Theorem 3.5 (iii).

Now that it is proved that for a finite $\aleph$ (signifying a finite number of changes in the actuator failure pattern), the tracking error $z(t) \in \mathcal{L}_2[0,\ \infty) \cap \mathcal{L}_\infty[0,\ \infty)$ and its derivative $\dot{z}(t) \in \mathcal{L}_\infty[0,\ \infty)$. Hence, invoking Barbalat's Lemma, asymptotic stability of the tracking error dynamics is proved and $\lim_{t\to\infty} z(t) = 0$. The proofs are complete. □

Remark 3.2. *The essential attributes of the proposed control scheme in regards to infinitely occurring actuator failures and their subsequent effect on the bounds of tracking error vector $z(t)$ is illustrated in Figure 3.4. It is a schematic representation of the stability properties and inferences drawn from Theorem 3.4 and 3.5 to support a quick understanding of the interdependence between the transit time T^* between two successive changes in actuator failure pattern, controller gains and the $\mathcal{L}_\infty$ bound on the tracking error $z(t)$. From Theorem 3.4 and 3.5, the condition $T^* > 0$ is derived to be a principal criterion which must be satisfied to yield boundedness of closed loop system trajectories. Figure 3.4 demonstrates that a decrease in the transition time T^* results in increased magnitude of output overshoots which however can also be decreased by incrementing the controller gains accordingly. Moreover, it is observed that decrementing T^* gradually effects the output transient performance adversely until the transit time reaches a neighborhood close to zero which results in $\|z(t)\|$ escaping to infinity.*

Remark 3.3. *It is worth mentioning that the adaptive fault tolerant controller proposed herein is general in the sense that it can be easily applied to control design problems dealing with no failure,*

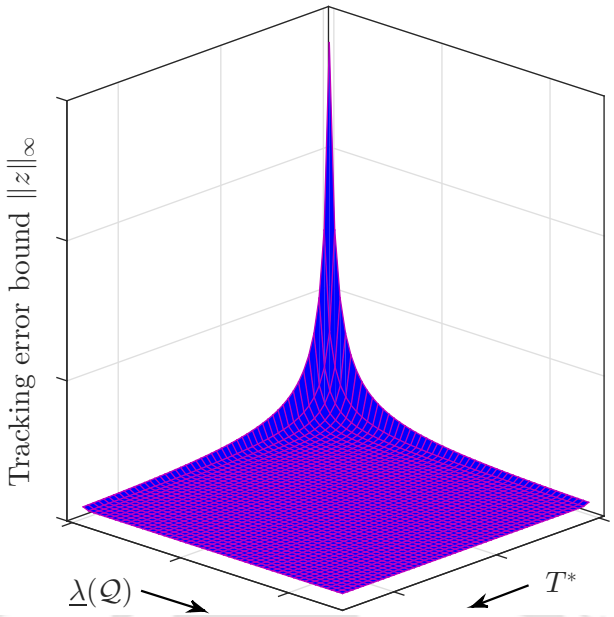

Figure 3.4: Illustration explaining the interdependence between $\|z\|_\infty$, controller gain parameters and actuator failure transit time T^*

finite actuator failures and infinite actuator failures. The bounds on the tracking error derived for the case of infinite actuator failures can be utilized to calculate similar bounds in finite actuator failure scenarios by considering the limiting value of the inequality (3.70) *as* $T^* \to \infty$. *Further, unlike the works in [5, 31, 32, 71], apart from yielding closed loop stability in the case of intermittently changing actuator failure patterns, the proposed adaptive controller is also capable of compensating a larger class of actuator faults modeled as* $u_j(t) = K_{j,h}u_{Hj} + \bar{u}_{Fj,h} + \sum_{i=1}^{n_j} k_{jh,i}f_{jh,i}(t)$, *where* $K_{j,h}$, $\bar{u}_{Fj,h}$, $k_{jh,i}$ *for* $j = \overline{1,m}$ *are unknown constants and* $f_{jh,i}(t)$ *are unknown bounded basis functions. The proposed scheme is also believed to yield promising results when applied to nonlinear uncertain systems with frequently varying unknown parameters and external disturbances.*

3.2.3.2 Transient Performance Analysis for the Proposed AMMFTC

In this section, it is shown that the proposed adaptive control methodology using multiple adaptive identification models results in an improved transient performance compared to the results achieved using a single identifier based backstepping controller. To proceed with the analysis, we state the following result,

Theorem 3.6. *Let us consider the nonlinear uncertain system* (3.1), *the control law* (3.37), *the identifier* (3.11) *and the adaptive law* (3.12) *at the first layer followed by the second layer of parameter adaptation yielding* $\hat{\theta}_s = \sum_{\mu=1}^{p+m+2} \hat{w}_\mu \hat{\theta}_{(\mu)}$ *with the weight learning law* (3.23). *With the choice of* $P_\mu = P = I_\wp$, $A_{\mu_0} = A_0$ *as a Hurwitz matrix,* $\gamma > 0$, $A_0^T P + PA_0 = -Q$ *and the adaptive rate parameter* $\Gamma_\mu > 0$, *the*

following inequality holds for $t \in [T_h,\ T_{h+1}),\ h \in \mathbb{W}$,

$$\|z\| \leq \|z(T_h)\|e^{-\rho t} + \frac{1}{\sqrt{\rho}}\Big(\frac{1}{2\bar{\bar{c}}} + \frac{1}{\gamma\epsilon}\Big)^{\frac{1}{2}}\Big\|\sum_{\mu=1}^{N}\hat{w}_\mu(T_h)\tilde{\theta}_{(\mu)}(T_h)\Big\|^2 \tag{3.105}$$

where, the parameters are defined as $\bar{\bar{c}} := \min\{\bar{c}, c_\wp, \bar{c}_\wp\}$ *and* $\rho := \min\{\underline{\lambda}(Q), \underline{\lambda}(\mathcal{Q})\}$.

Proof.

The derivation follows a similar procedure as given in [69]. With the choice of design parameters as stated in the Theorem 3.6 above, using (3.84) the identification error dynamics under second layer of adaptation is described by,

$$\dot{\tilde{x}}_s = (A_0 - \gamma\Phi(x,v)^T\Phi(x,v))\tilde{x}_s + \Phi(x,v)^T\tilde{\theta}_s \tag{3.106}$$

$$\dot{\tilde{\theta}}_s = \Gamma\Phi(x,v)\tilde{x}_s + \sum_{\mu=1}^{p+m+2}\dot{\hat{w}}_\mu\hat{\theta}_{(\mu)} \tag{3.107}$$

Therefore, it follows that, the differential inequality given below holds,

$$\frac{d}{dt}\Big(\frac{1}{2}\|\tilde{x}_s\|^2\Big) = -\tilde{x}_s^TQ\tilde{x}_s - \gamma\|\Phi(x,v)\tilde{x}_s\|^2 + \tilde{x}_s^T\Phi^T(x,v)\tilde{\theta}_s \tag{3.108}$$

Applying Peter Paul inequality to the above equality with the factor $\gamma > 0$ yields,

$$\frac{d}{dt}\Big(\frac{1}{2}\|\tilde{x}_s\|^2\Big) \leq -\tilde{x}_s^TQ\tilde{x}_s - \gamma\|\Phi(x,v)\tilde{x}_s\|^2 + \frac{\gamma\|\Phi(x,v)\tilde{x}_s\|^2}{2} + \frac{\|\tilde{\theta}_s\|^2}{2\gamma} \tag{3.109}$$

Thereafter, substituting the inequality $\|\Phi(x,v)\tilde{x}_s\|^2 \geq \underline{\lambda}(\Gamma^{-2})(\|\dot{\tilde{\theta}}_s\|^2 + \|\dot{\tilde{w}}^T\tilde{\Theta}\|^2)$ in the inequality (3.109) results in,

$$\begin{aligned}\frac{d}{dt}\Big(\frac{1}{2}\|\tilde{x}_s\|^2\Big) &\leq -\tilde{x}_s^TQ\tilde{x}_s - \frac{\gamma\underline{\lambda}(\Gamma^{-2})}{2}\|\dot{\tilde{\theta}}_s\|^2 + \frac{\|\tilde{\theta}_s\|^2}{2\gamma}\\ &\leq -\underline{\lambda}(Q)\|\tilde{x}_s\|^2 - \frac{\gamma\underline{\lambda}(\Gamma^{-2})}{2}\|\dot{\tilde{\theta}}_s\|^2 + \frac{\|\tilde{\theta}_s\|^2}{2\gamma}\end{aligned} \tag{3.110}$$

Now using the tracking error dynamics (3.86) obtained by substituting the parameter estimate $\hat{\theta}_s$ after second layer of adaptation and the inequality (3.90) yields,

$$\frac{d}{dt}\Big(\frac{\epsilon\|z\|^2 + \|\tilde{x}_s\|^2}{2}\Big) \leq -\rho(\epsilon\|z\|^2 + \|\tilde{x}_s\|^2) + \left(\frac{\epsilon}{4\bar{\bar{c}}} + \frac{1}{2\gamma}\right)\|\tilde{\theta}_s\|^2 - \left(\frac{\gamma\underline{\lambda}(\Gamma^{-2})}{2} - \frac{\epsilon}{4\bar{g}}\right)\|\dot{\tilde{\theta}}_s\|^2 \tag{3.111}$$

Where, $\rho = \min\{\underline{\lambda}(\mathcal{Q}), \underline{\lambda}(Q)\}$. Thereafter choosing $\epsilon = \gamma\underline{\lambda}(\Gamma^{-2})\bar{g}$ and integrating both sides of the inequality from $T_h \sim t$ results in,

$$\epsilon\|z\|^2 + \|\tilde{x}_s\|^2 \leq (\epsilon\|z(T_h)\|^2 + \|\tilde{x}_s(T_h)\|^2)e^{-2\rho t} + \left(\frac{\gamma\epsilon + 2\bar{\bar{c}}}{2\bar{\bar{c}}\gamma\epsilon}\right)\int_{T_h}^{t} e^{-2\rho(t-\tau)}\|\tilde{\theta}_s(\tau)\|^2 d\tau \tag{3.112}$$

Finally, taking the supremum of $\tilde{\theta}_s(\tau)$ implies,

$$\|z(t)\| \leq \|z(T_h)\|e^{-\rho t} + \frac{1}{\sqrt{2\rho}}\left(\frac{1}{2\bar{\bar{c}}} + \frac{1}{\gamma\epsilon}\right)^{\frac{1}{2}}\|\tilde{\theta}_s\|_\infty \tag{3.113}$$

Thereafter performing trajectory initialization procedure mentioned in [69], that is setting $z(T_h) = 0$, the bound on $z(t)$ in (3.113) becomes,

$$\|z(t)\|_\infty \leq \frac{1}{\sqrt{2\rho}}\left(\frac{1}{2\bar{\bar{c}}} + \frac{1}{\gamma\epsilon}\right)^{\frac{1}{2}}\|\tilde{\theta}_s(T_h)\| \tag{3.114}$$

Further, the bound on $z(t)$ using a single identification model can be similarly derived in a straightforward manner as follows. Using the adaptive identifier with the parameter estimation law in (3.11) and (3.12), the inequality below holds with $P = I_\wp$.

$$\begin{aligned}\frac{d}{dt}\left(\frac{1}{2}\|\tilde{x}_{(\mu)}\|^2\right) &= -\tilde{x}_{(\mu)}^T Q_\mu \tilde{x}_{(\mu)} - \gamma\|\Phi(x,v)\tilde{x}_{(\mu)}\|^2 + \tilde{x}_{(\mu)}^T\Phi^T(x,v)\tilde{\theta}_{(\mu)} \\ &\leq -\underline{\lambda}(Q_\mu)\|\tilde{x}_{(\mu)}\|^2 - \gamma\|\Phi(x,v)\tilde{x}_{(\mu)}\|^2 + \frac{\gamma}{2}\|\Phi(x,v)\tilde{x}_{(\mu)}\|^2 + \frac{\|\tilde{\theta}_{(\mu)}\|^2}{2\gamma} \\ &\leq -\underline{\lambda}(Q_\mu)\|\tilde{x}_{(\mu)}\|^2 - \frac{\gamma\underline{\lambda}(\Gamma^{-2})}{2}\|\dot{\hat{\theta}}_{(\mu)}\|^2 + \frac{\|\tilde{\theta}_{(\mu)}\|^2}{2\gamma}\end{aligned} \tag{3.115}$$

In regards to the tracking error dynamics (3.41) by the parameter estimation from a single identifier, the following is satisfied,

$$\frac{d}{dt}\left(\frac{1}{2}\epsilon\|z\|^2\right) \leq -\underline{\lambda}(\mathcal{Q})\epsilon\|z\|^2 + \frac{\epsilon}{4\bar{\bar{c}}}\|\tilde{\theta}_{(\mu)}\|^2 + \frac{\epsilon}{4\bar{g}}\|\dot{\hat{\theta}}_{(\mu)}\|^2 \tag{3.116}$$

Adding (3.115) and (3.116), we get,

$$\frac{d}{dt}\left(\frac{\epsilon\|z\|^2 + \|\tilde{x}_{(\mu)}\|^2}{2}\right) \leq -\rho(\epsilon\|z\|^2 + \|\tilde{x}_{(\mu)}\|^2) + \left(\frac{\epsilon}{4\bar{\bar{c}}} + \frac{1}{2\gamma}\right)\|\tilde{\theta}_{(\mu)}\|^2 - \left(\frac{\gamma\underline{\lambda}(\Gamma^{-2})}{2} - \frac{\epsilon}{4\bar{g}}\right)\|\dot{\hat{\theta}}_{(\mu)}\|^2 \tag{3.117}$$

Choice of $\epsilon = \gamma\underline{\lambda}(\Gamma^{-2})\bar{g}$ leads to,

$$\frac{d}{dt}\left(\frac{\epsilon\|z\|^2 + \|\tilde{x}_{(\mu)}\|^2}{2}\right) \leq -\rho(\epsilon\|z\|^2 + \|\tilde{x}_{(\mu)}\|^2) + \left(\frac{\epsilon}{4\bar{\bar{c}}} + \frac{1}{2\gamma}\right)\|\tilde{\theta}_{(\mu)}\|^2 \tag{3.118}$$

Therefore solving the above differential inequality, the bound on $z(t)$ after simplifications and trajectory initializations ($z(T_h) = 0$) is found to be,

$$\|z(t)\|_\infty \leq \frac{1}{\sqrt{2\rho}}\left(\frac{1}{2\bar{\bar{c}}} + \frac{1}{\gamma\epsilon}\right)^{\frac{1}{2}}\|\tilde{\theta}_{(\mu)}(T_h)\| \tag{3.119}$$

Let us define (3.114) as $\|z(t)\|_{\mathcal{L}_\infty}(MM)$ being the $\mathcal{L}_\infty$ output transient bound using the proposed method and that in (3.119) using a single identification model as $\|z(t)\|_{\mathcal{L}_\infty}(SM)$. Dividing (3.114) by (3.119) yields,

$$\frac{\|z(t)\|_{\mathcal{L}_\infty}(MM)}{\|z(t)\|_{\mathcal{L}_\infty}(SM)} = \frac{\left\| \sum_{\mu=1}^{p+m+2} \hat{w}_\mu(T_h)\tilde{\theta}_{(\mu)}(T_h) \right\|}{\|\tilde{\theta}_{(\mu)}(T_h)\|} < 1 \tag{3.120}$$

The above inequality is derived using the fact that any convex combination of elements in a convex set even if they lie on the boundary always resides inside the convex hull formed by them. Based on (3.120), the following is concluded.

- When $h = 0$, inequalities (3.114) and (3.119) gives the $\mathcal{L}_\infty[0, T_1)$ norms for the tracking error $z(t)$ before the occurrence of the first actuator failure. Increasing the backstepping control gains c_i for $\overline{1, \wp}$ would result in an increment in $z(0)$. Although such a measure may improve the output performance for $t \in [0,\ T_1)$, it actually increases the upper bound of $z(t)$. This would result in an increased control effort and contribute to an cumulatively increasing magnitude of output overshoots with each change in the actuator failure pattern. However, if trajectory initialization is performed, i.e. setting $z(0) = 0$, the transient performance in the $\mathcal{L}_\infty$ sense can be improved by incrementing design parameters c_i and γ. With reference to (3.120), the proposed multiple model based control method additionally enhances the output performance by further decreasing the $\mathcal{L}_\infty[0,\ T_1)$ norm of the tracking error.
- The cases with $h > 0$, represents actuator failures at time instances $T_1,\ T_2, \ldots, T_h, \ldots,\ T_\aleph$ with each $T_h \in [0,\ T)$. Unlike the previous case with $h = 0$, attributed to the unknown time, pattern and magnitude of occurrence of actuator failures, trajectory initialization is not possible. Achieving a stable, fast and accurate output performance in indirect adaptive control directly translates from the fact that how rapidly and accurately are the unknown parameters estimated.The proposed controller exploits this distinct feature of indirect adaptive control. Instead of increasing the values of design parameters c_i $(i = \overline{1, \wp})$, γ and Γ_μ, it reduces the $\mathcal{L}_\infty$ norm of the parameter estimation error. Thereby the $\mathcal{L}_\infty$ norm, that is, $\|z(t)\|_{[T_h,\ T_h+1)}$ is reduced. Hence, the proposed control technique using multiple identification models offers an additional design freedom.

In conclusion, the adaptive control methodology proposed in this chapter proves to be beneficial in reducing the transient peaks at both instances of start up and post failures without trajectory initialization and increment in virtual control gains.

3.2.4 Simulation Studies

In this section, two examples of nonlinear dynamical systems are considered to illustrate the beneficial attributes of the proposed control method in compensating finite and infinitely occurring actuator failures. Further, as an addendo, the superior output transient and steady state performance obtained using AMMFTC compared to single identification model based control and the control technique proposed by [6] is demonstrated through plots and tabulations.

3.2.4.1 Numerical Example

Let us consider a multi input single output nonlinear uncertain system with unknown parametric uncertainties as,

$$\dot{\xi} = \varphi_0(\xi) + \varphi(\xi)\kappa^* + \sum_{j=1}^{2} b_j g_j(\xi) u_j$$
$$y = \xi_2 \tag{3.121}$$

where the state vector is defined as $\xi := [\xi_1,\ \xi_2,\ \xi_3]^T \in \mathbb{R}^3$ and $\kappa^* \in \mathbb{R}^3$ denotes the unknown system parameter vector. The nonlinear functions are defined as follows,

$$\varphi_0 = \begin{bmatrix} -\xi_1 \\ \xi_3 \\ \xi_2\xi_3 \end{bmatrix}, \varphi = \begin{bmatrix} 0 \\ \xi_2^2 \\ \dfrac{1-e^{-\xi_3}}{1+e^{-\xi_3}} \end{bmatrix} \tag{3.122}$$

$$g_1 = g_2 = \left[\frac{2+\xi_3^2}{1+\xi_3^2},\ 0,\ 1\right]^T. \tag{3.123}$$

The system model is the same as considered in [6]. Similar to [6], the nonlinear system in (3.121) can be transformed to the form in (3.1) by using the transformation $[\eta\ x_1\ x_2]^T := [\mathscr{T}_z(\xi),\ \mathscr{T}_c(\xi)]^T := [-\xi_1 + \xi_3 + \tan^{-1}\xi_3,\ \xi_2,\ \xi_3]$. The transformation $\mathscr{T}_z(\xi)$ is calculated by solving the partial differential equations, $\left[\sum_{k=1}^{3}\frac{\partial \mathscr{T}_z}{\partial \xi_k}g_1,\ \sum_{k=1}^{3}\frac{\partial \mathscr{T}_z}{\partial \xi_k}g_2\right]^T = [0,\ 0]^T$. Therefore, the transformed system is represented as follows,

$$\dot{\eta} = -\eta + x_2 + \tan^{-1}x_2 + \frac{2+x_2^2}{1+x_2^2}\left(x_1x_2 + \frac{1-e^{-x_2}}{1+e^{-x_2}}\kappa^*\right) \tag{3.124}$$

$$\dot{x}_1 = x_2 + x_1^2\kappa^*$$
$$\dot{x}_2 = x_1x_2 + \frac{1-e^{-x_2}}{1+e^{-x_2}}\kappa^* + \sum_{j=1}^{2} b_j u_j \tag{3.125}$$

It is seen that the internal dynamics in (3.125) is ISS since the functions $\tan^{-1}x_2$, $\frac{2+x_2^2}{1+x_2^2}$ and $\frac{1-e^{-x_2}}{1+e^{-x_2}}$ are bounded $\forall x_1,\ x_2$. Further the zero dynamics obtained by substituting $[x_1,\ x_2] = [0,\ 0]$ gives $\dot{\eta} = -\eta + 2\kappa^*$. Now since κ^* is a constant, therefore the zero dynamics is stable. Hence, the design Assumption 3.6 is satisfied.

Two scenarios are considered to demonstrate the effectiveness of AMMFTC in compensating finitely and intermittently occurring actuator failures, respectively. The unknown parameters considered in simulations are $\kappa^* = 2,\ b_1^* = 1,\ b_2^* = 1$. The reference trajectory to be tracked by the system output is $y_r = \sin(t)$. The reference signal is so chosen that it satisfies Assumption 3.4. The actuator failure

model representing Scenario 1 , is defined as follows,

$$u_1(t) = \begin{cases} 5, & t \in [50,\ 100) \\ u_{H1}(t), & t \in [0,\ 50) \cup [100,\ \infty) \end{cases}, \quad u_2(t) = \begin{cases} u_{H2}(t), & t \in [0,\ 100) \end{cases} \tag{3.126}$$

Further, the intermittently occurring actuator fault/failure considered in Scenario 2 is described in (3.127) below.

$$u_1(t) = \bar{u}_{Fj_1,h}, \quad t \in [hT^*,\ (h+1)T^*),\ h \in \mathbb{N}\backslash 2\mathbb{N} \tag{3.127}$$

The transition time between each change in the actuator failure pattern is considered to be $T^* = 5 > 0$. The value at which the actuator gets stuck corresponding to Scenario 2 is given by $\bar{u}_{Fj_1,h} = 5$. The bounds on the unknown parameters are given below.

$$1 \leq \kappa^* \leq 3,\ 0.8 \leq |b_1^*| \leq 1.4,\ 0.6 \leq |b_2^*| \leq 2 \tag{3.128}$$

$$0.5 \leq K_{j,h} \leq 1,\ |\bar{u}_{Fj_k,h}| \leq 6,\ j = 1, 2. \tag{3.129}$$

Hence, Assumptions 3.2 and 3.5 also hold. The initial conditions of the system are given by $\xi(0) = [0,\ 0.4,\ 0]$. The adaptive controller is designed using the AMMFTC methodology discussed in Section 3.3.2. The number of unknown parameters being 4, we choose $N = 5$ adaptive identifiers so that the initial parameter vector estimates from each of the identification models form a convex hull. The initial parameter estimates from each of the N estimators are $\hat{\theta}_{(1)}(0) = [1,\ 1,\ 0,\ 0]^T$, $\hat{\theta}_{(2)}(0) = [1.5,\ 2.5,\ 6,\ 6]^T$, $\hat{\theta}_{(3)}(0) = [2.5,\ 1,\ 0,\ 0]^T$, $\hat{\theta}_{(4)}(0) = [2.5,\ 2.5,\ -6,\ -6]^T$, $\hat{\theta}_{(5)}(0) = [2,\ 1.5,\ 0,\ 0]^T$. The controller design parameters for simulation are chosen to be $c_1 = c_2 = 5$, $\bar{c}_1 = \bar{c}_2 = 3$, $g_2 = 3$, $\gamma = 0.5$, $\Gamma_1 = \Gamma_2 = \Gamma_3 = \Gamma_4 = \Gamma_5 = 40 \times I_2$ and $A_0 = [\text{diag}(-5,\ -7)]$. In order to provide a fair comparison of the proposed control design with single model adaptive control and the modular backstepping control (MBSC) approach by Wang *et. al* [6], the values of controller gains and other relevant design parameters are chosen to be same. The output performance in regards to start-up and post fault transient peaks and settling times, is calculated using root mean square (RMS) and integral time absolute error (ITAE) metric of the output tracking error. A relatively lower value of ITAE and RMSE from the results obtained with other relevant control schemes, signify a faithful tracking with comparatively lower overshoots and faster settling time. Further, the input performance is quantified using control energy (CE) and the total variation (TV) of the control signal. Total variation is a very important measure which gives an insight on the frequency of input usage. The lower the value of TV and CE, better is the input performance. The control energy is measured using the $2-$norm of the control input whereas TV for each of the control inputs is measured using the expression $\sum_{i=1}^{N} |u_{j,i} - u_{j,i+1}|$ for $j = 1, 2$.

- *Scenario 1* (3.126): Under no fault conditions, the output tracking performance, the convergence of parameter estimates along with the remaining system states and the control signals are shown in Figures 3.5 and 3.6, respectively. As proved in the theoretical analysis earlier, fastness of parameter convergence and improvement in output transient performance using the proposed

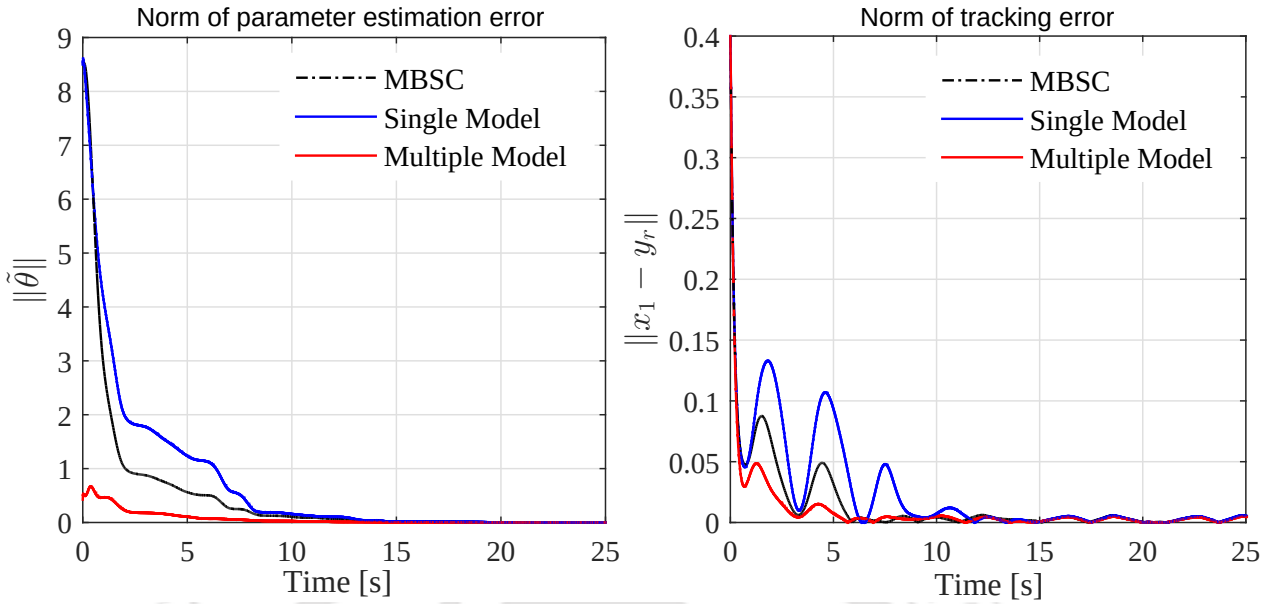

Figure 3.5: Comparison of start-up output transient performance and parameter convergence obtained with Modular Backstepping Control (MBSC) [6], single model adaptive control and proposed multiple model adaptive control

controller are clearly evident from Figure 3.5. The proposed controller using multiple models exhibits a superior output performance compared to a single model adaptive control scheme and modular backstepping control (MBSC) [6] without significantly increasing the control energy. Further, in the event of an abrupt actuator failure at $t = 50$ s, the proposed control methodology retains similar beneficial attributes in terms of rapid accommodation of actuator failure and fast post failure output tracking with minimal overshoots. The above inference is drawn from the simulation results provided in Figures 3.7 and 3.8. In addition, a consolidated performance chart summarizing the efficacy of the proposed controller relative to relevant existing adaptive control techniques is furnished in Table 3.1.

Table 3.1: Tabular comparison of output and input performance under Scenario 1 (3.126).

Control Schemes	**Output Performance**		**Input Performance**			
	ITAE	**RMSE**	**Control Energy**		**Total Variation**	
			u_1	u_2	u_1	u_2
Multiple Models	**18.69**	**0.0134**	3.644×10^3	3.126×10^3	131.72	297.48
Single Model	49.83	0.0268	3.643×10^3	3.102×10^3	147.78	305.48
MBSC	34.64	0.0195	3.639×10^3	3.106×10^3	127.97	286.34

- *Scenario 2* (3.127): This scenario demonstrates the robustness of the proposed adaptive controller to intermittently changing actuator failure patterns unknown in time, pattern and magnitude. The value at which u_1 is stuck is $\bar{u}_{Fj_1} = 5$. These eventualities are manifested in the form of infinitely occurring parameter jumps which are uncertain and unknown in all aspects except for

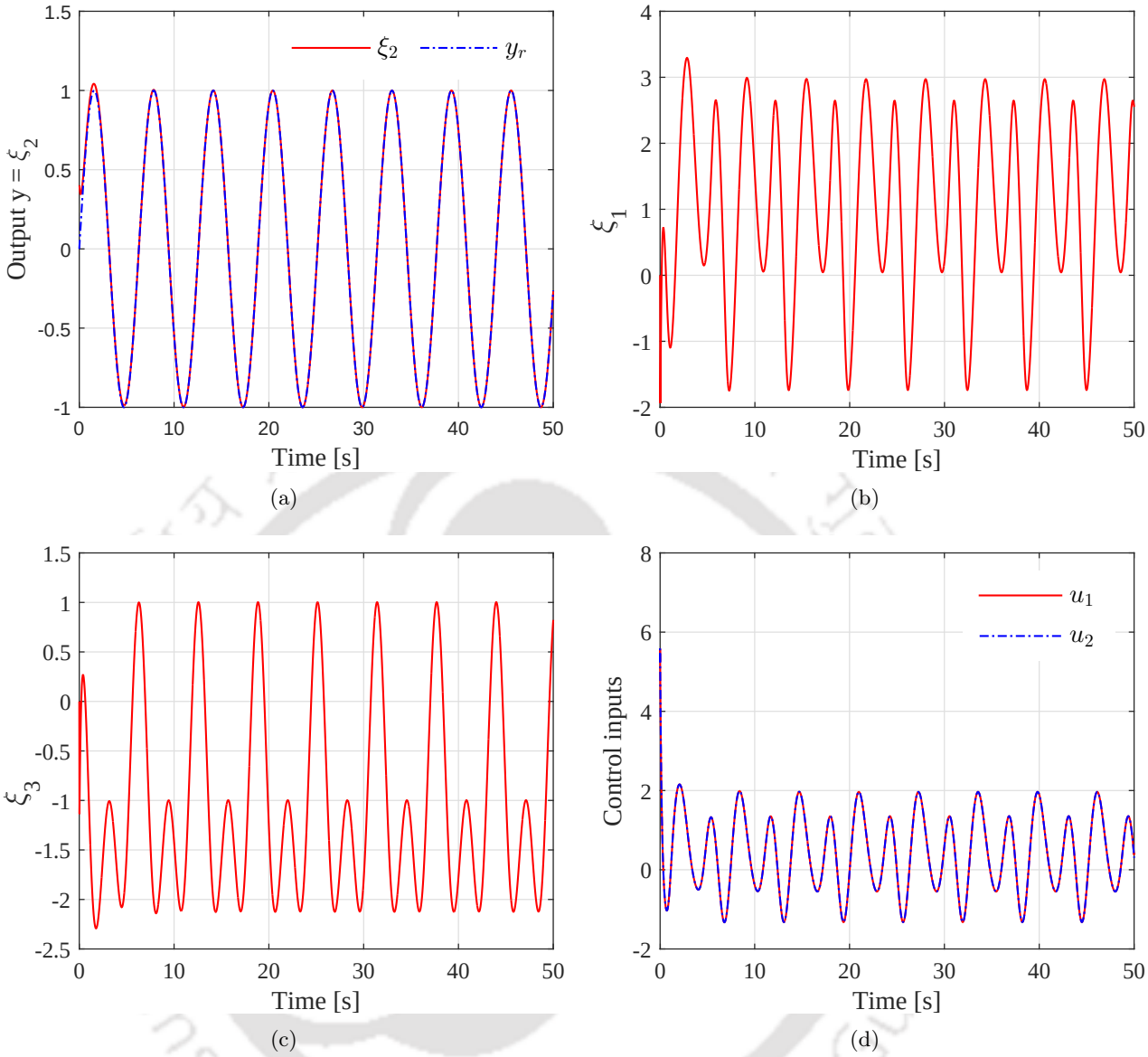

Figure 3.6: System states and control input with no actuator fault under Scenario 1 (3.126) from $t = 0 \sim 50$ s. (a) Output state $\xi_2 = x_1$;(b) state ξ_1;(c) state $\xi_3 = x_2$; (d) control inputs u_1 and u_2

the boundary set they reside in. Figure 3.10 shows the boundedness of all the system states and the control signals under this scenario with the transit time being $T^* = 5$ s. Further, the theoretical result claiming the improvement of output transient performance with an increasing T^*, is verified from the simulation results obtained with $T^* = 5$ s and $T^* = 15$ s in Figure 3.9 along with performance measures tabulated in Table 3.2. The superior features of the proposed adaptive control methodology are concluded from the tabulation of input and output performances obtained using the proposed method, single model adaptive control and modular adaptive backstepping control (MBSC) [6] techniques in Table 3.2.

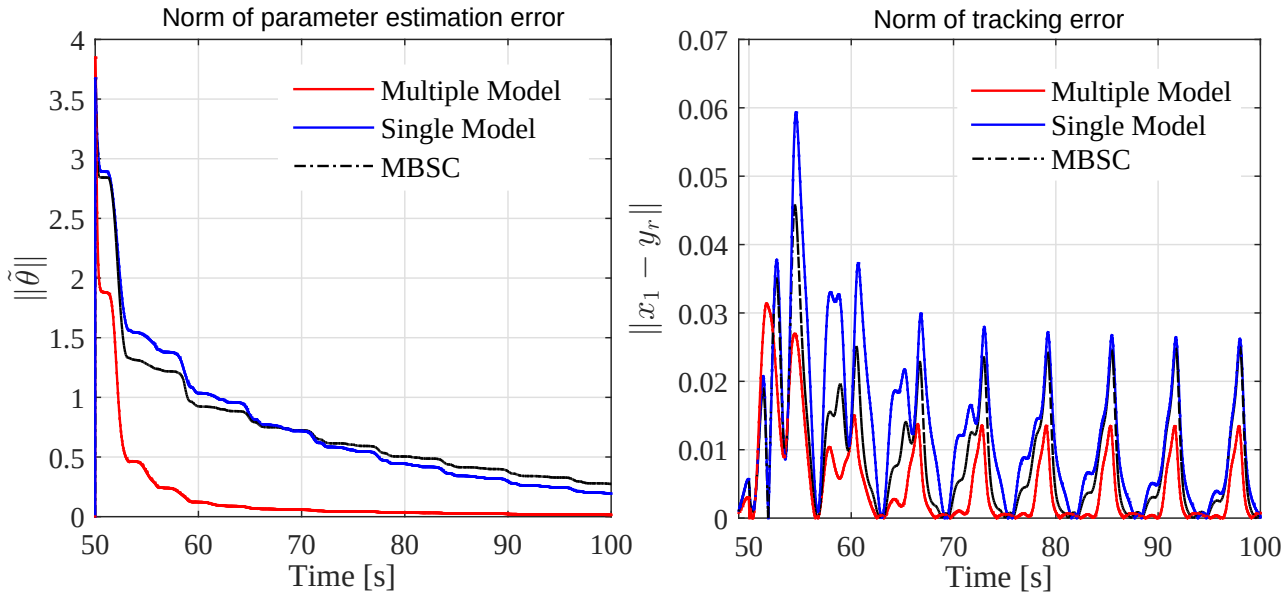

Figure 3.7: Scenario 1. Comparison of post-failure output transient performance and parameter convergence obtained with Modular Backstepping Control (MBSC) [6], single model adaptive control and proposed multiple model adaptive control

Table 3.2: Tabular comparison of output and input performance for Scenario 2 (3.127) describing infinite actuator failures with $T^* = 5$ s and $T^* = 15$ s

Transit time	**Control Schemes**	**Performance metrics**					
		ITAE	**RMSE**	**Control Energy**		**Total Variation**	
				u_1	u_2	u_1	u_2
$T^* = 5$ s	Multiple Models	**78.46**	**0.023**	3.64×10^3	3.09×10^3	293.64	359.15
	Single Model	124.44	0.039	3.74×10^3	3.22×10^3	309.69	380.27
	MBSC	111.08	0.032	3.67×10^3	3.14×10^3	291.05	362.00
$T^* = 15$ s	Multiple Models	**56.10**	**0.018**	3.48×10^3	2.99×10^3	180.41	299.11
	Single Model	85.75	0.033	3.47×10^3	2.93×10^3	200.45	319.21
	MBSC	62.93	0.026	3.47×10^3	2.94×10^3	181.15	327.89

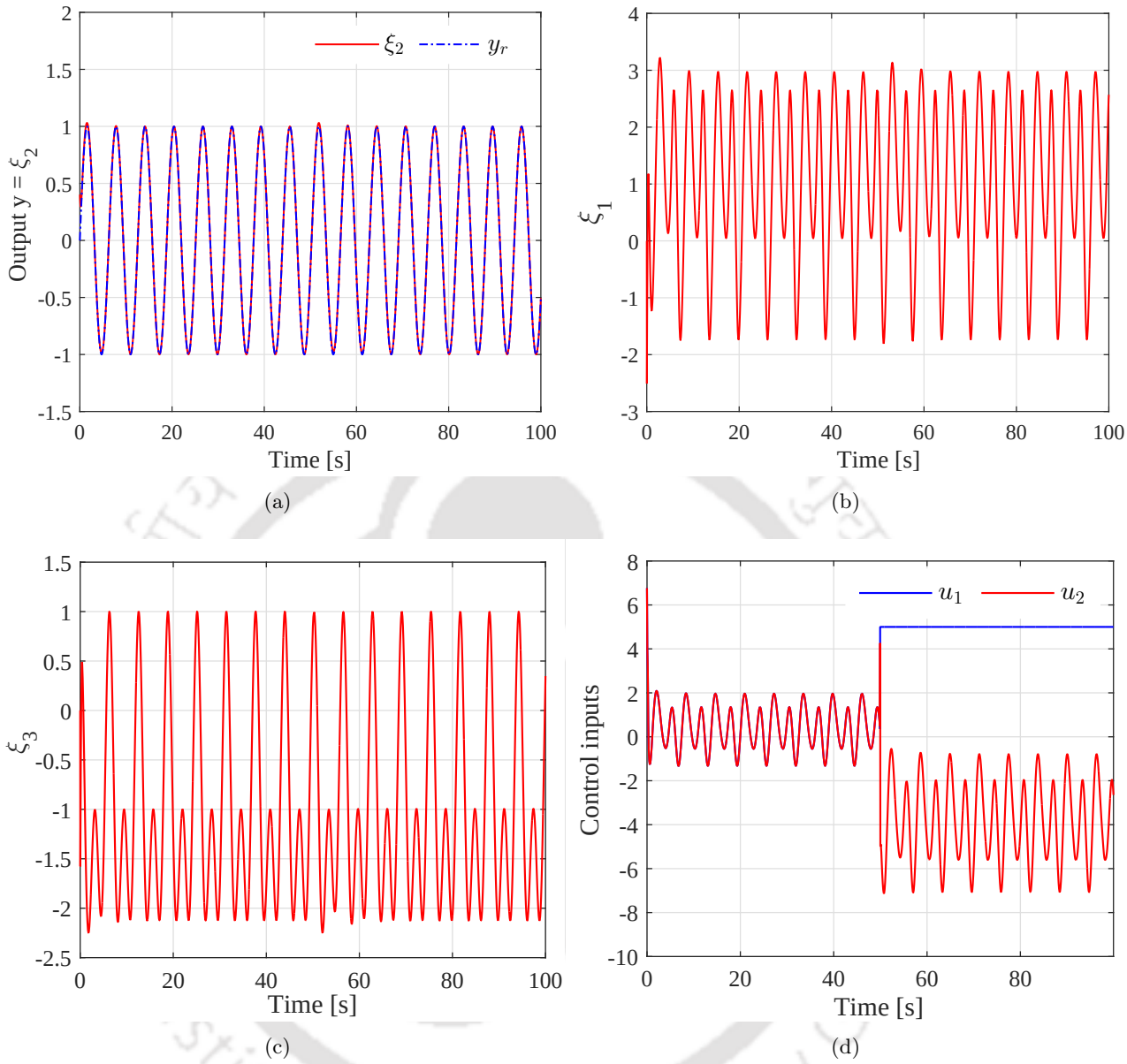

Figure 3.8: System states and control inputs with actuator fault under Scenario 1 (3.126) at $t = 50$ s. (a) Output state $\xi_2 = x_1$;(b) state ξ_1;(c) state $\xi_3 = x_2$; (d) control inputs u_1 and u_2

3.2.4.2 Application to an Aircraft System

In this section, a problem of longitudinal control of Boeing 747-100/200, a large transport aircraft is considered. It is assumed that the aircraft is subjected to infinite number of PLOE and LIP elevator failures at unknown time instants. This example would further demonstrate the applicability and proficiency of the proposed multiple model adaptive control scheme to practical systems. The aircraft model parameters chosen for simulations along with their respective notations and definitions are provided in Section 2.2.5. The longitudinal control dynamics of the aircraft can be referred to (2.57)-(2.58) and is not repeated here for brevity. The state variables are chosen as $[x_1,\ x_2,\ x_3,\ x_4]^T =$

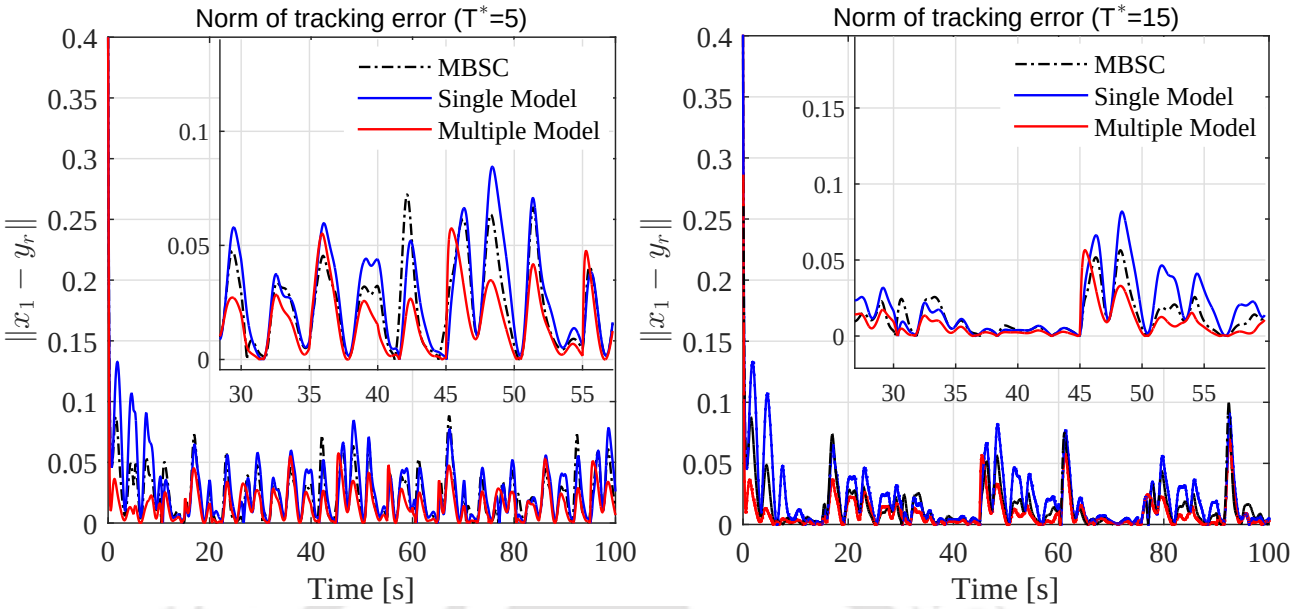

Figure 3.9: Comparison of post failure transient performance obtained with Modular Backstepping Control (MBSC), single model adaptive control and proposed multiple model adaptive control in case of infinite actuator failures

$[V,\ \alpha,\ \theta,\ q]^T$ and $u_1 = \delta_{e_1},\ u_2 = \delta_{e_2}$ are the control inputs. The system dynamics required for control design, are as follows,

$$\dot{x}_3 = x_4 \tag{3.130}$$

$$\dot{x}_4 = a(x,\eta) + a(x,\eta)\kappa^* + \sum_{j=1}^{m} b_j \beta_j(\xi,\eta) u_j \tag{3.131}$$

where $\kappa^* \in \mathbb{R}$ models the unknown factor of additive uncertainty in system dynamics. It basically denotes the deviation of the actual system model from its nominal model dynamics. The actuator failure model considered for the elevators is as follows,

$$u_1(t) = \bar{u}_{Fj_1,h},\quad u_2(t) = K_{2,h} u_{H2}\quad t \in [hT^*,\ (h+1)T^*),\ h \in \mathbb{N}\backslash 2\mathbb{N} \tag{3.132}$$

The above failure characteristics of the actuator assumes $T^* = 10$, the value at which the actuator is stuck $\bar{u}_{Fj_1,h} = 2$ and the LOE factor $K_{2,h} = 0.7$. Therefore, it is observed that the actuators switch from their healthy state of operation to a faulty state at each time interval of 10 s. The bounds on the unknown model and fault parameters are, $|\kappa^*| \leq 1,\ 0.5 \leq |b_j| \leq 2,\ 0.2 \leq K_{j,h} \leq 1$ and $\bar{u}_{Fj,h} \leq 5,\ j = 1, 2$. The initial state vector is considered to be $[0.0162,\ 230,\ 0.0162,\ 0]^T$ and $\hat{w}(t_0) = [0.25,\ 0.25,\ 0.25,\ 0.25]^T$. The reference signal for tracking is given by $y_r = 0.1\sin(0.05t)$. The controller design parameters are given as follows: $c_1 = 30$, $c_2 = 1$, $\bar{c}_1 = 0.1$, $\bar{c}_2 = 0.5$, $g_2 = 10^{-6}$ and $\ell = 0.01$. The observer design matrix $A_0 = 5I_{2\times 2}$ and adaptive rate matrix $\Gamma_1 = \Gamma_2 = \Gamma_3 = \Gamma_4 = 2I_{2\times 2}$ are considered in simulations. The number of models considered is $N = 4$. The minimum number of estimators are selected so as to satisfy that the set $\{\hat{\theta}_{(\mu)}(t_0)\}_{\mu=1}^{N}$ forms a convex hull $\forall t \geq t_0$.

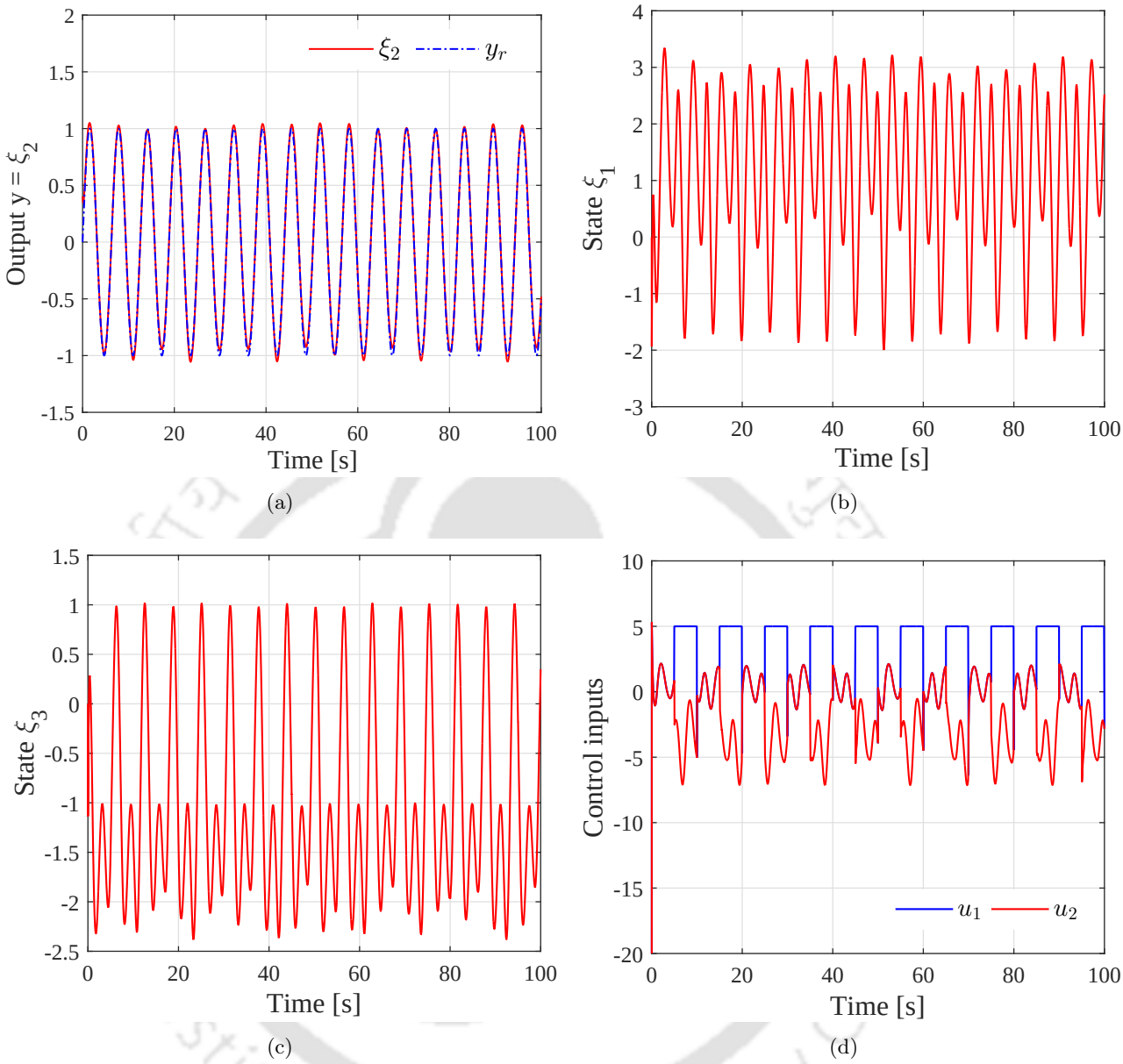

Figure 3.10: System states and control inputs with intermittent actuator fault/failures under Scenario 2 (3.127). (a) Output state $\xi_2 = x_1$;(b) state ξ_1;(c) state $\xi_3 = x_2$; (d) control inputs u_1 and u_2

Therefore, the initial parameter set is constructed using the initial parameter estimates from each of the N models defined as $\hat{\theta}_{(1)}(t_0) = [1,\ 0.4,\ 5]^T$, $\hat{\theta}_{(2)}(t_0) = [-1,\ 3,\ -5]^T$, $\hat{\theta}_{(3)}(t_0) = [1,\ 0.4,\ -5]^T$ and $\hat{\theta}_{(4)}(t_0) = [-1,\ 3,\ 5]^T$, respectively. Similar to the simulation illustration of the numerical example considered, the output transient and steady state performance is evaluated on the basis of ITAE and RMSE.

The simulation results obtained are provided in Figures 3.11 and 3.12. In such an event of infinitely occurring actuator failures, the boundedness of all the closed loop signals, namely, the pitch angle θ, pitch rate q, the angle of attack (AoA) α and velocity V along with the control inputs using the

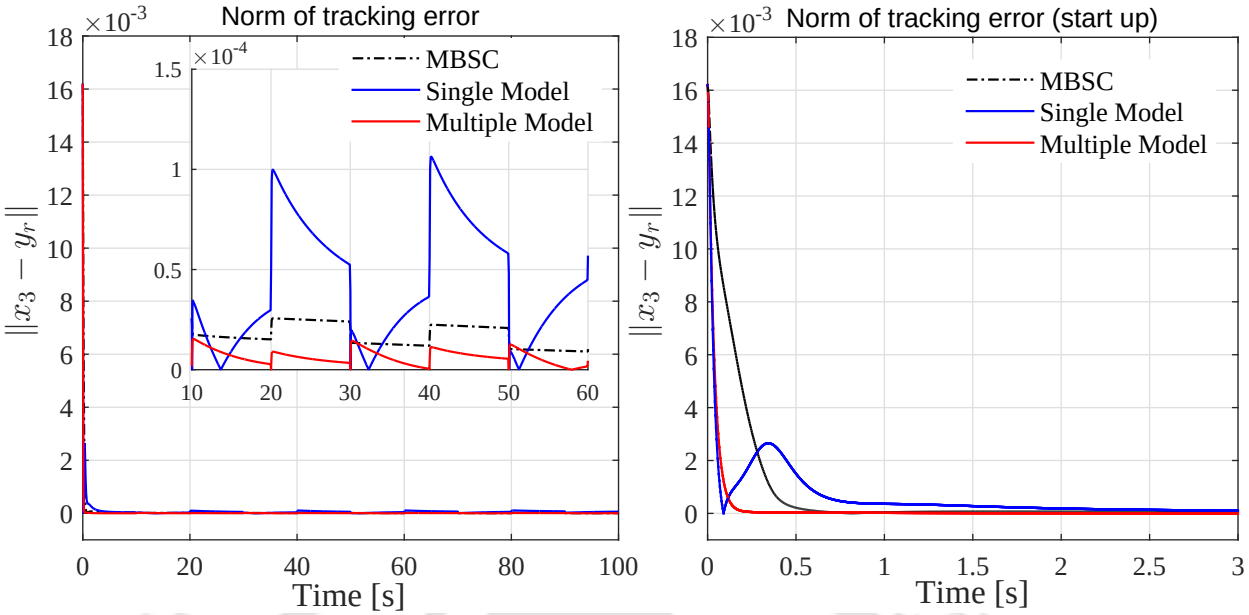

Figure 3.11: Comparison of start up and post failure transient performance obtained with Modular Backstepping Control (MBSC), single model adaptive control and multiple model adaptive control in case of infinite actuator failures

proposed adaptive controller is shown in Figure 3.12. Similar to the example considered in the previous section, the transient at start up and post failure in addition to the steady state behavior of the output is compared with those obtained using a single model adaptive controller and modular backstepping control (MBSC) [6]. For the sake of a fair comparison, all the relevant design parameters for all the three controllers are said to take identical values. The initial condition for the parameter estimate $\hat{\theta}$ in single model adaptive control and MBSC are taken to be $\hat{\theta}(t_0) = [-1,\ 3,\ 5]^T$ whereas the plant initial conditions are $x(t_0) = [0.794,\ 230,\ 0.0162,\ 0]^T$. The results in Figure 3.11 unveils the superior convergence of the tracking error norm compared to adaptive control using a single model and MBSC in terms fastness and accuracy of tracking. Quantitatively, the performance improvement is reflected from the ITAE and RMSE of the output tracking error at start up using each of the three control schemes. The ITAE values for the proposed method, single model adaptive control are recorded to be 0.00082 and 0.0898, respectively. Whereas, their RMSE measurements are calculated to be 0.00033 and 0.0079, respectively. Further, the enhanced performance for all time $0 \leq t < \infty$ is evident from the zoomed figure in Figure 3.11.

Remark 3.4. *From extensive simulations, it has been observed that the performance of the proposed control scheme is directly proportional to the choice of sampling frequency. Further, a judicious lowering of the sampling frequency while maintaining boundedness of the closed loop signals, impacts the performance of the proposed control design. Nevertheless, the magnitude of impact on performance due to increment in sampling time, is relatively insignificant compared to results obtained in simulation studies using adaptive control with single models and MBSC. For example, the MBSC based control system with the aircraft example renders a faithful performance with a sampling interval of 0.0001 s. While, a similar or rather a better performance is achieved utilizing the proposed multiple model*

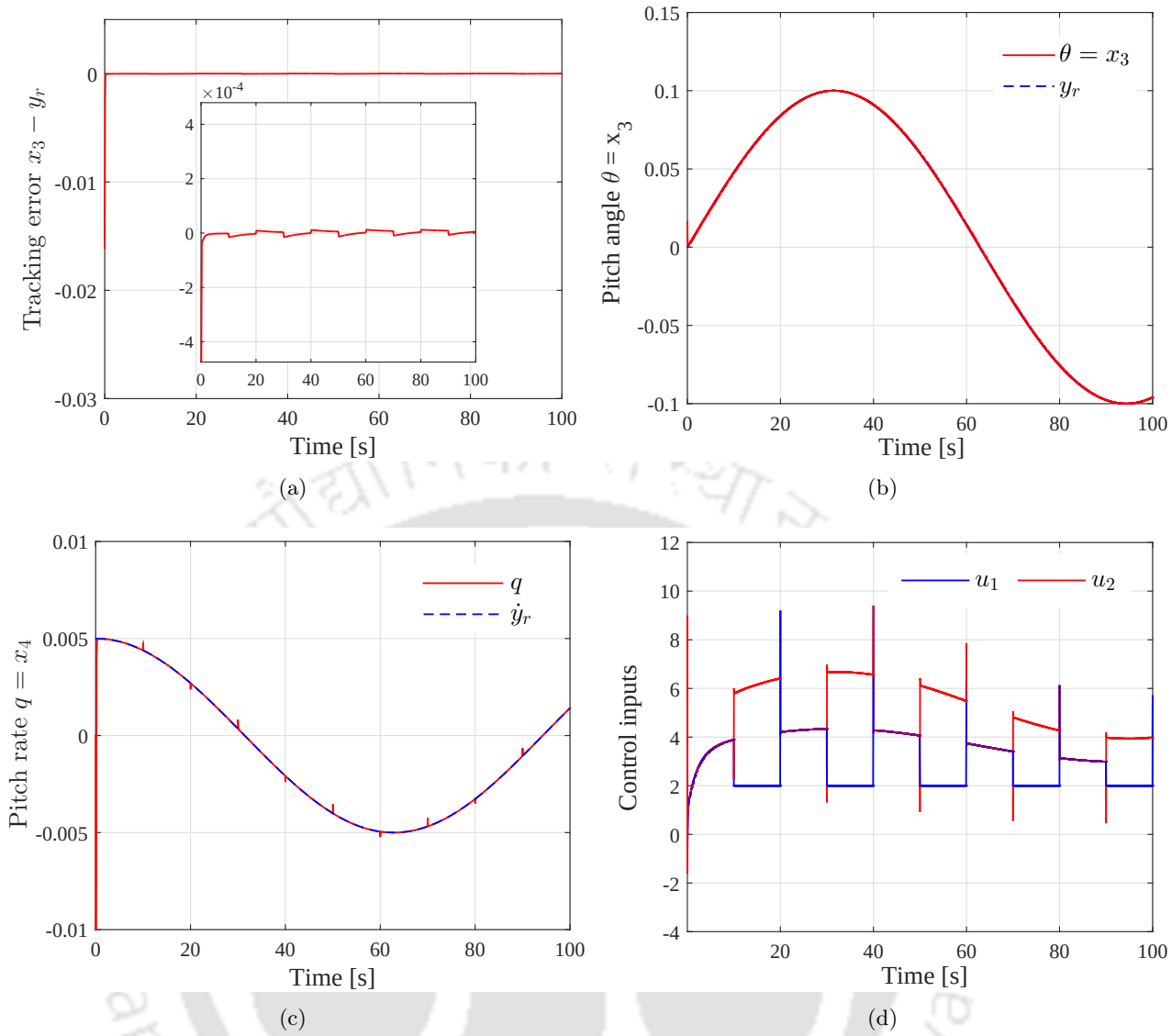

Figure 3.12: (a) aircraft pitch angle tracking error;(b) actual and desired aircraft pitch angle $\theta = x_3$; (c) aircraft pitch rate x_4; (d) control inputs u_1 and u_2;

adaptive control scheme with a sampling time of 0.005 s. Hence, it can be concluded, that the proposed algorithm is efficient and suitable for real time applications with limited bandwidth.

3.3 Adaptive Multiple Model Fault Tolerant Control (AMMFTC) for Uncertain Multi-Input-Multi-Output (MIMO) Nonlinear Systems

In what follows, the proposed multiple model adaptive control strategy is further applied to solve the FTC design problem in nonlinear uncertain MIMO systems. Incorporating the event of occurrence of abrupt uncertain actuator failures into the underlying system dynamics leads to several challenges in an effective control design. Apart from unknown system uncertainties and being affected by unanticipated

actuator faults and external perturbations, these systems inherently exhibit strong coupling effects between each of their subsystems. Withal, adaptive fault tolerant controller synthesis for such coupled MIMO nonlinear systems to effectively compensate actuator failures is indeed challenging. In the following, the FTC design problem for MIMO nonlinear systems affected by actuator failures, system uncertainties and unknown subsystem interactions is formulated and thereafter a control solution is derived.

3.3.1 Problem Formulation

Let us consider a MIMO nonlinear system as follows,

$$\sum_p : \begin{cases} \dot{\mathbf{x}} = \mathbf{f}_0(\mathbf{x}) + \sum\limits_{i=1}^{p} \kappa_i^* \mathbf{f}_i(\mathbf{x}) + \sum\limits_{j=1}^{m} \mathbf{g}_j(\mathbf{x}) u_j \\ \mathbf{y} = \mathbf{h}(\mathbf{x}) \end{cases} \tag{3.133}$$

The state vector of the system (3.133) is denoted by $\mathbf{x} := [x_1,\ x_2, \ldots, x_n]^T \in \mathbb{R}^n$. The vector $\mathbf{y} := [y_1,\ y_2,\ \ldots, y_q]^T \in \mathbb{R}^q$ represents the outputs while $\mathbf{h}(\mathbf{x})$ are defined as known smooth functions. Further, $\mathbf{f}_0, \mathbf{f}_i, \mathbf{g}_j : \mathbb{R}^n \to \mathbb{R}^n$ represent the vectors of known smooth nonlinear functions for $i = 1, \ldots, n$ and $j = 1, \ldots, m$. The terms u_j defines the control inputs, collectively denoted by the vector $\mathbf{u} := [u_1,\ u_2, \ldots,\ u_m]^T$ and $\kappa_i,\ i = 1, \ldots,\ p$ are unknown constants.
Considering the system dynamics in (3.133), the following assumptions are necessary.

Assumption 3.7. *The system* (3.133) *has well defined relative degrees* $\wp = \{\wp_1,\ \wp_2, \ldots,\ \wp_q\}$, $1 \leq \wp_i \leq n$, *for* $i = 1,\ 2, \ldots,\ n$. *Therefore the following equalities hold for* $j = \overline{1, m}$, $i = \overline{1, q}$ *and* $k = \overline{0, \wp_i - 2}$.

$$L_{\mathbf{g}_j} L_{\mathbf{f}_0}^k h_i(\mathbf{x}) = 0, \quad L_{\mathbf{g}_j} L_{\mathbf{f}_0}^{\wp_i - 1} h_i(\mathbf{x}) \neq 0$$

The operator $L_{\mathbf{f}}(\cdot)$ *defines the Lie derivative of the argument in the direction of* $\mathbf{f}(\mathbf{x})$. *Further, the nonlinear functions* $\mathbf{f}_i$ *satisfy the conditions given below [102] for* $k = \overline{1, p}$, $r_i = \overline{1, \wp_i - 1}$ *and* $i = \overline{1, q}$,

$$D_{\mathbf{x}}(L_{\mathbf{f}_k} L_{\mathbf{f}_0}^{r_i - 1} h_i(\mathbf{x})) \in span\{D_{\mathbf{x}}(h_1(\mathbf{x})), \ldots, D_{\mathbf{x}}(L_{\mathbf{f}_0}^{\wp_1 - \wp_i + r_i - 1} h_1(\mathbf{x})), D_{\mathbf{x}}(h_2(\mathbf{x})), \ldots, D_{\mathbf{x}}(L_{\mathbf{f}_0}^{\wp_2 - \wp_i + r_i - 1} h_2(\mathbf{x})),$$
$$D_{\mathbf{x}}(h_j(\mathbf{x})), \ldots, D_{\mathbf{x}}(L_{\mathbf{f}_0}^{\wp_j - \wp_i + r_i - 1} h_j(\mathbf{x})), D_{\mathbf{x}}(h_q(\mathbf{x})), \ldots, D_{\mathbf{x}}(L_{\mathbf{f}_0}^{\wp_q - \wp_i + r_i - 1} h_q(\mathbf{x}))\},$$

where, the operator $D_{\mathbf{x}}(\cdot)$ *denotes the partial differentiation of a function with respect to* $\mathbf{x} \in \mathbb{R}^n$ *resulting in a gradient vector* $D_{\mathbf{x}}(\cdot) := \left[\frac{\partial}{\partial x_1},\ \frac{\partial}{\partial x_2}, \ldots,\ \frac{\partial}{\partial x_n}\right]^T (\cdot)$.

In accordance with FTC literature, actuator fault in a system manifests itself in either of the forms as under, (i) partial loss of effectiveness (PLOE);(ii) lock-in-place (LIP);(iii) float failure. However in this work, LIP and float failures have been considered. Such types of actuator faults can be characterized by a unified mathematical model with a piecewise defined input-output relationship as given

below [100].

$$u_j = \begin{cases} K_j u_{Hj} + \bar{u}_{Fj}, & \forall\ t \geq t_{Fj} \\ u_{Hj}, & \forall\ t < t_{Fj} \end{cases} \quad j = \overline{1,m} \tag{3.134}$$

The term u_{Hj} and $\bar{u}_{Fj}$ denote the controller output fed to the j^{th} actuator and the value at which the j^{th} actuator is stuck under LIP failure, respectively. Float failure is the condition when the j^{th} actuator fails with $\bar{u}_{Fj}$=0. Apart from the additive consequences of actuator failures, multiplicative actuator faults are modeled using the factor K_j. The actuator failure value $\bar{u}_{Fj}$, the actuation effectiveness index K_j, the failure time instant t_{Fj} and the actuator index j are all unknown. This means that the actuator failures are unknown in time, pattern as well as magnitude. The actuator index set is given by $\{j_1,\ j_2, \ldots,\ j_m\}$. Unlike the actuator fault modeling in multi-input single-output (MISO) systems wherein the actuators were assumed to have same/similar physical characteristics, MIMO systems have multiple inputs with actuators not necessarily reflecting the same physical behavior/features and functioning. Therefore, to design fault tolerant controllers for a MIMO nonlinear system, an actuator grouping scheme $\mathscr{G} := \{\mathscr{G}_1,\ \mathscr{G}_2, \ldots, \mathscr{G}_q\}$ is required [32]. Herein, each set $\mathscr{G}_k \subset \{j_1,\ j_2, \ldots,\ j_m\}$ represents the set of actuators with similar operational characteristics and such a classification is done on the basis of $\wp := \{\wp_1,\ \wp_2, \ldots,\ \wp_q\}$. Further to effectively exploit the actuator redundancy, a proportional actuation scheme is utilized similar to [32]. Therefore, considering such a grouping and actuation scheme $\mathscr{G}$, the control input to be fed to each actuator included in the set $\mathscr{G}_k$ is given by,

$$u_{Hj} = b_{jk} v_k \quad \forall u_j \in \mathscr{G}_k,\ j = \overline{1,\ m}\ \&\ k = \overline{1,q} \tag{3.135}$$

where, b_{jk} defines a certain design function associated with each actuator group $\mathscr{G}_k$. Further, the choice of such design functions satisfy the relation $b_{jk} = b_j$ if the j^{th} actuator belong to $\mathscr{G}_k$ under the grouping scheme $\mathscr{G}$. Thereafter, to facilitate control design, under assumption 3.7 and (3.133)-(3.135), there exists a diffeomorphism $\mathscr{T}(\mathbf{x}) := [\boldsymbol{\xi}, \boldsymbol{\eta}]^T = [\xi_{1,1}, \xi_{1,2}, \ldots, \xi_{1,\wp_1}, \ldots, \xi_{q,1}, \xi_{q,2}, \ldots, \xi_{q,\wp_q}, \boldsymbol{\eta}] = [\mathscr{T}_c(\mathbf{x}), \mathscr{T}_z(\mathbf{x})]^T$ such that

$$\mathscr{T}_c(\mathbf{x}) := [h_1(\mathbf{x}), L_{\mathbf{f}_0} h_1(\mathbf{x}), \ldots, L_{\mathbf{f}_0}^{\wp_1 - 1} h_1(\mathbf{x}), \ldots, h_q(\mathbf{x}), L_{\mathbf{f}_0} h_q(\mathbf{x}), \ldots, L_{\mathbf{f}_0}^{\wp_q - 1} h_q(\mathbf{x})] \in \mathbb{R}^{\wp_1 + \wp_2 + \ldots + \wp_q}$$

and $\mathscr{T}_z \in \mathbb{R}^{\ell}$ transforms the system (3.133) to the following form with a controllable part $\sum_c$ and internal dynamics $\sum_z$,

$$\sum\nolimits_{c_1} : \begin{cases} \dot{\xi}_{1,r_1} = \xi_{1,r_1+1} + \boldsymbol{\varphi}_{1,r_1}^T \boldsymbol{\kappa}^* \\ \dot{\xi}_{1,\wp_1} = a_1(\xi,\eta) + \boldsymbol{\varphi}_{1,\wp_1}^T \boldsymbol{\kappa}^* + \sum\limits_{j \in \{j_1,\ldots,j_d\}} \beta_{1,j}(\xi,\eta)\bar{u}_{Fj} + \sum\limits_{k=1}^{q} \bar{\beta}_{1,k}(\xi,\eta) v_k \end{cases} \tag{3.136}$$

$$\vdots$$

$$\sum\nolimits_{c_q}: \begin{cases} \dot{\xi}_{q,r_q} = \xi_{q,r_q+1} + \boldsymbol{\varphi}_{q,r_q}^T \boldsymbol{\kappa}^* \\ \dot{\xi}_{q,\wp_q} = a_q(\xi,\eta) + \boldsymbol{\varphi}_{q,\wp_q}^T \boldsymbol{\kappa}^* + \sum\limits_{j\in\{j_1,\ldots,j_d\}} \beta_{q,j}(\xi,\eta)\bar{u}_{Fj} + \sum\limits_{k=1}^{q} \bar{\beta}_{q,k}(\xi,\eta)v_k \end{cases} \tag{3.137}$$

$$\sum\nolimits_z : \dot{\boldsymbol{\eta}} = \boldsymbol{\Lambda}_0(\boldsymbol{\xi},\boldsymbol{\eta}) + \boldsymbol{\Lambda}_1^T(\boldsymbol{\xi},\boldsymbol{\eta})\boldsymbol{\kappa}^* + \boldsymbol{\Lambda}_2^T(\boldsymbol{\xi},\boldsymbol{\eta})\bar{\mathbf{u}} \tag{3.138}$$

$$\mathbf{y} = [\xi_{1,1},\ \xi_{2,1},\ \xi_{3,1},\ldots,\ \xi_{i,1},\ldots,\ \xi_{q,1}]^T \tag{3.139}$$

where $\boldsymbol{\varphi}_{i,r_i}(\boldsymbol{\xi},\boldsymbol{\eta}) := [L_{\mathbf{f}_1}^{r_i}h_i(\mathbf{x}),\ldots,\ L_{\mathbf{f}_p}^{r_i}h_i(\mathbf{x})]^T$, $a_i(\boldsymbol{\xi},\boldsymbol{\eta}) := L_{\mathbf{f}_0}^{\wp_i}h_i(\mathbf{x})$, $\beta_{i,j}(\boldsymbol{\xi},\boldsymbol{\eta}) := L_{\mathbf{g}_j}L_{\mathbf{f}_0}^{\wp_i-1}h_i(\mathbf{x})$, $\boldsymbol{\beta}_i(\boldsymbol{\xi},\boldsymbol{\eta}) := [\{L_{\mathbf{g}_j}L_{\mathbf{f}_0}^{\wp_i-1}h_i(\mathbf{x})\}_{j=1}^m]$, $\bar{\beta}_{i,k} := \sum\limits_{j\notin\{j_1,\ldots,j_d\}\cap\mathscr{G}_k} b_{jk}K_j\beta_{i,j}(\boldsymbol{\xi},\boldsymbol{\eta})\ \forall k = 1,\ldots,q$

$\boldsymbol{\Lambda}_0(\boldsymbol{\xi},\boldsymbol{\eta}) := \frac{\partial\mathscr{T}_z}{\partial\mathbf{x}}\mathbf{f}_0(\mathbf{x})$, $\boldsymbol{\Lambda}_1^T(\boldsymbol{\xi},\boldsymbol{\eta}) := \dfrac{\partial\mathscr{T}_z}{\partial\mathbf{x}}[\mathbf{f}_1(\mathbf{x}),\ \mathbf{f}_2(\mathbf{x}),\ldots,\ \mathbf{f}_p(\mathbf{x})]$ and

$\boldsymbol{\Lambda}_2^T(\boldsymbol{\xi},\boldsymbol{\eta}) := \dfrac{\partial\mathscr{T}_z}{\partial\mathbf{x}}[\mathbf{g}_1(\mathbf{x}),\ \mathbf{g}_2(\mathbf{x}),\ldots,\ \mathbf{g}_m(\mathbf{x})]$ for $i = \overline{1,q}$, $r_i = \overline{1,\wp_i-1}$ and $j = \overline{1,m}$. At this point, we are well equipped to state the following additional assumptions.

Assumption 3.8. *The zero dynamics* (3.138) *of the system* (3.133)*, given by* $\sum\limits_z := \boldsymbol{\Lambda}_0(\boldsymbol{\xi},\boldsymbol{\eta}) + \boldsymbol{\Lambda}_1^T(\boldsymbol{\xi},\boldsymbol{\eta})\boldsymbol{\kappa}^* + \boldsymbol{\Lambda}_2^T(\boldsymbol{\xi},\boldsymbol{\eta})\bar{\mathbf{u}}$ *is input-to-state-stable (ISS) for each failure pattern with* $\boldsymbol{\xi}$ *as the input. With a supposition that there are* M *possible actuator failure patterns, the equivalent actuation matrix given by the argument of det operator in* (3.140)*, for the entire system corresponding to an actuator failure pattern* $\Xi_\jmath \in \Xi$, $\jmath = \overline{1,M}$ *under the grouping scheme* $\mathscr{G}$ *should be non-singular* $\forall\mathbf{x}\in\mathbb{R}^n$*, that is,*

$$det\left(\begin{bmatrix} \sum\limits_{j\notin\{j_1,\ldots,j_d\}\cap\mathscr{G}_1} b_{j1}K_jL_{\mathbf{g}_j}L_{\mathbf{f}_0}^{\wp_1-1}h_1(\mathbf{x}) & \ldots & \sum\limits_{j\notin\{j_1,\ldots,j_d\}\cap\mathscr{G}_q} b_{jq}K_jL_{\mathbf{g}_j}L_{\mathbf{f}_0}^{\wp_1-1}h_1(\mathbf{x}) \\ \sum\limits_{j\notin\{j_1,\ldots,j_d\}\cap\mathscr{G}_1} b_{j1}K_jL_{\mathbf{g}_j}L_{\mathbf{f}_0}^{\wp_2-1}h_2(\mathbf{x}) & \ldots & \sum\limits_{j\notin\{j_1,\ldots,j_d\}\cap\mathscr{G}_q} b_{jq}K_jL_{\mathbf{g}_j}L_{\mathbf{f}_0}^{\wp_2-1}h_2(\mathbf{x}) \\ \vdots & \ddots & \vdots \\ \sum\limits_{j\notin\{j_1,\ldots,j_d\}\cap\mathscr{G}_1} b_{j1}K_jL_{\mathbf{g}_j}L_{\mathbf{f}_0}^{\wp_q-1}h_q(\mathbf{x}) & \ldots & \sum\limits_{j\notin\{j_1,\ldots,j_d\}\cap\mathscr{G}_q} b_{jq}K_jL_{\mathbf{g}_j}L_{\mathbf{f}_0}^{\wp_q-1}h_q(\mathbf{x}) \end{bmatrix}_{\mathscr{G}(\Xi_\jmath)}\right) \neq 0. \tag{3.140}$$

Herein, Ξ *defines a set with cardinality* $M = \binom{m}{q}$*, whose elements are* $m\times m$ *diagonal matrices representing all possible actuator failure topologies. Further, the diagonal elements of each of such matrices in* Ξ *are either zero or unity depending on the state of health of the corresponding actuator. It is to be mentioned at this point in time that all of the* M *actuator failure patterns are not compensable and hence it is required to classify failures as compensable and non-compensable ones. The basis of such a classification are the actuation matrices corresponding to all possible failure topologies. The non-singularity of the actuation matrix for an actuator failure pattern is the deciding factor which defines an actuator failure pattern to be compensable or not. In other words, this classification criterion, if satisfied, guarantees the existence of an adaptive fault tolerant controller which can ensure stability of the closed-loop system in the event of actuator failures.*

Assumption 3.9. *The nonlinear dynamical system in* (3.133) *is so designed that the desired output performance can only be achieved in the event of atmost* $d \leq (m-q)$ *actuator failures unknown in time, pattern and magnitude. Further, under the grouping scheme* $\mathscr{G}$*, since the actuators are grouped on the basis of their similarity in structural characteristics, atleast one actuator in each of the groups* $\mathscr{G}_k$ *should be operational corresponding to an actuator failure pattern.*

Assumption 3.10. *The respective reference trajectories* $\mathbf{y_r}(t) := [y_{r,1},\ y_{r,2}, \ldots,\ y_{r,q}]^T \in \mathbb{R}^q$ *to be tracked by the system outputs are known, piecewise continuous and bounded. Further,* $\dot{\mathbf{y}}_\mathbf{r},\ \ddot{\mathbf{y}}_\mathbf{r}, \ldots, \mathbf{y}_\mathbf{r}^{(\wp)} \in \mathbb{R}^q$ *are also piecewise continuous, bounded and belong to a known compact set.*

Having stated all the necessary definitions and assumptions, we are now well equipped to state the FTC design problem. Considering the nonlinear uncertain MIMO system (3.133) and the assumptions 3.7-3.10, the control problem and its objectives can be framed as follows:

- To design the control inputs v_k corresponding to each actuator group $\mathscr{G}_k$ for $k = \overline{1,q}$ such that the closed loop system is stable and the output vector $\mathbf{y}(t)$ tracks the desired reference vector $\mathbf{y_r}(t)$ in the event of atmost $d \leq (m-q)$ unknown actuator failures $\forall\ t \in [0,\ \infty)$. The design assumes no prior knowledge of the magnitude, pattern and time t_{jF} of the occurrence of actuator failures/faults.
- To ensure an improved start-up and post failure output transient performance without any significant expense of control energy
- Asymptotic stability of output tracking error vector, i.e. $\lim_{t\to\infty} \mathbf{y}(t) - \mathbf{y_r}(t) = 0$ under no failure and past fault scenarios.
- Guaranteeing robustness towards parametric uncertainties, external perturbations and consequences of strong unknown cross coupling arising from subsystem interactions through estimation and subsequent compensation instead of merely alleviating their adverse effects.

3.3.2 Adaptive Multiple Model Fault Tolerant Control (AMMFTC) Design

Referring to the transformed system dynamics in (3.137)-(3.138), to simplify the control design procedure, the unknown system and failure induced parameters are denoted as $\boldsymbol{\theta}_2^* = \boldsymbol{\kappa^*}$, $\boldsymbol{\theta}_1^* = [\theta_{1,1}^*, \ldots, \theta_{1,m}^*]^T = [\{K_j\}_{j=1}^m]^T$ and $\boldsymbol{\theta}_3^* = [\theta_{3,1}^*, \ldots, \theta_{3,m}^*]^T = [\{\bar{u}_{Fj}\}_{j=1}^m]^T$. Further, the overall unknown parameter vector is defined as $\boldsymbol{\theta}^* := [\boldsymbol{\theta}_1^*,\ \boldsymbol{\theta}_2^*,\ \boldsymbol{\theta}_3^*]^T$. The control design procedure follows similar steps as discussed in Section 3.2.2 wherein the same control design problem was considered for single output nonlinear systems with operationally similar multiple inputs. Firstly, we proceed with an input-state-stable (ISS) controller design assuming the availability of parameter estimates from a faithful parameter estimator to ensure modularity between the controller-observer pair. Thereafter, the proposed multiple model parameter estimator is constructed to yield the parameter estimates to be fed to the controller for subsequent compensation preserving closed loop system stability $\forall\ t \in [0,\ \infty)$.

3.3.2.1 Controller Synthesis

For simplicity and ease of understanding, the control design is explained following a stepwise procedure as given below.

Step 1.1: Let us choose the first output error variable as $z_{1,1} = y_1 - y_{r,1} = \xi_{1,1} - y_{r,1}$. Further, define $z_{1,2} = \xi_{1,2} - \alpha_{1,1} - \dot{y}_{r,1}$ and $\tilde{\boldsymbol{\theta}} := \boldsymbol{\theta}^* - \hat{\boldsymbol{\theta}}$. Where α_{i,r_i} with $r_i = \overline{1, \wp_i}$ are stabilizing input functions for each of the subsystems incurred during control design. The error dynamics are given by,

$$\dot{z}_{1,1} = \xi_{1,2} + \boldsymbol{\varphi}_{1,1}^T \boldsymbol{\theta}_2^* - \dot{y}_{r,1} \tag{3.141}$$

$$= z_{1,2} + \alpha_{1,1} + \dot{y}_{r,1} \tag{3.142}$$

The first virtual control law $\alpha_{1,1}$ is so chosen as to stabilize the $z_{1,1}$ dynamics and is defined as follows,

$$\alpha_{1,1} = -c_{1,1} z_{1,1} - \bar{c}_{1,1} \|\boldsymbol{\psi}_{1,1}\|^2 z_{1,1} - \boldsymbol{\varphi}_{1,1}^T \hat{\boldsymbol{\theta}}_2 \tag{3.143}$$

Substituting $\alpha_{1,1}$ from (3.143) in (3.142) results in,

$$\dot{z}_{1,1} = -c_{1,1} z_{1,1} - \bar{c}_{1,1} \|\boldsymbol{\psi}_{1,1}\|^2 z_{1,1} + z_{1,2} + \boldsymbol{\varphi}_{1,1}^T (\boldsymbol{\theta}_2^* - \hat{\boldsymbol{\theta}}_2) \tag{3.144}$$

Step 1.r$_1$: For $r_1 = \overline{2, \wp_1 - 1}$, the steps of control design are similar wherein the r_1^{th} error variable is chosen as $z_{1,r_1} := \xi_{1,r_1} - \alpha_{1,r_1-1} - y_{r,1}^{(r_1-1)}$. Therefore,

$$\begin{aligned}
\dot{z}_{1,r_1} &= \xi_{1,r_1+1} + \boldsymbol{\varphi}_{1,r_1}^T \boldsymbol{\theta}_2^* - \sum_{k=1}^{r_1-1} \frac{\partial \alpha_{1,r_1-1}}{\partial \xi_{1,k}} \boldsymbol{\varphi}_{1,k}^T \boldsymbol{\theta}_2^* - \frac{\partial \alpha_{1,r_1-1}}{\partial \hat{\boldsymbol{\theta}}_2} \dot{\hat{\boldsymbol{\theta}}}_2 - \sum_{k=1}^{r_1-1} \frac{\partial \alpha_{1,r_1-1}}{\partial \xi_{1,k}} \xi_{1,k+1} - \sum_{k=1}^{r_1-1} \frac{\partial \alpha_{1,r_1-1}}{\partial y_{r,1}^{k-1}} y_{r,1}^{(k)} \\
&= z_{1,r_1+1} + \alpha_{1,r_1} + \underbrace{\left(\boldsymbol{\varphi}_{1,r_1}^T - \sum_{k=1}^{r_1-1} \frac{\partial \alpha_{1,r_1-1}}{\partial \xi_{1,k}} \boldsymbol{\varphi}_{1,k}^T \right)}_{\boldsymbol{\psi}_{1,r_1}} \boldsymbol{\theta}_2^* - \frac{\partial \alpha_{1,r_1-1}}{\partial \hat{\boldsymbol{\theta}}_2} \dot{\hat{\boldsymbol{\theta}}}_2 \\
&\quad - \left(\sum_{k=1}^{r_1-1} \frac{\partial \alpha_{1,r_1-1}}{\partial \xi_{1,k}} \xi_{1,k+1} + \sum_{k=1}^{r_1-1} \frac{\partial \alpha_{1,r_1-1}}{\partial y_{r,1}^{k-1}} y_{r,1}^{(k)} \right)
\end{aligned} \tag{3.145}$$

To stabilize the above subsystem (3.145), the virtual control law α_{1,r_1} is formulated to be,

$$\begin{aligned}
\alpha_{1,r_1} &= -z_{1,r_1-1} - c_{1,r_1} z_{1,r_1} - \bar{c}_{1,r_1} \|\boldsymbol{\psi}_{1,r_1}\|^2 z_{1,r_1} - g_{1,r_1} \left\| \frac{\partial \alpha_{1,r_1-1}}{\partial \hat{\boldsymbol{\theta}}_2} \right\|^2 z_{1,r_1} - \boldsymbol{\psi}_{1,r_1}^T \hat{\boldsymbol{\theta}}_2 \\
&\quad + \left(\sum_{k=1}^{r_1-1} \frac{\partial \alpha_{1,r_1-1}}{\partial \xi_{1,k}} \xi_{1,k+1} + \sum_{k=1}^{r_1-1} \frac{\partial \alpha_{1,r_1-1}}{\partial y_{r,1}^{k-1}} y_{r,1}^{(k)} \right)
\end{aligned} \tag{3.146}$$

Such a choice of the stabilizing functions at the r_1^{th} step yields,

$$\dot{z}_{1,r_1} = -z_{1,r_1-1} + z_{1,r_1+1} - c_{1,r_1} z_{1,r_1} - \left(\bar{c}_{1,r_1} \|\boldsymbol{\psi}_{1,r_1}\|^2 + g_{1,r_1} \left\| \frac{\partial \alpha_{1,r_1-1}}{\partial \hat{\boldsymbol{\theta}}_2} \right\|^2 \right) z_{1,r_1}$$
$$- \frac{\partial \alpha_{1,r_1-1}}{\partial \hat{\boldsymbol{\theta}}_2} \dot{\hat{\boldsymbol{\theta}}}_2 + \boldsymbol{\psi}_{1,r_1}^T (\boldsymbol{\theta}_2^* - \hat{\boldsymbol{\theta}}_2) \tag{3.147}$$

Step i.r$_i$: Following similar steps as detailed in the immediately preceding text for the error variables, $z_{2,1},\ z_{2,2}, \ldots,\ z_{2,\wp_2-1}, \ldots,\ z_{q,1},\ z_{q,2}, \ldots,\ z_{q,\wp_q-1}$, where

$$z_{i,1} = y_i - y_{r,i} = \xi_{i,1} - y_{r,i};\quad i = 2, \ldots, q \tag{3.148}$$
$$z_{i,r_i} = \xi_{i,r_i} - \alpha_{i,r_i-1} - y_{r,i}^{(r_i-1)};\ r_i = 2, \ldots, \wp_i - 1 \tag{3.149}$$

the virtual control laws α_{i,r_i} are obtained as given below satisfying the input-to-state-stable(ISS) criterion with respect to z_{i,r_i+1} as the input.

$$\alpha_{2,1} = -c_{2,1} z_{2,1} - \bar{c}_{2,1} \|\boldsymbol{\psi}_{2,1}\|^2 z_{2,1} - \boldsymbol{\varphi}_{2,1}^T \hat{\boldsymbol{\theta}}_2 \tag{3.150}$$

$$\alpha_{i,r_i} = -z_{i,r_i-1} - c_{i,r_i} z_{i,r_i} - \left(\bar{c}_{i,r_i} \|\boldsymbol{\psi}_{i,r_i}\|^2 + g_{i,r_i} \left\| \frac{\partial \alpha_{i,r_i-1}}{\partial \hat{\boldsymbol{\theta}}_2} \right\|^2 \right) z_{i,r_i} - \boldsymbol{\psi}_{i,r_i}^T \hat{\boldsymbol{\theta}}_2$$
$$+ \left(\sum_{k=1}^{r_i-1} \frac{\partial \alpha_{i,r_i-1}}{\partial \xi_{i,k}} \xi_{i,k+1} + \sum_{k=1}^{r_i-1} \frac{\partial \alpha_{i,r_i-1}}{\partial y_{r,i}^{k-1}} y_{r,i}^{(k)} \right) \tag{3.151}$$

In the expression for α_{i,r_i} for $r_i = \overline{2, \wp_i - 1}$, the regressor term $\boldsymbol{\psi}_{i,r_i}(\cdot)$ is defined as

$$\boldsymbol{\psi}_{i,r_i} = \boldsymbol{\varphi}_{i,r_i} - \sum_{k=1}^{r_i-1} \frac{\partial \alpha_{i,r_i-1}}{\partial \xi_{i,k}} \boldsymbol{\varphi}_{i,k}.$$

Therefore, with the above choice of α_{i,r_i}, the dynamics of z_{i,r_i} for $i = 2, \ldots, q$ are described as,

$$\dot{z}_{2,1} = -c_{2,1} z_{2,1} - \bar{c}_{2,1} \|\boldsymbol{\psi}_{2,1}\|^2 z_{2,1} + z_{2,2} + \boldsymbol{\varphi}_{2,1}^T (\boldsymbol{\theta}_2^* - \hat{\boldsymbol{\theta}}_2) \tag{3.152}$$
$$\vdots \quad \vdots$$
$$\dot{z}_{i,r_i} = -z_{i,r_i-1} + z_{i,r_i+1} - c_{i,r_i} z_{i,r_i} - \left(\bar{c}_{i,r_i} \|\boldsymbol{\psi}_{i,r_i}\|^2 + g_{i,r_i} \left\| \frac{\partial \alpha_{i,r_i-1}}{\partial \hat{\boldsymbol{\theta}}_2} \right\|^2 \right) z_{i,r_i}$$
$$- \frac{\partial \alpha_{i,r_i-1}}{\partial \hat{\boldsymbol{\theta}}_2} \dot{\hat{\boldsymbol{\theta}}}_2 + \boldsymbol{\psi}_{1,r_1}^T (\boldsymbol{\theta}_2^* - \hat{\boldsymbol{\theta}}_2) \tag{3.153}$$

Step 1.$\wp_1$: The formulation of the control input at $\wp_1^{th}$ step is quite different from those derived in the previous $\wp_1 - 1$ steps. The $\wp_1^{th}$ error variable is first defined as, $z_{1,\wp_1} := \xi_{1,\wp_1} - \alpha_{1,\wp_1-1} - y_{r,1}^{\wp_1-1}$

which thereby yields its dynamics as,

$$\dot{z}_{1,\wp_1} = a_1(\boldsymbol{\xi},\boldsymbol{\eta}) + \boldsymbol{\varphi}_{1,\wp_1}^T\boldsymbol{\theta}_2^* - \sum_{k=1}^{\wp_1-1}\frac{\partial\alpha_{1,\wp_1-1}}{\partial\xi_{1,k}}\boldsymbol{\varphi}_{1,k}^T\boldsymbol{\theta}_2^* - \frac{\partial\alpha_{1,\wp_1-1}}{\partial\hat{\boldsymbol{\theta}}_2}\dot{\hat{\boldsymbol{\theta}}}_2 - \sum_{k=1}^{\wp_1-1}\frac{\partial\alpha_{1,\wp_1-1}}{\partial\xi_{1,k}}\xi_{1,k+1}$$
$$- \sum_{k=1}^{\wp_1-1}\frac{\partial\alpha_{1,\wp_1-1}}{\partial y_{r,1}^{k-1}}y_{r,1}^{(k)} - y_{r,1}^{(\wp_1)} + \boldsymbol{\beta}_1(\boldsymbol{\xi},\boldsymbol{\eta})\boldsymbol{\theta}_3^* + \boldsymbol{\beta}_1(\boldsymbol{\xi},\boldsymbol{\eta})\left(\sum_{j=1}^{m}\theta_{1,j}^*N_j\right)\mathbf{B}\mathbf{v}(t) \tag{3.154}$$

where, the matrix $\mathbf{B} := \begin{bmatrix} b_{11} & \dots & b_{1q} \\ \vdots & \ddots & \vdots \\ b_{m1} & \dots & b_{mq} \end{bmatrix}$ defines the known proportional actuation matrix derived from (3.135) and N_j is also an $m \times m$ matrix wherein the j^{th} element of the main diagonal is 1 while all the other elements of the matrix are zero.

Step i.$\wp_i$: (for $i = \overline{2,q}$) The remaining dynamics for $z_{2,\wp_2},\ z_{3,\wp_3},\dots,\ z_{q,\wp_q}$ can be formulated in a similar manner on the lines of (3.154) as given below.

$$\dot{z}_{i,\wp_i} = a_i(\boldsymbol{\xi},\boldsymbol{\eta}) + \boldsymbol{\varphi}_{i,\wp_i}^T\boldsymbol{\theta}_2^* - \sum_{k=1}^{\wp_i-1}\frac{\partial\alpha_{i,\wp_i-1}}{\partial\xi_{i,k}}\boldsymbol{\varphi}_{i,k}^T\boldsymbol{\theta}_2^* - \frac{\partial\alpha_{i,\wp_i-1}}{\partial\hat{\boldsymbol{\theta}}_2}\dot{\hat{\boldsymbol{\theta}}}_2 - \sum_{k=1}^{\wp_i-1}\frac{\partial\alpha_{i,\wp_i-1}}{\partial\xi_{i,k}}\xi_{i,k+1}$$
$$- \sum_{k=1}^{\wp_i-1}\frac{\partial\alpha_{i,\wp_i-1}}{\partial y_{r,i}^{k-1}}y_{r,i}^{(k)} - y_{r,i}^{(\wp_i)} + \boldsymbol{\beta}_i(\boldsymbol{\xi},\boldsymbol{\eta})\boldsymbol{\theta}_3^* + \boldsymbol{\beta}_i(\boldsymbol{\xi},\boldsymbol{\eta})\left(\sum_{j=1}^{m}\theta_{1,j}^*N_j\right)\mathbf{B}\mathbf{v}(t) \tag{3.155}$$

Let us now define $\mathbf{v}(t) = \hat{\mathbf{v}}(t) + \bar{\mathbf{v}}(t)$, $\mathbf{v}(t) := [v_1,\ v_2,\dots,\ v_q]^T \in \mathbb{R}^q$. At this point, it is to be admitted that finding the actual control input is not at all straightforward for MIMO systems and hence the detailed derivation is discussed herein to lend more clarity in understanding. With this thought from a reader's perspective, we first define a state vector $\mathbf{z}_{\boldsymbol{\wp}} := [z_{1,\wp_1},\ z_{1,\wp_2},\ z_{1,\wp_3},\dots,\ z_{1,\wp_q}]^T$ and thereafter calculate its time derivative as,

$$\dot{\mathbf{z}}_{\boldsymbol{\wp}} = \begin{bmatrix} a_1(\boldsymbol{\xi},\boldsymbol{\eta}) \\ a_2(\boldsymbol{\xi},\boldsymbol{\eta}) \\ \vdots \\ a_q(\boldsymbol{\xi},\boldsymbol{\eta}) \end{bmatrix} + \begin{bmatrix} \boldsymbol{\psi}_{1,\wp_1}^T \\ \boldsymbol{\psi}_{2,\wp_2}^T \\ \vdots \\ \boldsymbol{\psi}_{q,\wp_q}^T \end{bmatrix}\boldsymbol{\theta}_2^* + \begin{bmatrix} \boldsymbol{\beta}_1(\boldsymbol{\xi},\boldsymbol{\eta}) \\ \boldsymbol{\beta}_2(\boldsymbol{\xi},\boldsymbol{\eta}) \\ \vdots \\ \boldsymbol{\beta}_q(\boldsymbol{\xi},\boldsymbol{\eta}) \end{bmatrix}\boldsymbol{\theta}_3^* - \mathbf{F}_{\boldsymbol{\xi}}(\boldsymbol{\xi},\ \eta) - \mathbf{F}_{\mathbf{y_r}}(\dot{\mathbf{y}}_\mathbf{r},\ \ddot{\mathbf{y}}_\mathbf{r},\dots,\mathbf{y}_\mathbf{r}^{(\wp)})$$
$$+ \underbrace{\begin{bmatrix} \boldsymbol{\beta}_1(\boldsymbol{\xi},\boldsymbol{\eta})\left(\sum_{j=1}^{m}\theta_{1,j}^*N_j\right)\mathbf{B} \\ \boldsymbol{\beta}_2(\boldsymbol{\xi},\boldsymbol{\eta})\left(\sum_{j=1}^{m}\theta_{1,j}^*N_j\right)\mathbf{B} \\ \vdots \\ \boldsymbol{\beta}_q(\boldsymbol{\xi},\boldsymbol{\eta})\left(\sum_{j=1}^{m}\theta_{1,j}^*N_j\right)\mathbf{B} \end{bmatrix}}_{\bar{\boldsymbol{\beta}}\left(\sum_{j=1}^{m}\theta_{1,j}^*N_j\right)\mathbf{B}}\mathbf{v} + \begin{bmatrix} y_{r,1}^{(\wp_1)} \\ y_{r,2}^{(\wp_2)} \\ \vdots \\ y_{r,q}^{(\wp_q)} \end{bmatrix} + \begin{bmatrix} -\frac{\partial\alpha_{1,\wp_1-1}}{\partial\hat{\boldsymbol{\theta}}_2} \\ -\frac{\partial\alpha_{2,\wp_2-1}}{\partial\hat{\boldsymbol{\theta}}_2} \\ \vdots \\ -\frac{\partial\alpha_{q,\wp_q-1}}{\partial\hat{\boldsymbol{\theta}}_2} \end{bmatrix}\dot{\hat{\boldsymbol{\theta}}}_2. \tag{3.156}$$

The function vectors $\mathbf{F}_{\boldsymbol{\xi}}$ and $\mathbf{F}_{\mathbf{y_r}}$ are defined as,

$$\mathbf{F}_{\boldsymbol{\xi}} = \left[\sum_{k=1}^{\wp_1-1}\frac{\partial\alpha_{1,\wp_1-1}}{\partial\xi_{1,k}}\xi_{1,k+1},\ \sum_{k=1}^{\wp_2-1}\frac{\partial\alpha_{2,\wp_2-1}}{\partial\xi_{2,k}}\xi_{2,k+1},\ldots,\ \sum_{k=1}^{\wp_q-1}\frac{\partial\alpha_{q,\wp_q-1}}{\partial\xi_{q,k}}\xi_{q,k+1}\right]^T$$

$$\mathbf{F}_{\mathbf{y_r}}(\dot{\mathbf{y}}_\mathbf{r},\ \ddot{\mathbf{y}}_\mathbf{r},\ldots,\mathbf{y}_\mathbf{r}^{(\wp)}) = \left[\sum_{k=1}^{\wp_1-1}\frac{\partial\alpha_{1,\wp_1-1}}{\partial y_{r,1}^{(k-1)}}y_{r,1}^{(k)},\ \sum_{k=1}^{\wp_2-1}\frac{\partial\alpha_{2,\wp_2-1}}{\partial y_{r,2}^{(k-1)}}y_{r,2}^{(k)},\ldots,\ \sum_{k=1}^{\wp_q-1}\frac{\partial\alpha_{q,\wp_q-1}}{\partial y_{r,q}^{(k-1)}}y_{r,q}^{(k)}\right]^T$$

Further, define $\bar{\boldsymbol{\beta}}(\boldsymbol{\xi},\boldsymbol{\eta}) := [\boldsymbol{\beta}_1(\boldsymbol{\xi},\boldsymbol{\eta}),\ \boldsymbol{\beta}_2(\boldsymbol{\xi},\boldsymbol{\eta}),\ldots,\ \boldsymbol{\beta}_q(\boldsymbol{\xi},\boldsymbol{\eta})]^T \in \mathbb{R}^{q\times m}$, $\boldsymbol{\psi}^T := [\boldsymbol{\psi}_{1,\wp_1}^T,\ \boldsymbol{\psi}_{2,\wp_2}^T,\ldots,\ \boldsymbol{\psi}_{q,\wp_q}^T]^T \in \mathbb{R}^{q\times p}$, $\boldsymbol{\psi}_{i,\wp_i}^T := \boldsymbol{\varphi}_{i,\wp_i}^T - \sum_{k=1}^{\wp_i-1}\frac{\partial\alpha_{i,\wp_i-1}}{\partial\xi_{i,k}}\boldsymbol{\varphi}_{i,k}^T,\ i=\overline{1,q},\ \frac{\partial\boldsymbol{\alpha}_{\boldsymbol{\wp}-1}}{\partial\hat{\boldsymbol{\theta}}_2} := \left[\frac{\partial\boldsymbol{\alpha}_{1,\wp_1-1}}{\partial\hat{\boldsymbol{\theta}}_2},\ \frac{\partial\boldsymbol{\alpha}_{2,\wp_2-1}}{\partial\hat{\boldsymbol{\theta}}_2},\ldots,\ \frac{\partial\boldsymbol{\alpha}_{q,\wp_q-1}}{\partial\hat{\boldsymbol{\theta}}_2}\right]^T$, $\boldsymbol{a}(\boldsymbol{\xi},\boldsymbol{\eta}) := [a_1(\boldsymbol{\xi},\boldsymbol{\eta}),\ a_2(\boldsymbol{\xi},\boldsymbol{\eta}),\ldots,\ a_q(\boldsymbol{\xi},\boldsymbol{\eta})]^T$ and $\mathbf{y}_\mathbf{r}^{(\boldsymbol{\wp})} := [y_{r,1}^{(\wp_1)},\ y_{r,2}^{(\wp_2)},\ldots,\ y_{r,q}^{(\wp_q)}]^T$. These terminologies allow us to rewrite the dynamics (3.156) in a more compact form as given below.

$$\dot{\mathbf{z}}_{\boldsymbol{\wp}} = \boldsymbol{a}(\boldsymbol{\xi},\boldsymbol{\eta}) + \boldsymbol{\psi}_{\boldsymbol{\wp}}^T\boldsymbol{\theta}_2^* + \bar{\boldsymbol{\beta}}\boldsymbol{\theta}_3^* - \mathbf{F}_{\boldsymbol{\xi}} - \mathbf{F}_{\mathbf{y_r}} - \frac{\partial\boldsymbol{\alpha}_{\boldsymbol{\wp}-1}}{\partial\hat{\boldsymbol{\theta}}_2}\dot{\hat{\boldsymbol{\theta}}}_2 + \bar{\boldsymbol{\beta}}\left(\sum_{j=1}^{m}\theta_{1,j}^*N_j\right)\mathbf{B}(\hat{\mathbf{v}}+\bar{\mathbf{v}}) - \mathbf{y}_\mathbf{r}^{(\boldsymbol{\wp})} \tag{3.157}$$

Hereafter, let us choose the first part of the control input given by $\hat{\mathbf{v}}(t)$ as,

$$\hat{\mathbf{v}}(t) = \left(\bar{\boldsymbol{\beta}}\sum_{j=1}^{m}\hat{\theta}_{1,j}N_j\mathbf{B}\right)^{-1}(-\boldsymbol{a}(\boldsymbol{\xi},\boldsymbol{\eta}) - \boldsymbol{\psi}_{\boldsymbol{\wp}}^T\hat{\boldsymbol{\theta}}_2 - \bar{\boldsymbol{\beta}}\hat{\boldsymbol{\theta}}_3 - \mathbf{z}_{\boldsymbol{\wp}-\mathbf{1}} + \mathbf{F}_{\boldsymbol{\xi}} + \mathbf{F}_{\mathbf{y_r}} + \mathbf{y}_\mathbf{r}^{(\boldsymbol{\wp})}) \tag{3.158}$$

Substituting $\hat{\mathbf{v}}(t)$ in (3.158) in (3.157) leads to the following dynamics,

$$\dot{\mathbf{z}}_{\boldsymbol{\wp}} = -\mathbf{z}_{\boldsymbol{\wp}-\mathbf{1}} + \bar{\boldsymbol{\beta}}\left(\sum_{j=1}^{m}\theta_{1,j}^*N_j\right)\mathbf{B}\bar{\mathbf{v}} + \bar{\boldsymbol{\beta}}\left(\sum_{j=1}^{m}\tilde{\theta}_{1,j}N_j\right)\mathbf{B}\hat{\mathbf{v}} + \boldsymbol{\psi}_{\boldsymbol{\wp}}^T\tilde{\boldsymbol{\theta}}_2 + \bar{\boldsymbol{\beta}}\tilde{\boldsymbol{\theta}}_3 - \frac{\partial\boldsymbol{\alpha}_{\boldsymbol{\wp}-1}}{\partial\hat{\boldsymbol{\theta}}_2}\dot{\hat{\boldsymbol{\theta}}}_2 \tag{3.159}$$

In accordance with the design assumptions, one actuator in each group $\mathscr{G}_k,\ k=\overline{1,q}$ under the grouping scheme $\mathscr{G}$ should be alive to satisfy the condition for existence of an adaptive solution to the FTC problem. Thus, it is reasonable to assume that there exists a constant ℓ such that $\left\|\sum_{j=1}^{m}\theta_{1,j}^*N_j\right\|_{\mathscr{F}} > \ell$. The control signal $\bar{\mathbf{v}}(t)$ is then designed as

$$\bar{\mathbf{v}}(t) = \left(\ell\bar{\boldsymbol{\beta}}\mathbf{B}\right)^{-1}\begin{bmatrix} -c_{1,\wp_1}z_{1,\wp_1} - \bar{c}_{1,\wp_1}(\|\boldsymbol{\psi}_{1,\wp_1}\|^2 + \|\boldsymbol{\beta}_1\|^2 + \|\bar{\boldsymbol{\beta}}_u^1\|^2)z_{1,\wp_1} - g_{1,\wp_1}\left\|\frac{\partial\alpha_{1,\wp_1-1}}{\partial\hat{\boldsymbol{\theta}}_2}\right\|^2 z_{1,\wp_1} \\ -c_{2,\wp_2}z_{2,\wp_2} - \bar{c}_{2,\wp_2}(\|\boldsymbol{\psi}_{2,\wp_2}\|^2 + \|\boldsymbol{\beta}_2\|^2 + \|\bar{\boldsymbol{\beta}}_u^2\|^2)z_{2,\wp_2} - g_{2,\wp_2}\left\|\frac{\partial\alpha_{2,\wp_2-1}}{\partial\hat{\boldsymbol{\theta}}_2}\right\|^2 z_{2,\wp_2} \\ \vdots \\ -c_{q,\wp_q}z_{q,\wp_q} - \bar{c}_{q,\wp_q}(\|\boldsymbol{\psi}_{q,\wp_q}\|^2 + \|\boldsymbol{\beta}_q\|^2 + \|\bar{\boldsymbol{\beta}}_u^q\|^2)z_{q,\wp_q} - g_{q,\wp_q}\left\|\frac{\partial\alpha_{q,\wp_q-1}}{\partial\hat{\boldsymbol{\theta}}_2}\right\|^2 z_{q,\wp_q} \end{bmatrix}.$$

Ultimately, the control law $\mathbf{v}(t)$ is calculated to be as follows.

$$\mathbf{v}(t) = \left(\bar{\boldsymbol{\beta}}\sum_{j=1}^{m}\hat{\theta}_{1,j}N_j\mathbf{B}\right)^{-1}\begin{bmatrix} -a_1(\boldsymbol{\xi},\ \boldsymbol{\eta}) - \boldsymbol{\psi}_{1,\wp_1}^T\hat{\boldsymbol{\theta}}_2 - \boldsymbol{\beta}_1\hat{\boldsymbol{\theta}}_3 - z_{1,\wp_1-1} + F_{\boldsymbol{\xi}_1} + F_{\mathbf{y_r},1} + y_{r,1}^{(\wp_1)} \\ -a_2(\boldsymbol{\xi},\ \boldsymbol{\eta}) - \boldsymbol{\psi}_{2,\wp_2}^T\hat{\boldsymbol{\theta}}_2 - \boldsymbol{\beta}_2\hat{\boldsymbol{\theta}}_3 - z_{2,\wp_2-1} + F_{\boldsymbol{\xi}_2} + F_{\mathbf{y_r},2} + y_{r,2}^{(\wp_2)} \\ \vdots \\ -a_q(\boldsymbol{\xi},\ \boldsymbol{\eta}) - \boldsymbol{\psi}_{q,\wp_q}^T\hat{\boldsymbol{\theta}}_2 - \boldsymbol{\beta}_q\hat{\boldsymbol{\theta}}_3 - z_{q,\wp_q-1} + F_{\boldsymbol{\xi}_q} + F_{\mathbf{y_r},q} + y_{r,q}^{(\wp_q)} \end{bmatrix} +$$

$$\left(\ell\bar{\boldsymbol{\beta}}\mathbf{B}\right)^{-1}\begin{bmatrix} -c_{1,\wp_1}z_{1,\wp_1} - \bar{c}_{1,\wp_1}(\|\boldsymbol{\psi}_{1,\wp_1}\|^2 + \|\boldsymbol{\beta}_1\|^2 + \|\bar{\boldsymbol{\beta}}_u^1\|^2)z_{1,\wp_1} - g_{1,\wp_1}\left\|\frac{\partial\alpha_{1,\wp_1-1}}{\partial\hat{\boldsymbol{\theta}}_2}\right\|^2 z_{1,\wp_1} \\ -c_{2,\wp_2}z_{2,\wp_2} - \bar{c}_{2,\wp_2}(\|\boldsymbol{\psi}_{2,\wp_2}\|^2 + \|\boldsymbol{\beta}_2\|^2 + \|\bar{\boldsymbol{\beta}}_u^2\|^2)z_{2,\wp_2} - g_{2,\wp_2}\left\|\frac{\partial\alpha_{2,\wp_2-1}}{\partial\hat{\boldsymbol{\theta}}_2}\right\|^2 z_{2,\wp_2} \\ \vdots \\ -c_{q,\wp_q}z_{q,\wp_q} - \bar{c}_{q,\wp_q}(\|\boldsymbol{\psi}_{q,\wp_q}\|^2 + \|\boldsymbol{\beta}_q\|^2 + \|\bar{\boldsymbol{\beta}}_u^q\|^2)z_{q,\wp_q} - g_{q,\wp_q}\left\|\frac{\partial\alpha_{q,\wp_q-1}}{\partial\hat{\boldsymbol{\theta}}_2}\right\|^2 z_{q,\wp_q} \end{bmatrix} \tag{3.160}$$

Where $\bar{\boldsymbol{\beta}}_u$ is defined as

$$\bar{\boldsymbol{\beta}}_u = \begin{bmatrix} \beta_{1,1}\hat{u}_{H1} & \beta_{1,2}\hat{u}_{H2} & \dots & \beta_{1,m}\hat{u}_{Hm} \\ \dots & \dots & \vdots & \dots \\ \beta_{q,1}\hat{u}_{H1} & \beta_{q,2}\hat{u}_{H2} & \dots & \beta_{q,m}\hat{u}_{Hm} \end{bmatrix}.$$

and $\bar{\boldsymbol{\beta}}_u^i$ denotes the i-th row vector of the matrix $\bar{\boldsymbol{\beta}}_u$. It should be mentioned that the choice of the control law $\mathbf{v}(t)$ is aimed at achieving stable solution trajectories under a closed loop operation. Thus, the controller design is primarily driven by a Lyapunov analysis to arrive at the final control law ensuring overall system stability under unforeseen circumstances of parametric/structural variations and actuator failures. This fact would be evident while conducting stability analysis of the closed-loop dynamics to follow.

3.3.2.2 Design of Parameter Estimator using Multiple Identification Models

The design the estimator, the transformed system is represented as a parametric $\boldsymbol{\xi}-$ model as follows.

$$\underbrace{\begin{bmatrix} \dot{\xi}_{1,1} \\ \vdots \\ \dot{\xi}_{q,1} \\ \vdots \\ \dot{\xi}_{1,\wp_1} \\ \vdots \\ \dot{\xi}_{q,\wp_q} \end{bmatrix}}_{\dot{\boldsymbol{\xi}}} = \underbrace{\begin{bmatrix} \xi_{1,2} \\ \vdots \\ \xi_{q,2} \\ \vdots \\ a_1(\boldsymbol{\xi},\ \boldsymbol{\eta}) \\ \vdots \\ a_q(\boldsymbol{\xi},\ \boldsymbol{\eta}) \end{bmatrix}}_{\bar{\boldsymbol{a}}(\boldsymbol{\xi},\boldsymbol{\eta})} + \underbrace{\begin{bmatrix} 0 & \dots & 0 & \boldsymbol{\varphi}_{1,1}^T & 0 \\ \vdots & \vdots & \vdots & \vdots & \vdots \\ 0 & \dots & 0 & \boldsymbol{\varphi}_{q,1}^T & 0 \\ \vdots & \vdots & \ddots & \vdots & \vdots \\ \beta_{1,1}u_{H1} & \dots & \beta_{1,m}u_{Hm} & \boldsymbol{\varphi}_{1,\wp_1}^T & \boldsymbol{\beta}_1 \\ \vdots & \ddots & \vdots & \vdots & \vdots \\ \beta_{q,1}u_{H1} & \dots & \beta_{q,m}u_{Hm} & \boldsymbol{\varphi}_{q,\wp_q}^T & \boldsymbol{\beta}_q \end{bmatrix}\begin{bmatrix} \theta_{1,1}^* \\ \vdots \\ \theta_{1,m}^* \\ \boldsymbol{\theta}_2^* \\ \boldsymbol{\theta}_3^* \end{bmatrix}}_{\boldsymbol{\Phi}^T(\boldsymbol{\xi},\mathbf{u})\boldsymbol{\theta}^*} \tag{3.161}$$

Where $u_{Hj} := \sum_{k=1}^{q} b_{jk} w_k$ for $j = \overline{1,m}$. The estimation model can now be simply written as, $\dot{\boldsymbol{\xi}} = \bar{\boldsymbol{a}}(\boldsymbol{\xi},\boldsymbol{\eta}) + \Phi^T(\boldsymbol{\xi},\boldsymbol{u})\boldsymbol{\theta}^*$. The function vector $\bar{\boldsymbol{a}}(\boldsymbol{\xi},\boldsymbol{\eta}) \in \mathbb{R}^{\wp_1+\ldots+\wp_q}$ and the regressor matrix $\boldsymbol{\Phi}^T(\boldsymbol{\xi},\boldsymbol{u}) \in \mathbb{R}^{\sum_k \wp_k \times (2m+p)}$. It is observed that irrespective of the system being characterized by multiple inputs and outputs, the estimation model bears the same structure as (3.9). Let us now define the parameter set $\mathcal{S}_{\boldsymbol{\theta}^*}$ as

$$\mathcal{S}_{\boldsymbol{\theta}^*} := [\underline{\theta}^*_{1,1}, \overline{\theta}^*_{1,1}] \times \ldots \times [\underline{\theta}^*_{1,m}, \overline{\theta}^*_{1,m}] \times [\underline{\theta}^*_{21}, \overline{\theta}^*_{21}] \times \ldots \times [\underline{\theta}^*_{2p}, \overline{\theta}^*_{2p}] \times [\underline{\theta}^*_{31}, \overline{\theta}^*_{31}] \times \ldots \times [\underline{\theta}^*_{3m}, \overline{\theta}^*_{3m}].$$

The notation $\overline{\theta}^*_i$ and $\underline{\theta}^*_i$ is used to denote the upper and lower bounds (may be sufficiently large in magnitude) of the elements of the unknown parameter vector $\boldsymbol{\theta}^*$. Hence, in accordance to the design assumptions stated apriori, the design of the parameter estimator at the first layer and second layer of adaptation is stated in the following subsections.

A. First Layer of Adaptation

The N adaptive identifiers are described by the following dynamics with non-zero initial values of the estimates of the unknown parameter vector in each of the identification models.

$$\dot{\hat{\boldsymbol{\xi}}}_{(\mu)} = \mathbf{A}_\mu(\boldsymbol{\xi},t)(\hat{\boldsymbol{\xi}}_{(\mu)} - \boldsymbol{\xi}) + \bar{\boldsymbol{a}}(\boldsymbol{\xi},\boldsymbol{\eta}) + \boldsymbol{\Phi}^T(\boldsymbol{\xi},\mathbf{u})\hat{\boldsymbol{\theta}}_{(\mu)} \tag{3.162}$$

$$\dot{\hat{\boldsymbol{\theta}}}_{(\mu)}(t) = \boldsymbol{\Gamma}_\mu \text{Proj}[\boldsymbol{\Phi}(\boldsymbol{\xi},\mathbf{u})P_\mu(\boldsymbol{\xi} - \hat{\boldsymbol{\xi}}_{(\mu)})] \tag{3.163}$$

Herein, the subscript $\mu = \overline{1,N}$ is used to index each of the adaptive identification models to distinctly figure out the signals associated with the μ-th adaptive identifier. The signal vectors $\hat{\boldsymbol{\xi}}_{(\mu)}$ and $\hat{\boldsymbol{\theta}}_{(\mu)}$ define the predicted state vector and the estimates of $\boldsymbol{\theta}^*$, respectively for each of the μ identification models. The initial conditions of parameter estimates corresponding to each of the N adaptive identifiers are so chosen that the unknown parameter vector $\boldsymbol{\theta}^*$ resides within the parameter space $\mathcal{S}_{\boldsymbol{\theta}^*}$ spanned by these N initialized estimates of the parameter vector $\hat{\boldsymbol{\theta}}_{(\mu)}$ for $\mu = \overline{1,N}$. The operator Proj$\{\cdot\}$ is a smooth projection operator which helps in restricting the parameter estimates $\hat{\boldsymbol{\theta}}_{(\mu)}$ within the set $\mathcal{S}_{\boldsymbol{\theta}^*}$. Further, $\mathbf{A}_\mu(\boldsymbol{\xi},t) := \mathbf{A}_{\mu 0} - \gamma\boldsymbol{\Phi}(\boldsymbol{\xi},\mathbf{u})^T\boldsymbol{\Phi}(\boldsymbol{\xi},\mathbf{u})\mathbf{P}_\mu$ is so chosen to guarantee boundedness of the μ-th estimator error dynamics irrespective of the boundedness of the regressor matrix $\boldsymbol{\Phi}(\boldsymbol{\xi},\mathbf{u})$. The matrix $\boldsymbol{\Gamma}_\mu \in \mathbb{R}^{(2m+p)\times(2m+p)}$ is a positive definite diagonal matrix defining the rate of adaptation for the $\mu-$th adaptive identifier and $\mathbf{A}_{\mu 0}$ denotes a Hurwitz matrix satisfying the Lyapunov equation, $\mathbf{A}^T_{\mu 0}\mathbf{P}_\mu + \mathbf{P}_\mu\mathbf{A}_{\mu 0} = -\mathbf{Q}_\mu$ with $\mathbf{P}_\mu,\ \mathbf{Q}_\mu > 0$.

To arrive at the prediction error dynamics of the μ-th estimator, let us define the state prediction error as $\tilde{\boldsymbol{\xi}}_{(\mu)} := \boldsymbol{\xi} - \hat{\boldsymbol{\xi}}_{(\mu)}$ and the parameter estimation error as $\tilde{\boldsymbol{\theta}}_{(\mu)} := \boldsymbol{\theta}^* - \hat{\boldsymbol{\theta}}_{(\mu)}$. Thereafter using (3.162)-(3.163), the identification error dynamics are derived as

$$\dot{\tilde{\boldsymbol{\xi}}}_{(\mu)} = (\mathbf{A}_{\mu 0} - \gamma\boldsymbol{\Phi}(\boldsymbol{\xi},\mathbf{u})^T\boldsymbol{\Phi}(\boldsymbol{\xi},\mathbf{u})\mathbf{P}_\mu)\tilde{\boldsymbol{\xi}}_{(\mu)} + \boldsymbol{\Phi}^T(\boldsymbol{\xi},\mathbf{u})\tilde{\boldsymbol{\theta}}_{(\mu)} \tag{3.164}$$

The identification error dynamics is similar to the one derived in (3.14). Now, unlike Section 3.2, herein our interest lies in compensating abrupt actuator failures which are finite in their occurrence meaning that the system is subjected to at most $(m-q)$ actuator failures $\forall t \in [0,\infty)$. As mentioned earlier, actuator failures unknown in time, pattern and magnitude introduce large parametric uncertainties in

to the system. Thus, actuator failure induced uncertain parameter vector $\boldsymbol{\theta}_1^*$ and $\boldsymbol{\theta}_3^*$ are time varying leading to $\dot{\boldsymbol{\theta}}_1^*, \dot{\boldsymbol{\theta}}_3^* \neq 0$. These parameters experience jumps at the occurrence of abrupt faults or failures. However, the magnitude of such jumps are bounded and an upper bound on the same can be calculated at time instant t encountering a partial loss or total loss of actuators. This statement implies that $\int_0^\infty |\dot{\boldsymbol{\theta}}^*(s)|ds < \infty$. The above conclusion is drawn from the following facts. Invoking assumption 3.5 and the discussion immediately following (3.159), it is shown that $\|\boldsymbol{\theta}_1^*\| \geq \ell > 0$, $\|\boldsymbol{\theta}_1^*(t^+) - \boldsymbol{\theta}_1^*(t^-)\| \leq \sum_{j=1}^{m} \overline{\theta}_{1,j} - \ell$ and $\|\theta_{3j}^*(t^+) - \theta_{3j}^*(t^-)\| \leq 2\overline{u}$. Let us define $\Delta^\dagger = \max\{\sum_{j=1}^{m} \overline{\theta}_{1,j} - \ell,\ 2\overline{u}\} < \infty$. Now, due to occurrence of actuator faults/failures at a time instant $t = t_f$, the elements of the parameter vector $\boldsymbol{\theta}^*(t)$ exhibit jumps whose magnitude is bounded as $\|\dot{\boldsymbol{\theta}}^*(t)\| \leq \Delta^\dagger \delta(t - t_f)$. The function $\delta(\cdot)$ denotes the dirac delta function. Taking integral from $0 \sim \infty$ on both sides of the resulting inequality and invoking the properties of delta functions leads to the property of $\boldsymbol{\theta}^*(t)$ stated above, i.e., $\dot{\boldsymbol{\theta}}^*(t) \in \mathcal{L}_1[0, \infty)$. Thus the following assumption is reasonable.

Assumption 3.11. *The time derivative of the unknown parameter vector $\boldsymbol{\theta}^*(t)$ representing system and actuator failure induced parametric uncertainties satisfy $\dot{\boldsymbol{\theta}}^*(t) \in \mathcal{L}_1[0, \infty)$, i.e.,*

$$\int_0^\infty \|\dot{\boldsymbol{\theta}}^*(s)\|ds \leq (m - q)\Delta^\dagger < \infty$$

where $\Delta^\dagger := \max\{\sum_{j=1}^{m} \overline{\theta}_{1,j} - \ell,\ 2\overline{u}\} < \infty$ and $\ell := \min_{j \notin \{j_1, \ldots, j_d\}} \{\sum_j \underline{\theta}_{1,j}\}$, $d = (m - q)$. The quantities $\overline{u}$, $\overline{\theta}_{1,j}$ and $\underline{\theta}_{1,j}$ define the upper bound of the stuck value due to lock-in-place failure, upper and lower bound on the actuation gain characterizing partial actuator failures, respectively.

The following theorem summarizes the properties of the signals associated with each of N adaptive identifiers which are similar to those stated in Theorem 3.1 with minor modifications.

Theorem 3.7. *Let us consider that the solutions of the adaptive identifiers given by* (3.162)-(3.163) *and the identification error dynamics in* (3.164) *for $\mu = \{1, \ldots, N\}$, with their maximal interval of existence being $[0,\ \infty)$. Then the following properties hold under the framework of first layer of adaptation for each of the N adaptive identification models for $\boldsymbol{\Gamma}_\mu,\ \mathbf{P}_\mu,\ \mathbf{Q}_\mu > 0$.*

(i) $\tilde{\boldsymbol{\theta}}_{(\mu)}(t) \in \mathcal{L}_\infty[0, \infty)$

(ii) $\tilde{\boldsymbol{\xi}}_{(\mu)}(t) \in \mathcal{L}_2[0, \infty) \cap \mathcal{L}_\infty[0, \infty)$, $\dot{\tilde{\boldsymbol{\xi}}}_{(\mu)}(t) \in \mathcal{L}_\infty[0, \infty)$

(iii) $\dot{\hat{\boldsymbol{\theta}}}_{(\mu)}(t) \in \mathcal{L}_2[0, \infty)$

Proof.

Let us consider a Lyapunov function $V_{(\mu)}(\tilde{\boldsymbol{\xi}}_{(\mu)}, \tilde{\boldsymbol{\theta}}_{(\mu)}, t) : \mathbb{R}^{\sum_k \wp_k} \times \mathbb{R}^{(2m+p)} \times [0, \infty)$ for $k = \overline{1, q}$ as,

$$V_{(\mu)} = \frac{1}{2}\tilde{\boldsymbol{\xi}}_{(\mu)}^T \mathbf{P}_\mu \tilde{\boldsymbol{\xi}}_{(\mu)} + \frac{1}{2}\tilde{\boldsymbol{\theta}}_{(\mu)}^T \boldsymbol{\Gamma}_\mu^{-1} \tilde{\boldsymbol{\theta}}_{(\mu)}$$

In view of the identification error dynamics (3.164) and owing to the fact that the failure induced unknown parameters are time varying $\forall\ t \in [0,\infty)$ results in, $\dot{\tilde{\boldsymbol{\theta}}} = \dot{\boldsymbol{\theta}}^* - \dot{\hat{\boldsymbol{\theta}}}$. The first time derivative of $V_{(\mu)}$ yields the following,

$$\dot{V}_{(\mu)} = -\tilde{\boldsymbol{\xi}}_{(\mu)}^T \mathbf{Q}_\mu \tilde{\boldsymbol{\xi}}_{(\mu)} - \gamma \tilde{\boldsymbol{\xi}}_{(\mu)}^T \mathbf{P}_\mu \boldsymbol{\Phi}^T \boldsymbol{\Phi} \mathbf{P}_\mu \tilde{\boldsymbol{\xi}}_{(\mu)} + \tilde{\boldsymbol{\theta}}_{(\mu)}^T \boldsymbol{\Phi} \mathbf{P}_\mu \tilde{\boldsymbol{\xi}}_{(\mu)} - \tilde{\boldsymbol{\theta}}_{(\mu)}^T \boldsymbol{\Gamma}_\mu^{-1} \dot{\hat{\boldsymbol{\theta}}}_{(\mu)} + \tilde{\boldsymbol{\theta}}_{(\mu)}^T \boldsymbol{\Gamma}_\mu^{-1} \dot{\boldsymbol{\theta}}_{(\mu)}^* \tag{3.165}$$

where the matrix $\mathbf{Q}_\mu := -(\mathbf{A}_{\mu 0}^T \mathbf{P}_\mu + \mathbf{P}_\mu \mathbf{A}_{\mu 0})/2 > 0$ and $\mathbf{P}_\mu$ is a positive definite symmetric matrix owing to $\mathbf{A}_{\mu 0}$ being Hurwitz. Substituting the parameter update law (3.163) in (3.165) and using the properties of projection operator from [69] as $-\tilde{\boldsymbol{\theta}}_{(\mu)}^T \boldsymbol{\Gamma}_\mu^{-1} \mathrm{Proj}(\boldsymbol{\Gamma}_\mu \boldsymbol{\Phi} \mathbf{P}_\mu \tilde{\boldsymbol{\xi}}_{(\mu)}) \leq -\tilde{\boldsymbol{\theta}}_{(\mu)}^T \boldsymbol{\Gamma}_\mu^{-1} \boldsymbol{\Gamma}_\mu \boldsymbol{\Phi} \mathbf{P}_\mu \tilde{\boldsymbol{\xi}}_{(\mu)}$, yields,

$$\dot{V}_{(\mu)} \leq -\underline{\lambda}(\mathbf{Q}_\mu) \|\tilde{\boldsymbol{\xi}}_{(\mu)}\|^2 - \gamma \|\boldsymbol{\Phi} \mathbf{P}_\mu \tilde{\boldsymbol{\xi}}_{(\mu)}\|^2 + \tilde{\boldsymbol{\theta}}_{(\mu)}^T \boldsymbol{\Gamma}_\mu^{-1} \dot{\boldsymbol{\theta}}_{(\mu)}^* \tag{3.166}$$

The above inequality (3.166) is derived after using Rayleigh's inequality $\underline{\lambda}(\mathbf{Q}) \|\tilde{\boldsymbol{\xi}}\|^2 \leq \boldsymbol{\xi}^T \mathbf{Q} \boldsymbol{\xi} \leq \overline{\lambda}(\mathbf{Q}) \|\tilde{\boldsymbol{\xi}}\|^2$ in (3.165). Now integrating the above inequality (3.166) for the time interval $[0,\infty)$, and using Hölder's inequality, we get,

$$\underline{\lambda}(\mathbf{Q}_\mu) \int_0^\infty \|\tilde{\boldsymbol{\xi}}_{(\mu)}\|^2 dt - \|\tilde{\boldsymbol{\theta}}_{(\mu)}\|_\infty \|\boldsymbol{\Gamma}_\mu^{-1}\|_\infty \int_0^\infty \|\dot{\boldsymbol{\theta}}^*\| dt \leq -\int_0^\infty \dot{V}_{(\mu)} dt \leq V_{(\mu)}(0) - V_{(\mu)}(\infty) \leq V_\mu(0) < \infty \tag{3.167}$$

$$\int_0^\infty \|\tilde{\boldsymbol{\xi}}_{(\mu)}\|^2 dt < \frac{1}{\underline{\lambda}(\mathbf{Q}_\mu)} (V_{(\mu)}(0) + (m-q)\Delta^\dagger \|\tilde{\boldsymbol{\theta}}_{(\mu)}\|_\infty \|\boldsymbol{\Gamma}_\mu^{-1}\|_\infty) \tag{3.168}$$

Now due to the projection operation on the adaptive laws in (3.164), the parameter estimation error $\tilde{\boldsymbol{\theta}} \in \mathcal{L}_\infty[0,\infty)$. Therefore from (3.168) and the inequality $\tilde{\boldsymbol{\xi}}_{(\mu)}^T \mathbf{P}_\mu \tilde{\boldsymbol{\xi}}_{(\mu)} \leq 2V_{(\mu)}(t) \leq 2V_{(\mu)}(0) < \infty$, the signal properties $\tilde{\boldsymbol{\xi}} \in \mathcal{L}_2 \cap \mathcal{L}_\infty$ and $\dot{\tilde{\boldsymbol{\xi}}} \in \mathcal{L}_\infty$ follows. Thereafter, the claims (i) and (ii) are proved.
To prove the $\mathcal{L}_2$-integrability of $\dot{\hat{\boldsymbol{\theta}}}_{(\mu)}(t)$, we first evaluate $\|\dot{\hat{\boldsymbol{\theta}}}_{(\mu)}\|^2 \leq \overline{\lambda}(\boldsymbol{\Gamma}_\mu^2) \|\boldsymbol{\Phi} \mathbf{P}_\mu \tilde{\boldsymbol{\xi}}_{(\mu)}\|^2$. Now, substituting $\|\boldsymbol{\Phi} \mathbf{P}_\mu \tilde{\boldsymbol{\xi}}_{(\mu)}\|^2 \geq \|\dot{\hat{\boldsymbol{\theta}}}_{(\mu)}\|^2 / \overline{\lambda}(\boldsymbol{\Gamma}_\mu^2)$ in (3.166) and rearranging the inequality results in,

$$\int_0^\infty \|\dot{\hat{\boldsymbol{\theta}}}_{(\mu)}(t)\|^2 dt \leq \frac{\overline{\lambda}(\boldsymbol{\Gamma}_\mu^2)}{\gamma} (V_{(\mu)}(0) + (m-q)\Delta^\dagger \|\tilde{\boldsymbol{\theta}}_{(\mu)}\|_\infty \|\boldsymbol{\Gamma}_\mu^{-1}\|_\infty) \tag{3.169}$$

Since, $V_{(\mu)}(0)$, $\Delta^\dagger$, $\|\tilde{\boldsymbol{\theta}}_{(\mu)}\|_\infty$ and $\|\boldsymbol{\Gamma}_\mu^{-1}\|_\infty$ are finite, the conclusion $\dot{\hat{\boldsymbol{\theta}}} \in \mathcal{L}_2[0,\ \infty)$ follows. Claim (iii) is proved. □

B. Second Layer of Adaptation

The parameter estimate obtained from the second layer of adaptation is fed to the controller for subsequent compensation and faithful realization of the control objective. The final parameter estimate

at the second layer of adaptation is mathematically represented as,

$$\hat{\boldsymbol{\theta}}_{\mathbf{s}} := \sum_{\mu=1}^{(2m+p+1)} w_{\mu}^{*}\hat{\boldsymbol{\theta}}_{(\mu)}, \quad w_{\mu}^{*} \in [0,1] \text{ and } \sum_{\mu=1}^{(2m+p+1)} w_{\mu}^{*} = 1$$

where, w_{μ}^{*} for $\mu = \{1, \ldots, 2m+p+1\}$ are the weights assigned to the parameters estimated for the $N = 2m+p+1$ identification models. The minimum number of models required to make the smallest convex set in which the unknown parameter vector resides is $N = 2m+p+1$. Similar to the weight learning law in Section 3.2.2.1 B, a Lyapunov based adaptive weight learning law is formulated which eliminates the requirement of the knowledge of weight parameters w_{μ}^{*}. The tuning law for weight adaptation herein, is stated as,

$$\dot{\hat{\tilde{\mathbf{w}}}}(t) = -\triangle\tilde{\boldsymbol{X}}(t)^{T}\triangle\tilde{\boldsymbol{X}}\hat{\tilde{\mathbf{w}}}(t) + \triangle\tilde{\boldsymbol{X}}(t)^{T}\mathbf{r}(t) \tag{3.170}$$

The $(2m+p+1)^{th}$ identification model weight is calculated as $\hat{w}_{2m+p+1} = 1 - \sum_{\mu=1}^{2m+p+1} \hat{w}_{\mu}$. Finally, the unknown parameter vector $\boldsymbol{\theta}^{*}$ is estimated as $\hat{\boldsymbol{\theta}}_{s} := \sum_{\mu=1}^{2m+p+1} \hat{w}_{\mu}\hat{\boldsymbol{\theta}}_{(\mu)}$. The stability properties of the estimation under the second layer of adaptation are $\hat{\boldsymbol{\theta}}_{\mathbf{s}} \in \mathcal{L}_{\infty}[0,\infty)$, $\hat{\mathbf{w}} \in \mathcal{L}_{\infty}[0,\infty)$ and $\dot{\hat{\mathbf{w}}} \in \mathcal{L}_{\infty}[0,\infty)$. These results directly follow from the proof of Theorem 3.2.

The next section presents the stability properties of the closed loop signals. These theoretical results are helpful in substantiating the claims and meet the contemplated design objectives of the proposed adaptive controller.

3.3.3 Main Results: Stability Analysis of the Proposed Control System

In this section, the input-to-state-stability (ISS) of the tracking error dynamics with $\tilde{\boldsymbol{\theta}}(t)$ and $\dot{\hat{\boldsymbol{\theta}}}(t)$ as the inputs will be proved first. Instead of repeating the ISS analysis with respect to $\tilde{\boldsymbol{\theta}}_{(\mu)}(t)$ and $\dot{\hat{\boldsymbol{\theta}}}_{\mu}(t)$ from each of the μ adaptive identification models, we present the closed loop stability results by directly considering the parameter estimate $\tilde{\boldsymbol{\theta}}_{\mathbf{s}}$ and $\dot{\hat{\boldsymbol{\theta}}}_{\mathbf{s}}$ at the second layer of adaptation. This is done to elude a comprehensive treatment of results at this stage which would help us to focus on the main results. Since, the procedure of inferring stability properties are similar, the interested reader is referred to Theorem 3.4 for a clear understanding. Continuing with the analysis, the tracking error dynamics obtained under the action of the proposed adaptive controller given by (3.160) is given by

$$\dot{\mathbf{z}} = \boldsymbol{\mathcal{A}}_{\mathbf{z}}(\mathbf{z}, \hat{\boldsymbol{\theta}}, t)\mathbf{z} + \mathbf{B}_{\boldsymbol{\theta}^{*}}(\mathbf{z}, \hat{\boldsymbol{\theta}}, t)\tilde{\boldsymbol{\theta}}_{\mathbf{s}} + \mathbf{B}_{\dot{\hat{\boldsymbol{\theta}}}}(\mathbf{z}, \hat{\theta}, t)\dot{\hat{\boldsymbol{\theta}}}_{\mathbf{s}}. \tag{3.171}$$

Where $\mathbf{z}(t) := [z_{1,1}, z_{2,1}, \ldots, z_{q,1}, z_{1,2}, z_{2,2}, \ldots, z_{q,2}, \ldots, z_{1,\wp_1}, z_{2,\wp_2}, \ldots, z_{q,\wp_q}]^{T} = [\mathbf{z}_{i,1}^{T}, \mathbf{z}_{i,2}^{T}, \ldots, \mathbf{z}_{i,q}^{T}]^{T}$ for $i = \overline{1,q}$ and the matrices $\boldsymbol{\mathcal{A}}_{\mathbf{z}}$ is defined in (3.173), respectively. The matrices $\mathbf{B}_{\boldsymbol{\theta}^{*}}$ and $\mathbf{B}_{\dot{\hat{\boldsymbol{\theta}}}}$ are

defined as follows.

$$\mathbf{B}_{\boldsymbol{\theta}^*} := \left[\begin{array}{cccc|c|cccc} 0 & 0 & \dots & 0 & & 0 & 0 & \dots & 0 \\ 0 & 0 & \dots & 0 & \boldsymbol{\psi}_{1,1}^T & 0 & 0 & \dots & 0 \\ \vdots & \ddots & \ddots & \vdots & \vdots & \vdots & \ddots & \ddots & \vdots \\ 0 & \dots & \dots & 0 & \boldsymbol{\psi}_{q,1}^T & 0 & \dots & \dots & 0 \\ \hline 0 & 0 & \dots & 0 & & 0 & 0 & \dots & 0 \\ 0 & 0 & \dots & 0 & \boldsymbol{\psi}_{1,2}^T & 0 & 0 & \dots & 0 \\ \vdots & \ddots & \ddots & \vdots & \vdots & \vdots & \ddots & \ddots & \vdots \\ 0 & \dots & \dots & 0 & \boldsymbol{\psi}_{q,2}^T & 0 & \dots & \dots & 0 \\ \hline & \vdots & & & \vdots & & \vdots & & \\ \hline 0 & 0 & \dots & 0 & & 0 & 0 & \dots & 0 \\ 0 & 0 & \dots & 0 & \boldsymbol{\psi}_{1,\wp_1-1}^T & 0 & 0 & \dots & 0 \\ \vdots & \ddots & \ddots & \vdots & \vdots & \vdots & \ddots & \ddots & \vdots \\ 0 & \dots & \dots & 0 & \boldsymbol{\psi}_{q,\wp_q-1}^T & 0 & \dots & \dots & 0 \\ \hline \beta_{1,1}\hat{u}_{H1} & \dots & \beta_{1,m}\hat{u}_{Hm} & & \boldsymbol{\psi}_{1,\wp_1}^T & \beta_{1,1} & \dots & \beta_{1,m} & \\ \vdots & \ddots & \vdots & & \vdots & \vdots & \ddots & \vdots & \\ \beta_{q,1}\hat{u}_{H1} & \dots & \beta_{q,m}\hat{u}_{Hm} & & \boldsymbol{\psi}_{q,\wp_q}^T & \beta_{q,1} & \dots & \beta_{q,m} & \end{array}\right]$$

$$\mathbf{B}_{\dot{\hat{\boldsymbol{\theta}}}_2} := -\left[\begin{array}{c|ccc|c|ccc} 0 & \dfrac{\partial \alpha_{1,1}}{\partial \hat{\boldsymbol{\theta}}_2} & \dots & \dfrac{\partial \alpha_{q,1}}{\partial \hat{\boldsymbol{\theta}}_2} & \dots & \dfrac{\partial \alpha_{1,\wp_1-1}}{\partial \hat{\boldsymbol{\theta}}_2} & \dots & \dfrac{\partial \alpha_{q,\wp_q-1}}{\partial \hat{\boldsymbol{\theta}}_2} \end{array}\right]^T \tag{3.172}$$

The matrix in left most lower block of the matrix $\mathbf{B}_{\boldsymbol{\theta}^*}$ is denoted by

$$\bar{\boldsymbol{\beta}}_{\hat{u}} := [\bar{\boldsymbol{\beta}}_{\hat{u}}^1,\ \bar{\boldsymbol{\beta}}_{\hat{u}}^2, \dots,\ \bar{\boldsymbol{\beta}}_{\hat{u}}^q]^T = \begin{bmatrix} \beta_{1,1}\hat{u}_{H1} & \dots & \beta_{1,m}\hat{u}_{Hm} \\ \beta_{2,1}\hat{u}_{H1} & \dots & \beta_{2,m}\hat{u}_{Hm} \\ \vdots & \ddots & \vdots \\ \beta_{q-1,1}\hat{u}_{H1} & \dots & \beta_{q-1,m}\hat{u}_{Hm} \\ \beta_{q,1}\hat{u}_{H1} & \dots & \beta_{q,m}\hat{u}_{Hm} \end{bmatrix}.$$

Such a notation is preferred to lend simplicity in matrix calculations to follow in the sequel. The closed loop system matrix and the relevant input matrices with reference to (3.171), namely, $\boldsymbol{\mathcal{A}}_{\mathbf{z}}$, $\mathbf{B}_{\boldsymbol{\theta}^*}$ and $\mathbf{B}_{\dot{\hat{\boldsymbol{\theta}}}_2}$ are of order $\sum_{i=1}^{q} \wp_i \times \sum_{i=1}^{q} \wp_i$, $\sum_{i=1}^{q} \wp_i \times (2m+p)$ and $\sum_{i=1}^{q} \wp_i \times p$ with elements from $\mathbb{R}$.

$$\mathcal{A}_{\mathbf{z}} := \left[\begin{array}{cccc|cccc|cccc|c|cccc} -a_{11} & 0 & \dots & 0 & 1 & 0 & \dots & 0 & 0 & 0 & \dots & 0 & & 0 & 0 & \dots & 0 \\ 0 & -a_{21} & \dots & 0 & 0 & 1 & \dots & 0 & 0 & 0 & \dots & 0 & & 0 & 0 & \dots & 0 \\ \vdots & \ddots & \ddots & \vdots & \vdots & \ddots & \ddots & \vdots & \vdots & \ddots & \ddots & \vdots & \dots & \vdots & \ddots & \ddots & \vdots \\ 0 & \dots & \dots & -a_{q1} & 0 & \dots & \dots & 1 & 0 & \dots & \dots & 0 & & 0 & \dots & \dots & 0 \\ \hline -1 & 0 & \dots & 0 & -a_{12} & 0 & \dots & 0 & 1 & 0 & \dots & 0 & & 0 & 0 & \dots & 0 \\ 0 & -1 & \dots & 0 & 0 & -a_{22} & \dots & 0 & 0 & 1 & \dots & 0 & & 0 & 0 & \dots & 0 \\ \vdots & \ddots & \ddots & \vdots & \vdots & \ddots & \ddots & \vdots & \vdots & \ddots & \ddots & \vdots & \dots & \vdots & \ddots & \ddots & \vdots \\ 0 & \dots & \dots & -1 & 0 & \dots & \dots & -a_{q2} & 0 & \dots & \dots & 1 & & 0 & \dots & \dots & 0 \\ \hline & \vdots & & & & \ddots & & & & \ddots & & & \ddots & & \vdots & & \\ & \vdots & & & & \ddots & & & & \ddots & & & \ddots & & \vdots & & \\ \hline & & & & & & & & & & & & & 1 & 0 & \dots & 0 \\ & \vdots & & & & \ddots & & & & \ddots & & & \ddots & 0 & 1 & \dots & 0 \\ & & & & & & & & & & & & & \vdots & \ddots & \ddots & \vdots \\ & & & & & & & & & & & & & 0 & \dots & \dots & 1 \\ \hline 0 & 0 & \dots & 0 & 0 & 0 & \dots & 0 & & & & & -1 & 0 & \dots & 0 & \\ 0 & 0 & \dots & 0 & 0 & 0 & \dots & 0 & & \dots & & & 0 & -1 & \dots & 0 & -\frac{\bar{\boldsymbol{\beta}} \sum_{j} \theta^{*}_{1,j} N_j \bar{\boldsymbol{\beta}}^{\dagger}}{\ell} \begin{pmatrix} a_{1\wp_1} & \dots & 0 \\ \vdots & \ddots & \vdots \\ 0 & \dots & a_{q\wp_q} \end{pmatrix} \\ \vdots & \ddots & \ddots & \vdots & \vdots & \ddots & \ddots & \vdots & & & & & \vdots & \ddots & \ddots & \vdots & \\ 0 & \dots & \dots & 0 & 0 & \dots & \dots & 0 & & & & & 0 & \dots & \dots & -1 & \end{array}\right] \tag{3.173}$$

Further, the shorthand notation used to represent the elements of the matrix $\boldsymbol{\mathcal{A}}_{\mathbf{z}}$ is explained as, $a_{i,j} := c_{i,j} + s_{i,j}$ for $i = \overline{1,q}$ and $j = \overline{1,\wp_q}$. The terms $c_{i,j}$ are constant controller gains and the damping factors $s_{i,j}$ are defined as,

$$s_{1,1} = \bar{c}_{1,1}\|\boldsymbol{\psi}_{1,1}\|^2 \tag{3.174}$$

$$s_{1,r_1} = \bar{c}_{1,r_1}\|\boldsymbol{\psi}_{1,r_1}\|^2 + g_{1,r_1}\left\|\frac{\partial \alpha_{1,r_1-1}}{\partial \hat{\boldsymbol{\theta}}_2}\right\|^2, \quad r_1 = \overline{2,\wp_1 - 1} \tag{3.175}$$

$$s_{1,\wp_1} = \bar{c}_{1,\wp_1}(\|\boldsymbol{\psi}_{1,\wp_1}\|^2 + \|\boldsymbol{\beta}_1\|^2 + \|\hat{v}_1\|^2) + g_{1,\wp_1}\left\|\frac{\partial \alpha_{1,\wp_1-1}}{\partial \hat{\boldsymbol{\theta}}_2}\right\|^2 \tag{3.176}$$

.....

$$s_{i,r_i} = \bar{c}_{i,r_i}\|\boldsymbol{\psi}_{i,r_i}\|^2 + g_{i,r_i}\left\|\frac{\partial \alpha_{i,r_i-1}}{\partial \hat{\boldsymbol{\theta}}_2}\right\|^2, \quad r_i = \overline{2,\wp_i - 1},\ i = \overline{1,q} \tag{3.177}$$

$$s_{i,\wp_i} = \bar{c}_{i,\wp_i}(\|\boldsymbol{\psi}_{i,\wp_i}\|^2 + \|\boldsymbol{\beta}_i\|^2 + \|\hat{v}_i\|^2) + g_{i,\wp_i}\left\|\frac{\partial \alpha_{i,\wp_i-1}}{\partial \hat{\boldsymbol{\theta}}_2}\right\|^2 \tag{3.178}$$

Referring to the closed loop tracking error dynamics in (3.171), the stability results are summarized in the following theorem.

Theorem 3.8. *Let us consider the multi-input-multi-output(MIMO) nonlinear uncertain system described by* (3.136)-(3.137) *with unknown parameters and affected by finite number of actuator failures whose occurrence is unknown in time, pattern and magnitude. Under assumptions 3.8-3.10, the proposed adaptive controller* (3.160) *along with parameter estimates from the multiple model estimators* (3.162)-(3.163) *under the second layer of adaptation given by* $\hat{\boldsymbol{\theta}}_{\mathbf{s}} = \sum_{\mu=1}^{2m+p+1} \hat{w}_\mu \hat{\boldsymbol{\theta}}_{(\mu)}$*, the weight adaptation law* $\dot{\hat{\mathbf{w}}}$ *in* (3.170)*, renders the following closed loop properties. The maximal interval of existence of all the closed loop signals is* $[0,\infty)$.

(i) The triple $(\mathbf{z},\ \tilde{\boldsymbol{\xi}}_{\mathbf{s}},\ \tilde{\boldsymbol{\theta}}_{\mathbf{s}})$ *has stable trajectories and all other associated closed loop signals are bounded.*

(ii) The output tracking error is energy integrable, i.e., $\mathbf{z}(\mathbf{t}) \in \mathcal{L}_2[0,\infty)$ *and asymptotically converges to the origin implying* $\lim_{t\to\infty}(\mathbf{y} - \mathbf{y_r}) = \mathbf{0}$.

Proof of (i).

At the beginning, let us prove the input to state stability of the closed loop tracking error dynamics with $\tilde{\boldsymbol{\theta}}_{\mathbf{s}}$ and $\dot{\tilde{\boldsymbol{\theta}}}_{\mathbf{s}}$ as the input. From (3.171)-(3.173), we have

$$z_{i,1}\dot{z}_{i,1} = -(c_{i,1} + s_{i,1})z_{i,1}^2 + z_{i,1}z_{i,2} + z_{i,1}\boldsymbol{\psi}_{i,1}^T\tilde{\boldsymbol{\theta}}_{\mathbf{2s}} \tag{3.179}$$

$$z_{i,r_i}\dot{z}_{i,r_i} = -z_{i,r_i}z_{i,r_i-1} + z_{i,r_i}z_{i,r_i+1} - (c_{i,r_i} + s_{i,r_i})z_{i,r_i}^2 - z_{i,r_i}\boldsymbol{\psi}_{i,r_i}^T\tilde{\boldsymbol{\theta}}_{\mathbf{2s}} - z_{i,r_i}\frac{\partial \alpha_{i,r_i-1}}{\partial \hat{\boldsymbol{\theta}}_{\mathbf{2s}}}\dot{\hat{\boldsymbol{\theta}}}_{\mathbf{2s}} \tag{3.180}$$

The procedure of analysis at the $\wp_i$-th step for each of the outputs is not straightforward. Therefore, the error dynamics at this step has to be simplified to a suitable form to facilitate the Lyapunov stability analysis. For the $\wp_i$-th step for $i = \overline{1,q}$, recalling $\boldsymbol{\theta}_1^* = \hat{\boldsymbol{\theta}}_{\mathbf{1s}} + \tilde{\boldsymbol{\theta}}_{\mathbf{1s}}$, the tracking error dynamics

satisfy the following vector differential equation.

$$\mathbf{z}_{\wp}^T\dot{\mathbf{z}}_{\wp} = -\mathbf{z}_{\wp-1}^T\mathbf{z}_{\wp} - \ell^{-1}\mathbf{z}_{\wp}^T\bar{\boldsymbol{\beta}}\left(\sum_{j=1}^{m}\hat{\theta}_{1,j}N_j\right)\bar{\boldsymbol{\beta}}^{\dagger}\begin{bmatrix}(c_{1,\wp_1}+s_{1,\wp_1})z_{1,\wp_1}\\ \vdots \\ (c_{q,\wp_q}+s_{q,\wp_q})z_{q,\wp_q}\end{bmatrix} + \mathbf{z}_{\wp}^T\boldsymbol{\psi}_{\wp}^T\tilde{\boldsymbol{\theta}}_{\mathbf{2s}} + \mathbf{z}_{\wp}^T\bar{\boldsymbol{\beta}}_u\tilde{\boldsymbol{\theta}}_{\mathbf{1s}}$$
$$+ \mathbf{z}_{\wp}^T\bar{\boldsymbol{\beta}}\tilde{\boldsymbol{\theta}}_{\mathbf{3s}} - \mathbf{z}_{\wp}^T\frac{\partial\boldsymbol{\alpha}_{\wp-1}}{\partial\hat{\boldsymbol{\theta}}_{\mathbf{2s}}}\dot{\hat{\boldsymbol{\theta}}}_{\mathbf{2s}} \tag{3.181}$$

where the new term $\bar{\boldsymbol{\beta}}_u$ is defined as

$$\bar{\boldsymbol{\beta}}_u = \begin{bmatrix}\beta_{1,1}u_{H1} & \beta_{1,2}u_{H2} & \dots & \beta_{1,m}u_{Hm}\\ \dots & \dots & \vdots & \dots \\ \beta_{q,1}u_{H1} & \beta_{q,2}u_{H2} & \dots & \beta_{q,m}u_{Hm}\end{bmatrix}.$$

With the assumption that atleast q actuators must be healthy (although partial failure is allowed) and $\theta_{1,j}^*$ for $j=\overline{1,m}$ is lower bounded by $\underline{\theta}_{1,j}$, the following inequality given by $\bar{\boldsymbol{\beta}}\left(\sum_{j=1}^{m}\hat{\theta}_{j,1}N_j\right)\bar{\boldsymbol{\beta}}^{\dagger} \geq \ell I_q$ holds. Since a projection operator is used for parameter adaptation, the estimate $\hat{\theta}_{j,1}$ is always positive and does not exceed unity nor violates its lower bound. Hence equation (3.181) can be transformed into an inequality suitable for stability analysis as shown below.

$$\mathbf{z}_{\wp}^T\dot{\mathbf{z}}_{\wp} \leq -\mathbf{z}_{\wp-1}^T\mathbf{z}_{\wp} - \mathbf{z}_{\wp}^T\begin{bmatrix}(c_{1,\wp_1}+s_{1,\wp_1})z_{1,\wp_1}\\ \vdots \\ (c_{q,\wp_q}+s_{q,\wp_q})z_{q,\wp_q}\end{bmatrix} + \mathbf{z}_{\wp}^T\boldsymbol{\psi}_{\wp}^T\tilde{\boldsymbol{\theta}}_{\mathbf{2s}} + \mathbf{z}_{\wp}^T\bar{\boldsymbol{\beta}}_u\tilde{\boldsymbol{\theta}}_{\mathbf{1s}}$$
$$+ \mathbf{z}_{\wp}^T\bar{\boldsymbol{\beta}}\tilde{\boldsymbol{\theta}}_{\mathbf{3s}} - \mathbf{z}_{\wp}^T\frac{\partial\boldsymbol{\alpha}_{\wp-1}}{\partial\hat{\boldsymbol{\theta}}_{\mathbf{2s}}}\dot{\hat{\boldsymbol{\theta}}}_{\mathbf{2s}} \tag{3.182}$$

Therefore, from relation (3.182), the inequality for the tracking error variable $z_{i,\wp_i}$ for step $i.\wp_i$ $(i=\overline{1,q})$ is simplified yielding

$$z_{i,\wp_i}\dot{z}_{i,\wp_i} \leq -z_{\wp_i-1}z_{\wp_i} - (c_{i,\wp_i}+s_{i,\wp_i})z_{i,\wp_i}^2 + z_{\wp_i}\boldsymbol{\psi}_{i,\wp_i}^T\tilde{\boldsymbol{\theta}}_{\mathbf{2s}} + z_{i,\wp_i}\bar{\boldsymbol{\beta}}_u^i\tilde{\boldsymbol{\theta}}_{\mathbf{1s}}$$
$$+ z_{i,\wp_i}\boldsymbol{\beta}_i\tilde{\boldsymbol{\theta}}_{\mathbf{3s}} - z_{i,\wp_i}\frac{\partial\alpha_{i,\wp_i-1}}{\partial\hat{\boldsymbol{\theta}}_{\mathbf{2s}}}\dot{\hat{\boldsymbol{\theta}}}_{\mathbf{2s}} \tag{3.183}$$

where $\bar{\boldsymbol{\beta}}_u^i$ denotes the i-th row vector of the matrix $\bar{\boldsymbol{\beta}}_u$. Substituting $s_{i,\wp_i}$ as in (3.180) in (3.183), yields,

$$z_{i,\wp_i}\dot{z}_{i,\wp_i} \leq -z_{\wp_i-1}z_{\wp_i} - c_{i,\wp_i}z_{i,\wp_i}^2 - \bar{c}_{i,\wp_i}\left(\|\boldsymbol{\psi}_{\boldsymbol{i,\wp_i}}\|^2 z_{i,\wp_i}^2 - \frac{z_{\wp_i}\boldsymbol{\psi}_{i,\wp_i}^T\tilde{\boldsymbol{\theta}}_{\mathbf{2s}}}{\bar{c}_{i,\wp_i}}\right) - \bar{c}_{i,\wp_i}\left(\|\bar{\boldsymbol{\beta}}_u^i\|^2 z_{i,\wp_i}^2 - \frac{z_{\wp_i}\bar{\boldsymbol{\beta}}_u^i\tilde{\boldsymbol{\theta}}_{\mathbf{1s}}}{\bar{c}_{i,\wp_i}}\right)$$
$$- \bar{c}_{i,\wp_i}\left(\|\boldsymbol{\beta}_i\|^2 z_{i,\wp_i}^2 - \frac{z_{i,\wp_i}\boldsymbol{\beta}_i\tilde{\boldsymbol{\theta}}_{\mathbf{3s}}}{\bar{c}_{i,\wp_i}}\right) - g_{i,\wp_i}\left(z_{i,\wp_i}^2\left\|\frac{\partial\alpha_{i,\wp_i-1}}{\partial\hat{\boldsymbol{\theta}}_{\mathbf{2s}}}\right\|^2 - \frac{1}{g_{i,\wp_i}}\frac{\partial\alpha_{i,\wp_i-1}}{\partial\hat{\boldsymbol{\theta}}_{\mathbf{2s}}}\dot{\hat{\boldsymbol{\theta}}}_{\mathbf{2s}}\right) \tag{3.184}$$

Using the identity $-(a^2-2ab) = -(a-b)^2+b^2$ in simplifying the bracketed terms in (3.184) results in

$$\begin{aligned} z_{i,\wp_i}\dot{z}_{i,\wp_i} \leq & -z_{\wp_i-1}z_{\wp_i} - c_{i,\wp_i}z_{i,\wp_i}^2 - \bar{c}_{i,\wp_i}\left\|\boldsymbol{\psi}_{i,\wp_i}z_{i,\wp_i} - \frac{\tilde{\boldsymbol{\theta}}_{2\mathbf{s}}}{2\bar{c}_{i,\wp_i}}\right\|^2 + \frac{\|\tilde{\boldsymbol{\theta}}_{2\mathbf{s}}\|^2}{4\bar{c}_{i,\wp_i}} \\ & - \bar{c}_{i,\wp_i}\left\|\bar{\boldsymbol{\beta}}_u^{i^T}z_{i,\wp_i} - \frac{\tilde{\boldsymbol{\theta}}_{1\mathbf{s}}}{2\bar{c}_{i,\wp_i}}\right\|^2 + \frac{\|\tilde{\boldsymbol{\theta}}_{1\mathbf{s}}\|^2}{4\bar{c}_{i,\wp_i}} - \bar{c}_{i,\wp_i}\left\|\boldsymbol{\beta}_i^T z_{i,\wp_i} - \frac{\tilde{\boldsymbol{\theta}}_{3\mathbf{s}}}{2\bar{c}_{i,\wp_i}}\right\|^2 + \frac{\|\tilde{\boldsymbol{\theta}}_{3\mathbf{s}}\|^2}{4\bar{c}_{i,\wp_i}} \\ & - g_{i,\wp_i}\left\|\frac{\partial\alpha_{i,\wp_i-1}}{\partial\hat{\boldsymbol{\theta}}_{2\mathbf{s}}}^T z_{i,\wp_i} - \frac{\dot{\hat{\boldsymbol{\theta}}}_{2\mathbf{s}}}{2g_{i,\wp_i}}\right\|^2 + \frac{\|\dot{\hat{\boldsymbol{\theta}}}_{2\mathbf{s}}\|^2}{4g_{i,\wp_i}} \end{aligned} \tag{3.185}$$

$$z_{i,\wp_i}\dot{z}_{i,\wp_i} \leq -z_{\wp_i-1}z_{\wp_i} - c_{i,\wp_i}z_{i,\wp_i}^2 + \frac{1}{4}\left(\frac{\|\tilde{\boldsymbol{\theta}}_{1\mathbf{s}}\|^2}{\bar{c}_{i,\wp_i}} + \frac{\|\tilde{\boldsymbol{\theta}}_{2\mathbf{s}}\|^2}{\bar{c}_{i,\wp_i}} + \frac{\|\tilde{\boldsymbol{\theta}_{3\mathbf{s}}}\|^2}{4\bar{c}_{i,\wp_i}} + \frac{\|\dot{\hat{\boldsymbol{\theta}}}_{2\mathbf{s}}\|^2}{g_{i,\wp_i}}\right) \tag{3.186}$$

In a similar manner the following inequality can be derived.

$$z_{i,r_i}\dot{z}_{i,r_i} \leq -z_{i,r_i-1}z_{i,r_i} - c_{i,r_i}z_{i,r_i}^2 + z_{i,r_i}z_{i,r_i+1} + \frac{1}{4}\left(\frac{\|\tilde{\boldsymbol{\theta}}_{1\mathbf{s}}\|^2}{\bar{c}_{i,r_i}} + \frac{\|\tilde{\boldsymbol{\theta}}_{2\mathbf{s}}\|^2}{\bar{c}_{i,r_i}} + \frac{\|\tilde{\boldsymbol{\theta}_{3\mathbf{s}}}\|^2}{4\bar{c}_{i,r_i}} + \frac{\|\dot{\hat{\boldsymbol{\theta}}}_{2\mathbf{s}}\|^2}{g_{i,r_i}}\right) \tag{3.187}$$

Having derived the aforementioned inequalities, the ISS of tracking error dynamics is found as follows.

$$\frac{\epsilon}{2}\frac{d}{dt}\left(\mathbf{z}^T\mathbf{z}\right) = \frac{\epsilon}{2}\frac{d}{dt}\left(\sum_{i=1}^{q}\sum_{r_i=1}^{\wp_i} z_{i,r_i}^2\right) \leq -\sum_{i=1}^{q}\sum_{r_i=1}^{\wp_i-1} z_{i,r_i}\dot{z}_{i,r_i} + \sum_{i=1}^{q} z_{i,\wp_i}\dot{z}_{i,\wp_i} \tag{3.188}$$

Substituting inequalities (3.186) and (3.187) in (3.188) yields

$$\frac{\epsilon}{2}\frac{d}{dt}\left(\sum_{i=1}^{q}\sum_{r_i=1}^{\wp_i} z_{i,r_i}^2\right) \leq -\epsilon\sum_{i=1}^{q}\sum_{r_i=1}^{\wp_i-1} c_{i,r_i}z_{i,r_i}^2 + \epsilon\sum_{i=1}^{q} c_{i,\wp_i}z_{i,\wp_i}^2 + \frac{\epsilon}{4}\left(\frac{\|\tilde{\boldsymbol{\theta}}_{1\mathbf{s}}\|^2}{\bar{\bar{c}}} + \frac{\|\tilde{\boldsymbol{\theta}}_{2\mathbf{s}}\|^2}{\bar{c}} + \frac{\|\tilde{\boldsymbol{\theta}_{3\mathbf{s}}}\|^2}{4\bar{\bar{c}}} + \frac{\|\dot{\hat{\boldsymbol{\theta}}}_{2\mathbf{s}}\|^2}{\bar{g}}\right) \tag{3.189}$$

$$\leq -\epsilon\sum_{i=1}^{q}\sum_{r_i=1}^{\wp_i} c_{i,r_i}z_{i,r_i}^2 + \frac{\epsilon}{4}\left(\frac{\|\tilde{\boldsymbol{\theta}}_{\mathbf{s}}\|^2}{\breve{c}} + \frac{\|\dot{\hat{\boldsymbol{\theta}}}_{2\mathbf{s}}\|^2}{\bar{g}}\right) \tag{3.190}$$

$$\leq -2\mathscr{C}\epsilon\sum_{i=1}^{q}\sum_{r_i=1}^{\wp_i} z_{i,r_i}^2 + \frac{\epsilon}{4}\left(\frac{\|\tilde{\boldsymbol{\theta}}_{\mathbf{s}}\|^2}{\breve{c}} + \frac{\|\dot{\hat{\boldsymbol{\theta}}}_{2\mathbf{s}}\|^2}{\bar{g}}\right) \tag{3.191}$$

where $\bar{\bar{c}} = \left(\sum_{i=1}^{q}\frac{1}{\bar{c}_{i,\wp_i}}\right)^{-1}$, $\bar{c} = \left(\sum_{i=1}^{q}\sum_{r_i=1}^{\wp_i}\frac{1}{\bar{c}_{i,r_i}}\right)^{-1}$, $\bar{g} = \left(\sum_{i=1}^{q}\sum_{r_i=2}^{\wp_i}\frac{1}{\bar{g}_{i,r_i}}\right)^{-1}$, $\breve{c} = \min\{\bar{\bar{c}},\bar{c}\}$ and $\mathscr{C} = \min_{\substack{1\leq i\leq q\\ 1\leq r_i\leq\wp_i}}\{c_{i,r_i}\}$. Now from (3.191), ISS of $\mathbf{z}(t)$ depends on the boundedness of $\tilde{\boldsymbol{\theta}}_{\mathbf{s}}$ and $\dot{\hat{\boldsymbol{\theta}}}_{2\mathbf{s}}$. Thus, we now commence with the analysis of the stability properties of the adaptive estimator under the second layer of adaptation. While developing this proof, stability properties of the first layer adapted estimator stated in Theorem 3.7 will be invoked wherever their need is felt. It is to be noticed that irrespective of the system being MISO or MIMO, the structure of the prediction error dynamics is invariably the same. This implies that similar stability characteristics hold for the second layer adapted estimator proposed

herein for MIMO systems as derived in the proof of Theorem 3.5 (ii) (ineq. (3.99), (3.102)). Therefore, the estimation error dynamics at the second layer can be directly referred to from (3.84)-(3.85) and is written as,

$$\dot{\tilde{\boldsymbol{\xi}}}_{\mathbf{s}} = (\mathbf{A}_0 - \gamma \boldsymbol{\Phi}(\boldsymbol{\xi}, \mathbf{u})^T \boldsymbol{\Phi}(\boldsymbol{\xi}, \mathbf{u}) \mathbf{P}) \tilde{\boldsymbol{\xi}}_{\mathbf{s}} + \boldsymbol{\Phi}(\boldsymbol{\xi}, \mathbf{u})^T \tilde{\boldsymbol{\theta}}_{\mathbf{s}} \tag{3.192}$$

$$\dot{\tilde{\boldsymbol{\theta}}}_{\mathbf{s}} = \boldsymbol{\Gamma} \boldsymbol{\Phi}(\boldsymbol{\xi}, \mathbf{u}) \mathbf{P} \tilde{\boldsymbol{\xi}}_{\mathbf{s}} + \sum_{\mu=1}^{2m+p+1} \dot{\hat{w}}_{\mu} \hat{\boldsymbol{\theta}}_{(\mu)} \tag{3.193}$$

From Section 3.3.2.2 B, it can be directly inferred that the estimated weight vector $\hat{\mathbf{w}} \in \mathcal{L}_{\infty}[0, \infty)$ and so is its time derivative, that is, $\dot{\hat{\mathbf{w}}} \in \mathcal{L}_{\infty}[0, \infty)$. It is known that $\hat{\boldsymbol{\theta}}_{\mathbf{s}} := \sum_{\mu=1}^{p+m+2} \hat{w}_{\mu} \hat{\boldsymbol{\theta}}_{(\mu)}$ is a adaptive weighted combination of parameter estimates $\hat{\boldsymbol{\theta}}_{(\mu)}$ for $\mu = \{1, \ldots, p+m+2\}$. Owing to $\hat{\boldsymbol{\theta}}_{(\mu)} \in \mathcal{L}_{\infty}[0, \infty)$ and $\hat{\mathbf{w}} \in \mathcal{L}_{\infty}[0, \infty)$, the parameter estimation error signals are bounded, which means $\tilde{\boldsymbol{\theta}}_{\mathbf{s}} \in \mathcal{L}_{\infty}[0, \infty)$. Now in (3.193), the expression for $\dot{\tilde{\boldsymbol{\theta}}}_{\mathbf{s}}$ can be further simplified as follows.

$$\dot{\tilde{\boldsymbol{\theta}}}_{\mathbf{s}} = \boldsymbol{\Gamma} \boldsymbol{\Phi}(\boldsymbol{\xi}, \mathbf{u}) \mathbf{P} \tilde{\boldsymbol{\xi}}_{\mathbf{s}} - \sum_{\mu=1}^{p+m+1} \dot{\hat{w}}_{\mu} (\hat{\boldsymbol{\theta}}_{(p+m+2)} - \hat{\boldsymbol{\theta}}_{(\mu)}) = \boldsymbol{\Gamma} \boldsymbol{\Phi}(\boldsymbol{\xi}, \mathbf{u}) \mathbf{P} \tilde{\boldsymbol{\xi}}_{\mathbf{s}} - \dot{\hat{\tilde{\mathbf{w}}}}^T \tilde{\boldsymbol{\Theta}} \tag{3.194}$$

where the vector $\hat{\tilde{\mathbf{w}}} := [\hat{\tilde{w}}_1, \ldots, \hat{\tilde{w}}_{p+m+1}]^T$ and $\tilde{\boldsymbol{\Theta}} := [\{\hat{\boldsymbol{\theta}}_{(p+m+2)} - \hat{\boldsymbol{\theta}}_{(\mu)}\}_{\mu=1}^{p+m+1}]^T$. Considering $\mathbf{P} = \mathbf{I}_{\sum_{i=1}^{q} \wp_i}$ and using equations (3.192)-(3.194), the following is deduced.

$$\begin{aligned} \frac{d}{dt} \left(\frac{1}{2} \|\tilde{\boldsymbol{\xi}}_{\mathbf{s}}\|^2 + \frac{1}{2} \tilde{\boldsymbol{\theta}}_{\mathbf{s}}^T \boldsymbol{\Gamma}^{-1} \tilde{\boldsymbol{\theta}}_{\mathbf{s}} \right) &\leq -\tilde{\boldsymbol{\xi}}_{\mathbf{s}}^T \mathbf{Q} \tilde{\boldsymbol{\xi}}_{\mathbf{s}} - \gamma \|\boldsymbol{\Phi} \tilde{\boldsymbol{\xi}}_{\mathbf{s}}\|^2 + \underline{\lambda}(\boldsymbol{\Gamma}) \|\tilde{\boldsymbol{\theta}}_{\mathbf{s}}\| \|\dot{\hat{\tilde{\mathbf{w}}}}^T \tilde{\boldsymbol{\Theta}}\| + \underline{\lambda}(\boldsymbol{\Gamma}) \|\tilde{\boldsymbol{\theta}}_{\mathbf{s}}\| \|\dot{\boldsymbol{\theta}}^*\| \\ &\leq -\tilde{\boldsymbol{\xi}}_{\mathbf{s}}^T \mathbf{Q} \tilde{\boldsymbol{\xi}}_{\mathbf{s}} + \underline{\lambda}(\boldsymbol{\Gamma}) \|\tilde{\boldsymbol{\theta}}_{\mathbf{s}}\| \|\dot{\hat{\tilde{\mathbf{w}}}}^T \tilde{\boldsymbol{\Theta}}\| + \underline{\lambda}(\boldsymbol{\Gamma}) \|\tilde{\boldsymbol{\theta}}_{\mathbf{s}}\| \|\dot{\boldsymbol{\theta}}^*\| \end{aligned} \tag{3.195}$$

Integrating both sides of (3.194) from $t = 0 \sim \infty$ yields

$$\left(\frac{1}{2} \|\tilde{\boldsymbol{\xi}}_{\mathbf{s}}\|^2 + \frac{1}{2} \tilde{\boldsymbol{\theta}}_{\mathbf{s}}^T \boldsymbol{\Gamma}^{-1} \tilde{\boldsymbol{\theta}}_{\mathbf{s}} \right) \Bigg|_{t=0}^{t=\infty} \leq -\int_o^{\infty} \tilde{\boldsymbol{\xi}}_{\mathbf{s}}^T \mathbf{Q} \tilde{\boldsymbol{\xi}}_{\mathbf{s}} dt + \underline{\lambda}(\boldsymbol{\Gamma}) \int_0^{\infty} \|\tilde{\boldsymbol{\theta}}_{\mathbf{s}}\| \|\dot{\hat{\tilde{\mathbf{w}}}}^T \tilde{\boldsymbol{\Theta}}\| dt + \underline{\lambda}(\boldsymbol{\Gamma}) \int_0^{\infty} \|\tilde{\boldsymbol{\theta}}_{\mathbf{s}}\| \|\dot{\boldsymbol{\theta}}^*\| dt \tag{3.196}$$

Applying Hölder's inequality to the second and the third term on the RHS of (3.195) and then rearranging leads to

$$\begin{aligned} \int_o^{\infty} \|\tilde{\boldsymbol{\xi}}_{\mathbf{s}}\|^2 dt \leq \frac{1}{2\underline{\lambda}(\mathbf{Q})} \left(\|\tilde{\boldsymbol{\xi}}_{\mathbf{s}}(0)\|^2 + \tilde{\boldsymbol{\theta}}_{\mathbf{s}}^T(0) \boldsymbol{\Gamma}^{-1} \tilde{\boldsymbol{\theta}}_{\mathbf{s}}(0) \right) + \frac{\underline{\lambda}(\boldsymbol{\Gamma})}{\underline{\lambda}(\mathbf{Q})} \|\tilde{\boldsymbol{\theta}}_{\mathbf{s}}\|_{\infty} \|\tilde{\boldsymbol{\Theta}}\|_{\infty} \int_0^{\infty} \|\dot{\hat{\tilde{\mathbf{w}}}}\| dt + \\ \frac{\underline{\lambda}(\boldsymbol{\Gamma})}{\underline{\lambda}(\mathbf{Q})} \|\tilde{\boldsymbol{\theta}}_{\mathbf{s}}\|_{\infty} \int_0^{\infty} \|\dot{\boldsymbol{\theta}}^*\| dt \end{aligned} \tag{3.197}$$

From the relation $\Delta \tilde{\boldsymbol{X}}(t) \bar{\mathbf{w}}^* = \mathbf{r}(t)$, $\tilde{\bar{\mathbf{w}}} = \bar{\mathbf{w}}^* - \hat{\bar{\mathbf{w}}}$ and (3.170), the inequality in (3.197) can be further

reframed as

$$\int_o^\infty \|\tilde{\boldsymbol{\xi}}_{\mathbf{s}}\|^2 dt \leq \frac{1}{2\underline{\lambda}(\mathbf{Q})}\left(\|\tilde{\boldsymbol{\xi}}_{\mathbf{s}}(0)\|^2 + \tilde{\boldsymbol{\theta}}_{\mathbf{s}}^T(0)\boldsymbol{\Gamma}^{-1}\tilde{\boldsymbol{\theta}}_{\mathbf{s}}(0)\right) + \frac{\underline{\lambda}(\boldsymbol{\Gamma})}{\underline{\lambda}(\mathbf{Q})}\|\tilde{\boldsymbol{\theta}}_{\mathbf{s}}\|_\infty\|\tilde{\boldsymbol{\Theta}}\|_\infty \int_0^\infty \|\triangle\tilde{\boldsymbol{X}}(t)^T\triangle\tilde{\boldsymbol{X}}(t)\tilde{\mathbf{w}}\|dt+$$

$$\frac{\underline{\lambda}(\boldsymbol{\Gamma})}{\underline{\lambda}(\mathbf{Q})}\|\tilde{\boldsymbol{\theta}}_{\mathbf{s}}\|_\infty \int_0^\infty \|\dot{\boldsymbol{\theta}}^*\|dt \tag{3.198}$$

$$\leq \frac{1}{2\underline{\lambda}(\mathbf{Q})}\left(\|\tilde{\boldsymbol{\xi}}_{\mathbf{s}}(0)\|^2 + \tilde{\boldsymbol{\theta}}_{\mathbf{s}}^T(0)\boldsymbol{\Gamma}^{-1}\tilde{\boldsymbol{\theta}}_{\mathbf{s}}(0)\right) + \frac{\underline{\lambda}(\boldsymbol{\Gamma})}{\underline{\lambda}(\mathbf{Q})}\|\tilde{\boldsymbol{\theta}}_{\mathbf{s}}\|_\infty\|\tilde{\boldsymbol{\Theta}}\|_\infty\|\tilde{\mathbf{w}}\|_\infty \int_0^\infty \|\triangle\tilde{\boldsymbol{X}}(t)^T\triangle\tilde{\boldsymbol{X}}(t)\|dt+$$

$$\frac{\underline{\lambda}(\boldsymbol{\Gamma})}{\underline{\lambda}(\mathbf{Q})}\|\tilde{\boldsymbol{\theta}}_{\mathbf{s}}\|_\infty \int_0^\infty \|\dot{\boldsymbol{\theta}}^*\|dt < \infty \tag{3.199}$$

Since $\tilde{\boldsymbol{\xi}} \in \mathcal{L}_2[0,\infty) \cap \mathcal{L}_\infty[0,\infty)$, by definition, $\triangle\tilde{\boldsymbol{X}}(t) \in \mathcal{L}_2[0,\infty) \cap \mathcal{L}_\infty[0,\infty)$. Finally, the finiteness of the integral in (3.198) is concluded by invoking Assumption 3.11 and the fact that $\tilde{\boldsymbol{\theta}}_{\mathbf{s}} \in \mathcal{L}_\infty[0,\infty)$ and $\tilde{\mathbf{w}} \in \mathcal{L}_\infty[0,\infty)$. Thus, $\tilde{\boldsymbol{\xi}}_{\mathbf{s}} \in \mathcal{L}_2[0,\infty)$. Further, $\|\tilde{\boldsymbol{\xi}}_{\mathbf{s}}\|^2 \leq \|\tilde{\boldsymbol{\xi}}_{\mathbf{s}}(0)\|^2 + \tilde{\boldsymbol{\theta}}_{\mathbf{s}}^T(0)\boldsymbol{\Gamma}^{-1}\tilde{\boldsymbol{\theta}}_{\mathbf{s}}(0)$ is obvious. In view of the aforementioned arguments, the energy and absolute boundedness of $\tilde{\boldsymbol{\xi}}_{\mathbf{s}}$ is concluded, meaning $\tilde{\boldsymbol{\xi}}_{\mathbf{s}} \in \mathcal{L}_2[0,\infty) \cap \mathcal{L}_\infty[0,\infty)$. In addition, the $\mathcal{L}_2$ boundedness of $\dot{\tilde{\boldsymbol{\theta}}}_{\mathbf{s}}$ is proved as follows.
It is justified to state $\|\boldsymbol{\Phi}(\boldsymbol{\xi},\mathbf{u})\tilde{\boldsymbol{\xi}}_{\mathbf{s}}\|^2 \geq \underline{\lambda}(\boldsymbol{\Gamma}^{-2})\left(\|\dot{\tilde{\boldsymbol{\theta}}}_{\mathbf{s}}\|^2 + \|\dot{\tilde{\mathbf{w}}}^T\tilde{\boldsymbol{\Theta}}\|^2\right)$. Using this mathematical inequality, the following holds from (3.195).

$$\frac{d}{dt}\left(\frac{1}{2}\|\tilde{\boldsymbol{\xi}}_{\mathbf{s}}\|^2 + \frac{1}{2}\tilde{\boldsymbol{\theta}}_{\mathbf{s}}^T\boldsymbol{\Gamma}^{-1}\tilde{\boldsymbol{\theta}}_{\mathbf{s}}\right) \leq -\gamma\underline{\lambda}(\boldsymbol{\Gamma}^{-2})\left(\|\dot{\tilde{\boldsymbol{\theta}}}_{\mathbf{s}}\|^2 + \|\dot{\tilde{\mathbf{w}}}\tilde{\boldsymbol{\Theta}}\|^2\right) + \underline{\lambda}(\boldsymbol{\Gamma})\|\tilde{\boldsymbol{\theta}}_{\mathbf{s}}\|\|\dot{\tilde{\mathbf{w}}}\tilde{\boldsymbol{\Theta}}\| + \underline{\lambda}(\boldsymbol{\Gamma})\|\tilde{\boldsymbol{\theta}}_{\mathbf{s}}\|\|\dot{\boldsymbol{\theta}}^*\| \tag{3.200}$$

$$\leq -\gamma\underline{\lambda}(\boldsymbol{\Gamma}^{-2})\left(\|\dot{\tilde{\boldsymbol{\theta}}}_{\mathbf{s}}\|^2 + \|\dot{\tilde{\mathbf{w}}}\tilde{\boldsymbol{\Theta}}\|^2\right) + \underline{\lambda}(\boldsymbol{\Gamma})\|\tilde{\boldsymbol{\theta}}_{\mathbf{s}}\|\|\dot{\boldsymbol{\theta}}^*\| + \underline{\lambda}(\boldsymbol{\Gamma})\|\tilde{\boldsymbol{\theta}}_{\mathbf{s}}\|\|\triangle\tilde{\boldsymbol{X}}(t)^T\triangle\tilde{\boldsymbol{X}}(t)\|\|\tilde{\mathbf{w}}\|\|\tilde{\boldsymbol{\Theta}}\| \tag{3.201}$$

Integrating the above inequality over $t = 0 \sim \infty$ and simultaneous application of the Hölder's inequality to the resulting integrals yield

$$\int_0^\infty \|\dot{\tilde{\boldsymbol{\theta}}}_{\mathbf{s}}\|^2 dt \leq \frac{1}{2\gamma\underline{\lambda}(\boldsymbol{\Gamma}^{-2})}\left(\|\tilde{\boldsymbol{\xi}}_{\mathbf{s}}(0)\|^2 + \tilde{\boldsymbol{\theta}}_{\mathbf{s}}(0)^T\boldsymbol{\Gamma}^{-1}\tilde{\boldsymbol{\theta}}_{\mathbf{s}}(0)\right) + \frac{\underline{\lambda}(\boldsymbol{\Gamma})}{\gamma\underline{\lambda}(\boldsymbol{\Gamma}^{-2})}\|\tilde{\boldsymbol{\theta}}_{\mathbf{s}}\|_\infty \int_0^\infty \|\dot{\boldsymbol{\theta}}^*\|dt$$

$$+ \frac{\underline{\lambda}(\boldsymbol{\Gamma})\|\tilde{\boldsymbol{\theta}}_{\mathbf{s}}\|_\infty\|\tilde{\mathbf{w}}\|_\infty\|\tilde{\boldsymbol{\Theta}}\|_\infty}{\gamma\underline{\lambda}(\boldsymbol{\Gamma}^{-2})} \int_0^\infty \|\triangle\tilde{\boldsymbol{X}}(t)^T\triangle\tilde{\boldsymbol{X}}(t)\|dt \tag{3.202}$$

The RHS of the above inequality (3.202) is finite since $\dot{\boldsymbol{\theta}}^* \in \mathcal{L}_1[0,\infty)$ and $\tilde{\boldsymbol{\xi}} \in \mathcal{L}_2[0,\infty) \cap \mathcal{L}_\infty[0,\infty)$ implying $\tilde{\boldsymbol{X}}(t) \in \mathcal{L}_2[0,\infty)$. Thus, the energy boundedness of $\dot{\tilde{\boldsymbol{\theta}}}_{\mathbf{s}}$ is proved from (3.202).
Finally, as $\tilde{\boldsymbol{\theta}}_{\mathbf{s}} \in \mathcal{L}_\infty[0,\infty)$ and $\dot{\tilde{\boldsymbol{\theta}}}_{\mathbf{s}} \in \mathcal{L}_2[0,\infty)$ is proved, invoking inequality (3.191), the tracking error

$z(t)$ is shown to be upper bounded from its solution

$$\|z(t)\| \leq \|z(0)\|e^{-\mathscr{C}t} + \frac{1}{2\sqrt{\mathscr{C}}}\left(\frac{\|\tilde{\boldsymbol{\theta}}_{\mathbf{s}}\|_{\infty}^{2}}{\breve{c}} + \frac{\|\dot{\hat{\boldsymbol{\theta}}}_{2\mathbf{s}}\|_{2}^{2}}{\bar{g}}\right)^{\frac{1}{2}} \tag{3.203}$$

Therefore, the ISS of the tracking error dynamics in $z(t)$ with respect to $\tilde{\boldsymbol{\theta}}_{\mathbf{s}}$ and $\dot{\hat{\boldsymbol{\theta}}}_{\mathbf{s}}$ as the inputs is proved from (3.203). The proof of Claim (i) is complete. The triple $(\mathbf{z}, \tilde{\boldsymbol{\xi}}_{\mathbf{s}}, \tilde{\boldsymbol{\theta}}_{\mathbf{s}}) \in \mathcal{L}_{\infty}[0,\infty)$. □

Proof of (ii).

To proceed with the proof of Claim (ii), the closed loop tracking error dynamics is rewritten as,

$$\dot{\mathbf{z}}(t) = \bar{\boldsymbol{\mathcal{A}}}_{\mathbf{z}}(\mathbf{z}, \hat{\boldsymbol{\theta}}_{\mathbf{s}}, t)\mathbf{z}(t) + \bar{\mathbf{B}}_{\boldsymbol{\theta}^{*}}(\mathbf{z}, \hat{\boldsymbol{\theta}}_{\mathbf{s}}, t)\tilde{\boldsymbol{\theta}}_{\mathbf{s}} + \mathbf{B}_{\dot{\hat{\boldsymbol{\theta}}}_{2}}(\mathbf{z}, \hat{\boldsymbol{\theta}}_{\mathbf{s}}, t)\dot{\hat{\boldsymbol{\theta}}}_{2\mathbf{s}} \tag{3.204}$$

where the matrices are defined in (3.207)-(3.208). Thereafter, it is be noted that the matrix $\mathbf{B}_{\tilde{\boldsymbol{\theta}}}$ can be factorized as $\mathbf{B}_{\tilde{\boldsymbol{\theta}}} = \boldsymbol{\mathcal{M}}\boldsymbol{\Phi}^{T}(\boldsymbol{\xi}, \mathbf{u})$. Where, the matrix $\boldsymbol{\mathcal{M}}$ is calculated to be

$$\boldsymbol{\mathcal{M}} = \left[\begin{array}{ccccc}
1 & 0 & 0 & \dots & 0 \\
\vdots & \vdots & \vdots & \ddots & \vdots \\
1 & 0 & 0 & \dots & 0 \\
\hline
-\dfrac{\partial \alpha_{1,1}}{\partial \xi_{1,1}} & 1 & 0 & \dots & 0 \\
\vdots & \vdots & \vdots & \ddots & \vdots \\
-\dfrac{\partial \alpha_{q,1}}{\partial \xi_{q,1}} & 1 & 0 & \dots & 0 \\
\hline
\dots & \dots & \dots & \dots & \dots \\
\hline
-\dfrac{\partial \alpha_{1,\wp_1-2}}{\partial \xi_{1,1}} & \dots & -\dfrac{\partial \alpha_{1,\wp_1-2}}{\partial \xi_{1,\wp_1-2}} & 1 & 0 \\
\vdots & \vdots & \vdots & \ddots & \vdots \\
-\dfrac{\partial \alpha_{q,\wp_q-2}}{\partial \xi_{q,1}} & \dots & -\dfrac{\partial \alpha_{q,\wp_q-2}}{\partial \xi_{q,\wp_q-2}} & 1 & 0 \\
\hline
-\dfrac{\partial \alpha_{1,\wp_1-1}}{\partial \xi_{1,1}} & -\dfrac{\partial \alpha_{1,\wp_1-1}}{\partial \xi_{1,2}} & \dots & -\dfrac{\partial \alpha_{1,\wp_1-1}}{\partial \xi_{1,\wp_1-1}} & 1 \\
\vdots & \vdots & \ddots & \ddots & \vdots \\
-\dfrac{\partial \alpha_{q,\wp_q-1}}{\partial \xi_{q,1}} & -\dfrac{\partial \alpha_{q,\wp_q-1}}{\partial \xi_{q,2}} & \dots & -\dfrac{\partial \alpha_{q,\wp_q-1}}{\partial \xi_{q,\wp_q-1}} & 1
\end{array}\right] \tag{3.205}$$

Secondly, to facilitate the proof procedure an auxiliary state variable is defined as, $\boldsymbol{\vartheta} := \mathbf{z} - \boldsymbol{\mathcal{M}}\tilde{\boldsymbol{\xi}}_{\mathbf{s}}$. Its subsequent dynamics is derived to be

$$\dot{\boldsymbol{\vartheta}} = \bar{\boldsymbol{\mathcal{A}}}_{\mathbf{z}}\boldsymbol{\vartheta} + \underbrace{[-\dot{\boldsymbol{\mathcal{M}}} + \bar{\boldsymbol{\mathcal{A}}}_{\mathbf{z}}\boldsymbol{\mathcal{M}} - \boldsymbol{\mathcal{M}}(\mathbf{A}_0 - \gamma\boldsymbol{\Phi}^{T}\boldsymbol{\Phi}\mathbf{P})]}_{\widehat{\boldsymbol{\mathcal{M}}}}\tilde{\boldsymbol{\xi}}_{\mathbf{s}} + \mathbf{B}_{\dot{\hat{\boldsymbol{\theta}}}_{2}}(\mathbf{z}, \hat{\boldsymbol{\theta}}_{\mathbf{s}}, t)\dot{\hat{\boldsymbol{\theta}}}_{2\mathbf{s}}. \tag{3.206}$$

$$\bar{\mathcal{A}}_{\boldsymbol{z}} := \left[\begin{array}{cccc|cccc|cccc|c|cccc} -a_{11} & 0 & \dots & 0 & 1 & 0 & \dots & 0 & 0 & 0 & \dots & 0 & & 0 & 0 & \dots & 0 \\ 0 & -a_{21} & \dots & 0 & 0 & 1 & \dots & 0 & 0 & 0 & \dots & 0 & & 0 & 0 & \dots & 0 \\ \vdots & \ddots & \ddots & \vdots & \vdots & \ddots & \ddots & \vdots & \vdots & \ddots & \ddots & \vdots & \cdots & \vdots & \ddots & \ddots & \vdots \\ 0 & \dots & \dots & -a_{q1} & 0 & \dots & \dots & 1 & 0 & \dots & \dots & 0 & & 0 & \dots & \dots & 0 \\ \hline -1 & 0 & \dots & 0 & -a_{12} & 0 & \dots & 0 & 1 & 0 & \dots & 0 & & 0 & 0 & \dots & 0 \\ 0 & -1 & \dots & 0 & 0 & -a_{22} & \dots & 0 & 0 & 1 & \dots & 0 & & 0 & 0 & \dots & 0 \\ \vdots & \ddots & \ddots & \vdots & \vdots & \ddots & \ddots & \vdots & \vdots & \ddots & \ddots & \vdots & \cdots & \vdots & \ddots & \ddots & \vdots \\ 0 & \dots & \dots & -1 & 0 & \dots & \dots & -a_{q2} & 0 & \dots & \dots & 1 & & 0 & \dots & \dots & 0 \\ \hline & \vdots & & & & \ddots & & & & \ddots & & & \ddots & & \vdots & & \\ & \vdots & & & & \ddots & & & & \ddots & & & \ddots & & \vdots & & \\ \hline & \vdots & & & & \ddots & & & & \ddots & & & \ddots & 1 & 0 & \dots & 0 \\ & \vdots & & & & \ddots & & & & \ddots & & & \ddots & 0 & 1 & \dots & 0 \\ & & & & & & & & & & & & & \vdots & \ddots & \ddots & \vdots \\ & & & & & & & & & & & & & 0 & \dots & \dots & 1 \\ \hline 0 & 0 & \dots & 0 & 0 & 0 & \dots & 0 & & & & & -1 & 0 & \dots & 0 & \\ 0 & 0 & \dots & 0 & 0 & 0 & \dots & 0 & & & \dots & & 0 & -1 & \dots & 0 & -\frac{\bar{\boldsymbol{\beta}}\sum_j \hat{\theta}_{1,j} N_j \bar{\boldsymbol{\beta}}^\dagger}{\ell} \begin{pmatrix} a_{1\wp_1} & \dots & 0 \\ \vdots & \ddots & \vdots \\ 0 & \dots & a_{q\wp_q} \end{pmatrix} \\ \vdots & \ddots & \ddots & \vdots & \vdots & \ddots & \ddots & \vdots & & & & & \vdots & \ddots & \ddots & \vdots & \\ 0 & \dots & \dots & 0 & 0 & \dots & \dots & 0 & & & & & 0 & \dots & \dots & -1 & \end{array}\right] \tag{3.207}$$

$$\bar{\mathbf{B}}_{\boldsymbol{\theta}^*} := \left[\begin{array}{ccc|c|ccc} 0 & 0 & \dots & 0 & & 0 & 0 & \dots & 0 \\ 0 & 0 & \dots & 0 & \boldsymbol{\psi}_{1,1}^T & 0 & 0 & \dots & 0 \\ \vdots & \ddots & \ddots & \vdots & \vdots & \vdots & \ddots & \ddots & \vdots \\ 0 & \dots & \dots & 0 & \boldsymbol{\psi}_{q,1}^T & 0 & \dots & \dots & 0 \\ \hline & \vdots & & \vdots & & & \vdots & & \\ \hline \beta_{1,1}u_{H1} & \dots & \beta_{1,m}u_{Hm} & \boldsymbol{\psi}_{1,\wp_1}^T & & \beta_{1,1} & \dots & \beta_{1,m} \\ \vdots & \ddots & \vdots & \vdots & & \vdots & \ddots & \vdots \\ \beta_{q,1}u_{H1} & \dots & \beta_{q,m}u_{Hm} & \boldsymbol{\psi}_{q,\wp_q}^T & & \beta_{q,1} & \dots & \beta_{q,m} \end{array}\right] \tag{3.208}$$

With the auxiliary error dynamics in (3.206), what remains is to prove the $\mathcal{L}_2$-integrability of the auxiliary variable $\boldsymbol{\vartheta}$. This would essentially lead us to proving $z(t) \in \mathcal{L}_2[0,\infty)$. In view of this objective, we compute the following.

$$\begin{aligned}\frac{d}{dt}\left(\frac{1}{2}\|\boldsymbol{\vartheta}\|^2\right) &\leq \boldsymbol{\vartheta}^T\bar{\boldsymbol{\mathcal{A}}}_{\mathbf{z}}\boldsymbol{\vartheta} + \boldsymbol{\vartheta}\widehat{\boldsymbol{\mathcal{M}}}\tilde{\boldsymbol{\xi}}_{\mathbf{s}} + \boldsymbol{\vartheta}^T\mathbf{B}_{\hat{\boldsymbol{\theta}}_2}\dot{\hat{\boldsymbol{\theta}}}_{2\mathbf{s}} \\ &\leq -\mathscr{C}\|\boldsymbol{\vartheta}\|^2 - \sum_{i=1}^{q}\sum_{r_i=2}^{\wp_i} g_{i,r_i}\left\|\frac{\partial\alpha_{i,r_i-1}}{\partial\hat{\boldsymbol{\theta}}_{2\mathbf{s}}}\right\|^2\vartheta_{i,r_i}^2 + \sum_{i=1}^{q}\sum_{r_i=2}^{\wp_i}\frac{\partial\alpha_{i,r_i-1}}{\partial\hat{\boldsymbol{\theta}}_{2\mathbf{s}}}\dot{\hat{\boldsymbol{\theta}}}_{2\mathbf{s}}\vartheta_{i,r_i} + \boldsymbol{\vartheta}^T\widehat{\boldsymbol{\mathcal{M}}}\tilde{\boldsymbol{\xi}}_{\mathbf{s}} \\ &\leq -\mathscr{C}\|\boldsymbol{\vartheta}\|^2 + \frac{\|\dot{\hat{\boldsymbol{\theta}}}_{2\mathbf{s}}\|^2}{4\bar{g}} + \boldsymbol{\vartheta}^T\widehat{\boldsymbol{\mathcal{M}}}\tilde{\boldsymbol{\xi}}_{\mathbf{s}} \end{aligned} \tag{3.209}$$

Applying Peter-Paul inequality to the third term in (3.209) with the factor $\mathscr{C}$ results in

$$\boldsymbol{\vartheta}^T\widehat{\boldsymbol{\mathcal{M}}}\tilde{\boldsymbol{\xi}}_{\mathbf{s}} \leq \mathscr{C}\frac{\|\boldsymbol{\vartheta}\|^2}{2} + \frac{1}{2\mathscr{C}}\|\widehat{\boldsymbol{\mathcal{M}}}\|_{\mathscr{F}}^2\|\tilde{\boldsymbol{\xi}}_{\mathbf{s}}\|^2 \tag{3.210}$$

Substituting RHS of the inequality (3.210) in (3.209) yields

$$\frac{d}{dt}\left(\frac{1}{2}\|\boldsymbol{\vartheta}\|^2\right) \leq -\frac{\mathscr{C}}{2}\|\boldsymbol{\vartheta}\|^2 + \frac{\|\dot{\hat{\boldsymbol{\theta}}}_{2\mathbf{s}}\|^2}{4\bar{g}} + \frac{\|\widehat{\boldsymbol{\mathcal{M}}}\|_{\mathscr{F}}^2\|\tilde{\boldsymbol{\xi}}_{\mathbf{s}}\|^2}{2\mathscr{C}} \tag{3.211}$$

Since, all the closed loop signals are bounded, it is justified to infer that $\boldsymbol{\mathcal{M}}$, $\dot{\boldsymbol{\mathcal{M}}}$, $\bar{\boldsymbol{\mathcal{A}}}_{\mathbf{z}}$ and $(\mathbf{A}_0 - \gamma\boldsymbol{\Phi}^T\boldsymbol{\Phi}\mathbf{P})$ are bounded. Thus, the matrix $\widehat{\boldsymbol{\mathcal{M}}}$ is bounded. The following integral if proved to be finite would imply the energy integrability of $\boldsymbol{\vartheta}$.

$$\int_0^\infty\|\boldsymbol{\vartheta}\|^2dt \leq \frac{\|\boldsymbol{\vartheta}(0)\|^2}{2\mathscr{C}} + \frac{1}{4\bar{g}\mathscr{C}}\int_0^\infty\|\dot{\hat{\boldsymbol{\theta}}}_{2\mathbf{s}}\|^2dt + \frac{\|\widehat{\boldsymbol{\mathcal{M}}}\|_{\mathscr{F}}^2}{2\mathscr{C}^2}\int_0^\infty\|\tilde{\boldsymbol{\xi}}_{\mathbf{s}}\|^2dt \tag{3.212}$$

Owing to the following properties, that is, $\dot{\hat{\boldsymbol{\theta}}}_{2\mathbf{s}}$, $\tilde{\boldsymbol{\xi}}_{\mathbf{s}} \in \mathcal{L}_2[0,\infty)$, the above integral (3.212) is finite. Thus, $\boldsymbol{\vartheta} \in \mathcal{L}_2[0,\infty)$ follows. With this result, the tracking error $\mathbf{z}(t) \in \mathcal{L}_2[0,\infty)$ is concluded from its definition as $\mathbf{z} = \boldsymbol{\vartheta} + \boldsymbol{\mathcal{M}}\tilde{\boldsymbol{\xi}}_{\mathbf{s}}$.
Since. $\mathbf{z}(t) \in \mathcal{L}_2[0,\infty) \cap \mathcal{L}_\infty[0,\infty)$ and $\dot{\mathbf{z}}(t) \in \mathcal{L}_\infty[0,\infty)$, invoking Barbalat's Lemma [122], the asymptotic stability of $\mathbf{z}(t) = 0$ is proved. The proof is complete. □

3.3.4 Simulation Study

In this section, simulation results for a coupled mass-spring-damper system are considered to demonstrate the effectiveness of the proposed adaptive FTC methodology using multiple models. The mass-spring-damper system taken into consideration is depicted in Figure (3.13) and it essentially characterizes a nonlinear coupled MIMO dynamical system. In fact, these type of systems essentially coexist in large scale systems, for instance, in active vehicle suspension (AVS) systems . AVS technologies embedded in a car renders high ride quality and car handling by keeping the tires perpendicular to the road in corners, ensuring better road hold, traction and control. An automobile embedded

with AVS eliminates body roll and pitch variation during turning at medium/high speeds, cornering, accelerating, and braking. Assuming that the AVS has actuation redundancy , the actuators may be partially effective under unanticipated situations and also some of the actuators may totally fail. If left unattended with no corrective action, such failures unknown in time and magnitude would culminate to severe accidents. To deal with these situations, the AVS must be equipped with an FTC module. Hence, the suitability of a mass-spring-damper system as a benchmark example to illustrate the prolific features of the proposed adaptive FTC methodology is justified.

Prior to control design, dynamical modeling of the system is necessary. The equations of motion for the concerned mass-spring-damper system are expressed as vector differential equations as

$$\mathbf{M}(\boldsymbol{y},\dot{\boldsymbol{y}})\ddot{\boldsymbol{y}} + \mathbf{F_B}(\boldsymbol{y},\dot{\boldsymbol{y}})\dot{\boldsymbol{y}} + \mathbf{F_K}(\boldsymbol{y}) = \mathbf{u}(t) + \mathbf{d}(t). \tag{3.213}$$

where $\mathbf{F_B} := \begin{bmatrix} 4.2 + 0.05\dot{y}_1 & -2.2 + 0.3\dot{y}_1 - 0.15\dot{y}_2 \\ 2 + 0.2\dot{y}_1 & 0 \end{bmatrix}$ and $\mathbf{F_K} := \begin{bmatrix} k_{10}y_1 + k_{11}y_1^3 \\ k_{20}(y_2 - y_1) + k_{21}(y_2 - y_1)^3 \end{bmatrix}$ represent the matrices related to friction forces and the spring forces, respectively. The control inputs are defined by $\mathbf{u} = [u_1,\ u_2]^T$ and the unknown exogenous disturbance is given by $\mathbf{d} = [d_1,\ d_2]^T$. The matrix $\mathbf{M}(\boldsymbol{y},\dot{\boldsymbol{y}}) := \text{diag}\{m_1,\ m_2\} \in \mathbb{R}^{2\times 2}$ defines the inertia of the system. Further, the parameters of the system are totally unknown to the control designer. The output vector of the system is denoted by $\boldsymbol{y} = [y_1,\ y_2]^T$. For simulations, the values of unknown parameters are assumed to be $m_1 = 0.25$ kg, $m_2 = 0.2$ kg, $k_{10} = 1$ N/m, $k_{11} = 0.1$ N/m, $k_{20} = 2$ N/m and $k_{21} = 0.12$ N/m. As had been mentioned earlier, the system considered exhibits strong output coupling and also captures the nonlinearities of the spring as well as damping through the nonlinear terms. The system has two outputs driven by two inputs, hence the case of total actuator failure has not been considered in this example, to satisfy the design assumptions. We show the effectiveness of the proposed FTC approach in improving the start up and post fault transient/steady state performances in the event of partial loss of effectiveness of each of the actuators. Further, such improvements are obtained without any substantial increment in the input usage when compared to single model adaptive control and modular backstepping control [6].

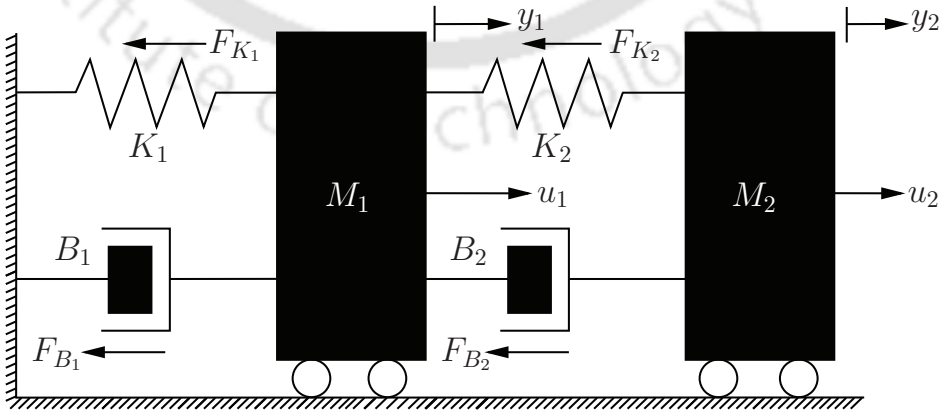

Figure 3.13: Schematic diagram of a coupled mass-spring-damper system

In simulations, the actuator failure occurs as per the following piecewise definition.

$$u_1(t) = \begin{cases} 0.5u_{H1}, & t \geq 30s \\ u_{H1}, & \text{otherwise} \end{cases} \tag{3.214}$$

$$u_2(t) = \begin{cases} 0.5u_{H2}, & t \geq 60s \\ u_{H2}, & \text{otherwise} \end{cases} \tag{3.215}$$

The reference trajectories to be tracked by the system outputs y_1 and y_2 are given by $y_{r,1} = 0.2\sin(0.5t)$ and $y_{r,2} = 0.5\sin(0.5t)$. The relative degree of the system with respect to each of the outputs is found to be $\wp_1 = \wp_2 = 2$. In order to translate the proposed control design procedure, let us first choose the state variables as $\xi_{1,1} = y_1$, $\xi_{2,1} = y_2$, $\xi_{1,2} = \dot{y}_1$ and $\xi_{2,2} = \dot{y}_2$ such that $\boldsymbol{\xi}_1 := [\xi_{1,1}, \xi_{2,1}]^T$ and $\boldsymbol{\xi}_2 := [\xi_{1,2}, \xi_{2,2}]^T$. With this choice of states, the state vector $\boldsymbol{\xi} := [\boldsymbol{\xi}_1,\ \boldsymbol{\xi}_2]$ and the partial actuator failure model, the entire dynamical system is rewritten as

$$\dot{\boldsymbol{\xi}}_1 = \boldsymbol{\xi}_2 \tag{3.216}$$

$$\dot{\boldsymbol{\xi}}_2 = \boldsymbol{\varphi}^T\boldsymbol{\theta}_2^* + \sum_{j=1}^{2}\theta_{1,j}^* N_j \mathbf{u}_H. \tag{3.217}$$

Where $\boldsymbol{\varphi}^T := [\text{diag}\{\boldsymbol{\varphi}_{1,2}^T,\ \boldsymbol{\varphi}_{2,2}^T\}]^T$ and $\mathbf{u}_H = [u_{H1},\ u_{H2}]^T$. The regressor matrices are defined as $\boldsymbol{\varphi}_{1,2} := [-\xi_{1,1},\ -\xi_{1,1}^3,\ -\xi_{1,2},\ -\xi_{1,2}^2,\ (\xi_{2,2} - \xi_{1,2}),\ (\xi_{2,2} - \xi_{1,2})^2]^T$ and $\boldsymbol{\varphi}_{2,2} := [-(\xi_{2,1} - \xi_{1,1}),\ -(\xi_{2,1} - \xi_{1,1})^3,\ -\xi_{1,2},\ -\xi_{1,2}^2]^T$. Further, the estimation model for the considered nonlinear dynamical system (3.213) is framed as

$$\dot{\boldsymbol{\xi}} = \begin{bmatrix} \xi_{1,2} \\ \xi_{2,2} \\ 0 \\ 0 \end{bmatrix} + \underbrace{\left[\begin{array}{c|c|c|c} 0 & \mathbf{0}_{1\times 6} & 0 & \mathbf{0}_{1\times 4} \\ 0 & \mathbf{0}_{1\times 6} & 0 & \mathbf{0}_{1\times 4} \\ u_{H1} & \boldsymbol{\varphi}_{1,2}^T & 0 & \mathbf{0}_{1\times 4} \\ \mathbf{0}_{1\times 9} & \mathbf{0}_{1\times 6} & u_{H2} & \boldsymbol{\varphi}_{2,2}^T \end{array}\right]}_{\boldsymbol{\Phi}^T} \boldsymbol{\theta}^*. \tag{3.218}$$

Herein $\boldsymbol{\theta}^* := [\theta_{1,1}^*, \theta_{2,1}^*, \ldots, \theta_{2,6}^*, \theta_{1,2}, \theta_{2,7}, \ldots, \theta_{2,10}]^T$. The adaptive controller is thereafter developed in accordance with (3.160). Whereas the unknown parameter vector $\boldsymbol{\theta}^*$ is estimated using (3.162)-(3.163) followed by the second layer adaptation. The total number of unknown parameters is 12. Hence, as per the proposed design, the number of identification models to be considered is $N = 13$ to satisfy the conditions of a convex hull. In simulations, the initial conditions of the system are $\boldsymbol{\xi}(0) = [0, 0, 0, 0]^T$. The controller gains are selected as, $c_{1,1} = 15$, $c_{1,2} = c_{2,1} = c_{2,2} = 5$ and the damping factors as, $\bar{c}_{1,2} = \bar{c}_{2,2} = 5$. The matrices $\mathbf{A}_{\mu 0} = [\text{diag}\{-14, -14, -16, -16\}]$ and $\gamma = 2$ are chosen to be the same for all μ identification models; however with different initial parameter estimates. Lastly, the adaptive rate matrix for the parameter update law is considered to be $\Gamma_\mu = 20\mathbf{I}_{12}$.

The strongly coupled mass-spring-damper system with unknown parametric uncertainties was simulated in MATLAB. To illustrate the robustness of the proposed AMMFTC scheme to actuator failures, the system is deliberately subjected to abrupt and unknown actuator faults consistent with equations

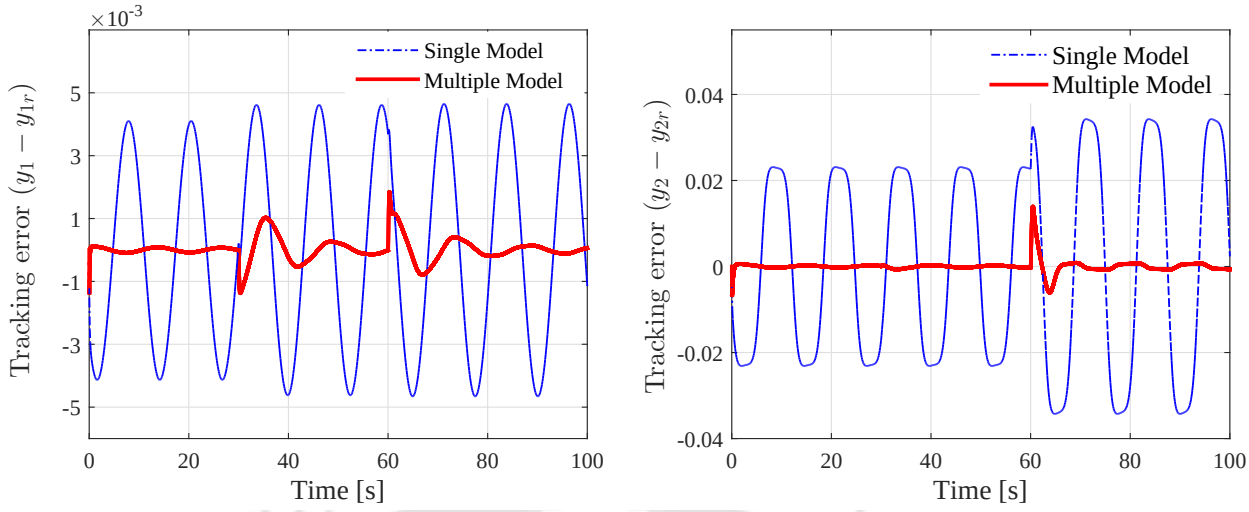

(a) (b)

Figure 3.14: (a) Tracking error comparison in displacement output y_1;(b) Tracking error comparison in displacement output y_2; using the proposed adaptive FTC using multiple models and under a single model adaptive FTC strategy.

(3.214)-(4.174). The simulation results obtained are depicted in Figures 3.16-3.15. As claimed in our theoretical developments, stability of the closed loop system is evident from the time evolution of the outputs y_1, y_2 and their respective velocity profiles $\dot{y}_1$ and $\dot{y}_2$ in Figure 3.15 for all time even inspite of occurrence of unknown faults at $t = 30$s and $t = 60$s. As can be observed from Figure 3.15(c), the control inputs u_1 and u_2 are also bounded. A comparison of output tracking errors and control inputs obtained using the proposed AMM(Adaptive Multiple Model) FTC strategy and single identification model based adaptive control are provided in Figure 3.16 and Figure 3.15(c)-(d) to further substantiate our theoretical claims.

Strong output and input interactions between y_1- subsystem and y_2-subsystem allow the propaga-

Table 3.3: Tabular comparison of output and input performances under proposed AMMFTC and adaptive FTC using a single identification model

Control Schemes	**Output Performance metrics**				**Input Performance metrics**			
	ITAE		**RMSE**		**Control Energy**		**Total Variation**	
	y_1	y_2	y_1	y_2	u_1	u_2	u_1	u_2
Multiple Models	**1.1727**	**3.5234**	**0.00036**	**0.0015**	285.26	637.09	14.85	29.04
Single Model	13.01	116.66	0.0028	0.0231	285.26	573.73	14.20	27.04

tion of adverse effects of actuator faults occurring in any of the subsystems to the other. These are widely known as cross coupling effects. In addition to the accommodation of uncertain and unknown actuator faults, these cross coupling effects should also be minimized which otherwise may jeopardize the stability of the system. In this simulation study, the system has been so considered that fault induced perturbations and subsystem interactions are categorically placed under the same class of

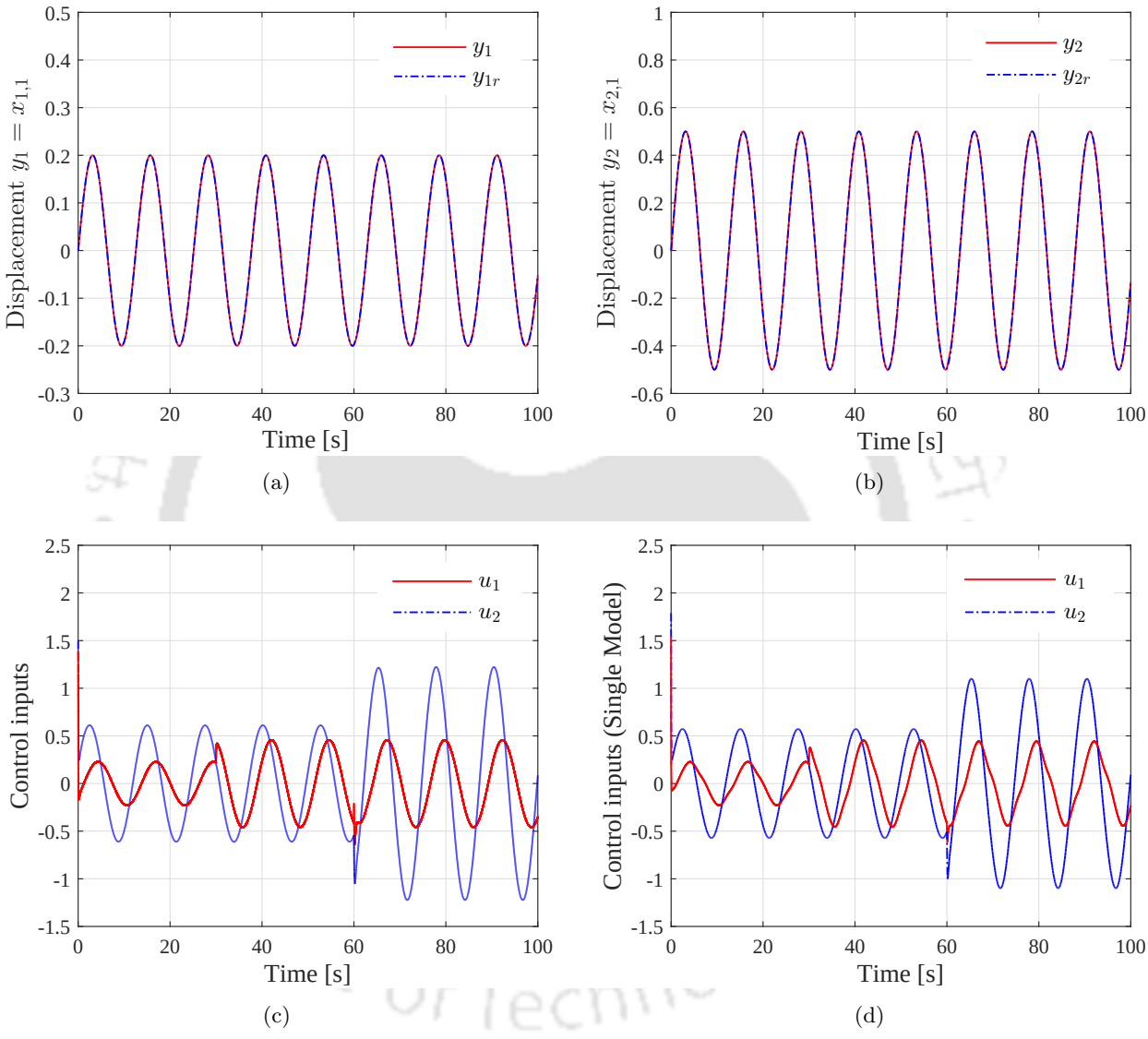

Figure 3.15: (a) Time evolution of $y_1(t)$ under the proposed adaptive FTC using multiple models;(b) Time evolution of $y_2(t)$ under the proposed adaptive FTC using multiple models;(c) Control inputs u_1 and u_2 under the proposed FTC scheme using multiple models; (d) Control inputs u_1 and u_2 under adaptive FTC scheme using a single model.

uncertainties affecting system performance. Therefore, improvement of transient performance in terms of $\mathcal{L}_\infty$ bounds at start up and post fault scenarios in both the outputs would definitely reflect better mitigation of coupling effects. The tracking error comparison in Figure 3.16 demonstrate superior transient and steady state performance as claimed in theory over single model adaptive FTC; besides achieving substantial alleviation of coupling effects. The output tracking error performance in both the outputs, that is, displacements of masses m_1 and m_2 denoted by y_1 and y_2 is indeed promising. On the contrary, as evident from Figures 3.16-3.15, the single model adaptive FTC suffers from a fairly unsatisfactory output tracking while its multiple model counterpart shows remarkable performance without any considerable increase in the control usage. Furthermore, the output tracking performance and the extent of control usage or rather the input energy spent under the proposed control and its single model equivalent, are quantified in terms of relevant and suitable performance metrics in Table 3.3 . Thereafter, as an added testament to our claims, a tabular comparison of such calculated input and output performances are drawn. In fact, as anticipated, the comparison reverberates the prolific features of the proposed adaptive FTC methodology.

3.3.5 Experimental Study on a Twin Rotor MIMO System

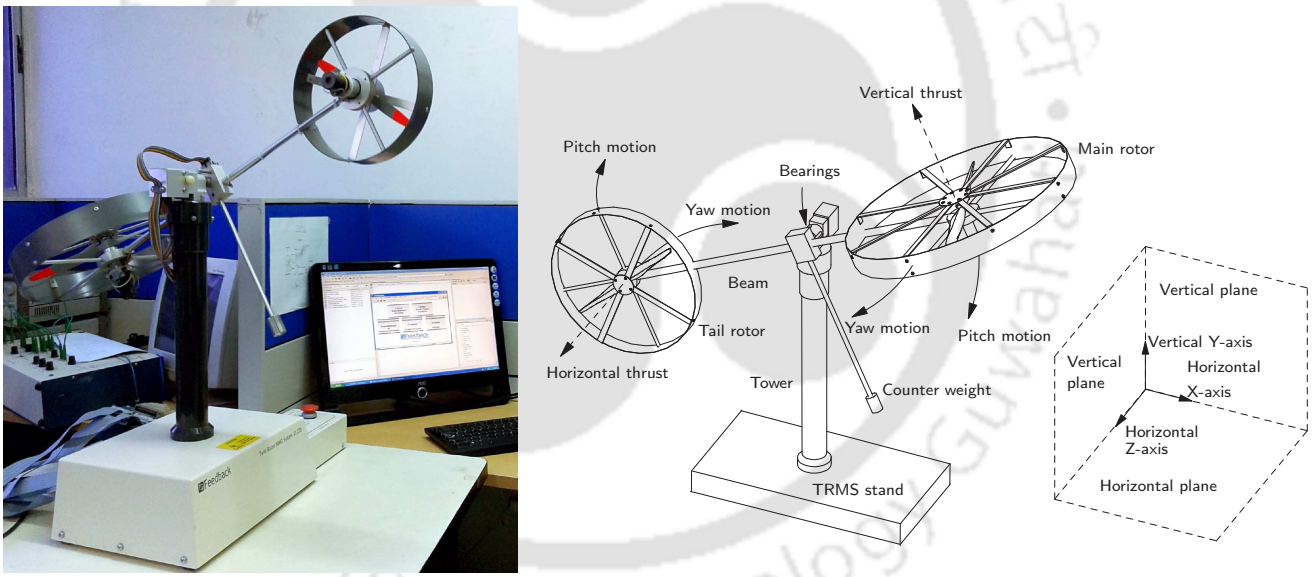

(a) (b)

Figure 3.16: (a) The experimental setup of a twin rotor MIMO system (TRMS) emulating a 2-DOF helicopter; (b) Schematic physical description of the twin rotor MIMO system (TRMS).

To validate the real time applicability of the proposed adaptive controller, it was applied to the problem of attitude control in a 2DOF helicopter experimental prototype in the laboratory. This experimental setup, popularly known as the twin rotor MIMO system (TRMS) emulates a 2 DOF helicopter and characterizes a strongly coupled nonlinear dynamical system with uncertainties. Thus, it serves as a benchmark example to validate the claims in regards to the proposed adaptive controller. Figures 3.16(a)-(b) show the laboratory setup and the schematic description of the TRMS, respectively.

To physically describe the TRMS system, is indeed necessary to lend clear understanding of the

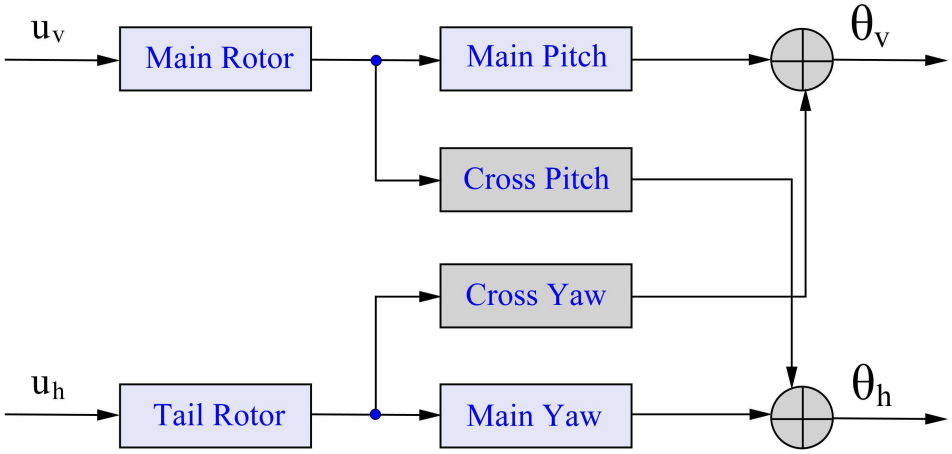

Figure 3.17: Schematic of cross-coupled twin rotor MIMO system or a 2-DOF helicopter for control development

system and its desired objective. Referring to Figure 3.16(b), the TRMS has two propellers driven by dc motors, place perpendicular to each other. These propellers are attached to both ends of a beam pivoted at its base in a manner that the assembly of beam and the rotors, can rotate freely in both vertical and horizontal planes. A counterbalance arm with a weight at its end is fixed to the horizontal beam at its pivot to stabilize the TRMS. The main rotor produces a vertical thrust allowing the beam to rise vertically. This vertical movement is called pitch motion. While, the tail rotor generates a horizontal thrust and provides yaw stabilization by appropriately moving along the horizontal plane either towards left or right. The set-up is so constructed taht the angle of attack is fixed. It is easy to observe that TRMS comprises of two subsystems, namely, the pitch and yaw subsystems controlled by varying the speed of the main rotor and tail rotor, respectively. Further, the speed of the propellers are controlled by varying the armature voltage of the corresponding DC motors. In fact, DC motors herein act as actuators producing the desired speed equivalent to the control input voltages. In addition, the inherent dynamic input and output interactions between each of the subsystems in the TRMS are shown in Figure 3.17, where θ_v and θ_h represent the pitch angle and the yaw angle; and u_v and u_h are control input voltages to the main and tail rotors, respectively. The pitch and the yaw angle are measured using position encoders fitted at the pivot. Since, it has been obvious from various simulations and experiments that pitch and yaw interactions play a crucial role in determining the performance of a controlled system. Inputs to any of the rotors influence both the position angles. Hence, apart from other design objectives including fault tolerance, alleviating these strong coupling effects is indeed imperative for any adaptive control synthesis for TRMS.

To complete the description, the TRMS set-up is interfaced with a Windows 7 PC (4 GB RAM), installed with Matlab/Simulink R2011a using PCL-812 card. Two position encoders are available to communicate the pitch and yaw angle measurements to the PC. The control inputs are generated using these measurements and the reference signals along with their derivatives, in the data acquisition and control block in the form of digital signals. These digital signals are thereafter converted to analog

signals through an embedded D/A converter and sent to the two d.c. motors attached to the rotors to achieve the desired attitude control.

Deviating our attention to mathematical modeling, the differential equations describing the dynamics of TRMS are given below [123].

$$I_v\ddot{\theta}_v = M_1 - M_{FG} - M_{B\theta_v} - M_G \tag{3.219}$$

$$I_h\ddot{\theta}_h = M_2 - M_{B\theta_h} - M_R \tag{3.220}$$

Where M_1 and M_2 denote the nonlinear static characteristics, M_{FG} represents the gravity momentum, $M_{B\theta_v}$ and $M_{B\theta_h}$ are momenta corresponding to friction forces, M_G is the gyroscopic momentum and M_R defines the cross reaction momentum. Further, their mathematical definitions are as follows.

$$M_1 = a_1L_m^2 + b_1L_m;\ M_2 = a_2L_t^2 + b_2L_t \tag{3.221}$$

$$M_{FG} = M_g\sin\theta_v;\ M_G = k_{gy}M_1\dot{\theta}_h\cos\theta_v \tag{3.222}$$

$$M_{B\theta_v} = B_{1\theta_v}\dot{\theta}_v - \frac{0.0326}{2}\dot{\theta}_h^2\sin 2\theta_v;\ M_{B\theta_h} = B_{1\theta_h}\dot{\theta}_h \tag{3.223}$$

$$M_R = \left[\frac{k_c(T_0s+1)}{(T_ps+1)}\right]M_1 \tag{3.224}$$

The terms L_m and L_t define the momentum of the main rotor and the tail rotor, respectively. These momentum functions are related to their corresponding control input(armature) voltages $u_v(t)$ and $u_h(t)$ as

$$L_m = \left[\frac{k_m}{T_{11}s+T_{10}}\right]u_v; \quad L_t = \left[\frac{k_t}{T_{21}s+T_{20}}\right]u_h \tag{3.225}$$

All other remaining parameters in equations (3.219)-(3.225) and their respective values are defined and listed in Table 3.4. Equations (3.219) and (3.220) are derived using Newton's laws of rotational motion. To obtain a state space model of the TRMS dynamics, the state variables are chosen as $\mathbf{x} := [x_1, x_2, x_3, x_4, x_5, x_6]^T := [\theta_v, \dot{\theta}_v, \theta_h, \dot{\theta}_h, L_m, L_t]^T$. Herein, x_1 defines the pitch angle, x_2 is the pitch angular velocity, x_3 denotes the yaw angle, the variable x_4 is the yaw angular velocity. Further, x_5 and x_6 represent the momentum of the main and tail rotor, respectively. Using the above relations from (3.221)-(3.225) in (3.219) and (3.220) leads to the formulation of the following dynamics describing the motion of a TRMS.

$$\begin{aligned}
\dot{x}_1 &= x_2\\
\dot{x}_3 &= x_4\\
\dot{x}_2 &= \theta_1^*{x_5}^2 + \theta_2^*x_5 - \theta_3^*\sin x_1 - \theta_4^*x_2 + \theta_5^*{x_4}^2\sin(2x_2)\\
&\quad -\theta_6^*x_4{x_5}^2\cos(x_1) - \theta_7^*x_4x_5\cos(x_1)\\
\dot{x}_4 &= \theta_8^*{x_6}^2 + \theta_9^*x_6 - \theta_{10}^*x_4 - \theta_{11}^*{x_5}^2 - \theta_{12}^*x_5\\
\dot{x}_5 &= -\theta_{13}^*x_5 + \theta_{14}^*u_v\\
\dot{x}_6 &= -\theta_{15}^*x_6 + \theta_{16}^*u_h\\
y_1 &= x_1, \quad y_2 = x_3
\end{aligned} \tag{3.226}$$

Table 3.4: Physical parameters of the TRMS

Symb.	Description, Value & Unit		
I_v	Moment of inertia of vertical rotor	0.068	kg-m^2
I_h	Moment of inertia of horizontal rotor	0.02	kg-m^2
a_1	Static characteristic parameter	0.0135	-
b_1	Static characteristic parameter	0.0294	-
a_2	Static characteristic parameter	0.02	-
b_2	Static characteristic parameter	0.09	-
M_g	Gravity momentum	0.32	N-m
$B_{1\alpha_v}$	Friction momentum function parameter	0.006	N-m-s/rad
$B_{1\alpha_h}$	Friction momentum function parameter	0.1	N-m-s/rad
k_{gy}	Gyroscopic momentum parameter	.0155	s/rad
k_m	Main rotor gain	1.1	-
k_t	Tail rotor gain	0.8	-
T_{11}	Main rotor denominator parameter	1.1	-
T_{10}	Main rotor denominator parameter	1	-
T_{21}	Tail rotor denominator parameter	1	-
T_{20}	Tail rotor denominator parameter	1	-
T_p	Cross reaction momentum parameter	2	-
T_0	Cross reaction momentum parameter	3.5	-
k_c	Cross reaction momentum gain	-0.2	-

The outputs of the TRMS are pitch and yaw angles and are denoted by y_1 and y_2. The unknown parameter vector is defined as $\boldsymbol{\theta}^* := [\theta_1^*, \theta_2^*, \ldots, \theta_{14}^*, \theta_{15}^*, \theta_{16}^*]^T$. The definition of all the unknown parameters θ_i for $i = 1, \ldots, 14$ are as follows.

$$\begin{aligned}
&\theta_1^* = a_1/I_v;\ \theta_2^* = b_1/I_v;\ \theta_3^* = M_g/I_v;\ \theta_4^* = B_{1\alpha_v}/I_v;\ \theta_5^* = 0.0326/2I_v;\ \theta_6^* = k_{gy}a_1/I_v;\\
&\theta_7^* = k_{gy}b_1/I_v;\ \theta_8^* = a_2/I_h;\ \theta_9^* = b_2/I_h;\ \theta_{10}^* = B_{1\alpha_h}/I_h;\ \theta_{11}^* = -1.75k_c a_1/I_h;\\
&\theta_{12}^* = -1.75k_c b_1/I_h;\ \theta_{13}^* = T_{10}/T_{11};\ \theta_{14}^* = k_m/T_{11};\ \theta_{15}^* = T_{20}/T_{21};\ \theta_{16}^* = k_t/T_{21}
\end{aligned} \tag{3.227}$$

The parametric model for unknown parameter estimation is written as,

$$\dot{\mathbf{x}} = \begin{bmatrix} \dot{x}_1 \\ \dot{x}_3 \\ \dot{x}_2 \\ \dot{x}_4 \\ \dot{x}_5 \\ \dot{x}_6 \end{bmatrix} = \begin{bmatrix} x_2 \\ x_4 \\ 0 \\ 0 \\ 0 \\ 0 \end{bmatrix} + \underbrace{\left[\begin{array}{c|c|c|c} \mathbf{0}_{1\times 7} & \mathbf{0}_{1\times 5} & \mathbf{0}_{1\times 2} & \mathbf{0}_{1\times 2} \\ \mathbf{0}_{1\times 7} & \mathbf{0}_{1\times 5} & \mathbf{0}_{1\times 2} & \mathbf{0}_{1\times 2} \\ \hline \boldsymbol{\varphi}_{1,2}^T & \mathbf{0}_{1\times 5} & \mathbf{0}_{1\times 2} & \mathbf{0}_{1\times 2} \\ \mathbf{0}_{1\times 7} & \boldsymbol{\varphi}_{2,2}^T & \mathbf{0}_{1\times 2} & \mathbf{0}_{1\times 2} \\ \hline \mathbf{0}_{1\times 7} & \mathbf{0}_{1\times 5} & \boldsymbol{\varphi}_{1,3}^T & \mathbf{0}_{1\times 2} \\ \mathbf{0}_{1\times 7} & \mathbf{0}_{1\times 5} & \mathbf{0}_{1\times 2} & \boldsymbol{\varphi}_{2,3}^T \end{array}\right]}_{\boldsymbol{\Phi}(\mathbf{x},\mathbf{u})} \underbrace{\begin{bmatrix} \theta_1^* \\ \theta_2^* \\ \vdots \\ \theta_{14}^* \\ \theta_{15}^* \\ \theta_{16}^* \end{bmatrix}}_{\boldsymbol{\theta}^*}. \tag{3.228}$$

The regressors are defined as $\boldsymbol{\varphi}_{1,2} := [x_5^2, x_5, -\sin x_1, -x_2, -x_4^2 \sin 2x_2, -x_4 x_5^2 \cos x_1, -x_4 x_5 \cos x_1]^T$, $\boldsymbol{\varphi}_{2,2} := [x_6^2, x_6, -x_4, -x_5^2, -x_5]^T$, $\boldsymbol{\varphi}_{1,3} := [-x_5, u_v]^T$ and $\boldsymbol{\varphi}_{2,3} := [-x_6, u_h]^T$. The multiple identification models for parameter estimation are designed using the above estimation model (3.228) consistent with equations (3.162)-(3.163). The parameter estimates from each of the identification models are thereafter utilized for second layer of adaptation to yield the final estimate of the parameter vector $\boldsymbol{\theta}^*$. Following the estimation of unknown parameters, the proposed adaptive controller is developed

following the backstepping methodology detailed in Section 3.3.2.1.

For experimental implementation of the proposed adaptive controller using multiple models, all the states of the system should be available. However, among the six states in the state vector $\mathbf{x}(t)$, only x_1 (pitch angle) and x_3 (yaw angle) are available for measurement. Therefore, an Extended Kalman Filter (EKF, Kalman-Bucy filter) [124] is used to estimate the remaining states of the nonlinear system. The detailed design of the EKF is provided in Appendix A.3. The initial conditions of the system are $\mathbf{x}(0) = [0,0,0,0,0,0]^T$. Similarly the EKF states and the states of the identification models are also initialized at zero. Since the number of unknown parameters is 16, the number of identification models required to satisfy the conditions of proposed design N=17. The relative degree of the pitch and yaw subsystems are found to be $\wp_1 = \wp_2 = 3$ and hence the controller gains are selected as $c_1 = [\{c_{1,i}\}_{i=1}^{3}]$=$[15, 2.5, 2.5]$ and $c_2 = [\{c_{2,i}\}_{i=1}^{3}]$=$[10, 2.5, 2]$. The damping gains are chosen as$\bar{c}_{1,2} = \bar{c}_{2,2} = \bar{g}_{1,3} = \bar{g}_{2,3} = 0.5$. The gain matrices of the adaptive identification models are considered as $\mathbf{A}_{\mu 0} = [\text{diag}\{-14,-14,-16,-16,-14,-14\}]$ for $\mu = \overline{1,17}$ and $\gamma = 2$. The adaptive rate parameter $\mathbf{\Gamma}_\mu$ is chosen as $\mathbf{\Gamma}_\mu = 20\mathbf{I}_{16}$. The adaptive weight parameters $\hat{w}_\mu$ for second layer of adaptation are initialized at $\hat{\mathbf{w}}(0) = \frac{1}{17}\mathbf{1}_{17\times 1}$. The control input voltages u_h and u_v are maintained within their allowable range of $[-2.5, 2.5]$V. The reference trajectories $y_{r,1}$ and $y_{r,2}$ to be tracked by the outputs $y_1 = \theta_v$ and $y_2 = \theta_h$ are the outputs of the reference system $\mathbf{G_r}(s) = \left[\text{diag}\left\{\frac{0.2}{9s^2+10s+4}, \frac{0.2}{9s^2+10s+4}\right\}\right]$ with $y_{d,1}$ and $y_{d,2}$ as the inputs. In the following, the system is subjected two scenarios of step signal and sinusoidal signal tracking to illustrate the tracking capability of the proposed multiple model adaptive controller featuring transient performance improvement without significantly increasing the control energy.

- *Scenario I*: This scenario demonstrates sine command tracking performance of the proposed adaptive controller. The inputs to the reference system are chosen as $y_{d,1} = 6 + 4\sin(0.05\pi t)$ and $y_{d,2} = 12\cos(0.05\pi t)$. Figure 3.18(b)-(c) shows satisfactory output tracking capability for both pitch and yaw angles $\theta_v = x_1$ and $\theta_h = x_3$ with the proposed control scheme. From a closer glance at the tracking performance in Figure 3.18(a), it is observed that the pitch and yaw error signals exhibit no substantial transients and ultimately oscillates in the range $[-0.02, 0.04]$ and $[-0.02, 0.15]$ at steady state. The maximum percentage of steady state error in tracking with reference to the peak value of $y_{r,1}$ and $y_{r,2}$ corresponding to each of the outputs y_1 and y_2 is approximately found to be 6% and 14%, respectively. The control input voltages u_v and u_h are bounded within their limits. To further our insights on the prolific features of the proposed adaptive control methodology, a tabulation of output and input performances are provided in Table 3.5. A low value of root mean square error (RMSE) and integral of absolute error (IAE) essentially hints at a good steady state performance. Whereas, the integral of time absolute error (ITAE) metric is meant to measure the transient performance and is desired be of a small magnitude for fast tracking and stabilization. The inferences drawn from quantifications of the output tracking performance in Table 3.5 are fairly consistent with our claims of acceptable transient and steady state performance. The input performance is measured using control energy(CE) defined as the second norm of the control signal and total variation

Table 3.5: Tabulation of input and output performances quantified using suitable performance measures

Reference Signal		Output Performance					Input Performance		
		RMSE	IAE	ITAE	M_p	M_u		CE	TV
Sine tracking	θ_v	0.027	2.364	117.42	-	-	u_v	298.93	217.72
	θ_h	0.062	5.389	276.63	-	-	u_h	164.11	809.38
Step tracking	θ_v	0.011	1.023	20.56	19%	14%	u_v	288.96	59.40
	θ_h	0.032	3.336	84.08	-	-	u_h	86.15	25.95

(TV) [113] which indicates how frequent the control is used. A small value of TV for a control scheme is beneficial for practical applications as mentioned in Remark 3.5. The CE and TV of the control inputs u_v and u_h corresponding to the proposed controller indicate a fairly good input performance without excessive chattering. Nevertheless, on a critical assessment of the error performances, the reader may find the steady state error bounds on a slightly higher side. However, it is to be mentioned that the performance of the TRMS under the action of the proposed controller is indeed appreciable given the fact that real time experiments on the TRMS are subjected to noise, air gust, voltage fluctuations and other unforeseen external disturbances.

- *Scenario II*: In this case, we study the performance of the proposed control methodology under step command tracking. Considering the same reference system $\mathbf{G_r}(s)$ driven by inputs $y_{d,1} = 4U(t) + 4U(t-25) - 4U(t-75)$ and $y_{d,2} = 6U(t)$, its outputs $y_{r,1}$ and $y_{r,2}$ serve as the desired trajectories for system output tracking. Here, $U(t)$ is defined as the unit step input. From the results in Figure 3.19, it is evident that the proposed control scheme is capable of rendering a good tracking performance for step reference inputs with minimum chattering in the control input voltages. Further, the control inputs reside within their permissible ranges while realizing the desired control objective. The pitch tracking error show some transient behaviour with an overshoot of 19% and an undershoot of 14% with reference to $y_{r,1} = 0.2$ while the yaw tracking error exhibits no peaks beyond $y_{r,2} = 0.3$. The maximum steady state error is approximately calculated to be 5% for θ_v and 9% for θ_h. Tabulation of calculated ITAE, IAE, and RMSE values under step tracking in Table 3.5 reveals a satisfactory and appreciable output performance. Further, the TV and CE values in Table 3.5 are reasonably low, indicating a promising input performance. The effect of cross-coupling The yaw tracking performance can be however further improved using an integral action in the proposed controller. Taking into consideration several issues in real time implementation as mentioned in the preceding scenario, the performance of the proposed adaptive control system is certainly acceptable. The authors do believe that the obtained results are indeed appreciable and encouraging.

Remark 3.5. *At this juncture, it should be remarked upon that the proposed adaptive control methodology contributes in two directions. Firstly, it offers a control solution to the tracking problem in unknown nonlinear uncertain systems featuring an improved output transient performance. Secondly,*

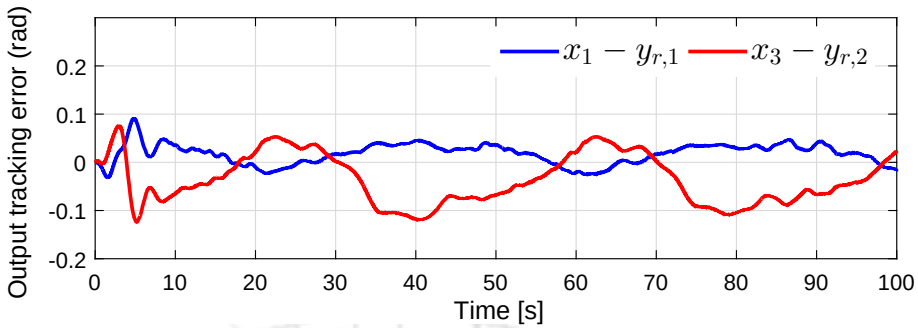

(a)

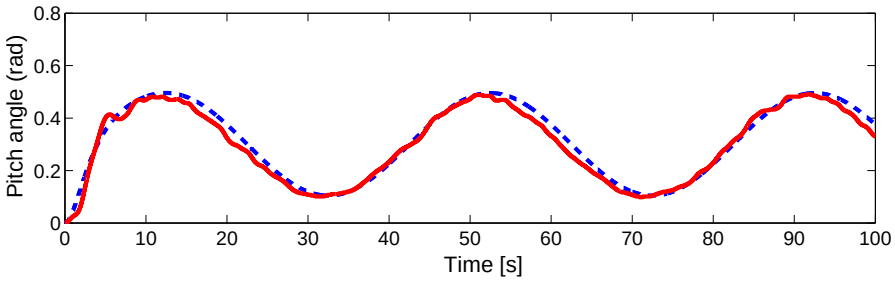

(b)

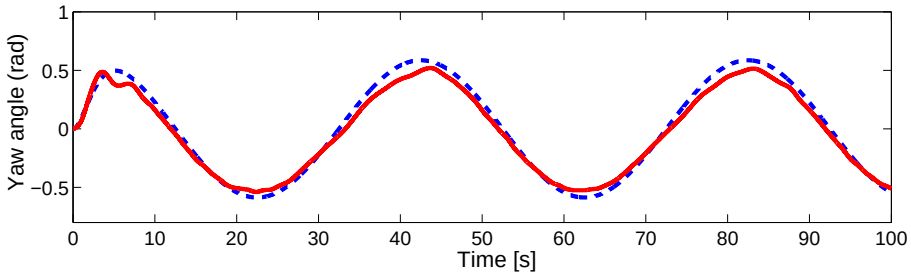

(c)

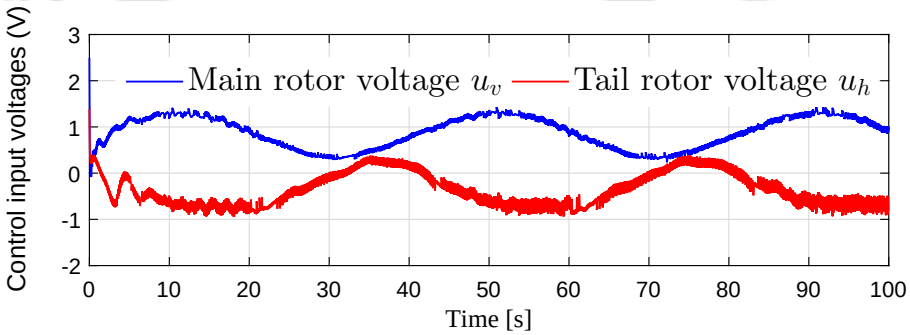

(d)

Figure 3.18: (a) pitch and yaw angle tracking error (rad) ; (b) pitch angle $\theta_v = x_1$(rad); (c) yaw angle $\theta_h = x_3$(rad); (d) control input voltages u_v and u_h (V).

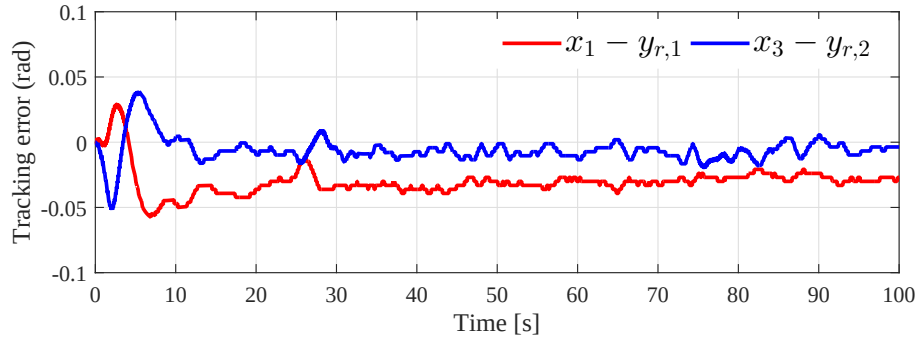

(a)

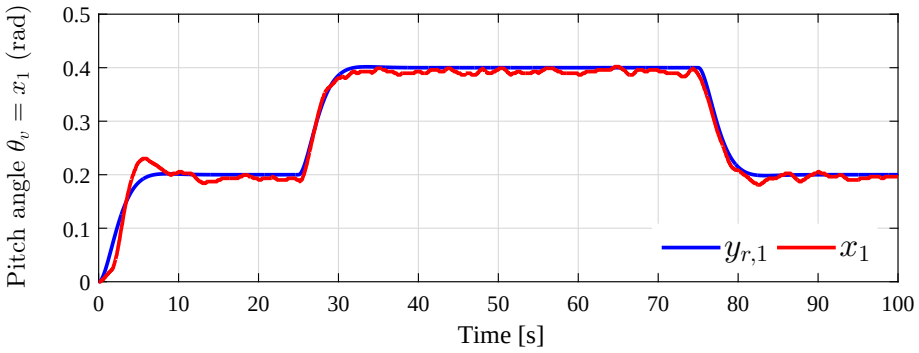

(b)

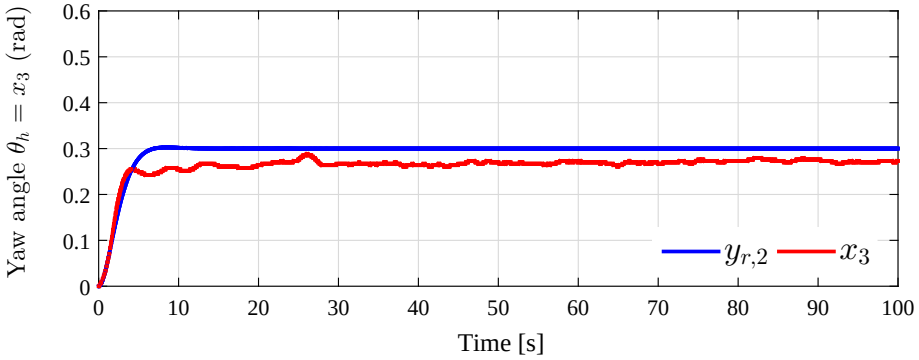

(c)

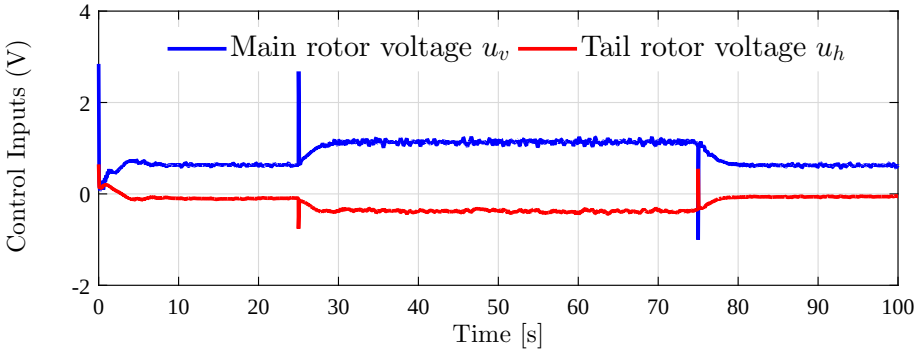

(d)

Figure 3.19: (a) pitch and yaw angle tracking error (rad) ; (b) pitch angle $\theta_v = x_1$(rad); (c) yaw angle $\theta_h = x_3$(rad); (d) control input voltages u_v and u_h (V)

the obtained solution can be further utilized to solve FTC problems using adaptive control and cater to the requirements of enhanced post failure transient performance without substantial increase in control usage. Adhering to the aim of FTC, the performance of the proposed AMMFTC scheme was demonstrated for control of MIMO nonlinear uncertain systems affected by abrupt actuator faults through extensive simulations in Section 3.3.4. Further, the proposed control methodology was experimentally implemented to control the attitude of a twin rotor MIMO system (TRMS). Given the fact, an abrupt decrease in thrust forces generated by the rotors would emulate the occurrence of actuator faults, it is certainly not possible to practically realize actuator faults in such an experimental set-up. It should be clearly understood that scaling the parameters θ_{14}^* and θ_{16}^* associated with the control voltages u_v and u_h do not model partial loss of effectiveness of actuators. Hence, the experiments were conducted without considering the occurrence of actuator faults. Nevertheless, the parameters of the TRMS were assumed to be unknown and estimated using the adaptation algorithm proposed in this chapter. The results obtained are promising. Any loss of actuation effectiveness will lead to change in the values of constant unknown parameters associated with L_m and L_t. Therefore, under this scenario, if a satisfactory transient and steady state performance is achieved at start up, it is reasonable to assume that the proposed adaptive controller would exhibit similar attributes at post fault scenarios.

3.4 Summary

In this chapter, a new actuator failure compensation strategy was presented for nonlinear uncertain systems. The design methodology followed a multiple model adaptive backstepping procedure without switching and tuning. The proposed method exhibits a simpler structure compared to [54], [24] and [100] in the sense that a single controller is utilized in the design of failure compensation in the event of unknown actuator LOE, LIP and float free failures. The proposed controller was developed in a manner so as to be able to compensate infinite actuator failures. Unlike existing literature on adaptive FTC in regards to intermittent actuator failures, explicit output error bounds in terms of $\mathcal{L}_\infty$ and $\mathcal{L}_2$ signal measures are derived by formulating the closed loop dynamics as a random impulsive hybrid system. Besides, the improvement of output transient performance using the proposed FTC strategy is proved theoretically through an appropriate quantification. Finally, the proposed controller fed with parameter estimation from a minimum number of estimation models adds up to the computational simplicity of the method presented. Thereafter, the AMMFTC algorithm is extended to control of MIMO nonlinear systems with actuator failures. Similar design attributes were observed and the controller was able to suppress overshoots due to actuator failures as well as those due to cross coupling effects. In addition, the control input performance was also observed to be acceptable. Thus, the proposed control algorithm conforms with the desired FTC design requirements and qualifies to be a suitable scheme for practical applications. It is expected to achieve promising results in large scale MIMO systems as well. Simulation results illustrate the effectiveness of the proposed FTC method in the case of actuator faults/failures for both single input multi output and MIMO nonlinear uncertain systems.

4

Finite Time Adaptation based Compensation (FTAC) of Actuator Failures in Nonlinear Uncertain Systems

Contents

4.1 Introduction 128

4.2 Finite Time Adaptation based Compensation (FTAC) of Infinite Actuator Failures 132

4.3 Finite Time Adaptation based Compensation (FTAC) of Actuator Failures in Multi-Input-Multi-Output (MIMO) Nonlinear Uncertain Systems 165

4.4 Summary 187

4.1 Introduction

Pertinent to nonlinear systems, the adaptive multiple model based fault estimator (FE) integrated FTC algorithm proposed in Chapter 3, is certainly a promising attempt to overcome the design limitations encountered in direct adaptive FTC and existing ARFTC methods. Such an algorithm enjoys the merits of (1) modularity between the controller-estimator pair; (2) enhanced output transient performance without decreased stability margins at start up and post-failure; (3) faithful compensation of infinite actuator failures; (4) globally asymptotically stable fault tolerant output tracking; and (5) increased design freedom. Despite exhibiting a plethora of prolific features, the computational complexity is only alleviated to an extent on account of a significant decrease in the number of identifiers. Although the multiple model estimator with two layer of adaptation in Chapter 3, exhibits comparatively faster convergence, it can only guarantee boundedness of parameter estimates. Moreover, the parameter estimates converge to their true values if and only if the restrictive persistence of excitation (PE) condition is met by the regressor signals. Further, the parameter convergence time cannot be exactly characterized. It is always a good practice to explore new rewarding adaptive control methods for FTC applications which offer excellent robust performance and at the same time are computationally appealing. Along similar lines, the search for algorithms to arrive at an *ideal* adaptive solution, is indeed akin to the infinite quest for the "*Holy Grail*" in active FTC design for nonlinear uncertain systems. Within the proposed active FTC architecture, the time available for fault estimation and subsequent recovery plays a crucial role in deciding the existence of stable adaptive solutions. Considering practical situations such as in mission critical systems, where the time window in which the faulty system is stabilizable is very short [8, 94], this time is strictly small. As a matter of fact, if the actuator fault/failure is not accommodated within a specific finite time, the inputs and outputs will encroach their safety limits and eventually lead to mission failures, which is undesirable.

In view of the design objectives of fast failure recovery, transient improvement, acceptable control usage (within predefined physical limits) and computational simplicity; the strong controller developed in Chapter 3, when augmented with a finite time parameter estimator would be a promising choice for FTC applications, where time is a critical parameter. Introduction of finite time stable parameter estimators into the design allows for an upper bound on the time required for fault estimation. Thus, such a modification will add to the design freedom of the FE/FTC architecture proposed in Chapter 3. In consequence, the damping parameters can be tuned accordingly to maintain the design modularity and obtain a control input within its allowable limits. It is well known that output performance in an indirect adaptive control approach is directly related to the estimation performance. Hence, the estimator featuring finite time convergence will ensure accurate estimation of failure induced parameters and contribute to the improvement of output transient performance. Besides, stability margins remain unaffected and are certainly enhanced, if not decreased. Motivated by the above insights and reasonable arguments, a finite time adaptation based control (FTAC) is designed in this chapter for application to the development of failure resilient nonlinear control systems. The control design herein utilizes an ISS backstepping controller augmented with a novel finite time parameter estimator. The design features of the proposed finite time parameter estimator will be discussed in the sequel. To the best of authors' knowledge, there are still no results available in FTC literature which propose an integrated

FE/FTC design framework featuring finite time fault/failure estimation in linearly parameterizable nonlinear uncertain systems. Further, an FTAC solution to the problem of compensating possible infinite actuator failures followed by a rigorous analysis is also not attempted so far. Therefore, the FTAC method developed in this chapter is also extended to adaptive compensation design for intermittent actuator failures followed by rigorous analysis of signal convergence properties. The results obtained are indeed encouraging. Compared to AMMFTC method, the proposed technique obviates the usage of multiple identification models and hence the computational burden is expected to be further reduced. In summary, the proposed control method exhibits all the desirable attributes of an *ambitious* FTC strategy.

Apart from its promising contributions to FTC literature, the proposed algorithm is also anticipated to be a value addition to existing control schemes with finite time parameter estimation. Such a claim certainly requires well substantiated and strong arguments to endorse the proposed controller and to arrive at conclusions justifying its design uniqueness. In what follows, we discuss the FTAC methodology in brief and its contributions compared to relevant existing results on adaptive control with finite time adaptation.

With reference to the FTAC algorithm developed in this chapter, parameter convergence is justified to be a fundamental design element which decides performance improvement and also contributes to the enhancement of robust stability of the closed loop adaptive system. Recent years have witnessed an influx of generalized second order sliding mode ideas to solve the problem of finite time parameter identification in nonlinear systems as a part of observer design [125–128]. The resulting robust parameter adaptation algorithms claim exact estimation of unknown parameters in finite time. However, the following drawbacks restrict their applicability to general nonlinear systems with linearly parameterized uncertainties.

- Finite time parameter estimation is possible only for linear stable systems and Lipschitz nonlinear systems.
- Apart from assuming that the system states are accessible for measurement, these observer based parameter estimation approaches also require the measurement or computation of the velocity state vector.
- The invertibility of the regressor matrix has to be continuously checked online and the matrix inverse has to be computed for parameter estimation.
- Inapplicable for unstable systems regardless of their dynamics being linear or nonlinear.

In addition to the above-mentioned shortcomings, it is also observed that integration of these parameter estimators driven by state predictor/observer error, with a controller fails to yield parameter convergence to their true values. As a result, output performance is adversely affected. The disadvantages of observer based adaptive parameter estimation approaches have immensely motivated the design of parameter prediction error dependent estimators to improve estimator convergence characteristics. Certainly, to the best of our knowledge, finite time parameter estimation in adaptive control of nonlinear systems has been pioneered by Adetola and Guay in [129]. The adaptation algorithm proposed

in [129], ensures exact estimation of unknown parameters after a finite time whose magnitude is dependent on the observed excitation of the filtered regressor signals. The estimation performance superiority in comparison to standard parameter estimators has been well demonstrated therein. In [130], an integrated finite time adaptive estimation based controller is designed to improve output performance and achieve asymptotic stability of the tracking error. In [130], the adaptation algorithm resorts to the finite time parameter estimation algorithm in [129] and uses both the tracking error and parameter prediction error for performance enhancement. In [129], the PE condition on the regressor signals transforms to online checking for non-singularity of the time integrated function of filtered regressor matrix for each sampling interval. This is indeed obligatory for the algorithm proposed in [129] in the sense that the estimation method explicitly computes the inverse of the foregoing integral of interest on the run to arrive at the parameter estimate. From a computational perspective, it is natural to conclude that such continuous online check for existence and subsequent computation of inverses lead to increased computational complexity with increase in the dimension of unknown parameter vector. Thus, to make the design amenable to practical computational constraints, the authors suggested the invertibility check from $t = 0$ to a time t_c after which the integral of the filtered regressor function is positive definite. The parameter adaptation is stopped after time t_c. However, actuator failures are unanticipated both in time and magnitude. Therefore, in regards to FTC design, such a remedial measure to lend computational simplicity is practically infeasible. Besides, no closed form expression has been provided in [129] to determine the convergence time of the parameter estimation error. Adaptive parameter estimators utilizing ideas from sliding mode control (SMC) have also been proposed recently [131] to guarantee finite time convergence. The parameter estimation obtained from an SMC estimator contains high frequency components and is not smooth. As a consequence, the input performance is compromised whenever sliding mode parameter estimation is incorporated into an integrated estimation based control design.

A novel finite time adaptive parameter estimator driven by *parameter prediction error*, is proposed in this chapter. Apart from assuring finite time parameter estimation, the proposed algorithm eliminates all the limitations of the above cited literature. From the view point of finite time parameter estimation based adaptive control, the proposed method builds upon the work of Adetola and Guay in [129]. The proposed estimator design initiates by introducing several stable filters to obtain the filtered versions of the state vector and regressor matrix. On account of a passivity based low pass filtering of the regressor matrix, stability of estimation error and inherent signals are ensured irrespective of the boundedness of the regressor matrix. Thereafter, two additional low pass filters with their inputs being functions of filtered regressor matrix and state vector are introduced to yield two auxiliary design variables. The parameter estimation error is then defined using these auxiliary variables. Finally, the proposed adaptive law is developed utilizing concepts from second order sliding mode control [132]. The parameter update law does not require any knowledge of the time derivative of parameter prediction error. The estimation is continuous and smooth without chattering. Unlike [129], the usage of low pass filters in arriving at the expression for parameter error circumvents the online check for existence and computation of inverse for the filtered regressor matrix. The integral laws proposed in [129] to relax PE condition, may result in integrator wind up and hence unboundedness of adaptation may occur.

This drawback is very serious, especially when practical applications are considered and is eliminated by the proposed adaptation algorithm. Furthermore, as an added advantage, robustness of parameter estimation to external disturbances is also guaranteed. Parameter convergence to their true values is guaranteed, using the proposed estimator without the need of the PE condition. However, a more relaxed initial excitation (IE) condition [133] needs to be satisfied to achieve faithful parameter estimation. Exponential stability of tracking error is guaranteed provided the IE condition is fulfilled. The parameter prediction error and its time derivative using the proposed adaptation technique converge to zero at steady state. Under the integrated estimator based FTC scheme proposed herein, such an attribute indeed adds to further improvement of input performance and accuracy of output tracking at steady state.

As the third contribution in this chapter, the proposed FTAC method is also applied to solve the adaptive FTC design problem in nonlinear coupled MIMO systems affected by large unknown parametric uncertainties and actuator failures/faults. Although not straightforward, the design methodology is utilized to develop the proposed FE/FTC control architecture. Similar to the results obtained for MISO systems, convergence and stability properties of the output error, estimation error and other intermediate signals do not change when the FE/FTC scheme with finite time adaptation is applied to control of MIMO nonlinear systems. Further, to investigate its suitability for practical applications, the proposed FTAC algorithm is utilized to design an adaptive attitude controller for the laboratory prototype of a 2-DOF helicopter (Twin Rotor MIMO system, TRMS) assuming that its parameters are totally unknown. The results obtained are satisfactory which prove that performance efficacy and robustness of the proposed FTAC strategy.

Rest of the chapter is organized as follows: Section 4.2 presents the design of finite time adaptation based controller (FTAC) for nonlinear uncertain systems to compensate finite and infinite actuator failures. Prior to the description of the design methodology, some preliminary definitions are stated in subsection 4.2.1. Further, the problem formulation and design assumptions appear in subsection 4.2.2. Thereafter, the proposed controller and finite time estimator are discussed in subsection 4.2.3. A rigorous closed loop stability analysis is provided in subsection 4.2.4. A detailed simulation study is conducted in subsection 4.2.5. Section 4.3 deals with the extension of FTAC strategy coupled MIMO nonlinear systems with unknown parameters and actuator failures. Subsection 4.3.1 formulates the FTC design problem along with the necessary assumptions for MIMO nonlinear systems while subsection 4.3.2 describes the FTAC design procedure. Subsection 4.3.3 presents the closed-loop stability analysis of the proposed control system. In subsection 4.3.4, simulation studies are described and the results obtained are illustrated. Subsection 4.3.5 presents the experimental results obtained by applying the proposed FTAC methodology to attitude control of a twin rotor MIMO system. Finally, the summary of Chapter 4 is drawn in Section 4.4.

4.2 Finite Time Adaptation based Compensation (FTAC) of Infinite Actuator Failures

4.2.1 Some Preliminary Definitions

Definition 4.1. *Let us consider a signal $x(t) \in \mathbb{R}^n$ and consider the set,*

$$\mathcal{S}_1(\nu) = \left\{ x : [0,\infty) \mapsto \mathbb{R}^n \Big| \int_t^{t+T} |x(s)|ds \leq \lambda_0 \nu T + \lambda_1,\ \forall t,\ T > 0 \right\}$$

for a given constant $\nu \geq 0$ with $\lambda_0,\ \lambda_1 > 0$ are finite constants. The signal $x(t)$ is said to be $\nu-$small in the absolute sense (a.b.s) if $x(t) \in \mathcal{S}_1(\nu)$.

Definition 4.2. *Let us consider a signal $x(t) \in \mathbb{R}^n$ and consider the set,*

$$\mathcal{S}_2(\nu) = \left\{ x : [0,\infty) \mapsto \mathbb{R}^n \Big| \int_t^{t+T} x^T(s)x(s)ds \leq (\lambda_0 \nu^2 + \lambda_1 \nu)T + \lambda_2,\ \forall t,\ T > 0 \right\}$$

for a given constant $\nu \geq 0$ with $\lambda_0,\ \lambda_1,\ \lambda_2 > 0$ are finite constants. The signal $x(t)$ is said to be $\nu-$small in the mean square sense (m.s.s) if $x(t) \in \mathcal{S}_2(\nu)$.

Definition 4.3. *A bounded signal $x(t) \in \mathbb{R}^n$ is* persistently exciting *(PE) for $t \in [0,\ \infty)$ provided $\exists T > 0$ and $\lambda > 0$ such that the following condition holds ([133], [134]),*

$$\int_t^{t+T} x(s)x^T(s)ds \geq \lambda I_n, \quad \forall t \geq 0$$

where I_n denotes an identity matrix of order n.

Definition 4.4. *A bounded signal $x(t) \in \mathbb{R}^n$ is* exciting *over the finite time interval $[t_0,\ t_0 + T)$ with $T > 0$ and $t_0 \geq 0$, provided $\exists\ \lambda > 0$ such that the following condition holds ([133]),*

$$\int_{t_0}^{t_0+T} x(s)x^T(s)ds \geq \lambda I_n$$

where I_n denotes an identity matrix of order n.

Theorem 4.1. *Let us consider a continuously differentiable function $V : \mathcal{D} \times [0,\infty) \to \mathbb{R}_+$, finite positive numbers $\Gamma > 0$, $\mu \in (0,1)$, and a neighborhood $\mathcal{N} \subset \mathcal{D}$ of the origin such that V is positive definite over $\mathcal{N}$ and $\dot{V} + \Gamma V^\mu$ is negative semi-definite over $\mathcal{N}$ where $\dot{V}(x) \triangleq \frac{\partial V(x)}{\partial x} f(x)$. Then the origin is a finite-time-stable equilibrium of the dynamics $\dot{x} = f(x)$. Further, if T_s defines the settling time function, then $T_s(x) \leq \frac{1}{\Gamma(1-\mu)} V(x)^{1-\mu}\ \forall x$ in the open neighborhood of the origin [106].*

4.2.2 Problem Formulation

On similar lines as in 3.2, let us consider a class of nonlinear uncertain systems transformable to a parametric strict feedback form as follows.

$$\dot{x}_i = x_{i+1} + f_i(\bar{x}_i)^T \kappa^*, \quad i = \overline{1, \wp - 1} \tag{4.1}$$

$$\dot{x}_\wp = f_0(x, \eta) + f_\wp(x, \eta)^T \kappa^* + \sum_{j=1}^{m} b_j \beta_j(x, \eta) u_j \tag{4.2}$$

$$y = x_1 \tag{4.3}$$

$$\dot{\eta} = \Lambda_0(x, \eta) + \sum_{i=1}^{p} \kappa_i^* \Lambda_i(x, \eta) \tag{4.4}$$

where $x_i(t)$ for $i = \overline{1, \wp}$ represent the states of the dynamical system (4.1)-(4.2) and $\wp$ defines the relative degree of the plant with reference to its output. The notation $\bar{x}_i(t)$ is meant to denote a $i-$tuple state vector and $x(t) = [x_1, \ldots, x_\wp]^T \in \mathbb{R}^\wp$ defines the full state vector. The system output is given by y defined by a state or a smooth function of the states. The functions $f_i(\cdot, \cdot) : \mathbb{R}^\wp \times \mathbb{R}^{n-\wp} \to \mathbb{R}^p$ for $i = \overline{1, \wp}$ are assumed to be vectors of known smooth linear/nonlinear functions. Further, $f_0(\cdot, \cdot)$ is also a known nonlinear function which is infinitely continuously differentiable. The actuation functions $\beta_j(\cdot, \cdot) : \mathbb{R}^\wp \times \mathbb{R}^{n-\wp} \to \mathbb{R} \in \mathfrak{C}^\infty$ for $j = \overline{1, m}$ are known and may not be necessarily linear. The factors b_j for $j = \overline{1, m}$ define the unknown control coefficients. Further, the uncontrollable dynamics of the system is described by $\dot{\eta}$. The unknown vector of system parametric uncertainty is denoted by $\kappa^* \in \mathbb{R}^p$ where its elements are unknown constants or may be time varying.

Prior to the formulation of the FTC problem, the input-output characteristics of the actuators encompassing their healthy, faulty and failure states of operation are to be defined. Given that u_{Hj} defines the input and $K_{j,h}$ describing the state of health of the $j-$th actuator during time $t \in [t_{j,h}^o, t_{j,h}^e) \subset [0, \infty)$, the actuator failure model is described as,

$$u_j(t) = \begin{cases} K_{j,h} u_{Hj} + \bar{u}_{Fj,h}, & t \in [t_{j,h}^o, t_{j,h}^e) \\ u_{Hj}, & t \in [t_{j,h}^e, t_{j,h+1}^o) \end{cases} \tag{4.5}$$

The suffix 'o' and 'e' is used to denote the onset and end of a particular actuator failure pattern for the time interval $t \in [t_h, \ t_{h+1})$. The notation $\bar{u}_{Fj,h}$ is used to represent the magnitude at which the $j-th$ actuator is jammed after it fails completely. It has been discussed in Section 3.2 that the above modeling encompasses three forms of actuator faults and failures, namely; loss of effectiveness(LOE), lock-in-place(LIP) and float failure.

Now assuming that actuators in the system may undergo abrupt and sudden faults/failures, the control design objectives are as follows,

- Guaranteeing stability of the closed-loop system under occurrence of the considered types of actuator failures unknown in time pattern and magnitude for all time $t \in [0, \infty)$.
- Fast, accurate and finite time estimation of unknown system and failure induced parameters leading to an improved output transient and steady state performance.

- Output tracking is robust to unknown system and actuator failure parameters assumed to vary intermittently across all time $t \in [0,\ \infty)$. Given that the system undergoes possible infinite parameter jumps not necessarily known, the output tracking error $y(t) - y_r(t)$ is ensured to be stable and $\nu-$small in the absolute sense (a. b. s.), i.e., $z_1(t) := (y(t) - y_r(t)) \in \mathcal{S}_1(\nu)$.

- In case the total number of actuator failures and system parameter jumps are finite, asymptotic convergence of output tracking error to the origin is ensured, that means, $\lim_{t\to\infty} z_1(t) = 0$.

4.2.2.1 Design Assumptions

The same set of *assumptions* as in Section 3.2 are invoked prior to controller design to meet the aforementioned objectives. The assumptions are not repeated in detail here for the sake of brevity in presentation. In summary, the fault tolerant control design assumes that the system is controllable with respect to $(m-1)$ actuator failures adding to the non-singularity of the resulting actuation function, that is, $\beta_j(x,\eta) \neq 0$. This condition guarantees the existence of an adaptive control solution to the concerned actuator FTC problem. The signs of the actuation coefficients $sign(b_j)$ for $j = \overline{1,m}$ is known. The internal dynamics (4.4) of order $(n-\wp)$ is input-to-state-stable(ISS) with respect to the controllable states $(x(t))$ as its input. The reference trajectory $y_r(t)$ and their successive time derivatives until $\wp-$th order are continuous, bounded and belong to a compact set. Besides, the unknown failure and system parameters satisfy Assumption 3.5 meaning that $0 < \underline{b}_j \leq |b_j| \leq \overline{b}_j$, $|\bar{u}_{Fj,h}| < \bar{u}$ and $0 < \underline{K}_j \leq K_j \leq 1$ and $\underline{b}_j$, $\overline{b}_j$, $u_{\max}$ and $\underline{K}_j$ for $j = \overline{1,m}$ are known finite positive constants. The unknown parameter vector κ^* belongs to a known convex compact set, i.e., $\kappa^* \in \mathcal{S}_{\kappa^*} \subset \mathbb{R}^p$. The set $\mathcal{S}_{\kappa^*}$ is the convex compact set where the parameter vector $\kappa^* \in \mathbb{R}^p$ resides and $\forall \kappa_1, \kappa_2 \in \mathcal{S}_{\kappa^*}$, the relation $\|\kappa_1 - \kappa_2\| \leq \kappa_{\max}$ holds.

4.2.3 Fault Tolerant Control Design with Finite Time Adaptation

Actuator redundancy is indispensable in achieving failure tolerance in any dynamical system. Hence, considering that the actuators of the nonlinear system (4.1)-(4.4) have similar physical and operational characteristics, the $j-$th control input can be designed in parallel as,

$$u_{Hj}(t) = \frac{1}{\beta_j} v(t) sign(b_j) \tag{4.6}$$

where $v(t)$ is designed using a backstepping technique with finite time adaptation to improve the performance. Let us define the actuator index set as $\mathscr{B} := \{j_1, \ldots, j_m\}$ and two of its subsets comprising of failed and healthy actuator indices as $\mathscr{B}_{tot_F} = \{j_1, \ldots, j_{q_h}\}$ and $\mathscr{B}_{tot_H} := \mathscr{B}/\mathscr{B}_{tot_F}$, respectively. The notation q_h is used to denote the number of totally failed actuators at a failure time instant $t = T_h$ and varies as $0 \leq q_h \leq (m-1)$ all throughout the interval $[T_h,\ T_{h+1})$ until the onset of the next consecutive actuator failure pattern at $t = T_{h+1}$.
Incorporating the actuator failure model (4.5) and the expression for $v(t)$ (4.6) into the system dynamics

(4.1)-(4.2), the unified model with actuator failure parameters can be formulated as,

$$\begin{aligned}\dot{x}_i &= x_{i+1} + f_i(\bar{x}_i)^T\kappa^*, \quad i = \overline{1, \wp-1}\\ \dot{x}_\wp &= f_0(x,\eta) + f_\wp(x,\eta)^T\kappa^* + b^*v + \beta^T\bar{u}^*\end{aligned} \tag{4.7}$$

where,

$$b^* := \begin{cases} \sum\limits_{j=1}^{m} |b_j|, & \text{for } K_{j,h} = 1 \text{ and } \bar{u}_{Fj,h} = 0 \forall\ j\ \in \mathscr{B} \\ \sum\limits_{j\in\mathscr{B}_{tot_H}} K_{j,h}|b_j|, & \text{for } K_{j,h} \in [0,1) \text{ and } \bar{u}_{Fj,h} \neq 0\ \forall\ j\ \in \mathscr{B}_{tot_F} \end{cases} \tag{4.8}$$

$$\bar{u}^* := [0,\ldots,0]^T \in \mathbb{R}^m, \text{ for } K_{j,h} = 1 \text{ and } \bar{u}_{Fj,h} = 0\ \forall\ j\ \in \mathscr{B} \tag{4.9}$$

$$\bar{u}^* := [\{b_{j_k}\bar{u}_{Fj_k,h}\}_{k=1}^{q_h}, 0,\ldots,0]^T \in \mathbb{R}^m \text{ for } K_{j,h} \in [0,1) \text{ and } \bar{u}_{Fj,h} \neq 0\ \forall\ j\ \in \mathscr{B}_{tot_F} \tag{4.10}$$

Finally, the vector of unknown parameters due to abrupt actuator faults/failures and unknown parameters in modeling is defined by $\theta^* := [\theta_1^*\ \theta_2^*\ \theta_3^*]^T = [b^*\ \kappa^*\ \bar{u}^*]^T \in \mathbb{R}^{p+m+1}$. The parameter θ_1^* and θ_3^* are actuator fault/failure induced perturbations and hence are time varying with $\dot{\theta}_1^*$,$\dot{\theta}_3^* \neq 0$ implying $\dot{\theta}^*(t) \neq 0$. Nevertheless, $\dot{\theta}_1^*$ and $\dot{\theta}_3^*$ can be considered to be approximately zero if the cardinality of occurrence of actuator failure is finite and the inter-event time between two successive failure events is substantially large. Owing to intermittent changes in the failure induced parameters resulting from changes in the actuator failure pattern for every $T^* := (T_{h+1} - T_h) > 0$, for $h \in \mathbb{W}$ and $t \in [0,\ \infty)$, $\dot{\theta}^*(t)$ satisfies the following property [6] stated in Lemma 4.1.

Lemma 4.1. *The time derivative of the unknown parameter vector $\theta^*(t)$ representing system and actuator failure induced parametric uncertainties satisfy $\dot{\theta}^*(t) \in \mathcal{S}_1(\nu)$, i.e.,*

$$\int_t^{t+T} \|\dot{\theta}^*(s)\|ds \leq \sqrt{m+p+1}\Delta^\dagger\nu T + \sqrt{m+p+1}\Delta^\dagger;\ \ \forall t \in [t,\ t+T) \tag{4.11}$$

where $\nu = \frac{1}{T^*} > 0$, $\Delta^\dagger = \max\{\sum\limits_{j=1}^{m} \overline{b}_j - \ell,\ 2\overline{b}_j\overline{u}\} < \infty$ and $\ell = \min\limits_{1\leq j\leq m}\{\underline{K}_j\underline{b}_j\}$. The time span T^* is the minimum of all the time intervals between two consecutive changes in the actuator fault/failure pattern and the constants $\overline{b}_j$, $\overline{u} > 0$ are derived from the design assumptions in Section 4.2.2.

Proof. The proof is provided in Appendix A.4.

Remark 4.1. *It is well known that unknown parameters in any dynamical system vary with time. Given the fact that their variation with time is sufficiently slow, it is an universal assumption to consider them as constants and that their time derivatives are zero. This assumption is widely cited in the design and stability analysis of any adaptive or adaptive robust control methodologies in literature. Unlike the works in literature, since the adaptive control design concerns compensation of time varying actuator faults and failures, the proposed FTC design does not consider the time derivative of the unknown*

parameter vector $\dot{\theta}^*(t)$ to be zero. For the case of finite variations in actuator failure patterns and system parameters not assumed to be sufficiently close, taking the integral in (A.4.3) *from $0 \sim T$ and $T^* \to \infty(\nu \to 0)$, we get $\dot{\theta}^*(t) \in \mathcal{L}_1[0, T)$. Where, $[0,\ T)$ denotes the maximal interval of existence of $\dot{\theta}^*(t)$. This result would be utilized later to prove the asymptotic stability of the tracking error dynamics in the event of changes in actuator failure patterns with finite cardinality. At this juncture, it is worth mentioning that in presence of unknown piecewise constant time varying parameters, the property of $\dot{\theta}^*(t)$ in* (A.4.3) *and its subsequent usage in the stability analysis, will provide a clear insight to infer the signal characteristics of the output tracking error $z(t)$ for all $t \in [0,\ \infty)$.*

4.2.3.1 Design of Finite Time Parameter Estimator

In this subsection, a new parameter estimator featuring fast and finite time convergence to the actual parameter is proposed. Some necessary filters are introduced and boundedness properties of filtered signals and their derivatives are studied a priori. The adaptive law guaranteeing accurate and finite time parameter estimation is presented thereafter followed by derivation of stability properties of the estimator.

The estimator design procedure starts with representing the nonlinear dynamical system with failure parametrization (4.7) as a parametric $x-$model as given below.

$$\dot{x} = f(x) + \Phi^T(x, v)\theta^* \tag{4.12}$$

where, $f(x)$ and $\Phi(x, v)$ are defined as follows,

$$f(x) = [x_2,\ x_3, \ldots,\ x_\wp,\ f_0(x, \eta)]^T \in \mathbb{R}^\wp \ \&\ \Phi^T(x, \eta) = \begin{bmatrix} 0 & f_1(x_1)^T & 0_{1\times m} \\ 0 & f_2(\bar{x}_2)^T & 0_{1\times m} \\ \vdots & \vdots & \vdots \\ v & f_p(x, \eta)^T & \beta^T \end{bmatrix} \in \mathbb{R}^{\wp\times p+m+1}.$$

At this point, let us introduce the following filters.

$$\dot{\Omega}^T = A(x, t)\Omega^T + \Phi^T(x, v); \quad \Omega \in \mathbb{R}^{(m+p+1)\times\wp} \tag{4.13}$$

$$\dot{\Omega}_0 = A(x, t)(\Omega_0 + x) - f(x); \quad \Omega_0 \in \mathbb{R}^\wp \tag{4.14}$$

where, $A(x, t) = A_0 - \gamma\Phi(x, v)^T\Phi(x, v)P$. Further, A_0 is a constant Hurwitz matrix with a positive definite matrix $P = P^T > 0$ as the solution to the equality $A_0^T P + PA_0 + Q = 0$ with a chosen $Q > 0$. Additionally, we define another two filters with filtered variables $R(t)$ and $S(t)$ as,

$$\dot{R}(t) = -\mathscr{K}R(t) + \Omega\Omega^T; \quad R(0) = 0,\ R(t) \in \mathbb{R}^{(m+p+1)\times(m+p+1)} \tag{4.15}$$

$$\dot{S}(t) = -\mathscr{K}S(t) + \Omega(\Omega_0 + x); \quad S(0) = 0,\ S(t) \in \mathbb{R}^{m+p+1} \tag{4.16}$$

where $\mathscr{K} > 0$ is another design scalar. Now, we have the following lemmas which are essential prior to development of stability properties of the proposed controller.

Lemma 4.2. *Let the maximal interval of existence of solutions of filter dynamics* (4.13) *be* $[0,\ T)$. *Then filtered signal* $\Omega(t)$ *is bounded irrespective of the boundedness of the regressor matrix* Φ, *i.e.,* $\Omega(t) \in \mathcal{L}_\infty[0,\ T)$. *The* $\mathcal{L}_\infty$ *bound is given by,*

$$\|\Omega\|_\infty \leq \sqrt{\wp}\left(\sqrt{\frac{\overline{\lambda}(P)}{\underline{\lambda}(P)}}\|\Omega(0)\|_{\mathscr{F}} + \sqrt{\frac{m+p+1}{2\gamma\underline{\lambda}(Q)}}\right)$$

where $\|\cdot\|_{\mathscr{F}}$ *denotes the Frobenius norm of the argument matrix.*

Proof.

The proof follows a similar procedure as outlined in Section 4 of Chapter 6 in [69]. The boundedness of $\Omega(t)$ is derived as follows.

$$\begin{aligned}\frac{d}{dt}(\Omega P\Omega^T) &= \Omega(A_0^T P + PA_0)\Omega^T - 2\gamma\Omega P\Phi^T\Phi P\Omega^T + \Omega P\Phi^T + \Phi P\Omega^T \\ &= -\Omega Q\Omega^T - 2\gamma\left[\Omega P\Phi^T\Phi P\Omega^T - 2\frac{1}{2\gamma}\Phi P\Omega^T + \frac{1}{4\gamma^2}I_{m+p+1}\right] + \frac{1}{2\gamma}I_{m+p+1} \\ &= -\Omega Q\Omega^T - 2\gamma\left[\Phi P\Omega^T - \frac{1}{2\gamma}I_{m+p+1}\right]^T\left[\Phi P\Omega^T - \frac{1}{2\gamma}I_{m+p+1}\right] + \frac{1}{2\gamma}I_{m+p+1} \qquad (4.17)\end{aligned}$$

Now taking $trace(\cdot)$ operator on both sides of the equality (4.17) yields,

$$\begin{aligned}\frac{d}{dt}trace(\Omega P\Omega^T) &\leq -\underline{\lambda}(Q)\|\Omega\|_{\mathscr{F}}^2 - 2\gamma\|\Phi P\Omega^T - \frac{1}{2\gamma}I_{m+p+1}\|_{\mathscr{F}}^2 + \frac{1}{2\gamma}trace(I_{m+p+1}) \qquad (4.18) \\ &\leq -\underline{\lambda}(Q)\|\Omega\|_{\mathscr{F}}^2 + \frac{m+p+1}{2\gamma} \qquad (4.19)\end{aligned}$$

Now using the fact that $\underline{\lambda}(P)\|\Omega\|_{\mathscr{F}}^2 \leq trace(\Omega P\Omega^T)$ and the property of norm inequalities (Page 47, [122]) $\|\Omega\|_\infty \leq \sqrt{\wp}\|\Omega\|_2$ along with $\|\Omega\|_2 \leq \|\Omega\|_{\mathscr{F}}$, the following is obtained.

$$\|\Omega\|_\infty \leq \sqrt{\wp}\left(\sqrt{\frac{\overline{\lambda}(P)}{\underline{\lambda}(P)}}\|\Omega(0)\|_{\mathscr{F}} + \sqrt{\frac{m+p+1}{2\gamma\underline{\lambda}(Q)}}\right) \qquad (4.20)$$

The proof is complete. □

Combining (4.12) and (4.14), let us define an auxiliary variable $\mathscr{Y} := \Omega_0 + x$ such that,

$$\dot{\mathscr{Y}} = (A_0 - \gamma\Phi(x,v)^T\Phi(x,v))\mathscr{Y} + \Phi(x,v)^T\theta^* \qquad (4.21)$$

Before proceeding further, stating the following lemma is necessary.

Lemma 4.3. *The filtered regressor matrix* $R(t)$ *obtained as solution of* (4.15) *is positive definite if and only if* $\Phi(x,v)$ *in* (4.12) *is persistently exciting (PE).*

Proof.

From the proof of Lemma 4.2, the presence of the matrix $A(x,t) = (A_0 - \gamma\Phi(x,v)^T\Phi(x,v))$ in (4.13) yields strongly stable and bounded trajectories of Ω even though the regressor matrix is unbounded.

Hence $A(x,t)$ is inferred to be a stable matrix. Now, in accordance with the statement of the proof, it is apriori assumed that $\Phi(x,v)$ is PE. Since, the filter dynamics (4.13) is stable and minimum phase, the PE for Ω holds straightaway and hence $\int_t^{t+T} \Omega(s)\Omega^T(s)ds \geq \int_t^{t+T} \min\{\sqrt{\lambda(\Omega(s)\Omega^T(s))}\}I_{m+p+1}ds \geq \varpi I_{m+p+1}$ [133]. Here $\lambda(\cdot)$ denotes the eigen values of its argument and I_{m+p+1} is the identity matrix of order $(m+p+1)$. Now the solution $R(t)$ of the additional filter in (4.15) is given by,

$$R(t) = \int_t^{t+T} e^{-\mathscr{K}(T-s)}\Omega(s)\Omega^T(s)ds \tag{4.22}$$

The above equality (4.22) is further reiterated in the form of an inequality as stated below.

$$R(t) = e^{-\mathscr{K}T}\int_{t-T}^{t} e^{\mathscr{K}s}\Omega(s)\Omega^T(s)ds \geq e^{-\mathscr{K}T}\int_{t-T}^{t} \min\left\{\sqrt{\lambda(\Omega\Omega^T)}\right\}I_{m+p+1} \geq e^{-\mathscr{K}T}\varpi I_{m+p+1} \tag{4.23}$$

The inequality derived in (4.23) holds for $t > T$ and directs the readers to the conclusion that $R(t) \geq \underline{\lambda}(R(t))I_{m+p+1} > e^{-\mathscr{K}T}\varpi I_{m+p+1} > 0$. Hence, $R(t)$ is positive definite. Therefore, it is concluded that the PE condition on the regressor matrix $\Phi(x,v)$ now translates to ensuring the positive definiteness of $R(t)$. □

Now, defining $\tilde{\mathscr{Y}} := \mathscr{Y} - \Omega^T\theta^*$, the derivative of $\tilde{\mathscr{Y}}$ is calculated from (4.21) as,

$$\dot{\tilde{\mathscr{Y}}} = (A_0 - \gamma\Phi^T\Phi)\mathscr{Y} + \Phi^T\theta^* - ((A_0 - \gamma\Phi^T\Phi)\Omega^T + \Phi^T)\theta^* - \Omega^T\dot{\theta}^* \tag{4.24}$$

$$\leq \underbrace{(A_0 - \gamma\Phi^T\Phi)}_{A(x,t)}\mathscr{Y} - \Omega^T\dot{\theta}^* \tag{4.25}$$

Lemma 4.4. *Considering the $\mathscr{Y}-$error dynamics in (4.25), the error signal $\tilde{\mathscr{Y}}$ is bounded and is both $\nu-$small in the absolute sense (a.b.s.) as well as in the mean square sense (m.s.s), i.e., $\tilde{\mathscr{Y}} \in \mathcal{S}_1(\nu) \cap \mathcal{S}_2(\nu)$. Where $\nu = \frac{1}{T^*}$ is a finite positive number and T^* is the minimum elapse time between two successive variation of actuator failure patterns.*

Proof.

The solutions along (4.25) is described by,

$$\tilde{\mathscr{Y}}(t) \leq e^{-A(x,t)t}\tilde{\mathscr{Y}}(0) - \int_0^t e^{-A(t-s)}\Omega^T(s)\dot{\theta}^*(s)ds \tag{4.26}$$

Using Lemma 3.3 and Lemma 4.2, (4.26) reduces to an inequality as follows,

$$\|\tilde{\mathscr{Y}}(t)\| \leq \breve{k}e^{-c_0 t}\|\tilde{\mathscr{Y}}(0)\| + \breve{k}\|\Omega\|_\infty \int_0^t e^{-c_0(t-s)}\|\dot{\theta}^*(s)\|ds \tag{4.27}$$

The first term in (4.27) is undoubtedly bounded above and the integral in the second term is calculated

by following the procedure outlined on Pages 84-85 in [110]. Therefore, invoking the result in Lemma 4.1 with the inequality (4.27) yields,

$$\breve{k}\|\Omega\|_\infty \int_0^t e^{-c_0(t-s)}\|\dot{\theta}^*(s)\|ds \leq \frac{\breve{k}\|\Omega\|_\infty\Delta^\ddagger}{1-e^{-c_0}}\nu e^{c_0} + \frac{\breve{k}\|\Omega\|_\infty\Delta^\ddagger}{1-e^{-c_0}}e^{c_0} < \infty \tag{4.28}$$

Hence the ultimate bound on the signal $\tilde{\mathscr{Y}}(t)$ is given by,

$$\|\tilde{\mathscr{Y}}(t)\|_\infty = \frac{\breve{k}\|\Omega\|_\infty\Delta^\ddagger}{1-e^{-c_0}}\nu e^{c_0} + \frac{\breve{k}\|\Omega\|_\infty\Delta^\ddagger}{1-e^{-c_0}}e^{c_0} + \breve{k}\|\tilde{\mathscr{Y}}(0)\| \tag{4.29}$$

Equality (4.29) shows the boundedness of $\tilde{\mathscr{Y}}(t)$ provided ν is finite. The first part of the proof is complete.

Next, it is to be proved that $\tilde{\mathscr{Y}}(t) \in \mathcal{S}_1(\nu)$ followed by $\tilde{\mathscr{Y}}(t) \in \mathcal{S}_2(\nu)$. The procedure starts with the computation of the following integral.

$$\int_t^{t+T}\|\tilde{\mathscr{Y}}(s)\|ds \leq \int_t^{t+T}\breve{k}e^{-c_0 s}\|\tilde{\mathscr{Y}}(0)\|ds + \breve{k}\|\Omega\|_\infty \int_t^{t+T}\int_0^s e^{-c_0(s-\tau)}\|\dot{\theta}^*(\tau)\|d\tau ds \tag{4.30}$$

$$\leq \frac{\breve{k}}{c_0}(e^{-c_0 t} - e^{-c_0(t+T)})\|\tilde{\mathscr{Y}}(0)\| + \breve{k}\|\Omega\|_\infty \int_t^{t+T} e^{-c_0 s}\int_0^s e^{c_0\tau}\|\dot{\theta}^*(\tau)\|d\tau ds \tag{4.31}$$

$$\int_t^{t+T}\|\tilde{\mathscr{Y}}(s)\|ds \leq \frac{\breve{k}}{c_0}(e^{-c_0 t} - e^{-c_0(t+T)})\|\tilde{\mathscr{Y}}(0)\| + \breve{k}\|\Omega\|_\infty \int_t^{t+T} e^{-c_0 s}\int_0^t e^{c_0\tau}\|\dot{\theta}^*(\tau)\|d\tau ds$$
$$+ \breve{k}\|\Omega\|_\infty \int_t^{t+T} e^{-c_0 s}\int_t^s e^{c_0\tau}\|\dot{\theta}^*(\tau)\|d\tau ds \tag{4.32}$$

$$\leq \frac{\breve{k}}{c_0}(e^{-c_0 t} - e^{-c_0(t+T)})\|\tilde{\mathscr{Y}}(0)\| + \frac{\breve{k}\|\Omega\|_\infty}{c_0}(e^{-c_0 t} - e^{-c_0(t+T)})\int_0^t e^{c_0\tau}\|\dot{\theta}^*(\tau)\|d\tau ds$$
$$+ \breve{k}\|\Omega\|_\infty \int_t^{t+T} e^{-c_0 s}\int_t^s e^{c_0\tau}\|\dot{\theta}^*(\tau)\|d\tau ds \tag{4.33}$$

Utilizing the inequality $(e^{-c_0 t} - e^{-c_0(t+T)}) \leq e^{-c_0 t}$, the inequality (4.33) reduces to,

$$\int_t^{t+T}\|\tilde{\mathscr{Y}}(s)\|ds \leq \frac{\breve{k}\|\tilde{\mathscr{Y}}(0)\|}{c_0}e^{-c_0 t} + \frac{\breve{k}\|\Omega\|_\infty}{c_0}e^{-c_0 t}\int_0^t e^{c_0\tau}\|\dot{\theta}^*(\tau)\|d\tau + \breve{k}\|\Omega\|_\infty \int_t^{t+T} e^{-c_0 s}\int_t^s e^{c_0\tau}\|\dot{\theta}^*(\tau)\|d\tau ds \tag{4.34}$$

Similar to the proof of boundedness of $\tilde{\mathscr{Y}}(t)$ [110], let us substitute the integral in the second term on

the right hand side of (4.34) as,

$$\int_0^t e^{-c_0(t-\tau)}\|\dot{\theta}^*(\tau)\|d\tau \leq \frac{\Delta^\ddagger e^{c_0}}{1-e^{-c_0}}\nu + \frac{\Delta^\ddagger e^{c_0}}{1-e^{-c_0}} \tag{4.35}$$

Substituting (4.35) in (4.34) yields,

$$\int_t^{t+T}\|\tilde{\mathscr{Y}}(s)\|ds \leq \frac{\breve{k}\|\tilde{\mathscr{Y}}(0)\|}{c_0} + \frac{\breve{k}\|\Omega\|_\infty\Delta^\ddagger e^{c_0}}{c_0(1-e^{-c_0})}\nu + \frac{\breve{k}\|\Omega\|_\infty\Delta^\ddagger e^{c_0}}{c_0(1-e^{-c_0})} + \breve{k}\|\Omega\|_\infty\int_t^{t+T} e^{-c_0 s}\int_t^s e^{c_0\tau}\|\dot{\theta}^*(\tau)\|d\tau ds \tag{4.36}$$

Utilizing the identity for change of sequence of integration [110], i.e.,

$$\int_t^{t+T} f(s)\int_t^s g(\tau)d\tau ds = \int_t^{t+T} g(\tau)\int_\tau^{t+T} f(s)ds d\tau \tag{4.37}$$

for (4.36), a further simplified inequality is obtained as given below.

$$\int_t^{t+T}\|\tilde{\mathscr{Y}}(s)\|ds \leq \frac{\breve{k}\|\tilde{\mathscr{Y}}(0)\|}{c_0} + \frac{\breve{k}\|\Omega\|_\infty\Delta^\ddagger e^{c_0}}{c_0(1-e^{-c_0})}\nu + \frac{\breve{k}\|\Omega\|_\infty\Delta^\ddagger e^{c_0}}{c_0(1-e^{-c_0})} + \breve{k}\|\Omega\|_\infty\int_t^{t+T} e^{c_0\tau}\|\dot{\theta}^*(\tau)\|\int_\tau^{t+T} e^{-c_0 s}ds d\tau \tag{4.38}$$

$$\leq \frac{\breve{k}\|\tilde{\mathscr{Y}}(0)\|}{c_0} + \frac{\breve{k}\|\Omega\|_\infty\Delta^\ddagger e^{c_0}}{c_0(1-e^{-c_0})}\nu + \frac{\breve{k}\|\Omega\|_\infty\Delta^\ddagger e^{c_0}}{c_0(1-e^{-c_0})} + \frac{\breve{k}\|\Omega\|_\infty}{c_0}\int_t^{t+T}\|\dot{\theta}^*(\tau)\|d\tau \tag{4.39}$$

Finally invoking Lemma 4.1, it is shown that,

$$\int_t^{t+T}\|\tilde{\mathscr{Y}}(s)\|ds \leq \underbrace{\frac{\breve{k}\|\Omega\|_\infty\Delta^\ddagger}{c_0}}_{B_1}\nu T + \underbrace{\frac{\breve{k}}{c_0}\Big(\|\tilde{\mathscr{Y}}(0)\| + \|\Omega\|_\infty\Delta^\ddagger\Big[\frac{e^{c_0}(\nu+1)}{1-e^{-c_0}}+1\Big]\Big)}_{B_0} \tag{4.40}$$

Hence, the resulting inequality $\int_t^{t+T}\|\mathscr{Y}(s)\|ds \leq B_1\nu T + B_0$ with $B_0,\ B_1 > 0$ derived to be finite constants prove $\tilde{\mathscr{Y}}(t) \in \mathcal{S}_1(\nu)$. The second part of the proof is complete.

To prove $\tilde{\mathscr{Y}}(t) \in \mathcal{S}_2(\nu)$, let us first recall the upper bound of $\tilde{\mathscr{Y}}(t)$ from (4.29) and thereafter invoke Hölder's inequality to compute the bound of the following integral,

$$\int_t^{t+T}\tilde{\mathscr{Y}}(s)^T\tilde{\mathscr{Y}}(s)ds \leq \|\tilde{\mathscr{Y}}\|_\infty\int_t^{t+T}\|\tilde{\mathscr{Y}}(s)\|ds$$

$$\leq \left(\frac{\breve{k}\|\Omega\|_\infty\Delta^\ddagger}{1-e^{-c_0}}\nu e^{c_0} + \frac{\breve{k}\|\Omega\|_\infty\Delta^\ddagger}{1-e^{-c_0}}e^{c_0} + \breve{k}\|\tilde{\mathscr{Y}}(0)\|\right)(B_1\nu T + B_0) \tag{4.41}$$

Finally, $\tilde{\mathscr{Y}}(t)$ is $\nu-$small in m.s.s that is $\tilde{\mathscr{Y}}(t) \in \mathcal{S}_2(\nu)$ with

$$\int_t^{t+T} \tilde{\mathscr{Y}}(s)^T \tilde{\mathscr{Y}}(s) ds \leq \underbrace{\left(\frac{\breve{k}\|\Omega\|_\infty \Delta^\ddagger B_1 e^{c_0}}{1-e^{-c_0}}\right)}_{B_4} \nu^2 T + \underbrace{\left(\frac{\breve{k}\|\Omega\|_\infty \Delta^\ddagger B_1 e^{c_0}}{1-e^{-c_0}} + \breve{k} B_1 \|\tilde{\mathscr{Y}}(0)\|\right)}_{B_3} \nu T + \underbrace{\left(\frac{\breve{k}\|\Omega\|_\infty \Delta^\ddagger e^{c_0} B_0}{1-e^{-c_0}}(\nu+1) + \breve{k}\|\tilde{\mathscr{Y}}(0)\| B_0\right)}_{B_2} \tag{4.42}$$

where, $B_2,\ B_3,\ B_4 > 0$ are calculated to be finite constants. The proof is complete. □ The following lemma is helpful in developing the adaptive law for finite time parameter estimation by utilizing the "prediction error" of the unknown parameter rather than the states. The notion of prediction error herein is defined with the help of the result stated in the below mentioned Lemma.

Lemma 4.5. *Considering the regressor matrix $\Phi(x,v)$ to be persistently exciting (PE) and the definitions of $R(t)$ and $S(t)$ in (4.15) and (4.16), the unknown parameter vector θ^* can be found as $\theta^* := R^{-1}(t)S(t)$. This definition of θ^* will play an important role in the development of the proposed finite time adaptation law guaranteeing a fast and accurate estimation.*

Proof.

The proof is straightforward and can be left for the readers. However, for the sake of completeness, the procedure to arrive at the final conclusion, that is, $\theta^* := R^{-1}(t)S(t)$ follows next. From their dynamics described in (4.15)-(4.16), the rudiments of linear system theory allows us to define the solutions of $R(t)$ and $S(t)$ as,

$$R(t) = \int_0^t e^{-\mathscr{K}(t-s)} \Omega(s) \Omega^T(s) ds \tag{4.43}$$

$$S(t) = \int_0^t e^{-\mathscr{K}(t-s)} \Omega(s) (\Omega_0(s) + x(s)) ds \tag{4.44}$$

The solution $\mathscr{Y}(t)$ of the differential equation (4.21) is described as,

$$\mathscr{Y}(t) := \int_0^t e^{-A(x,t)(t-s)} \Phi(x(s), v(s))^T \theta^* ds = \Omega^T(t)\theta^* \tag{4.45}$$

Since $\mathscr{Y} := \Omega_0 + x$ and substituting $(\Omega_0 + x) = \Omega^T\theta^*$ in the expression for $S(t)$ in (4.44) yields,

$$S(t) = \int_0^t e^{-\mathscr{K}(t-s)} \Omega(s) \Omega^T(s) \theta^* ds \tag{4.46}$$

From the solution of $R(t)$ in (4.43) and θ^* considered to be a vector with constant elements, the equality (4.46) reduces to $S(t) = R(t)\theta^*$. Pre-multiplying both sides by $R^{-1}(t)$ yields $\theta^* = R^{-1}(t)S(t)$. □ In what follows, it is shown that the adaptive parameter estimation strategy proposed does not rely on explicit calculation of matrix $R^{-1}(t)$ online and hence all involved numerical issues are circumvented.

Unlike the parameter update laws proposed in literature largely dependent on the identification error, the adaptive law presented herein is formulated on the basis of the parameter estimation error. At this stage, let us define the prediction of $S(t)$ as $\hat{S}(t) = R(t)\hat{\theta}(t)$ and hence the prediction error $\mathscr{E} := S(t) - R(t)\hat{\theta}$. Thereafter, unlike the commonly used robust gradient or least squares based adaptive laws and their normalized versions ([122] [110]), the parameter update law proposed herein is stated in the following proposition along with its signal stability properties guaranteeing finite time stability.

Proposition 4.1. *Let us consider the prediction error $\mathscr{E}(t) = S(t) - R(t)\hat{\theta}(t)$ with $R(t) > 0$ and $S(t)$ defined as solutions of (4.15) and (4.16), respectively. Assuming that the regressor matrix $\Phi(x, v)$ is PE such that $R(t) > \underline{\lambda}(R(t)) > \varpi > 0$, the proposed parameter estimation law given by,*

$$\dot{\hat{\theta}} = \Gamma_1 \frac{\mathscr{E}(t)}{\|\mathscr{E}(t)\|^{1/2}} + \Gamma_2 \int_0^t \frac{\mathscr{E}(s)}{\|\mathscr{E}(s)\|} ds \tag{4.47}$$

bears the following attributes; (i) finite time stability of $\tilde{\theta} = 0$ from any initial condition $\tilde{\theta}(0)$ characterized by an explicit settling time function $T_s(\tilde{\theta}(t_0 = 0), t_0 = 0)$ satisfying $0 \leq T_s(\tilde{\theta}(0), 0) < +\infty$(ii) $\tilde{\theta}(t) \in \mathcal{S}_1(\nu)$ and $\dot{\hat{\theta}}(t) \in \mathcal{S}_1(\nu)$ (for the case of intermittently changing unknown parameters) provided that a projection operator is utilized with the proposed adaptive law, (iii) $\tilde{\theta}(t) \in \mathcal{L}_1 \cap \mathcal{L}_\infty$ and $\dot{\hat{\theta}}(t) \in \mathcal{L}_1$ (for the case of variations with finite cardinality in system parameters and actuator failure patterns). Herein, $\underline{\lambda}(R(t))$ and ϖ denote the minimum eigen value of $R(t)$ and the level of excitation of the regressor matrix, respectively.

Proof of (i).

In this part, the claim of finite time convergence of the parameter estimation error $\tilde{\theta}$ to the origin is proved. To proceed further, in this part of the proof, the finite time convergence of $\tilde{\theta}(t)$ to the origin for every piecewise variation in the system and failure induced parameters defined by the vector θ^* is proved. The unknown parameters defined by θ^* is therefore a piecewise constant vector and hence $\dot{\theta}^* = 0$ for $t \in [T_h,\ T_{h+1})$, $h \in \mathbb{W}$ with initial time $T_0 = 0$. T_h is the time of occurrence of an actuator failure while T_{h+1} denotes the time at which the system is subjected to the next successive actuator failure pattern. From the foregoing arguments, it can now be assumed that $\dot{\theta}^* = 0$ holds, in a piecewise fashion though.

To prove the finite time stability, let us first define the vector $\tilde{\Theta} := \begin{bmatrix} \frac{\tilde{\theta}}{\|\tilde{\theta}\|^{\frac{1}{2}}} & \tilde{\theta}_a \end{bmatrix}^T$. Where, $\tilde{\theta}_a = -\Gamma_2 \int_0^t \frac{\mathscr{E}(s)}{\|\mathscr{E}(s)\|} ds$ is an auxiliary state variable chosen and whose usefulness would be evident in the sequel. Let us consider the Lyapunov function candidate $V_{\tilde{\Theta}} : \mathcal{S}_{\tilde{\Theta}} \subseteq \mathbb{R}^{2(m+p+1)} \setminus \{0\} \times [T_h,\ T_{h+1}) \to \mathbb{R}_+$

as $(\tilde{\Theta}, t) \mapsto \tilde{\Theta}^T P \tilde{\Theta}$. The first time derivative of $\tilde{\Theta}$ is calculated as follows,

$$\dot{\tilde{\Theta}} = \begin{bmatrix} \frac{1}{2}\|\tilde{\theta}\|^{-\frac{1}{2}}\dot{\tilde{\theta}} \\ \dot{\tilde{\theta}}_a \end{bmatrix} = \begin{bmatrix} \frac{1}{2}\|\tilde{\theta}\|^{-\frac{1}{2}}\left(-\Gamma_1\frac{\mathscr{E}}{\|\mathscr{E}\|^{\frac{1}{2}}} + \tilde{\theta}_a\right) \\ -\Gamma_2\frac{\mathscr{E}}{\|\mathscr{E}\|} \end{bmatrix} \tag{4.48}$$

Since, as per the definition of prediction error $\mathscr{E}(t)$, it can be reexpressed as $\mathscr{E}(t) = R(t)\tilde{\theta}$. Therefore substituting the same in (4.48) yields,

$$\dot{\tilde{\Theta}} \leq \|\tilde{\theta}\|^{-\frac{1}{2}} \begin{bmatrix} -\frac{\Gamma_1}{2}\frac{R\tilde{\theta}}{\sqrt{\overline{\lambda}(R)}\|\tilde{\theta}\|^{\frac{1}{2}}} + \frac{\tilde{\theta}_a}{2} \\ -\Gamma_2\frac{R\tilde{\theta}}{\overline{\lambda}(R)\|\tilde{\theta}\|^{\frac{1}{2}}} \end{bmatrix} \leq \|\tilde{\theta}\|^{-\frac{1}{2}} \underbrace{\left[\begin{array}{c|c} -\frac{\underline{\lambda}(R)}{2\sqrt{\overline{\lambda}(R)}}\Gamma_1 & \frac{1}{2}I_{m+p+1} \\ \hline -\frac{\underline{\lambda}(R)}{\overline{\lambda}(R)}\Gamma_2 & 0 \end{array}\right]}_{F} \begin{bmatrix} \frac{\tilde{\theta}}{\|\tilde{\theta}\|^{\frac{1}{2}}} \\ \tilde{\theta}_a \end{bmatrix} \tag{4.49}$$

Clearly, the matrix $F := \frac{1}{2}\left[\begin{array}{c|c} -\frac{\underline{\lambda}(R)}{\sqrt{\overline{\lambda}(R)}}\Gamma_1 & I_{m+p+1} \\ \hline -\frac{2\underline{\lambda}(R)}{\overline{\lambda}(R)}\Gamma_2 & 0 \end{array}\right]$ is Hurwitz in view of Lemma 4.3 which states $\|R(t)\| \geq \underline{\lambda}(R(t)) > \varpi > 0$. Here, ϖ denotes the level of excitation. Continuing with the stability proof, the time derivative of the Lyapunov function $V_{\tilde{\Theta}}$ is calculated as,

$$\dot{V}_{\tilde{\Theta}} = \tilde{\Theta}^T P\dot{\tilde{\Theta}} + \dot{\tilde{\Theta}}^T P\tilde{\Theta} \leq \|\tilde{\theta}\|^{-\frac{1}{2}}\tilde{\Theta}^T(F^TP + PF)\tilde{\Theta} \tag{4.50}$$

$$\leq -\|\tilde{\theta}\|^{-\frac{1}{2}}\tilde{\Theta}^T Q\tilde{\Theta} < 0 \tag{4.51}$$

The inequality (4.51) is derived using the fact that matrix F is Hurwitz and satisfies the Lyapunov criterion given by, $F^TP + FA = -Q$ with $Q > 0$. Now, from Rayleigh principle [109], $\|\tilde{\theta}\|^{\frac{1}{2}} \leq \|\tilde{\Theta}\|_2 < \underline{\lambda}^{-\frac{1}{2}}(P)V_{\tilde{\Theta}}^{\frac{1}{2}}$. Then $\dot{V}_{\tilde{\Theta}}$ (4.51) can be represented as,

$$\dot{V}_{\tilde{\Theta}} \leq -\|\tilde{\theta}\|^{-\frac{1}{2}}\underline{\lambda}(Q)\|\tilde{\Theta}\|_2^2 \leq -\underline{\lambda}^{\frac{1}{2}}(P)V_{\tilde{\Theta}}^{-\frac{1}{2}}\underline{\lambda}(Q)\|\tilde{\Theta}\|_2^2 \tag{4.52}$$

$$\leq -\frac{\underline{\lambda}^{\frac{1}{2}}(P)\underline{\lambda}(Q)}{\overline{\lambda}(P)}V_{\tilde{\Theta}}^{\frac{1}{2}} \leq -\Gamma\sqrt{V_{\tilde{\Theta}}} \tag{4.53}$$

where $\Gamma = \frac{\underline{\lambda}^{\frac{1}{2}}(P)\underline{\lambda}(Q)}{\overline{\lambda}(P)}$, $\overline{\lambda}(\cdot)$ and $\underline{\lambda}(\cdot)$ denote the maximum and minimum eigen values of a square matrix. Since the transformed error dynamics $\tilde{\Theta}$ is continuous, it follows that $\tilde{\Theta}$ decays to zero in finite time, which in turn implies that the parameter estimation error $\tilde{\theta}(t)$ converge to the origin in finite time. Therefore, using Theorem 2.1 in [106], and from (4.53), the pair $(\tilde{\theta}(t),\ \tilde{\theta}_a)$ are inferred to be finite time stable. This completes the proof of finite time stability of $\tilde{\Theta} = 0$.

To formulate the settling time function T_s, for simplicity, let us consider the time interval $t \in [T_0,\ T_1)$

for $h = 0$ with initial time $t_0 = T_0 = 0$ and $T_s \leq T_1$. Thereafter, it is stated that $V_{\tilde{\Theta}}(t_0 = 0) = V_{\tilde{\Theta}}(0)$ holds. The expression for T_s is calculated by considering $V_{\tilde{\Theta}}(T_s) = 0$ due to negative definiteness of $\dot{V}_{\tilde{\Theta}}$. From (4.53) it follows that,

$$\begin{aligned} &\dot{V}_{\tilde{\Theta}} + \Gamma\sqrt{V_{\tilde{\Theta}}} \leq 0 \\ &\Rightarrow \int_{V_{\tilde{\Theta}}(0)}^{V_{\tilde{\Theta}}(T_s)} \frac{dV_{\tilde{\Theta}}}{\sqrt{V_{\tilde{\Theta}}}} \leq -\Gamma(T_s - 0) \\ &\Rightarrow 2(\sqrt{V_{\tilde{\Theta}}(T_s)} - \sqrt{V_{\tilde{\Theta}}(0)}) \leq -\Gamma T_s. \end{aligned} \tag{4.54}$$

As $V_{\tilde{\Theta}}(T_s) = 0$, it is substituted in the above inequality, to get closed form expression for the convergence (settling) time T_s in terms of initial conditions and gains $\Gamma_1,\ \Gamma_2 > 0$ as defined below.

$$T_s(\tilde{\theta}(t_0 = 0), t_0 = 0) \leq \frac{2V_{\tilde{\Theta}}(0)^{\frac{1}{2}}}{\Gamma} \tag{4.55}$$

Therefore, (4.55) reflects that the relevant parameter characterizing finite time convergence, is the bound on the convergence time given by T_s. On the contrary, such closed form definition of the upper bound on the convergence time for any arbitrary initial condition is not possible in case of commonly existing asymptotic (exponentially converging) parameter estimators in literature. The proof is complete. □

Proof of (ii).

The solution of $R(t)$ in (4.44), can be expanded by solving the involved integral followed by invoking Hölder's inequality and Lemma 4.2, yielding,

$$R(t) \leq e^{-\mathscr{K} I_{m+p+1} t} \frac{\|\Omega(t)\|_\infty^2}{\mathscr{K}} (e^{\mathscr{K} I_{m+p+1} t} - I_{m+p+1}) \leq \frac{\|\Omega(t)\|_\infty^2}{\mathscr{K}} I_{m+p+1} < \infty \tag{4.56}$$

Hence, $\|R(t)\|_\infty = \|\Omega(t)\|_\infty^2/\mathscr{K}$ and $R(t),\ \dot{R}(t) \in \mathcal{L}_\infty$. In this section of the proof, we do consider the occurrence of infinitely varying actuator failure patterns resulting in intermittently varying unknown parameters affecting the system. Therefore, the time derivative of θ^* is considered to be nonzero, i.e., $\dot{\theta}^* \neq 0$ and satisfies the property stated in Lemma 4.1. Further, use of a projection operator is necessary in order to ensure $\tilde{\theta}(t) \in \mathcal{L}_\infty$ and other beneficial stability properties which would be clear as the proof procedure herein develops. With subsequent application of Rayleigh's inequality, the following can be derived utilizing a similar procedure as in the earlier proof yielding (4.54) with an additional term in $\dot{\theta}^*$,

$$\dot{V}_{\tilde{\Theta}} \leq -\underbrace{\Gamma\sqrt{\underline{\lambda}(P)}}_{\overline{\Gamma}} \|\tilde{\Theta}\| + \overline{\lambda}(P)\|\dot{\theta}^*\| \tag{4.57}$$

By integrating (4.57) on both sides and application of Hölder's inequality from $t \sim t+T$ leads to,

$$\int_t^{t+T} \dot{V}_{\tilde{\Theta}} ds \leq -\overline{\Gamma} \int_t^{t+T} \|\tilde{\Theta}\| ds + \overline{\lambda}(P) \int_t^{t+T} \|\dot{\theta}^*\| ds \tag{4.58}$$

$$\int_t^{t+T} \|\tilde{\Theta}\| ds \leq \frac{\overline{\lambda}(P)}{\sqrt{\underline{\lambda}(P)}\Gamma} \left(\|\tilde{\Theta}(t)\|^2 - \|\tilde{\Theta}(t+T)\|^2 \right) + \frac{\overline{\lambda}(P)}{\Gamma\sqrt{\underline{\lambda}(P)}} \int_t^{t+T} \|\dot{\theta}^*\| ds \tag{4.59}$$

$$\leq \frac{\overline{\lambda}(P)}{\sqrt{\underline{\lambda}(P)}\Gamma} \|\tilde{\Theta}\|_\infty^2 + \frac{\overline{\lambda}(P)}{\sqrt{\underline{\lambda}(P)}\Gamma} \left(\sqrt{m+p+1}\Delta^\dagger(\nu T+1) \right) \tag{4.60}$$

$$\leq \underbrace{\overline{\lambda}(P)\Gamma^{-1}\Delta^\dagger \sqrt{\overline{\lambda}(P)(m+p+1)}}_{B_6} \nu T + \underbrace{\overline{\lambda}(P)\Gamma^{-1}\Delta^\dagger \sqrt{\overline{\lambda}(P)(m+p+1)} + \Gamma^{-1}\overline{\lambda}(P)^{\frac{3}{2}} \|\tilde{\Theta}\|_\infty^2}_{B_5} \tag{4.61}$$

Therefore, from (4.61), it is proved that $\tilde{\Theta} \in \mathcal{S}_1(\nu)$. The last inequality (4.61) is derived using the result from Lemma 4.1.Using the fact that $\frac{\|\tilde{\theta}\|}{\|\tilde{\theta}\|^{\frac{1}{2}}} \leq \|\tilde{\Theta}\|$ and thereafter invoking integral inequalities, it is straightforward to conclude that the signal $\frac{\tilde{\theta}(t)}{\|\tilde{\theta}(t)\|^{\frac{1}{2}}} \in \mathcal{S}_1(\nu)$. Similarly, since the auxiliary variable $\tilde{\theta}_a$ also satisfies $\|\tilde{\theta}_a\| \leq \|\tilde{\Theta}\|$, the property $\tilde{\theta}_a(t) \in \mathcal{S}_1(\nu)$ follows.

Derivation of the signal space to which $\tilde{\theta}$ belongs is shown in the following. The claim is to prove $\tilde{\theta} \in \mathcal{S}_1(\nu)$. Therefore, utilizing that fact that use of a projection operator yield a bounded parameter estimation and the Hölder's inequality, the following is obtained.

$$\int_t^{t+T} \|\tilde{\theta}(s)\| ds \leq \|\tilde{\theta}\|_\infty^{\frac{1}{2}} \int_t^{t+T} \left\| \frac{\tilde{\theta}(s)}{\|\tilde{\theta}(s)\|^{\frac{1}{2}}} \right\| ds \leq \underbrace{\|\tilde{\theta}\|_\infty^{\frac{1}{2}} B_6}_{B_8} \nu T + \underbrace{\|\tilde{\theta}|_\infty^{\frac{1}{2}} B_5}_{B_7} \tag{4.62}$$

Hence, from (4.62), the claim follows that the parameter estimation error $\tilde{\theta}(t)$ is absolute integrable, i.e., $\tilde{\theta}(t) \in \mathcal{S}_1(\nu)$.

Now what remains, is to show that $\dot{\hat{\theta}}(t) \in \mathcal{S}_1(\nu)$. With this objective, the integral of the parameter update law is considered followed by the application of Minkowski inequality as shown below,

$$\int_t^{t+T} \|\dot{\hat{\theta}}\| ds \leq \frac{\overline{\lambda}(\Gamma_1)\|R\|_\infty}{\sqrt{\underline{\lambda}(R)}} \int_t^{t+T} \left\| \frac{\tilde{\theta}(s)}{\|\tilde{\theta}(s)\|^{\frac{1}{2}}} \right\| ds + \int_t^{t+T} \|\tilde{\theta}_a(s)\| ds \tag{4.63}$$

$$\leq \underbrace{\left(\frac{\overline{\lambda}(\Gamma_1)\|R\|_\infty}{\sqrt{\underline{\lambda}(R)}} + 1 \right) B_6}_{B_{10}} \nu T + \underbrace{\left(\frac{\overline{\lambda}(\Gamma_1)\|R\|_\infty}{\sqrt{\underline{\lambda}(R)}} + 1 \right) B_5}_{B_9} \leq B_{10}\nu T + B_9 \tag{4.64}$$

From (4.64) and the foregoing discussions it is obvious now to conclude $\dot{\hat{\theta}}(t) \in \mathcal{S}_1(\nu)$. The proof of (ii) is complete. □

Proof of (iii).
To prove: $\tilde{\theta}(t),\ \dot{\hat{\theta}}(t) \in \mathcal{L}_1$, provided the cardinality of occurrence of changes in unknown parameters duly induced in the event of uncertain actuator failures is finite. As a corollary to the results of Lemma 4.1, it has already been stated in Remark 4.1 that $\dot{\theta}^*(t)$ is absolutely integrable, i.e. $\dot{\hat{\theta}}^*(t) \in \mathcal{L}_1[0, \infty)$ (the maximal interval of existence is considered to be $[0,\ \infty)$ in the case of finite occurrence of actuator failures. Following the same procedure as in the proof of Proposition 4.1(ii) and repeated citing of the $\mathcal{L}_1-$integrability property of $\dot{\theta}^*(t)$ proves the claim. The proof is easy and hence its details are avoided to support a concise presentation. □

Remark 4.2. *The results of Proposition 4.1 can be utilized to infer the stability property of $\mathscr{E}(t)$. Since $\mathscr{E}(t) = R(t)\tilde{\theta}(t)$, usage of the derived result stating $R(t) \in \mathcal{L}_\infty$ along with $\tilde{\theta} \in \mathcal{S}_1(\nu)$ proves that $\mathscr{E}(t)$ is absolutely integrable, i.e., $\mathscr{E}(t) \in \mathcal{S}_1(\nu)$. Moving to the case of finite changes in actuator failure patterns reflecting the case of finite actuator failures, it is easy to infer that $\mathscr{E}(t) \in \mathcal{L}_1[0,\ \infty) \cap \mathcal{L}_\infty[0,\ \infty)$ with similar arguments and the property $\dot{\theta}^*(t) \in \mathcal{L}_1[0,\ \infty)$. Further, the signal $\dot{\mathscr{E}}$ is also bounded which directs the property that $\dot{\tilde{\theta}}(t) \in \mathcal{L}_\infty$. Therefore, it is concluded from signal convergence lemma [122] that both $\tilde{\theta}(t)$ and $\dot{\tilde{\theta}}$ characterize asymptotic convergence to the origin. This attribute of the proposed estimation scheme is highly beneficial for real time applications since a significant improvement in the estimation performance is achieved without any substantial increment in the control usage. Such an advantage directly translates to the enhancement in output transient performance as well.*

Remark 4.3. *In addition, applying a homogeneity transformation $\mathscr{T}_k : (t,\ \tilde{\theta}) \mapsto (kt,\ k^{3-i}\tilde{\theta})$ to the unperturbed parameter estimation error dynamics derived from (4.48), yields the degree of homogeneity of the associated vector fields to be $-1 < 0$. Hence, from the definition of finite time stability based on the concept of homogeneity [106, 132, 135] (negative homogeneity of vector fields+asymptotic stability of the dynamics⇒Finite Time Stability), the estimated parameter $\hat{\theta}(t)$ converges to its actual value θ^* in finite time. The proposed estimator offers the advantages of fast and accurate estimation in addition to a precise calculation of the convergence rate. This result is very helpful in calculating a lower bound on the transit time/elapse time T^* between two successive changes in the actuator failure pattern. Therefore, when the minimum time between consecutive variations in failure induced parameters/system parameters is greater than the calculated T^*, piecewise output asymptotic stability to the origin as well as asymptotic and finite time convergence of the tracking error dynamics and the parameter estimation error $\tilde{\theta}(t)$, respectively over all time $t > 0$ is ensured. In a nut shell, the proposed estimation scheme offers a fast, accurate and effective estimation of non-smooth time varying unknown parameters. These estimated parameters when fed to the controller for subsequent compensation, yields a robust and improved output performance of the closed loop system.*

4.2.3.2 Controller Design

The controller is designed under a backstepping framework guaranteeing ISS with respect to parameter estimation error and its time derivative as disturbance inputs to the controlled closed loop

system. The synthesis of the control law starts with the definition of the tracking error variables as,

$$z_1 = x_1 - y_r, \tag{4.65}$$

$$z_i = x_i - \alpha_{i-1} - y_r^{(i-1)} \tag{4.66}$$

where $i = \overline{2, \wp}$. Now utilizing the plant dynamics in (4.7), and taking the first time derivative of the error variables yields,

$$\dot{z}_i = z_{i+1} + \alpha_i + f_i(\bar{x}_i)\theta_2^* - \dot{\alpha}_{i-1} \tag{4.67}$$

$$\dot{z}_\wp = f_0(x,\eta) + f_\wp(x,\eta)^T\theta_2^* + \theta_1^* v + \beta^T\theta_3^* - \dot{\alpha}_{\wp-1} \tag{4.68}$$

Here $i = \overline{1, \wp - 1}$. The variables α_i are the virtual control inputs stabilizing each of the tracking error subsystem dynamics in z_i. These subsystem dynamics are described by the set of differential equations (4.66)-(4.67). The stabilizing functions α_i for each of the ith step is given by (4.68).

$$\alpha_i = -z_{i-1} - c_i z_i - \bar{c}_i\|\psi_i\|^2 z_i - g_i\left\|\frac{\partial \alpha_{i-1}}{\partial \hat{\theta}_2}\right\|^2 z_i - \psi_i^T\hat{\theta}_2 + \sum_{k=1}^{i-1}\Big(\frac{\partial \alpha_{i-1}}{\partial x_k}x_{k+1} + \frac{\partial \alpha_{i-1}}{\partial y_r^{(k-1)}}y_r^{(k)}\Big) \tag{4.69}$$

with $i = \overline{1, \wp - 1}$ and $\psi_i := f_i(\bar{x}_i) - \sum_{k=1}^{i-1}\frac{\partial \alpha_{i-1}}{\partial x_k}f_k(\bar{x}_k)$. In Step $\wp$, the controller design is initiated by defining the $z_\wp$-dynamics in an expanded form with the actual control law v, as follows.

$$\dot{z}_\wp = f_0(x,\eta) + f_\wp(x,\eta)^T\hat{\theta}_2 + \beta^T\hat{\theta}_3 + \hat{\theta}_1 v + \tilde{\theta}_1 v + \theta_1^* v - y_r^{(\wp)} - \sum_{k=1}^{\wp-1}\Big(\frac{\partial \alpha_{\wp-1}}{\partial x_k}x_{k+1} - \frac{\partial \alpha_{\wp-1}}{\partial y_r^{(k-1)}}y_r^{(k)}\Big)$$
$$+ \Big(\beta^T\tilde{\theta}_3 + \psi_\wp^T\tilde{\theta}_2 - \frac{\partial \alpha_{\wp-1}}{\partial \hat{\theta}_2}\dot{\hat{\theta}}_2\Big) \tag{4.70}$$

The final control law to stabilize the $z_\wp-$dynamics is given by,

$$v(t) = \frac{1}{\hat{\theta}_1}(-f_0(x,\eta) - f_\wp(x,\eta)^T\hat{\theta}_2 - \beta^T\hat{\theta}_3 - z_{\wp-1} + \sum_{k=1}^{\wp-1}\Big(\frac{\partial \alpha_{\wp-1}}{\partial x_k}x_{k+1} - \frac{\partial \alpha_{\wp-1}}{\partial y_r^{(k-1)}}y_r^{(k)}\Big) + y_r^{(\wp)}) +$$
$$\ell^{-1}\big(-c_\wp z_\wp - \bar{c}_\wp\big(|v_1|^2 + \|\beta\|^2 + \|\psi_\wp\|^2\big)z_\wp - g_\wp\Big\|\frac{\partial \alpha_{\wp-1}}{\partial \hat{\theta}_2}\Big\|^2 z_\wp\big) \tag{4.71}$$

The control design procedure is involving and is not discussed here in details for the sake of compactness. Instead, the reader is referred to Section 3.2.2.2 for details of derivation of the control law $v(t)$.
A schematic block diagrammatic implementation of the proposed finite time parameter estimation based FTC is shown in Figure 4.1.

4.2.4 Stability Analysis

At this juncture, a couple of statements and consequences of pre-design assumptions will be elucidated in a compact form prior to the main results. From the design assumptions, it is known that

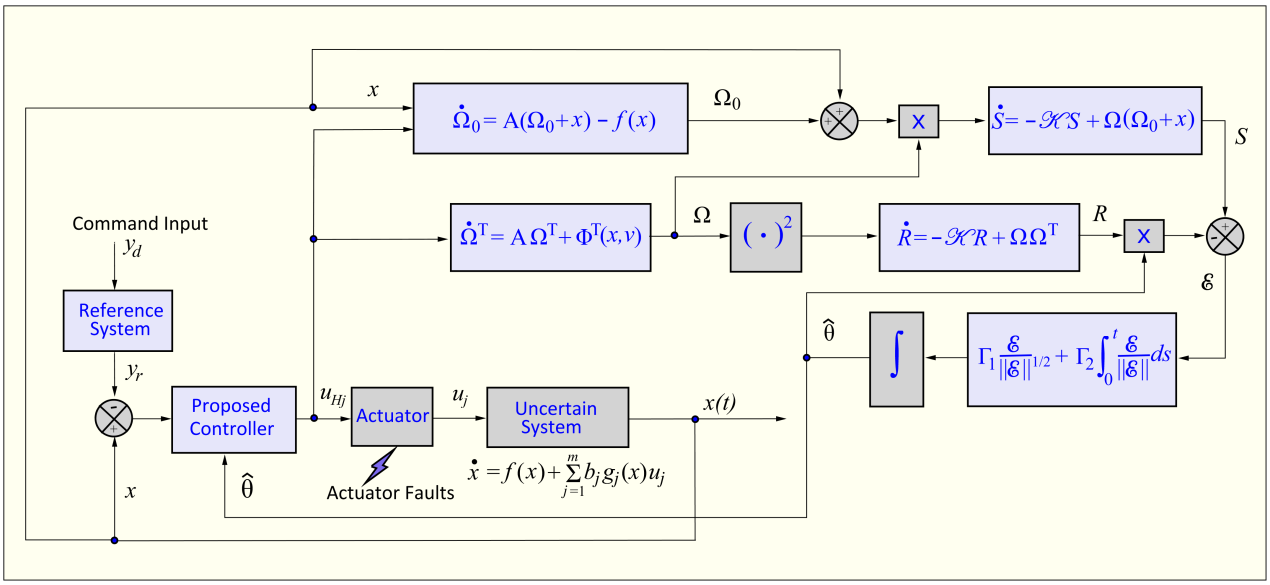

Figure 4.1: Block diagrammatic representation of the proposed FTAC strategy

the unknown parameter vector θ^* belong to a known convex and compact set $\mathcal{S}_{\theta^*}$. Hence, as a result, it is natural to conclude from property (iii) in Lemma 3.2 that a projection operated adaptation law ensures boundedness of parameter estimation error $\tilde{\theta}(t)$ within the convex compact set $\mathcal{S}_{\theta^*}$ defined by the known upper and lower bounds of the unknown parameter vector. Therefore the upper-bound on the parameter estimation error $\tilde{\theta}(t)$ is given by,

$$\|\tilde{\theta}\| \leq \sqrt{(\sum_{j=1}^{m} \overline{b}_j - \ell)^2 + \kappa_{\max}^2 + 4\sum_{j=1}^{m} \overline{b}_j^2 \bar{u}_j^2} := \overline{\theta},\ \mu = \overline{1,\ p+m+1} \tag{4.72}$$

where, $\overline{b}_j,\ \kappa_{\max},\ \bar{u}_j$ for $j = \overline{1, m}$ are constants with their respective definitions provided in the section on design assumptions.

Now, to this end, the dynamical description of the closed loop system under the action of the proposed adaptive control is required to set the stage for presenting the main results. In this direction, substituting the stabilizing functions α_i in (4.69), the control input $v(t)$ given by (4.71) and the parameter estimation law $\dot{\hat{\theta}}_{(\mu)}(t)$ in (4.47) in Proposition 4.1, into the fault parameterized system dynamics (4.7), thereby yielding,

$$\dot{z} = \underbrace{\begin{bmatrix} -(c_1+s_1) & 1 & \dots & 0 \\ -1 & -(c_2+s_2) & \dots & 0 \\ \vdots & \dots & \dots & 1 \\ 0 & \dots & -1 & -(c_\wp + s_\wp)\frac{b^*}{\ell} \end{bmatrix}}_{\mathcal{A}} z + \underbrace{\begin{bmatrix} 0 & \psi_1^T & 0 \\ 0 & \psi_2^T & 0 \\ \vdots & \vdots & \vdots \\ v_1 & \psi_\wp^T & \beta^T \end{bmatrix}}_{B_{\theta^*}} \tilde{\theta} + \underbrace{\begin{bmatrix} 0 \\ -\frac{\partial \alpha_1}{\partial \hat{\kappa}} \\ \vdots \\ -\frac{\partial \alpha_{\wp-1}}{\partial \hat{\kappa}} \end{bmatrix}}_{B_{\dot{\hat{\kappa}}}} \dot{\hat{\kappa}} \tag{4.73}$$

where $z := [\{z_i\}_{i=1}^{\wp}]^T$ is the tracking error vector and the matrices in (4.73) are denoted by $\mathcal{A}(x,t) \in \mathbb{R}^{\wp\times\wp}$, $B_{\theta^*} \in \mathbb{R}^{\wp\times(p+m+1)}$ and $B_{\hat{\kappa}} \in \mathbb{R}^{\wp}$. For simplicity of representation, the short hand notation s_i in the matrix $\mathcal{A}$, is used for the following expressions given below.

$$s_1 = \bar{c}_1\|\psi_1\|^2,\ s_i = \bar{c}_2\|\psi_i\|^2 + g_i\left\|\frac{\partial\alpha_{i-1}}{\partial\hat{\kappa}}\right\|^2$$
$$s_\wp = \bar{c}_\wp(\|\psi_\wp\|^2 + |v_1|^2 + \|\beta\|^2) + g_\wp\left\|\frac{\partial\alpha_{\wp-1}}{\partial\hat{\kappa}}\right\|^2$$

As defined earlier, the parameters $c_i,\ \bar{c}_i$ and g_j for $i = \overline{1,\wp}$ and $j = \overline{2,\wp}$ are positive design constants chosen by the designer. It is now possible to state the main results of this paper in the following theorem.

Theorem 4.2. *Let us consider the output tracking error dynamics in* (4.72) *obtained under the action of the control law* (4.71) *and the finite time parameter adaptation law* $\dot{\hat{\theta}}(t)$ *in* (4.47). *By virtue of the design assumptions in section 4.2.2.1 and further assuming that the system is affected by infinite actuator failures, the following results are stated: (i) Closed loop signal boundedness for all* $t \in [0,\ \infty)$ *as long as the minimum transit time* T^* *between successive changes in actuator failure patterns is strictly nonzero and positive; (ii) The tracking error* $z_1(t) = y(t) - y_r(t) \in \mathcal{S}_1(\nu)$, *that is, it is small in the absolute sense; (iii) Asymptotic convergence of tracking error to the origin in the case of finite number of actuator failures or faults.*

Proof of (i).
From (4.72), the parameter estimation error $\tilde{\theta} \in \mathcal{L}_\infty[0,\ \infty)$. Further, the filtered regressor matrix $\Omega(t) \in \mathcal{L}_\infty[0,\ \infty)$ is concluded from Lemma 4.2. Lemma 4.4 and (4.29) shows the boundedness of $\tilde{\mathscr{Y}}, i.e., \tilde{\mathscr{Y}} \in \mathcal{L}_\infty[0,\ \infty)$ as long as ν is finite. Since $\mathscr{E} = R(t)\tilde{\theta} \in \mathcal{L}_\infty$ owing to the boundedness of $R(t)$ from (4.56) and $\tilde{\theta}$, the signal $\dot{\hat{\theta}}$ is bounded or $\dot{\hat{\theta}} \in \mathcal{L}_\infty$. These properties render a closed-loop system (4.73) which is similar to the tracking error system dynamics in (3.41). Hence using (3.29),(3.30), (3.36) and invoking the sum of squares inequality with $\theta^* := [\theta_1^*\ \theta_2^*\ \theta_3^*]^T =: [b\ \kappa^*\ \bar{u}]^T$ yields,

$$\frac{d}{dt}\left(\frac{\|z\|^2}{2}\right) \leq -\underline{\lambda}(\mathcal{Q})\|z\|^2 + \frac{1}{4}\left[\frac{\|\tilde{\theta}\|}{\bar{\bar{c}}} + \frac{\|\dot{\hat{\theta}}\|^2}{\bar{g}}\right] \tag{4.74}$$

where $\mathcal{Q} := \text{diag}\{c_1, \ldots, c_{\wp-1}, \frac{\theta_1^*}{\ell}c_\wp\} > 0$, $\bar{c} := \sum_{i=1}^{\wp}\left(\frac{1}{\bar{c}_i}\right)^{-1}$, $\bar{\bar{c}} := \min\{\bar{c}, \bar{c}_\wp, c_\wp\}$ and $\bar{g} := \left(\sum_{i=2}^{\wp}\frac{1}{\bar{g}_i}\right)^{-1}$. The inequality (4.74) holds for all $t \geq 0$ in the event of occurrence of intermittent actuator faults/failures within the time interval $[0,\ \infty)$. The foregoing conclusions on stability properties of the estimation error $\tilde{\theta}$ and its time derivative $\dot{\hat{\theta}}$ allows us to infer $z(t) \in \mathcal{L}_\infty[0,\ \infty)$ with,

$$\|z(t)\| \leq \|z(0)\|e^{-\underline{\lambda}(\mathcal{Q})t} + \frac{1}{2\sqrt{\underline{\lambda}(\mathcal{Q})}}\left[\frac{\|\tilde{\theta}\|_\infty^2}{\bar{\bar{c}}} + \frac{\|\dot{\hat{\theta}}\|_\infty^2}{\bar{g}}\right]^{\frac{1}{2}} \tag{4.75}$$

Now since the reference trajectory $y_r(t)$ and its successive time derivatives are bounded and belong to a compact set, $x(t) \in \mathcal{L}_\infty[0,\ \infty)$. Besides, as per the design assumptions, $\eta(t)$ is bounded with

$x(t) \in \mathcal{L}_\infty[0,\ \infty)$, the virtual control laws α_i (4.69) and the actual control law (4.71) are also bounded. Therefore, the closed loop system is stable. □

Proof of (ii).

To proceed, let us rewrite the closed loop tracking error dynamics (4.73) as,

$$\dot{z} = \mathcal{A}(z,\hat{\theta},t)z + B_{\theta^*}(z,\hat{\theta},t)\tilde{\theta} + B_{\dot{\hat{\kappa}}}(z,\hat{\theta},t)\dot{\hat{\kappa}} \tag{4.76}$$

where, $\mathcal{A}(z,\hat{\theta},t) = \begin{bmatrix} -(c_1+s_1) & 1 & \dots & 0 \\ -1 & -(c_2+s_2) & \dots & 0 \\ \vdots & \dots & \dots & 1 \\ 0 & \dots & -1 & -(c_{\wp}+s_{\wp})\frac{b^*}{\ell} \end{bmatrix}$ and $B_{\theta^*} = \begin{bmatrix} 0 & \psi_1^T & 0 \\ 0 & \psi_2^T & 0 \\ \vdots & \vdots & \vdots \\ v_1 & \psi_{\wp}^T & \beta^T \end{bmatrix}$.

Before the proof begins, the reader should bear in mind that unlike the usage of Lyapunov stability approach to prove the energy integrability of the tracking error $z(t)$ in direct adaptive control, herein the derivation of $z(t) \in \mathcal{S}_1(\nu)(z(t) \in \mathcal{L}_1(\nu)$ in the case of finite number of changes in the actuator failure pattern) is not so straightforward. So let us begin by introducing an additional state variable $\chi^T(t) \in \mathbb{R}^{\wp\times(m+p+1)}$, whose dynamics are described by,

$$\dot{\chi}^T = \mathcal{A}(z,\hat{\theta},t)\chi^T + B_{\theta^*}(z,\hat{\theta},t) \tag{4.77}$$

From the concepts of linear systems theory, the solution of the above additional subsystem is derived to be,

$$\chi^T(t) = e^{-\mathcal{A}t}\chi^T(0) + \int_0^t e^{-\mathcal{A}(t-s)}B_{\theta^*}(s)ds \tag{4.78}$$

From Lemma 3.3, it is concluded that $\|e^{-\mathcal{A}(z,\hat{\theta},t)t}\| \leq \breve{\breve{k}}e^{-\bar{c}_0 t}$ where $\breve{\breve{k}},\ \bar{c}_0 > 0$ are finite constants. Since all the closed loop signals exhibit a stable behavior from the immediate earlier proof, B_{θ^*} is also bounded. Therefore,

$$\|\chi\| \leq \|\chi(0)\| + \frac{\breve{\breve{k}}\|B_{\theta^*}\|_\infty}{\bar{c}_0} \tag{4.79}$$

From (4.79), $\chi \in \mathcal{L}_\infty$. Further, let us define another additional variable ϑ as,

$$\vartheta(t) = z(t) - \chi^T\tilde{\theta}(t) \tag{4.80}$$

Now with the above definition of $\vartheta(t)$, if $\chi^T\tilde{\theta}(t),\ \vartheta(t) \in \mathcal{S}_1(\nu)$, it directs us to conclude $z(t) \in \mathcal{S}_1(\nu)$. This result is derived using the *closed under addition* property of function spaces. First, we set out to prove $\chi^T\tilde{\theta}(t) \in \mathcal{S}_1(\nu)$ followed by the proof of $\vartheta(t) \in \mathcal{S}_1(\nu)$.

(i) ***To prove:*** $\chi^T\tilde{\theta}(t) \in \mathcal{S}_1(\nu)$.

Let us consider the following integral and thereafter apply Hölder's inequality along with (4.79) yields,

$$\int_{t}^{t+T} \|\chi^T\tilde{\theta}\|ds \leq \|\chi\|_\infty \int_{t}^{t+T} \|\tilde{\theta}\|ds \tag{4.81}$$

Citing (4.62) stating $\tilde{\theta}(t) \in \mathcal{S}_1(\nu)$, it is proved that $\chi^T\tilde{\theta}(t) \in \mathcal{S}_1(\nu)$.

(ii) ***To prove:*** $\vartheta(t) \in \mathcal{S}_1(\nu)$.

The proof requires the dynamics of the auxiliary variable $\vartheta(t)$ and hence its dynamical description is deduced as follows,

$$\begin{aligned}\dot{\vartheta} &= \dot{z} - \dot{\chi}^T\tilde{\theta} + \chi^T\dot{\hat{\theta}} - \chi^T\dot{\theta}^* \\ &= \mathcal{A}z + B_{\theta^*}\tilde{\theta} + B_{\hat{\kappa}}\dot{\hat{\kappa}} - \mathcal{A}\chi^T\tilde{\theta} - B_{\theta^*}\tilde{\theta} + \chi^T\dot{\hat{\theta}} - \chi^T\dot{\theta}^* \\ &= \mathcal{A}\vartheta + B_{\hat{\kappa}}\dot{\hat{\kappa}} + \chi^T\dot{\hat{\theta}} - \chi^T\dot{\theta}^*\end{aligned} \tag{4.82}$$

The solution of (4.82) is obtained as,

$$\begin{aligned}\vartheta(t) = e^{-\mathcal{A}t}\vartheta(0) &+ \int_0^t e^{-\mathcal{A}(t-s)}B_{\hat{\kappa}}(z(s),\hat{\theta}(s),s)\dot{\hat{\kappa}}(s)ds \\ &+ \int_0^t e^{-\mathcal{A}(t-s)}\chi^T(s)\dot{\hat{\theta}}(s)ds - \int_0^t e^{-\mathcal{A}(t-s)}\chi^T(s)\dot{\theta}^*(s)ds\end{aligned} \tag{4.83}$$

To this end, from the deduced information about the closed loop system, it is known that $\chi(t),\ B_{\theta^*} \in \mathcal{L}_\infty[0,\ \infty)$. Since, our interest lies in deriving the signal property of $\vartheta(t)$, we proceed by imposing the norm operator on both sides of (4.83) followed by the application of Lemma 3.3 and Hölder's inequality, ultimately results in,

$$\begin{aligned}\|\vartheta(t)\| \leq \underbrace{\breve{\breve{k}}e^{-\bar{c}_0 t}\|\vartheta(0)\|}_{\text{I}} &+ \underbrace{\breve{\breve{k}}\|B_{\hat{\kappa}}\|_\infty \int_0^t e^{-\bar{c}_0(t-s)}\|\dot{\hat{\kappa}}(s)\|ds}_{\text{II}} \\ &+ \underbrace{\breve{\breve{k}}\|\chi\|_\infty \int_0^t e^{-\bar{c}_0(t-s)}\|\dot{\hat{\theta}}(s)\|ds}_{\text{III}} + \underbrace{\breve{\breve{k}}\|\chi\|_\infty \int_0^t e^{-\bar{c}_0(t-s)}\|\dot{\theta}^*(s)\|ds}_{\text{IV}}\end{aligned} \tag{4.84}$$

Integrating both sides of inequality (4.84) from $t \sim t+T$ and thereafter calculating the integral to be finite (for finite νT) would prove the claim. Therefore, for simplicity and ease of understanding, we will seperately take the integrals of the terms `I-IV` and prove each one of them to be finite (for finite νT) to arrive at our claim. The following integrals of `I-IV` are calculated in the same order aiming at

our interests discussed above as shown below,

$$\int_{t}^{t+T} \breve{\breve{k}} e^{-\bar{c}_0 s} \|\vartheta(0)\| ds = \frac{\breve{\breve{k}}}{\bar{c}_0} \|\vartheta(0)\| < \infty \tag{4.85}$$

Integration of II in(4.84) from $t \sim t+T$ leads to the following.

$$\begin{aligned}
&\int_{t}^{t+T} \breve{\breve{k}} \|B_{\dot{\hat{\kappa}}}\|_\infty \int_{0}^{s} e^{-\bar{c}_0(s-\tau)} \|\dot{\hat{\kappa}}(\tau)\| d\tau ds \leq \breve{\breve{k}} \|B_{\dot{\hat{\kappa}}}\|_\infty \int_{t}^{t+T} \int_{0}^{s} e^{-\bar{c}_0(s-\tau)} \|\dot{\hat{\kappa}}(\tau)\| d\tau ds \\
&\leq \breve{\breve{k}} \|B_{\dot{\hat{\kappa}}}\|_\infty \int_{t}^{t+T} e^{-\bar{c}_0 s} \int_{0}^{t} e^{\bar{c}_0 \tau} \|\dot{\hat{\kappa}}(\tau)\| d\tau ds + \breve{\breve{k}} \|B_{\dot{\hat{\kappa}}}\|_\infty \int_{t}^{t+T} e^{-\bar{c}_0 s} \int_{t}^{s} e^{\bar{c}_0 \tau} \|\dot{\hat{\kappa}}(\tau)\| d\tau ds \\
&\leq \frac{\breve{\breve{k}} \|B_{\dot{\hat{\kappa}}}\|_\infty}{\bar{c}_0} \left[e^{-\bar{c}_0 t} - e^{-\bar{c}_0(t+T)} \right] \int_{0}^{t} e^{\bar{c}_0 \tau} \|\dot{\hat{\kappa}}(\tau)\| d\tau + \breve{\breve{k}} \|B_{\dot{\hat{\kappa}}}\|_\infty \int_{t}^{t+T} e^{-\bar{c}_0 s} \int_{t}^{s} e^{\bar{c}_0 \tau} \|\dot{\hat{\kappa}}(\tau)\| d\tau ds \\
&\leq \frac{\breve{\breve{k}} \|B_{\dot{\hat{\kappa}}}\|_\infty}{\bar{c}_0} \int_{0}^{t} e^{-\bar{c}_0(t-\tau)} \|\dot{\hat{\kappa}}(\tau)\| d\tau + \breve{\breve{k}} \|B_{\dot{\hat{\kappa}}}\|_\infty \int_{t}^{t+T} e^{-\bar{c}_0 s} \int_{t}^{s} e^{\bar{c}_0 \tau} \|\dot{\hat{\kappa}}(\tau)\| d\tau ds
\end{aligned} \tag{4.86}$$

Inequality (4.86) is derived using the property $e^{-\bar{c}_0 t} - e^{-\bar{c}_0(t+T)} \leq e^{-\bar{c}_0 t}$. Further simplifications follow as,

$$\begin{aligned}
\int_{t}^{t+T} \breve{\breve{k}} \|B_{\dot{\hat{\kappa}}}\|_\infty \int_{0}^{s} e^{-\bar{c}_0(s-\tau)} \|\dot{\hat{\kappa}}(\tau)\| d\tau ds \leq \frac{\breve{\breve{k}} \|B_{\dot{\hat{\kappa}}}\|_\infty}{\bar{c}_0} \int_{0}^{t} e^{-\bar{c}_0(t-\tau)} \|\dot{\hat{\kappa}}(\tau)\| d\tau + \\
\breve{\breve{k}} \|B_{\dot{\hat{\kappa}}}\|_\infty \int_{t}^{t+T} e^{-\bar{c}_0 s} \int_{t}^{s} e^{\bar{c}_0 \tau} \|\dot{\hat{\kappa}}(\tau)\| d\tau ds
\end{aligned} \tag{4.87}$$

The first expression on the right hand side of (4.87) can be solved in a similar manner to arrive at (4.35). Therefore, using (4.35) and (4.64), the result below follows,

$$\frac{\breve{\breve{k}} \|B_{\dot{\hat{\kappa}}}\|_\infty}{\bar{c}_0} \int_{0}^{t} e^{-\bar{c}_0(t-\tau)} \|\dot{\hat{\kappa}}(\tau)\| d\tau \leq \frac{\breve{\breve{k}} \|B_{\dot{\hat{\kappa}}}\|_\infty B_{10} e^{\bar{c}_0}}{\bar{c}_0(1-e^{-\bar{c}_0})} \nu + \frac{\breve{\breve{k}} \|B_{\dot{\hat{\kappa}}}\|_\infty B_9 e^{\bar{c}_0}}{\bar{c}_0(1-e^{-\bar{c}_0})} < \infty \quad (\nu < \infty) \tag{4.88}$$

Now, the identity for the change of sequence of integration (4.37) is applied to the the remaining

integral on the RHS of (4.87) as shown below.

$$\begin{aligned}\breve{\breve{k}}\|B_{\dot{\hat{\kappa}}}\|_\infty \int_t^{t+T} e^{-\bar{c}_0 s}\int_t^s e^{\bar{c}_0\tau}\|\dot{\hat{\kappa}}(\tau)\|d\tau ds &= \breve{\breve{k}}\|B_{\dot{\hat{\kappa}}}\|_\infty \int_t^{t+T} e^{\bar{c}_0\tau}\|\dot{\hat{\kappa}}(\tau)\|\int_\tau^{t+T} e^{-\bar{c}_0 s}dsd\tau \\ &\leq \breve{\breve{k}}\|B_{\dot{\hat{\kappa}}}\|_\infty \int_t^{t+T} e^{\bar{c}_0\tau}\|\dot{\hat{\theta}}(\tau)\|\int_\tau^{t+T} e^{-\bar{c}_0 s}dsd\tau \leq \frac{\breve{\breve{k}}\|B_{\dot{\hat{\kappa}}}\|_\infty}{\bar{c}_0}\int_t^{t+T}\|\dot{\hat{\theta}}(\tau)\|d\tau \\ &\leq \underbrace{\frac{\breve{\breve{k}}\|B_{\dot{\hat{\kappa}}}\|_\infty B_{10}}{\bar{c}_0}}_{B_{12}}\nu T + \underbrace{\frac{\breve{\breve{k}}\|B_{\dot{\hat{\kappa}}}\|_\infty B_9}{\bar{c}_0}}_{B_{11}} = B_{12}\nu T + B_{11} \end{aligned} \tag{4.89}$$

Similar to (4.88) and (4.89), the integral of `III` in (4.84) is obtained to be,

$$\int_t^{t+T}\breve{\breve{k}}\|\chi\|_\infty\int_0^s e^{-\bar{c}_0(s-\tau)}\|\dot{\hat{\theta}}(\tau)\|d\tau ds \leq \frac{\breve{\breve{k}}\|\chi\|_\infty B_{10}e^{\bar{c}_0}}{\bar{c}_0(1-e^{-\bar{c}_0})}\nu + \frac{\breve{\breve{k}}\|\chi\|_\infty B_9 e^{\bar{c}_0}}{\bar{c}_0(1-e^{-\bar{c}_0})} + \frac{\breve{\breve{k}}\|\chi\|_\infty B_{10}}{\bar{c}_0}\nu T + \frac{\breve{\breve{k}}\|\chi\|_\infty B_9}{\bar{c}_0} \tag{4.90}$$

Finally, the upper bound on the definite integral in (4.90) is derived to be,

$$\underbrace{\frac{\breve{\breve{k}}\|\chi\|_\infty B_{10}}{\bar{c}_0}}_{B_{14}}\nu T + \underbrace{\frac{\breve{\breve{k}}\|\chi\|_\infty B_{10}e^{\bar{c}_0}}{\bar{c}_0(1-e^{-\bar{c}_0})}\nu + \frac{\breve{\breve{k}}\|\chi\|_\infty B_9 e^{\bar{c}_0}}{\bar{c}_0(1-e^{-\bar{c}_0})} + \frac{\breve{\breve{k}}\|\chi\|_\infty B_9}{\bar{c}_0}}_{B_{13}}$$

Likewise, the time integration of the `IV` term (4.84) is calculated as,

$$\begin{aligned}\int_t^{t+T}\breve{\breve{k}}\|\chi\|_\infty\int_0^s e^{-\bar{c}_0(s-\tau)}\|\dot{\theta}^*(\tau)\|d\tau ds &\leq \frac{\breve{\breve{k}}\|\chi\|_\infty\Delta^\ddagger e^{\bar{c}_0}}{\bar{c}_0(1-e^{-\bar{c}_0})}\nu + \frac{\breve{\breve{k}}\|\chi\|_\infty\Delta^\ddagger e^{\bar{c}_0}}{\bar{c}_0(1-e^{-\bar{c}_0})} + \frac{\breve{\breve{k}}\|\chi\|_\infty\Delta^\ddagger}{\bar{c}_0}\nu T + \frac{\breve{\breve{k}}\|\chi\|_\infty\Delta^\ddagger}{\bar{c}_0} \\ &\leq \underbrace{\frac{\breve{\breve{k}}\|\chi\|_\infty\Delta^\ddagger}{\bar{c}_0}}_{B_{16}}\nu T + \underbrace{\frac{\breve{\breve{k}}\|\chi\|_\infty\Delta^\ddagger e^{\bar{c}_0}}{\bar{c}_0(1-e^{-\bar{c}_0})}\nu + \frac{\breve{\breve{k}}\|\chi\|_\infty\Delta^\ddagger e^{\bar{c}_0}}{\bar{c}_0(1-e^{-\bar{c}_0})} + \frac{\breve{\breve{k}}\|\chi\|_\infty\Delta^\ddagger}{\bar{c}_0}}_{B_{15}}\end{aligned} \tag{4.91}$$

From (4.85) and (4.88)-(4.91), it is mathematically proved that,

$$\int_t^{t+T}\|\vartheta(s)\|ds \leq B_{18}\nu T + B_{17} \tag{4.92}$$

where $B_{17} = \frac{\breve{\breve{k}}}{\bar{c}_0}\|\vartheta(0)\| + \frac{\breve{\breve{k}}\|B_{\dot{\hat{\kappa}}}\|_\infty B_{10}e^{\bar{c}_0}}{\bar{c}_0(1-e^{-\bar{c}_0})}\nu + \frac{\breve{\breve{k}}\|B_{\dot{\hat{\kappa}}}\|_\infty B_9 e^{\bar{c}_0}}{\bar{c}_0(1-e^{-\bar{c}_0})} + B_{11} + B_{13} + B_{15}$ and $B_{18} = B_{12} + B_{14} + B_{16}$. Hence, $\vartheta(t) \in \mathcal{S}_1(\nu)$. Now from the property of *closed under addition* of function spaces, since $z(t) = \vartheta(t) + \chi^T\tilde{\theta}(t)$, the signal property $z(t) \in \mathcal{S}_1(\nu)$ is proved. □

Proof of (iii). In the case of finite actuator failures or occurrence of actuator faults, it has already been discussed that $\dot{\theta}^* \in \mathcal{L}_1[0,\ \infty)$. Through a similar analysis and taking the limiting value of the derived bounds with $\nu \to 0$, we arrive at $z(t) \in \mathcal{L}_1[0,\ \infty)$ for finite number of changes in actuator failure/fault patterns and even intermittent changes in system parameters. From (4.73), we have $\dot{z}(t) \in \mathcal{L}_\infty[0,\ \infty)$. Hence, by using Barbalat's Lemma [110], the tracking error $z(t)$ is proved to exhibit asymptotic convergence to the origin. □

In what follows, we state an important feature of the proposed controller, i.e., *nominal performance recovery*. The term "*nominal performance recovery*" is actually meant to convey the recovery of the region of attraction of the nominal system and recovering the fault-free transient and steady state performance followed by restoring the exponential stability properties of the origin. By nominal system, we mean an exponentially stable system void of uncertainties and external disturbances. In the following theorem, it is shown as to how the proposed adaptive controller ensures robustness towards uncertain unknown inputs, starts recovering its performance and eventually the tracking error vector $z(t)$ converges to the nominal exponentially decaying solution of the unperturbed error dynamics (the dynamics in (4.73) with $\tilde{\theta} = 0,\ \dot{\hat{\theta}} = 0$) in finite time T_s. Besides, the recovery of performance is in the global sense. Herein, apart from ensuring reinforced immunity towards unknown failure induced adversities/system parameters and pre/post fault transient performance enhancement, global exponential stability rather than asymptotic stability of tracking error dynamics is achieved. The following theorem legitimize our conclusions in the aforementioned discussion. For the sake of simplicity in theoretical development and clarity in understanding the philosophy of nominal performance recovery, we abandon the assumption on the system being affected by infinite actuator failures. Instead, a general nonlinear system unknown in parameters is resorted to with the presumption that the actual parameter vector θ^* is a vector of constant scalars. It is to be noted that the preceding assumption just serves for mere simplicity and the extension of these results to the case of time varying parameters is quite straightforward.

Theorem 4.3. *The tracking error dynamics described in* (4.73) *under the action of the proposed controller* (4.71) *and estimator* (4.47) *is exponentially stable provided* $\exists\ \epsilon^* > 0$ *satisfying* $0 < \epsilon \leq \epsilon^*$. *Given any* $\varrho > 0$ *and the filtered regressor matrix* $R(t) > 0$, *there exists* $\epsilon^* > 0$ *such that the solution* $\bar{z}(t)$ *of the nominal closed loop system* ((4.73) *with* $\tilde{\theta} = 0,\ \dot{\hat{\theta}} = 0$) *and* $z(t, \epsilon^*)$ *of the uncertain closed loop dynamics* (4.73) *satisfy* $\|z(t, \epsilon^*) - \bar{z}(t)\| \leq \varrho$ *for all* $t \geq 0$. (*This result proves that the trajectory* $z(t, \tilde{\theta}, \dot{\hat{\theta}})$ *converges to the nominal solution* $z(t, 0, 0)$.)

Proof. The proof is developed in two parts. The exponential stability of $z(t) = 0$ is shown mathematically followed by the proof of finite time trajectory convergence of $z(t, \tilde{\theta}, \dot{\hat{\theta}})$ to its nominal solution $z(t, 0, 0)$. Herein, the analysis will primarily adopt the method of singular perturbations (decomposing the closed loop system into fast dynamics and a predominantly slower dynamics) and thereafter invoke certain results from Filippov's theory of differential equations (Theorem 6 on Page 105 in [105]) to arrive at our claim. The proof is rendered as follows. From (4.73) and (4.47), the closed-loop tracking

error system along with the dynamical description of its inputs $\tilde{\theta}(t)$ and $\dot{\hat{\theta}}(t)$ are re-iterated as,

$$\dot{z} = \mathcal{A}(z, \tilde{\theta}, t)z + B_{\theta^*}\tilde{\theta}(t) + B_{\hat{\kappa}}\dot{\hat{\theta}}(t) \tag{4.93}$$

$$\dot{\mathscr{E}}(t) = -R(t)\Gamma_1 \frac{\mathscr{E}(t)}{\|\mathscr{E}(t)\|^{\frac{1}{2}}} - R(t)\Gamma_2 \int_0^t \frac{\mathscr{E}(s)}{\|\mathscr{E}(s)\|} ds + \dot{R}(t)\tilde{\theta}(t) \tag{4.94}$$

$$\ddot{\tilde{\theta}}(t) = \Gamma_1 \|\mathscr{E}(t)\|^{-\frac{1}{2}} \left(-R(t)\dot{\tilde{\theta}}(t) + \frac{\Gamma_1^{-1}\Gamma_2 R(t)\tilde{\theta}(t)}{\|\mathscr{E}(t)\|^{\frac{1}{2}}} + \dot{R}(t)\tilde{\theta}(t) \right) \tag{4.95}$$

To retrofit the intended analysis, we factorize the adaptive rate matrices Γ_1 and Γ_2 as $\Gamma_1 = \epsilon^{-1}\bar{\Gamma}_1$, $\Gamma_2 = \epsilon^{-2}\bar{\Gamma}_2$ and introduce a formal change of coordinates for (4.94) as,

$$(\mathscr{E},\ \tilde{\theta}_a,\ \dot{\tilde{\theta}}) \mapsto \left(\frac{\mathscr{E}}{\|\mathscr{E}\|^{\frac{1}{2}}},\ \epsilon\tilde{\theta}_a,\ \epsilon^2\dot{\tilde{\theta}} \right) \triangleq (\bar{\mathscr{E}}_1,\ \bar{\mathscr{E}}_2,\ \bar{\mathscr{E}}_3) \tag{4.96}$$

where $\bar{\Gamma}_1,\ \bar{\Gamma}_2$ are positive definite symmetric matrices, $\epsilon \in (0, 1)$, $\tilde{\theta}_a = -\Gamma_2 \int_0^t \frac{\mathscr{E}(s)}{\|\mathscr{E}(s)\|} ds$ and $\bar{\mathscr{E}} \triangleq [\bar{\mathscr{E}}_1,\ \bar{\mathscr{E}}_2]^T$. Defining the off-manifold vector (state vector of the fast subsystem) as,

$$\begin{bmatrix} \bar{\mathscr{E}}_1 \\ \bar{\mathscr{E}}_2 \\ \bar{\mathscr{E}}_3 \end{bmatrix} = \begin{bmatrix} \mathscr{E}/\|\mathscr{E}\|^{\frac{1}{2}} \\ \epsilon\tilde{\theta}_a \\ \epsilon^2\dot{\tilde{\theta}} \end{bmatrix}, \tag{4.97}$$

the closed loop system can be reframed as a composition of slow and fast dynamical subsystems in $z(t)$ and $(\bar{\mathscr{E}}(t),\ \dot{\tilde{\theta}}(t))$, respectively as,

$$\dot{z} = \mathcal{A}(z, \tilde{\theta}, t)z + B_{\theta^*}\tilde{\theta} + B_{\hat{\kappa}}\dot{\tilde{\theta}} \tag{4.98}$$

$$\epsilon\dot{\bar{\mathscr{E}}} = R\|\mathscr{E}\|^{-\frac{1}{2}} \left(\begin{bmatrix} -\bar{\Gamma}_1 & I_{m+p+1} \\ -R^{-1}\bar{\Gamma}_2 & 0 \end{bmatrix} \bar{\mathscr{E}} + \epsilon \begin{bmatrix} R^{-1} \\ 0 \end{bmatrix} \dot{R}\tilde{\theta} \right) \tag{4.99}$$

$$\epsilon\dot{\bar{\mathscr{E}}}_3 = \bar{\Gamma}_1 \|\mathscr{E}\|^{-\frac{1}{2}} \left(-R\bar{\mathscr{E}}_3 + \epsilon^2 \bar{D}\tilde{\theta} \right) \tag{4.100}$$

where, $\bar{D} := \dfrac{\bar{\Gamma}_1^{-1}\bar{\Gamma}_2 R}{\epsilon\|\mathscr{E}\|^{\frac{1}{2}}} + \dot{R}$. Since R is positive definite from its definition, the prediction error $\mathscr{E}$ decaying to zero implicates the convergence of $\tilde{\theta}$ invariably to zero. Further, the common multiplier functions $R\|\mathscr{E}\|^{-\frac{1}{2}}$ and $\bar{\Gamma}_1\|\mathscr{E}\|^{-\frac{1}{2}}$ in (4.99)-(4.100) are strictly positive. Therefore from Filippov's Theorem [105], the set of differential equations (4.99)-(4.100) and

$$\epsilon \begin{bmatrix} \dot{\bar{\mathscr{E}}} \\ \dot{\bar{\mathscr{E}}}_3 \end{bmatrix} = \left[\begin{array}{cc|c} -\bar{\Gamma}_1 & I_{m+p+1} & 0 \\ -R^{-1}\bar{\Gamma}_2 & 0 & 0 \\ \hline 0 & 0 & -R \end{array}\right] \begin{bmatrix} \bar{\mathscr{E}} \\ \bar{\mathscr{E}}_3 \end{bmatrix} + \left[\begin{array}{c|c} R^{-1} & 0 \\ 0 & 0 \\ \hline 0 & I_{m+p+1} \end{array}\right] \begin{bmatrix} \epsilon\dot{R}\tilde{\theta} \\ \epsilon^2\bar{D}\tilde{\theta} \end{bmatrix}, \tag{4.101}$$

have same trajectories with identical signal properties. Thus, from this point in the proof, the analysis

of the estimation error is conducted using the reduced dynamical description in (4.101). It is known from Theorem 4.2 that all closed loop signals are bounded. This implies that $z(t)$ resides inside a compact set. Designating $\mathcal{F}(t,z,\bar{\mathscr{E}},\dot{\hat{\theta}},\epsilon) \triangleq \mathcal{A}z + B_{\theta^*}\tilde{\theta} + B_{\hat{\kappa}}\dot{\hat{\theta}}$ and $\mathcal{G} \triangleq [\mathcal{G}_1,\ \mathcal{G}_2]^T$ as,

$$\begin{bmatrix} \mathcal{G}_1(t,z,\bar{\mathscr{E}},\dot{\hat{\theta}},\epsilon) \\ \mathcal{G}_2(t,z,\bar{\mathscr{E}},\dot{\hat{\theta}},\epsilon) \end{bmatrix} \triangleq \left[\begin{array}{cc|c} -\bar{\Gamma}_1 & I_{m+p+1} & 0 \\ -R^{-1}\bar{\Gamma}_2 & 0 & 0 \\ \hline 0 & 0 & -R \end{array}\right] \begin{bmatrix} \bar{\mathscr{E}}_1 \\ \bar{\mathscr{E}}_2 \\ \bar{\mathscr{E}}_3 \end{bmatrix} + \left[\begin{array}{c|c} R^{-1} & 0 \\ 0 & 0 \\ \hline 0 & I_{m+p+1} \end{array}\right] \begin{bmatrix} \epsilon\dot{R}\tilde{\theta} \\ \epsilon^2\bar{D}\tilde{\theta} \end{bmatrix}, \quad (4.102)$$

the simplified closed loop system for the forthcoming analysis with $\bar{\bar{\mathscr{E}}} \triangleq [\bar{\mathscr{E}}_1,\ \bar{\mathscr{E}}_2,\ \bar{\mathscr{E}}_3]^T$ is written as,

$$\dot{z} = \mathcal{F}(t,z,\bar{\mathscr{E}},\dot{\hat{\theta}},\epsilon) \quad (4.103)$$

$$\epsilon\dot{\bar{\bar{\mathscr{E}}}} = \mathcal{G}(t,z,\bar{\mathscr{E}},\dot{\hat{\theta}},\epsilon) \quad (4.104)$$

Referring to (4.103)-(4.104), the following conditions are satisfied;

- The functions $\mathcal{F}$ and $\mathcal{G}$ satisfy, $\mathcal{F}(t,0,0,0,\epsilon) = 0$ and $\mathcal{G}(t,0,0,0,\epsilon) = 0$.
- Further, the equation $\mathcal{G}(t,z,\bar{\bar{\mathscr{E}}},\dot{\hat{\theta}},0) = 0$ yields $\tilde{\theta} = 0$ and $\dot{\hat{\theta}} = 0$.
- Since all the closed loop signals are bounded, on account of the same, $\mathcal{F}$ and $\mathcal{G}$ and their partial derivatives are bounded for $z(t)$ residing inside a compact set.
- The origin of the closed loop tracking error dynamics with $\tilde{\theta} = 0$ and $\dot{\hat{\theta}} = 0$, that is, $\dot{z} = \mathcal{F}(t,z,0,0,0)$ can be easily derived to be exponentially stable.
- Finally, the origin of the boundary layer system operating under a time scale $\tau = t/\epsilon$ given by,

$$\frac{d\bar{\bar{\mathscr{E}}}}{d\tau} = \mathcal{G}(t,z,\bar{\mathscr{E}},\dot{\hat{\theta}},0) \quad (4.105)$$

  again can be easily verified to be uniformly exponentially stable.

Therefore, by virtue of the aforementioned satisfied conditions and invoking Theorem 11.4 in [109], there exists $\epsilon^* > \epsilon > 0$ ensuring the origin of (4.103) is exponentially stable. □

Starting with the proof of the second claim, we follow the approach presented in [136–138]. The time span $[0,\ \infty]$ is divided into three intervals, namely, $[0,\ T_1)$, $[T_1,\ T_2)$ and $[T_2,\ \infty)$ and it is required to prove that $\|z(t,\epsilon^*) - \bar{z}(t)\| \leq \varrho$ for each of these time intervals with selected values of T_1 and T_2. It has been shown in the foregoing proof that $z(t)$ exponentially converges to the origin. Further, it is well known that the parameter estimation error $\tilde{\theta}$ and $\dot{\hat{\theta}}$ converge to zero in a finite time T_s. Therefore, the time instant T_2 can be chosen to be T_s such that $\exists\epsilon \in (0,\epsilon^*)$, the solution $z(t)$ of (4.73) and that of the nominal tracking error dynamics $\bar{z}(t)$ satisfy the following,

$$\|z(t,\epsilon)\| \leq \frac{\varrho}{2}; \quad \|\bar{z}(t)\| \leq \frac{\varrho}{2}, \quad t \geq T_s. \quad (4.106)$$

Hence, $\|z(t,\epsilon) - \bar{z}(t)\| \leq \varrho$ holds true for the interval $[T_s,\ \infty)$.

The choice of time instant T_1 resorts to the property of continuous time dependence of differential

equations on initial conditions and perturbation $\bar{\bar{\mathscr{E}}}$. As mentioned in [109] (Chapter 3, Theorem 3.5), there exists a number $N(\varrho)$ such that if the following conditions,

$$\|\bar{z}(T_1) - z(T_1,\ \epsilon)\| \leq N(\varrho); \quad \|\bar{\bar{\mathscr{E}}}(t)\| \leq N(\varrho), \quad \forall t \in [T_1,\ T_s), \tag{4.107}$$

are satisfied then $\|z(t,\epsilon) - \bar{z}(t)\| \leq \varrho$ follows. Therefore, in this direction , it is known that the trajectories of the system under the action of the proposed controller is bounded. Hence, the function $\mathcal{F}$ on the RHS of (4.103) is bounded in magnitude by a constant k_1 which means,

$$\|z(T_1,\epsilon) - z(0)\| \leq k_1 T_1; \quad \|\bar{z}(T_1) - z(0)\| \leq k_1 T_1 \tag{4.108}$$

The inequalities in (4.108) implicates that the first inequality in (4.107) is satisfied if $T_1 = \dfrac{N(\varrho)}{2k_1}$. Thereafter to guarantee that $\|\bar{\bar{\mathscr{E}}}(t)\| \leq N(\varrho),\ \forall t \in [T_1,\ T_s)$ holds, let

$$k_2 = \|\dot{R}\tilde{\theta}\|_\infty \tag{4.109}$$

$$k_3 = \|\bar{D}\tilde{\theta}\|_\infty \tag{4.110}$$

with $k_2,\ k_3 > 0$ are finite constants. The above fact follows from the boundedness of all closed loop trajectories proved in Theorem 4.2. Besides, assuming the above mentioned condition, the solution of the differential equation (4.104) is given by,

$$\|\bar{\bar{\mathscr{E}}}\| \leq e^{-\bar{a}\frac{t}{\epsilon}}\|\bar{\bar{\mathscr{E}}}(0)\| + \epsilon k_2 + \epsilon^2 k_3 \tag{4.111}$$

herein $\bar{a} = \min\{\underline{\lambda}\left(\begin{bmatrix} \bar{\Gamma}_1 & 1 \\ R^{-1}\bar{\Gamma}_2 & 0 \end{bmatrix}\right),\ \underline{\lambda}(R)\}$. Thus for given $N(\varrho),\ T_1$ and $\bar{\bar{\mathscr{E}}}(0)$ residing in a compact set, there exists ϵ^{**} for $\epsilon \in (0,\ \epsilon^{**})$ such that the second inequality in (4.107) simply follows from (4.111). The proof is complete. □

It is immediately conjectured from Theorem 4.3, that augmenting a finite time parameter estimator with the proposed adaptive controller yields nominal performance recovery in the event of unforseen failures in finite time, that is, finite time convergence of output tracking error trajectories $z(t)$ of the perturbed system to their nominal trajectories $\bar{z}(t)$. This attribute increases the design freedom apart from achieving an improved output performance in the sense that the magnitude of time for estimation T_s is finite and can be represented as a closed form expression in terms of initial conditions. The expression of T_s is derived using a strict Lyapunov function approach. In contrary to other research approaches in adaptive control wherein the time of convergence to the origin from any initial condition is undefined, the settling time to reach the origin herein can be explicitly calculated. Thus, at this point, it is assertive to claim that the proposed scheme allows the system to recover from its failure state in finite time. Further, in the case of infinite actuator failures, finite time parameter convergence allows a lower bound on the transit time T^* between two successive changes in actuator failure pattern given by T_s which adds to an enhanced performance of the proposed scheme. It is reiterated that T_s denotes the finite settling time of the estimation error signals, namely $\tilde{\theta}$ and $\dot{\tilde{\theta}}$ to the origin.

4.2.5 Simulation Studies

This section illustrates the advantages offered by the proposed control through numerical simulation studies. The tracking control problem of a multi-input single output (MISO) nonlinear dynamical system is considered assuming unknown parametric uncertainties and occurrence of finite and intermittent changes in the failure induced unknown parameters (infinitely changing actuator failure patterns). The claimed theoretical results on stability and asymptotic stability of the system in presence of infinite and finite actuator failures are verified through extensive simulation studies. Fast finite time convergence of parameter estimation to their actual values is also justified through necessary simulations. Finally, robustness and significant improvement in output transient and steady state performance in all the cases of no failure, finite actuator failures and intermittently changing actuator failure configurations are demonstrated.

The superior performance of the proposed FTC methodology at start up and post failure scenarios are justified through a comparison of results with those obtained using single model adaptive FTC, MBSC [6] and multiple model adaptive control (AMMFTC, Chapter 3). Besides, a tabular comparison of the output performance in terms of ITAE and RMSE is drawn which suggests similar trend in improvement of transients. In addition, to correlate the enhancement in transient performance with the increment in control usage, corresponding input performances of single model adaptive FTC, MBSC [6] and AMMFTC are also quantified using 2-norm and total variation (TV) of the control input and a tabular comparison is drawn. It should be emphasized that the proposed FTC methodology ensures transient performance improvement in the output with no substantial increase in control usage.

Let us consider a multi input single output nonlinear uncertain system with unknown parametric uncertainties as,

$$\begin{aligned}\dot{\xi} &= \varphi_0(\xi) + \varphi(\xi)\kappa^* + \sum_{j=1}^{2} b_j g_j(\xi) u_j \\ y &= \xi_2 \end{aligned} \tag{4.112}$$

where the state vector is defined as $\xi := [\xi_1,\ \xi_2,\ \xi_3]^T \in \mathbb{R}^3$ and $\kappa^* \in \mathbb{R}^3$ denotes the unknown system parameter vector. The nonlinear functions are defined as follows,

$$\varphi_0 = \begin{bmatrix} -\xi_1 \\ \xi_3 \\ \xi_2\xi_3 \end{bmatrix}, \varphi = \begin{bmatrix} 0 \\ \xi_2^2 \\ \dfrac{1-e^{-\xi_3}}{1+e^{-\xi_3}} \end{bmatrix} \tag{4.113}$$

$$g_1 = g_2 = \left[\frac{2+\xi_3^2}{1+\xi_3^2},\ 0,\ 1\right]^T. \tag{4.114}$$

The system model is the same as considered in Section 3.2.4 of the previous chapter and [6]. By using the transformation $[\eta\ x_1\ x_2]^T := [\mathscr{T}_z(\xi),\ \mathscr{T}_c(\xi)]^T := [-\xi_1 + \xi_3 + \tan^{-1}\xi_3,\ \xi_2,\ \xi_3]$, the system conforms to the description in (4.7). The transformation $\mathscr{T}_z(\xi)$ is calculated by solving the partial differential

equations, $\left[\sum_{k=1}^{3}\frac{\partial \mathscr{T}_z}{\partial \xi_k}g_1,\ \sum_{k=1}^{3}\frac{\partial \mathscr{T}_z}{\partial \xi_k}g_2\right]^T = [0,\ 0]^T$. Therefore, the transformed system is represented as follows,

$$\dot{\eta} = -\eta + x_2 + \tan^{-1}x_2 + \frac{2+x_2^2}{1+x_2^2}\left(x_1x_2 + \frac{1-e^{-x_2}}{1+e^{-x_2}}\kappa^*\right) \tag{4.115}$$

$$\dot{x}_1 = x_2 + x_1^2\kappa^*$$

$$\dot{x}_2 = x_1x_2 + \frac{1-e^{-x_2}}{1+e^{-x_2}}\kappa^* + \sum_{j=1}^{2}b_ju_j \tag{4.116}$$

As deduced in Section 3.2.4 of Chapter 3, the internal dynamics described by (4.115) is input-to-state stable (ISS).

Two cases of finite and infinite changes in actuator failure pattern are considered to demonstrate the performance robustness of the proposed control methodology with finite time adaptation. The unknown parameters considered in simulations are $\kappa^* = 2,\ b_1^* = 1,\ b_2^* = 1$. The reference trajectory to be tracked by the system output is $y_r = \sin(t)$. The reference signal is so chosen that it satisfies the design assumptions in Section 4.2.2.1. The actuator failure model representing Case 1 , is defined as follows,

$$u_1(t) = \begin{cases} 5, & t \in [50,\ 100) \\ u_{H1}(t), & t \in [0,\ 50)\cup[100,\ \infty) \end{cases}, \quad u_2(t) = \begin{cases} u_{H2}(t), & t \in [0,\ 100) \end{cases} \tag{4.117}$$

Further, the intermittently occurring actuator fault/failure considered in Case 2 is described in (4.118) below.

$$u_1(t) = \bar{u}_{Fj_1,h},\quad t \in [hT^*,\ (h+1)T^*),\ h \in \mathbb{N}\backslash 2\mathbb{N} \tag{4.118}$$

The transition time between each change in the actuator failure pattern is considered to be $T^* = 5 > 0$. The bounds on the unknown parameters are given below.

$$1 \le \kappa^* \le 3,\ 0.8 \le |b_1^*| \le 1.4,\ 0.6 \le |b_2^*| \le 2 \tag{4.119}$$
$$0.5 \le K_{j,h} \le 1,\ |\bar{u}_{Fj_k,h}| \le 6,\ j = 1, 2.$$

The stuck actuator failure is characterized by $K_{j_1,h} = 0$ and $\bar{u}_{Fj_1,h} = 5$. The initial conditions of the system are given by $\xi(0) = [0,\ 0.4,\ 0]$. The adaptive controller is designed using proposed finite time adaptation based control methodology discussed in Section 4.2.3. The controller design parameters for simulation are chosen to be $c_1 = c_2 = 5,\ \bar{c}_1 = \bar{c}_2 = 3,\ g_2 = 3,\ \gamma = 0.5,\ \Gamma_1 = 2\times I_2,\ \Gamma_2 = 4\times I_2,\ \mathscr{K} = 1$ and $A_0 = [\text{diag}(-5,\ -7)]$. In order to ensure a fair comparison of the proposed control design with single model adaptive control and the modular backstepping control (MBSC) approach by Wang *et. al* [6] and AMMFTC design, the values of controller gains and other relevant design parameters are chosen to be same. The output performance in regards to start-up and post fault transient peaks and settling times, is calculated using root mean square (RMS) and integral time absolute error (ITAE) metric of

the output tracking error. A relatively lower value of ITAE and RMSE from the results obtained with other relevant control schemes, signify a faithful tracking with comparatively lower overshoots and faster settling time. Further, the input performance is quantified using control energy (CE) and the total variation (TV) of the control signal. Total variation is a very important measure which gives an insight on the effectiveness of the controller with a limited communication network in the loop. Hence, a lower value of TV with the proposed scheme allows its application to the trending cyber-physical systems and networked control and it is expected to yield fruitful results in such scenarios. The control energy is measured using the $2-$norm of the control input whereas TV for each of the control inputs is measured using the expression $\sum_{i=1}^{N} |u_{j,i} - u_{j,i+1}|$ for $j = 1, 2$.

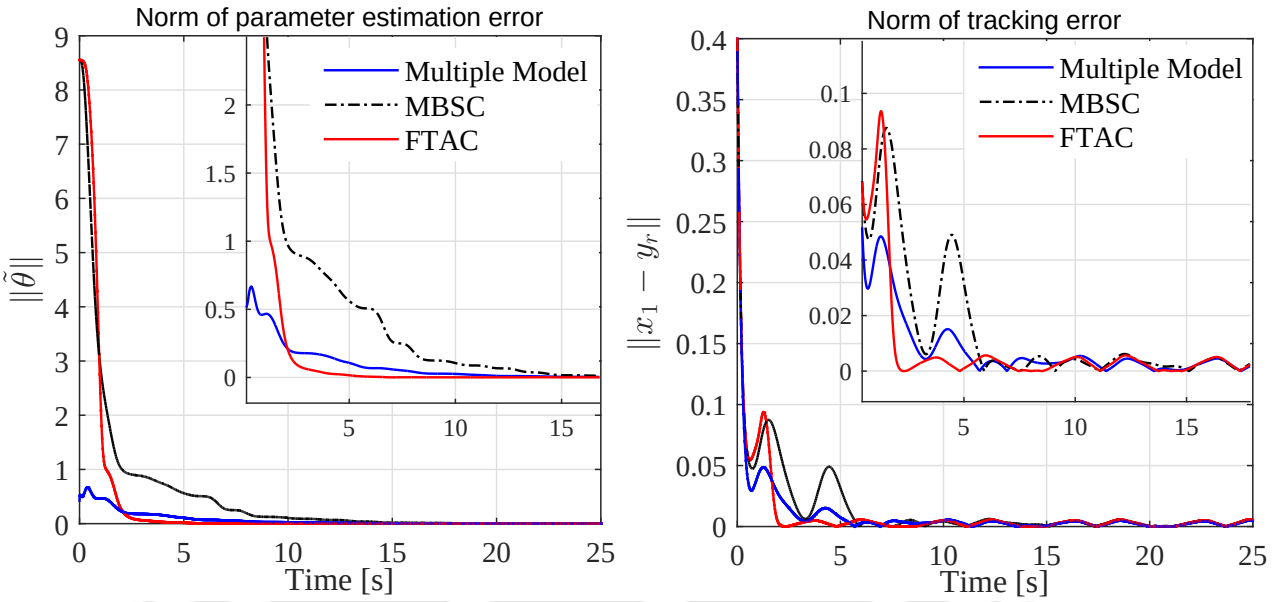

Figure 4.2: (Left) Comparison of parameter estimation performance; (Right) Comparison of start up transient performance; obtained with AMMFTC, Modular Backstepping Control (MBSC) and proposed FTAC method under no failure from $t = 0s - 25s$.

- *Case 1* (4.117): The output tracking performance and the convergence of parameter estimates at start up and post actuator failure scenario along with the remaining system states and the control signals are shown in Figures 4.2 and 4.3, respectively. The superiority of the proposed control strategy in terms of parameter estimation speed and accuracy along with the speed of convergence of output tracking error in both the phases of start up and in the event of actuator failure is justified from the comparison drawn in Figure 4.2 and Figure 4.3. The proposed controller with finite time adaptation further improves upon the output performance (transient and steady state) and parameter convergence obtained using adaptive control with multiple models. The above inference is drawn from the simulation results provided in Figure 4.4. In addition, a consolidated performance chart summarizing the efficacy of the proposed controller relative to relevant existing adaptive control techniques is furnished in Table 4.1.

- *Case 2* (4.118): The robustness of the proposed adaptive controller to intermittently changing

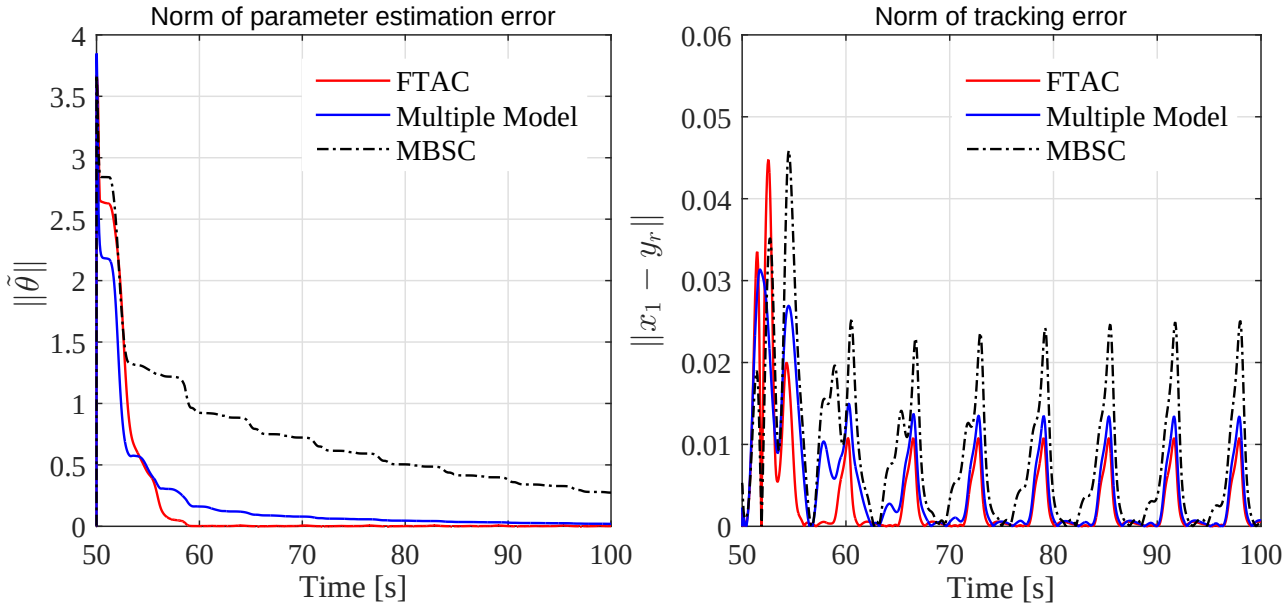

Figure 4.3: (Left) Comparison of parameter estimation performance; (Right) Comparison of post failure transient and steady state performance; obtained with AMMFTC, Modular Backstepping Control (MBSC) and proposed FTAC method under no failure from $t = 50s - 100s$.

Table 4.1: Tabular comparison of output and input performance under Case 1 (4.117).

Control Schemes	**Output Performance**		**Input Performance**			
	ITAE	**RMSE**	**Control Energy**		**Total Variation**	
			u_1	u_2	u_1	u_2
FTAC	**12.64**	**0.015**	3.663×10^3	3.143×10^3	147.57	307.65
Multiple Models	18.69	0.0134	3.644×10^3	3.126×10^3	131.72	297.48
Single Model	49.83	0.0268	3.643×10^3	3.102×10^3	147.78	305.48
MBSC	34.64	0.0195	3.639×10^3	3.106×10^3	127.97	286.34

actuator failure patterns unknown in time, pattern and magnitude is illustrated in this case study. The value at which u_1 is stuck is $\bar{u}_{Fj_1} = 5$. These eventualities are manifested in the form of infinitely occurring parameter jumps which are uncertain and unknown in all aspects except for the boundary set they reside in. Figure 4.5 shows the boundedness of all the system states and the control signals under this scenario with the transit time being $T^* = 5$ s. Further, the improvement of output transient performance with an increasing T^*, is verified from the simulation results obtained with $T^* = 5$ s and $T^* = 15$ s in Figure 4.6 along with performance measures tabulated in Table 4.2. The superior features of the proposed adaptive control methodology are concluded from the tabulation of input and output performances obtained using the proposed method, multiple model adaptive control, single model adaptive control and modular adaptive backstepping control (MBSC) [6] techniques in Table 4.2.

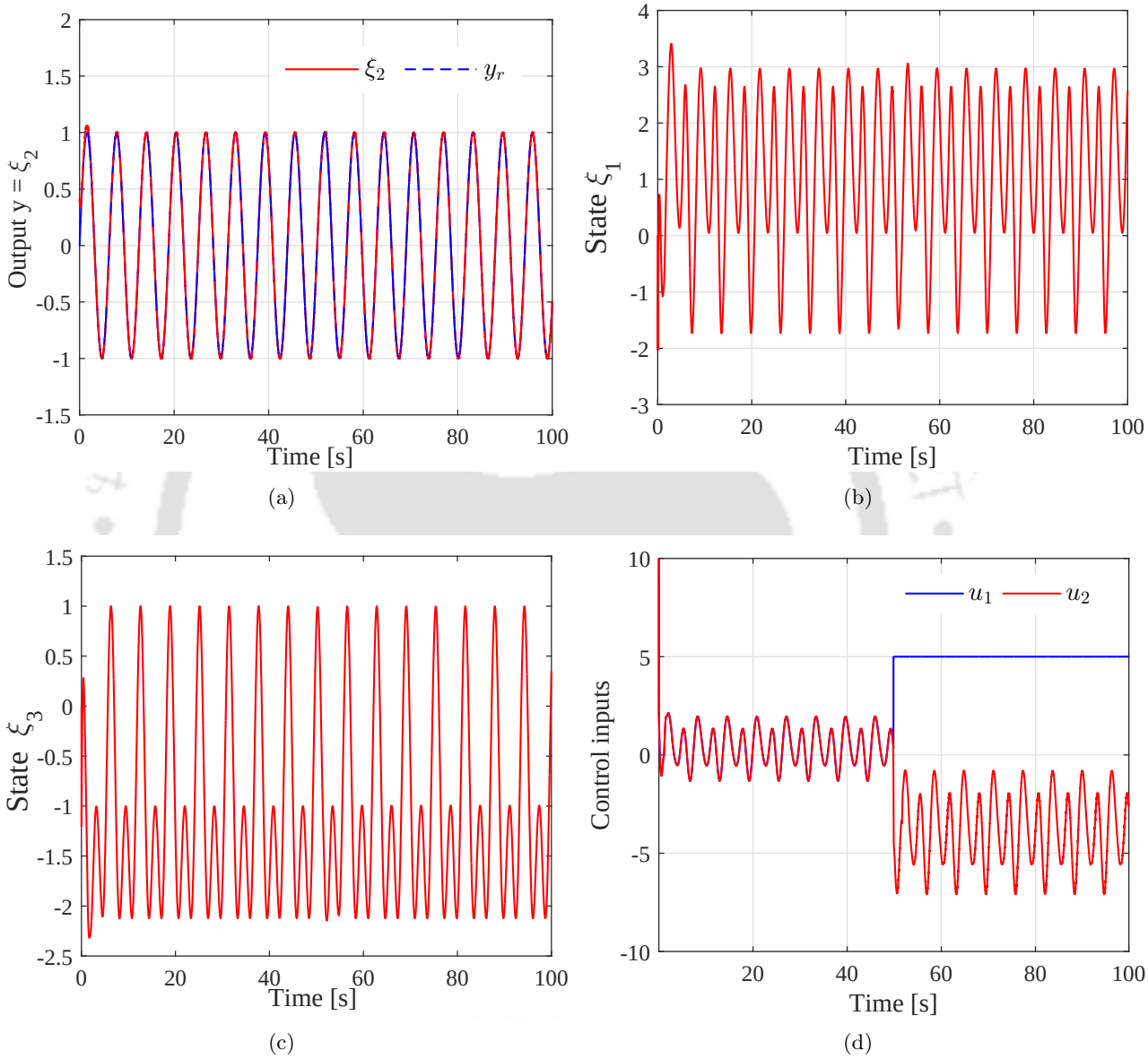

Figure 4.4: System states and control inputs with actuator fault under Case 1 (4.117) at $t = 50$ s. (a) Output state $\xi_2 = x_1$;(b) state ξ_1;(c) state $\xi_3 = x_2$; (d) control inputs u_1 and u_2

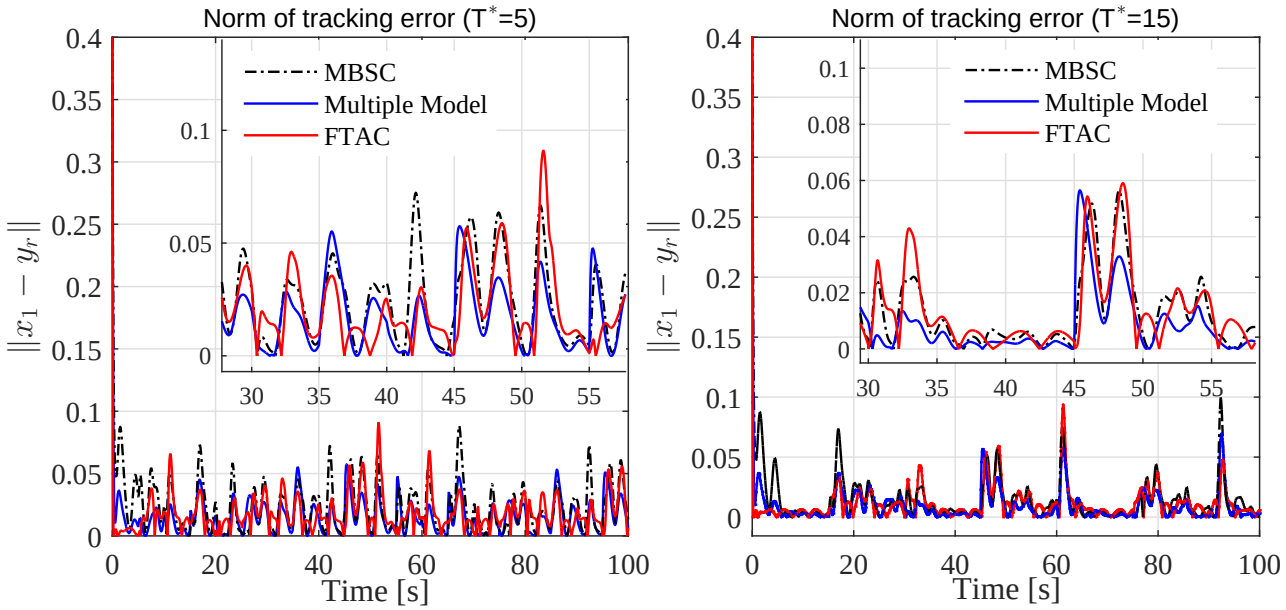

Figure 4.5: Comparison of tracking performance under infinite actuator failures Case 2 (4.118) showing performance improvement with increasing T^*; (Left) tracking error performance for $T^* = 5s$; (Right) tracking error performance for $T^* = 15s$; between Modular Backstepping Control (MBSC) [6], Multiple Model (AMMFTC) and FTAC method in case of infinite actuator failures

Table 4.2: Case 2: Performance Comparison between three adaptive control schemes, namely, finite time adaptation based control (FTAC), adaptive control using multiple models, single model adaptive control and modular backstepping control (MBSC) [6]

Transit time	**Control Schemes**	**Performance metrics**					
		ITAE	**RMSE**	**Control Energy**		**Total Variation**	
				u_1	u_2	u_1	u_2
$T^* = 5$ s	FTAC	**95.04**	**0.023**	3.67×10^3	3.15×10^3	316.76	404.78
	Multiple Models	78.46	0.023	3.64×10^3	3.09×10^3	293.64	359.15
	Single Model	124.44	0.039	3.74×10^3	3.22×10^3	309.69	380.27
	MBSC	111.08	0.032	3.67×10^3	3.14×10^3	291.05	362.00
$T^* = 15$ s	FTAC	**57.87**	**0.017**	3.49×10^3	2.98×10^3	202.63	327.89
	Multiple Models	**56.10**	**0.018**	3.48×10^3	2.99×10^3	180.41	299.11
	Single Model	85.75	0.033	3.47×10^3	2.93×10^3	200.45	319.21
	MBSC	62.93	0.026	3.47×10^3	2.94×10^3	181.15	327.89

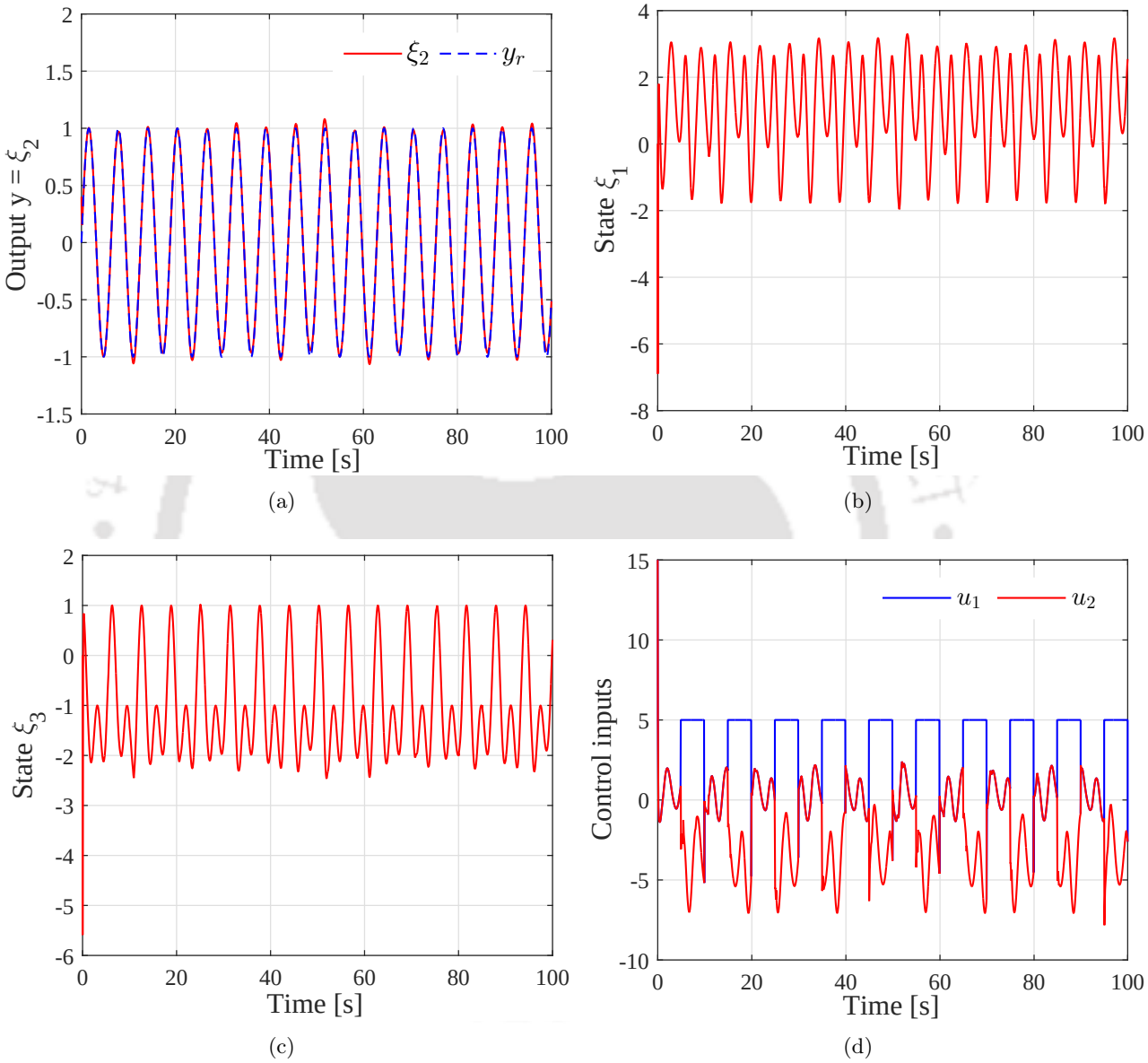

Figure 4.6: System states and control inputs for Case 2 (4.118) with $T^* = 5$s. (a) Output state $\xi_2 = x_1$;(b) state ξ_1;(c) state $\xi_3 = x_2$; (d) control inputs u_1 and u_2

4.3 Finite Time Adaptation based Compensation (FTAC) of Actuator Failures in Multi-Input-Multi-Output (MIMO) Nonlinear Uncertain Systems

In this section, the proposed finite time adaptation based control (FTAC) strategy is extended to the tracking control problem in MIMO nonlinear systems with immanent parametric uncertainties (totally unknown system parameters) and abrupt actuator failures unknown in time pattern and magnitude. In general, owing to the presence of strong coupling among inherent subsystems, the FTC design problem for MIMO nonlinear systems and obtaining promising solutions, is certainly challenging. In the following, an uncertain nonlinear dynamical system with multiple inputs and outputs incorporating actuator failure input-output characteristics is described first. Thereafter, the adaptive FTC design with the proposed finite time parameter estimator is put forward. Since, the inherent design assumptions for the proposed control algorithm are essentially the same as in Chapter 3, Section 3.3.1, we restrain from repeating the same herein to avoid repetition and preserve brevity of presentation all throughout this chapter. Besides, the proposed finite time bound parameter estimation, the controller developed under an indirect adaptive backstepping framework is exactly similar to what has been presented in (3.160) (Section 3.3.2.1). Hence, the controller design procedure is not elucidated further. Instead, only some of the important steps would be presented. Further, the stability analysis of the closed loop control system under the action of the proposed control will be sketched briefly.

4.3.1 Problem Formulation

Let us consider the class of MIMO nonlinear systems affected by parametric uncertainties transformed to a strict-feedback form as follows.

$$\begin{cases} \dot{\xi}_{1,r_1} = \xi_{1,r_1+1} + \boldsymbol{\varphi}_{1,r_1}^T \boldsymbol{\kappa}^* \\ \quad \dot{\xi}_{1,\wp_1} = a_1(\xi,\eta) + \boldsymbol{\varphi}_{1,\wp_1}^T \boldsymbol{\kappa}^* + \sum_{j=1}^{m} \beta_{1,j}(\xi,\eta) u_j \end{cases} \tag{4.120}$$

$$\vdots$$

$$\begin{cases} \dot{\xi}_{q,r_q} = \xi_{q,r_q+1} + \boldsymbol{\varphi}_{q,r_q}^T \boldsymbol{\kappa}^* \\ \quad \dot{\xi}_{q,\wp_q} = a_q(\xi,\eta) + \boldsymbol{\varphi}_{q,\wp_q}^T \boldsymbol{\kappa}^* + \sum_{j=1}^{m} \beta_{q,j}(\xi,\eta) u_j \end{cases} \tag{4.121}$$

$$\dot{\boldsymbol{\eta}} = \boldsymbol{\Lambda}_0(\boldsymbol{\xi},\boldsymbol{\eta}) + \boldsymbol{\Lambda}_1^T(\boldsymbol{\xi},\boldsymbol{\eta})\boldsymbol{\kappa}^* \tag{4.122}$$

$$\mathbf{y} = [\xi_{1,1},\ \xi_{2,1},\ \xi_{3,1},\ldots,\ \xi_{i,1},\ldots,\ \xi_{q,1}]^T \tag{4.123}$$

where $\boldsymbol{\xi} := [\xi_{1,1}, \xi_{1,2}, \ldots, \xi_{1,\wp_1}, \ldots, \xi_{q,1}, \xi_{q,2}, \ldots, \xi_{q,\wp_q}]^T \in \mathbb{R}^{\wp_1+\ldots+\wp_q}$ denotes the state vector and $\boldsymbol{\varphi}_{i,r_i}$ for $i = \overline{1,q}$ and $r_i = \overline{1,\wp_i}$ define the regressor matrices associated with unknown parameter vector $\boldsymbol{\kappa}^*$. The elements of the regressor matrices are linear and nonlinear smooth functions of the state

vector $\boldsymbol{\xi}$. The output of the system (4.120)-(4.121) is represented by the vector $\mathbf{y} = [\{y_i\}_{i=1}^{q}]^T \in \mathbb{R}^q$ while $\{\wp_1, \wp_2, \ldots, \wp_q\}$ define the relative degrees of each of the q subsystems corresponding to their outputs y_i. The functions $a_i(\boldsymbol{\xi}, \boldsymbol{\eta})$ for $i = \overline{1,q}$ are known nonlinear smooth functions. The functions $\beta_{i,j}(\boldsymbol{\xi}, \boldsymbol{\eta})$ define the actuation functions for system dynamics corresponding to output y_i with $i = \overline{1,q}$ and $j = \overline{1,m}$. The internal dynamics of the system are described by (4.122) and are assumed to be ISS with respect to state vector $\boldsymbol{\xi}(t)$ as the input.

Undoubtedly, the actuators realizing the control inputs u_j for $j = \overline{1,m}$ are vulnerable to uncertain faults and failures in their due course of operation over time. Similar to the actuator input-output characterization presented in the previous chapters, the actuator failure model considered here is given by,

$$u_j = \begin{cases} K_j u_{Hj} + \bar{u}_{Fj}, & \forall\ t \geq t_{Fj} \\ u_{Hj}, & \forall\ t < t_{Fj} \end{cases} \quad j = \overline{1,m} \tag{4.124}$$

The term u_{Hj} denotes the derived control signal to be fed as input to the j^{th} actuator. While $\bar{u}_{Fj}$ defines the value at which the j^{th} actuator is stuck under stuck or lock-in-place (LIP) failure. The term $\bar{u}_{Fj}$=0 models float failure of the j^{th} actuator. The factor K_j defines the partial loss of effectiveness (PLOE) of the j^{th} actuator. The actuator failures considered are unknown in time, pattern as well as magnitude. The actuator index set is given by $\{j_1,\ j_2, \ldots,\ j_m\}$. It is assumed that the number of inputs m is greater than the number of outputs q. Inspired from [32], the actuators are thereafter classified under a grouping scheme $\mathscr{G}$ into q groups $\mathscr{G}_1, \ldots, \mathscr{G}_q$ according to their similarity in physical structure and operational characteristics. This means that actuators reflecting the same physical structure and functioning are placed together in a single group $\mathscr{G}_k \subset \{j_1,\ j_2, \ldots,\ j_m\}$, $k = \overline{1,q}$. In other words, let us assume that out of m actuators, m_i of them exhibit similar operation and bear structural resemblance. These m_i actuators are allotted to group $\mathscr{G}_i$ and so on for $i = \overline{1,q}$. A proportional actuation scheme is utilized similar to [32] to effectively exploit the actuator redundancy. Now, considering such a grouping and actuation scheme $\mathscr{G}$, the control input to be fed to each actuator included in the set $\mathscr{G}_k$ is given by,

$$u_{Hj} = b_{jk} v_k \quad \forall u_j \in \mathscr{G}_k,\ j = \overline{1,\ m}\ \&\ k = \overline{1,q} \tag{4.125}$$

where, b_{jk} defines a certain known design function or constant associated with each actuator group $\mathscr{G}_k$. Further, the choice of such design functions satisfy the relation $b_{jk} = b_j$ if the j^{th} actuator belong to $\mathscr{G}_k$ under the grouping scheme $\mathscr{G}$.

Incorporating the actuator failure model in (4.124) along with the grouping $\mathscr{G}$ and a proportional actuation scheme, the nonlinear uncertain system in (4.120)-(4.121) is reframed as,

$$\begin{cases} \dot{\xi}_{1,r_1} = \xi_{1,r_1+1} + \boldsymbol{\varphi}_{1,r_1}^T \boldsymbol{\kappa}^* \\ \dot{\xi}_{1,\wp_1} = a_1(\xi,\eta) + \boldsymbol{\varphi}_{1,\wp_1}^T \boldsymbol{\kappa}^* + \sum\limits_{j \in \{j_1,\ldots,j_d\}} \beta_{1,j}(\xi,\eta)\bar{u}_{Fj} + \sum\limits_{k=1}^{q} \bar{\beta}_{1,k}(\xi,\eta) v_k \end{cases} \tag{4.126}$$

$$\begin{cases} \dot{\xi}_{2,r_2} = \xi_{2,r_2+1} + \boldsymbol{\varphi}_{2,r_2}^T \boldsymbol{\kappa}^* \\ \dot{\xi}_{2,\wp_2} = a_2(\xi,\eta) + \boldsymbol{\varphi}_{2,\wp_2}^T \boldsymbol{\kappa}^* + \sum\limits_{j\in\{j_1,\ldots,j_d\}} \beta_{2,j}(\xi,\eta)\bar{u}_{Fj} + \sum\limits_{k=1}^{q} \bar{\beta}_{2,k}(\xi,\eta)v_k \end{cases} \tag{4.127}$$

$$\vdots$$

$$\begin{cases} \dot{\xi}_{q,r_q} = \xi_{q,r_q+1} + \boldsymbol{\varphi}_{q,r_q}^T \boldsymbol{\kappa}^* \\ \dot{\xi}_{q,\wp_q} = a_q(\xi,\eta) + \boldsymbol{\varphi}_{q,\wp_q}^T \boldsymbol{\kappa}^* + \sum\limits_{j\in\{j_1,\ldots,j_d\}} \beta_{q,j}(\xi,\eta)\bar{u}_{Fj} + \sum\limits_{k=1}^{q} \bar{\beta}_{q,k}(\xi,\eta)v_k \end{cases} \tag{4.128}$$

where $\bar{\beta}_{i,k} := \sum\limits_{j\notin\{j_1,\ldots,j_d\}\cap\mathscr{G}_k} b_{jk}K_j\beta_{i,j}(\boldsymbol{\xi},\boldsymbol{\eta})\ \forall k = 1,\ldots,q$ and $j = \overline{1,m}$. The term $\bar{u}_{Fj}$ denotes the value at which the j^{th} actuator is stuck after it fails completely. The subscript d is delimited as $d \leq (m-q)$. To ensure that an adaptive control solution exists to compensate for the actuator faults and failures apart from parametric uncertainties, the following condition must hold for a particular pattern of actuator failure $\forall\boldsymbol{\xi} \in \mathbb{R}^{\wp_1+\ldots+\wp_q}$ under the defined grouping scheme $\mathscr{G}$.

$$\det\left(\begin{bmatrix} \bar{\beta}_{1,1} & \bar{\beta}_{1,2} & \ldots & \bar{\beta}_{1,q} \\ \bar{\beta}_{2,1} & \bar{\beta}_{1,2} & \ldots & \bar{\beta}_{2,q} \\ \vdots & \ddots & \ldots & \vdots \\ \bar{\beta}_{q,1} & \bar{\beta}_{q,2} & \ldots & \bar{\beta}_{q,q} \end{bmatrix}_{\mathscr{G}(\Xi_j)}\right) \neq 0. \tag{4.129}$$

For the above condition to hold true for the grouping scheme $\mathscr{G}$, a maximum of (m_i-1) actuator failures are allowed in each of the groups $\mathscr{G}_i$. This condition ensures controllability of the nonlinear MIMO system in presence of actuator faults and total failures; guaranteeing the existence of an adaptive control solution to the FTC problem. The control design assumptions are fundamental and are no different than what have been previously stated in Assumptions 3.9-3.10.

By virtue of all the necessary assumptions and the system dynamics under actuator faults/failures described in (4.126)-(4.128), the control problem and its objectives are stated below.

- To design the control inputs v_k for each of the actuator groups $\mathscr{G}_k$ with $k = \overline{1,q}$ to ensure boundedness of all closed loop signals.
- Adaptive estimation of unknown system parameters and actuator fault/failure induced parametric uncertainties in *finite time*, meaning $\lim\limits_{t\to T_s} \boldsymbol{\theta}^*(t) - \hat{\boldsymbol{\theta}}(t) = 0$. Where $\boldsymbol{\theta}^*$ and $\hat{\boldsymbol{\theta}}$ denote the actual parameter vector and its estimated equivalent, respectively. T_s defines the settling time.
- Asymptotic exponential convergence of the output tracking error $(\mathbf{y}-\mathbf{y_r})$ to origin under nominal (fault-free) conditions and in the event of actuator faults and failures unknown in their time of occurrence, failure patterns and magnitudes, i.e., $\lim\limits_{t\to\infty} \mathbf{y}(t) - \mathbf{y_r}(t) = 0$.
- Improvement in output transient performance both at start up and post fault/failure scenarios without any substantial increase in the control usage. Unknown subsystem interactions in MIMO nonlinear systems are known play a decisive role in determining the system output transient

behavior. Thus, reinforced robustness towards consequences of unknown strong cross coupling effects arising from such interactions is an additional design objective to be accomplished.

4.3.2 Proposed Finite Time Adaptation based Controller (FTAC)

Prior to the proposed controller design, the faulty system in (4.126)-(4.128) is first parameterized to identify the unknown parameters associated with actuator faults and failures. Following the parametrization, the unknown system parameters are represented by $\boldsymbol{\theta}_2^* = \boldsymbol{\kappa}^*$; while large parametric uncertainties introduced into the system due to occurrence of actuator failures are defined as $\boldsymbol{\theta}_1^* = [\theta_{1,1}^*, \ldots, \theta_{1,m}^*]^T = [K_1, K_2, \ldots, K_m]^T$ and $\boldsymbol{\theta}_3^* = [\theta_{3,1}^*, \ldots, \theta_{3,m}^*]^T = [\bar{u}_{F1}, \bar{u}_{F2}, \ldots, \bar{u}_{Fm}]^T$. After the preceding definitions, the vector comprising of all the aforementioned unknown parameters is defined as $\boldsymbol{\theta}^* := [\boldsymbol{\theta}_1^*,\ \boldsymbol{\theta}_2^*,\ \boldsymbol{\theta}_3^*]^T$. In what follows, the controller design is presented which helps in realizing the "*modularity*" between control and parameter estimation thereby guaranteeing a unidirectional interaction between the controller-observer pair as desired. Thereafter, the parameter estimator featuring finite time convergence of the parameter estimation error to the origin is proposed. It is worth mentioning that the adaptive parameter estimator to be proposed in the sequel is independent of the boundedness of the regressor vector and hence the signals associated with the estimation module are bounded.

4.3.2.1 Controller Synthesis

Let us first augment all the q inputs denoted by v_k for $k = \overline{1,q}$ together to form the vector $\mathbf{v} := [v_1, v_2, \ldots, v_q]^T$. Now, the design of $\mathbf{v}(t)$ entirely follows the same procedure in Chapter 3 (Section 3.3.2.1). Thus, only some important steps are provided for the sake of completeness. Firstly, the following error variables are introduced.

$$\begin{aligned}
z_{1,1} &= \xi_{1,1} - y_{r,1};\ \ z_{1,r_1} = \xi_{1,r_1} - \alpha_{1,r_1-1} - y_{r,1}^{(r_1-1)};\\
z_{2,1} &= \xi_{2,1} - y_{r,2};\ \ z_{2,r_2} = \xi_{2,r_2} - \alpha_{2,r_2-1} - y_{r,2}^{(r_2-1)};\\
&\vdots \qquad\quad \vdots\\
z_{q,1} &= \xi_{q,1} - y_{r,q};\ \ z_{q,r_q} = \xi_{q,r_q} - \alpha_{q,r_q-1} - y_{r,q}^{(r_q-1)}
\end{aligned} \tag{4.130}$$

where $r_i = \overline{2,\wp_i}$, $i = \overline{1,q}$, $y_{r,i}^{(r_i-1)}$ denotes $(r_i-1)^{th}$ derivative of the i^{th} reference signal $y_{r,i}$ and α_{i,r_i} are the stabilizing control laws known as virtual inputs determined at the r_i^{th} step (for $r_i = \overline{1,\wp_i - 1}$) as

$$\alpha_{i,1} = -c_{i,1}z_{i,1} - \bar{c}_{i,1}\|\boldsymbol{\psi}_{i,1}\|^2 z_{i,1} - \boldsymbol{\varphi}_{i,1}^T\hat{\boldsymbol{\theta}}_2 \tag{4.131}$$

$$\begin{aligned}
\alpha_{i,r_i} = &-z_{i,r_i-1} - c_{i,r_i}z_{i,r_i} - \left(\bar{c}_{i,r_i}\|\boldsymbol{\psi}_{i,r_i}\|^2 + g_{i,r_i}\left\|\frac{\partial\alpha_{i,r_i-1}}{\partial\hat{\boldsymbol{\theta}}_2}\right\|^2\right)z_{i,r_i} - \boldsymbol{\psi}_{i,r_i}^T\hat{\boldsymbol{\theta}}_2\\
&+\left(\sum_{k=1}^{r_i-1}\frac{\partial\alpha_{i,r_i-1}}{\partial\xi_{i,k}}\xi_{i,k+1} + \sum_{k=1}^{r_i-1}\frac{\partial\alpha_{i,r_i-1}}{\partial y_{r,i}^{k-1}}y_{r,i}^{(k)}\right).
\end{aligned} \tag{4.132}$$

Where, $\boldsymbol{\psi}_{i,r_i} = \boldsymbol{\varphi}_{i,r_i} - \sum_{k=1}^{r_i-1} \frac{\partial \alpha_{i,r_i-1}}{\partial \xi_{i,k}} \boldsymbol{\varphi}_{i,k}$ for $i = \overline{1,q}$ and $r_i = \overline{2, \wp_i - 1}$. The actual control input $\mathbf{v}(t)$ is then derived to be

$$\mathbf{v}(t) = \left(\bar{\boldsymbol{\beta}} \sum_{j=1}^{m} \hat{\theta}_{1,j} N_j \mathbf{B} \right)^{-1} \begin{bmatrix} -a_1(\boldsymbol{\xi},\ \boldsymbol{\eta}) - \boldsymbol{\psi}_{1,\wp_1}^T \hat{\boldsymbol{\theta}}_2 - \boldsymbol{\beta}_1 \hat{\boldsymbol{\theta}}_3 - z_{1,\wp_1-1} + F_{\boldsymbol{\xi}_1} + F_{\mathbf{r},1} + y_{r,1}^{(\wp_1)} \\ -a_2(\boldsymbol{\xi},\ \boldsymbol{\eta}) - \boldsymbol{\psi}_{2,\wp_2}^T \hat{\boldsymbol{\theta}}_2 - \boldsymbol{\beta}_2 \hat{\boldsymbol{\theta}}_3 - z_{2,\wp_2-1} + F_{\boldsymbol{\xi}_2} + F_{\mathbf{r},2} + y_{r,2}^{(\wp_2)} \\ \vdots \\ -a_q(\boldsymbol{\xi},\ \boldsymbol{\eta}) - \boldsymbol{\psi}_{q,\wp_q}^T \hat{\boldsymbol{\theta}}_2 - \boldsymbol{\beta}_q \hat{\boldsymbol{\theta}}_3 - z_{q,\wp_q-1} + F_{\boldsymbol{\xi}_q} + F_{\mathbf{y_r},q} + y_{r,q}^{(\wp_q)} \end{bmatrix} +$$

$$\left(\ell \bar{\boldsymbol{\beta}} \mathbf{B}\right)^{-1} \begin{bmatrix} -c_{1,\wp_1} z_{1,\wp_1} - \bar{c}_{1,\wp_1} (\|\boldsymbol{\psi}_{1,\wp_1}\|^2 + \|\boldsymbol{\beta}_1\|^2 + \|\bar{\boldsymbol{\beta}}_u^1\|^2) z_{1,\wp_1} - g_{1,\wp_1} \left\| \frac{\partial \alpha_{1,\wp_1-1}}{\partial \hat{\boldsymbol{\theta}}_2} \right\|^2 z_{1,\wp_1} \\ -c_{2,\wp_2} z_{2,\wp_2} - \bar{c}_{2,\wp_2} (\|\boldsymbol{\psi}_{2,\wp_2}\|^2 + \|\boldsymbol{\beta}_2\|^2 + \|\bar{\boldsymbol{\beta}}_u^2\|^2) z_{2,\wp_2} - g_{2,\wp_2} \left\| \frac{\partial \alpha_{2,\wp_2-1}}{\partial \hat{\boldsymbol{\theta}}_2} \right\|^2 z_{2,\wp_2} \\ \vdots \\ -c_{q,\wp_q} z_{q,\wp_q} - \bar{c}_{q,\wp_q} (\|\boldsymbol{\psi}_{q,\wp_q}\|^2 + \|\boldsymbol{\beta}_q\|^2 + \|\bar{\boldsymbol{\beta}}_u^q\|^2) z_{q,\wp_q} - g_{q,\wp_q} \left\| \frac{\partial \alpha_{q,\wp_q-1}}{\partial \hat{\boldsymbol{\theta}}_2} \right\|^2 z_{q,\wp_q} \end{bmatrix} \tag{4.133}$$

. Wherein the terms have their respective meanings with

$$\mathbf{F}_{\boldsymbol{\xi}} = \left[\sum_{k=1}^{\wp_1-1} \frac{\partial \alpha_{1,\wp_1-1}}{\partial \xi_{1,k}} \xi_{1,k+1},\ \sum_{k=1}^{\wp_2-1} \frac{\partial \alpha_{2,\wp_2-1}}{\partial \xi_{2,k}} \xi_{2,k+1}, \ldots,\ \sum_{k=1}^{\wp_q-1} \frac{\partial \alpha_{q,\wp_q-1}}{\partial \xi_{q,k}} \xi_{q,k+1} \right]^T$$

$$\mathbf{F}_{\mathbf{y_r}}(\dot{\mathbf{y}}_\mathbf{r},\ \ddot{\mathbf{y}}_\mathbf{r}, \ldots, \mathbf{y}_\mathbf{r}^{(\wp)}) = \left[\sum_{k=1}^{\wp_1-1} \frac{\partial \alpha_{1,\wp_1-1}}{\partial y_{r,1}^{(k-1)}} y_{r,1}^{(k)},\ \sum_{k=1}^{\wp_2-1} \frac{\partial \alpha_{2,\wp_2-1}}{\partial y_{r,2}^{(k-1)}} y_{r,2}^{(k)}, \ldots,\ \sum_{k=1}^{\wp_q-1} \frac{\partial \alpha_{q,\wp_q-1}}{\partial y_{r,q}^{(k-1)}} y_{r,q}^{(k)} \right]^T$$

$$\bar{\boldsymbol{\beta}}(\boldsymbol{\xi}, \boldsymbol{\eta}) := [\boldsymbol{\beta}_1(\boldsymbol{\xi}, \boldsymbol{\eta}),\ \boldsymbol{\beta}_2(\boldsymbol{\xi}, \boldsymbol{\eta}), \ldots,\ \boldsymbol{\beta}_q(\boldsymbol{\xi}, \boldsymbol{\eta})]^T \in \mathbb{R}^{q \times m}$$

Further, $N_j \in \mathbb{R}^{m \times m}$ is a square matrix with the j^{th} element on the main diagonal being 1 and all other entries as 0. While the known proportional actuation matrix $\mathbf{B}$ and $\bar{\boldsymbol{\beta}}_u$ are defined as

$$\mathbf{B} := \begin{bmatrix} b_{11} & \ldots & b_{1q} \\ \vdots & \ddots & \vdots \\ b_{m1} & \ldots & b_{mq} \end{bmatrix};\quad \bar{\boldsymbol{\beta}}_u = \begin{bmatrix} \beta_{1,1}\hat{u}_{H1} & \beta_{1,2}\hat{u}_{H2} & \ldots & \beta_{1,m}\hat{u}_{Hm} \\ \ldots & \ldots & \vdots & \ldots \\ \beta_{q,1}\hat{u}_{H1} & \beta_{q,2}\hat{u}_{H2} & \ldots & \beta_{q,m}\hat{u}_{Hm} \end{bmatrix}.$$

and $\bar{\boldsymbol{\beta}}_u^i$ denotes the i^{th} row vector of the matrix $\bar{\boldsymbol{\beta}}_u$. $\hat{\boldsymbol{\theta}}_1$, $\hat{\boldsymbol{\theta}}_2$ and $\hat{\boldsymbol{\theta}}_3$ are the estimates of the unknown parameters $\boldsymbol{\theta}_1^*$, $\boldsymbol{\theta}_2^*$ and $\boldsymbol{\theta}_2^*$, respectively. It has been mentioned earlier that one actuator in each group $\mathscr{G}_k,\ k = \overline{1,q}$ under the grouping scheme $\mathscr{G}$ should be alive to satisfy the controllability condition in (4.129). Thus, the assumption $\|\boldsymbol{\theta}^*\| > \ell$ and hence $\left\| \sum_{j=1}^{m} \theta_{1,j}^* N_j \right\| > \ell$ with $\ell > 0$ is justified. The parameter estimates are obtained from a faithful finite time bound estimator with $\tilde{\boldsymbol{\theta}} = \boldsymbol{\theta}^* - \hat{\boldsymbol{\theta}} = 0$ within an explicitly calculated finite time T_s. The design of the estimator will be discussed in the

section hereafter.

4.3.2.2 Design of Parameter Estimator with Finite Time Convergence

Firstly, the design of the parameter estimator requires the nonlinear system dynamics in (4.126)-(4.128) to be represented as a parametric $\boldsymbol{\xi}$ model as given below.

$$\underbrace{\begin{bmatrix} \dot{\xi}_{1,1} \\ \vdots \\ \dot{\xi}_{q,1} \\ \vdots \\ \dot{\xi}_{1,\wp_1} \\ \vdots \\ \dot{\xi}_{q,\wp_q} \end{bmatrix}}_{\dot{\boldsymbol{\xi}}} = \underbrace{\begin{bmatrix} \xi_{1,2} \\ \vdots \\ \xi_{q,2} \\ \vdots \\ a_1(\boldsymbol{\xi},\ \boldsymbol{\eta}) \\ \vdots \\ a_q(\boldsymbol{\xi},\ \boldsymbol{\eta}) \end{bmatrix}}_{\bar{\boldsymbol{a}}(\boldsymbol{\xi},\boldsymbol{\eta})} + \underbrace{\begin{bmatrix} 0 & \dots & 0 & \boldsymbol{\varphi}_{1,1}^T & 0 \\ \vdots & \vdots & \vdots & \vdots & \vdots \\ 0 & \dots & 0 & \boldsymbol{\varphi}_{q,1}^T & 0 \\ \vdots & \vdots & \ddots & \vdots & \vdots \\ \beta_{1,1}u_{H1} & \dots & \beta_{1,m}u_{Hm} & \boldsymbol{\varphi}_{1,\wp_1}^T & \boldsymbol{\beta}_1 \\ \vdots & \ddots & \vdots & \vdots & \vdots \\ \beta_{q,1}u_{H1} & \dots & \beta_{q,m}u_{Hm} & \boldsymbol{\varphi}_{q,\wp_q}^T & \boldsymbol{\beta}_q \end{bmatrix} \begin{bmatrix} \theta_{1,1}^* \\ \vdots \\ \theta_{1,m}^* \\ \boldsymbol{\theta}_2^* \\ \boldsymbol{\theta}_3^* \end{bmatrix}}_{\boldsymbol{\Phi}^T(\boldsymbol{\xi},\mathbf{u})\boldsymbol{\theta}^*} \tag{4.134}$$

Where $u_{Hj} := \sum_{k=1}^{q} b_{jk}w_k$ for $j = \overline{1,m}$. From (4.134), it can be well observed that the structure of the above estimation model is essentially the same as (4.12) regardless of the number of inputs and outputs of the system. In view of an exactly similar structural description of the parametric $\boldsymbol{\xi}-$model, the parameter estimator along with the necessary prerequisite filters are stated with direct reference from Section 4.2.3.1. Further, the convergence properties of the filtered signals, as we would observe in the sequel, will essentially follow from the results deduced in Lemmas 4.1-4.5 and Proposition 4.1. Let us therefore introduce the necessary filters as

$$\dot{\boldsymbol{\Omega}}^T = \mathbf{A}(\boldsymbol{\xi},t)\boldsymbol{\Omega}^T + \boldsymbol{\Phi}^T(\mathbf{x},\mathbf{v}); \quad \boldsymbol{\Omega} \in \mathbb{R}^{(2m+p)\times\sum_k \wp_k} \tag{4.135}$$

$$\dot{\boldsymbol{\Omega}}_0 = \mathbf{A}(\boldsymbol{\xi},t)(\boldsymbol{\Omega}_0 + \boldsymbol{\xi}) - \bar{\boldsymbol{a}}(\boldsymbol{\xi}); \quad \boldsymbol{\Omega}_0 \in \mathbb{R}^{\sum_k \wp_k} \tag{4.136}$$

Where $k = \overline{1,q}$ and $\mathbf{A}(\boldsymbol{\xi},t) = \mathbf{A_0} - \gamma\boldsymbol{\Phi}^T(\mathbf{x},\mathbf{v})\boldsymbol{\Phi}(\mathbf{x},\mathbf{v})\mathbf{P}$. Further, $\mathbf{A_0}$ is a constant Hurwitz matrix with a positive definite matrix $\mathbf{P} = \mathbf{P}^T > 0$ as the solution to the equality $\mathbf{A_0}^T\mathbf{P} + \mathbf{P}\mathbf{A_0} + \mathbf{Q} = 0$ with a chosen $\mathbf{Q} > 0$. Additionally, we define another two filters with filtered variables $\mathbf{R}(t)$ and $\mathbf{S}(t)$ as,

$$\dot{\mathbf{R}}(t) = -\mathscr{K}\mathbf{R}(t) + \boldsymbol{\Omega}\boldsymbol{\Omega}^T; \quad \mathbf{R}(0) = 0,\ \mathbf{R}(t) \in \mathbb{R}^{(2m+p)\times(2m+p)} \tag{4.137}$$

$$\dot{\mathbf{S}}(t) = -\mathscr{K}\mathbf{S}(t) + \boldsymbol{\Omega}(\boldsymbol{\Omega}_0 + \boldsymbol{\xi}); \quad \mathbf{S}(0) = 0,\ \mathbf{S}(t) \in \mathbb{R}^{2m+p} \tag{4.138}$$

where $\mathscr{K} > 0$ is another design scalar. Thereafter, defining the *prediction error* as $\mathscr{E} := \mathbf{S}(t) - \mathbf{R}(t)\hat{\boldsymbol{\theta}}$, the parameter update law exhibiting finite time stable solutions is obtained as follows.

$$\dot{\hat{\boldsymbol{\theta}}} = \boldsymbol{\Gamma}_1\frac{\mathscr{E}(t)}{\|\mathscr{E}(t)\|^{1/2}} + \boldsymbol{\Gamma}_2\int_0^t \frac{\mathscr{E}(s)}{\|\mathscr{E}(s)\|}ds \tag{4.139}$$

Herein $\boldsymbol{\Gamma}_1, \boldsymbol{\Gamma}_2 > 0$ define the rate of adaptation and decides the speed of convergence of the parameter estimates to their actual values. The following proposition, the stability properties of the proposed finite time parameter estimator and other auxiliary signals are summarized.

Proposition 4.2. *Let us assume that the regressor* $\boldsymbol{\Phi}(\boldsymbol{\xi}, \mathbf{u})$ *in the estimation model* (4.134) *is PE such that the solution of* (4.137) *given by* $\mathbf{R}(t)$ *is positive definite. Thus, the proposed adaptive parameter estimation law described by* (4.139) *ensures the finite time convergence of the parameter estimation error* $\tilde{\boldsymbol{\theta}}$ *to the origin from any initial condition. Further, the convergence time is defined by a explicit settling time function* $T_s(\tilde{\boldsymbol{\theta}}(t_0 = 0), t_0 = 0)$ *dependent on initial conditions and satisfies* $0 \leq T_s(\tilde{\boldsymbol{\theta}}(0), 0) < +\infty$. *In addition, the following properties hold in the sense of the solutions of* (4.139)*; (i)* $\tilde{\boldsymbol{\theta}}(t) \in \mathcal{L}_1 \cap \mathcal{L}_\infty$ *and (ii)* $\dot{\tilde{\boldsymbol{\theta}}}(t) \in \mathcal{L}_1$.

Proof.

Proving finite time stability of $\tilde{\boldsymbol{\theta}} = 0$ and the derivation of the settling time function T_s follows the same procedure as in the proof of Proposition 4.1 (i). Hence the proof is straightforward and the results directly follow from Proposition 4.1 (i). Nevertheless, the important milestones of the proof are provided in the succeeding text for ease of understanding.

To prove finite time stability, a new vector is defined as $\tilde{\boldsymbol{\theta}} := \left[\frac{\tilde{\boldsymbol{\theta}}}{\|\tilde{\boldsymbol{\theta}}\|^{\frac{1}{2}}},\ \tilde{\boldsymbol{\theta}}_{\boldsymbol{a}}\right]^T$. Where $\tilde{\boldsymbol{\theta}}_{\boldsymbol{a}} = -\boldsymbol{\Gamma}_2 \int_0^t \frac{\mathscr{E}(s)}{\|\mathscr{E}(s)\|} ds$ is an auxiliary state variable. The Lyapunov function candidate $V_{\tilde{\boldsymbol{\Theta}}} : \mathbb{R}^{2(2m+p)} \setminus \{0\} \times [0, \infty) \to \mathbb{R}_+$ as $(\tilde{\boldsymbol{\Theta}}, t) \mapsto \tilde{\boldsymbol{\Theta}}^T \mathbf{P} \tilde{\boldsymbol{\Theta}}$ with $\mathbf{P} > 0$ as a symmetric matrix. Thereafter taking the first time derivative of $V_{\tilde{\boldsymbol{\Theta}}}$ and following similar steps as in the proof of Proposition 4.1 (i), results in

$$\dot{V}_{\tilde{\boldsymbol{\Theta}}} \leq -\boldsymbol{\Gamma} \sqrt{V_{\tilde{\boldsymbol{\Theta}}}} < 0 \tag{4.140}$$

where $\boldsymbol{\Gamma} = \frac{\underline{\lambda}^{\frac{1}{2}}(\mathbf{P}) \underline{\lambda}(\mathbf{Q})}{\overline{\lambda}(\mathbf{P})}$, $\overline{\lambda}(\cdot)$ and $\underline{\lambda}(\cdot)$ denote the maximum and minimum eigen values of a square matrix. The matrix $\mathbf{Q} = -(\mathbf{F}^T \mathbf{P} + \mathbf{P}\mathbf{F})$ and $\mathbf{F} = \frac{1}{2} \left[\begin{array}{c|c} -\frac{\underline{\lambda}(\mathbf{R})}{\sqrt{\overline{\lambda}(\mathbf{R})}} \boldsymbol{\Gamma}_1 & \mathbf{I}_{2m+p} \\ \hline -\frac{2\underline{\lambda}(\mathbf{R})}{\overline{\lambda}(\mathbf{R})} \boldsymbol{\Gamma}_2 & \mathbf{0}_{2m+p} \end{array}\right]$ Invoking Theorem 2.1 in [106] and from the inequality obtained in (4.140), finite time stability of $\tilde{\boldsymbol{\Theta}} = 0$ is proved. The derivation of the expression for settling time T_s follows from inequality (4.140). For any initial condition $V_{\tilde{\boldsymbol{\Theta}}}(t_0 = 0) = V_{\tilde{\boldsymbol{\Theta}}}(0)$, the time taken by $\tilde{\boldsymbol{\Theta}}(t)$ to converge to the origin is atmost $T_s = 2V_{\tilde{\boldsymbol{\Theta}}}(0)^{\frac{1}{2}} / \boldsymbol{\Gamma}$ seconds. Thus, the first part of the proof is complete.

In the proof above, $\boldsymbol{\theta}^*$ is considered to be constant vector. However, occurrence of actuator failures will result in $\dot{\boldsymbol{\theta}}^* \neq 0$ at failure instances. Herein, we are interested in inferring the stability properties of signals for all $0 \leq t < \infty$ instead of concluding about their piecewise characteristics with respect to time. It has already been explained in Remark 4.1 that $\dot{\boldsymbol{\theta}}^*$ is $\mathcal{L}_1$-integrable provided the number of changes in the unknown parameter vector due to actuator failures is finite. From Lemma 4.2, the

boundedness of $\mathbf{\Omega}$ is inferred. The solution $\mathbf{R}(t)$ of the matrix differential equation (4.137) is given by

$$\mathbf{R}(t) \leq \mathbf{R}(0)e^{-\mathscr{K}\mathbf{I}_{2m+p}t}\frac{\|\mathbf{\Omega}(t)\|_{\infty}^{2}}{\mathscr{K}}(e^{\mathscr{K}\mathbf{I}_{2m+p}t} - \mathbf{I}_{2m+p}) \leq \frac{\|\mathbf{\Omega}(t)\|_{\infty}^{2}}{\mathscr{K}}\mathbf{I}_{2m+p} < \infty \tag{4.141}$$

Hence, $\|\mathbf{R}(t)\|_{\infty} = \sqrt{2m+p}\|\mathbf{\Omega}(t)\|_{\infty}^{2}/\mathscr{K}$ and $\mathbf{R}(t),\ \dot{\mathbf{R}}(t) \in \mathcal{L}_{\infty}$. To prove $\tilde{\boldsymbol{\theta}} \in \mathcal{L}_1$, the signal $\tilde{\mathbf{\Theta}}$ to be $\mathcal{L}_1$-integrable. Thus, with $\dot{\boldsymbol{\theta}}^* \neq 0$ the expression of $\dot{V}_{\tilde{\mathbf{\Theta}}}$ takes the following form.

$$\dot{V}_{\tilde{\mathbf{\Theta}}} \leq -\underbrace{\mathbf{\Gamma}\sqrt{\underline{\lambda}(\mathbf{P})}}_{\overline{\mathbf{\Gamma}}}\|\tilde{\mathbf{\Theta}}\| + \overline{\lambda}(\mathbf{P})\|\dot{\boldsymbol{\theta}}^*\| \tag{4.142}$$

Therefore, integrating the immediately above inequality and subsequent application of HÖlder's inequality from $0 \sim \infty$ yields,

$$\int_0^{\infty}\dot{V}_{\tilde{\mathbf{\Theta}}}ds \leq -\overline{\mathbf{\Gamma}}\int_0^{\infty}\|\tilde{\mathbf{\Theta}}\|ds + \overline{\lambda}(\mathbf{P})\int_0^{\infty}\|\dot{\boldsymbol{\theta}}^*\|ds \tag{4.143}$$

$$\int_0^{\infty}\|\tilde{\mathbf{\Theta}}\|ds \leq \frac{\overline{\lambda}(\mathbf{P})}{\sqrt{\underline{\lambda}(\mathbf{P})}\mathbf{\Gamma}}\|\tilde{\Theta}(0)\|^2 + \frac{\overline{\lambda}(\mathbf{P})}{\mathbf{\Gamma}\sqrt{\underline{\lambda}(\mathbf{P})}}\int_0^{\infty}\|\dot{\boldsymbol{\theta}}^*\|ds \tag{4.144}$$

From inequality (4.144) and invoking $\dot{\boldsymbol{\theta}}^* \in \mathcal{L}_1$, the $\mathcal{L}_1$-integrability of $\tilde{\mathbf{\Theta}}$ is concluded. Therefore $\tilde{\boldsymbol{\theta}}, \tilde{\boldsymbol{\theta}}_{\boldsymbol{a}} \in \mathcal{L}_1 \cap \mathcal{L}_{\infty}$ follows. Further, since $\mathbf{R}(t), \dot{\mathbf{R}}(t) \in \mathcal{L}_{\infty}$, it is straightforward to prove $\dot{\hat{\boldsymbol{\theta}}} \in \mathcal{L}_1$. The proof is complete. □

4.3.3 Stability Analysis of the Proposed Control System

The stability properties of the closed loop signals under the proposed control scheme are summarized in Theorem 4.4. Prior to the theoretical conclusions on the convergence features offered by the proposed control scheme; let us first reiterate the tracking error dynamics of the closed loop controlled system. The closed loop tracking error dynamics is described by

$$\dot{\mathbf{z}} = \boldsymbol{\mathcal{A}}_{\mathbf{z}}(\mathbf{z}, \hat{\boldsymbol{\theta}}, t)\mathbf{z} + \mathbf{B}_{\boldsymbol{\theta}^*}(\mathbf{z}, \hat{\boldsymbol{\theta}}, t)\tilde{\boldsymbol{\theta}} + \mathbf{B}_{\dot{\hat{\boldsymbol{\theta}}}}(\mathbf{z}, \hat{\theta}, t)\dot{\tilde{\boldsymbol{\theta}}}. \tag{4.145}$$

Where $\mathbf{z}(t) := [z_{1,1}, z_{2,1}, \ldots, z_{q,1}, z_{1,2}, z_{2,2}, \ldots, z_{q,2}, \ldots, z_{1,\wp_1}, z_{2,\wp_2}, \ldots, z_{q,\wp_q}]^T = [\mathbf{z}_{i,1}^T,\ \mathbf{z}_{i,2}^T, \ldots,\ \mathbf{z}_{i,q}^T]^T$ for $i = \overline{1,q}$ and the matrices $\boldsymbol{\mathcal{A}}_{\mathbf{z}}$ is defined in (4.152), respectively. The matrices $\mathbf{B}_{\boldsymbol{\theta}^*}$ and $\mathbf{B}_{\dot{\hat{\boldsymbol{\theta}}}}$ are

defined as follows.

$$\mathbf{B}_{\boldsymbol{\theta}^*} := \left[\begin{array}{ccc|c|ccc} 0 & 0 & 0 & & 0 & 0 & 0 \\ 0 & 0 & 0 & \boldsymbol{\psi}_{1,1}^T & 0 & 0 & 0 \\ \vdots & \ddots & \ddots & \vdots & \vdots & \ddots & \vdots \\ 0 & 0 & 0 & \boldsymbol{\psi}_{q,1}^T & 0 & 0 & 0 \\ \hline 0 & 0 & 0 & & 0 & 0 & 0 \\ 0 & 0 & 0 & \boldsymbol{\psi}_{1,2}^T & 0 & 0 & 0 \\ \vdots & \ddots & \ddots & \vdots & \vdots & \ddots & \vdots \\ 0 & 0 & 0 & \boldsymbol{\psi}_{q,2}^T & 0 & 0 & 0 \\ \hline & \vdots & & \vdots & & \vdots & \\ \hline 0 & 0 & 0 & & 0 & 0 & 0 \\ 0 & 0 & 0 & \boldsymbol{\psi}_{1,\wp_1-1}^T & 0 & 0 & 0 \\ \vdots & \ddots & \ddots & \vdots & \vdots & \ddots & \vdots \\ 0 & 0 & 0 & \boldsymbol{\psi}_{q,\wp_q-1}^T & 0 & 0 & 0 \\ \hline \beta_{1,1}\hat{u}_{H1} & \dots & \beta_{1,m}\hat{u}_{Hm} & \boldsymbol{\psi}_{1,\wp_1}^T & \beta_{1,1} & \dots & \beta_{1,m} \\ \vdots & \ddots & \vdots & \vdots & \vdots & \ddots & \vdots \\ \beta_{q,1}\hat{u}_{H1} & \dots & \beta_{q,m}\hat{u}_{Hm} & \boldsymbol{\psi}_{q,\wp_q}^T & \beta_{q,1} & \dots & \beta_{q,m} \end{array}\right]$$

$$\mathbf{B}_{\dot{\hat{\boldsymbol{\theta}}}_2} := -\left[\begin{array}{c|ccc|c|ccc} 0 & \dfrac{\partial \alpha_{1,1}}{\partial \hat{\boldsymbol{\theta}}_2} & \dots & \dfrac{\partial \alpha_{q,1}}{\partial \hat{\boldsymbol{\theta}}_2} & \dots & \dfrac{\partial \alpha_{1,\wp_1-1}}{\partial \hat{\boldsymbol{\theta}}_2} & \dots & \dfrac{\partial \alpha_{q,\wp_q-1}}{\partial \hat{\boldsymbol{\theta}}_2} \end{array}\right]^T \tag{4.146}$$

The matrix in left most lower block of the matrix $\mathbf{B}_{\boldsymbol{\theta}^*}$ is denoted by

$$\bar{\boldsymbol{\beta}}_{\hat{u}} := [\bar{\boldsymbol{\beta}}_{\hat{u}}^1,\ \bar{\boldsymbol{\beta}}_{\hat{u}}^2, \dots,\ \bar{\boldsymbol{\beta}}_{\hat{u}}^q]^T = \begin{bmatrix} \beta_{1,1}\hat{u}_{H1} & \dots & \beta_{1,m}\hat{u}_{Hm} \\ \beta_{2,1}\hat{u}_{H1} & \dots & \beta_{2,m}\hat{u}_{Hm} \\ \vdots & \ddots & \vdots \\ \beta_{q-1,1}\hat{u}_{H1} & \dots & \beta_{q-1,m}\hat{u}_{Hm} \\ \beta_{q,1}\hat{u}_{H1} & \dots & \beta_{q,m}\hat{u}_{Hm} \end{bmatrix}.$$

Such a notation is preferred to lend simplicity in matrix calculations to follow in the sequel. The closed loop system matrix and the relevant input matrices with reference to (4.145), namely, $\boldsymbol{\mathcal{A}}_{\mathbf{z}}$, $\mathbf{B}_{\boldsymbol{\theta}^*}$ and $\mathbf{B}_{\dot{\hat{\boldsymbol{\theta}}}_2}$ are of order $\sum_{i=1}^{q} \wp_i \times \sum_{i=1}^{q} \wp_i$, $\sum_{i=1}^{q} \wp_i \times (2m+p)$ and $\sum_{i=1}^{q} \wp_i \times p$ with elements from $\mathbb{R}$. Further, the shorthand notation used to represent the elements of the matrix $\boldsymbol{\mathcal{A}}_{\mathbf{z}}$ is explained as, $a_{i,j} := c_{i,j} + s_{i,j}$ for $i = \overline{1,q}$ and $j = \overline{1,\wp_q}$. The terms $c_{i,j}$ are constant controller gains and the damping factors $s_{i,j}$ are

defined as,

$$s_{1,1} = \bar{c}_{1,1}\|\boldsymbol{\psi}_{1,1}\|^2 \tag{4.147}$$

$$s_{1,r_1} = \bar{c}_{1,r_1}\|\boldsymbol{\psi}_{1,r_1}\|^2 + g_{1,r_1}\left\|\frac{\partial \alpha_{1,r_1-1}}{\partial \hat{\boldsymbol{\theta}}_2}\right\|^2, \quad r_1 = \overline{2, \wp_1 - 1} \tag{4.148}$$

$$s_{1,\wp_1} = \bar{c}_{1,\wp_1}(\|\boldsymbol{\psi}_{1,\wp_1}\|^2 + \|\boldsymbol{\beta}_1\|^2 + \|\hat{v}_1\|^2) + g_{1,\wp_1}\left\|\frac{\partial \alpha_{1,\wp_1-1}}{\partial \hat{\boldsymbol{\theta}}_2}\right\|^2 \tag{4.149}$$

.....

$$s_{i,r_i} = \bar{c}_{i,r_i}\|\boldsymbol{\psi}_{i,r_i}\|^2 + g_{i,r_i}\left\|\frac{\partial \alpha_{i,r_i-1}}{\partial \hat{\boldsymbol{\theta}}_2}\right\|^2, \quad r_i = \overline{2, \wp_i - 1},\ i = \overline{1, q} \tag{4.150}$$

$$s_{i,\wp_i} = \bar{c}_{i,\wp_i}(\|\boldsymbol{\psi}_{i,\wp_i}\|^2 + \|\boldsymbol{\beta}_i\|^2 + \|\hat{v}_i\|^2) + g_{i,\wp_i}\left\|\frac{\partial \alpha_{i,\wp_i-1}}{\partial \hat{\boldsymbol{\theta}}_2}\right\|^2 \tag{4.151}$$

In what follows, the theorem states the stability characteristics of the closed loop signals when the system is affected by finite number of actuator failures. By finite number of actuator failures, we mean that the system can be subjected to a maximum of $(m-q)$ actuator failures satisfying (4.129) to enable the existence of an adaptive FTC strategy to recover its performance.

Theorem 4.4. *Let us consider the MIMO nonlinear uncertain system dynamics in* (4.126)-(4.128) *with unknown parameters, affected by finite number of actuator failures. Considering the immanent design assumptions 3.8-3.10, the proposed adaptive controller* (4.133) *augmented with the finite time parameter estimator in* (4.139) *renders the following properties with the maximal interval of existence of signals being* $[0, \infty)$.

(i) All closed loop signals have stable trajectories and $\mathbf{z}(t) \in \mathcal{L}_\infty$.

(ii) The tracking error vector $\mathbf{z}(t) \in \mathcal{L}_1$ *and the output tracking error asymptotically converges to the origin, i.e.,* $\lim_{t\to\infty}(\mathbf{y} - \mathbf{y_r}) = 0$.

$$\mathcal{A}_{\mathbf{z}} := \left[\begin{array}{cccc|cccc|cccc|c|cccc} -a_{11} & 0 & \dots & 0 & 1 & 0 & \dots & 0 & 0 & 0 & \dots & 0 & & 0 & 0 & \dots & 0 \\ 0 & -a_{21} & \dots & 0 & 0 & 1 & \dots & 0 & 0 & 0 & \dots & 0 & & 0 & 0 & \dots & 0 \\ \vdots & \ddots & \ddots & \vdots & \vdots & \ddots & \ddots & \vdots & \vdots & \ddots & \ddots & \vdots & \dots & \vdots & \ddots & \ddots & \vdots \\ 0 & \dots & \dots & -a_{q1} & 0 & \dots & \dots & 1 & 0 & \dots & \dots & 0 & & 0 & \dots & \dots & 0 \\ \hline -1 & 0 & \dots & 0 & -a_{12} & 0 & \dots & 0 & 1 & 0 & \dots & 0 & & 0 & 0 & \dots & 0 \\ 0 & -1 & \dots & 0 & 0 & -a_{22} & \dots & 0 & 0 & 1 & \dots & 0 & & 0 & 0 & \dots & 0 \\ \vdots & \ddots & \ddots & \vdots & \vdots & \ddots & \ddots & \vdots & \vdots & \ddots & \ddots & \vdots & \dots & \vdots & \ddots & \ddots & \vdots \\ 0 & \dots & \dots & -1 & 0 & \dots & \dots & -a_{q2} & 0 & \dots & \dots & 1 & & 0 & \dots & \dots & 0 \\ \hline & \vdots & & & & \ddots & & & & \ddots & & & \ddots & & \vdots & & \\ & \vdots & & & & \ddots & & & & \ddots & & & \ddots & & \vdots & & \\ \hline & & & & & & & & & & & & & 1 & 0 & \dots & 0 \\ & & & & & & & & & & & & & 0 & 1 & \dots & 0 \\ & \vdots & & & & \ddots & & & & \ddots & & & \ddots & \vdots & \ddots & \ddots & \vdots \\ & & & & & & & & & & & & & 0 & \dots & \dots & 1 \\ \hline 0 & 0 & \dots & 0 & 0 & 0 & \dots & 0 & & & & & -1 & 0 & \dots & 0 & \\ 0 & 0 & \dots & 0 & 0 & 0 & \dots & 0 & & & \dots & & 0 & -1 & \dots & 0 & -\frac{\bar{\boldsymbol{\beta}} \sum_{j} \theta^{*}_{1,j} N_j \bar{\boldsymbol{\beta}}^{\dagger}}{\ell} \begin{pmatrix} a_{1_{\wp 1}} & \dots & 0 \\ \vdots & \ddots & \vdots \\ 0 & \dots & a_{q_{\wp q}} \end{pmatrix} \\ \vdots & \ddots & \ddots & \vdots & \vdots & \ddots & \ddots & \vdots & & & & & \vdots & \ddots & \ddots & \vdots & \\ 0 & \dots & \dots & 0 & 0 & \dots & \dots & 0 & & & & & 0 & \dots & \dots & -1 & \end{array}\right] \tag{4.152}$$

Proof of (i).

From Proposition 4.2, the boundedness of $\tilde{\boldsymbol{\theta}}$ and $\dot{\hat{\boldsymbol{\theta}}} \in \mathcal{L}_1$ is proved. Thereafter following exactly similar steps as in the proof of Theorem 3.8(i) with the substitution $\tilde{\boldsymbol{\theta}}_{\mathbf{s}} = \tilde{\boldsymbol{\theta}}$ yields the following.

$$\frac{1}{2}\frac{d}{dt}\left(\sum_{i=1}^{q}\sum_{r_i=1}^{\wp_i} z_{i,r_i}^2\right) \leq -\sum_{i=1}^{q}\sum_{r_i=1}^{\wp_i-1} c_{i,r_i} z_{i,r_i}^2 + \sum_{i=1}^{q} c_{i,\wp_i} z_{i,\wp_i}^2 + \frac{1}{4}\left(\frac{\|\tilde{\boldsymbol{\theta}}_1\|^2}{\bar{\bar{c}}} + \frac{\|\tilde{\boldsymbol{\theta}}_2\|^2}{\bar{c}} + \frac{\|\tilde{\boldsymbol{\theta}}_3\|^2}{4\bar{\bar{c}}} + \frac{\|\dot{\hat{\boldsymbol{\theta}}}_2\|^2}{\bar{g}}\right) \tag{4.153}$$

$$\leq -\sum_{i=1}^{q}\sum_{r_i=1}^{\wp_i} c_{i,r_i} z_{i,r_i}^2 + \frac{1}{4}\left(\frac{\|\tilde{\boldsymbol{\theta}}\|^2}{\breve{c}} + \frac{\|\dot{\hat{\boldsymbol{\theta}}}_2\|^2}{\bar{g}}\right) \tag{4.154}$$

$$\leq -2\mathscr{C}\sum_{i=1}^{q}\sum_{r_i=1}^{\wp_i} z_{i,r_i}^2 + \frac{1}{4}\left(\frac{\|\tilde{\boldsymbol{\theta}}\|^2}{\breve{c}} + \frac{\|\dot{\hat{\boldsymbol{\theta}}}_2\|^2}{\bar{g}}\right) \tag{4.155}$$

where $\bar{\bar{c}} = \left(\sum_{i=1}^{q}\frac{1}{\bar{c}_{i,\wp_i}}\right)^{-1}$, $\bar{c} = \left(\sum_{i=1}^{q}\sum_{r_i=1}^{\wp_i}\frac{1}{\bar{c}_{i,r_i}}\right)^{-1}$, $\bar{g} = \left(\sum_{i=1}^{q}\sum_{r_i=2}^{\wp_i}\frac{1}{\bar{g}_{i,r_i}}\right)^{-1}$, $\breve{c} = \min\{\bar{\bar{c}}, \bar{c}\}$ and $\mathscr{C} = \min_{\substack{1\leq i\leq q\\ 1\leq r_i\leq \wp_i}}\{c_{i,r_i}\}$. Invoking the boundedness of $\tilde{\boldsymbol{\theta}}$ and $\dot{\hat{\boldsymbol{\theta}}} \in \mathcal{L}_1$ in (4.155), directs the conclusion that $\mathbf{z}(t) \in \mathcal{L}_\infty$. □

Proof of (ii).

The closed loop tracking error dynamics is first rewritten as,

$$\dot{\mathbf{z}}(t) = \bar{\boldsymbol{\mathcal{A}}}_{\mathbf{z}}(\mathbf{z}, \hat{\boldsymbol{\theta}}_{\mathbf{s}}, t)\mathbf{z}(t) + \bar{\mathbf{B}}_{\boldsymbol{\theta}^*}(\mathbf{z}, \hat{\boldsymbol{\theta}}_{\mathbf{s}}, t)\tilde{\boldsymbol{\theta}}_{\mathbf{s}} + \mathbf{B}_{\dot{\hat{\boldsymbol{\theta}}}_2}(\mathbf{z}, \hat{\boldsymbol{\theta}}_{\mathbf{s}}, t)\dot{\hat{\boldsymbol{\theta}}}_{2\mathbf{s}} \tag{4.156}$$

where the matrices $\bar{\boldsymbol{\mathcal{A}}}_{\mathbf{z}}$ and $\bar{\mathbf{B}}_{\boldsymbol{\theta}^*}$ are defined in (4.159)-(4.160). The matrix $\mathbf{B}_{\dot{\hat{\boldsymbol{\theta}}}_2}$ has the same definition as given in (4.146). Needless to mention, the procedure to arrive at the $\mathcal{L}_1-$integrability of the tracking error vector $\mathbf{z}(t)$, although not trivial is same as what has been followed in the proof of Theorem 4.2 (ii) with slight modifications. The essential steps are mentioned herein to abstain from a too comprehensive treatment and more importantly to avert redundant calculations.

Let us begin by introducing an auxiliary state variable $\boldsymbol{\chi}^T \in \mathbb{R}^{\sum_k \wp_k \times (2m+p)}$ whose dynamics are described by the following matrix differential equation,

$$\dot{\boldsymbol{\chi}}^T = \bar{\boldsymbol{\mathcal{A}}}_{\mathbf{z}}(\mathbf{z}, \hat{\boldsymbol{\theta}}, t)\boldsymbol{\chi}^T + \bar{\mathbf{B}}_{\boldsymbol{\theta}^*}(\mathbf{z}, \hat{\boldsymbol{\theta}}, t) \tag{4.157}$$

The solution of (4.157) is described by

$$\boldsymbol{\chi}^T = \boldsymbol{e}^{-\bar{\boldsymbol{\mathcal{A}}}_{\mathbf{z}}t}\boldsymbol{\chi}^T(0) + \int_0^t \boldsymbol{e}^{-\bar{\boldsymbol{\mathcal{A}}}_{\mathbf{z}}(t-s)}\bar{\mathbf{B}}_{\boldsymbol{\theta}^*}(s)ds \tag{4.158}$$

$$\bar{\mathcal{A}}_{\mathbf{z}} := \left[\begin{array}{cccc|cccc|cccc|c|cccc} -a_{11} & 0 & \dots & 0 & 1 & 0 & \dots & 0 & 0 & 0 & \dots & 0 & & 0 & 0 & \dots & 0 \\ 0 & -a_{21} & \dots & 0 & 0 & 1 & \dots & 0 & 0 & 0 & \dots & 0 & & 0 & 0 & \dots & 0 \\ \vdots & \ddots & \ddots & \vdots & \vdots & \ddots & \ddots & \vdots & \vdots & \ddots & \ddots & \vdots & \dots & \vdots & \ddots & \ddots & \vdots \\ 0 & \dots & \dots & -a_{q1} & 0 & \dots & \dots & 1 & 0 & \dots & \dots & 0 & & 0 & \dots & \dots & 0 \\ \hline -1 & 0 & \dots & 0 & -a_{12} & 0 & \dots & 0 & 1 & 0 & \dots & 0 & & 0 & 0 & \dots & 0 \\ 0 & -1 & \dots & 0 & 0 & -a_{22} & \dots & 0 & 0 & 1 & \dots & 0 & & 0 & 0 & \dots & 0 \\ \vdots & \ddots & \ddots & \vdots & \vdots & \ddots & \ddots & \vdots & \vdots & \ddots & \ddots & \vdots & \dots & \vdots & \ddots & \ddots & \vdots \\ 0 & \dots & \dots & -1 & 0 & \dots & \dots & -a_{q2} & 0 & \dots & \dots & 1 & & 0 & \dots & \dots & 0 \\ \hline \multicolumn{4}{c|}{\vdots} & \multicolumn{4}{c|}{\ddots} & \multicolumn{4}{c|}{\ddots} & \ddots & \multicolumn{4}{c}{\vdots} \\ \multicolumn{4}{c|}{} & \multicolumn{4}{c|}{\ddots} & \multicolumn{4}{c|}{\ddots} & \ddots & \multicolumn{4}{c}{\vdots} \\ \hline \multicolumn{4}{c|}{\vdots} & \multicolumn{4}{c|}{\ddots} & \multicolumn{4}{c|}{\ddots} & \ddots & 1 & 0 & \dots & 0 \\ \multicolumn{4}{c|}{} & \multicolumn{4}{c|}{} & \multicolumn{4}{c|}{} & & 0 & 1 & \dots & 0 \\ \multicolumn{4}{c|}{} & \multicolumn{4}{c|}{} & \multicolumn{4}{c|}{} & & \vdots & \ddots & \ddots & \vdots \\ \multicolumn{4}{c|}{} & \multicolumn{4}{c|}{} & \multicolumn{4}{c|}{} & & 0 & \dots & \dots & 1 \\ \hline 0 & 0 & \dots & 0 & 0 & 0 & \dots & 0 & \multicolumn{4}{c|}{} & -1 & 0 & \dots & 0 & -\frac{\bar{\boldsymbol{\beta}}\sum_j \hat{\theta}_{1,j} N_j \bar{\boldsymbol{\beta}}^\dagger}{\ell} \begin{pmatrix} a_{1\wp_1} & \dots & 0 \\ \vdots & \ddots & \vdots \\ 0 & \dots & a_{q\wp_q} \end{pmatrix} \\ 0 & 0 & \dots & 0 & 0 & 0 & \dots & 0 & \multicolumn{4}{c|}{} & 0 & -1 & \dots & 0 & \\ \vdots & \ddots & \ddots & \vdots & \vdots & \ddots & \ddots & \vdots & \multicolumn{4}{c|}{\dots} & \vdots & \ddots & \ddots & \vdots & \\ 0 & \dots & \dots & 0 & 0 & \dots & \dots & 0 & \multicolumn{4}{c|}{} & 0 & \dots & \dots & -1 & \end{array}\right] \tag{4.159}$$

$$\bar{\mathbf{B}}_{\boldsymbol{\theta}^*} := \left[\begin{array}{ccc|c|ccc} 0 & 0 & \dots & 0 & & 0 & 0 & \dots & 0 \\ 0 & 0 & \dots & 0 & \boldsymbol{\psi}_{1,1}^T & 0 & 0 & \dots & 0 \\ \vdots & \ddots & \ddots & \vdots & \vdots & \vdots & \ddots & \ddots & \vdots \\ 0 & \dots & \dots & 0 & \boldsymbol{\psi}_{q,1}^T & 0 & \dots & \dots & 0 \\ \hline \multicolumn{3}{c|}{\vdots} & \vdots & & \multicolumn{3}{c}{\vdots} \\ \hline \beta_{1,1}u_{H1} & \dots & \beta_{1,m}u_{Hm} & \boldsymbol{\psi}_{1,\wp_1}^T & & \beta_{1,1} & \dots & \beta_{1,m} \\ \vdots & \ddots & \vdots & \vdots & & \vdots & \ddots & \vdots \\ \beta_{q,1}u_{H1} & \dots & \beta_{q,m}u_{Hm} & \boldsymbol{\psi}_{q,\wp_q}^T & & \beta_{q,1} & \dots & \beta_{q,m} \end{array}\right] \tag{4.160}$$

Using the inequality $\|e^{-\bar{\mathcal{A}}_{\mathbf{z}}t}\| \leq \breve{\breve{k}}e^{-\bar{c}_0 t}$, $\bar{c}_0, \breve{\breve{k}} > 0$ in (4.158) and the fact that $\bar{\mathbf{B}}_{\boldsymbol{\theta}^*}$ is bounded (since all closed loop trajectories are bounded) results in

$$\|\boldsymbol{\chi}\| \leq \|\boldsymbol{\chi}(0)\| + \frac{\breve{\breve{k}}\|\bar{\mathbf{B}}_{\boldsymbol{\theta}^*}\|_\infty}{\bar{c}_0} \tag{4.161}$$

Hence the auxiliary state variable $\boldsymbol{\chi}^T(t) \in \mathcal{L}_\infty$ is ascertained from (4.161). At this point, let us define another additional variable $\boldsymbol{\vartheta}$ as follows

$$\boldsymbol{\vartheta}(t) = \mathbf{z}(t) - \boldsymbol{\chi}^T\tilde{\boldsymbol{\theta}}(t) \tag{4.162}$$

Thus from the definition of $\boldsymbol{\vartheta}(t)$, to prove that $\mathbf{z}(t) \in \mathcal{L}_1$ requires $\boldsymbol{\vartheta}(t)$ and $\boldsymbol{\chi}^T\tilde{\boldsymbol{\theta}}(t)$ to be $\mathcal{L}_1-$integrable. Proving $\boldsymbol{\chi}^T\tilde{\boldsymbol{\theta}} \in \mathcal{L}_1$ is straightforward as shown below. Integrating $\|\boldsymbol{\chi}^T\tilde{\boldsymbol{\theta}}\|$ from $t = 0 \sim \infty$ and thereafter applying Hölder's inequality to the integral results in,

$$\int_0^\infty \|\boldsymbol{\chi}^T\tilde{\boldsymbol{\theta}}\|dt \leq \|\boldsymbol{\chi}\|_\infty \int_0^\infty \|\tilde{\boldsymbol{\theta}}\|ds \tag{4.163}$$

The above inequality uses the boundedness of $\boldsymbol{\chi}(t)$ derived in (4.161). Further $\tilde{\boldsymbol{\theta}}(t) \in \mathcal{L}_1$ is proved in Proposition 4.2. Hence $\boldsymbol{\chi}^T\tilde{\boldsymbol{\theta}} \in \mathcal{L}_1$ follows from (4.163).

Now what remains is to prove $\boldsymbol{\vartheta}(t) \in \mathcal{L}_1$. It should be reiterated that all the signal properties are derived considering their maximal interval of existence to be $[0, \infty)$. Adopting similar calculations as in (4.82), the following dynamics of $\boldsymbol{\vartheta}(t)$ is arrived at,

$$\dot{\boldsymbol{\vartheta}} = \bar{\boldsymbol{\mathcal{A}}}_{\mathbf{z}}\boldsymbol{\vartheta} + \mathbf{B}_{\dot{\hat{\boldsymbol{\theta}}}_2}\dot{\hat{\boldsymbol{\theta}}}_2 + \boldsymbol{\chi}^T\dot{\hat{\boldsymbol{\theta}}} - \boldsymbol{\chi}^T\dot{\boldsymbol{\theta}}^* \tag{4.164}$$

The solution of (4.164) is derived to be

$$\begin{aligned}\vartheta(t) = e^{-\bar{\boldsymbol{\mathcal{A}}}_{\mathbf{z}}t}\boldsymbol{\vartheta}(0) + \int_0^t e^{-\bar{\boldsymbol{\mathcal{A}}}_{\mathbf{z}}(t-s)}\mathbf{B}_{\dot{\hat{\boldsymbol{\theta}}}_2}(\mathbf{z}(s), \hat{\boldsymbol{\theta}}(s), s)\dot{\hat{\boldsymbol{\theta}}}_2(s)ds \\ + \int_0^t e^{-\bar{\boldsymbol{\mathcal{A}}}_{\mathbf{z}}(t-s)}\boldsymbol{\chi}^T(s)\dot{\hat{\boldsymbol{\theta}}}(s)ds - \int_0^t e^{-\bar{\boldsymbol{\mathcal{A}}}_{\mathbf{z}}(t-s)}\boldsymbol{\chi}^T(s)\dot{\boldsymbol{\theta}}^*(s)ds\end{aligned} \tag{4.165}$$

Thereafter imposing the norm operator on both sides of (4.165) and using the inequality $\|e^{-\bar{\boldsymbol{\mathcal{A}}}_{\mathbf{z}}t}\| \leq$

$\breve{\breve{k}}\boldsymbol{e}^{-\bar{c}_0 t}$, $\bar{c}_0, \breve{\breve{k}} > 0$ followed by Hölder's inequality, leads to

$$\|\boldsymbol{\vartheta}(t)\| \leq \underbrace{\breve{\breve{k}}\boldsymbol{e}^{-\bar{c}_0 t}\|\boldsymbol{\vartheta}(0)\|}_{\text{I}} + \underbrace{\breve{\breve{k}}\|\mathbf{B}_{\dot{\hat{\boldsymbol{\theta}}}}\|_\infty \int_0^t \boldsymbol{e}^{-\bar{c}_0(t-s)}\|\dot{\hat{\boldsymbol{\theta}}}(s)\|ds}_{\text{II}}$$
$$+ \underbrace{\breve{\breve{k}}\|\boldsymbol{\chi}\|_\infty \int_0^t \boldsymbol{e}^{-\bar{c}_0(t-s)}\|\dot{\hat{\boldsymbol{\theta}}}(s)\|ds}_{\text{III}} + \underbrace{\breve{\breve{k}}\|\boldsymbol{\chi}\|_\infty \int_0^t \boldsymbol{e}^{-\bar{c}_0(t-s)}\|\dot{\boldsymbol{\theta}}^*(s)\|ds}_{\text{IV}} \tag{4.166}$$

Now integrating both sides of inequality (4.166) from $t \sim t+T$ and thereafter calculating the integral to be finite would prove the claim. The integrals of `I`-`IV` are calculated in the same order as stated above for clarity. The integral of `I` is calculated to be

$$\int_t^{t+T} \breve{\breve{k}}\boldsymbol{e}^{-\bar{c}_0 s}\|\boldsymbol{\vartheta}(0)\|ds = \frac{\breve{\breve{k}}}{\bar{c}_0}\|\boldsymbol{\vartheta}(0)\| < \infty. \tag{4.167}$$

Integration of `II` in(4.166) from $t \sim t+T$ leads to the following.

$$\int_t^{t+T} \breve{\breve{k}}\|\mathbf{B}_{\dot{\hat{\boldsymbol{\theta}}}_2}\|_\infty \int_0^s \boldsymbol{e}^{-\bar{c}_0(s-\tau)}\|\dot{\hat{\boldsymbol{\theta}}}_2(\tau)\|d\tau ds \leq \breve{\breve{k}}\|\mathbf{B}_{\dot{\hat{\boldsymbol{\theta}}}_2}\|_\infty \int_t^{t+T}\int_0^s \boldsymbol{e}^{-\bar{c}_0(s-\tau)}\|\dot{\hat{\boldsymbol{\theta}}}_2(\tau)\|d\tau ds$$
$$\leq \breve{\breve{k}}\|\mathbf{B}_{\dot{\hat{\boldsymbol{\theta}}}_2}\|_\infty \int_t^{t+T} \boldsymbol{e}^{-\bar{c}_0 s}\int_0^t \boldsymbol{e}^{\bar{c}_0\tau}\|\dot{\hat{\boldsymbol{\theta}}}_2(\tau)\|d\tau ds + \breve{\breve{k}}\|\mathbf{B}_{\dot{\hat{\boldsymbol{\theta}}}_2}\|_\infty \int_t^{t+T}\boldsymbol{e}^{-\bar{c}_0 s}\int_t^s \mathbf{e}^{\bar{c}_0\tau}\|\dot{\hat{\boldsymbol{\theta}}}_2(\tau)\|d\tau ds$$
$$\leq \frac{\breve{\breve{k}}\|\mathbf{B}_{\dot{\hat{\boldsymbol{\theta}}}_2}\|_\infty}{\bar{c}_0}\int_0^t \boldsymbol{e}^{-\bar{c}_0(t-\tau)}\|\dot{\hat{\boldsymbol{\theta}}}_2(\tau)\|d\tau + \breve{\breve{k}}\|\mathbf{B}_{\dot{\hat{\boldsymbol{\theta}}}_2}\|_\infty \int_t^{t+T}\boldsymbol{e}^{-\bar{c}_0 s}\int_t^s \boldsymbol{e}^{\bar{c}_0\tau}\|\dot{\hat{\boldsymbol{\theta}}}_2(\tau)\|d\tau ds \tag{4.168}$$

Inequality (4.168) is derived using the property $\boldsymbol{e}^{-\bar{c}_0 t} - \boldsymbol{e}^{-\bar{c}_0(t+T)} \leq \boldsymbol{e}^{-\bar{c}_0 t}$. The first expression on the right hand side of the last inequality among the set of inequalities in (4.87) can be solved using the procedure adopted in [110] (Chapter 3, page 85) to arrive at the boundedness of Δ. Using the fact that $\dot{\hat{\boldsymbol{\theta}}}_2 \in \mathcal{L}_1$ (instead of $\mathcal{S}_1(\nu)$ since finite number of actuator failures are considered), and if its $\mathcal{L}_1-$bound is designated by $\|\dot{\hat{\boldsymbol{\theta}}}_2\|_{\mathcal{L}_1}$ the result below follows,

$$\frac{\breve{\breve{k}}\|\mathbf{B}_{\dot{\hat{\boldsymbol{\theta}}}_2}\|_\infty}{\bar{c}_0}\int_0^t \boldsymbol{e}^{-\bar{c}_0(t-\tau)}\|\dot{\hat{\boldsymbol{\theta}}}_2(\tau)\|d\tau \leq \frac{\breve{\breve{k}}\|\mathbf{B}_{\dot{\hat{\boldsymbol{\theta}}}_2}\|_\infty e^{\bar{c}_0}}{\bar{c}_0(1-e^{-\bar{c}_0})}\|\dot{\hat{\boldsymbol{\theta}}}_2\|_{\mathcal{L}_1} < \infty \tag{4.169}$$

Having determined the boundedness of the integral in (4.169), proving the finiteness of the remaining integral on the RHS of (4.168) is yet to be attempted. In this direction, the identity for the change of

sequence of integration (4.37) is applied to the underlying integral as shown below.

$$\breve{\breve{k}}\|\mathbf{B}_{\dot{\hat{\boldsymbol{\theta}}}_2}\|_\infty \int_t^{t+T} \boldsymbol{e}^{-\bar{c}_0 s} \int_t^s \boldsymbol{e}^{\bar{c}_0\tau}\|\dot{\hat{\boldsymbol{\theta}}}_2(\tau)\|d\tau ds = \breve{\breve{k}}\|\mathbf{B}_{\dot{\hat{\boldsymbol{\theta}}}_2}\|_\infty \int_t^{t+T} \boldsymbol{e}^{\bar{c}_0\tau}\|\dot{\hat{\boldsymbol{\theta}}}_2(\tau)\| \int_\tau^{t+T} \boldsymbol{e}^{-\bar{c}_0 s} ds d\tau$$

$$\leq \frac{\breve{\breve{k}}\|\mathbf{B}_{\dot{\hat{\boldsymbol{\theta}}}_2}\|_\infty}{\bar{c}_0} \int_t^{t+T} \|\dot{\hat{\boldsymbol{\theta}}}_2(\tau)\|d\tau \tag{4.170}$$

$$\tag{4.171}$$

Let us now consider the limits of the integral on the RHS of (4.170) in accordance with $t = 0$ and $T \to \infty$. Thereafter invoking the $\mathcal{L}_1-$integrability property of $\dot{\hat{\boldsymbol{\theta}}}$ proved earlier, the boundedness of (4.170) follows, that is,

$$\breve{\breve{k}}\|\mathbf{B}_{\dot{\hat{\boldsymbol{\theta}}}_2}\|_\infty \int_t^{t+T} \boldsymbol{e}^{-\bar{c}_0 s} \int_t^s \boldsymbol{e}^{\bar{c}_0\tau}\|\dot{\hat{\boldsymbol{\theta}}}_2(\tau)\|d\tau ds < \infty \tag{4.172}$$

Hence the integral of `II` is proved to have a finite bound. Eventually, since the integral of `III` and `IV` looks similar to that of `II`, the same procedure is followed to arrive at their boundedness. The derivation procedure involves the slicing of the interval $[0, s]$ to $[0, t]$ and $[t, s]$ and solving two resultant integrals using change of sequence of integration. The $\mathcal{L}_1-$integrability property of $\dot{\hat{\boldsymbol{\theta}}}$ and $\dot{\boldsymbol{\theta}}^*$ is invoked thereafter to infer the boundedness of the underlying integrals. The steps are indeed straightforward if the reader is familiar with the boundedness calculations culminating in (4.172). Hence for the sake of conciseness the proof is not repeated. Thus, from the foregoing arguments and discussions, it is mathematically proved that $\vartheta(t) \in \mathcal{L}_1$ from its inequality definition in (4.166). Now from the property of *closed under addition* of function spaces, since $\mathbf{z}(t) = \boldsymbol{\vartheta}(t) + \boldsymbol{\chi}^T\tilde{\boldsymbol{\theta}}(t)$, the signal property $\mathbf{z}(t) \in \mathcal{L}_1$ is proved. □

4.3.4 Simulation Study

To demonstrate the effectiveness of the proposed adaptive FTC approach featuring finite time adaptation, simulations are conducted on a coupled mass-spring-damper (MSD) system. The mass-spring-damper system taken into consideration is shown in Figure (3.13). Certainly, this system serves as a benchmark example of a nonlinear coupled MIMO dynamical system to validate the applicability and beneficial attributes of several nonlinear control schemes. The system description and modeling have been detailed in Section 3.3.4 in the previous chapter and hence not repeated.

Referring to the nonlinear uncertain dynamics of the coupled mass-spring-damper system in (3.213), the parameters of the system are the same as considered in the previous chapter. Further, the unknown failure induced uncertainty parameters are considered to be the same for simulations in order to ensure similar operating conditions necessary for comparison. The following actuator failure condition

considered reflects their partial loss of effectiveness (PLOE).

$$u_1(t) = \begin{cases} 0.5u_{H1}, & t \geq 30s \\ u_{H1}, & \text{otherwise} \end{cases} \tag{4.173}$$

$$u_2(t) = \begin{cases} 0.5u_{H2}, & t \geq 60s \\ u_{H2}, & \text{otherwise} \end{cases} \tag{4.174}$$

In order to translate the control design procedure to the system concerned, the dynamics in (3.213) is represented in a more appropriate form as

$$\dot{\boldsymbol{\xi}}_1 = \boldsymbol{\xi}_2 \tag{4.175}$$

$$\dot{\boldsymbol{\xi}}_2 = \boldsymbol{\varphi}^T \boldsymbol{\theta}_2^* + \sum_{j=1}^{2} \theta_{1,j}^* N_j \mathbf{u}_H. \tag{4.176}$$

Where the state vector $\boldsymbol{\xi} := [\boldsymbol{\xi}_1,\ \boldsymbol{\xi}_2]$, $\boldsymbol{\xi}_1 := [\xi_{1,1}, \xi_{2,1}]^T$, $\boldsymbol{\xi}_2 := [\xi_{1,2}, \xi_{2,2}]^T$ the entire dynamical system is rewritten as$\boldsymbol{\varphi}^T := [\text{diag}\{\boldsymbol{\varphi}_{1,2}^T,\ \boldsymbol{\varphi}_{2,2}^T\}]^T$ and $\mathbf{u}_H = [u_{H1},\ u_{H2}]^T$. The regressor matrices are defined as $\boldsymbol{\varphi}_{1,2} := [-\xi_{1,1},\ -\xi_{1,1}^3,\ -\xi_{1,2},\ -\xi_{1,2}^2,\ (\xi_{2,2} - \xi_{1,2}),\ (\xi_{2,2} - \xi_{1,2})^2]^T$ and $\boldsymbol{\varphi}_{2,2} := [-(\xi_{2,1} - \xi_{1,1}),\ -(\xi_{2,1} - \xi_{1,1})^3,\ -\xi_{1,2},\ -\xi_{1,2}^2]^T$. Further, the estimation model for the considered nonlinear dynamical system (3.213) is formulated as

$$\dot{\boldsymbol{\xi}} = \begin{bmatrix} \xi_{1,2} \\ \xi_{2,2} \\ 0 \\ 0 \end{bmatrix} + \underbrace{\left[\begin{array}{c|c|c|c} 0 & \mathbf{0}_{1\times 6} & 0 & \mathbf{0}_{1\times 4} \\ \hline 0 & \mathbf{0}_{1\times 6} & 0 & \mathbf{0}_{1\times 4} \\ \hline u_{H1} & \boldsymbol{\varphi}_{1,2}^T & 0 & \mathbf{0}_{1\times 4} \\ \hline \mathbf{0}_{1\times 9} & \mathbf{0}_{1\times 6} & u_{H2} & \boldsymbol{\varphi}_{2,2}^T \end{array}\right]}_{\boldsymbol{\Phi}^T} \boldsymbol{\theta}^*. \tag{4.177}$$

Herein $\boldsymbol{\theta}^* := [\theta_{1,1}^*, \theta_{2,1}^*, \ldots, \theta_{2,8}^*, \theta_{1,2}, \theta_{2,9}, \ldots, \theta_{2,12}]^T$. The reference trajectories to be tracked by the outputs $y_1 = \xi_{1,1}$ and $y_2 = \xi_{2,1}$ are given by $y_{r,1} = 0.2\sin(0.5t)$ and $y_{r,2} = 0.5\sin(0.5t)$. The controllers u_{H1} and u_{H2} are developed consistent with equation (4.133) and the parameter estimation $\hat{\boldsymbol{\theta}}$ follows (4.135) through (4.139). Unlike the control algorithm proposed in the previous chapter, there is only one single parameter estimator instead of a bank of multiple identification models identifying the same parameter vector. The initial states and parameter estimates are considered to be $\boldsymbol{\xi}(0) = [0, 0, 0, 0]^T$ and $\hat{\boldsymbol{\theta}}(0) = 0.1\mathbf{1}_{12\times 1}$, respectively. The controller gains are chosen as $c_{1,1} = 15,\ c_{1,2} = c_{2,1} = c_{2,2} = 5$ and the damping factors as, $\bar{c}_{1,2} = \bar{c}_{2,2} = 3$. The parameters for the filters (4.135) and (4.137)-(4.138) are selected as $\mathbf{A}_0 = [\text{diag}\{-14, -14, -16, -16\}]$, $\gamma = 2$ and $\mathscr{K} = 1$. The adaptive rate matrices of the proposed finite time estimator is selected as $\boldsymbol{\Gamma_1} = 20\mathbf{I}_{2m+p}$ and $\boldsymbol{\Gamma_2} = 10\mathbf{I}_{2m+p}$. It is apparent at this point that all the operating conditions and controller gains are deliberately chosen to be the same as in the previous chapter to ensure a fair and fruitful comparison between the performances obtained under both the adaptive FTC strategies.

The simulation results under start-up and under conditions of actuator failures/faults consistent with (4.173) are illustrated in Figures 4.7-4.8. From the tracking error performance for both the outputs y_1

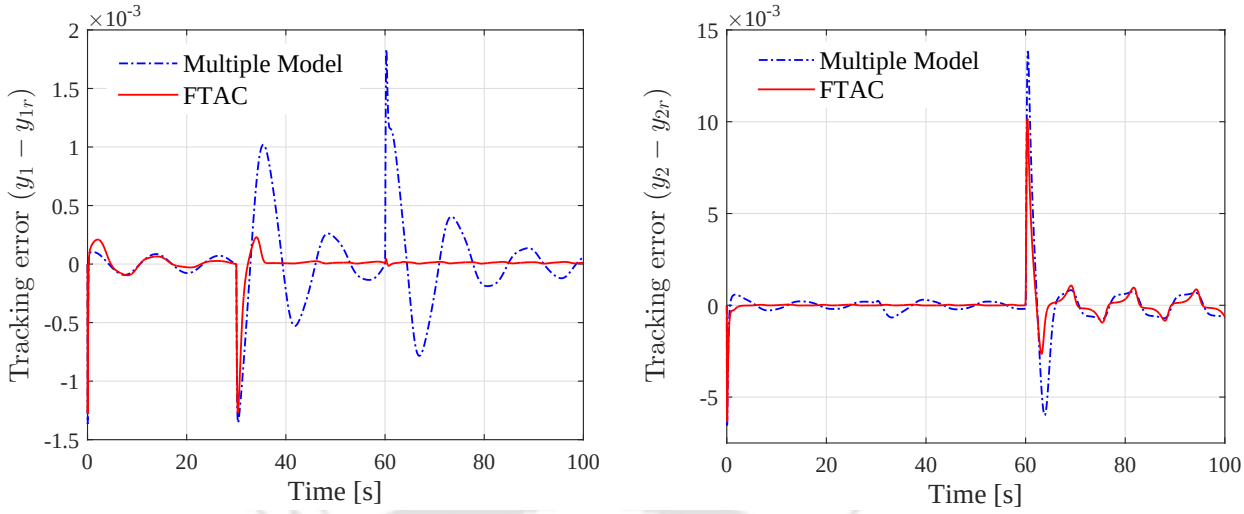

Figure 4.7: (a) Tracking error comparison in displacement output y_1;(b) Tracking error comparison in displacement output y_2; under the action of the proposed FTAC based FTC strategy and AMMFTC

and y_2 in Figure 4.7(a)-(b), the superiority of the proposed FTC methodology can be well ascertained. Compared to the tracking error profiles obtained under AMMFTC, the proposed FTAC methodology exhibits substantially low overshoots in the outputs with fast convergence to the origin. This is indeed an achievement especially when the improvement of output transient performance is ensured without a significant expense in the control energy. In this direction, the simulation results along with the quantification and subsequent comparison of the output and input performances in Table 4.3 successfully justify the theoretical claims. It is worth noticing from the calculated performance indices in Table 4.3 that the proposed FTAC strategy overrides the AMMFTC and the Single model adaptive FTC in terms of both input and output performances. Further, the strong robustness to adverse effects of cross coupling among subsystems under the action of the proposed controller should also be apprehended. It is well observable from Figure 4.7 that actuator fault in y_1-subsystem at $t = 30$s has negligible effect on the output y_2. Similarly, the output y_1 is almost unaffected in the event of occurrence of actuator failure in y_2-subsystem at $t = 60$s. Thus, the FTAC algorithm certainly emerges as a promising control technique for FTC applications demanding excellent output transient performance, precise tracking and economical control usage.

4.3.5 Experimental Study on a Twin Rotor MIMO System

Similar to Chapter 3, the proposed FTAC strategy is applied to the problem of attitude tracking in a 2-DOF helicopter. Experiments to validate and endorse the prolific features of the proposed control strategy with finite time adaptation are conducted on the 2-DOF helicopter prototype in the laboratory. The set-up is popularly known as a twin rotor MIMO system (TRMS). The physical description and operation of the TRMS has already been provided in Section 3.3.5 (Chapter 3). The specifications of the experimental set-up are also provided in the same section. The associated parameters definitions and

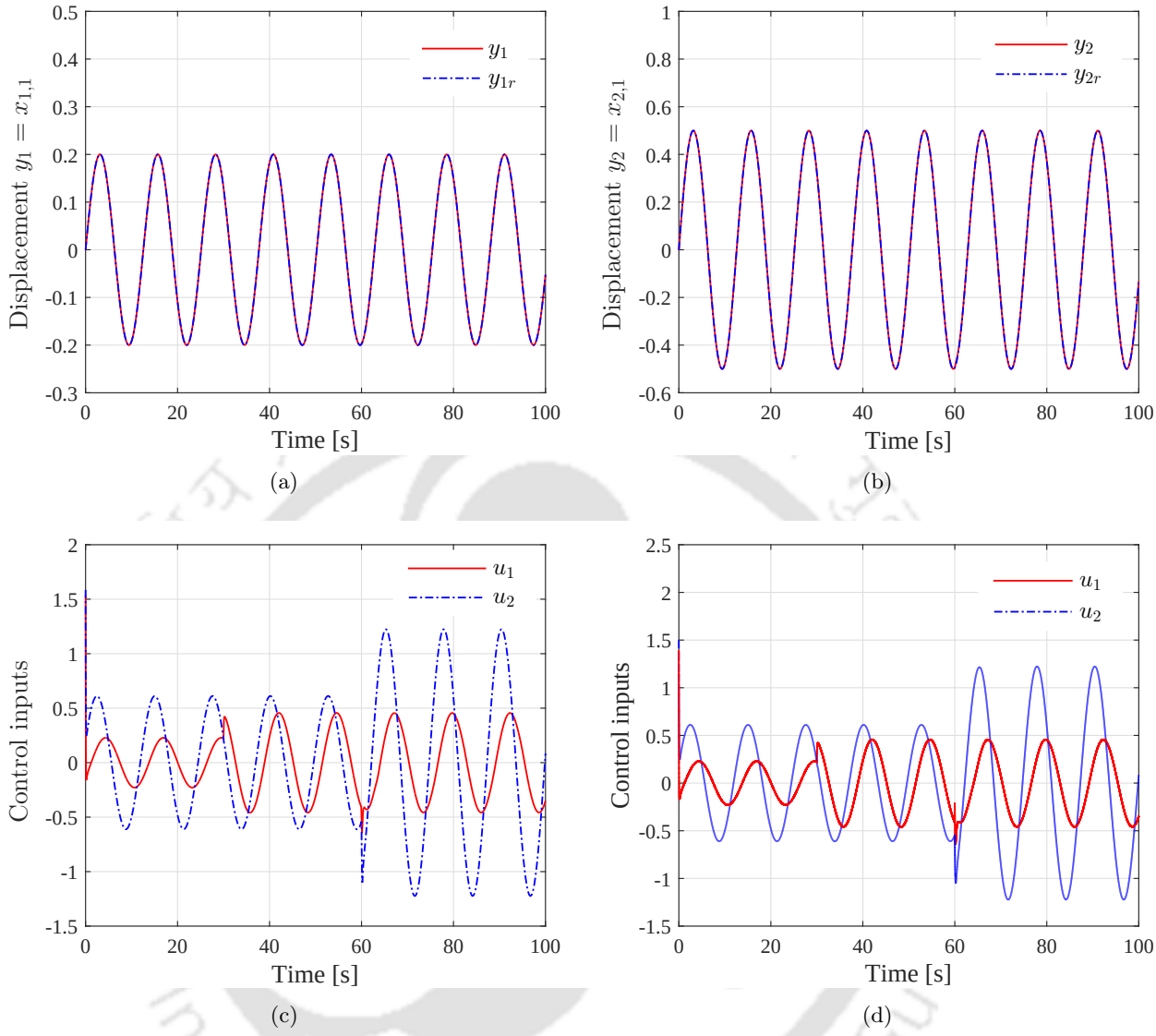

Figure 4.8: (a) Time evolution of $y_1(t)$ under the proposed adaptive FTC using FTAC;(b) Time evolution of $y_2(t)$ under the proposed adaptive FTC using FTAC;(c) Control inputs u_1 and u_2 under the proposed FTC scheme using FTAC; (d) Control inputs u_1 and u_2 under AMMFTC.

Table 4.3: Tabular comparison of output and input performances under proposed FTC under finite time adaptation based control (FTAC), AMMFTC and adaptive FTC using a single identification model

Control Schemes	**Output Performance metrics**				**Input Performance metrics**			
	ITAE		**RMSE**		**Control Energy**		**Total Variation**	
	y_1	y_2	y_1	y_2	u_1	u_2	u_1	u_2
FTAC	**0.1205**	**1.8399**	**0.00012**	**0.00094**	285.58	637.35	14.67	29.22
Multiple Models	1.1727	3.5234	0.00036	0.0015	285.26	637.09	14.85	29.04
Single Model	13.01	116.66	0.0028	0.0231	285.26	573.73	14.20	27.04

their nominal values appear in Table 3.4. Further the detailed dynamical modeling and parametrization in terms of unknown system parameters for the TRMS is discussed in Section 3.3.5 in equations (3.219) through (3.227). To ensure completeness, the dynamical model of the TRMS reiterated along with the formulation of the parametric model for parameter estimation. The dynamical description of the nonlinear coupled twin rotor MIMO system is as follows (please refer to Section 3.3.5 for details).

$$\begin{aligned}
\dot{x}_1 &= x_2 \\
\dot{x}_3 &= x_4 \\
\dot{x}_2 &= \theta_1^* {x_5}^2 + \theta_2^* x_5 - \theta_3^* \sin x_1 - \theta_4^* x_2 + \theta_5^* {x_4}^2 \sin(2x_2) \\
&\quad -\theta_6^* x_4 {x_5}^2 \cos(x_1) - \theta_7^* x_4 x_5 \cos(x_1) \\
\dot{x}_4 &= \theta_8^* {x_6}^2 + \theta_9^* x_6 - \theta_{10}^* x_4 - \theta_{11}^* {x_5}^2 - \theta_{12}^* x_5 \\
\dot{x}_5 &= -\theta_{13}^* x_5 + \theta_{14}^* u_v \\
\dot{x}_6 &= -\theta_{15}^* x_6 + \theta_{16}^* u_h \\
y_1 &= x_1, \qquad y_2 = x_3
\end{aligned} \tag{4.178}$$

The outputs of the TRMS are pitch and yaw angles and are denoted by y_1 and y_2. The unknown parameter vector is defined as $\boldsymbol{\theta}^* := [\theta_1^*, \theta_2^*, \ldots, \theta_{14}^*, \theta_{15}^*, \theta_{16}^*]^T$. The definition of all the unknown parameters θ_i for $i = 1, \ldots, 14$ are as follows.

$$\begin{aligned}
&\theta_1^* = a_1/I_v;\ \theta_2^* = b_1/I_v;\ \theta_3^* = M_g/I_v;\ \theta_4^* = B_{1\alpha_v}/I_v;\ \theta_5^* = 0.0326/2I_v;\ \theta_6^* = k_{gy}a_1/I_v; \\
&\theta_7^* = k_{gy}b_1/I_v;\ \theta_8^* = a_2/I_h;\ \theta_9^* = b_2/I_h;\ \theta_{10}^* = B_{1\alpha_h}/I_h;\ \theta_{11}^* = -1.75k_c a_1/I_h; \\
&\theta_{12}^* = -1.75k_c b_1/I_h;\ \theta_{13}^* = T_{10}/T_{11};\ \theta_{14}^* = k_m/T_{11};\ \theta_{15}^* = T_{20}/T_{21};\ \theta_{16}^* = k_t/T_{21}
\end{aligned} \tag{4.179}$$

Further, the parametric model for unknown parameter estimation is formulated as,

$$\dot{\mathbf{x}} = \begin{bmatrix} \dot{x}_1 \\ \dot{x}_3 \\ \dot{x}_2 \\ \dot{x}_4 \\ \dot{x}_5 \\ \dot{x}_6 \end{bmatrix} = \begin{bmatrix} x_2 \\ x_4 \\ 0 \\ 0 \\ 0 \\ 0 \end{bmatrix} + \underbrace{\left[\begin{array}{c|c|c|c} \mathbf{0}_{1\times 7} & \mathbf{0}_{1\times 5} & \mathbf{0}_{1\times 2} & \mathbf{0}_{1\times 2} \\ \mathbf{0}_{1\times 7} & \mathbf{0}_{1\times 5} & \mathbf{0}_{1\times 2} & \mathbf{0}_{1\times 2} \\ \hline \boldsymbol{\varphi}_{1,2}^T & \mathbf{0}_{1\times 5} & \mathbf{0}_{1\times 2} & \mathbf{0}_{1\times 2} \\ \mathbf{0}_{1\times 7} & \boldsymbol{\varphi}_{2,2}^T & \mathbf{0}_{1\times 2} & \mathbf{0}_{1\times 2} \\ \hline \mathbf{0}_{1\times 7} & \mathbf{0}_{1\times 5} & \boldsymbol{\varphi}_{1,3}^T & \mathbf{0}_{1\times 2} \\ \mathbf{0}_{1\times 7} & \mathbf{0}_{1\times 5} & \mathbf{0}_{1\times 2} & \boldsymbol{\varphi}_{2,3}^T \end{array}\right]}_{\boldsymbol{\Phi}(\mathbf{x},\mathbf{u})} \underbrace{\begin{bmatrix} \theta_1^* \\ \theta_2^* \\ \vdots \\ \theta_{14}^* \\ \theta_{15}^* \\ \theta_{16}^* \end{bmatrix}}_{\boldsymbol{\theta}^*}. \tag{4.180}$$

The regressors are defined as $\boldsymbol{\varphi}_{1,2} := [x_5^2, x_5, -\sin x_1, -x_2, -x_4^2 \sin 2x_2, -x_4 x_5^2 \cos x_1, -x_4 x_5 \cos x_1]^T$, $\boldsymbol{\varphi}_{2,2} := [x_6^2, x_6, -x_4, -x_5^2, -x_5]^T$, $\boldsymbol{\varphi}_{1,3} := [-x_5, u_v]^T$ and $\boldsymbol{\varphi}_{2,3} := [-x_6, u_h]^T$. The finite time parameter estimator and the requisite filters are designed using the above estimation model (4.180) and translating its use to the differential equations in (4.135)-(4.139). At this juncture, prior to control design, it is assumed that all the states of the system are available for measurement. However, the only states available for measurement is the pitch angle x_1 and yaw angle x_3. The remaining states, namely the pitch rate (x_2), the yaw rate (x_4), the momenta of the main rotor and tail rotor (L_m and L_t) are unavailable. Therefore, an Extended Kalman Filter (EKF) is designed to estimate the unavailable states of the TRMS. The details of EKF design are provided in Appendix A.3. The initial conditions of the

system are $\mathbf{x}(0) = [0,0,0,0,0,0]^T$. The EKF states are also initialized at zero. The relative degree of the pitch (x_1) and yaw (x_3) subsystems are found to be $\wp_1 = \wp_2 = 3$ with respect to the motor input voltages u_v and u_h. Hence the controller gains are selected as $c_1 = [\{c_{1,i}\}_{i=1}^3]$=[15, 2.5, 2.5] and $c_2 = [\{c_{2,i}\}_{i=1}^3]$=[10, 2.5, 2]. The damping gains are chosen as$\bar{c}_{1,2} = \bar{c}_{2,2} = \bar{g}_{1,3} = \bar{g}_{2,3} = 0.3$. The parameters associated with the estimation of $\hat{\boldsymbol{\theta}}$ are chosen as $\mathbf{A}_0 = [\text{diag}\{-14,-14,-16,-16,-14,-14\}]$, $\gamma = 2$ and $\mathscr{K} = 1$. The adaptive rate matrices are selected as $\boldsymbol{\Gamma}_1 = 20\mathbf{I}_{2m+p}$ and $\boldsymbol{\Gamma}_2 = 10\mathbf{I}_{2m+p}$. The control input voltages u_h and u_v are maintained within their allowable range of $[-2.5, 2.5]$V. The reference trajectories $y_{r,1}$ and $y_{r,2}$ to be tracked by the outputs $y_1 = \theta_v = x_1$ and $y_2 = \theta_h = x_3$ are the outputs of the reference system $\mathbf{G_r}(s) = \left[\text{diag}\left\{\frac{0.2}{9s^2+10s+4}, \frac{0.2}{9s^2+10s+4}\right\}\right]$ with $y_{d,1}$ and $y_{d,2}$ as the inputs. The inputs to the reference system are $y_{d,1} = 6 + 4\sin(0.05\pi t)$ and $y_{d,2} = 12\cos(0.05\pi t)$. Under the action of the proposed FTAC, the TRMS outputs are required to track the outputs of the reference model $\mathbf{G_r}(s)$ to analyze the superior tracking performance over that obtained using AMMFTC. Further, the tracking efficiency should not be achieved at the cost of excessive control usage. In the sequel, the experimental results obtained are illustrated and discussed to essentially arrive at certain conclusions substantiating all theoretical propositions in this chapter.

Given that the command reference inputs are sinusoidal signals defined by $y_{r,1}$ and $y_{r,2}$; the TRMS

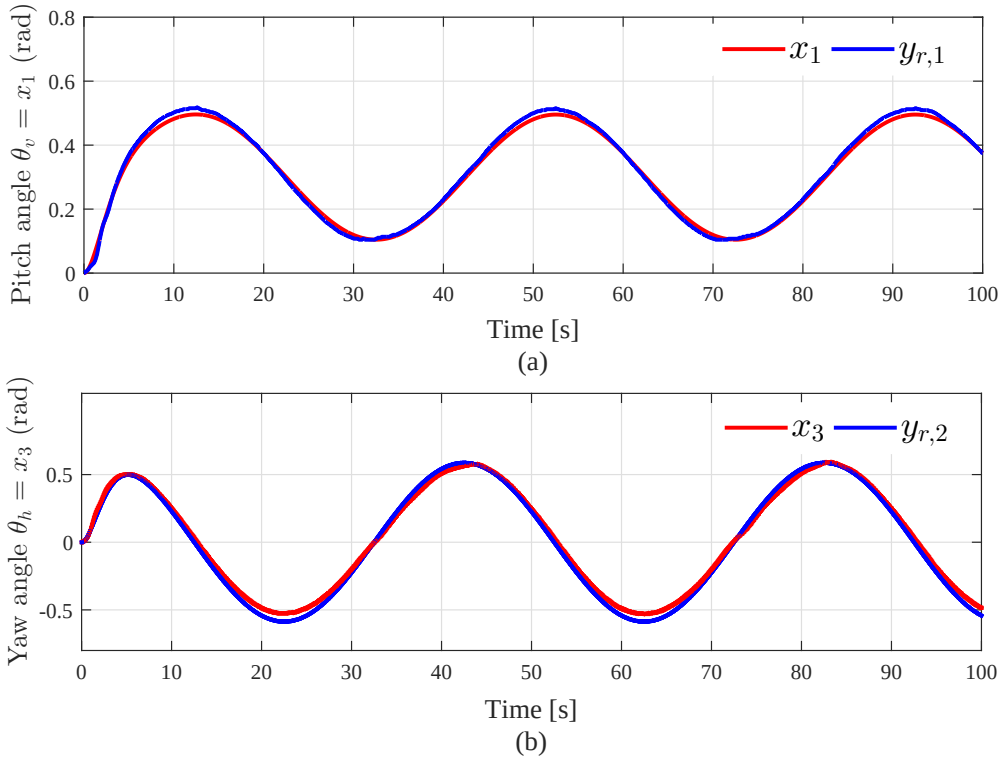

Figure 4.9: (a) Time evolution of the pitch angle $\theta_v = x_1$ (rad) tracking the reference signal $y_{r,1}$;(b) Time evolution of the yaw angle $\theta_h = x_3$ (rad) tracking the reference signal $y_{r,2}$.

equipped with the proposed FTAC methodology renders faithful attitude tracking. Besides, the control

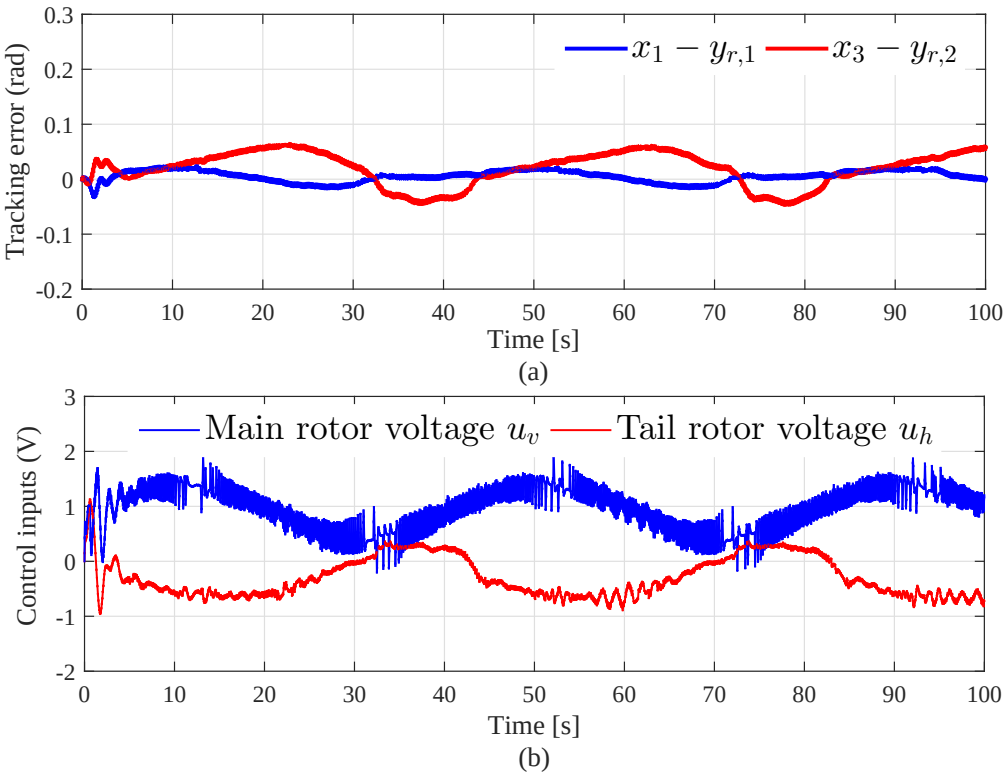

Figure 4.10: (a) pitch and yaw tracking error (rad); (b) control input voltages u_v and u_h for the main rotor and the tail rotor.

objective is achieved without encroaching the physical limits on the motor armature voltages driving the horizontal and vertical propellers. The experimental results are depicted in Figures 4.9-4.10. The proposed control scheme is indeed rewarding in the sense that a precise output tracking is observed in Figure 4.9. The output tracking error plotted seperately in Figure 4.9 further corroborates the theoretical claims of improved output transient and steady state performance. To elucidate the results further, the pitch and the yaw angle x_1 and x_3 exhibit no considerable transients and at steady state, the pitch and yaw tracking errors oscillate between $[-0.015, 0.015]$ and $[-0.05, 0.01]$, respectively. The maximum percentage of steady state error is determined with reference to the maximum peak magnitude of the respective reference signals. The average steady state error in outputs y_1 and y_2 are approximately calculated to be 3% and 5%, respectively. Further, Table 4.4 tabulates the calculated performance measures from experimental results obtained from proposed FTAC and AMMFTC schemes. While root mean square error (RMSE) and Integral absolute error (IAE) are indices measuring steady state performance, Integral time absolute error (ITAE) quantifies the transient performance in tracking control problems. As evident from ITAE values in Table 4.4, the tracking transient performance is almost at par with AMMFTC in experiments. However, ITAE and RMSE values corresponding to the proposed FTAC strategy indeed hints towards its promising and precise tracking abilities. Moreover, the input performance tabulations appearing on the same table displays no significant increment in control usage. Certainly, the transient and steady state performance improvement of the proposed FTAC

strategy over AMMFTC is appreciable and noteworthy. These encouraging and promising results obtained through extensive experimentation on a real time system are indeed testaments validating the theoretical assertions presented in this chapter. In other words, the conclusions drawn from an analysis of experimental results as mentioned above, acknowledge the conjectural attributes of the proposed control methodology.

Table 4.4: Tabulation of output and input performances using the proposed FTAC methodology when applied to attitude tracking problem of TRMS.

Control Methodology		Output Performance			Input Performance		
		RMSE	IAE	ITAE	CE		TV
FTAC	$\underline{\theta_v}$	0.011	0.466	22.31	$\underline{u_v}$	326.68	567.24
	θ_h	0.036	1.645	83.92	u_h	145.19	133.37
AMMFTC	$\underline{\theta_v}$	0.011	1.023	20.56	$\underline{u_v}$	298.93	217.72
	θ_h	0.032	3.336	84.08	u_t	164.10	809.38

4.4 Summary

A new finite time adaptive parameter estimation based backstepping controller is designed to accommodate finite as well as infinite number of actuator failures in nonlinear systems with large parametric uncertainties. The boundedness of the closed loop signals using the proposed control scheme in the case of finite and infinite actuator faults/failures, has been proved through a rigorous stability analysis. The output transient and steady state performances are improved without significantly increasing the control usage. Finite time estimation of unknown system parameters and failure induced parameters is guaranteed. Considering infinite actuator failures, the incorporation of a finite time parameter estimator into the proposed FE/FTC scheme allows us to define a lower bound on the minimum transition time T^* between two successive actuator failure patterns; in a sense that if $T^* \geq T_s$, the system recovers its nominal performance. Where T_s is the upper bound on the parameter convergence time. In addition, it is observed that the proposed FTAC method renders reinforced robustness of estimation towards unknown bounded external disturbances provided its frequency is higher than the tracking reference signal. By an accurate failure parameter estimation in finite time, we succeed in achieving a time bound recovery of the nominal exponential tracking performance of the plant. Different from AMMFTC strategy in Chapter 3 and other FE/FTC schemes with bounded or at best asymptotic parameter convergence, the proposed control scheme allows the existence of an explicit upper-bound on the convergence time of the parameter vector comprising of system and failure parameter estimates. This time is certainly equivalent to the time required by the system to transit from its faulty state to its nominal state conditions and hence serves as a measure of performance robustness of the FTC algorithm. Adding to the proficient attributes of the FTAC algorithm discussed above, it is actually our belief that one of the most important ones which plays an instrumental role in substantial performance improvement is the efficiency of the adaptation algorithm in terms of both

transient and steady-state behavior. Comparison of simulation results obtained under the proposed FTAC strategy with those using benchmark adaptive controllers and the one in Chapter 3 further justifies our conclusion.

Besides, application of the proposed FTAC methodology to coupled nonlinear MIMO systems also yields promising transient and steady state behavior. Comparison of simulation results obtained using the benchmark MBSC [6] method , single model adaptive control and AMMFTC methods proposed in Chapter 3 validates the theoretical claims and unveils the superiority of the proposed FTAC design. Experimentation on a twin rotor MIMO system also reveal encouraging performance and well justifies the suitability of the proposed adaptive control method for practical applications.

5

Parametrization-free Finite Time Estimation based Adaptive Compensation of Actuator Failures in Nonlinear Uncertain Systems

Contents

5.1 Introduction 190

5.2 Parametrization-free Finite Time Estimation based Adaptive Compensation of Actuator Failures in Nonlinear uncertain Systems 192

5.3 Summary 214

5.1 Introduction

At this juncture, it is evident that active FTC design for nonlinear systems has attracted the attention of researchers in view of the inherent nature of system dynamics, which is definitely not linear. In the context of FE based active FTC design, it is indeed apparent from the earlier chapters and the references therein that adaptive control methods have gained immense popularity due to their simplicity and effectiveness in compensating uncertain actuator faults/failures obviating the drawbacks and implementation issues in controller reconfiguration/failure prognosis unit. Focussing on FE based active FTC approaches, direct and indirect adaptive control strategies have been proposed in Chapters 2-4 for MISO and MIMO nonlinear uncertain systems assuming that the actuator failure induced perturbations are linearly parameterizable. Further, the matched uncertainties in the nonlinear system due to inaccurate modeling are considered to also exhibit linear parametrization. In this chapter, a parametrization-free finite time estimation based adaptive FTC built on the basis of an indirect FE/FTC design architecture is proposed to compensate more general class of actuator failures. Herein, the perturbations due to actuator failures or faults and matched uncertainties are not assumed to be linearly parameterized. Further, the lumped uncertainty due to modeling inaccuracies and fault/failure induced perturbations is considered to be state-dependent and may explicitly or implicitly vary with time. Besides, such an uncertainty is not necessarily assumed to be vanishing. The proposed FTC methodology is also utilized to compensate intermittent actuator failures in nonlinear systems considered in this work. Direct adaptive control methods, in large, have been found to be incapable of compensating infinite actuator failures in nonlinear uncertain systems. However, such schemes inherently offer a promising output transient performance. Now, infinite actuator failures induce changes in failure parameters at each instances of such variations while the system parametric uncertainties remain invariant to the occurrence of such faults/failures. Therefore, we intend to exploit the strong features of direct adaptive backstepping approach to ensure a rewarding transient performance in fault free situations while inducting an indirect approach through the use of finite time adaptive estimator based backstepping control at the last coordinate to counteract infinite actuator failures. Therefore, a unified adaptive control design has been proposed in this paper to primarily compensate parametrization free infinite actuator failures and maintain closed-loop signal boundedness for all time. Finite time bound exact estimation of fault induced perturbations and asymptotic output tracking with improved transients and steady state behavior are additional design objectives to be met. Adopting such an ideology with exact uncertainty estimation allows us to exactly (not approximately) recover nominal fault-free transient and steady state performance in the event of faults and failures as proved later.

Nonetheless, as pointed out in earlier chapters, such an estimator integrated control approach especially for nonlinear systems pose serious challenges in stability analysis on account of the bidirectional robustness interaction between the estimator and the controlled system. Such an interaction may manifest itself in the form of inaccurate estimation adversely affecting output performance. This interaction would be very clear from the stability analysis wherein the salient attributes of the proposed methodology namely, boundedness of all closed loop trajectories, output performance recovery, asymptotic exact output tracking, piecewise exact estimation of system and failure induced uncertainties;

and potential to compensate infinite actuator failures; are proved. Infinite actuator failures result in discontinuities in failure induced perturbations at time instances wherein the actuator failure pattern changes and essentially characterizes addition of fast varying non-smooth perturbations to the nonlinear system. Hence rigorous stability analysis of the closed-loop system using the proposed finite time uncertainty estimator integrated with a backstepping control strategy under infinite actuator failures for $t \in [0, \infty)$, is indeed not a trivial task.

Recently, uncertainty estimator/disturbance observer based controller design, popularly known as ADRC, have attracted considerable interest for control of linear and nonlinear systems [80–83, 92, 93]. Further, second order sliding mode based disturbance observation integrated with a suitable controller has been either proposed for linear or globally Lipschitz nonlinear uncertain systems with globally Lipschitz lumped uncertainties [139, 140]. Although significant progress has been made, almost all such methods in literature assume either the unknown uncertainty to be slowly varying or the uncertainties to be globally Lipschitz with precise knowledge of their bounds, which are indeed restrictive assumptions for practical systems more importantly prone to actuator failures. Although some of the works [80–83] address FTC of general affine in control non-Lipschitz nonlinear systems, only semi-global boundedness of trajectories is achieved. In addition, their application to the problem of FTC in nonlinear systems with uncertainties (not necessarily Lipschitz) with infinite actuator failures, have not yet been addressed.

Diverting our attention from FTC objectives, within the ambit of ADRC, disturbance observers inspired from the theory of high gain observers (HGOs) have been proposed in conjunction with a suitable controller to achieve tracking/stabilization in nonlinear uncertain systems [96, 137]. In order to circumvent the *peaking effect* due to high observer gains, such control schemes resort to saturating the control input beyond a compact region of interest chosen by the designer. This control strategy is known as globally bounded control (GBC). Nevertheless, the following shortcomings in the context of theoretical developments in control are of immense motivation in this work. Firstly, at most semi-global tracking/stabilization is guaranteed. On a second note, although *nominal performance recovery* in terms of trajectory convergence and regaining the region of attraction of the nominal system has been claimed, a crucial design aspect has still remained indiscernible. In fact, to enlarge the region of attraction as well as to ensure trajectory convergence to their nominal solutions using GBC, simultaneous increment in both the saturation limits and observer gains is required [136]. Theoretically, in order to attain the region of attraction of the nominal system and recover the nominal output performance, the observer gains must tend to infinity. Now, estimation using high gain disturbance observers are not robust to measurement noise. With the increase in observer gains, the noise is amplified and hence the signal to be estimated is lost. It is therefore imperative to design new disturbance observer based control approaches wherein there exists finite values of observer gains which guarantee exact nominal output transient and steady state performance recovery along with acceptable stability margins. At this point, it is clear that the avoidance of *peaking phenomenon* in such design strategies without resorting to the concept of GBC would definitely lead to the existence of global stability properties of closed-loop system trajectories. Hence, the proposed FTC design utilizes a backstepping procedure augmented with a finite time disturbance estimator and a damping injection at the last coordinate.

The incorporation of damping function allows the control design to ensure global stability of closed loop trajectories [69]. The peaking effect is circumvented by the use of an uncertainty estimator based on second order sliding modes [132] without the use of saturation. It is shown that there exist finite values of estimator/observer gains under which the integrated estimator based controller ensures nominal output performance recovery and restores the region of attraction of the nominal system . In addition, the disturbance/uncertainty estimator adopted in this work is robust to measurement noise and does not require the unknown lumped disturbance signal to be slowly varying. The estimation characterizes exact convergence to the actual time description of the lumped uncertainty (system uncertainty and failure induced uncertainty) in finite time and does not require any knowledge of the structure or upper bound of the same. Finally, a detailed and exhaustive stability proof showing the boundedness of all closed-loop trajectories obtained using the proposed finite time FE integrated FTC approach under infinitely occuring parametrization-free actuator failures is provided for all $t \in [0, \infty)$. Further, asymptotic exact output tracking with exact fault-free transient and steady state performance recovery is achieved using the proposed FTC scheme in the case of finite occurrence of actuator failures. Besides, the proposed FTC strategy allows the designer to define a lower bound on the transit time between two consecutive changes in actuator failure patterns to ensure exact recovery of fault-free system performance.

In order to investigate the practical applicability, the proposed methodology is evaluated on a nonlinear longitudinal model of large civil aircraft (Boeing 747-100/200) subject to modeling uncertainties and infinite actuator failures. Simulation results justify theoretical claims and prove the applicability of the proposed method to the problem of infinite actuator failures in nonlinear systems. The rest of the chapter is organized as follows. The FTC problem to be solved is formulated and stated in Section 5.2.2. In Section 5.2.3, the proposed unified adaptive FTC is explained. A detailed closed-loop stability analysis and output tracking performance are described in Section 5.2.4. In Section 5.2.5, extensive simulation studies are presented to illustrate the effectiveness in an aircraft control application. Finally, a summary of this chapter is provided in Section 5.3.

5.2 Parametrization-free Finite Time Estimation based Adaptive Compensation of Actuator Failures in Nonlinear uncertain Systems

5.2.1 Mathematical Notations and Definitions

Due to brevity of presentation, the definitions of terminologies and preliminary notions have discussed briefly yet in a lucid manner for ease of understanding of the control methodology developed in the sequel.

- Let us consider a vector $\xi(t) \in \mathbb{R}^n$. Then $\|\xi\|_p$ denotes its $\mathcal{L}_p$ norm for $p \in [1, \infty)$ such that $\|\xi\|_p := \left(\int_0^\infty |\xi(s)|^p ds\right)^{1/p}$. For $p = \infty$, the $\mathcal{L}_\infty$ norm is defined as $\|\xi\|_\infty := \sup_{t>0}\{|\xi(t)|\}$.
- Defining the family of dilations $\mathcal{D}_\varpi(\cdot)$ as a linear map associated with the weight vector $m = [m_1, m_2, \ldots, m_n]^T$, by $\mathcal{D}_\varpi : (\xi_1, \xi_2, \ldots, \xi_n) \mapsto (\varpi^{m_1}\xi_1, \varpi^{m_2}\xi_2, \ldots, \varpi^{m_n}\xi_n)$, a vector field $f : \mathbb{R}^n \to \mathbb{R}^n$ is said to be homogeneous with degree $\nu \in \mathbb{R}$ if $f(\mathcal{D}_\varpi \xi) = \varpi^\nu \mathcal{D}_\varpi f(\xi)\ \forall\ \varpi, m_i > 0$.

- Let the vector field $f(\xi)$ be homogeneous with degree ν. Therefore, the differential equation $\dot{\xi}(t) = f(\xi, t)$ is invariant with respect to the transformation $\mathcal{T}_\varpi : (t, \xi) \mapsto (\varpi^{-\nu} t, \mathcal{D}_\varpi \xi)$, implying *homogeneity* of solutions, i.e., $\xi(t, \varpi\xi_0) = \varpi\xi(\varpi^{-\nu}t, \xi_0)$. Further, the trivial solution $\xi = 0$ is globally *finite time stable* if it is asymptotically stable and $\nu < 0$ [141].

- A set Ω is called *dilation-retractable* if $\mathcal{D}_\varpi \Omega \subset \Omega$ for all $0 \leq \varpi \leq 1$ [132].

- $D_{(z,\tilde{\kappa})} \subseteq \mathbb{R}^{\wp+p}$ and $D_\sigma \subseteq \mathbb{R}^2$ denote the region of attraction for the tracking error dynamics and estimation error variables, respectively. The symbols $\wp$ defines the relative degree of the system and the number of unknown parameters κ_i is given by p.

- $\Omega_\sigma^\epsilon := \{\sigma \in D_\sigma : \sigma^T P_\sigma \sigma \leq \epsilon\tau\varepsilon^2,\ \epsilon > 1\}$ and $\Omega_\sigma^\epsilon \subset D_\sigma$; $\mathcal{N}_\sigma := \{\sigma \in D_\sigma : \sigma^T P_\sigma \sigma \leq \tau\varepsilon^2\} \subset \Omega_\sigma^\epsilon$ is a set, arbitrarily small in the direction of σ. The parameter $\tau > 0$ is a design parameter and is defined later.

- $\mathcal{M}_e := \{(z, \tilde{\kappa}) \in D_{(z,\tilde{\kappa})} : z = 0,\ F_e^T \tilde{\kappa} = 0\}$ is the largest positively invariant set wherein the tracking error variables finally reside under the action of control.

- $\mathcal{M}_{(z,\tilde{\kappa})} := \{(z, \tilde{\kappa}) \in D_{(z,\tilde{\kappa})} : \frac{1}{2}(z^T P_c z + \tilde{\kappa}^T \Gamma^{-1} \tilde{\kappa}) \leq c, c > 0\}$ and $\Omega_{(z,\tilde{\kappa})} \subset \mathcal{M}_{(z,\tilde{\kappa})}$ denotes the compact set wherein $(z(t_0), \tilde{\kappa}(t_0))$ are assumed to reside initially.

- $\overline{\lambda}(M)$ and $\underline{\lambda}(M)$ are meant to denote the maximum and minimum eigen values of a square matrix M.

5.2.2 Problem Formulation

Let us consider a class of multi input single output nonlinear system affine in control given by,

$$\sum\nolimits_p : \begin{cases} \dot{x} = f_0(x) + \sum\limits_{i=1}^{p} \kappa_i^* f_i(x) + \sum\limits_{j=1}^{m} g_j(x) u_j \\ y = h(x) \end{cases} \tag{5.1}$$

where $x := [x_1,\ x_2, \ldots, x_n]^T \in D \subseteq \mathbb{R}^n$ defines the state vector, $y \in \mathbb{R}$ is the system output and $u_j : [0, \infty) \to \mathbb{R}$ for $j = 1, \ldots, m$, denotes the jth control input (output of the jth actuator) whose actuators may undergo a fault or a failure in course of simultaneous operation over time. The functions $f_i(x), g_j(x) : D \subseteq \mathbb{R}^n \to \mathbb{R}$, for $i = 0, \ldots, p$ are smooth nonlinear functions of which the coefficients κ_i^* are assumed to be unknown. The output function $h(x) \in \mathbb{R}$ is assumed to be a known smooth function not necessarily nonlinear. The system $\sum_p$ can be transformed to a strict feedback form using a suitable diffeomorphism into a controllable subsystem of order $\wp$, as given below.

$$\sum\nolimits_c : \begin{cases} \dot{\xi}_i = \xi_{i+1} + f_i(\bar{\xi}_i)^T \kappa^*, \quad i = 1, ..., \wp - 1 \\ \dot{\xi}_\wp = a(\xi, \eta) + f_\wp(\bar{\xi}, \eta)^T \kappa^* + \sum\limits_{j=1}^{m} \beta_j(\xi, \eta) u_j \\ y = \xi_1 \end{cases}$$

where, $\bar{\xi}_i := [\xi_1, \xi_2, \ldots, \xi_i]^T$, $f_i(\bar{\xi}_i) := [\{L^i_{f_k} h(x)\}_{k=1}^p]^T$ for $i = \overline{1, \wp}$, $a(\xi, \eta) := L^{\wp}_{f_0} h(x)$ and $\beta_j(\xi, \eta) := L_{g_j} L^{\wp-1}_{f_0} h(x)$. Further, the subsystem $\sum_z : \dot{\eta} = \Lambda_0(\xi, \eta) + \sum_{i=1}^p \kappa_i^* \Lambda_i(\xi, \eta),\ \eta \in \mathbb{R}^{n-\wp}$ is input-to-state(ISS) stable with respect to ξ as its input.

Hereafter, we assume that the actuators in the system may experience a malfunctioning characterized by partial loss of effectiveness (PLOE) fault or actuator lock-in-place (LIP) failures. The input/output(i/o) characteristics of such faults and failures for $t \in [t^o_{j,h},\ t^e_{j,h}),\ h \in \mathbb{Z}_+$, can be modeled as [6]:

$$u_j(t) = \begin{cases} K_{j,h} u_{Hj} + \bar{u}_{Fj,h} \phi_{j,h}, & t \in [t^o_{j,h}, t^e_{j,h}) \\ u_{Hj}, & t \in [t^e_{j,h}, t^o_{j,h+1}) \end{cases} \tag{5.2}$$

where $h = 1, \ldots, \infty$ and $K_{j,h} \in [0, 1]$ represents the health factor of the jth actuator at the hth instant of the fault incurred. The terms u_{Hj} and u_j denote the controller output fed as input to the jth actuator and the output of the jth actuator respectively. The function $\phi_{j,h}(\cdot)$ denotes the basis function depending on which the partial, stuck, and oscillatory failures are characterized by the fault model in (5.2). In LIP/oscillatory failures, the magnitude at which the jth actuator is stuck/amplitude of oscillations is given by $\bar{u}_{Fj}$ with $\phi_{j,h} = 1$ or any piecewise continuous bounded function of time while $\phi_{j,h} = 0$ features partial loss. The time variables $t^o_{j,h}$ and $t^e_{j,h}$ denote the time instants at which hth failure of the jth actuator starts and ends, respectively. The jth actuator remains healthy for the time interval $t \in [t^e_{j,h}, t^o_{j,h+1})$ until the onset of the $(h+1)$th failure at $t = t^o_{j,h+1}$. Further, in contrast to the earlier works in [17,31,32], the basis function $\phi_{j,h}(\cdot)$ is assumed to be unknown with each actuator undergoing a transition from its normal mode of operation to various failure modes, infinitely many times. In addition, the transit time T^* between the occurrence of two consecutive actuator failure patterns is nonzero and finite. It is worth mentioning that the failure model (5.2) can be used to characterize the i/o behavior of a healthy actuator($k_{j,h} = 1,\ \bar{u}_{Fj,h} = 0$) as well. Hence, in order to proceed with controller design, the failure model (5.2) can be incorporated into the controllable plant dynamics $\sum_p$ irrespective of the actuators being healthy or affected by faults.

Assumption 5.1. *The plant $\sum_p$ under the action of a suitably designed failure compensation scheme can at most tolerate up to $(m-1)$ actuator failures at any particular instant of time. This ensures that the plant is associated with atleast one control input $\forall t > 0$ corresponding to any actuator failure pattern, to guarantee the existence of stable solutions. The actuator failures are assumed to be unknown in time, pattern and magnitude.*

Assumption 5.2. *The reference trajectory to be tracked by the output of the plant $\sum_p$ is the output of a stable linear reference model described as $[y_d(t)] = G_r(s)[y_r(t)]$. Where $G_r(s) = k_m/(s^{\wp} + a_{\wp-1}s^{\wp-1} + \ldots + a_1 s + a_0)$ and $y_r(t)$ being bounded and piecewise continuous. Therefore, the signals $(y_d, \dot{y}_d, \ldots, y_d^{(\wp)})$ are continuous, bounded and hence belong to a compact set.*

Having stated the preliminary assumptions, the problem lies in the design of an active fault tolerant controller aimed at achieving closed loop signal boundedness with asymptotic output tracking irrespective of finite and infinite actuator failures. In addition, attaining nominal transient performance recovery while being afflicted by such faults is another prime concern. With contextual reference to

FTC, apart from design of controllers rendering asymptotic stability, schemes ensuring the latter followed by proof of nominal transient performance recovery has not been addressed so far in literature. In the section that follows, we shall look into the challenges involved in adaptive control design to compensate possible infinite actuator failures. Accordingly, we shall come up with a unified optimal solution which would deliver to the design objectives while adhering to the basic assumptions in control synthesis.

5.2.3 Proposed Adaptive FTC Design for Infinite Actuator Failures

Considering $\beta_j u_{Hj} = u_0$ for $j = 1, \ldots, m$ and the fault model (5.2), the plant dynamics at the $\wp$th step exhibit two different forms corresponding to fault free and fault affected scenarios. Let us define the index set of actuators as $\mathscr{B} = \{j_1, j_2, \ldots, j_m\}$. Thereafter, two subsets $\mathscr{B}^h_{tot_F} := \{j_1, j_2, \ldots, j_k\}_h$ and $\mathscr{B}^h_{par_H} := \mathscr{B} \setminus \mathscr{B}^h_{tot_F}$ correspond to the index set for each of the possible/compensable failure patterns and loss of effectiveness faults encountered at the hth instant, respectively. Encompassing both the forms, the unified model for control design is represented as,

$$\begin{aligned} \dot{\xi}_i &= \xi_{i+1} + f_i(\bar{\xi}_i)^T \kappa^* \quad i = 1, \ldots, \wp - 1 \\ \dot{\xi}_\wp &= f_0(\xi, \eta) + f_\wp(\xi, \eta)^T \kappa^* + g u_0 + \beta^T \overline{u}_\phi \end{aligned} \tag{5.3}$$

with the terminologies defined as, $\beta = [\{\beta_j\}_{j=1}^m]^T$; $g := \sum_{j \in \mathscr{B}^h_{par_H}} K_{j,h}$, $\overline{u}_\phi := [\{\overline{u}_{j,h}\}_{j=1}^m]^T$ with $\overline{u}_{j,h} = 0$ with $j \notin \mathscr{B}^h_{tot_F}$ for cases of actuator failures while $g := m$, $\overline{u}_\phi := 0_{m \times 1}$ define a no fault scenario. At this juncture, it is suitable to assume that uncertainties induced due to feasibly infinite actuator faults are piecewise continuous and differentiable.

5.2.3.1 Controller Design

System parametric uncertainties due to modeling imperfections are invariant to changes in actuator failure pattern. Assuming the knowledge of full state vector, the controller is designed following a tuning function based backstepping until the $(\wp - 1)$th step finally followed by a finite time exact adaptive estimator based feedback control at the $\wp$th step to arrive at the actual control input u_0. The motivation behind the development of such a unified adaptive scheme has been discussed in the introduction. Proceeding with the control design, let us define the error variables as, $z_i = \xi_i - \alpha_{i-1} - y_d^{(i-1)}$, $i = \overline{1, \wp}$. The stabilizing control law α_i for each of the ith error subsystem are,

$$\begin{aligned} \alpha_i = &-c_i z_i - \bar{c}_i |\psi_i|^2 z_i - z_{i-1} - \psi_i^T \hat{\kappa} - \sum_{k=1}^{i-2} z_{k+1} \frac{\partial \alpha_k}{\partial \hat{\kappa}} \Gamma \psi_i \\ &- \frac{\partial \alpha_{i-1}}{\partial \hat{\kappa}} \Gamma \psi_i + \left(\sum_{k=1}^{i-1} \frac{\partial \alpha_{i-1}}{\partial \xi_k} \xi_{k+1} + \sum_{k=0}^{i-1} \frac{\partial \alpha_{i-1}}{\partial y_d^{(k)}} y_d^{k+1} \right) \end{aligned} \tag{5.4}$$

$$\dot{\hat{\kappa}} = -\Gamma \omega_{\wp-1}, \ \omega_{\wp-1} = \omega_{\wp-2} + \omega_{\wp-1} z_{\wp-1} \tag{5.5}$$

$$\psi_i = f_i(\bar{\xi}_i) - \sum_{k=1}^{i-1} \frac{\partial \alpha_{i-1}}{\partial \xi_k} f_k(\bar{\xi}_k) \tag{5.6}$$

Thereafter, the actual control input u_0 is finally derived following a backstepping technique integrated with a finite time exact estimator module to estimate system uncertainties and the intruding perturbations due to faults/failures. The expression for u_0 is derived as,

$$u_0 = (-z_{\wp-1} - (c_\wp + s_\wp)z_\wp - f_0(\xi,\eta) - \hat{\Delta}_\wp + y_d^{(\wp)})/m \tag{5.7}$$

wherein, $s_\wp = \bar{c}_\wp \left|\sqrt{\hat{\Delta}_\wp^2 + \varsigma}\right|$, $c_i, \bar{c}_i, \Gamma > 0$ denote the controller design parameters; $\hat{\kappa}$ and $\hat{\Delta}_\wp$ are notations meant to represent estimates of κ^* and stacked static and dynamic uncertainties $\Delta_\wp^*$ incurred due to modeling inaccuracies and actuator failures, respectively. $\Delta_\wp^*$ is mathematically defined in the upcoming sub-section. Nonlinear damping terms have been used in each of the virtual controls and the actual control law to ensure the input-to-state property of the tracking error dynamics with respect to $\tilde{\kappa} := \kappa^* - \hat{\kappa}$ and $\tilde{\Delta}_\wp := \hat{\Delta}_\wp - \Delta_\wp^*$ as the inputs.

5.2.3.2 Failure Induced Uncertainty Estimation

As discussed earlier, occurrence of faults and failures in actuators lead to changes in the structure of system dynamics immediately at the $\wp$th step. Therefore, the information of the $\wp$th error variable $z_\wp$ is used to design an adaptive estimator which would render an exact estimate of any uncertainty irrespective of its nature (static/dynamic/both) in finite time. On the lines of [142], the estimator is designed as given below. Invoking the dynamics of $z_\wp(t)$ derived from (5.4) and the fact that a multiplicative actuator fault can be converted to an additive one [143], the estimator dynamics is as follows.

$$\begin{aligned}
\dot{\hat{z}}_\wp &= f_0(\xi,\eta) + g_0 u_0 - y_d^{(\wp)} - k_1\sqrt{\mu}\lceil \hat{z}_\wp - z_\wp \rfloor^{1/2} + \hat{\Delta}_\wp \\
\dot{\hat{\Delta}}_\wp &= -k_2\mu \text{sign}(k_1\sqrt{\mu}\lceil \hat{z}_\wp - z_\wp \rfloor^{1/2} \text{sign}(\hat{z}_\wp - z_\wp))
\end{aligned} \tag{5.8}$$

where $\mu, k_1, k_2 > 0$ constitute the estimator gains, $\lceil \hat{z}_\wp - z_\wp \rfloor^{1/2} = |\hat{z}_\wp - z_\wp|^{\frac{1}{2}} \text{sign}(\hat{z}_\wp - z_\wp)$ and the uncertainty to be estimated is defined as $\Delta_\wp^* := f_\wp(\xi,\eta)^T\kappa^* + \dot{\alpha}_{\wp-1} + (g - g_0)u_0 + \sum_{j\in\mathscr{B}_{tot_F}^h} \beta_j \bar{u}_{Fj,h}\phi_{j,h}$ with $g_0 = m$. The variable $\hat{\Delta}_\wp$ gives the exact estimate of $\Delta_\wp^*$ using the estimator (5.8). The parameters $k_1, k_2 > 0$ are chosen so that the polynomial $(s^2 + k_1 s + k_2)$ is Hurwitz. In addition, it is important to mention that choice of $\mu > 0$ is the deciding factor to achieve exactness and rapidity of estimation thereby yielding exact asymptotic output tracking. Since faults/failures occur erratically with unknown degree of severity, a heuristic tuning of μ does not yield a fruitful estimation. Further, re-tuning the parameter μ at instances depending on the severity of fault incurred, is also infeasible. Hence an adaptive learning law is formulated to instantaneously estimate an appropriate gain online at the onset of failures to ensure a faithful estimation of uncertainties. The adaptive learning law is given by,

$$\mu(t) = \mu(t_0) + \gamma \int_{t_0}^{t} |\hat{z}_\wp(s) - z_\wp(s)|^{1/2} ds \tag{5.9}$$

However, prior to providing any insight or basis behind the adaptive law formulation, our primary aim is to prove boundedness of all closed loop trajectories for a finite μ. A dead-zone function with a

threshold $|\sigma_1| < \delta$ has been incorporated into the adaptive law so as to avoid unboundedness of gain estimation due to noisy measurements in practical scenarios.

5.2.4 Stability Analysis of the Proposed Control System under Infinite Actuator Failures

In the following, it is first shown that the proposed FE/FTC design approach ensures modularity between the estimator and the controller. Through the piecewise stability analysis to follow, it is shown that the proposed FTC strategy satisfies the *nonlinear separation principle* [69]. In consequence, the bidirectional robustness interaction between the controller-estimator pair is transformed to a unidirectional interaction from the observer to the controller. In the piecewise analysis below, a piece of time refers to the time interval between the onset and end of an actuator failure pattern. Within this time interval, the actuator failure pattern does not change and hence the failure induced uncertainty is also fixed. It does not exhibit any discontinuity within this time interval.

5.2.4.1 Piecewise Boundedness of Closed-Loop Signals

Considering the system dynamics (5.3), final control input $u_0(t)$ in (5.7) and the estimator dynamics (5.8), we arrive at the closed loop system represented in the following form.

$$\dot{z} = \mathcal{A}_z(z, \hat{\kappa}, t)z + \Psi_\kappa(z, \hat{\kappa}, t)^T\tilde{\kappa} + B_\sigma\sigma_2(\cdot) \tag{5.10}$$

$$\dot{\kappa} = -\Gamma\Psi_\kappa\bar{z} \tag{5.11}$$

$$\dot{\sigma}_1 = -k_1\sqrt{\mu}|\sigma_1|^{1/2}\text{sign}(\sigma_1) + \sigma_2 \tag{5.12}$$

$$\dot{\sigma}_2 = -k_2\mu\text{sign}(\sigma_1) - \dot{\Delta}^*_\wp \tag{5.13}$$

The state variables in (5.31)-(5.13) are defined as $\bar{z} := [z_1\ z_2 \dots z_{\wp-1}]^T; z := [\bar{z}\ z_\wp]^T; \sigma_1 = (\hat{z}_\wp - z_\wp), \sigma_2 = \tilde{\Delta}_\wp, \sigma := [|\sigma_1|^{1/2}\text{sign}(\sigma_1)\ \sigma_2]^T$. With the definitions $s_i := -\bar{c}_i|\psi_i|^2$ and $\zeta_{ik} := \frac{\partial\alpha_{i-1}}{\partial\hat{\kappa}}\Gamma\psi_k$, the remaining terms are described as follows. The matrix $\mathcal{A}_z$ is given by,

$$\begin{bmatrix} -(c_1+s_1) & 1 & 0 & \cdots & 0 \\ -1 & -(c_2+s_2) & \cdots & \zeta_{2(\wp-1)} & 0 \\ 0 & -1-\zeta_{23} & \ddots & \ddots & \vdots \\ \vdots & \vdots & \ddots & \ddots & 0 \\ 0 & -\zeta_{2(\wp-1)} & \cdots & -(c_{\wp-1}+s_{\wp-1}) & 1 \\ 0 & \cdots & \cdots & -1 & -(c_\wp+s_\wp) \end{bmatrix}$$

, $B_\sigma = [0 \cdots 0\ 1]^T$, $F(\xi) := [f_1(\xi_1)\ f_2(\bar{\xi}_2) \cdots f_{\wp-1}(\bar{\xi}_{\wp-1})]$,

$$\Psi^T_\kappa := \begin{bmatrix} 1 & 0 & \cdots & 0 \\ -\frac{\partial\alpha_1}{\partial\xi_1} & 1 & \ddots & \vdots \\ \vdots & \ddots & \ddots & 0 \\ -\frac{\partial\alpha_{\wp-2}}{\partial\xi_1} & \cdots & -\frac{\partial\alpha_{\wp-2}}{\partial\xi_{\wp-2}} & 1 \\ 0 & \cdots & 0 & 0 \end{bmatrix} F(\xi)^T := W(z,\hat{\kappa})F(\xi)^T$$

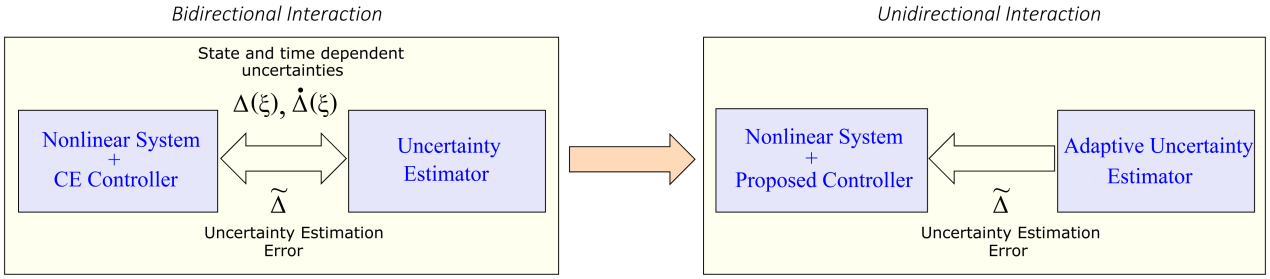

Figure 5.1: Bidirectional robustness interactions transformed to unidirectional interaction under the proposed FTC strategy

The bidirectional robustness interaction between the controller-estimator pair is evident from the closed loop equations in (5.31)-(5.13). As illustrated in Figure 5.1, through the proof of piecewise boundedness of closed-loop signals in Propositions 5.1-5.3, it is shown that the proposed FTC design ideology transforms the bidirectional interactions to a unidirectional one which in turn ensures a wide stability margin.

Therefore, in this spirit, let us consider a Lyapunov function $V_z : \mathbb{R}^{\wp} \times [0, \infty) \to \mathbb{R} = 0.5(z^T P_c z + \tilde{\kappa}^T \Gamma^{-1} \tilde{\kappa})$. With $P_c = I_{\wp}$, and in view of no change in system parameters κ due to faults resulting in $\dot{\tilde{\kappa}} = \dot{\hat{\kappa}} - \dot{\kappa}^* = \dot{\hat{\kappa}}$, the first time derivative of V_z yields,

$$\begin{aligned} \dot{V}_z &= -z^T \mathcal{Q} z + \bar{z}^T \Psi_{\kappa}^T \tilde{\kappa} + z_{\wp}\sigma_2 + \tilde{\kappa}^T \Gamma^{-1} \dot{\hat{\kappa}} \\ &= -\sum_{i=1}^{\wp} c_i z_i^2 - \sum_{i=1}^{\wp-1} \bar{c}_i |\psi_i|^2 z_i^2 - \bar{c}_{\wp} |\hat{\Delta}_{\wp} + \varsigma|^{\frac{1}{2}} z_{\wp}^2 + z_{\wp}\sigma_2 \\ &\leq -\sum_{i=1}^{\wp-1} c_i z_i^2 - \frac{c_{\wp}}{2} z_{\wp}^2 - \left[\frac{c_{\wp}}{2} + \bar{c}_{\wp} |\hat{\Delta}_{\wp} + \varsigma|^{\frac{1}{2}}\right] |z_{\wp}|(|z_{\wp}| - \bar{\bar{\sigma}}_2) \end{aligned} \tag{5.14}$$

where $\bar{\bar{\sigma}}_2 := |\sigma_2|/(0.5c_{\wp} + \bar{c}_{\wp}|\hat{\Delta}_{\wp} + \varsigma|^{1/2})$. Here, we see that when σ_2 term in the numerator grows, the nonlinear damping term in the denominator also increases correspondingly. Therefore, the effects of σ_2 can be curbed suitably to obtain, $|z(t)| \leq |z(t_0)|e^{-c_0 t} + \|\bar{\bar{\sigma}}_2\|_{\infty}$, with $c_0 = \min_{1 \leq i \leq \wp} \{c_i, c_{\wp}/2\}$ which is known to be the ISS property. Thus, at this point, it is important to state the following remarks.

Remark 5.1. *From assumption 2, the reference trajectories and its successive derivatives belong to a compact set $D_{y_d} \subset D_{\xi}$. The set D_{ξ} is also a compact set known as the domain of interest. Defining a compact set $\mathcal{M}_{(z,\tilde{\kappa})} := \{(z, \tilde{\kappa}) \in D_{(z,\tilde{\kappa})} : \frac{1}{2}(z^T P_c z + \tilde{\kappa}^T \Gamma^{-1} \tilde{\kappa}) \leq c_z + c_{\kappa} = c, \exists c, c_z > 0\} \subset D_{(z,\tilde{\kappa})}$, all initial conditions $(z(t_0), \tilde{\kappa}(t_0))$ reside within the compact set $\Omega_{(z,\tilde{\kappa})} \subset \mathcal{M}_{(z,\tilde{\kappa})}$. In the spirit of semi-global stability, the set $\Omega_{(z,\tilde{\kappa})} \subset \mathcal{M}_{(z,\tilde{\kappa})}$, for any finite c, can be made relatively large by suitable choice of controller gains. Thus, with $(z, \tilde{\kappa}) \in \mathcal{M}_{(z,\tilde{\kappa})}$, it follows that $\xi \in \mathcal{M}_{\xi} \subset D_{\xi}$, where $\xi \in \mathcal{M}_{\xi}$ is also a compact set.*

Remark 5.2. *On the other hand, incorporating nonlinear time varying damping into control design increases the stability and robustness which is indeed rewarding in the following sense. In the event of occurrence of actuator failures, the damping injection first drives the output trajectories to a bounded*

set whose boundaries are defined by $\bar{\bar{\sigma}}_2$ while the proposed estimator allows peaking-free estimation results without the use of saturation function. Hence these features when unified in the proposed FTC scheme, solely contribute to the attainment of global stability results. Provided there are no magnitude and rate constraints on the control signal (which is theoretically sound) and the tracking error dynamics is certainly input-to-state-stable (ISS) with respect to the uncertainty estimation error; there exists a control law which ensures globally stable adaptive output tracking.

At this stage, the following proposition is stated which testifies the convergence of tracking error to its nominal fault/failure-free solutions.

Proposition 5.1. ***(Boundedness)*** *Under the action of the control law* (5.7), $\exists\ \bar{\mu} > 0$, *such that for* $\mu \geq \bar{\mu}$, *all trajectories* $(z, \tilde{\kappa}, \sigma)$ *of the closed loop system* (5.31)-(5.13) *residing initially in the set* $\Omega_{(z,\tilde{\kappa})} \times \Omega_{\sigma}^{\epsilon}$ *are bounded for* $\forall t \geq 0$.

Proof. Proving boundedness of closed loop trajectories require positive invariance of an appropriately chosen set containing $\Omega_{(z,\tilde{\kappa})} \times \Omega_{\sigma}^{\epsilon}$ and existence of a finite time in which all trajectories starting in $\Omega_{(z,\tilde{\kappa})} \times \Omega_{\sigma}^{\epsilon}$ enter the chosen set and remain thereafter. It is clear from the expression of $\dot{V}_z$ in (5.14) that $\sigma_2 = 0$ implies the convergence of $(z, \tilde{\kappa})$ to the set $\mathcal{M}_e$ rendering $z = 0$ asymptotically stable with a region of attraction $D_{(z,\tilde{\kappa})}$. Since $V_z(z, \tilde{\kappa})$ is positive definite in $D_{(z,\tilde{\kappa})}$ (whose proof is trivial), there always exists a finite $c > \max_{(z,\tilde{\kappa})\in\Omega_{(z,\tilde{\kappa})}} V_z$ such that $\mathcal{M}_{(z,\tilde{\kappa})} := \{(z, \tilde{\kappa}) \in D_{(z,\tilde{\kappa})} : \frac{1}{2}(z^T P_c z + \tilde{\kappa}^T \Gamma^{-1} \tilde{\kappa}) \leq c, c > 0\}$ is a compact subset in $D_{(z,\tilde{\kappa})}$ and contains the set of initial conditions $\Omega_{(z,\tilde{\kappa})}$. In order to proceed with the analysis, let $\varepsilon^2 = \mu^{-1}$ and thereafter calculating $\dot{V}_z$ to be negative definite in the set $\mathcal{S} := \mathcal{M}_{(z,\tilde{\kappa})} \times \mathcal{N}_{\sigma}$ for $\epsilon \leq \epsilon_1$, shall prove the set $\mathcal{S}$ to be positively invariant. Therefore in the set, $(z, \tilde{\kappa}, \sigma) \in \{V_z(z, \tilde{\kappa}) = c\} \times \mathcal{N}_{\sigma}$, we have, $\dot{V}_z \leq -\sum_{i=1}^{\wp} c_i z_i^2 + \varepsilon \ell_1$ with $\ell_1 := \max_{\mathcal{M}_{(z,\tilde{\kappa})}} \|\frac{\partial V_z}{\partial z}\| K_1 \sqrt{\tau/\underline{\lambda}(P_\sigma)}$ and $\|\dot{V}_z(z, \tilde{\kappa}, \sigma_2) - \dot{V}_z(z, \tilde{\kappa}, 0)\| \leq K_2 K_1 \|\sigma\|$ in the set $\mathcal{S}$ with $K_2 = \max_{z\in\mathcal{M}_{(z,\tilde{\kappa})}} \|\frac{\partial V_z}{\partial z}\|$. Now, in the set, $\mathcal{M}_{(z,\tilde{\kappa})} \times \{V_\sigma := \sigma^T P_\sigma \sigma = \tau\varepsilon^2\}$, the following conditions $\|\dot{z}(z, \tilde{\kappa}, \sigma_2) - \dot{z}(z, \tilde{\kappa}, 0)\| \leq K_1$ and $\|\dot{\Delta}_{\wp}(z, \sigma)\| \leq K_3$, are obvious. In this direction, let us call upon the positive definite function $V_\sigma : D_\sigma \subset \mathbb{R}^2 \setminus \{0\} \times [0, \infty) \to \mathbb{R}$ such that $(\sigma, t) \mapsto \sigma^T P_\sigma \sigma$. Using (5.13), the first time derivative of σ is given by,

$$\dot{\sigma} = \begin{bmatrix} \frac{1}{2}|\sigma_1|^{-1/2}\dot{\sigma}_1 \\ \dot{\sigma}_2 \end{bmatrix} = \begin{bmatrix} \frac{1}{2}|\sigma_1|^{-1/2}(-\frac{k_1}{\varepsilon}\lceil\sigma_1\rfloor^{\frac{1}{2}} + \sigma_2) \\ -\frac{k_2}{\varepsilon^2}\text{sign}(\sigma_1) + \dot{\Delta}_{\wp}^*(\cdot) \end{bmatrix}$$

$$= |\sigma_1|^{-1/2} \begin{bmatrix} -\frac{k_1}{2\varepsilon}\lceil\sigma_1\rfloor^{1/2} + \frac{\sigma_2}{2} \\ -(\frac{k_2}{\varepsilon^2} - \dot{\Delta}_{\wp}^*(\cdot)\text{sign}(\sigma_1))\lceil\sigma_1\rfloor^{1/2} \end{bmatrix}$$

$$= |\sigma_1|^{-1/2} \underbrace{\begin{bmatrix} -\frac{k_1}{2\varepsilon} & \frac{1}{2} \\ -\frac{k_2}{\varepsilon^2} & 0 \end{bmatrix}}_{\bar{A}_\sigma} \begin{bmatrix} \lceil\sigma_1\rfloor^{1/2} \\ \sigma_2 \end{bmatrix} + \|\dot{\Delta}_{\wp}^*(\cdot)\|$$

$$= |\sigma_1|^{-1/2} \bar{A}_\sigma \sigma + \|\dot{\Delta}_{\wp}^*(\cdot)\| \tag{5.15}$$

Therefore, the $\dot{V}_\sigma$ can be written as, $\dot{V}_\sigma \leq -|\sigma_1|^{-1/2}\sigma^T \bar{Q}_\sigma \sigma + 2\sigma^T P_\sigma \|\dot{\Delta}_{\wp}^*(\cdot)\|$. The matrix $\bar{Q}_\sigma$ is positive

definite since $\bar{A}_\sigma$ is Hurwitz owing to $k_1, k_2, \varepsilon > 0$. Using the inequality $|\sigma_1|^{\frac{1}{2}} \leq \lceil \sigma_1 \rfloor^{\frac{1}{2}} \leq \|\sigma\|$ in the expression for $\dot{V}_\sigma$ yields, $\dot{V}_\sigma \leq -\underline{\lambda}(\bar{Q}_\sigma)\|\sigma\|^2 + 2\sigma^T P_\sigma \|\dot{\Delta}^*_\wp(\cdot)\|$. Hereafter, there exists a $\tau > 0$ satisfying the inequality $2\overline{\lambda}^2(P_\sigma)K_3 < \underline{\lambda}(P_\sigma)\underline{\lambda}(\bar{Q}_\sigma)$ and the above conditions, such that $\dot{V}_z \leq 0 \ \forall \ (z, \tilde{\kappa}, \sigma) \in \{V_z = c\} \times \mathcal{N}_\sigma$ and $\dot{V}_\sigma \leq 0 \ \forall \ (z, \tilde{\kappa}, \sigma) \in \mathcal{M}_{(z,\tilde{\kappa})} \times \{V_\sigma = \tau\varepsilon^2\}$. Finally, from the foregoing arguments and inequalities, it is proved that the set $\mathcal{S}$ is positively invariant.

To proceed next, we shall turn our interest on the σ-dynamics to eventually comment on the behavior of $(z, \tilde{\kappa})$ and prove the second claim. From the proof of positive invariance of $\mathcal{S}$, it is straightforward to conclude the existence of a finite time with which trajectories residing in the set $\Omega_{(z,\tilde{\kappa})} \times \Omega^\epsilon_\sigma$ ultimately converge to the set $\mathcal{S} := \mathcal{M}_{(z,\tilde{\kappa})} \times \mathcal{N}_\sigma$. The calculation of this finite time would be shown at the end of this proof. It is observed that the vector fields $\varphi(\sigma)$ of the estimation error system (5.12)-(5.13) are homogeneous with negative degree of homogeneity. With $\mathcal{D}_\varpi : (\sigma_1, \sigma_2) \mapsto (\varpi^2\sigma_1, \varpi\sigma_2)$, we get $\mathcal{T}_\varpi : (t, \sigma) \mapsto (\varpi^{-\nu}t, \varpi^{3-i}\sigma_i), \ i = 1, 2$, satisfying the relation $\varphi(\mathcal{D}_\varpi\sigma) = \varpi^{-1}\mathcal{D}_\varpi\varphi(\sigma)$ yielding homogeneity degree $\nu = -1$. The negative degree of homogeneity is the key to exact robustness of estimation towards $\dot{\Delta}^*_\wp$ while preserving the properties of homogeneity. Homogeneity of the vector fields in the proposed estimator contributes to the avoidance of the peaking effect in the proposed FTC [132].

Further, due to homogeneity of solutions (σ_1, σ_2), Lyapunov function V_σ, the negative definiteness of $\dot{V}_\sigma$ in $\mathcal{N}_\sigma \subset \Omega^\epsilon_\sigma$ is also true in the set Ω^ϵ_σ (local stability in homogeneous systems implies global stability). This in turn induces the property of dilation retractability of the set $\mathcal{N}_\sigma$ and hence $\Omega^\epsilon_\sigma := \{\sigma \in D_\sigma : \sigma^T P_\sigma \sigma \leq \epsilon\tau\varepsilon^2, \ \epsilon > 1\}$ to the origin. This is illustrated as follows.

Let us consider a ball $\mathcal{N}_\sigma \subset B_0 \subset \Omega^2_\sigma(\epsilon = 2)$ wherein $(\sigma_1(t_0), \sigma_2(t_0))$ reside. It is to be noted that the initial conditions now lie outside the set $\mathcal{N}_\sigma$. Now consider a sequence of balls obtained by dilation as, $B_{i+1} = \mathcal{D}_\varpi B_i, \ 0 < \varpi < 1$. Asymptotic stability (not exponential) and homogeneity of (σ_1, σ_2) infers that every trajectory starting in B_i will enter B_{i+1} before a finite time $\varpi^{-i\nu}T$. Let us consider that T is the time taken by the trajectories to travel from B_0 to B_1. The process of retractability of the sets to the origin is explained as follows. Due to negative definiteness of $\dot{V}_\sigma$, $\sigma \in B_0$ will enter the ball B_1, i.e., $\sigma(T, B_0) \in B_1$. Applying dilation on both sides of this immediate expression and using properties of trajectory invariance due to homogeneity, yields,

$$\mathcal{D}_\varpi(\sigma(T, B_0)) = \sigma(\varpi^{-\nu}T, \mathcal{D}_\varpi B_0) = \sigma(\varpi^{-\nu}T, B_1) \in \mathcal{D}_\varpi B_1$$

with $\mathcal{D}_\varpi B_1 = B_2$, i.e., trajectories $\sigma \in B_1$ enter the ball B_2 in a finite time $\varpi^{-\nu}T$. Repeating in the same manner, it is concluded that the ball $B_n (n >> 0)$ close to the origin is reached from a ball B_i, in a finite time T_s, represented as sum of a geometric series as,

$$T_s = \varpi^{-i\nu}T \sum_{i=0}^{\infty} (\varpi^{-\nu})^i = \frac{\varpi^{-i\nu}T}{1 - \varpi^{-\nu}} \tag{5.16}$$

Hence it is proved both through Lyapunov function and homogeneity approach that σ is bounded in finite time even when it lies initially outside the compact set $\mathcal{N}_\sigma$.

With the above arguments and $(z(t_0), \tilde{\kappa}(t_0)) \in \Omega_{(z,\tilde{\kappa})} \subset \mathcal{M}(z, \tilde{\kappa})$, it is relevant that $\|z(t) - z(t_0)\| \leq K_1 t$ with $K_1 > 0$(defined at the beginning of the proof) as long as $z(t) \in \mathcal{M}_{(z,\tilde{\kappa})}$. Thus, a finite time T_0 independent of ε exists such that $\forall \ t \in [0, T_0]$, $(z(t), \tilde{\kappa}) \in \mathcal{M}_{(z,\tilde{\kappa})}$. Within this time interval, with a

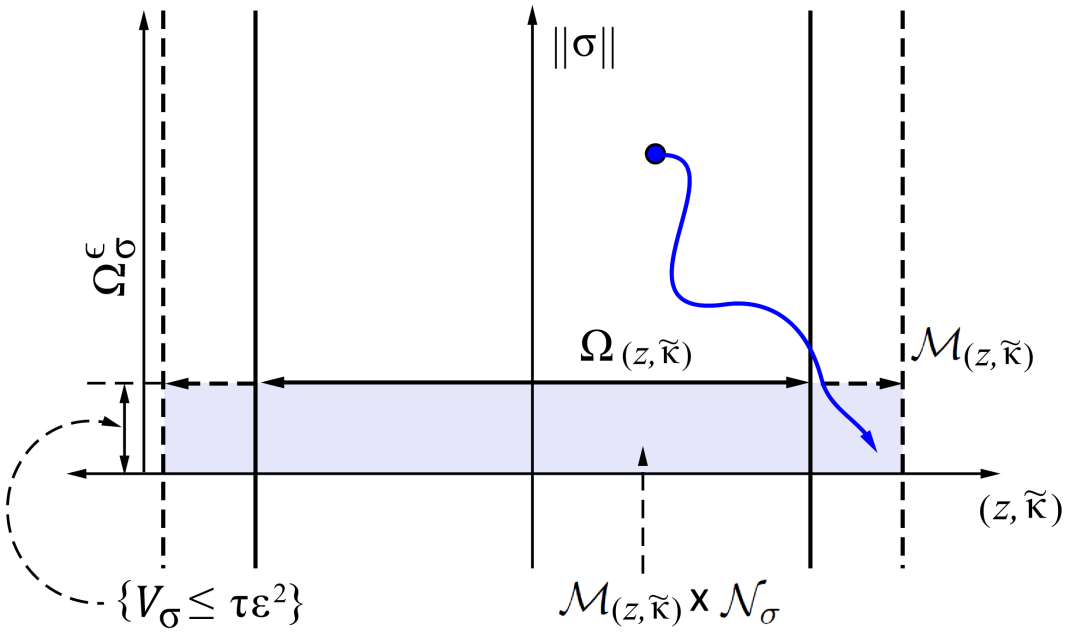

Figure 5.2: Illustration of the trajectory starting from $(z(0),\tilde{\kappa}(0)) \in \Omega_{(z,\tilde{\kappa})}$ and $\sigma(0) \notin \mathcal{N}_\sigma$ converges into $(z,\tilde{\kappa},\sigma) \in \mathcal{M}_{(z,\tilde{\kappa})} \times \mathcal{N}_\sigma$.

sufficiently small choice of $\varepsilon > 0$, $\exists\, T_s(\varepsilon)$ in which the trajectories of σ initially residing in $\Omega^{\epsilon}_{\sigma}$ also enter the compact set $\mathcal{N}_\sigma$ (a set sufficiently small in the direction of σ) and guarantee positive invariance of the set $\mathcal{S}$. Since, $\dot{V}_\sigma \leq -\underline{\lambda}(\bar{Q}_\sigma)\|\sigma\|^2$ for $\sigma \in \Omega^{\epsilon}_{\sigma}$ as shown earlier leads to another explicit closed form expression for T_s with $t_0 = 0$, given as,

$$T_s(\varepsilon) = \frac{\overline{\lambda}(P_\sigma)}{\underline{\lambda}(\bar{Q}_\sigma)} \ln(\epsilon) \tag{5.17}$$

Therefore, the time required by the trajectories $(\sigma_1,\sigma_2) \in \Omega^{\epsilon}_{\sigma}$ to enter $\mathcal{N}_\sigma$ is calculated as, $T_s(\varepsilon) = \frac{\overline{\lambda}(P_\sigma)}{\underline{\lambda}(\bar{Q}_\sigma)} \ln(\epsilon)$. A close observation of the forgoing formula of T_s reveals that $\varepsilon \to 0$ implies $\underline{\lambda}(\bar{Q}_\sigma) \to \infty$ and hence $T_s(\varepsilon) \to 0$. Therefore, there exists $\varepsilon \leq \bar{\varepsilon}_1 \leq \varepsilon_1$ such that $T_s(\varepsilon) < T_0/2$. This infers that $V_\sigma(\sigma(T(\varepsilon))) \leq \tau\varepsilon^2$ for every $0 < \varepsilon \leq \bar{\varepsilon}$ guaranteeing that the trajectory $(z(t),\sigma(t),\tilde{\kappa})$ enters $\mathcal{S} := \mathcal{M}_{z,\tilde{\kappa}} \times \mathcal{N}_\sigma$ within the time $T_s(\varepsilon)$ and stay there for all future time. Hence the closed loop trajectories are bounded $\forall t > T_s(\varepsilon)$. Further, boundedness of trajectories for $t < T_s(\varepsilon)$ is implied due to the use of damping functions which restrict the tracking error trajectories inside a compact set bounded by $\bar{\bar{\sigma}}_2$, while the estimation algorithm operates. Finally, re-substituting $\mu = \varepsilon^{-2}$, $\mu_1 = \varepsilon_1^{-2}$ and $\bar{\mu}_1 = \bar{\varepsilon}_1^{-2}$, boundedness of trajectories follow for $\mu \geq \bar{\mu} > 0$ with $\bar{\mu} := \max\{\mu_1, \bar{\mu}_1\}$. This completes the proof.□

The summary of the proof of piecewise boundedness of closed loop trajectories is schematically illustrated in Figure 5.2 for ease of understanding.

Proposition 5.2. ***(Ultimate boundedness)*** *The closed-loop trajectories obtained using the controller given by* (5.7) *are ultimately bounded. In other words, for any given* $\varrho > 0$ $\exists$ $\mu > \breve{\mu} \geq \bar{\mu}$ *and* T_1 *such*

that, $\|z(t)\| + \|\sigma(t)\| \leq \varrho \ \ \forall t \geq T_1$.

Proof. To prove the above proposition, it is to be shown that trajectories $(z, \tilde{\kappa}, \sigma)$ confined in set $\mathcal{S}$ as defined earlier for $t > T_s(\varepsilon)$ move towards compact sets nearing the origin. Thereafter, depending on ϱ, the trajectories must enter the corresponding compact set $\mathcal{S}^* \subset \mathcal{S}$ in a finite time T_1 and remain there forever. In simple words, the set $\mathcal{S}^*$ has to be proved positively invariant.
From Proposition 5.1, it is already proved that all trajectories starting in $\Omega_{(z,\tilde{\kappa})} \times \Omega_{\sigma}^{\epsilon}$ remain in the set $\mathcal{S}$ for all $t \geq T_s(\varepsilon)$. Hence, $\exists\ \breve{\mu}_1 > \bar{\mu}$ such that for every $\mu \geq \breve{\mu}_1$, the inequality $\|\sigma(t)\| \leq \varrho/2$ is satisfied for all $t \geq \bar{T}_1$. Now, from the proof of Proposition 5.1, for $(z, \tilde{\kappa}, \sigma) \in \mathcal{S}$, the Lyapunov function derivative is given by, $\dot{V}_z \leq -\sum_{i=1}^{\wp} c_i z_i^2 + \varepsilon \ell_1$ with $\ell_1 := \max_{\mathcal{M}_{(z,\tilde{\kappa})}} \|\frac{\partial V_z}{\partial z}\| K_1 \sqrt{\tau/\underline{\lambda}(P_\sigma)}$. Taking $\sum_{i=1}^{\wp} c_i z_i^2 \geq 2\varepsilon\ell_1$ assures $\dot{V}_z \leq -\sum_{i=1}^{\wp} c_i z_i^2/2$. Therefore, choosing $\mathcal{W}(z, \tilde{\kappa}) := \{z : \sum_{i=1}^{\wp} c_i z_i^2 \leq 2\varepsilon\ell_1\}$ as a compact set, there exists $\mu \geq \breve{\mu}_2 > \breve{\mu}_1$ such that the new set $\mathcal{S}^* := \{(z, \tilde{\kappa}) : V_z \leq c_0,\ c_0 = \max_{\mathcal{W}}\{V_z(z, \tilde{\kappa})\}\} \subset \mathcal{S}$ and $\{(z, \tilde{\kappa}) : V_z \leq c_0\}$ implies $\|z(t)\| \leq \varrho/2\ \forall\ t \geq \breve{T}_1$. The above argument proves that all $z(t)$ starting in $\mathcal{S}$ will eventually converge to the set $\mathcal{S}^* : \{(z, \tilde{\kappa}) : V_z \leq c_0\} \times \mathcal{N}_\sigma$ in finite time $T_1 = \max(\bar{T}_1, \breve{T}_1)$ considering $\mu \geq \max\{\breve{\mu}_1, \breve{\mu}_2\} \geq \bar{\mu}$. Hence the set $\mathcal{S}^*$ is positively invariant. The claim in Proposition 5.2 follows. □

Proposition 5.3. ***(Nominal Trajectory Convergence)*** *Given* $\varrho > 0$*, as defined in Proposition 5.2,* $\exists\ \breve{\mu}_3 > 0$ *such that* $\forall\ \mu \geq \breve{\mu}_3 > \max\{\breve{\mu}_1, \breve{\mu}_2\} (\forall\ \varepsilon \leq \breve{\varepsilon} < \min\{\breve{\varepsilon}_1, \breve{\varepsilon}_2\}; \varepsilon^2 = \mu^{-1})$ *and* $(z(t_0), \tilde{\kappa}(t_0)) \in \mathcal{M}_{(z,\tilde{\kappa})}$*, the solution* $\bar{z}(t)$ *and* $z(t, \varepsilon)$ *of the dynamics* $\dot{z}(t, z, 0)$ *and the perturbed dynamics* $\dot{z}(t, z, \sigma_2)$ *using the controller in* (5.7) *ensures* $\|z(t, \varepsilon) - \bar{z}(t)\| \leq \varrho,\ \forall\ t \geq 0$.

Proof. Firstly, it is assumed that the conditions of Proposition 5.1 and 5.2 are satisfied. Thereafter, exploiting the property of continuous dependence of solutions of differential equation (5.31) on initial conditions (i/c) and the estimation error σ_2, we invoke Theorem 2 of Chapter 2 in [105], to infer $\exists\ \varrho > 0$ such that for a time $T_s(\varepsilon) < t = T_2 \leq T_1$ (T_1 has been defined in the previous proposition), $\|z(T_2, \varepsilon) - \bar{z}(T_2)\| \leq \varrho$ with $\|\sigma(t)\| \leq \varrho;\ \forall t \geq T_2$. Since the trajectories $z(t)$ satisfy Proposition 5.1, it can be concluded that for $t \leq T_s(\varepsilon)$, $\|\bar{z}(T_s(\varepsilon)) - z(t_0)\| \leq K_1 T_s(\varepsilon)$ and $\|z(T_s(\varepsilon), \varepsilon) - z(t_0)\| \leq K_1 T_s(\varepsilon)$. Using these foregoing immediate relations and performing elementary operations, $\|z(T_s(\varepsilon), \varepsilon) - \bar{z}(T_s(\varepsilon))\| \leq 2K_1 T_s(\varepsilon)$ is arrived at. Again, using the feature of continuous dependence of solutions of differential equations on initial conditions (i/c) leads to the inequalities, $\|z(T_s(\varepsilon), \varepsilon) - \bar{z}(T_s(\varepsilon))\| \leq \mathcal{U}(\varrho)$ with $\|\sigma(t)\| \leq \mathcal{U}(\varrho)\ \forall\ t \geq T_2$ and $\mathcal{U}(\varrho) > 0$. Therefore during the interval $[t_0, T_s(\varepsilon)]$ and choosing $T_s = \mathcal{U}(\varrho)/2K_1$, the inequality $\|z(T_s(\varepsilon), \varepsilon) - \bar{z}(T_s(\epsilon))\| \leq \mathcal{U}(\varrho)$ holds true. Invoking the aforementioned arguments prove the claim as $\|z(t, \varepsilon) - \bar{z}(t)\| \leq \varrho,\ \forall\ t \geq 0$. □

This property of trajectory convergence is the most amazing property of the proposed control scheme which can be coined the term *performance recovery*. Therefore, Propositions 5.1-5.3 hold under the proposed FTC algorithm and hence fulfills all the conditions required to satisfy *nonlinear separation principle* [109]. Finally, modularity between controller and estimator is attained.

5.2.4.2 Further Results on Stability of the Closed-loop System under Infinite Actuator Failures

In the previous section, Proposition 5.2 states that the closed loop trajectories are ultimately bounded for $\mu > \breve{\mu} > \bar{\mu}$. These values of gain parameter μ depend on the magnitude of the ultimate bound. A larger value of μ yields a smaller ultimate bound of the closed loop signals. However, in the sense of piecewise stability, we are interested in achieving exact asymptotic output tracking which requires the ultimate bound of σ to be zero. In other words, it is now intended to find an estimator gain inequality from the estimator dynamics which when satisfied yields an exact estimation with the error variables converging to zero exactly. Solving the foregoing problem, let us call upon the inequality, $\dot{V}_\sigma \leq -|\sigma_1|^{-1/2}\sigma^T\bar{Q}_\sigma\sigma + 2\sigma^T P_\sigma\|\dot{\Delta}^*_\wp(\cdot)\|$ from the proof of Proposition 5.1. This inequality relation can be rearranged as $\dot{V}_\sigma \leq -|\sigma_1|^{-1/2}\sigma^T\bar{Q}_\sigma\sigma$. Where $\bar{Q}_\sigma = -(A_\sigma^T P_\sigma + P_\sigma A_\sigma)$ and

$$A_\sigma := \begin{bmatrix} -\frac{k_1}{2\varepsilon} & \frac{1}{2} \\ -\left(\frac{k_2}{\varepsilon^2} - |\dot{\Delta}^*_\wp|\right) & 0 \end{bmatrix}$$

Herein, it can be easily figured out that satisfying conditions for asymptotic stability of the origin (ultimate bound is zero) requires the matrix A_σ to be Hurwitz meaning $k_2\mu > \sup_{t^o_{j,h}\leq t<t^e_{j,h}}\{|\dot{\Delta}^*_\wp|\} = K_3$, yielding $\mu > K_3/k_2 = \mu^*$. For $k_2 = 1$ as chosen in the work, $\mu > \sup_{t^o_{j,h}\leq t<t^e_{j,h}}\{|\dot{\Delta}^*_\wp|\} = \mu^*$. To promote notational simplicity, the time interval between the onset and end of a particular actuator failure pattern defined by $[t^o_{j,h}, t^e_{j,h})$ is replaced by $[T_h, T_{h+1})$ from now onwards. Therefore, from Proposition 5.2, the following result $\mu > \mu^* > \breve{\mu} > \bar{\mu}$ on the choice of μ is derived. In addition, the estimation error dynamics exhibits negative degree of homogeneity. On account of the same, with the choice of $\mu > \mu^*$, finite time convergence of the estimation error signals is guaranteed. Further as proved in our works in [144], the estimation error exactly converges to zero in a predefined finite time. The expression for the upper bound on the convergence time to the origin is T_f defined as follows

$$T_f(V_\sigma(0), t_0) = \frac{2V_\sigma(0)}{K_4}$$

where $K_4 := \underline{\lambda}^{\frac{1}{2}}(P_\sigma)\underline{\lambda}(Q_\sigma)/\overline{\lambda}(P_\sigma)$. The detailed calculation is not shown for brevity and instead can be referred to [144].

Therefore, to this point it is clear that the FTC design scheme until now requires a precise knowledge of μ^* to ensure exact estimation of lumped uncertainty and exact asymptotic tracking. However, since the control problem considers the compensation of actuator failures which are unknown in time, pattern and magnitude, the knowledge of upper bounds of failure induced uncertainties and their first derivatives are not available. In Section 5.2.3.2, the motivation behind the design of uncertainty estimator (5.8) featuring adaptive gains (5.9) has been discussed briefly. Therefore, in this work, the gain parameters in the proposed uncertainty/disturbance estimator are estimated adaptively and hence promising performance can be guaranteed in all cases of actuator failures. However, stability properties of the proposed estimator are yet to be stated and proved. In the following, boundedness of estimation obtained from the finite time adaptive estimator in the event of infinite actuator failures

will be rigorously dealt with. Further, the stability and convergence properties of the tracking error under the action of the proposed adaptive FTC (5.7) for the case of infinite actuator failures, will be summarized in the in the form of theorems supported by proofs.

Theorem 5.1. ***(Piecewise stability properties of the proposed finite time adaptive estimator)*** *Assuming the lumped uncertainty $\Delta^*_{\wp}(\cdot)$ resulting from modeling imperfections, exogenous disturbances and failure induced uncertainties, to be at least once piecewise continuously differentiable, the finite time adaptive estimator given by* (5.8) *with the gain adaptation law in* (5.9)*, ensures finite time convergence of observer error variables σ_1 and σ_2 to the origin and yields an exact estimation of $\Delta^*_{\wp}(\cdot)$. Further, assuming the time interval between two consecutive changes in actuator failure pattern as $[T_h, T_{h+1})$, $h \in \mathbb{W}$, the estimation signals exhibit the following piecewise stability properties, i.e., $\sigma_1(t) \in \mathcal{L}_1[T_h, T_{h+1})$ and $\sigma_2(t) \in \mathcal{L}_2[T_h, T_{h+1})$. Here, the index h denotes the occurrence of h^{th} change in the actuator failure pattern and $h = 0$ represents initial time.*

Proof. Establishing finite time stability of $(\sigma_1 = 0, \sigma_2 = 0)$ necessitates, (1) negative homogeneity of the vector fields in the estimation error dynamics (5.12)-(5.13); (2) negative definiteness of time derivative of an appropriately chosen strict Lyapunov function. It has been shown in the proof of Proposition 5.1 that vector fields in (5.12)-(5.13) possess negative homogeneity of degree $\nu = -1 < 0$. Thereafter, to prove the second requirement, let us define $\tilde{\mu} := \mu - \mu^*$ and $\bar{k}_1 = k_1\sqrt{\mu}, \bar{k}_2 = k_2\mu$ for ease of calculation. Thereafter, let us consider a suitably chosen strict Lyapunov function $V_{\sigma,h} : \mathbb{R}^2 \setminus \{0\} \times \mathbb{R}_+ \times [T_h, T_{h+1}) \to \mathbb{R}_+$ defined as,

$$V_{\sigma,h}(\sigma, \mu) = \mu^{-\frac{3}{2}}\sigma^T P_\sigma \sigma + \frac{2 + 4\mu^{-1}\mu^*}{4\gamma}\bar{k}_1\mu^{-3/2}\tilde{\mu}^2 \tag{5.18}$$

where $P_\sigma = [\{p_{\sigma i,j}\}^2_{i,j=1}]$ is a user defined positive definite symmetric matrix with its elements chosen as $p_{\sigma 1,1} = 2\bar{k}_2 + \bar{k}_1^2/2$, $p_{\sigma 1,2} = p_{\sigma 2,1} = -\bar{k}_1/2$ and $p_{\sigma 2,2} = 1$. These elements $p_{\sigma i,j}$ are selected through back calculations to ensure that $\dot{V}_\sigma < 0$ and $V_\sigma > 0$ [145,146]. Hence to prove stability of the estimator with forward calculations, let us take the first time derivative of $V_{\sigma,h}$. Using the estimation error dynamics defined in (5.12)-(5.13) and the adaptive learning law (5.9), the equality obtained is given by (5.19)-(5.21). Using the conditions to infer negative definiteness of symmetric matrices and given the fact that $k_1 = k_2 = 1, \mu, \dot{\mu} > 0$, leads to $\dot{V}_{\sigma,h} < -\mu^{-3/2}\sigma^T\hat{Q}_\sigma\dot{\mu}\sigma \leq -\mu^{-3/2}\sigma^T\hat{Q}_\sigma\sigma < 0$, $\hat{Q}_\sigma > 0$ proving the piecewise boundedness and finite time stability of the estimation error dynamics, i.e., $(\sigma_1 = 0, \sigma_2 = 0)$ is reached in finite time. Further, the immediate inequality of $\dot{V}_{\sigma,h}$ shows that $\sigma \in \mathcal{L}_2[T_h, T_{h+1})$ implying that $\sigma_1 \in \mathcal{L}_1[T_h, T_{h+1})$ and $\sigma_2 \in \mathcal{L}_2[T_h, T_{h+1})$. □

Having proved the piecewise stability properties of the proposed adaptive uncertainty estimator, the results are now extended to the time interval $t \in [0, \infty)$ to prove estimation error boundedness in the case of infinite actuator failures.

Theorem 5.2. ***(Extension of piecewise stability properties to $t \in [0, \infty)$ interval of existence)*** *From Theorem 5.1, let us consider the stable solutions of the proposed adaptive uncertainty estimation error dynamics in* (5.12)-(5.13) *with the adaptive gain learning law* (5.9) *for the time interval $[T_h, T_{h+1})$, $h \in \mathbb{W}$. The following are inferred, (i) In the case of infinitely occurring actuator*

failures, the error dynamics of the proposed uncertainty estimator with adaptive gains yields stable solutions for the time interval $[0,\infty)$ *which means* $\sigma \in \mathcal{L}_\infty[0,\infty)$*; (ii) In the case of finite actuator failures, the estimation error signal* σ_1 *is* $\mathcal{L}_1$ *integrable, i.e.,* $\sigma_1 \in \mathcal{L}_1[0,\infty)$.

Proof of (i).

From the proof of Theorem 5.1, the following has already been proved. With the same definition of the piecewise Lyapunov function in Theorem 5.1 to verify the stability properties of the estimator, from (5.21) we get $\dot{V}_{\sigma,h} \leq -\sigma^T \hat{Q}_\sigma \sigma$. A dead-zone based adaptive tuning law is used to find the estimator gains. Therefore, invoking the properties of dead-zone based adaptation [110], the estimator gain μ always converges to a finite limit $\widehat{\mu} > \mu^*$. Given μ^* is a constant, this in turn implies the existence of a finite bound on $\tilde{\mu} = \mu - \mu^* \leq \bar{\tilde{\mu}}$. Hence the inequality for $\dot{V}_{\sigma,h}$ can be rewritten as

$$\dot{V}_{\sigma,h} \leq -\mu^{-3/2}\sigma^T \hat{Q}_\sigma \sigma - \frac{1}{2\gamma}\tilde{\mu}^2 + \frac{1}{2\gamma}\bar{\tilde{\mu}}^2 \tag{5.22}$$

The above inequality can be further simplified as

$$\dot{V}_{\sigma,h} \leq -\rho V_{\sigma,h} + \frac{1}{2\gamma}\bar{\tilde{\mu}}^2 \tag{5.23}$$

where $\rho := \min\{\underline{\lambda}(P_\sigma^{-1})\underline{\lambda}(\breve{Q}_\sigma),\ \frac{1}{\widehat{\mu}+2\mu^*}\}$ and $\breve{Q}_\sigma := \mu^{-3/2}\hat{Q}_\sigma$. Now let us consider the occurrence of infinite actuator failures and attempt to utilize the stability properties of the estimator between $[T_h, T_{h+1}),\ (h \in \mathbb{Z}_+)$ to extend the existence of such stable solutions for all $t \in [0,\infty)$. Therefore, in this

$$\begin{aligned}
\dot{V}_{\sigma,h} &= \mu^{-\frac{3}{2}}\sigma^T\dot{P}_\sigma\sigma + \mu^{-\frac{3}{2}}\dot{\sigma}^T P_\sigma\sigma + \mu^{-\frac{3}{2}}\sigma^T P_\sigma\dot{\sigma} + \frac{(2+4\mu^{-1}\mu^*)\bar{k}_1\tilde{\mu}\dot{\mu}}{\mu^{\frac{3}{2}}\gamma} + \frac{1}{2\gamma}\frac{d}{dt}\left(\frac{2+4\mu^{-1}\mu^*}{2\mu^{\frac{3}{2}}}\bar{k}_1\right)\tilde{\mu}^2 \\
&= \mu^{-\frac{3}{2}}\sigma^T\dot{P}_\sigma\sigma - \frac{\bar{k}_1}{2}\mu^{-\frac{3}{2}}|\sigma_1|^{-\frac{1}{2}}\left((2\bar{k}_2+\bar{k}_1^2-2\mu^*)|\sigma_1| - \left(\bar{k}_1 - \frac{2}{\bar{k}_1}|\dot{\Delta}_\wp|\right)|\sigma_1|\right) + \frac{1}{2\gamma}\frac{d}{dt}\left(\frac{2+4\mu^{-1}\mu^*}{2\mu^{\frac{3}{2}}}\bar{k}_1\right)\tilde{\mu}^2 \\
&\quad + \frac{1}{2\gamma}(2+4\mu^{-1}\mu^*)\bar{k}_1\mu^{-\frac{3}{2}}\tilde{\mu}\dot{\mu} - \frac{\bar{k}_1}{2}\mu^{-\frac{3}{2}}|\sigma_1|^{-\frac{1}{2}}\left(\sigma_2 - \left(\bar{k}_1 - \frac{2}{\bar{k}_1}|\dot{\Delta}_\wp|\right)|\sigma_1|^{\frac{1}{2}}\mathrm{sign}(\sigma_1)\right)^2 \qquad (5.19) \\
&= \mu^{-\frac{3}{2}}\sigma^T\dot{P}_\sigma\sigma - \frac{\bar{k}_1}{2}\mu^{-\frac{3}{2}}|\sigma_1|^{-\frac{1}{2}}\left((2\bar{k}_2+\bar{k}_1^2-2\mu^*)|\sigma_1| - \left(\bar{k}_1-\frac{2}{\bar{k}_1}\mu^*\right)^2|\sigma_1| + \left(\sigma_2 - \left(\bar{k}_1-\frac{2}{\bar{k}_1}\mu^*\right)|\sigma_1|^{\frac{1}{2}}\mathrm{sign}(\sigma_1)\right)^2\right) \\
&\quad + \frac{1}{2\gamma}(2+4\mu^{-1}\mu^*)\bar{k}_1\mu^{-\frac{3}{2}}\tilde{\mu}\dot{\mu} - \frac{1}{2\gamma}(\mu^{-2}+4\mu^{-3}\mu^*)\dot{\mu}\tilde{\mu}^2 \\
&= \sigma^T\begin{bmatrix} -\frac{(2k_2+k_1^2)}{2}\mu^{-\frac{3}{2}} & k_1\mu^{-2} \\ k_1\mu^{-2} & -\frac{3}{2}\mu^{-\frac{5}{2}}\end{bmatrix}\dot{\mu}\sigma - \frac{\bar{k}_1}{2}\mu^{-\frac{3}{2}}|\sigma_1|^{-\frac{1}{2}}\left((\mu-\mu^*)(2+4\mu^{-1}\mu^*)|\sigma_1|\right) - \frac{1}{2\gamma}(\mu^{-2}+4\mu^{-3}\mu^*)\dot{\mu}\tilde{\mu}^2 \\
&\quad - \frac{\bar{k}_1}{2}\mu^{-\frac{3}{2}}|\sigma_1|^{-\frac{1}{2}}\left(\sigma_2 - \left(\bar{k}_1-\frac{2}{\bar{k}_1}\mu^*\right)|\sigma_1|^{\frac{1}{2}}\mathrm{sign}(\sigma_1)\right)^2 + \frac{1}{2\gamma}\bar{k}_1(2+4\mu^{-1}\mu^*)\mu^{-\frac{3}{2}}(\mu-\mu^*)\dot{\mu} \qquad (5.20)
\end{aligned}$$

Using Remainder Theorem, the parameters (k_1, k_2) are found to satisfy $2k_1^2k_2 + 2k_1^2 - 4 = 0$, and using the adaptive law from (5.9) as $\dot{\mu} = \gamma|\sigma_1|^{1/2} > 0$ yields,

$$\dot{V}_{\sigma,h} = \mu^{-3/2}\sigma^T\underbrace{\begin{bmatrix} -\frac{3}{2} & \mu^{-1/2} \\ \mu^{-1/2} & -\frac{3}{2}\mu^{-1}\end{bmatrix}}_{\hat{Q}_\sigma}\dot{\mu}\sigma - \frac{\bar{k}_1}{2}\mu^{-\frac{3}{2}}|\sigma_1|^{-\frac{1}{2}}\left(\sigma_2 - \left(\lambda_1 - \frac{2}{\lambda_1}\mu^*\right)^2|\sigma_1|^{\frac{1}{2}}\mathrm{sign}(\sigma_1)\right)^2 - \frac{1}{2\gamma}(\mu^{-2}+4\mu^{-3}\mu^*)\dot{\mu}\tilde{\mu}^2 < 0 \tag{5.21}$$

direction, a Lyapunov function $V_\sigma : \mathbb{R}^2 \setminus \{0\} \times \mathbb{R} \times [0, \infty) \to \mathbb{R}_+$ is defined whose piecewise counterpart defined over the time interval $[T_h, T_{h+1})$ is $V_{\sigma,h}$. In the event of intermittently occurring changes in the actuator failure patterns affecting the system at time instances T_h, $(h \in \mathbb{Z}_+)$, discontinuities are encountered in the Lyapunov function as well as its value cumulatively increases at every time instance T_h. The magnitude change in the Lyapunov function at the failure instances T_h is calculated as,

$$V(T_h^+) - V(T_h^-) \leq \frac{2 + 4\mu^{-1}(T_h^+)\mu^*}{4\gamma}\mu^{-1}(T_h^+)\tilde{\mu}^2(T_h^+) - \frac{2 + 4\mu^{-1}(T_h^-)\mu^*}{4\gamma}\mu^{-1}(T_h^-)\tilde{\mu}^2(T_h^-) \tag{5.24}$$

$$V(T_h^+) \leq V(T_h^-) + \frac{2 + 4\widehat{\mu}^{-1}\mu^*}{4\gamma}\widehat{\mu}^{-1}\bar{\tilde{\mu}}^2 \leq V(T_h^-) + \overline{\Delta} \tag{5.25}$$

Here $\overline{\Delta} := \frac{2+4\widehat{\mu}^{-1}\mu^*}{4\gamma}\widehat{\mu}^{-1}\bar{\tilde{\mu}}^2$ is the maximum magnitude change in the Lyapunov function $V(t)$ at all failure instances T_h and $V(T_h^-) := \lim_{t \to T_h^-} V(t)$. Further, $\overline{\Delta}$ is finite due to the usage of dead-zone based gain adaptation. At this point, using (5.23) and (5.25), the overall system under infinitely varying actuator failure patterns can be represented as a hybrid system comprising of piecewise continuous dynamics, discrete dynamics and an impulse sequence $\{T_h\}$ $\forall h \in \mathbb{W}$ satisfying $0 \leq T_0 < T_1 < T_2 < \ldots < T_\aleph < T$ and $T \to \infty$. The notation $\aleph$ is used to denote the total number of changes in the actuator failure pattern within the time interval $[0, T) \supset [T_h, T_{h+1})$ and $\aleph(T_0, T) = (T - T_0)/T^*$ with $T_\aleph < T < \infty$, $T^* := \min\{T_{h+1} - T_h\}$ for $h \in \mathbb{W}$.

Repeating the same procedure as adopted in the proof of Theorem 3.4(i) with the recursive formulations (5.23) and (5.25) with the choice of $T_0 = 0$ yields,

$$V(T^-) \leq V(0)e^{-\rho T} + \frac{\bar{\tilde{\mu}}^2}{2\gamma\rho}\left(\frac{2 - e^{-\rho T^*}}{1 - e^{-\rho T^*}}\right) + \frac{\overline{\Delta}}{1 - e^{-\rho T^*}} \tag{5.26}$$

Finally from (5.26), the boundedness of the estimation error $\sigma(t)$ is proved in the case of infinite actuator failures, i.e., $\sigma(t) \in \mathcal{L}_\infty[0, \infty)$. □

Proof of (ii).

Using the inequality $\|\sigma\|^2 \geq |\sigma_1|^{1/2}$ in (5.21) yields the following,

$$\dot{V}_\sigma < -\gamma|\sigma_1|^{1/2}\sigma^T\breve{Q}_\sigma\sigma \leq -\gamma\underline{\lambda}(\breve{Q}_\sigma)|\sigma_1| \tag{5.27}$$

Integrating the above inequality over $[T_h, T_{h+1})$ proves that $\sigma_1 \in \mathcal{L}_1[T_h, T_{h+1})$. Besides the inequality can be expanded with respect to discrete time instants T_h and T_{h+1} using (5.25) and (5.27) as given below.

$$V_\sigma(T_{h+1}^-) \leq V_\sigma(T_h^+) - \gamma\underline{\lambda}(\breve{Q}_\sigma)\int_{T_h}^{T_{h+1}}|\sigma_1|dt \leq V_\sigma(T_h^-) - \gamma\underline{\lambda}(\breve{Q}_\sigma)\int_{T_h}^{T_{h+1}}|\sigma_1|dt + \overline{\Delta} \tag{5.28}$$

Utilizing the above inequality (5.28), the following holds for the final time T under $\aleph(0, T)$ changes in

actuator failure patterns within time $[0, T)$.

$$V_\sigma(T^-) \leq V_\sigma(T_\aleph^+) - \gamma \underline{\lambda}(\breve{Q}_\sigma) \int_{T_\aleph}^{T} |\sigma_1| dt \leq V_\sigma(T_\aleph^-) + \overline{\Delta} - \gamma \underline{\lambda}(\breve{Q}_\sigma) \int_{T_\aleph}^{T} |\sigma_1| dt \leq \ldots$$
$$\leq \ldots \leq V_\sigma(0) + \aleph(0, T)\overline{\Delta} - \gamma \underline{\lambda}(\breve{Q}_\sigma) \int_{0}^{T} |\sigma_1| dt \tag{5.29}$$

Hence, from (5.29), the $\mathcal{L}_1$ bound on σ_1 is calculated as follows with $T \to \infty$,

$$\int_0^\infty |\sigma_1| dt \leq \frac{V_\sigma(0) + \aleph(0, T)\overline{\Delta}}{\gamma \underline{\lambda}(\breve{Q}_\sigma)} < \infty \tag{5.30}$$

From (5.30), it is observed that if the occurrence of actuator failures is finite implying $\aleph(0, \infty)$ to be finite, the estimation error signal satisfies $\sigma_1 \in \mathcal{L}_1[0, \infty)$. □

Now, the final theorem summarizes the stability properties of the proposed adaptive estimator based backstepping controller to compensate actuator faults and failures followed by the boundedness of the closed loop trajectories and asymptotic stability of output tracking error dynamics, in the case of infinite actuator failures.

Theorem 5.3. ***(Stability of tracking error dynamics for*** $t \in [0, \infty)$ ***interval of existence)*** *Consider the closed-loop adaptive system consisting of the plant* (5.3) *affected by actuator faults/failures modeled in* (5.2)*, the controller* (5.7) *and the finite time adaptive estimator* (5.8) *with the adaptive law* (5.9)*. Under assumptions 5.1-5.2, the following holds. (i) All signals of the closed-loop system are globally ultimately bounded irrespective of the actuator failures being finite or infinite. (ii) Global asymptotic stability of the output tracking error dynamics is guaranteed, i.e.* $\lim_{t\to\infty} z(t) = 0$ *provided the occurrence of actuator failures is finite.*

Proof of (i).

From Theorem 5.2, the boundedness of $\sigma_2 = \tilde{\Delta}_\wp$ is guaranteed for all $t \in [0, \infty)$ in the case of infinite actuator failures with its piecewise finite time convergence to the origin. Further, the homogeneity property of the vector fields in the estimation error dynamics (5.12)-(5.13) also restricts the trajectories to reside within compact sets. With the adaptive learning law for μ starting from an arbitrary small nonzero initial condition and a suitably chosen adaptive rate γ, the conditions in Proposition 5.1 will be satisfied. The advantage of this adaptive finite time estimator is its inherent capability to adjust its gains online and react accordingly to the requirement of the plant so that the trajectories of $(z, \tilde{\kappa})$ do not escape the compact set $\mathcal{M}_{(z,\tilde{\kappa})}$ for all $t > t_0$ and eventually move towards the origin. A time varying damping injection contributes to the achievement of global stability results. The adaptive law $\dot{\mu}$ ensures $\mu \geq \mu^* = \sup_{T_h \leq t < T_{h+1}} \{|\dot{\Delta}_\wp^*|\}$ for $k_1 = k_2 = 1$. Such a value of μ satisfies both Proposition 5.1 and 5.2 inferring the piecewise ultimate boundedness of closed-loop trajectories. Further, the inequalities in (5.14) and $\sigma \in \mathcal{L}_\infty[0, \infty)$ prove $z(t) \in \mathcal{L}_\infty[0, \infty)$, $\dot{z}(t) \in \mathcal{L}_\infty[0, \infty)$ in the event of infinite actuator failures.

Proof of (ii).

The $\wp$-th order tracking error dynamics after substituting the virtual control laws α_i defined by (5.4),

is reframed in a linear state space form as follows,

$$\dot{z} = \mathcal{A}_z(z, \hat{\kappa}, t)z + \Psi_\kappa(z, \hat{\kappa}, t)^T\tilde{\kappa} + B_\sigma\sigma_2(\cdot) \tag{5.31}$$

$$\dot{\kappa} = -\Gamma\Psi_\kappa\bar{z} \tag{5.32}$$

The state variables in (5.31) are defined as $\bar{z} := [z_1\ z_2 \dots z_{\wp-1}]^T; z := [\bar{z}\ z_\wp]^T; \sigma_2 = \tilde{\Delta}_\wp$. The matrices $\mathcal{A}_z(z, \hat{\kappa}, t)$, B_σ and $\Psi_\kappa(z, \hat{\kappa}, t)^T$ are defined earlier in the beginning of Section 5.4.3. Let us introduce an auxiliary state $\chi(t) := z(t) - \mathcal{N}\bar{\sigma}_1(t)$ such that $\mathcal{N} := [0\ 0 \dots 0\ 1]^T_{1\times\wp}$ and $\bar{\sigma}_1(t) = \lceil\hat{z}_\wp - z_\wp\rfloor^{1/2}$ denoting the estimation error for the state $z_\wp$. With this choice of χ, we arrive at a dynamics in χ driven by σ_1 only. Firstly, to deduce such a dynamics from the definition of χ, a more compliant form of estimation error dynamics is needed so that the theory of $\mathcal{L}_p$ spaces can be applied.

In this direction, to begin with the proof, we first invoke the estimation error dynamics in (5.12)-(5.13). For convenience in analysis, the error dynamics has to be transformed to a more tractable form using a suitable diffeomorphism. Therefore, using the diffeomorphism $\sigma = [\bar{\sigma}_1\ \bar{\sigma}_2]^T := [\lceil\sigma_1\rfloor^{1/2}\ \sigma_2]^T$, the transformed error dynamics is given by,

$$\dot{\sigma} = \frac{|\sigma_1|^{-1/2}}{2}\left(\begin{bmatrix} -\bar{k}_1 & 1 \\ -2(\bar{k}_2 - \sup\{\dot{\Delta}^*_\wp\}) & 0 \end{bmatrix}\begin{bmatrix} \bar{\sigma}_1 \\ \bar{\sigma}_2 \end{bmatrix}\right) \tag{5.33}$$

Now, let us consider the additional dynamics in $(\bar{\sigma}_1, \bar{\sigma}_2)$ as,

$$\dot{\sigma} = \begin{bmatrix} -\bar{k}_1 & 1 \\ -2(\bar{k}_2 - \sup\{\dot{\Delta}^*_\wp\}) & 0 \end{bmatrix}\begin{bmatrix} \bar{\sigma}_1 \\ \bar{\sigma}_2 \end{bmatrix} \tag{5.34}$$

Using Filippov's Theorem 6 of Chapter 2 in [105], it is concluded that the dynamics described in (5.33) and (5.34) have the same trajectories with identical signal properties if the scaling function $\frac{|\sigma_1|^{-1/2}}{2}$ is positive definite. With the chosen diffeomorphism and $\mu > 0, \bar{k}_1 = \sqrt{\mu}, \bar{k}_2 = \mu$ for $k_1 = k_2 = 1$, the scaling function satisfies the positive definiteness condition. Hence, the equivalence of solutions of (5.33) and (5.34) is inferred from Filippov's Theorem. Thus, from now on the analysis of the the estimation error will be conducted using the auxiliary error dynamics in (5.34).

The dynamics of χ using the estimation error dynamics (5.34) is described by the following differential equation.

$$\dot{\chi} = \mathcal{A}_z(z, t)\chi + \Psi^T\tilde{\kappa} + \mathcal{N}(\bar{k}_1 - (c_\wp + s_\wp))\bar{\sigma}_1 \tag{5.35}$$

From Theorem 5.2, the estimation error signal $\sigma \in \mathcal{L}_\infty[0, \infty)$ in the event of finite actuator failures. Therefore, using Hölder's inequality, it is straightforward to prove that $\bar{\sigma}_1 \in \mathcal{L}_2[0, \infty)$ in the case of finite actuator failures. It can now be observed that (5.35) is driven by an $\mathcal{L}_2$-integrable input $\bar{\sigma}_1$. Therefore, our objective is to prove the $\mathcal{L}_2$-integrability of the auxiliary state $\chi(t)$. This is due to the fact that $\chi(t) \in \mathcal{L}_2[0, \infty)$ implies $z(t) \in \mathcal{L}_2[0, \infty)$. Defining $\bar{\chi} := [\{\chi_i\}_{i=1}^{\wp-1}]^T$, $\chi_\wp := z_\wp - \lceil\sigma_1(t)\rfloor^{1/2}$, $\chi := [\bar{\chi}\ \chi_\wp]^T$ and proceeding with this aim, we compute,

$$\frac{1d}{2dt}\left(\|\chi\|^2 + \Gamma^{-1}\|\tilde{\kappa}\|^2\right) \leq \chi^T\left(\frac{\mathcal{A}_z^T + \mathcal{A}_z}{2}\right)\chi + \chi^T\widehat{\mathcal{N}}\bar{\sigma}_1$$

$$\frac{1d}{2dt}\left(\|z\|^2+\Gamma^{-1}\|\tilde{\kappa}\|^2\right)\leq -\chi^T\mathcal{Q}\chi+\chi^T\widehat{\mathcal{N}}\bar{\sigma}_1 \tag{5.36}$$

$$\begin{aligned}&\leq -\underline{\lambda}(\mathcal{Q})\|\chi\|^2-\sum_{i=1}^{\wp-1}\bar{c}_i|\psi_i|^2\bar{\chi}_i^2-\bar{c}_\wp|\hat{\Delta}_\wp+\varsigma|^{\frac{1}{2}}\chi_\wp^2+\chi^T\widehat{\mathcal{N}}\bar{\sigma}_1\\&\leq -\underline{\lambda}(\mathcal{Q})\|\chi\|^2+\chi^T\widehat{\mathcal{N}}\bar{\sigma}_1\end{aligned} \tag{5.37}$$

where $\widehat{\mathcal{N}}:=\mathcal{N}(\bar{k}_1-(c_\wp+s_\wp))$. Using the Peter-Paul inequality with the factor $\underline{\lambda}(\mathcal{Q})$ for the second term in (5.37) leads to,

$$\chi^T\widehat{\mathcal{N}}\bar{\sigma}_1\leq\underline{\lambda}(\mathcal{Q})\frac{\|\chi\|^2}{2}+\frac{1}{2\underline{\lambda}(\mathcal{Q})}\|\widehat{\mathcal{N}}\|_\infty^2\|\bar{\sigma}_1\|^2 \tag{5.38}$$

Substituting (5.38) in (5.37) renders the inequality below,

$$\begin{aligned}\frac{1}{2}\frac{d}{dt}\left(\|\chi\|^2+\Gamma^{-1}\|\tilde{\kappa}\|^2\right)&\leq-\frac{\underline{\lambda}(\mathcal{Q})}{2}\|\chi\|^2\\&+\frac{1}{2\underline{\lambda}(\mathcal{Q})}\|\widehat{\mathcal{N}}\|_\infty^2\|\bar{\sigma}_1\|^2\end{aligned} \tag{5.39}$$

The boundedness of $\widehat{\mathcal{N}}$ is ensured by taking into account the boundedness of all closed-loop signals under the action of the proposed FTC. Finally, the inequality in (5.39) is re-arranged and then integrated for the time interval $[0,\infty)$ using $\bar{\sigma}_1\in\mathcal{L}_2[0,\infty)$ which yields,

$$\begin{aligned}\int_0^\infty\|\chi\|^2dt&\leq\frac{1}{\underline{\lambda}(\mathcal{Q})}\left(\|\chi(0)\|^2+\Gamma^{-1}\|\tilde{\kappa}(0)\|^2\right)\\&+\frac{1}{\underline{\lambda}(\mathcal{Q})}\|\widehat{\mathcal{N}}\|_\infty^2\int_0^\infty\|\bar{\sigma}_1\|^2dt\leq\infty\end{aligned} \tag{5.40}$$

Given the facts that $\chi(0)$ and $\tilde{\kappa}(0)$ are finite and $\bar{\sigma}_1\in\mathcal{L}_2[0,\infty)$, the signal property of $\chi\in\mathcal{L}_2[0,\infty)$ is easily concluded from (5.40). Therefore, $z(t)\in\mathcal{L}_2$ follows from the $\mathcal{L}_2$-integrability property of $\chi(t)$. Invoking Barbalat's Lemma, with the signal properties $z(t)\in\mathcal{L}_2[0,\infty)\cap\mathcal{L}_\infty[0,\infty)$ and $\dot{z}(t)\in\mathcal{L}_\infty[0,\infty)$ infers asymptotic stability of the tracking error vector $z(t)$. This completes the proof. □

The nominal performance recovery at time T_f and asymptotic convergence of the tracking error starting from $\Omega_{(z,\tilde{\kappa})}$ to the origin under the action of the proposed FTC strategy is schematically illustrated in Figure 5.3.

Further, it can be said that Theorem 5.3 been proved, the proposed controller satisfies the results in Propositions 5.1 and 5.2. Thereafter, invoking the result in Proposition 5.3, the transient performance recovery or the convergence of perturbed system trajectories to those of the nominal system (assuming known virtual control derivative and free of faults) under adaptive backstepping control is ensured. Since the estimator gain is adapted online with sufficiently fast adaptive rate γ, the condition of $\mu>\mu^*$ is always satisfied. This choice of estimator gains yields the ultimate bound on (σ_1,σ_2) to be zero within a finite time T_f. Hence the proposed design allows to exactly recover the output performance achieved by using a backstepping controller for the nominal system (free from faults/failures).

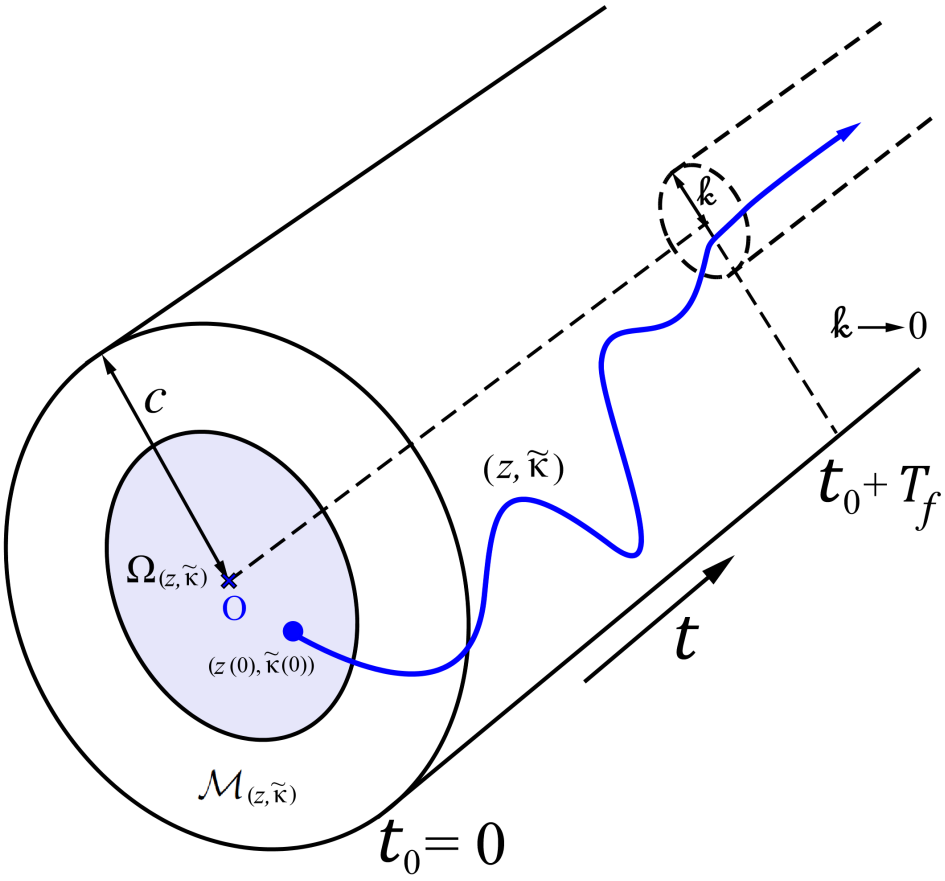

Figure 5.3: Time evolution of $z(t)$ and $\tilde{\kappa}(t)$ starting in $\Omega_{(z,\tilde{\kappa})}$ traversing through the set $\mathcal{M}_{(z,\tilde{\kappa})}$ and ultimately exponentially asymptotically converging to origin. The radius k defines the decaying exponential envelope along which $z(t)$ converges to the origin with $k \to 0$ as $t \to \infty$.

Remark 5.3. *It should be mentioned that the proposed control scheme can also be used in the case of the loss of effectiveness fault being state dependent. This is due to the fact that in the proposed adaptive estimator integrated control scheme, boundedness of all closed loop system trajectories have been proved by taking into consideration the interaction between the control system and estimator as a consequence of the interaction between the fault and the system states.*

5.2.5 Simulation Studies

In this section, the proposed methodology is applied to compensate infinite number of relatively frequent PLOE actuator faults and total actuator failures in a nonlinear longitudinal model of a Boeing 747-100/200 aircraft in presence of modeling uncertainties. This study illustrates the effectiveness of the proposed technique in guaranteeing stability, maintaining nominal fault-free performance (the most distinctive attribute) while ensuring a faithful and exact disturbance rejection. A Boeing 747-100/200 aircraft longitudinal nonlinear dynamics are considered from [4, 111, 112] similar to the one considered in (2.57)-(2.58). The detailed dynamical description along with the definitions and values of the aerodynamic parameters are referred to Section 2.2.5 in Chapter 2 of this thesis.

Choosing the state variables as $[\alpha\ V_T\ \theta\ q]^T = [x_1\ x_2\ x_3\ x_4]^T = [\eta\ \xi]^T$ and using Assumption 5.2, the system is transformed to a strict feedback form. The elevator deflection angles of the two piece augmented elevator is δ_{e1}=δ_{e2} and are the two actuators u_1 and u_2. Moreover, the thrust generated by each engine is chosen to be equal, i.e., $P_{n1} = P_{n2} = P_{n3} = P_{n4} = P_n$. The dynamics in $\eta := [x_1\ x_2]^T$ describe the internal dynamics of the system with $\xi = [x_3\ x_4]^T$ as the input. Input-to-State stability of the internal dynamics with ξ as the input, was shown in [95]. The transformed system Σ_c to be used for controller design is given as,

$$\dot{\xi}_3 = \xi_4,\ \dot{\xi}_4 = a(\xi,\eta) + \Delta_{\wp}(\xi,\eta) + \sum_{j=1}^{m} \beta_j(\xi,\eta)u_j \tag{5.41}$$

where $\xi = [\xi_3\ \ \xi_4]$. The infinite actuator faults/failures in both the scenarios are modeled similar to that in [6] as

$$\begin{cases} u_1 = \bar{u}_{F1,h}\phi_{1,h} \\ u_2 = (1 - K_{2,h})u_{H2} \end{cases}, t \in [hT^*, (h+1)T^*) \tag{5.42}$$

where $h = 1, 3, \ldots, \infty$. In simulations, the initial state is considered to be $[0.0162\ 230\ 0.0162\ 0]^T$. Further, the virtual control and actual control parameters are chosen as $c_1 = 20, c_2 = 5, \bar{c}_1 = 0.5, \bar{c}_2 = 0.05, \varsigma = 0.1$. The rate parameter in the estimator gain adaptation law is considered as $\gamma = 50$. The reference signal for tracking y_d is the output of a reference system as in [66], given by $G_{\mathrm{r}} = \frac{1}{s^2+5s+6}$ and $[y_d(t)] = G_{\mathrm{r}}(s)[y_r(t)]$ with $y_r = 0.1\sin(0.5t)$. The modeling uncertainty $\Delta a(\xi,\eta)$ is additive in nature and is given by $\Delta a(\xi,\eta) = \kappa^* a(\xi,\eta)$, where $|\kappa^*| \leq 1$.

The performance of the proposed methodology is compared with existing FTC scheme by [6] in the event of infinite actuator failures. The controller proposed by [6] is designed for the system in (5.41), based on modular backstepping control (MBSC). The notations followed for the control design based on the methodology of [6] are the same as considered in their work except for the modeling uncertainty θ which is substituted by the term κ^* here. For the scheme by [6], it is assumed that $|\kappa^*| \leq 1$ and $0.2 \leq K_{jh} \leq 1$ are known at the design phase. The design parameters of the controller by Wang and Wen [6] are as follows: $\zeta = 0.05, c_1 = 20, c_2 = 5, \kappa_2 = 10^{-6}, \Gamma = 0.5 \times I_4, \nu_1 = (0.05+2)/2, \nu_2 = \nu_3 = \nu_4 = 0, \sigma_1 = 1.025 - 0.05, \sigma_3 = \sigma_4 = 10, \varsigma = 0.5$ and $q = 20$.

Fault Scenario 1: $T^* = 10$s, $\bar{u}_{F1,h} = 5$, $K_{2,h} = 0.7$ and $\phi_{1,h} = 1$, it is observed that the proposed control scheme and the controller by Wang and Wen [6] yield a faithful output tracking while maintaining boundedness of all the closed loop signals. The tracking performance along with the control inputs for both the schemes are shown in Figures 5.4(a)-5.4(f).

Fault Scenario 2: Here, the failure parameters are assumed to be $T^* = 10$s, $\bar{u}_{F1,h} = 0$, $K_{2,h} = 0.5$ and $\phi_{1,h} = 1$. The output tracking of the desired pitch angle θ and pitch rate q using the proposed controller are illustrated in Figures 5.5(b)-5.5(c) while the tracking performance using both the methodologies are demonstrated in Figure 5.5(a). The profile of the control inputs u_1 and u_2 with the proposed control design and that by [6] are given in Figures 5.5(e)-5.5(f), respectively.

Fault Scenario 3: This is an extended case which demonstrates the potential of the proposed scheme in handling oscillatory failures in actuators. For the purpose of illustration of actuator oscillatory failures, the failure parameters are chosen as $\bar{u}_{F1,h} = 2$, $K_{2,h} = 0.5$, $\phi_{1,h} = \sin(2t)$, $T^* = 10$ and

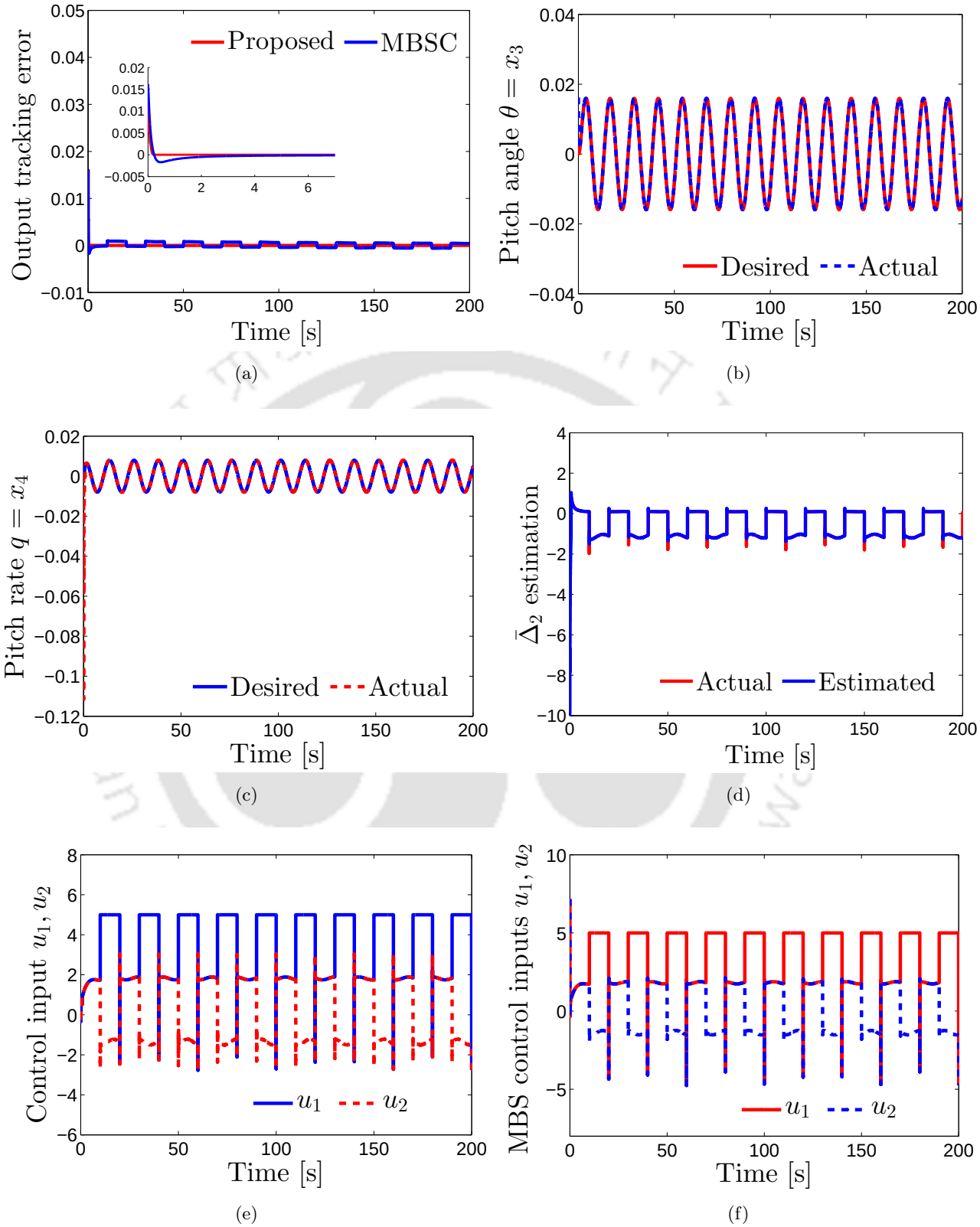

Figure 5.4: Scenario 1: System response with the proposed fault tolerant control scheme with T^*= 10s. (a) Comparison of output pitch angle tracking error $z_1 = x_3 - y_r$ using the proposed controller and modular backstepping control (MBSC) [6], (b) Pitch angle $x_3 = \theta$ using the proposed FTC scheme, (c) Pitch rate $x_4 = q$ using the proposed FTC, (d) The estimate of the lumped uncertainty $\hat{\bar{\Delta}}_2$ incurred due to actuator faults/failures and modeling uncertainties, (e) Proposed control inputs $u_1(t)$ and $u_2(t)$, (f) Control inputs $u_1(t)$ and $u_2(t)$ using modular backstepping control based FTC proposed by Wang & Wen [6]

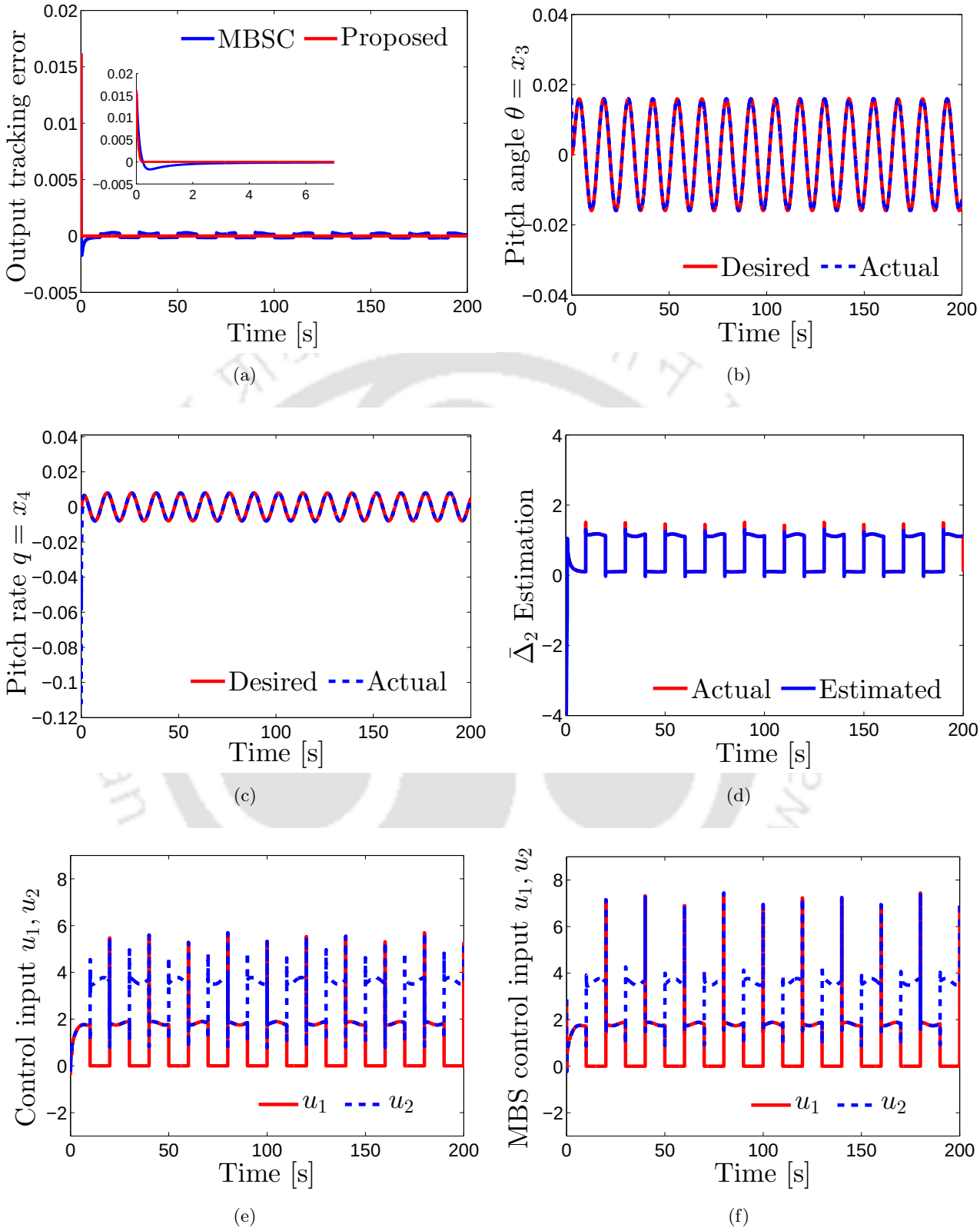

Figure 5.5: Scenario 2: System response with the proposed fault tolerant control scheme with T^*= 10s. (a) Comparison of output pitch angle tracking error $z_1 = x_3 - y_r$ using the proposed controller and modular backstepping control (MBSC) [6], (b) Pitch angle $x_3 = \theta$ using the proposed FTC scheme, (c) Pitch rate $x_4 = q$ using the proposed FTC, (d) The estimate of the lumped uncertainty $\hat{\bar{\Delta}}_2$ incurred due to actuator faults/failures and modeling uncertainties, (e) Proposed control inputs $u_1(t)$ and $u_2(t)$, (f) Control inputs $u_1(t)$ and $u_2(t)$ using modular backstepping control based FTC proposed by Wang & Wen [6]

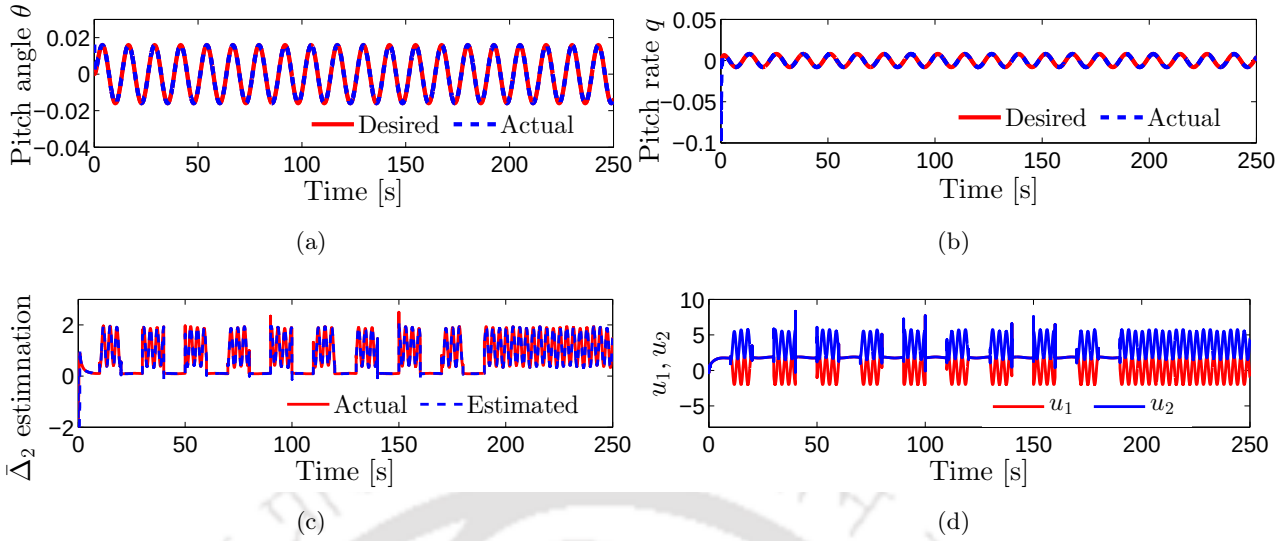

Figure 5.6: Scenario 3: System response with the proposed fault tolerant control scheme. (a) Pitch angle $x_3 = \theta$ using the proposed FTC scheme, (b) Pitch rate $x_4 = q$ using the proposed FTC, (c) The estimate of the lumped uncertainty $\hat{\bar{\Delta}}_2$ incurred due to actuator faults/failures and modeling uncertainties, (d) Proposed control inputs $u_1(t)$ and $u_2(t)$

$u_1 = 2\sin(2t)$ for $190\text{s} \leq t \leq 250\text{s}$. Results appear in Figures 5.6(a)-5.6(d).
Herein, we observe that the proposed scheme is still successful in maintaining the desired nominal output performance with an acceptable control input. This case had not been considered in the work in [6] and hence a performance comparison is not drawn.

5.3 Summary

In this chapter, the problem of accommodating infinite number of actuator failures in nonlinear uncertain systems was addressed. In this context, a new adaptive control scheme was proposed for nonlinear systems affected by infinite failures with inherent modeling uncertainties and matched/mismatched perturbations. The proposed controller appropriately utilizes direct adaptive backstepping approach to guarantee an appreciable transient performance in fault free situations and inducts a finite time adaptive estimator based control at the last step to counteract infinite actuator failures. The attributes of the proposed control methodology are boundedness of all closed loop trajectories; output transient and steady state performance recovery in the event of failures; asymptotic exact output tracking; finite time exact estimation of system and failure induced uncertainties; and potential to compensate infinite actuator failures. A rigorous stability analysis of the closed loop system using the proposed adaptive estimator integrated backstepping controller is conducted to prove stability of the overall controlled system. Unlike estimators based on HGOs, the adaptive uncertainty estimator does not induce peaking effect and exact estimation of the lumped uncertainty is achieved with finite values of estimator gain parameters. These estimator gains are also selected through an adaptive learning procedure. In addition, the introduction of damping function in the backstepping controller depending

on the lumped uncertainty estimation error allows for the existence of global stability of closed-loop trajectories irrespective of actuator failures being finite or infinite. Consequently, global exponential asymptotic exact convergence of the output tracking error to the origin is ensured in the event of finite occurrence of actuator failures without the use of GBC. Different from GBC, the proposed FTC design methodology also does not require the knowledge of the estimate of the region of attraction which is required by the former to tune the control saturation level. Besides, for real time applications, unlike GBC, no trade-off is required to be achieved between the choice of estimator gains for output fault-free performance recovery and sensitivity of estimation towards measurement noise. In order to study performance of the proposed methodology, it was applied for pitch control in nonlinear longitudinal model of Boeing 747-100/200 aircraft. Simulation results obtained illustrate the superiority of the proposed FTC scheme in compensating infinite actuator failures over existing approaches [6, 75, 76] designed under similar circumstances.

6

Conclusions and Scope for Future Work

Contents

6.1 Conclusions 217

6.2 Recommendations for Future Research 220

The research in this thesis is centered around the design, development, analysis and implementation of adaptive FTC strategies for nonlinear uncertain systems affected by unknown actuator failures. With the backstepping procedure being central to all the proposed control algorithms, some new adaptive backstepping algorithms in the context of promising applications to the problem of FTC design have been proposed. The proposed controllers are aimed at achieving closed loop signal boundedness asymptotic convergence of the tracking error to the origin with an acceptable transient behavior and a decent control usage, in the event of unanticipated actuator failures. Besides, the expansion of their applicability to a large class of dynamical systems is another important design concern. This thesis is an attempt to address the open issues in adaptive FTC discussed in Chapter 1. An FE/FTC architecture is adopted to design and investigate all the control algorithms proposed herein. Briefly, the work done has been summarized below followed by future research recommendations in adaptive FTC design for nonlinear uncertain systems.

6.1 Conclusions

In Chapter 2, an actuator failure compensation strategy based on direct adaptive control is designed for affine nonlinear uncertain systems affected by faults in the form of partial and total loss of effectiveness of actuators. The proposed strategy is based on backstepping and adaptive second order sliding mode control methodologies. The actuator fault/failure induced unknown parameters and the bounds on system uncertainties are estimated seperately using two adaptive update laws which utilize the output tracking error information. Asymptotic stability of the output error in nominal scenarios and in the event of actuator failures is ensured. Improvement of output transient behavior at the output is shown through a rigorous stability analysis. Compared to ABSC and ASMC based FTC strategies, the proposed controller reduces the conservatism of the tradeoff between output and input performance enhancement by rendering an excellent output performance without any increment in virtual control gains. Further, the cumulative increment of the $\mathcal{L}_\infty$ bounds on output tracking error with every instances of actuator failures is eluded. The incorporation of an adaptive second order sliding mode controller results in a finite time convergence of the last tracking error variable to zero. In view of the closed loop error analysis under ABSC, the tracking error variable corresponding to the last coordinate behaves as a disturbance to the remaining reduced closed loop tracking error dynamics. Further, occurrence of actuator failures directly affects the last error coordinate. Therefore, a finite time convergence of the last error variable translates to a nominal performance recovery of the reduced tracking error dynamics both at their transient and steady state phases. Thus , owing to fast and accurate convergence of the last error variable to the origin, output transient and steady performance is significantly improved. Such a design attribute also allows us an extra design freedom on defining a time bound on the nominal performance recovery in the event of actuator faults/failures or occurrences of external disturbances. In contrary to the performance recovery in the asymptotic sense, the nominal performance recovery herein is meant in the finite time sense which means that the actual output error not only remains close to the nominal trajectory as much is desired but also exhibits a time bound convergence to the latter, as time elapses. This property is indeed beneficial for FTC ap-

plications. Simulation results also confirm that the proposed controller yields enhanced transient and input performance with no chattering in the control input in comparison with a dedicated ABSC or relevant ASMC schemes proposed till date in literature. Hence, improvement of transient performance through the increment of virtual control gains/sliding surface parameters and trajectory initialization is circumvented. The stability and convergence properties of closed loop signals under the proposed control law are understood in the global sense.

Thereafter, in Chapter 3, the drawbacks of direct adaptive controllers under an FE/FTC framework, are discussed and their inability in compensating infinitely time varying failure patterns is mathematically proved. These shortcomings are circumvented by proposing a new actuator failure compensation strategy based on indirect adaptive control within the same FE/FTC architecture. Although direct adaptive strategies have been extensively used for FTC; to the best of author's knowledge, there are very few results available in literature which utilize indirect adaptive control to compensate even finite actuator failures in nonlinear uncertain systems. Such a lack of interest is accrued from the poor output transient performance obtained using an indirect adaptive scheme during the learning phase. However, indirect strategies are well known to assure faithful asymptotic tracking/stabilization with an economized usage of control effort. Therefore, Chapters 3-4 essentially focus on encashing the advantages of indirect adaptive control while concurrently exploring ways to improve the output transient and steady state performance without any substantial effect on system stability margins. These chapters consider the system parametric uncertainty and failure induced perturbations to be linearly parameterized. The functions in the regressor matrices associated with unknown parameters are smooth, not Lipschitz though. Thus, there exists a bidirectional robustness interaction between the certainty equivalence (CE) controller and the parameter estimator which breaks down the design modularity and inhibits the existence of global stability of closed loop signals. The region of attraction is decreased significantly and any increment in virtual control gains to improve the output performance will eventually manifest in decremented stability margins, which is undesirable. In Chapter 3, the multiple model adaptive FTC with two layer adaptation, proposed for the aforementioned nonlinear systems affected by finite as well as infinite actuator failures, obviates the foregoing design challenges. Multiple model adaptive estimation based FTC of general nonlinear systems (with linearly parametrized uncertainties) with transient performance characterization, has not yet been addressed in open literature even to compensate finite actuator failures. Therefore, contributions in Chapter 3 can be considered as filling the gap that exists in adaptive backstepping based actuator failure compensation strategies for nonlinear uncertain systems. The fastness and accuracy of estimation compared to single model adaptive control parameter estimation are ensured using the two layers of adaptation. As a result, the output performance of the proposed scheme is promising both at start up and post failure scenarios. The output transient performance under the proposed adaptive multiple model FTC (AMMFTC) is quantified and proved to be superior to that obtained using single identification model based adaptive FTC. Explicit $\mathcal{L}_\infty$ and $\mathcal{L}_2$ bounds on the tracking error for all time $t \in [0, \infty)$ are derived in the event of intermittently occurring actuator failures. These bounds provide the designer with an idea of choice of gains and estimator parameters to improve both input and output transient behavior. The proposed method exhibits a simpler structure compared to [56] in the sense that a single controller is utilized

in the design of failure compensation in the event of unknown actuator LOE, LIP float free failures and intermittent actuator failures. Simulation results illustrate the effectiveness of the proposed FTC method in the case of infinite actuator faults/failures. The proposed multiple model adaptive control method has also delivered to the expectations of achieving a fruitful output transient performance without any substantial increase in control effort.

In Chapter 4, to further enhance output transient performance and to make it more compliant with practical design requirements, a finite time parameter estimator is inserted within the same FE/FTC architecture. This ensures finite time exact estimation of the unknown parameters including those induced by actuator failures and hence a time bound convergence of the output to the nominal solutions of the healthy system is exhibited. Apart from the above attributes, the finite time adaptation based controller (FTAC) is also proposed to compensate possible infinite actuator failures. Closed loop signal boundedness and absolutely integrable property for the output tracking error is established for all $t \in [0, \infty)$. The finite time parameter estimation is exact at steady state and additionally robust to external disturbances. Indeed, Chapter 4 proposes the very first results on finite time estimation based adaptive FTC to compensate actuator failures. Asymptotic stability of tracking error dynamics, is guaranteed for finite/infinite number of actuator failures. Nominal performance recovery in the finite time sense is ensured provided the time between two successive changes in failure patterns is greater than the convergence time of the estimation error to the origin. The theoretical results obtained are undoubtedly novel and the algorithm would be a value addition to existing adaptive FTC literature.

Finally, in Chapter 5, the FTC problem is considered for a nonlinear system characterizing linearly parameterizable and parametrization free modeling uncertainties, affected by finite/infinite actuator failures. An integrated FE/FTC controller is developed using a backstepping methodology augmented with an adaptive disturbance observer which estimates total/lumped uncertainty arising due to modeling imperfections, external disturbances and actuator failures. Further, a tuning function approach is used to estimate the mismatched parametric uncertainties until the second last coordinate of backstepping. Following such an approach will avert the dependence on the derivative of parameter estimates and the closed loop tracking and performance recovery only depend on the total disturbance estimation error at the last coordinate. The modularity of the controller-disturbance pair is established by incorporating a new time varying damping term into the backstepping controller which decreases the effect of the disturbance estimation error on the tracking error and ensures its boundedness until the proposed adaptive disturbance observer estimates the total uncertainty in finite time. The standing assumption on the lumped uncertainties to be slowly varying with time, is removed. Such an FTC algorithm results in a precise control offering robust transient performance and successful recovery of the nominal output trajectory(without actuator failures) for the entire time period in the event of abrupt actuator faults and failures. Compared to existing approaches with similar design features, especially the most celebrated high gain observer(HGO) based methods, high gain instability due to peaking is avoided and hence the proposed control methodology also exhibits nominal input performance recovery in a finite time sense. The region of attraction corresponding to nominal conditions is also recovered largely. The avoidance of peaking indeed paves the way for achieving globally stable closed loop trajectories, global asymptotic stability of output tracking error dynamics and finite time nominal

performance recovery. The proposed scheme does not require any knowledge of the bounds of the total lumped uncertainty introduced into the system at the occurrence of eventualities of faults and failures.These design attributes have indeed been an unattained goal for a majority of DOB based control approaches in nonlinear systems which are not globally Lipschitz. The proposed control methodology is further extended for its application to the FTC problem of accommodating infinite actuator failures yielding promising and encouraging results. In contrast to bounded or asymptotically stable parameter/uncertainty estimation incurred due to actuator faults, a predefined exact finite time convergence of the disturbance estimates to their actual temporal profile, allows a lower bound on the minimum time lapse between two consecutive changes of actuator failure patterns, such that the nominal performance recovery in the sense of finite time is ensured. Finally, given that the control design is independent of the structural information of the total uncertainty, it enables the resulting FTC controllers to be applicable to a wide range of control systems with more general type of actuator failures.

6.2 Recommendations for Future Research

Future possible directions which are worth exploring based on the adaptive FTC algorithms proposed in this thesis are suggested as follows.

- Design and analysis of an adaptive FTC strategy which would not only exhibit finite time estimation but also achieve finite time compensation of actuator failures and unknown system uncertainties.
- Extension of the proposed multiple model adaptive backstepping FTC algorithms to the problem of compensating actuator failures and nonlinearly parameterized system and failure uncertainties.
- Application of the finite time parameter adaptation algorithm to adaptive control design in nonlinear uncertain systems with nonlinear parameterizations to improve its performance and robustness.
- All the adaptive FTC schemes proposed in this thesis assume that all the systems states are available for measurement. Relaxing this assumption, output feedback design based on the proposed FTC methodologies is also a research avenue worth exploring.
- Investigating the robustness of the proposed adaptive backstepping FTC methodologies in presence of input delays and thereafter calculate the time delay margin of such controllers.
- Extension of the proposed design methodologies to the problem of adaptive FTC in time delay systems.
- Design of optimal adaptive FTC algorithms for uncertain nonlinear systems using dynamic programming integrated with the proposed uncertainty estimators.
- Synthesis of adaptive controllers to compensate unknown actuator failures in non-minimum phase linear and nonlinear systems in presence of modeling uncertainties.

- Experimental validation of the proposed FTC schemes on real time systems such a mobile robot, quad-copters, axial rotor helicopters and variety of other dynamical systems requiring a self repairing module.
- Exploring promising possibilities of application of the proposed adaptive strategies to design controllers operating over a network. The control design would aim to achieve robust stability in presence of network uncertainties, for instance, limited channel bandwidth, loss of information packets, communication delay, etc. and also achieve an acceptable output performance.

A

Appendix

Contents

A.1 Definition of Performance Indices 223
A.2 Some Useful Definitions and Inequalities 224
A.3 Nonlinear State Estimation: Extended Kalman Filter (EKF) 226
A.4 Proof of Lemma 4.1 228

A.1 Definition of Performance Indices

- The performance indices like peak overshoot (M_p) and peak undershoot (M_u) are used to quantify the transient performance of the controlled system in regulation and set-point tracking problems.

- For tracking problems wherein the reference trajectory is a smooth time varying and bounded signal, the transient performance is measured using the integral time absolute error (ITAE). Whereas, the tracking accuracy (steady state performance) is measured using the integral of the absolute tracking error (IAE) and root mean square of the error (RMSE). All these performance metric together constitute the output performance measure of a controlled system. The respective mathematical definitions of the above stated performance indices are as follows.

$$ITAE = \int_0^T t|e(t)|dt \tag{A.1.1}$$

$$IAE = \int_0^T |e(t)|dt \tag{A.1.2}$$

$$RMSE = \sqrt{\frac{\sum_{l=1}^{n_s} e^2(l)}{n_s}} \tag{A.1.3}$$

where n_s denotes the total number of samples with the time interval $[0, T]$ with an appropriate sampling time.

- The control energy (CE) is defined by $\|u\|_2$ as the 2-norm of the control input and denotes the input performance. Further, total variation (TV) characterizes smoothness of the control signal and extent of usage of the control input [113] and is given as

$$TV = \sum_{l=1}^{n_s} |u_i(l+1) - u_i(l)\ | \tag{A.1.4}$$

where $u_i(1), u_i(2), ..., u_i(n_s)$ is the discretized sequence of the input signal. A low value of TV indicates smoothness of the control input.

A.2 Some Useful Definitions and Inequalities

A.2.1 Definition of Signal Norms and $\mathcal{L}_p$ Spaces

- Given, an interval $[a, b]$, the $\mathcal{L}_p$ norm of a continuous time vector function $f(t) \in \mathbb{R}^n$ is defined as, $\|f\|_{p[a,b]} := \int_a^b \|f(t)\|_p^p dt = \left(\int_a^b (|f_1(t)|^p + \ldots + |f_n(t)|^p) dt \right)^{\frac{1}{p}}$.
- Replacing $p = 1, 2, \infty$, the $\mathcal{L}_1[a, b]$, $\mathcal{L}_2[a, b]$ and $\mathcal{L}_\infty[a, b]$ norms are defined as,

$$\|f\|_{1[a,b]} := \int_a^b \|f(t)\|_1 dt, \quad \|f\|_{2[a,b]} := \left(\int_a^b \|f(t)\|_2^2 dt \right)^{\frac{1}{2}}, \quad \|f\|_{\infty[a,b]} := \sup_{t\in[a,b]} \max_{1\leq i\leq n} \|f_i(t)\|$$

- Given, an interval $[a, b]$, the $\mathcal{L}_p$ space is a vector space of functions with a finite $\mathcal{L}_p$ norm and defined as,

$$\mathcal{L}_p[a, b] := \left\{ f \in \mathbb{R}^n : \int_a^b \|f(t)\|_p^p < \infty \right\}$$

A.2.2 Signal Convergence Lemmas

Lemma A.1. *If $f(t), \dot{f}(t) \in \mathcal{L}_\infty$ and $f(t) \in \mathcal{L}_p$ for some $p \in [1, \infty)$, then $f(t) \to 0$ as $t \to \infty$.*

Proof. Please refer to [122].

Lemma A.2. *[Barbălat's Lemma] If $f(t), \dot{f}(t) \in \mathcal{L}_\infty$, which means that $f(t)$ is uniformly continuous and $\lim_{t\to\infty} \int_0^t f(s)ds$ exists and is finite, then $f(t) \to 0$ as $t \to \infty$.*

Proof. Please refer to [122].

A.2.3 Important Inequalities

The following inequalities are immensely useful for adaptive control design and stability analysis.

- **Hölder's Inequality:** For $p, q \in [1, \infty]$ and $\frac{1}{p} + \frac{1}{q} = 1$, then $f(t) \in \mathcal{L}_p$ and $g(t) \in \mathcal{L}_q$ implies $f(t)g(t) \in \mathcal{L}_1$ and $\|f(t)g(t)\|_1 \leq \|f(t)\|_p \|g(t)\|_q$.
- **Peter-Paul Inequality:** For $p, q \in [1, \infty]$ and $\frac{1}{p} + \frac{1}{q} = 1$, then $f(t) \in \mathcal{L}_p$ and $g(t) \in \mathcal{L}_q$ with $\varepsilon > 0$ implies $\|f(t)g(t)\|_1 \leq \frac{\|f(t)\|^2}{2\varepsilon} + \frac{\varepsilon \|g(t)\|^2}{2}$, where $p = q = 2$.
- **Minkowski Inequality:** For $p, q \in [1, \infty]$, $f(t) \in \mathcal{L}_p$ and $g(t) \in \mathcal{L}_p$, we have $\|f(t) + g(t)\|_p \leq \|f(t)\|_p + \|g(t)\|_p$ implying $f(t) + g(t) \in \mathcal{L}_p$.

A.2.4 Convex Sets

The following definitions and properties connected to convex sets are referred from [147] and the detailed proofs can be found therein.

Definition A.1. *Let $\theta_1, \theta_2, \ldots, \theta_N$ be points on a vector space $\mathcal{V}$. Let $\mathcal{S}$ be the set of all linear combinations $\sum_{i=1}^{N} w_i\theta_i$ with $w_i > 0$, $i = 1, \ldots, N$ and $\sum_{i=1}^{N} w_i = 1$. The set $\mathcal{S}$ is convex.*

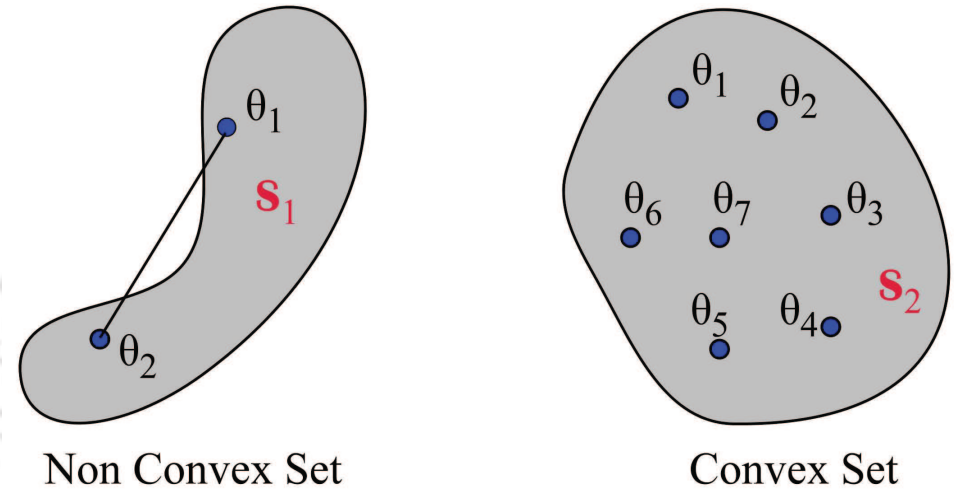

Figure A.1: Illustration of convex sets

Figure A.1 illustrates the convex sets wherein $\mathcal{S}_2$ is *convex* whereas $\mathcal{S}_1$ is not *convex*. The above conclusion is drawn from the following property of convex sets which is indeed important for the control methodology developed in Chapter 3.

Property of Convex Sets: Let $\theta_1, \theta_2, \ldots, \theta_N$ be points on a vector space V. Any convex set $\mathcal{S}$ which contains $\theta_1, \theta_2, \ldots, \theta_N$ also contains its linear combinations, $\sum_{i=1}^{N} w_i\theta_i$ satisfying $w_i > 0$, $i = 1, \ldots, N$ and $\sum_{i=1}^{N} w_i = 1$.

Definition A.2. *Considering the set $\mathcal{S}$ of points $\theta_1, \theta_2, \ldots, \theta_N$ on a vector space $\mathcal{V}$, the convex hull is defined as, $Conv(\mathcal{S}) := \{\sum_{i=1}^{N} w_i\theta_i | \forall i : w_i > 0$ and $\sum_{i=1}^{N} w_i = 1\}$. A minimum of $(n+1)$ points form a convex hull with a non-empty interior in an n-dimensional vector space.*

The concept of convex hull utilized in Chapter 3 to improve the output transient performance is schematically illustrated in Figure A.2. To obviate the drawbacks of switching, the control design in Chapter 3 resorts to a second layer of adaptation involving convex combination of parameter estimates from each of the identification models. In order to ensure a correct parameter estimation, the adaptive estimates from all the $N + 1$ identification models must together form a convex hull in the parameter space containing the actual parameter vector. Thereafter the algorithm is so constructed that the convex combination of their initial estimates dynamically converges to the actual parameter. Considering the dimension of actual parameter as N, Figure A.2 shows the convex hull (shaded portion for

N=2,3) formed by $N+1$ parameter estimates from $N+1$ identification models in an $N-$dimensional parameter space and is seen to contain the actual parameter $\theta^* \in \mathbb{R}^N$ for N=1,2,3.

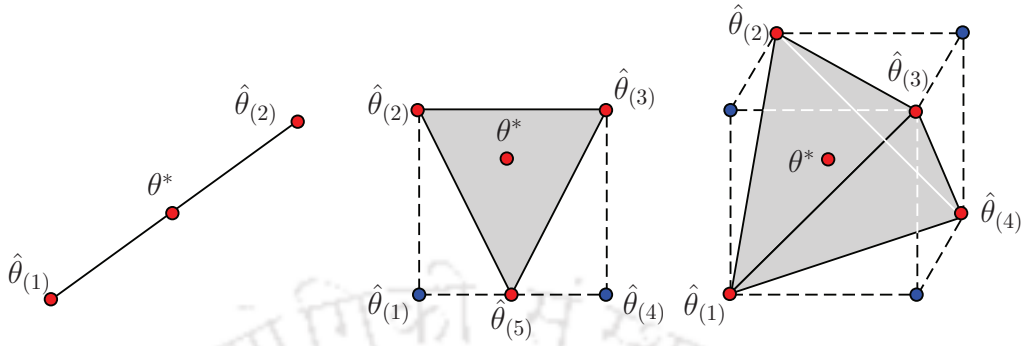

Figure A.2: Illustration of construction of convex hull in the parameter space for estimating a parameter of dimension $N = 1, 2, 3$ (from left to right).

A.3 Nonlinear State Estimation: Extended Kalman Filter (EKF)

A.3.1 Design Motivation

Kalman filter is used to find the best estimate of the unknown states of a dynamical system from the information available from the measured states in presence of noise [124]. The filter design primarily relies on the dynamic model of the system acted upon by the control inputs and affected by noise sources. Briefly, these filters are found useful in (a) extracting information about unmeasurable quantity from measurable quantity (b) estimating state of a system by combining the series of noisy measurements available from sensors.

It is obvious from (A.3.1)-(A.3.2) stated below that Kalman filtering is a two step procedure, starting with the prediction of current state variables, which are then updated once the next measurement is observed. Since both measurement and estimate may be subjected to some noise with finite covariance, these estimates are updated using weighted average gain known as the Kalman Gain (K). This Kalman Gain (K) is determined using the covariances as shown in A.3.2. TO explain the estimation process, let us consider a continuous-time linear system with the following dynamic and measurement equations:

$$\begin{aligned} \dot{x} &= Ax + Bu + w \\ y &= Cx + v \\ w &\sim \mathcal{N}(0, Q) \\ v &\sim \mathcal{N}(0, R) \end{aligned} \tag{A.3.1}$$

where $x \in \mathbb{R}^n$ is the state vector, $u \in \mathbb{R}^m$ is the control input, $y \in \mathbb{R}^q$ is the system output and w & v are zero mean process and measurement noises, respectively. Both the noise signals are assumed to be Gaussian with covariance Q and R, respectively. The Kalman filter equations used to estimate the

state of a system are:

$$\begin{aligned}
\hat{x}(0) &= E[x(0)] \\
P(0) &= E[(x(0) - \hat{x}(0))(x(0) - \hat{x}(0))^T] \\
K &= PC^T R^{-1} \\
\dot{\hat{x}} &= A\hat{x} + Bu + K(y - C\hat{x}) \\
\dot{P} &= -PC^T R^{-1} CP + AP + PA^T + Q
\end{aligned} \tag{A.3.2}$$

In first part of the equation, the system model is used to calculate initial state estimate $\hat{x}(0)$ and initial noise covariance $P(0)$. The second part of the equation uses these prior estimates and updates them to find posteriori estimates of the state and noise covariance. This algorithm repeats itself until the optimal estimate of the state is calculated.

The Kalman filter defined above can be applied to linear systems only. In case of nonlinear systems, applying Kalman filter directly may not lead to convergence to optimal states. So, the nonlinear system is first linearized around nominal values which are based on initial guess of system trajectory. The system whose states represent the deviation of a true state from this nominal state forms an incremental system which is exactly the linearized system dynamics around the nominal state. Thus, Kalman filter design methodology can be applied on the linearized system dynamics to estimate the deviation $\Delta\hat{x}$, and hence an estimate of true state vector is obtained. However, it is not always straightforward to predict the nominal state trajectory. In such a case, Extended Kalman Filter (EKF) can be implemented, which linearizes the nonlinear function around current state estimate obtained from Kalman Filter itself, and then the resulting Jacobian matrices are used in prediction and updation stages of Kalman filter algorithm.

A.3.2 Design of Extended Kalman Filter (EKF)

As explained in the preceding text, the design of an EKF seems to follow a 'bootstrapping procedure'. Let us consider a general non-linear system as follows.

$$\begin{aligned}
\dot{x} &= f(x, u, w, t) \\
y &= h(x, v) \\
w &\sim \mathcal{N}(0, Q) \\
v &\sim \mathcal{N}(0, R)
\end{aligned} \tag{A.3.3}$$

where $x \in \mathbb{R}^n$ is the state vector, $u \in \mathbb{R}^m$ is the control input, $y \in \mathbb{R}^q$ is the system output and w & v are zero mean process and measurement noises, respectively. The functions $f : \mathbb{R}^n \times \mathbb{R}^m \times \mathbb{R}^n \times \mathbb{R}_+ \to \mathbb{R}^n$ and $h : \mathbb{R}^n \times \mathbb{R}^q \to \mathbb{R}^q$ are smooth nonlinear and linear functions. Thereafter, using Taylor series, these

equations (A.3.3) can be linearized around the current state estimate $\hat{x}$ resulting in:

$$\begin{aligned} \dot{x} &= f(\hat{x}, u_0, w_0, t) + A\Delta x + B\Delta u + L\Delta w \\ y &= h(\hat{x}, v_0, t) + C\Delta x + M\Delta v \end{aligned} \tag{A.3.4}$$

where the matrices A, B, L, C and M are evaluated at each time step as

$$\begin{aligned} A &= \frac{\partial f}{\partial x}\Big|_{\hat{x}} & B &= \frac{\partial f}{\partial u}\Big|_{\hat{x}} & L &= \frac{\partial f}{\partial w}\Big|_{\hat{x}} \\ C &= \frac{\partial h}{\partial x}\Big|_{\hat{x}} & M &= \frac{\partial h}{\partial v}\Big|_{\hat{x}} \end{aligned} \tag{A.3.5}$$

Assuming that nominal noise values w_0 and u_0 are zero, the final equations describing the Extended Kalman Filter (EKF) are

$$\begin{aligned} \hat{x}(0) &= E[x(0)] \\ P(0) &= E[(x(0) - \hat{x}(0))(x(0) - \hat{x}(0))^T] \\ \dot{\hat{x}} &= f(\hat{x}, u_0, w_0, t) + K(y - h(\hat{x}, v_0, t)) \\ K &= PC^T\tilde{R}^{-1} \\ \dot{P} &= AP + PA^T + \tilde{Q} - PC^T\tilde{R}^{-1}CP \end{aligned} \tag{A.3.6}$$

where $\tilde{Q} = LQL^T$ and $\tilde{R} = MRM^T$. Thus using this approach, state estimate, $\hat{x}$, of a nonlinear system (approximated by linearization) is obtained directly. However, for highly nonlinear systems, linearization does not provide good approximation, and calculating Jacobians analytically may get complicated. Moreover, the state transition and measurement model needs to be differentiable for Jacobians to exist. Otherwise advanced filters need to employed for estimation, which are computationally more expensive than EKF.

A.4 Proof of Lemma 4.1

Proving that $\dot{\theta}^*(t) \in \mathcal{S}_1(\nu)$ is very straightforward. In the worst case, at least one actuator should be alive to satisfy the controllability condition and ensure the existence of a solution to the FTC problem. Therefore there exists a lower bound on θ_1^*. The lower bound can be derive straightaway as $\theta_1^* \geq \min\{\underline{K}_1\underline{b}_1, \ldots, \underline{K}_m\underline{b}_m\} =: \ell$. Further, it can be easily derived from the design assumptions that parameters jump at time instant T_h due to change in the actuator failure pattern. The fault/failure pattern does not change until the $T_{h+1}-$th instant of occurrence of the next failure/fault pattern for $h \in \mathbb{W}$. Therefore, if the failure parameter jumps at time t, the following holds.

$$|\theta_1^*(t^+) - \theta_1^*(t^-)| \leq \sum_{j=1}^{m} \overline{b}_j - \ell \tag{A.4.1}$$

$$|\theta_{3j}^*(t^+) - \theta_{3j}^*(t^-)| \leq 2\overline{b}_j\overline{u} \tag{A.4.2}$$

Defining $\Delta^{\dagger} = \max\{\sum_{j=1}^{m} \overline{b}_j - \ell,\ 2\overline{b}_j\overline{u}\} < \infty$. Now, due to change in actuator faults/failure pattern at $t = T_h$, the parameter $\theta^*(t)$ exhibits a jump whose magnitude is bounded as $\|\dot{\theta}^*(t)\| \leq \Delta^{\dagger}\delta(t - T_h)$. Therefore, $\forall h \in \mathbb{W}$, it is inferred that $\|\dot{\theta}^*(t)\| \leq \Delta^{\ddagger} \sum_{h} \delta(t - T_h)$ with $\Delta^{\ddagger} := \sqrt{m + p + 1}\Delta^{\dagger}$ (derived from norm inequalities [110, 122]). The function $\delta(\cdot)$ denotes the dirac delta function. At this point, it is easy to assume that $T \geq T^*$ and $t + T \geq T_{h+\aleph}$ where, $\aleph = T/T^* = \nu T$ is a positive number. Hence, the number of changes in the actuator failure pattern between the time $t \sim t + T$ is $\aleph + 1$. Utilizing this immediate assumption along with the assertion and thereafter invoking the properties of delta functions, the following is obtained,

$$\int_{t}^{t+T} \|\dot{\theta}^*(s)\| ds \leq \Delta^{\ddagger} \int_{t}^{t+T} \sum_{h} \delta(s - T_h) ds \leq \Delta^{\ddagger}(\aleph + 1) \tag{A.4.3}$$

The above integral (A.4.3) leads to the property of $\dot{\theta}^*(t)$ stated above, i.e., $\dot{\theta}^*(t) \in \mathcal{S}_1(\nu)$. The proof is complete. □

References

[1] J. C. Maxwell, "I. on governors," *Proceedings of the Royal Society of London*, vol. 16, pp. 270–283, 1868.

[2] M. T. Hamayun, C. Edwards, and H. Alwi, *Fault Tolerant Control Schemes Using Integral Sliding Modes*, ser. Studies in Systems, Decision and Control. Switzerland: Springer International Publishing, 2016, vol. 61, no. 1.

[3] "Reconfigurable fault-tolerant control: A tutorial introduction," *European Journal of Control*, vol. 14, no. 5, pp. 359 – 386, 2008.

[4] T. Wang, W. Xie, and Y. Zhang, "Sliding mode fault tolerant control dealing with modeling uncertainties and actuator faults," *ISA Transactions*, vol. 51, no. 3, pp. 386 – 392, 2012.

[5] X. Tang, G. Tao, and S. M. Joshi, "Adaptive actuator failure compensation for parametric strict feedback systems and an aircraft application," *Automatica*, vol. 39, no. 11, pp. 1975 – 1982, 2003.

[6] W. Wang and C. Wen, "Adaptive compensation for infinite number of actuator failures or faults," *Automatica*, vol. 47, no. 10, pp. 2197 – 2210, 2011.

[7] R. Eslinger and P. R. Chandler, "Self-repairing flight control system program overview," in *in Proceedings of the IEEE National Aerospace and Electron. Conference*, Dayton, OH, 1988.

[8] Y. Zhang and J. Jiang, "Bibliographical review on reconfigurable fault-tolerant control systems," *Annual Reviews in Control*, vol. 32, no. 2, pp. 229 – 252, 2008.

[9] X. Yu and J. Jiang, "A survey of fault-tolerant controllers based on safety-related issues," *Annual Reviews in Control*, vol. 39, pp. 46 – 57, 2015.

[10] J. Jiang and X. Yu, "Fault-tolerant control systems: A comparative study between active and passive approaches," *Annual Reviews in Control*, vol. 36, no. 1, pp. 60 – 72, 2012.

[11] F. Burcham, C. Fullerton, and T. Maine, "Manual manipulation of engine throttles for emergency flight control," NASA, Technical report NASA/TM-2004-212045, 2004.

[12] K. Ehsan, "Jet airways' pilot's act in goa was as miraculous as landing the aircraft on water," *Janta Ka Reporter*, 2016.

[13] "Goa jet airways accident: 15 passengers suffer minor injuries; dgca begins probe," *The Indian Express*, 2016.

[14] C. Yuan, Y. Zhang, and Z. Liu, "A survey on technologies for automatic forest fire monitoring, detection, and fighting using unmanned aerial vehicles and remote sensing techniques," *Canadian Journal of Forest Research*, vol. 45, no. 7, pp. 783–792, 2015.

[15] L. Zhixiang, Y. Chi, Y. Xiang, and Z. Youmin, "Retrofit faultâĂŘtolerant tracking control design of an unmanned quadrotor helicopter considering actuator dynamics," *International Journal of Robust and Nonlinear Control*, vol. 0, no. 0, 2017.

[16] H. Wu and M. Deng, "Robust adaptive control scheme for uncertain non-linear model reference adaptive control systems with time-varying delays," *IET Control Theory Applications*, vol. 9, no. 8, pp. 1181–1189, 2015.

[17] G. Tao, S. Joshi, and X. Ma, "Adaptive state feedback and tracking control of systems with actuator failures," *IEEE Transactions on Automatic Control*, vol. 46, no. 1, pp. 78–95, 2001.

[18] M.-H. Liu and W. Lin, "Multivariable self-tuning control with decoupling robotic manipulators," *IEE Proceedings D - Control Theory and Applications*, vol. 135, no. 1, pp. 43–48, 1988.

[19] H. Alwi and C. Edwards, "Fault tolerant control using sliding modes with on-line control allocation," *Automatica*, vol. 44, no. 7, pp. 1859 – 1866, 2008.

[20] M. Hamayun, C. Edwards, and H. Alwi, "A fault tolerant control allocation scheme with output integral sliding modes," *Automatica*, vol. 49, no. 6, pp. 1830 – 1837, 2013.

[21] S. S. Tohidi, A. K. Sedigh, and D. Buzorgnia, "Fault tolerant control design using adaptive control allocation based on the pseudo inverse along the null space," *International Journal of Robust and Nonlinear Control*, pp. n/a–n/a, 2016.

[22] P. S. Maybeck, "Multiple model adaptive algorithms for detecting and compensating sensor and actuator/surface failures in aircraft flight control systems," *International Journal of Robust and Nonlinear Control*, vol. 9, no. 14, pp. 1051–1070, 1999.

[23] G. Yen and L.-W. Ho, "Online multiple-model-based fault diagnosis and accommodation," *IEEE Transactions on Industrial Electronics*, vol. 50, no. 2, pp. 296–312, April, 2003.

[24] S.-J. Zhang, X.-W. Qiu, B. Jiang, and C.-S. Liu, "Adaptive actuator failure compensation control based on mmst grouping for a class of mimo nonlinear systems with guaranteed transient performance," *International Journal of Control*, vol. 88, no. 3, pp. 593–601, 2015.

[25] Y. Yin, P. Shi, and F. Liu, "Gain-scheduled robust fault detection on time-delay stochastic nonlinear systems," *IEEE Transactions on Industrial Electronics*, vol. 58, no. 10, pp. 4908–4916, 2011.

[26] S. Montes de Oca, S. Tornil-Sin, V. Puig, and D. Theilliol, "Fault-tolerant control design using the linear parameter varying approach," *International Journal of Robust and Nonlinear Control*, vol. 24, no. 14, pp. 1969–1988, 2014.

[27] B. A. Siddiqui, S. El-Ferik, and M. Abdelkader, "Fault tolerant flight control using sliding modes and subspace identification-based predictive control," *IFAC-PapersOnLine*, vol. 49, no. 9, pp. 124 – 129, 2016, 6th IFAC Symposium on System Structure and Control SSSC 2016.

[28] Y. Alain, M. Seron, and A. De Doná José, "Robust multiactuator fault-tolerant mpc design for constrained systems," *International Journal of Robust and Nonlinear Control*, vol. 23, no. 16, pp. 1828–1845, 2012.

[29] Alwi, H. and Edwards, C., "Fault detection and fault-tolerant control of a civil aircraft using a sliding-mode-based scheme," *IEEE Transactions on Control Systems Technology*, vol. 16, no. 3, pp. 499 –510, May 2008.

[30] F. Chen, B. Jiang, and G. Tao, "An intelligent self-repairing control for nonlinear MIMO systems via adaptive sliding mode control technology," *Journal of the Franklin Institute*, vol. 351, no. 1, pp. 399 – 411, 2014.

[31] W. Wang and C. Wen, "Adaptive actuator failure compensation control of uncertain nonlinear systems with guaranteed transient performance," *Automatica*, vol. 46, no. 12, pp. 2082 – 2091, 2010.

[32] X. Tang, G. Tao and S.M. Joshi, "Adaptive actuator failure compensation for nonlinear MIMO systems with an aircraft control application," *Automatica*, vol. 43, no. 11, pp. 1869 – 1883, 2007.

[33] X. Yu and J. Jiang, "Hybrid fault-tolerant flight control system design against partial actuator failures," *IEEE Transactions on Control Systems Technology*, vol. 20, no. 4, pp. 871–886, July 2012.

[34] M. Khosrowjerdi, "Mixed $\mathcal{H}_2/\mathcal{H}_\infty$ approach to fault-tolerant controller design for lipschitz non-linear systems," *IET Control Theory & Applications*, vol. 5, pp. 299–307, January 2011.

[35] Q. Hu, B. Xiao, and M. Friswell, "Robust fault tolerant control for spacecraft attitude stabilization under actuator faults and bounded disturbance," *Journal of Dynamic Systems, Measurement and Control*, vol. 133, pp. 051 006–1–051 006–8, 2011.

[36] ——, "Fault tolerant control with $\mathcal{H}_\infty$ performance for attitude tracking of flexible spacecraft," *IET Control Theory Applications*, vol. 6, no. 10, pp. 1388–1399, 2012.

[37] H. Niemann and J. Stoustrup, "Passive fault tolerant control of a double inverted pendulum: a case study," *Control Engineering Practice*, vol. 13, no. 8, pp. 1047 – 1059, 2005.

[38] B. Liang and G. Duan, "Robust $\mathcal{H}_\infty$ fault-tolerant control for uncertain descriptor systems by dynamical compensators," *Journal of Control Theory and Applications*, vol. 2, no. 3, pp. 288–292, 2004.

[39] M. Benosman and K.-Y. Lum, "Application of absolute stability theory to robust control against loss of actuator effectiveness," *IET Control Theory Applications*, vol. 3, no. 6, pp. 772–788, 2009.

[40] M. Corradini and G. Orlando, "A sliding mode controller for actuator failure compensation," in *Proceedings of 42nd IEEE Conference on Decision and Control*, vol. 4, Maui, Hawaii, December 2003, pp. 4291–4296.

[41] Corradini, M.L. and Orlando, G. and Parlangeli, G., "Actuator failures compensation: a sliding mode control approach," in *14th Mediterranean Conference on Control and Automation*, 2003, pp. 1–6.

[42] Corradini, M.L. and Monteriu, A. and Orlando, G., "An actuator failure tolerant control scheme for an underwater remotely operated vehicle," *IEEE Transactions on Control Systems Technology*, vol. 19, no. 5, pp. 1036–1046, 2011.

[43] M. Hamayun, C. Edwards, and H. Alwi, "Design and analysis of an integral sliding mode fault-tolerant control scheme," *IEEE Transactions on Automatic Control*, vol. 57, no. 7, pp. 1783 –1789, July 2012.

[44] ——, "Augmentation scheme for fault-tolerant control using integral sliding modes," *IEEE Transactions onControl Systems Technology,*, vol. 22, no. 1, pp. 307–313, Jan 2014.

[45] P. Baldi, M. Blanke, P. Castaldi, N. Mimmo, and S. Simani, "Adaptive ftc based on control allocation and fault accommodation for satellite reaction wheels," in *2016 3rd Conference on Control and Fault-Tolerant Systems (SysTol)*, Sept 2016, pp. 672–677.

[46] C. Andrea, P. M. M., and J. T. Arne, "Fault-Řtolerant control allocation for overactuated nonlinear systems," *Asian Journal of Control*, vol. 20, no. 2, pp. 621–634.

[47] A. Casavola and E. Garone, "Fault-tolerant adaptive control allocation schemes for overactuated systems," *International Journal of Robust and Nonlinear Control*, vol. 20, no. 17, pp. 1958–1980, 2010.

[48] Q. Shen, B. Jiang, P. Shi, and C. C. Lim, "Novel neural networks-based fault tolerant control scheme with fault alarm," *IEEE Transactions on Cybernetics*, vol. 44, no. 11, pp. 2190–2201, Nov 2014.

[49] J. Han, H. Zhang, Y. Wang, and X. Liu, "Robust state/fault estimation and fault tolerant control for ts fuzzy systems with sensor and actuator faults," *Journal of the Franklin Institute*, vol. 353, no. 2, pp. 615 – 641, 2016.

[50] X. Zhang, M. M. Polycarpou, and T. Parisini, "Adaptive fault diagnosis and fault-tolerant control of mimo nonlinear uncertain systems," *International Journal of Control*, vol. 83, no. 5, pp. 1054–1080, 2010.

[51] X. Zhang, T. Parisini, and M. M. Polycarpou, "Adaptive fault-tolerant control of nonlinear uncertain systems: an information-based diagnostic approach," *IEEE Transactions on Automatic Control*, vol. 49, no. 8, pp. 1259–1274, Aug 2004.

[52] X. Zhang, M. M. Polycarpou, and T. Parisini, "Fault diagnosis of a class of nonlinear uncertain systems with lipschitz nonlinearities using adaptive estimation," *Automatica*, vol. 46, no. 2, pp. 290 – 299, 2010.

[53] C. Tan, X. Yao, G. Tao, and R. Qi, "A multiple-model based adaptive actuator failure compensation scheme for control of near-space vehicles," *IFAC Proceedings Volumes*, vol. 45, no. 20, pp. 594 – 599, 2012, 8th IFAC Symposium on Fault Detection, Supervision and Safety of Technical Processes.

[54] X. L. Yao, G. Tao, R. Y. Qi, and B. Jiang, "An adaptive actuator failure compensation scheme for a class of nonlinear mimo systems," *Journal of the Franklin Institute*, vol. 350, no. 9, pp. 2423–2441, November 2013.

[55] M. A. Yajie, B. Jiang, and G. Tao, "A new multiple-model adaptive actuator failure compensation scheme for a class of nonlinear mimo systems," in *Proceedings of the 34th Chinese Control Conference*, vol. 4, July 2015, pp. 6274 –6279.

[56] X. Yao, G. Tao, and B. Jiang, "Adaptive actuator failure compensation for multivariable feedback linearizable systems," *International Journal of Robust and Nonlinear Control*, vol. 26, no. 2, pp. 252–285, 2016.

[57] Q. Yang, S. S. Ge, and Y. Sun, "Adaptive actuator fault tolerant control for uncertain nonlinear systems with multiple actuators," *Automatica*, vol. 60, pp. 92 – 99, 2015.

[58] G. P. Incremona, A. Ferrara, and L. Magni, "Hierarchical model predictive/sliding mode control of nonlinear constrained uncertain systems," *IFAC-PapersOnLine*, vol. 48, no. 23, pp. 102 – 109, 2015, 5th IFAC Conference on Nonlinear Model Predictive Control NMPC 2015.

[59] S. E. Boukani, M. J. Khosrowjerdi, and R. Amjadifard, "Terminal sliding mode control allocation for nonlinear systems," *Canadian Journal of Electrical and Computer Engineering*, vol. 40, no. 3, pp. 162–170, Summer 2017.

[60] H. Alwi, "Fault tolerant longitudinal aircraft control using non-linear integral sliding mode," *IET Control Theory Applications*, vol. 8, pp. 1803–1814(11), November 2014.

[61] C.-C. Chen and Y.-W. Liang, "Fault tolerant control of nonlinear systems via a ca-based integral sliding mode technique," in *Decision and Control (CDC), 2013 IEEE 52nd Annual Conference on*, Dec 2013, pp. 19–24.

[62] B. Xu, R. Qi, B. Jiang, and X. Yao, "Nussbaum gain adaptive fault tolerant control for hypersonic vehicles with uncertain parameters and actuator faults," *IFAC-PapersOnLine*, vol. 50, no. 1, pp. 5256 – 5262, 2017, 20th IFAC World Congress.

[63] H. Jingjing, Q. Ruiyun, and J. Bin, "Adaptive fault-tolerant control design for hypersonic flight vehicles based on feedback linearization," in *Proceedings of the 33rd Chinese Control Conference*, July 2014, pp. 3197–3202.

[64] X. Ma and G. Tao, "Adaptive actuator compensation control with feedback linearization," *IEEE Transactions on Automatic Control*, vol. 45, no. 9, pp. 1705–1710, Sep 2000.

[65] J. He, R. Qi, B. Jiang, and J. Qian, "Adaptive output feedback fault-tolerant control design for hypersonic flight vehicles," *Journal of the Franklin Institute*, no. 0, pp. –, 2015.

[66] S. Kendrick Amezquita, L. Yan, and W. A. Butt, "Adaptive dynamic surface control for a class of mimo nonlinear systems with actuator failures," *International Journal of Systems Science*, vol. 44, no. 3, pp. 479–492, 2013.

[67] S. Kendrick Amezquita, Y. Lin, W. Butt, and C. Y. P. Chen, "Dynamic surface control for a class of nonlinear feedback linearizable systems with actuator failures," *IEEE Transactions on Neural Networks and Learning Systems*, vol. PP, no. 99, pp. 1–6, June 2016.

[68] S. Sastry, *Nonlinear Systems: Analysis, Stability, and Control*, ser. Interdisciplinary Applied Mathematics.

[69] M. Krstić, I. Kanellakopoulos, and P. Kokotović, *Nonlinear and adaptive control design*, ser. Adaptive and learning systems for signal processing, communications, and control. Wiley, 1995.

[70] D. Swaroop, J. Hedrick, P. Yip, and J. Gerdes, "Dynamic surface control for a class of nonlinear systems," *IEEE Transactions on Automatic Control*, vol. 45, no. 10, pp. 1893–1899, Oct 2000.

[71] X. Tang, G. Tao, and S. M. Joshi, "Adaptive output feedback actuator failure compensation for a class of non-linear systems," *International Journal of Adaptive Control and Signal Processing*, vol. 19, no. 6, pp. 419–444, 2005.

[72] Z. Zhang and W. Chen, "Adaptive output feedback control of nonlinear systems with actuator failures," *Information Sciences*, vol. 179, no. 24, pp. 4249 – 4260, 2009.

[73] Z. Zhang, S. Xu, Y. Guo, and Y. Chu, "Robust adaptive output-feedback control for a class of nonlinear systems with time-varying actuator faults," *International Journal of Adaptive Control and Signal Processing*, vol. 24, no. 9, pp. 743–759, 2010.

[74] T. Wang, W. Xie, and Y. Zhang, "Sliding mode reconfigurable fault tolerant control for nonlinear aircraft systems," *Journal of Aerospace Engineering*, vol. 28, no. 3, p. 04014086, May 2015.

[75] C. Wang and L. Guo, "Adaptive compensation for infinite number of actuator failures with an application to flight control," *International Journal of Adaptive Control and Signal Processing*, vol. 30, no. 3, pp. 443–455, 2016.

[76] G. Lai, C. Wen, Z. Liu, Y. Zhang, C. PhilipÂăChen, and S. Xie, "Adaptive compensation for infinite number of actuator failures based on tuning function approach," *Automatica*, vol. 87, pp. 365 – 374, 2018.

[77] L. Jianglin and P. R. J., "Integrated fault estimation and fault-Řtolerant control for uncertain lipschitz nonlinear systems," *International Journal of Robust and Nonlinear Control*, vol. 27, no. 5, pp. 761–780, July 2016.

[78] P. Castaldi, N. Mimmo, and S. Simani, "Differential geometry based active fault tolerant control for aircraft," *Control Engineering Practice*, vol. 32, pp. 227 – 235, 2014.

[79] B. Jiang, D. Xu, P. Shi, and C. C. Lim, "Adaptive neural observer-based backstepping fault tolerant control for near space vehicle under control effector damage," *Control Theory Applications, IET*, vol. 8, no. 9, pp. 658–666, June 2014.

[80] F. Chen, W. Lei, K. Zhang, G. Tao, and B. Jiang, "A novel nonlinear resilient control for a quadrotor uav via backstepping control and nonlinear disturbance observer," *Nonlinear Dynamics*, vol. 85, no. 2, pp. 1281–1295, Jul 2016.

[81] Y. l. Zhou and M. Chen, "Disturbance-observer-based fault tolerant control for near space vehicles with input saturation," in *Proceedings of the 33rd Chinese Control Conference*, July 2014, pp. 2101–2105.

[82] Q. Y. Fan and G. H. Yang, "Adaptive fault-tolerant control for affine non-linear systems based on approximate dynamic programming," *IET Control Theory Applications*, vol. 10, no. 6, pp. 655–663, 2016.

[83] Z. Ma, S. Tong, and Y. Li, "Adaptive output feedback fault-tolerant control for mimo non-affine non-linear systems based on disturbance observer," *IET Control Theory Applications*, vol. 10, no. 18, pp. 2422–2436, 2016.

[84] M. Chen, S. Y. Shao, and B. Jiang, "Adaptive neural control of uncertain nonlinear systems using disturbance observer," *IEEE Transactions on Cybernetics*, vol. 47, no. 10, pp. 3110–3123, Oct 2017.

[85] M. Chen, P. Shi, and C. C. Lim, "Adaptive neural fault-tolerant control of a 3-dof model helicopter system," *IEEE Transactions on Systems, Man, and Cybernetics: Systems*, vol. 46, no. 2, pp. 260–270, Feb 2016.

[86] Y. Yang and D. Yue, "Observer-based decentralized adaptive nns fault-tolerant control of a class of large-scale uncertain nonlinear systems with actuator failures," *IEEE Transactions on Systems, Man, and Cybernetics: Systems*, pp. 1–15, 2017.

[87] S. Yin, H. Yang, H. Gao, J. Qiu, and O. Kaynak, "An adaptive nn-based approach for fault-tolerant control of nonlinear time-varying delay systems with unmodeled dynamics," *IEEE Transactions on Neural Networks and Learning Systems*, vol. 28, no. 8, pp. 1902–1913, Aug 2017.

[88] M. Chen and G. Tao, "Adaptive fault-tolerant control of uncertain nonlinear large-scale systems with unknown dead zone," *IEEE Transactions on Cybernetics*, vol. 46, no. 8, pp. 1851–1862, Aug 2016.

[89] C. Jérôme, E. Denis, and H. David, "Transient management of a supervisory fault-Řtolerant control scheme based on dwell-time conditions," *International Journal of Adaptive Control and Signal Processing*, vol. 29, no. 1, pp. 123–142, 2014.

[90] J. Cieslak, D. Efimov, and D. Henry, "Supervisory fault tolerant control scheme based on bumpless scheme and dwell-time conditions," *IFAC Proceedings Volumes*, vol. 45, no. 20, pp. 385 – 390, 2012, 8th IFAC Symposium on Fault Detection, Supervision and Safety of Technical Processes.

[91] I. D. Landau, R. Lozano, and M. M'Saad, *Adaptive Control*, J. W. Modestino, A. Fettweis, J. L. Massey, M. Thoma, E. D. Sontag, and B. W. Dickinson, Eds. Berlin, Heidelberg: Springer-Verlag, 1998.

[92] D. Ginoya, P. Shendge, and S. Phadke, "Disturbance observer based sliding mode control of nonlinear mismatched uncertain systems," *Communications in Nonlinear Science and Numerical Simulation*, vol. 26, no. 13, pp. 98 – 107, 2015.

[93] H. Sun and L. Guo, "Composite adaptive disturbance observer based control and back-stepping method for nonlinear system with multiple mismatched disturbances," *Journal of the Franklin Institute*, vol. 351, no. 2, pp. 1027 – 1041, 2014.

[94] H. Niemann and J. Stoustrup, "Passive fault tolerant control of a double inverted pendulum-a case study," *Control Engineering Practice*, vol. 13, no. 8, pp. 1047 – 1059, 2005, fault Detection, Supervision and Safety of Technical Processes (S afeprocess 2003).

[95] A. Chakravarty and C. Mahanta, "Actuator fault-tolerant control (ftc) design with post-fault transient improvement for application to aircraft control," *International Journal of Robust and Nonlinear Control*, vol. 26, no. 10, pp. 2049–2074, 2016.

[96] S. Kwon and W. Chung, "A robust tracking controller design with hierarchical perturbation compensation," *ASME. J. Dyn. Sys., Meas., Control*, vol. 124, no. 2, pp. 261–271, 2002.

[97] A. Levant, "Universal single-input-single-output (siso) sliding-mode controllers with finite-time convergence," *IEEE Transactions on Automatic Control*, vol. 46, no. 9, pp. 1447–1451, 2001.

[98] R. Y. Qi, Y. H. Huang, B. Jiang, and G. Tao, "Adaptive backstepping control for hypersonic vehicle with uncertain parameters and actuator faults," *Journal of Systems and Control Engineering*, vol. 227, no. 1, pp. 51–61, January 2013.

[99] Q. Shen, B. Jiang, and V. Cocquempot, "Adaptive fault-tolerant backstepping control against actuator gain faults and its applications to an aircraft longitudinal motion dynamics," *International Journal of Robust and Nonlinear Control*, vol. 23, no. 15, pp. 1753–1779, 2013.

[100] J. Boskovic and R. Mehra, "Stable multiple model adaptive flight control for accommodation of a large class of control effector failures," in *Proceedings of the American Control Conference*, vol. 3, San Diego, CA, June 1999, pp. 1920–1924.

[101] C. Tan, G. Tao, and R. Qi, "A discrete-time indirect adaptive multiple-model actuator failure compensation scheme," *International Journal of Adaptive Control and Signal Processing*, pp. n/a–n/a, 2015.

[102] R. Marino and P. Tomei, *Nonlinear Control Design: Geometric, Adaptive and Robust.* Hertfordshire,UK: Prentice Hall International (UK) Ltd., 1996.

[103] V. Utkin and J. Shi, "Integral sliding mode in systems operating under uncertainty conditions," in *Proceedings of the 35th IEEE Conference on Decision and Control*, vol. 4, Kobe, Japan, December 1996, pp. 4591–4596.

[104] A. Chakravarty and C. Mahanta, "Actuator fault tolerant control scheme for nonlinear uncertain systems using backstepping based sliding mode," in *Annual IEEE India Conference (INDICON), 2013*, Dec 2013, pp. 1–6.

[105] A. Filippov, *Differential Equations with Discontinuous Righthand Sides*, ser. Mathematics and its Applications, F. Arscott, Ed. Springer, 1988, vol. 18.

[106] S. Bhat and D. Bernstein, "Geometric homogeneity with applications to finite-time stability," *Math. Control Signals Systems*, vol. 17, pp. 101–127, 2005.

[107] M. Defoort, T. Floquet, A. Kokosyd, and W. Perruquetti, "A novel higher order sliding mode control scheme," *System and Control Letters*, vol. 58, pp. 102–108, 2009.

[108] W. Gao and J. C. Hung, "Variable structure control of nonlinear systems: A new approach," *IEEE Transactions on Industrial Electronics*, vol. 40, (1), pp. 45–50, 1993.

[109] H. K. Khalil, *Nonlinear Systems (2nd ed.).* Upper Saddle River, NJ: Prentice Hall, 1996.

[110] P. Ioannou and J. Sun, *Robust Adaptive Control*, ser. Control theory. PTR Prentice-Hall, 1996, no. v. 1.

[111] J. Y. Shin, C. Belcastro, and T. Khong, "Closed-loop evaluation of an integrated failure identification and fault tolerant control system for a transport aircraft," in *AIAA Guidance, Navigation, and Control Conference and Exhibit.* American Institute of Aeronautics and Astronautics, 2006.

[112] A. Marcos and G. J. Balas, "Development of linear-parameter-varying models for aircraft," *Journal of Guidance, Control, and Dynamics*, vol. 27, no. 2, pp. 218–228, 2004.

[113] S. Skogestad, "Simple analytic rules for model reduction and pid controller tuning," *Journal of Process Control*, vol. 13, pp. 291–309, 2003.

[114] N. Hovakimyan and C. Cao, *L1 Adaptive Control Theory: Guaranteed Robustness with Fast Adaptation*, ser. Advances in Design and Control. Society for Industrial and Applied Mathematics (SIAM, 3600 Market Street, Floor 6, Philadelphia, PA 19104), 2010.

[115] K. S. Narendra and J. Balakrishnan, "Improving transient response of adaptive control systems using multiple models and switching," *IEEE Transactions on Automatic Control*, vol. 39, no. 9, pp. 1861–1866, 1994.

[116] K. S. Narendra, J. Balakrishnan, and M. K. Ciliz, "Adaptation and learning using multiple models, switching, and tuning," *IEEE Control Systems*, vol. 15, no. 3, pp. 37 –51, June 1995.

[117] K. S. Narendra and K. George, "Adaptive control of simple nonlinear systems using multiple models," in *Proceedings of the American Control Conference*, vol. 3, 2002, pp. 1779 – 1784 vol.3.

[118] A. Cezayirli and M. K. Ciliz, "Increased transient performance for the adaptive control of feedback linearizable systems using multiple models," *International Journal of Control*, vol. 79, no. 10, pp. 1205–1215, 2006.

[119] ——, "Indirect adaptive control of non-linear systems using multiple identification models and switching," *International Journal of Control*, vol. 81, no. 9, pp. 1434–1450, 2008.

[120] M. Huang, W. Xin, and W. Zhenlei, "Multiple model adaptive control for a class of linear-bounded nonlinear systems," *IEEE Transactions on Automatic Control*, vol. 60, no. 1, pp. 271–276, May 2014.

[121] Z. Han and K. S. Narendra, "New concepts in adaptive control using multiple models," *IEEE Transactions on Automatic Control*, vol. 57, no. 1, pp. 78 –89, Jan 2012.

[122] G. Tao, *Adaptive Control Design and Analysis (Adaptive and Learning Systems for Signal Processing, Communications and Control Series)*. New York, NY, USA: John Wiley & Sons, Inc., 2003.

[123] TRMS, *Twin Rotor MIMO System Control Experiments 33-949S*, 33rd ed., Feedback Instruments Ltd., Crowborough, U.K., 1997.

[124] D. Simon, *Optimal State Estimation: Kalman, H Infinity, and Nonlinear Approaches*. New York, NY, USA: Wiley-Interscience, 2006.

[125] J. Davila, M. Basin, and L. Fridman, "Finite-time parameter identification via high-order sliding mode observer," in *Proceedings of the 2010 American Control Conference*, June 2010, pp. 2960–2964.

[126] Y. Shen and X. Xia, "Nonlinear adaptive observers with finite-time convergence for a class of lipschitz nonlinear systems," in *2012 IEEE 51st IEEE Conference on Decision and Control (CDC)*, Dec 2012, pp. 320–325.

[127] Y. Shen, H. Yu, and J. Jian, "Finite-time adaptive observers for a class of nonlinear systems and its application to robot systems," in *2014 IEEE International Conference on Robotics and Biomimetics (ROBIO 2014)*, Dec 2014, pp. 2613–2618.

[128] J. A. Moreno and E. Guzman, "A new recursive finite-time convergent parameter estimation algorithm," *IFAC Proceedings Volumes*, vol. 44, no. 1, pp. 3439 – 3444, 2011, 18th IFAC World Congress.

[129] V. Adetola and M. Guay, "Finite-time parameter estimation in adaptive control of nonlinear systems," *IEEE Transactions on Automatic Control*, vol. 53, no. 3, pp. 807–811, April 2008.

[130] ——, "Performance improvement in adaptive control of linearly parameterized nonlinear systems ," *IEEE Transactions on Automatic Control*, vol. 55, no. 9, pp. 2182–2186, Sept 2010.

[131] J. Na, M. N. Mahyuddin, G. Herrmann, and X. Ren, "Robust adaptive finite-time parameter estimation for linearly parameterized nonlinear systems," in *Proceedings of the 32nd Chinese Control Conference*, July 2013, pp. 1735–1741.

[132] A. Levant, "Homogeneity approach to high-order sliding mode design," *Automatica*, vol. 41, no. 5, pp. 823 – 830, 2005.

[133] S. B. Roy, S. Bhasin, and I. N. Kar, "Parameter convergence via a novel pi-like composite adaptive controller for uncertain euler-lagrange systems," in *2016 IEEE 55th Conference on Decision and Control (CDC)*, Dec 2016, pp. 1261–1266.

[134] ——, "Robust gradient-based adaptive control of nonlinearly parametrized plants," *IEEE Control Systems Letters*, vol. 1, no. 2, pp. 352–357, Oct 2017.

[135] S. P. Bhat and D. S. Bernstein, "Continuous finite-time stabilization of the translational and rotational double integrators," *IEEE Tansactions on Automatic Control*, vol. 43 (5), pp. 678–682, 1998.

[136] A. N. Atassi and H. K. Khalil, "A separation principle for the stabilization of a class of nonlinear systems," *IEEE Transactions on Automatic Control*, vol. 44, no. 9, pp. 1672–1687, Sep 1999.

[137] ——, "A separation principle for the control of a class of nonlinear systems," *IEEE Transactions on Automatic Control*, vol. 46, no. 5, pp. 742–746, May 2001.

[138] H. K. Khalil, "High-gain observers in feedback control: Application to permanent magnet synchronous motors," *IEEE Control Systems*, vol. 37, no. 3, pp. 25–41, June 2017.

[139] J. Davila, "Exact tracking using backstepping control design and high-order sliding modes," *IEEE Transactions on Automatic Control*, vol. 58, no. 8, pp. 2077–2081, Aug 2013.

[140] A. Ferreira de Loza, J. Cieslak, D. Henry, A. Zolghadri, and L. M. Fridman, "Output tracking of systems subjected to perturbations and a class of actuator faults based on hosm observation and identification," *Automatica*, vol. 59, no. C, pp. 200–205, Sep. 2015.

[141] L. Rosier, "Homogeneous lyapunov function for homogeneous continuous vector field," *Syst. Control Lett.*, vol. 19, no. 6, pp. 467–473, Dec. 1992.

[142] Y. B. Shtessel, I. A. Shkolnikov, and A. Levant, "Smooth second-order sliding modes: Missile guidance application," *Automatica*, vol. 43, no. 8, pp. 1470 – 1476, 2007.

[143] "A new strategy for integration of fault estimation within fault-tolerant control," *Automatica*, vol. 69, pp. 48 – 59, 2016.

[144] T. K. Nizami, A. Chakravarty, and C. Mahanta, "Analysis and experimental investigation into a finite time current observer based adaptive backstepping control of buck converters," *Journal of the Franklin Institute*, 2018.

[145] J. A. Moreno and M. Osorio, "Strict lyapunov functions for the super-twisting algorithm," *IEEE Transactions on Automatic Control*, vol. 57, no. 4, pp. 1035–1040, April 2012.

[146] H. Alwi and C. Edwards, "An adaptive sliding mode differentiator for actuator oscillatory failure case reconstruction," *Automatica*, vol. 49, no. 2, pp. 642 – 651, 2013.

[147] S. Lang, *Linear Algebra*, ser. Springer Undergraduate Texts in Mathematics and Technology. Springer, 1987.